

2012

Aminostratigraphy of semi-enclosed basins

William Anthony Nicholas
University of Wollongong

Recommended Citation

Nicholas, William Anthony, Aminostratigraphy of semi-enclosed basins, Doctor of Philosophy thesis, School of Earth & Environmental Sciences, University of Wollongong, 2012. <http://ro.uow.edu.au/theses/3536>

Research Online is the open access institutional repository for the University of Wollongong. For further information contact Manager Repository Services: morgan@uow.edu.au.

UNIVERSITY OF WOLLONGONG

COPYRIGHT WARNING

You may print or download ONE copy of this document for the purpose of your own research or study. The University does not authorise you to copy, communicate or otherwise make available electronically to any other person any copyright material contained on this site. You are reminded of the following:

Copyright owners are entitled to take legal action against persons who infringe their copyright. A reproduction of material that is protected by copyright may be a copyright infringement. A court may impose penalties and award damages in relation to offences and infringements relating to copyright material. Higher penalties may apply, and higher damages may be awarded, for offences and infringements involving the conversion of material into digital or electronic form.

**Aminostratigraphy
of semi-enclosed basins**

**A thesis submitted in fulfilment of the requirement for the
award of the degree of**

Doctor of Philosophy

**from
University of Wollongong**

by

W. A. (Tony) Nicholas, BSc Hons (Geology)

School of Earth & Environmental Sciences

2012

Thesis Certification

Certification

I, William Anthony (Tony) Nicholas, declare that this thesis, submitted in fulfilment of the requirements for the award of Doctor of Philosophy, in the School of Earth & Environmental Sciences, University of Wollongong, is wholly my own work unless otherwise referenced or acknowledged. This document has not been submitted for qualifications at any other academic institution.

W. A. (Tony) Nicholas

Date

ABSTRACT

Estimates on the extent of time-averaging and age-mixing in sediments from semi-enclosed shallow marine systems (deltas, aggrading clastic shelves, and carbonate platforms) are sparse. Yet, semi-enclosed basins are particularly important for palaeoclimatic studies, because they commonly retain proxy evidence related to oscillations in the level of the sea, at both local (relative) and global (eustatic) scales. However, an accurate and realistic chronology of semi-enclosed basins can be especially difficult to formulate due to the repeated oscillation of sea level, the consequent inundation by and regression of the sea, and the invariably repetitive and alternating cycles of prompt growth and death of populations of marine, brackish and non-marine assemblages upon which dating techniques are commonly applied. Thus, this may result in punctuated stratigraphies, significant hiatuses in the chronological record, particularly because of the mixing of non-, marginal- and fully marine sediments during transitions from one hydrodynamic regime to another.

This project investigates the extent of time-averaging in three semi-enclosed basins, the Gulf of Carpentaria, and Gulf St Vincent, Australia; and the Black Sea. These basins vary in scale and depth, climate, and the extent to which they are open to the ocean, the latter being particularly influenced by the depth of the entrance or sill. Amino acid racemization, accelerator mass spectrometry ^{14}C and uranium-series dating were utilised to estimate the degree to which mixed-age fossil assemblages contribute to the sedimentary record in Gulf St Vincent basin, at Kingscote, Kangaroo Island, South Australia, at Karumba, Queensland, and the central Gulf of Carpentaria, Northern Australia, and at Kerch Strait, Northeastern Black Sea, the Danube Delta coast, and the Northwest shelf of the Black Sea.

The extent of time-averaging in Holocene sediments from these basins was determined to be: Gulf St Vincent – 30-40 ka; Gulf of Carpentaria, ~ 10-12 ka; the Black Sea shelves, 5-6 ka. Broadly speaking, these results indicate that in large shallow basins moderately open to the influence of the global ocean (here, the Gulf of Carpentaria), reworking of sediment is an issue for chronology, and perhaps to a greater extent for defining palaeo-environments, because sediments and fossils from several different niches may regularly contribute to each sedimentary stratum, and thus though the extent of time-averaging may not be significant in numbers of years, the presence of mixed-source sediments can be problematic for defining a reliable chronology. Small fluctuations in water-level about the level of the enclosing sill can result in the inundation and/or exposure and subsequent reworking of material for dating from unrelated environments.

In smaller shallow estuarine basins (here Gulf St Vincent), where the sill has less influence on the volume of water held within the basin, the ingress and regress of marine water results

in stratigraphies that are punctuated. In contrast, large semi-enclosed basins whose interaction with the marine realm is strongly controlled by the sill or entrance (the Black Sea) typically contain punctuated stratigraphies that are easily discernable in broad shelf settings, similar to Gulf St Vincent, but also commonly have on their coastal margins strata that are mixed.

The scale of time-averaging in these and similar basins is a function of the availability, and preservation of fossils as source material. In the samples examined, the scale of time-averaging for the Gulf of Carpentaria may be up to 12 ka and indicated by the presence of early Holocene non-marine shells in surface sediments from the central basin; in Gulf St Vincent, the extent of time-averaging in sediments recovered from the central basin is up to 30-40 ka, indicated by the presence of individually dated MIS 3 age *Elphidium* in Holocene sediments; whereas in the Black Sea the extent of time-averaging in Holocene shelf environments is comparatively small, being only 5-6 ka. The principal difference in the sedimentary record among these basins is that little sediment is removed from the two shallow Australian marginal marine basins, whereas in contrast, a large proportion of sediment originating from coastal environments and deposited on the shelves of the Black Sea is transported ultimately from the shelves to the continental slopes and distal deep basin.

These results indicate that the chronological recognition of reworked fossils at high resolution is a requisite for determining accurate palaeoenvironments and ages, especially over Holocene time. Given the capability of modern analytical instruments, it is insufficient, especially in young marginal marine sediments which may be stratigraphically and chronologically mixed, to estimate an age for a population of fossils based on the assemblage alone, or on bulk samples from an assemblage. Modern dating methods must be utilised in determining the age of individual bioclasts in sediments prior to associating an environment to the sediments being studied because chronological and palaeoenvironmental estimates based on bulk samples or assemblages have a large likelihood of being unreliable.

ACKNOWLEDGEMENTS

I wish to thank a large number of people to whom I owe a debt of gratitude for their help and guidance with this project. Unfortunately there is not space to list everyone, and my memory may not be perfect, but everyone's help is gratefully acknowledged whether included here or not. This journey started when I first was introduced to Bess and Ross McDonald by Sarah McDonald in 1993 who in turn all introduced me to geology. This work began in earnest when I met Prof Allan Chivas about 10 years later. Thanks go to Allan and Prof Colin Murray-Wallace, supervisors, for their patience, guidance, and willingness to help over these past few years. I am extremely grateful for the opportunities I have been given by you – I hope that some of this shows here in this work.

Many other people contributed to this project, either by reading drafts of chapters, journal articles, poster contributions or abstracts, or by sharing their samples and/or their mind with me. These include Adriana García, Paul Carr, Brian Jones and Craig Sloss (Wollongong), John Cann (Adelaide), Mary-Anne Binnie (Adelaide), Valentina Yanko-Hombach (Odessa, Ukraine), Sergei Kadurin (Odessa, Ukraine), Yvgeny Konikov (Odessa, Ukraine) and others. Fieldwork undertaken in the Gulf of Carpentaria, Kangaroo Island and Gulf St Vincent, and the Black Sea region was helped enormously by the company of some of those above, but also by the following teachers and colleagues: Andrei Chepalyga (Russia), Nicolae Panin (Romania), Gheorge Oiaie (Romania), Cristina Vasiliu (Romania), Darrell Kaufman (USA), Paul Hearty (USA), Brent Peterson, Anders Hallam, Terry Lachlan and Richard Gillespie (Wollongong).

I must also thank staff and fellow students in the School of Earth & Environmental Sciences at the University of Wollongong. The guidance, kindness, help and suggestions I received from you all has contributed, in a large measure, to ensuring the completion of this thesis. To Penny, Heidi, Jose and Dave – I owe you guys! Thanks.

The final part of this work was a fieldtrip to the Danube Delta, funded in part by GeoQuESt, School of Earth & Environmental Sciences, University of Wollongong, and by GeoEcoMar, the Romanian coastal and Marine Research and Development Institute, based in Bucharest. During this fieldwork many people contributed to a successful and profoundly insightful period which strongly influenced and re-inforced some of my thoughts on the Black Sea, and where to go next! To Silviu Radan, and the captain and crew of the R. V. *Istros*, and to the research crew - Corneliu Cosovanu, Livius Popa, Sorin Ballan, Irina Catianis, Madelaine Bonta, and Danny – thank you many many times over.

This research has been supported by AINSE grants; 09017, Chronostratigraphy of coastal sedimentary sequences at Eltigen (Prof A. R. Chivas, Prof D. Fink, T. Nicholas); grant 06134,

Identification of remanié microfossils, and the timing of transgressive and regressive events on the Australian margin (Prof C. Murray-Wallace, Dr U. Zoppi, T. Nicholas); grant 05220, Pilot Study: Black Sea palaeoenvironments (Prof A. R. Chivas, T. Nicholas); and by CcASH project (Prof D. Fink).

Table of Contents

Abstract	iv
Acknowledgements	vi
Table of contents	viii
List of figures	xvi
List of tables	xix

Chapter 1 Introduction to the thesis and outline of the project

1.1	Semi-enclosed basins	1
1.2	Aims and study locations	2
1.3	Thesis design	3
1.4	Outline of this report	4

Chapter 2 From amino acids to aminostratigraphy

2.1	Introduction and outline	6
2.2	Amino acids and biomineralisation	7
2.2.1	Amino acids	7
2.2.2	Proteins	9
2.2.3	Amino acids in biominerals	10
2.3	Racemization, rates and temperature dependency of the reaction	13
2.3.1	Racemization	13
2.3.2	The Arrhenius equation and temperature dependency	15
2.3.3	Time dependent racemization	16
2.3.4	Relative rates of racemization	17
2.4	Measurement of D/L values	19
2.5	Aminostratigraphy	20
2.5.1	Aminostratigraphy and aminozones	20
2.5.2	Amino acids used in AAR studies	21
2.6	The impact of taphonomy on aminostratigraphic results	24
2.6.1	Variations in results	24
2.6.2	Biostratinomy and reworking	26
2.6.3	Dissolution	27

2.6.4	Diagenesis	28
2.6.5	Hydrolysis	29
2.6.6	Decompositon reactions	29
2.6.7	Destruction or alteration by microorganisms	29
2.6.8	Condensation reactions	30
2.6.9	Contamination	30
2.6.10	Diffusive leaching of indigenous amino acids	30
2.7	Chapter summary	31
2.8	The analytical approach used in this thesis	32

Chapter 3 Field and Laboratory methods

3.1	Outline and introduction	33
3.2	Fieldwork and sample collection	33
3.3	Sample preparation and chromatography (RP-HPLC)	34
3.3.1	Chromatography	34
3.3.2	HPLC equipment	35
3.3.3	Sample picking	38
3.3.4	Sample preparation	38
3.3.5	Sample types	38
3.3.6	Cleaning and cutting of shell samples	38
3.3.7	Carbonate content in whole-rock samples	38
3.3.8	Ultrasonic cleaning	39
3.3.9	Etching of shell	39
3.3.10	Bleach treatment and contaminant removal	40
3.3.11	Isolation of the intracrystalline amino acid pool	40
3.3.12	Demineralisation	41
3.3.13	Hydrolysis	41
3.3.14	Derivatisation	42
3.3.15	Guard column	43
3.3.16	D/L area and height measurements	43
3.3.17	Gradient program	43
3.3.18	Column	45
3.3.19	Manipulation of chromatographic data	45
3.4	Testing uncertainties and reproducibility	46
3.4.1	Evaluation of the repeatability of amino acid D/L results	46

3.4.2	Repeatability of results for a near-racemic amino acid mixture	47
3.4.3	Repeatability of 2 and 4 µL injections of modern geological samples	48
3.4.4	Repeat analysis of interlaboratory standards	49
3.5	Taphonomic analysis	53
3.5.1	Previous taphonomic analysis	53
3.5.2	Corrasion	54
3.5.3	Completeness	55
3.5.4	Discolouration	56
3.6	¹⁴ C dating	56
3.7	Uranium-series dating	57
3.7.1	Uranium-series sample preparation and measurement of isotopic activities	57

Chapter 4 Amino acid racemization dating of a raised gravel beach at Kingscote, Kangaroo Island, South Australia

4.1	Outline	59
4.2	Introduction	59
4.2	Methods	62
4.3	Regional setting	63
4.4	Field observations	65
4.4.1	Kingscote cobble beach	65
4.4.2	Location 3, northeastern Kingscote	67
4.4.3	Bluff Road and northern carpark	68
4.4.4	Summary of field and sedimentological investigations	69
4.5	Results	71
4.5.1	Amino acid racemization data	71
4.5.2	Summary of AAR data	72
4.6	Uranium-series dating	75
4.7	Fossil preservation	75
4.8	Discussion	76
4.8.1	AAR results	76
4.8.2	Palaeo- sea-levels	80
4.8.3	Sea surface temperatures, the Leeuwin current, and palaeoenvironments	81
4.8	Chapter summary	83

Chapter 5 Aminostratigraphy of Gulf St Vincent

5.1	Outline	85
5.2	Introduction	85
5.3	Aims	87
5.4	Methods	88
5.5	Regional setting	90
5.5.1	Core SV5 and adjacent sampling locations, Gulf St Vincent	91
5.6	Results	92
5.6.1	Paired AAR and AMS ^{14}C dating of bulk samples of <i>Elphidium</i>	92
5.6.2	Single foraminifer data, SV5: Sample screening	94
5.6.3	Preservation and D/L values	95
5.6.4	Single <i>Elphidium</i> results (SV5) and ^{14}C calibration of ages	97
5.6.5	Modern and grab samples	104
5.7	Discussion	106
5.7.1	Previous ^{14}C dating in Gulf St Vincent	106
5.7.2	Relative extents of racemization and comparison with previous AAR data	107
5.7.3	Age mixing	109
5.7.4	MIS3 Bathymetry	116
5.8	Chapter Summary	119

Chapter 6 Transgression of the Holocene Black Sea

6.1	Outline	120
6.2	Introduction	120
6.3	The problem of radiocarbon ages and sea-level curves in the Black Sea	121
6.4	The modern environment	124
6.5	Methods	126
6.6	AMS ^{14}C ages, and observations on chronology	126
6.6.1	Cores BS37-82 and BS37A-82	126
6.6.2	Core 721, Sukhumi Bay, Georgia	131
6.6.3	Core 342, Ukrainian shelf	132
6.6.4	Core 45B, Ukrainian shelf	134
6.7	Amino acid racemization data and implications	136
6.6.1	Cores BS37-82 and BS37A-82, Ukrainian shelf	136
6.7.2	Core 342, Ukrainian shelf	140
6.7.3.	Core 45B, Ukrainian shelf	142

6.7.4	Modern shoreline deposits	142
6.7.5	Amino acid racemization data, age-mixing and implications for chronology	143
6.8	Revisiting the radiocarbon data	144
6.8.1	AMS dating and age-depth relationships of coastal peat deposits	144
6.8.2	Evidence from the northwestern shelf of the Black Sea	146
6.8.3	Radiocarbon ages on peat deposits	147
6.9	Palaeoclimate: the post Younger Dryas in the Black Sea	154
6.10	Prompt transgression and gradual salinisation of the Holocene Black Sea	156
6.11	Reservoir ages and water level	157
6.12	Synthesis	160
6.13	Conclusions	162

Chapter 7 An aminostratigraphic study of Kerch Strait, northwestern Black Sea

7.1	Outline	163
7.2	Introduction	163
7.3	Regional geology and geomorphology	165
7.4	Methods	167
7.5	Field observations and study site descriptions	168
7.5.1	Eltigen (BS 3-8 inclusive)	168
7.5.2	Cape Tuzla (BS 9)	169
7.5.3	Cape Krotkov (BS 10)	169
7.5.4	Maly Kut (BS 11)	170
7.6	Results, total hydrolysable amino acids	170
7.6.1	Whole-rock samples	170
7.6.2	<i>Elphidium</i>	176
7.6.3	<i>Cardium edule</i>	177
7.6.4	<i>Chione gallina</i>	178
7.6.5	Uranium-series dating and calibration of D/L values	186
7.6.6	Terrestrial gastropods	191
7.6.7	Intra-crystalline amino acids in <i>Cardium edule</i> and <i>Chione gallina</i>	193
7.7	Discussion	198
7.7.1	Palaeoenvironment of the Karangatian transgression in Kerch Strait	198
7.8	Chapter summary	201

Chapter 8 Amino acid racemization dating of the Gulf of Carpentaria

8.1	Outline	202
8.2	Introduction	202
8.3	Study location	204
8.4	Previous amino acid racemization studies	206
8.5	Methods	209
8.6	Results	210
8.6.1	Karumba beach ridges	210
8.6.2	Data on shells and foraminifers from cores using THAA	212
8.6.3	Age calibration using bivalve molluscs	214
8.6.4	Shell data and calibrated ages	217
8.6.5	Hydrolysable amino acids in bulk samples of <i>Ammonia beccarii</i>	223
8.7	Intracrystalline amino acids	224
8.7.1	Intracrystalline amino acids in <i>Lentidium</i> (bivalve mollusc)	224
8.7.2	Intracrystalline amino acids: <i>Ammonia beccarii</i>	225
8.8	Discussion	230
8.9	Summary	236

Chapter 9 Summary, conclusions and suggestions for further research

9.1	Introduction	237
9.2	Reworked fossils in the sedimentary record of semi-enclosed basins	237
9.2.1	Time-averaging	237
9.2.2	Mass of samples	238
9.2.3	Analytical time-averaging	239
9.2.4	Reworking in semi-enclosed basins	240
9.2.5	Scales of time-averaging	241
9.2.6	The utility of the intracrystalline approach	242
9.3	Suggestions for further research	243

References	245
Appendices	270
Abstracts A-G	270
Prompt Transgression and Gradual Salinisation of the Holocene Black Sea constrained by amino acid racemisation and radiocarbon dating	287

List of Figures

Figure 1.1	Some present semi-enclosed seas and basins	2
Figure 1.2	The semi-enclosed regions of interest	4
Figure 2.1	Zwitterion form of an amino acid	8
Figure 2.2	Covalent catenation of two generic amino acids	9
Figure 2.3	Amino acid concentrations and extent of racemization	12
Figure 2.4	L and D form of a generic amino acid	14
Figure 2.5	Reaction path model for racemization	14
Figure 2.6	Example of an Arrhenius plot	16
Figure 2.7	Example of a parabolic model	17
Figure 2.8	Heating studies at constant temperature	22
Figure 2.9	Uncertainty in D/L values	25
Figure 3.1	Beach ridges at Karumba, Gulf of Carpentaria	34
Figure 3.2	Agilent 1100 HPLC	36
Figure 3.3	Screenshot of Chemstation instrument control	37
Figure 3.4	Screenshot of Chemstation offline mode for data analysis	37
Figure 3.5	Screenshot of solvent gradient	44
Figure 3.6	Eluent flow rates	44
Figure 3.7	Data entry form for data input to database	46
Figure 3.8	Bivalve mollusc <i>Anadara trapezia</i> collected alive	48
Figure 3.9	Corresponding pairs of D/L values for ILC standards	51
Figure 3.10	All results for ILC A interlaboratory comparison standard	51
Figure 3.11	All results for ILC B interlaboratory comparison standard	52
Figure 3.12	All results for ILC C interlaboratory comparison standard	52
Figure 3.13	All results for ILC Z interlaboratory comparison standard	53
Figure 4.1	Location of Kangaroo Island, South Australia	61
Figure 4.2	Sampling locations at Kingscote	64
Figure 4.3	Location 1, Rolls Point	66
Figure 4.4	Location 2, Kingscote limestone masked by flowstone	67
Figure 4.5	Location 3, basalt cobble to boulder conglomerate	68
Figure 4.6	Location 5, northern carpark, Kingscote	70
Figure 4.7	Schematic cross section of last interglacial shoreline, Kingscote	70
Figure 4.8	Taphonomic variation among samples	78
Figure 4.9	Contamination indices, taphonomic values and valine D/L values	79
Figure 4.10	CMAT vs valine D/L values of <i>Katetyisia</i> and <i>Anadara</i>	80

Figure 4.11	Last interglacial (MIS 5e) sea-level heights for South Australia	81
Figure 5.1	Location of core and surface sampling locations, Gulf St Vincent	88
Figure 5.2	Variation in D/L values from bulk foraminifer samples	94
Figure 5.3	Mean preservation grades for individual <i>Elphidium</i> tests	95
Figure 5.4	Grades of completeness of <i>Elphidium</i> tests	96
Figure 5.5	Extent of corrosion of <i>Elphidium</i> tests	96
Figure 5.6	Grades of discolouration of <i>Elphidium</i> tests	97
Figure 5.7	Covariance of D/L values among best preserved and all tests	99
Figure 5.8	Variation in D/L values for single <i>Elphidium</i> in core SV5	102
Figure 5.9	Parabolic curve fitting for glutamic and aspartic acid D/L values	103
Figure 5.10	Variations in ^{14}C -calibrated AAR ages for core SV5	104
Figure 5.11	Results from randomly chosen one-centimetre horizons	105
Figure 5.12	Covariance of aspartic and glutamic acid D/L values	106
Figure 5.13	Similarities in radiocarbon ages	107
Figure 5.14	D/L values for <i>Elphidium</i> and <i>Katelsia</i>	108
Figure 5.15	Comparison among valine AAR data for <i>Katelsia</i> sp.	109
Figure 5.16	Screening of D/L values in SV5	113
Figure 5.17	D/L values and calibrated ages in single <i>Elphidium</i> tests	114
Figure 5.18	Concentration of amino acids in single <i>Elphidium</i> tests	115
Figure 5.19	Spatial distribution of MIS 3 sediments in Gulf St Vincent	118
Figure 5.20	Estimates for MIS 3 sea-level heights	118
Figure 6.1	The Black Sea	121
Figure 6.2	Difference in age-depth distribution of radiocarbon-dated samples	123
Figure 6.3	AMS ^{14}C ages in cores BS37-82 and BS37A-82	127
Figure 6.4	AMS ^{14}C chronology on cores BS37-82 and BS37A-82	128
Figure 6.5	Radiocarbon ages for core 721, Sukhumi Bay, Georgian shelf	131
Figure 6.6	Stratigraphic log of core 342, inner Ukrainian shelf	133
Figure 6.7	Correlation between core 45B and B2KS24	135
Figure 6.8	D/L values for <i>Cardium edule</i> from core BS37-82	137
Figure 6.9	D/L values in core 342, 45B and modern samples	140
Figure 6.10	Mean ^{14}C -calibrated AAR ages on Black Sea molluscs	143
Figure 6.11	AMS radiocarbon-dated samples from core 721 and Lake Aligol	144
Figure 6.12	Spatial distribution of bivalve molluscs on the northwestern shelf	146
Figure 6.13	Sea-level curve, Sukhumi Bay	148
Figure 6.14	Sukhumi sea-level curve applied to peat ages	149
Figure 6.15	Sea-level curve for the post-glacial Black Sea	150

Figure 6.16a	Composite sea-level curve from molluscs and peat samples	152
Figure 6.16b	Summary figure for Younger Dryas to late Holocene Black Sea	153
Figure 7.1	Location of Kerch Strait, northwestern Black Sea	166
Figure 7.2	Coastal cliffs at Eltigen, Kerch Peninsula	168
Figure 7.3	Whole-rock data from Eltigen, Kerch Strait	172
Figure 7.4	D/L values from individual <i>Elphidium</i> tests, BS-5-2, Eltigen	177
Figure 7.5	D/L values in <i>Cardium edule</i> , Kerch Strait	179
Figure 7.6	D/L values for individual articulated <i>Chione gallina</i> , Kerch Strait	180
Figure 7.7	Comparison of D/L values in disarticulated <i>Chione</i> and <i>Cardium</i>	181
Figure 7.8	D/L values and study sites	182
Figure 7.9	Mean D/L values for <i>Chione</i> , <i>Mytilus</i> and <i>Cardium</i> from	186
Figure 7.10	D/L values in last interglacial (MIS 5e) age bivalve molluscs	188
Figure 7.11	Parabolic equations for <i>Cardium edule</i>	190
Figure 7.12	Parabolic equations for <i>Chione gallina</i>	191
Figure 7.13	D/L values for the terrestrial gastropod <i>Helicella</i> , Kerch Strait	192
Figure 7.14	D/L values from intracrystalline amino acids, <i>Chione</i> and <i>Cardium</i>	197
Figure 7.15	<i>Mytilus</i> and <i>Ostrea</i> -rich strata, Eltigen	199
Figure 8.1	The Gulf of Carpentaria and study sites	205
Figure 8.2	Log of core MD32	207
Figure 8.3	Extent of racemization in <i>Tridacna</i> samples	208
Figure 8.4	D/L values for alloisoleucine from <i>Tridacna</i>	212
Figure 8.5	Holocene alloisoleucine D/L values	214
Figure 8.6	Possible ages based on D/L values in calibration samples	216
Figure 8.7	THAA D/L values in <i>Lentidium</i> sp	221
Figure 8.8	Distribution of amino acid D/L values from <i>Lentidium</i> in core MD32	222
Figure 8.9	Distribution of mean calibrated ages on molluscs from core MD 32	223
Figure 8.10	Amino acids in the foraminifer <i>Ammonia beccarii</i>	229
Figure 8.11	D/L values against depth for <i>Ammonia beccarii</i> , MD 32	230
Figure 8.12	Summary diagram for core MD32	232

List of Tables

Table 3.1	2 and 4 µL injections of a synthetic racemic amino acid mixture	47
Table 3.2	AAR analyses of modern <i>Anadara trapezia</i> from Lake Illawarra	50
Table 3.3	Mean D/L values for interlaboratory comparison samples	50
Table 3.4	Visual preservation index	55
Table 4.1	Assessed indicators of physical preservation	64
Table 4.2	Results for the HIAA pool in bivalve molluscs	73
Table 4.3	Mean results from <i>Katelsia</i> , at individual study locations Kingscote	74
Table 4.4	Mean D/L values for all <i>Katelsia</i>	74
Table 4.5	Results from uranium-series dating of <i>Goniopora lobata</i>	75
Table 5.1	Preservation features examined in <i>Elphidium</i> tests	90
Table 5.2	AMS ¹⁴ C and AAR data from bulk samples of <i>Elphidium</i>	93
Table 5.3	Mean D/L values downcore SV5 for single <i>Elphidium</i>	98
Table 5.4	Results removed from Table 5.3	100
Table 5.5	Previous ¹⁴ C dating of SV5	107
Table 5.6	Results from samples in adjacent cores and surface samples	112
Table 5.7	Variations in D/L values among <i>Elphidium</i> tests	116
Table 6.1	Location of cores and coastal sampling stations	127
Table 6.2	AMS ¹⁴ C data for the Black Sea obtained during this study	129
Table 6.3	Amino acid racemization data, post-glacial Black Sea	137
Table 7.1	THAA data for whole-rock, bivalve molluscs and foraminifers	173
Table 7.2	Uranium-series data from <i>Cardium edule</i> and <i>Chione gallina</i>	187
Table 7.3	Calibrated ages on THAA D/L values in <i>Cardium</i> and <i>Chione</i>	189
Table 7.4	AMS ¹⁴ C ages on individual <i>Helicella</i> , Kerch Strait	192
Table 7.5	HIAA D/L values in bivalve molluscs, Kerch Strait	195
Table 7.6	Calibrated ages on HIAA D/L values in <i>Cardium</i> and <i>Chione</i>	198
Table 8.1	D/L values for shells from Chivas <i>et al.</i> (2001)	209
Table 8.2	THAA in <i>Tridacna</i> , <i>Anadara trapezia</i> and <i>Lentidium</i>	211
Table 8.3	D/L values and radiocarbon ages on calibration samples	213
Table 8.4	Radiocarbon ages from core MD 32	217
Table 8.5	AAR data from THAA in core MD32 and MD31	219
Table 8.6	THAA D/L values from bulk samples of <i>Ammonia beccarii</i>	224
Table 8.7	Intracrystalline amino acid D/L values in <i>Lentidium</i> , core MD32	225
Table 8.8	D/L values from HIAA fraction of bulk <i>Ammonia beccarii</i>	227

Chapter 1

Aminostratigraphy in semi-enclosed basins: Introduction to the thesis, and outline of the project

1.1 Semi-enclosed basins

Semi-enclosed basins and their associated marine systems are marginal seas bounded by land along more than half of their periphery, and separated from the global ocean by either one or more of the following: a strait, a sill, or a front, that separates the enclosed water from the open ocean (Einsle, 1992; Urban *et al.*, 2009). Examples include large basins such as the Gulf of California, the Black Sea, and the Baltic Sea (Fig. 1). Smaller estuaries including for example, Sydney Harbour are semi-enclosed, yet because they lack a defined strait, or sill, they are not formally classified as semi-enclosed. The term ‘sea’ refers to a subdivision of an ocean, and each marginal semi-enclosed sea will have several or many estuaries.

These basins commonly have restricted circulation, and are found on both continental and oceanic crust (Einsle, 1992). Semi-enclosed and restricted basins act as effective amplifiers of global and regional palaeoenvironmental events. The nature of these basins is principally determined by mechanisms that vary their connection with the global ocean, the extent to which freshwater and associated sediments impact on the basin, and the nature of exchange of water-masses between the restricted sea and the open ocean. Semi-enclosed basins commonly become partially, to completely isolated from the world’s oceans during glacio-eustatic lowstands of sea-level (Oxburgh *et al.*, 2007). Isolation may result in stranded shorelines, lowered water-levels, and mixing of geochemical and faunal elements during reconnection (transgressions). This may result in stratigraphic records that are difficult to unravel, and incorrect palaeo-environmental interpretations may ensue. However, varved sedimentary records tend to be preserved during low-stand and lacustrine phases in these basins. These are important databases for palaeo-climatic studies (Hendy *et al.*, 2002). Large human populations inhabit many of these areas and recently the environmental consequences of anthropogenic forcing on these modern ecosystems has become a topic of interest (e.g. Urban *et al.*, 2009). Many of these modern studies rely however, on a palaeo-environmental context to build models for modern and future impacts of environment and climate change.



Figure 1.1. Some present semi-enclosed seas and basins (Middelburg *et al.* 1991; Desrosiers *et al.* 2000; Otsmann *et al.* 2001; Keigwin, 2002; Oguz and Su, 2004; Robert, 2004; Urban *et al.*, 2009; Van Daele *et al.* 2011)

A limited number of studies using amino acid racemization methods have been undertaken on semi-enclosed basins, employing gas and ion-exchange chromatography to create aminostratigraphic frameworks for the timing of environmental change in those regions. Basins investigated include the North Sea (Sejrup *et al.*, 1989,1999), Delaware Bay, New Jersey (O’Neal *et al.*, 2000). Studies in Australia include several focusing on the central gulfs of southern Australia (e.g. Cann *et al.*, 1988; Murray-Wallace *et al.*, 1993; Murray-Wallace 1995, 2000), and on the Gulf of Carpentaria (Chivas *et al.*, 2001).

1.2. Aims and Study locations

Uncertainties exist in the differences in the timing of environmental change within restricted and semi-enclosed basins when compared with the global marine sedimentary record during regressive, low-stand phases when isolation of these basins from the world’s ocean has commonly occurred. Many temporal scales and processes may be recorded within individual sedimentary units, and any attempt at understanding these records at fine scales of resolution requires an attention to the individual elements of such assemblages. Understanding the differences in depositional and chronological histories between semi-enclosed basins and the global marine record requires an attention to detail.

This thesis examines Late Quaternary sea-level and associated environmental change in three semi-enclosed basins using the amino acid racemization (AAR) geochronological method as the prime investigative tool (Kaufman and Manley, 1998). The study locations are Gulf St Vincent, the Gulf of Carpentaria and the Black Sea (Fig. 1.2). The objectives for each basin (detailed in each chapter) were principally achieved through the application of aminostratigraphic methods to refine previous chronologies where they exist (Gulf St Vincent and Gulf of Carpentaria), and where they did not exist to build an aminostratigraphic framework for further studies (the Black Sea).

The presence of reworked fossils and time-averaged sediments can be an underlying problem when attempting to construct temporal frameworks and refine previous chronologies. This is because relevant chronologies depend on the recognition of the stratigraphic disorder and mixing of fossil material where it exists. The basins targeted for study are representative of depositional environments and regions in which few studies have quantified the extent to which reworked fossils are present. These include perched lake, estuarine, raised beach, near-shore and off-shore shallow marine sediments. The attempt to recognise mixed-age populations and obtain numeric estimates of the duration of time-averaging in these siliciclastic (Gulf of Carpentaria and Black Sea) and carbonate rich (Gulf St Vincent) settings, is a further development of recent studies in quantitative estimates of reworking which have focused on Late Pleistocene and Holocene strata (Murray-Wallace and Belperio, 1994; Goodfriend and Stanley, 1996; Martin *et al.*, 1996).

Amino acid racemization dating using reverse-phase high performance liquid chromatography (RP-HPLC) on single microfossils is a relatively new technique, and because of the possibility of using smaller samples, the extent to which this method can be applied to Quaternary investigations is, by comparison with for example AAR studies using gas chromatography, less well understood. This thesis stretches these boundaries by applying, where possible, AAR methods to single microfossils from the basins in question and by doing so may assist in the further development of this relative and chronostratigraphic tool.

1.3. Thesis design

This thesis is designed as a compilation of research articles focusing on a common theme, that of aminostratigraphy in Late Quaternary semi-enclosed basins, and the recognition of reworked fossils where they exist, with the intended purpose of publication. Much of the literature is reviewed on a 'per chapter' basis because each of the research chapters (i.e. Chapters 4-9) focuses on the specific question (or questions) to be resolved.

Subsequent chapters also individually include a methods section because of variation in the objectives of the particular studies.

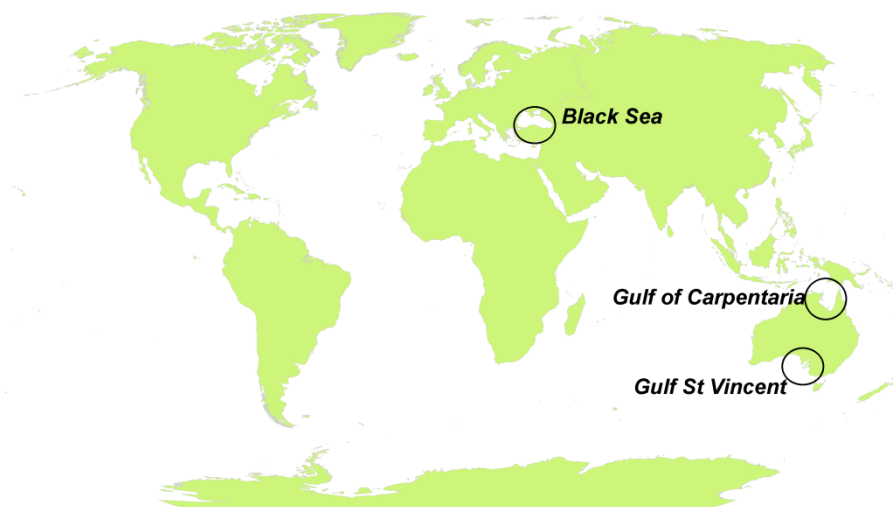


Figure 1.2. The semi-enclosed regions of interest. Coolwater temperate carbonate Gulf St Vincent and tropical Gulf of Carpentaria are shallow basins. The Gulf of Carpentaria has a very shallow slope when compared either to Gulf St Vincent, or the warm temperate Black Sea which has shelves down to in places -150 m depth, and a basin depth of over 3 km. In comparison, Gulf St Vincent is the shallowest at 40 m depth, and the Gulf of Carpentaria has a maximum depth of 70 m. These three basins have differing sedimentary environments, stratigraphies and fauna. The principal question of interest was how much reworking of shelly material occurs during transgressions within these basins. Despite a number of recent studies (Murray-Wallace and Belperio, 1994; Goodfriend and Stanley, 1996; Martin *et al.*, 1996; Cann *et al.*, 2006) little is known about this question, and this becomes an issue when samples are used consisting of bulk material, used for example, for chronology based on radiocarbon methods.

1.4 . Outline of this report

The basis of the amino acid racemization geochronological method is outlined in Chapter 2, and the methods used in this study are presented in Chapter 3. These include the chromatographic method, reverse-phase high performance liquid chromatography, and supporting methods of taphonomic analysis, radiocarbon dating, and uranium-series dating.

The results of the investigation into the age of a raised shoreline deposit at Kingscote, Kangaroo Island are presented in Chapter 4. The presence of last interglacial (MIS 5e) aged coral at this location has significant implications for palaeo-environmental studies within this basin, and for the broader southern Australian setting during that previous highstand of sea-level.

An aminostratigraphy for Late Quaternary sediments in Gulf St Vincent, South Australia is described Chapter 5. This assessment of the extent of reworking within this basin was undertaken by using single tests of the foraminifer *Elphidium* for dating by AAR methods, and a discussion on sea level during MIS 3 is presented based on these results.

Chapter 6 describes sea-level change in the post-glacial Black Sea. Radiocarbon and amino acid racemization dating indicate a prompt transgression of the early Holocene Black Sea by Mediterranean-sourced marine water following drawdown of the pre-existing lake during and after the Younger Dryas.

The Late Pleistocene, aminostratigraphic age of the clastic cliffs at Eltigen and adjacent locations in Kerch Strait, northeastern Black Sea are presented in Chapter 7. These predominantly marine sedimentary sequences are dated here to between MIS 5e and MIS 5c. Overlying loess is of MIS4 and 3 age.

Chapter 8 describes an aminostratigraphy of the Gulf of Carpentaria. Bivalve molluscs and foraminifers were the subject matter. This study focused on dating shells in core MD32 from the central part of the basin, on the most recent (MIS 2 and 3 age) lacustrine phase using bulk samples of the foraminifer *Ammonia beccarii*.

Chapter 9 presents a summary of this research into time-averaging and mixed-age assemblages within the sedimentary environments of semi-enclosed basins, and presents some recommendations for future research.

Conference abstracts (A-F) and publications (Nicholas *et al.*, 2011) arising from this thesis are in the Appendices.

Chapter Two

From Amino Acids to Aminostratigraphy

2.1. Introduction and outline

The focus of this study is the application of the amino acid racemization (AAR) geochronological method to assess the extent of reworking and mixed-age sediments in marginal semi-enclosed basins (Chapter 1). In doing so, this chapter follows a broadly similar route to that of Abelson (1956) by investigating protein in 'shell', by discussing the method of separating amino acids by chromatography, and by describing how amino acids are useful for chronology. However, this chapter develops these topics a little further by discussing how reworked fossils are problematic for chronology, and how the AAR method is especially useful in attempts to understand and recognise this phenomenon where it exists.

Reviews of the principles, methods and applications of amino acid racemization dating include those of Kvenvolden (1975), Schroeder and Bada (1976), Williams and Smith (1977), Miller and Brigham-Grette (1989), Rutter and Blackwell (1995) and Johnson and Miller (1997). Reviews by Wehmiller (1984) and, Wehmiller and Miller (2000) focus on aminostratigraphy. Two volumes dedicated to amino acid and protein geochemistry were compiled from their related conference papers. These are, *Biogeochemistry of Amino Acids* (Hare *et al.*, 1980), and *Perspectives in Amino Acid and Protein Geochemistry* (Goodfriend *et al.*, 2000).

The subject of amino acid racemization and its application to geological problems in coastal/marginal marine environments can be categorised into five principal topics. These are: biomineralisation, the racemization reaction, methods for determining amino acid D- and L- values in carbonate fossils, aminostratigraphy, and factors affecting results. This chapter therefore first reviews concepts of biogeochemistry using amino acids, proteins and biominerals as the subject matter. The process of racemization, and factors that affect it are subsequently discussed, followed by measurement of D/L values. An overview of the concept of aminostratigraphy is presented. Taphonomic and diagenetic factors that affect the results and interpretation of D/L values are discussed. The final section outlines the approach used in this thesis.

2.2 Amino acids and biomineralisation

2.2.1. Amino acids.

Protein-synthesising amino acids are crystalline organic molecules (carboxylic acids) that exist as one of two non-superimposable forms – L- and D-stereoisomers, or enantiomers. In modern environments, amino acids exist primarily in the L-enantiomeric form. L-amino acids reversibly interconvert to their corresponding D- form by way of the racemization reaction, and may eventually form equilibrium mixtures of D- and L-enantiomers (Kvenvolden *et al.*, 1973). In short-lived organisms such as molluscs and foraminifers, enzymatic cessation of suppression of D-amino acid formation generally corresponds with the time of death. In Quaternary studies, the ratio of D- to L-enantiomers allows the time since death to be estimated.

Each amino acid is identified by its side chain. The genetic code specifies twenty individual side chains for protein synthesis. Nineteen of these amino acids are L- α -amino acids (James & Schrek, 1982) and, seventeen have one central asymmetric carbon atom – the α -carbon (Kvenvolden *et al.*, 1973). The α -carbon has a valency of four, and in amino acids a hydrogen atom, a functional amino group (NH₂), and a functional carboxyl group (COOH) are covalently attached. The side chain (the R group) is attached by the fourth covalent bond (Brandon and Tooze, 1999). For glycine the side chain is a single hydrogen atom (R = H).

The direction of rotation of light about the tetrahedral carbon atom is a chiral property. Therefore α -amino acids are optically active (Hart, 1991). Using a polarimeter, the rotation direction of light passing through chiral molecules can be observed. If the polarimeter prism must be rotated to the right in order to allow light through, the chiral molecule is termed dextrorotatory (+), and levorotatory (-) if the prism must be rotated to the left. Chiral molecules with one central asymmetric carbon atom may exist as one of two stereoisomeric forms – as enantiomers. Compounds with more than one chiral centre are diastereomers. These molecules may be interconverted from their L- to D- form by rotation about a single bond, or, interconverted by breaking and remaking covalent bonds. If the groups attached to the α -carbon display a clockwise arrangement of higher to lower atomic numbers, the configuration is designated R (from rectus (latin) = right, correct), while the anticlockwise configuration is designated S (latin, sinister = left). This convention is known as the Cahn-Ingold-Prelog (CIP) system (Hart, 1991). There is no direct relationship between rotation direction (+ or -), and molecular configuration (R or S), however, the specific rotation of amino acids vary with temperature, concentration, and solvent used (Neuberger, 1948). In the geological literature the term D- and L- are consistently used instead of R and S.

A 50:50 ratio of enantiomers ($D = L$) is optically inactive because the optical rotations of the two enantiomers cancel out – this is the racemic mixture that Pasteur originally described. The interconversion of L- to D-amino acids can (but may not necessarily) continue until an equilibrium is reached. This equilibrium ratio of D- to L-amino acids is 1 for enantiomers, and approximately 1.3 for diastereomers. Isoleucine and threonine, having two carbon atoms may exist as four stereoisomers: a set of mirror image isomers (optical enantiomers) and a set of non-mirror image isomers (diastereomers). Intermediate-racemising L-isoleucine has two carbon atoms, and interconverts to its non-protein synthesising diastereomer D-alloisoleucine (Wehmiller and Hare, 1971; Bada, 1972). This reaction is termed epimerisation, and is analogous to racemization (Clarke *et al.*, 2007). The term racemization is used here to express both concepts.

Amino acids are primarily composed of carbon, hydrogen, oxygen, and nitrogen. The amino acids cysteine and methionine also contain sulfur. Protein-synthesising amino acids form peptide chains when the carboxyl (COOH) group (C-terminal) of one amino acid condenses with the amino (NH_2) group (N-terminal) of the next, forming the peptide bond through an amide linkage (Brandon and Tooze, 1999). This condensation reaction results in the expulsion of H_2O . Hydrolysis, the opposite reaction, results in the production of monomer units – the amino acids. In the living organisms these reactions occur at neutral pH, and the amino acids in this environment exist as zwitterions (Fig. 2.1). Zwitterions are electrically neutral molecules with a positive and negative charge on different sites (i.e. they exist as dipolar ions). In strongly acidic media the amino group exists as a cation, while in strongly alkaline conditions the carboxyl group is anionic (Jakubke and Jeschkeit, 1977). Amino acids tend to be more soluble in water than in non-polar solvents, and this allows their separation by reverse-phase liquid chromatography.

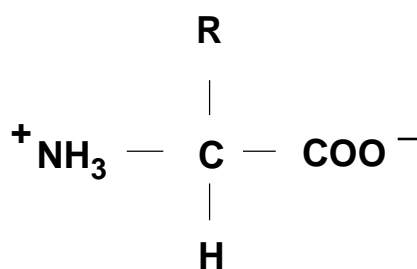


Figure 2.1. Zwitterion form of an amino acid. R is a side-chain at the α -carbon that determines the identity of the amino acid.

2.2.2. Proteins

Amino acids exist in proteins as catenated molecules covalently attached by way of the peptide bond (Fig. 2.2). Proteins are folded structures composed of polypeptide chains and exist with a specific conformation or direction of folding. The primary three-dimensional structure and functionality of protein is determined by the sequence of amino acid residues in the polypeptide. Hydrophobic interactions between amino acids and hydrogen bonds determine the orientation of the secondary structure, i.e. the way in which the polypeptide strand has coiled. The major secondary structure is the α -helix, commonly a dextrally coiling structure. A second major secondary structure, a β -pleated sheet is a side-by-side array of polypeptide units, and is the dominant feature of fibroin, a silk-like protein typical of molluscs. Further folding of the secondary structures gives rise to the tertiary structure of proteins. Quaternary structures are the result of the aggregation of two or more polypeptides, forming the native protein structure. The native protein is the biological functional unit required for that protein to work in the cell, and the protein properties depend on the interaction of, and between, their side chains. These are typically folded so that hydrophilic amino acid residues Aspartic (Asp), Glutamic (Glu), Lysine (Lys), Arginine (Arg) and Histidine (His) are exposed on the outside of the protein, and the hydrophobic amino acids Phenylalanine (Phe), Tyrosine (Tyr), Tryptophan (Trp), Leucine (Leu), Isoleucine (Ile), and Valine (Val) are enclosed in the interior of the structure (Reubsaet *et al.*, 1998). The route from simple peptide to native protein is one of increasing molecular weight. In contrast, during diagenesis the opposite pathway, occurs in fossils.

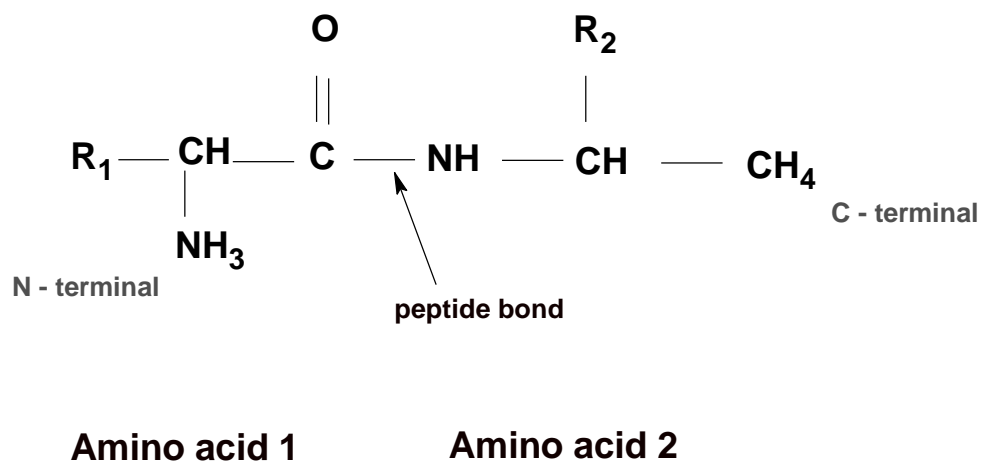


Figure 2.2. Covalent catenation of two generic amino acids to form a dipeptide by way of an amide bond - the peptide bond.

Genetically determined variations in protein composition are preserved in biomineralised skeletons and lead to differences in racemization rates in fossils (Hare and Abelson, 1965; Pietrzak *et al.*, 1973; Wehmiller, 1984; Walton and Curry, 1994). Biominerals are the predominant source of proteinaceous amino acids preserved *in situ* in the geological record (Endo *et al.*, 1995). Several aspects of biominerals have a significant impact on the utility of AAR studies for geochronological applications. This is because variations in amino acid content and concentration in samples are principally dependent on the biomineral involved, the type and size of proteins, and *post-mortem* environmental conditions. These issues are discussed below.

2.2.3. Amino acids in biominerals

Amino acids and proteins are incorporated into invertebrate ‘shell’ (e.g. mollusc shell, foraminifera tests, and ostracod valves) at inter- and intra-crystalline (occluded) locations through the process of biomineralisation (Crenshaw, 1972; Aizenberg *et al.*, 1997; Bédouet *et al.*, 2006; Penkman *et al.*, 2008). For example, soluble proteins, SM 50 and SM 30, of a sea urchin have both been found to be both inter-crystalline and intra-crystalline (Seto *et al.*, 2004). Similarly, the soluble protein caspartin, found within the inter-crystalline prismatic calcitic lamellae of the Mediterranean fan mussel *Pinna nobilis* was also found to exist as an intra-crystalline molecule (Marin *et al.*, 2007). The mineral phase in molluscs and similar invertebrates accounts for 95 to 99 wt % calcium carbonate, with the remaining 1 to 5 wt % being the organic matrix, a mixture of proteins, glycoproteins and polysaccharides (Marin and Luquet, 2004). Of this, approximately 5 wt % of the organic matrix consists of intracrystalline amino acids. Amino acids within both the inter- and intra-crystalline organic matrix exist as protein bound and free molecules.

Biomineralisation is organically mediated, and biologically and chemically controlled (Wilbur, 1964; Lowenstam, 1980; Falini *et al.*, 1996). Invertebrate ‘shells’ are similarly constructed as a layer or layers of microcrystalline (colloidal, or hydrated) calcium carbonate crystals separated from the next layer by an organic matrix (Weiner and Erez, 1984; Albeck *et al.*, 1993; Debenay *et al.*, 1999; Addadi *et al.*, 2006). The organic matrix is a multi-protein assemblage (Seto *et al.*, 2004), and includes amino acids, proteins, Ca-binding acidic glycoproteins, and polysaccharides. Acidic amino acids in glycoproteins provide templates or domains for binding of Ca^{2+} , principally at crystal step edges (Mann, 1993; Orme *et al.*, 2001). Aspartic and glutamic acids appear to be involved in stabilizing amorphous CaCO_3 permanently (Aizenberg *et al.*, 1996). By way of contrast, basic proteins are commonly rich in the amino acids, valine and glycine (Bowen and Tang, 1996).

Individual biominerals can exist in a range of morphologies. These include simple tabular and prismatic aragonite, prismatic and foliated calcite, and more complex structures (Chateigner *et al.*, 2000; Marin and Luquet, 2004). Metastable aragonite (nacre) is the most commonly studied biomineral (e.g. Grégoire *et al.*, 1955; Gregoire, 1957) and consists of uniformly thick layers of aragonite tablets delineated by interlamellar layers of organic matrix sheets, with crystallites connected to each other by tablet bridges (Michenfelder *et al.*, 2003; Su *et al.*, 2002). In contrast, calcitic crystallites do not have interconnecting structures, and therefore the intra-crystalline amino acid pool within these individual crystals are isolated (Sykes *et al.*, 1995).

The solubility of protein is dependent on the solvent used (Levi-Kalishman *et al.*, 2001). Matrix proteins are generally described as being either water and acid soluble or water and acid insoluble (Crenshaw, 1972; Weiner and Traub, 1984; Rousseau *et al.*, 2003; see Section 2.6.10 below). The insoluble fraction refers to the conchiolin of Grégoire (1957). Proteins recovered from the soluble organic matrix have been found to be either acidic residue (aspartic acid) rich (e.g. in protein shematin-5 from the bivalve *Pinctada fucata* (Yano *et al.*, 2006) or basic residue rich, that is, having relatively high concentrations of alanine, serine and glycine, (e.g protein P60 from *Pinctada fucata* (Lao *et al.*, 2007)). Similarly, it seems that there is no clear relationship between calcite and aragonite, and their particular amino acid constituents. For example, prismatic calcite may have higher concentrations of Glu, Ala and Val while tabular aragonite typically contains greater concentrations of Asp, Ser and Gly (e.g. Lee and Choi, 2006). Or, aspartic acid in modern shell typically constitutes between 30 and 40 mole percent of the aragonitic layer, while in calcite this value can be greater than 50 mole percent (Gotliv *et al.*, 2003). Of greater interest here is that amino acid concentrations reduce significantly over the course of burial of the fossil (e.g. Whitelaw *et al.*, 2001; Hearty *et al.*, 2004) (Fig. 2.3a, b). Loss of indigenous amino acids over time appears to be lowest in foraminifers (Fig. 2.3a, b). This is possibly due to the higher degree of stability of tests in geological conditions, because of their calcitic composition, compared to for example, metastable aragonite in molluscs.

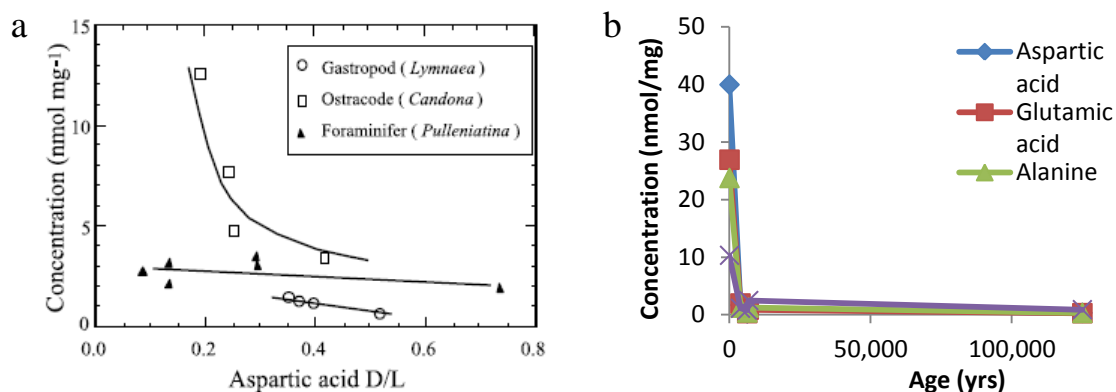


Figure 2.3. Amino acid concentrations and extent of racemization. Figure 2.3a Aspartic acid concentration variation with increasing racemization (representing time) in microfossils and gastropods (Hearty *et al.*, 2004). Figure 2.3b Depletion of total hydrolysable amino acid concentration of four amino acids from the bivalve mollusc *Anadara trapezia* over time (drawn from data in Whitelaw *et al.*, 2001). See also chapter 5, where the results from bleaching of single Foraminifera, *Elphidium*, are presented.

The majority of previous AAR studies on coastal sedimentary sequences have utilised the total hydrolysable amino acid (THAA) content in molluscs (the total hydrolysable amino acid pool, equates with the total acid soluble organic matrix) with or without the use of the free amino acid (FAA) population (e.g. Hollin and Hearty, 1990; Goodfriend and Meyer, 1991; Murray-Wallace, 1995). Some recent studies have used the hydrolysable intracrystalline amino acid (HIAA) fraction, but the extent of racemization between these fractions are different. It is not possible at present to directly compare the results between each pool for stratigraphic or chronological purposes, principally because there is insufficient data, and it is therefore problematic for aminostratigraphic studies. A number of studies have utilised the free amino acid pool in geological samples to assist in determining if the results from the THAA fraction are reliable (e.g. Murray-Wallace and Kimber, 1989). Free amino acids are readily found in sediment and water (e.g. Terashima, 1991; Keil *et al.*, 1998; Yamashita and Tanoue, 2004) and are dominated by the acidic (aspartic and glutamic) amino acids. Despite their presence, routine replicate analyses on suitably prepared molluscs have generally demonstrated that indigenous amino acids are not normally contaminated by exogenous free amino acids from the burial environment. Yet most of these studies have used non-acidic amino acids for geochronological purposes (i.e. valine and alloseleucine), and therefore the relative proportions of exogenous (free amino acids) to indigenous populations of valine and alloseleucine for example, in Pleistocene molluscs are very low.

A significant worry for those using the AAR method, and perhaps more so for those who use this type of data for comparison with other ‘dating’ results, is that the extent of recrystallisation can affect results. The stability of acidic amino acids may be a key to identifying the affects of recrystallisation in aragonite. This is because site-specific binding of

D- and L-aspartic acid residues to calcite surface steps change the step-edge free energies. This leads to chiral modification of the growing calcium carbonate biomineral by giving rise to direction-specific binding energies unique to individual acidic amino acids (Orme *et al.*, 2001). It is not known if the interconversion of L- to D-amino acids (i.e. racemization) in fossil carbonate changes the conformation of their associated biomineral molecules during or after racemization (and thereby possibly enhancing the degradation process). But given the above, this seems likely. If there is recrystallisation from aragonite to calcite, the Ca^{2+} binding acidic amino acids are likely to be lost from the occluded organic matrix. This may be evident in results as a noticeable reduction in concentration of aspartic and glutamic acids in chromatograms in older samples, but would not be readily evident in young examples because in young samples the THAA fraction is dominated by inter-crystalline amino acids. Over time the intracrystalline pool becomes a larger proportion of the THAA fraction. However, there is no work documenting the proportion of amino acids in the organic matrix onto which the calcium carbonate binds, and therefore no data on which to evaluate relative changes in concentrations of these molecules. This therefore requires a conservative approach to using D/L values for chronological purposes.

2.3. Racemization, rates, and temperature dependency of the reaction

2.3.1. Racemization

Racemization refers to the interconversion of a left handed (Laevorotatory) stereoisomer of a chiral molecule to its right handed (Dextro-rotatory), non-superimposable, mirror-image. This occurs because L-enantiomers by themselves are thermodynamically unstable (Johnson and Miller, 1997). There are several pathways for racemization (Van Duin and Collins, 1998; Van Duin and Collins, 2000). These include 1) direct isomerisation by formation of carbanions, 2) dipeptide condensation at the N-terminal of the polypeptide by way of diketopiperazine (DKP) formation, and 3) deamidation (Fig. 2.5) of specific amino acid residues (aspartic and asparagines) to form succinimide intermediates (Van Duin and Collins, 2000). Peptide-bound aspartic acid racemises via the formation of a cyclic succinimide (Asu) intermediate (Van Duin and Collins, 1998).

The racemization reaction in calcium-carbonate fossils is base-catalysed (i.e. under alkaline conditions) – any nucleophilic species may initiate the reaction by removing the α -proton, and in aqueous solution the nucleophile is the hydroxide ion (or H_2O) (Neuberger, 1948; Schroeder and Bada, 1976). Acid-catalysed racemization also occurs, commonly in the presence of clay species (Kroepelin, 1968; Frenkel and Heller-Kallai, 1977) but the rate of reaction is slow when compared to base-catalysed epimerisation.

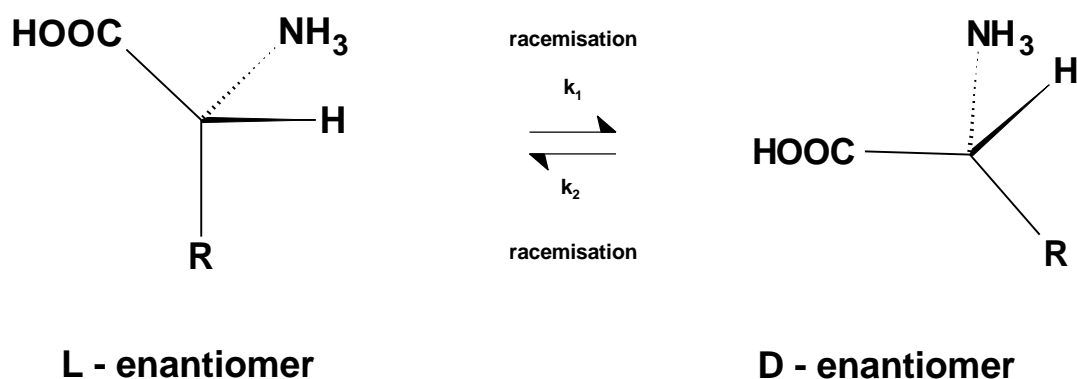


Figure 2.4. L and D form of a generic amino acid, k_1 and k_2 are the forward and reverse rate constants for the racemization reaction.

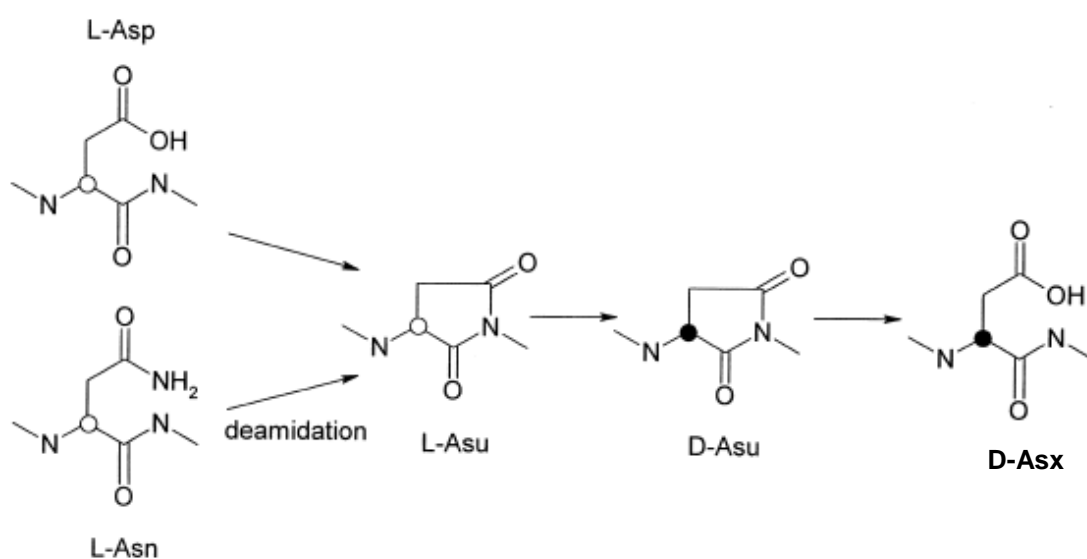


Figure 2.5. Reaction path model for racemization of L-Asp and deamidation of L-Asn and production of D-Asx. Redrawn from Van Duin and Collins, 1998.

In fossils the basic mechanism for racemization of biomineral-bound α -amino acids is believed to be ionisation of the α -hydrogen atom (bound to the α -carbon), to leave a carbanion intermediate (i.e. a carbon atom which has a negative electrical charge – a carbon anion) (Neuberger, 1948; Smith and Evans, 1980). This is followed by the readdition of a proton with equal probability of forming a D- or L-enantiomer (Schroeder and Bada, 1976).

In geological environments, the rate of the racemization reaction in fossils is dependent on the α -amino acid in question, and its spatial relationship to the peptide chain – i.e. whether it is on the surface or internally situated, but many interrelated reactions affect the stereochemistry of amino acids (Kvenvolden, 1975; Smith and Evans, 1980) and the racemization process within fossils is sensitive to the diagenetic environment outside the biomineral, particularly temperature (Murray-Wallace and Kimber, 1993).

Factors influencing the rate of diagenetic racemization include the above, and also the pH, ionic strength and buffering affects, the presence of clay surfaces, metallic cations, and the presence of water (Smith and Evans, 1980). All these factors being equal, for individual amino acids, the diagenetic temperature history has the greatest impact on racemization (Murray-Wallace and Kimber, 1993). This temperature dependency of racemization is demonstrated empirically using data from kinetic studies with the Arrhenius equation (Figure 2.6).

2.3.2. The Arrhenius equation and temperature dependency

The Arrhenius equation is utilised to express the dependent relationship of reaction rate on temperature. It is a mathematical model, derived from empirical evidence (i.e., laboratory studies using isothermal conditions), as being the best fit to changes observed in reaction rates with known changes in temperature. Isothermal conditions are employed to measure trends in the rate of racemization, and the temperature sensitivity of the racemization reaction in modern and fossil samples (Clarke and Murray-Wallace, 2006).

The Arrhenius equation is $k = Ae^{(-E_a/RT)}$ (1)

or $\ln(k) = \ln(A) - E_a / RT$ (2)

where k is the rate constant of racemization, A is the pre-exponential or frequency factor, also described as the Arrhenius factor, E_a is the activation energy, $R = 8.315 \text{ J mol}^{-1} \text{ K}^{-1}$ is the gas constant, and T is the thermodynamic temperature measured in Kelvin.

Rate constants have been empirically obtained for foraminifera (Kaufman, 2006), ostracods (Kaufman, 2000, Figure 2.6), molluscs (Manley *et al.*, 2000), and individual amino acids (Smith *et al.*, 1978). For most amino acids the forward and reverse rate constants k_1 and k_2 are equal and therefore $K = 1$ (Smith *et al.*, 1978; Miller and Clarke, 2007). However, for isoleucine $k_1 > k_2$. Thus, for the interconversion of L-ile to D-ile, $k_1/k_2 = 1.0/1.3 = 0.77$ (Clarke and Murray-Wallace, 2006).

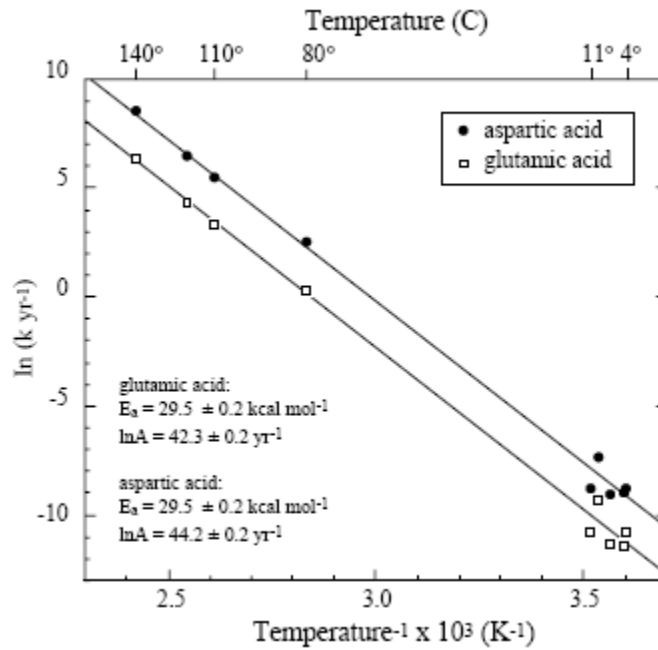


Figure 2.6. Example of an Arrhenius plot used to determine activation energies (E_a) from laboratory heated and ^{14}C dated *Candona* shells (Kaufman, 2000).

2.3.3. Time-dependent racemization

The onset of the racemization reaction does not necessarily commence with death. However, for most short lived organisms it is not possible to distinguish this event and so the event dated is regarded as the death of the organism. The time interval over which the AAR geochronological method is viable will vary, principally with the temperature of the burial environment because the reaction rate is exponentially dependent on temperature (Miller and Clarke, 2007). Over Quaternary timescales there is a strong correlation between palaeotemperatures and modern temperature values, and modern variability in air temperatures are reflected in burial environments (Wehmiller *et al.*, 2000). Over these timescales, changes in the effective burial temperature appear to follow climatic variations. Therefore, current mean annual temperature (CMAT), and by proxy, geographic setting, are reasonable indicators of the possible range of D/L values and ages for which AAR studies will be viable for a given location. For example, near equilibrium D-allo/L-Ile values were obtained in molluscs of last interglacial (MIS 5e) age (125 ka BP) from the Huon Peninsula, Papua New Guinea (CMAT 28 deg C) (Hearty and Aharon, 1988). In contrast, D-allo/L-Ile values of approximately 0.1 were reported from last interglacial (MIS 5e) deposits from the Lower Thames Valley, southeastern England (CMAT = 10°C) (Bowen, 2000).

Several mathematical approaches have been used to estimate ages from D/L values (Clarke and Murray-Wallace, 2006). The method used here is parabolic curve fitting. Numeric ages may be derived by using the equation

$$t = [(D/L)_s / M_c]^2 \quad (3)$$

where M is the slope of the line obtained from a plot of the square root of calibration ages (e.g. radiocarbon) against D/L values, and (D/L)_s is the value for a modern sample (Mitterer and Kriausakul, 1989; Murray-Wallace and Kimber, 1993), (Figure 2.7). The value of this approach is that it does not require a detailed knowledge of the thermal history of the fossils concerned, yet the temperature sensitivity of the samples can be assessed using kinetic studies undertaken with modern equivalents (e.g. Sloss *et al.*, 2004).

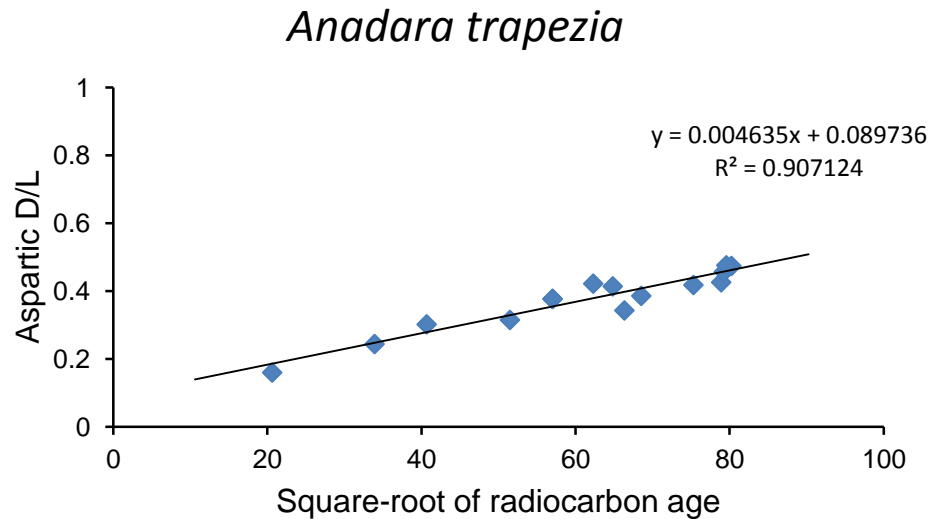


Figure 2.7. Example of a parabolic model for the calibration of numeric ages, drawn as a diagram of square root of age versus D/L ratio for the bivalve mollusc *Anadara trapezia*. Redrawn from data in Sloss *et al* (2004).

2.3.4. Relative rates of racemization

Rates of racemization vary according to the location of amino acids within peptide chains (Mitterer and Kriausakul, 1984), genus (Lajoie *et al.*, 1980), diagenetic temperature history, pH, and moisture regime (Murray-Wallace, 1993). Because different amino acids undergo contrasting rates of racemization their geochronological utility varies. For example, alanine and aspartic acid undergo the fastest rates of racemization and are more suited for the dating of Holocene materials, whereas valine and glutamic acid which racemise more slowly are more appropriate for Pleistocene fossils (Murray-Wallace, 2008). In modern shells almost all

amino acids are peptide-bound and exist in interior positions (Kriausakul and Mitterer, 1980). Racemization rates are hydrolysis dependent (Goodfriend *et al.*, 1997). This is evident in pyrolysis studies for example, where vials dry out with the result that the rate of racemization is substantially reduced (this study). Hydrolysis results in internal residues being exposed at either the NH₂ or COOH terminal, or as free amino acids. Racemization is faster at terminal positions (Kriausakul and Mitterer, 1980) than for interior sites, or for free amino acids. For isoleucine, faster rates of epimerisation occur at the COOH terminal than for the NH₂ terminal (Kriausakul and Mitterer, 1983).

Invertebrate skeletons such as molluscs, foraminifera and ostracods are composed of either aragonite or calcite. These carbonate forms are typically acidic residue rich (Asp, Glu) or rich in basic amino acids (Ala, Lys, His, Arg) (Weiner and Traub, 1984; Addadi *et al.*, 2006; Marin *et al.*, 2007). In general, up to D/L values of approximately 0.5, peptide-bound aspartic acid racemises at higher rates over other amino acids (Van Duin and Collins, 1998; Goodfriend and Weidman, 2001; this study) and is closely followed by alanine. This is in part because L-aspartic acid (Asp) racemises and L-asparagine (Asn) deamidates during the early phase of racemization, both giving rise to D-Asx (Asx denotes combined Asp and Asn). At higher values, alanine racemises faster (this study), and/or inversion of aspartic acid racemization may occur (Kimber *et al.*, 1986; Kimber and Griffin, 1987; this study). Slower racemising amino acids include valine and isoleucine.

Amino acid compositions in higher molecular weight fractions are more stable than in low molecular weight and free fractions (Kaufman and Miller, 1995). Over time hydrolysis reactions progressively break peptide bonds. This appears to occur to a greater extent in smaller molecules, with diagenetically-driven compositional changes affecting those lower molecular weight molecules, including those free of the peptide chain, more than those of the higher molecular weight molecules. These changes of increasing reactivity with decreasing molecular size (mass) are consistent with the concept of lower weight molecules in fossils being derived from those higher weight polypeptides (Wehmiller, 1980; Kaufman and Miller, 1995; Kaufman and Sejrup, 1995), and are affected by the position of an amino acid within a polypeptide. These influence the observed D/L values obtained from amino acid racemization analyses. Racemization of internally-bound amino acids has been found to occur more slowly than for amino acids that are terminally-bound (N- or C- terminal) producing lower D/L values, and slower than for free amino acids (Kriausakul and Mitterer, 1980a). This is because the activation energies required for racemization vary for these locations (Kriausakul and Mitterer, 1980b) with, for example, less energy being required for racemization at terminal positions than at positions internal to the peptide.

D/L values have been found to vary across shells and between shell layers (Hare, 1963; Goodfriend *et al.*, 1997; Goodfriend and Weidman, 2001). This variation across the shell from umbo to growth edge has been hypothesised to reflect differences in composition of the proteins involved in shell growth (Goodfriend and Weidman, 2001).

Relative rates of racemization among individual amino acids have been found to be similar in different molluscan genera (Lajoie *et al.*, 1980), such that the relative rates are; proline \geq phenylalanine \geq leucine $>$ glutamic acid $>$ valine. Similar relationships were found for Foraminifera from deep sea cores (Kvenvolden *et al.*, 1973). Valine, glutamic acid and leucine were found to racemise at slower rates than phenylalanine, alanine, aspartic acid and proline. Isoleucine, the authors note, epimerises about as slowly as valine racemises. Free amino acids were found to generally have higher D/L ratio values over those obtained for the total hydrolysable amino acid content of a sample (Kvenvolden *et al.*, 1973).

Comparisons of individual amino acid racemization rates are complicated by taxonomy (Wehmiller, 1980). Differences in racemization rate exist between genera such that molluscs have been classified as fast-racemising (e.g. *Tegula*, *Macoma*) or slow-racemising (e.g. *Chione*, *Saxidomus*), with a 20-30% difference in rate being noticeable between these groups (Wehmiller, 1980). These differences are likely to be in part because of differences in protein composition among genera. Furthermore, warm-water and cold-water species of the same genus, or other taxon, differ in their proportion of calcite to aragonite. Warm-water species favour aragonite composition, while colder species favour calcite biomineralisation (Hudson, 1968). This implies that the amino acid composition will also differ in monogeneric samples from sources with strong latitudinal gradients given that aragonitic species are typically rich in acidic (e.g. Asp) amino acids. This is because, for example, higher rates of aspartic acid racemization are associated with higher relative concentrations of acidic amino acids (Asp, Glu and ala) (Goodfriend and Weidman, 2001). Principally for the above reasons, and those outlined in Section 2.2, monogeneric samples are preferred subjects for aminostratigraphic studies, and where possible this was the approach taken here.

2.4. Measurement of D/L values

The process of amino acid racemization (AAR) has allowed the development of a geochronological and stratigraphic tool that has been studied for more than 50 years (e.g. Abelson, 1954; Miller and Clarke, 2007). The racemization process results in the production of a relative geo-chronometer in the form of D- and L- protein synthesising amino acids (e.g. aspartic, glutamic, serine, alanine, valine, alloisoleucine) that are routinely used in this study, separated with Reverse-phase High Performance Liquid Chromatography.

The four principal chromatographic methods used in racemization studies to date are paper chromatography (e.g. Abelson, 1954), gas chromatography (e.g. Kvenvolden *et al.*, 1973), ion-exchange liquid chromatography, and reverse-phase high performance liquid chromatography (e.g. Kaufman and Manley, 1998). The most recent developments (e.g. Bruckner *et al.*, 1991; Kaufman and Manley, 1998; Kaufman, 2000) of enantiomeric chromatography, allow for calibrated age estimates on individual macro- and micro-fossils, where they are suitably preserved, and of sufficient mass.

2.5. Aminostratigraphy

2.5.1. Aminostratigraphy and aminozones

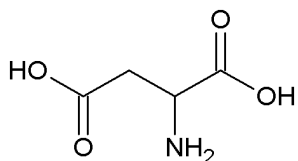
Amino acid D/L values from fossils obtained from regions with similar palaeotemperature can be used directly as stratigraphic correlation tools (Miller *et al.*, 1979; Miller and Hare, 1980; Miller and Mangerud, 1986; Murray-Wallace and Kimber, 1989). The basis of this method lies in the premise that within a geographic region of broadly similar CMAT and having had a similar geological history, the diagenetic temperature history of the fossils would be similar (Wehmiller, 1982; Murray-Wallace, 1993). At mid-latitudes, CMAT for air and ground measurements are in close agreement (Miller and Mangerud, 1986). Aminostratigraphy involves the application of amino acid racemization reactions in ‘shell’ material to the chronostratigraphic subdivision of the Quaternary (Murray-Wallace, 1995). It is a chemostratigraphic method based on chronostratigraphic principles, with aminozones being the fundamental chronostratigraphic unit (Murray-Wallace, 1995).

Aminostratigraphy can be used to correlate and differentiate between strata, and when calibrated, can be used to provide a regional chronostratigraphy. The simplest application of this principle is in defining aminozones (Murray-Wallace, 1993). Measurements are best made on the same or comparable species throughout a deposit or sedimentary sequence because of different rates of racemization among taxa (Johnson and Miller, 1997; and discussed elsewhere in this chapter). Aminozones represent discrete time intervals, and are characterised using scatter plots by the clustering of similar D/L values obtained on similar fossils contained within these stratigraphic units and commonly related to isotope stages (Keenan *et al.*, 1987; Murray-Wallace and Kimber, 1987). It is unnecessary to assess racemization kinetics nor palaeotemperatures in detail for this purpose when using monogeneric samples and therefore this is a relatively unambiguous method to use (Miller and Clarke, 2007).

2.5.2. Amino acids used in AAR studies

Not all of the twenty protein synthesising amino acids have been used in AAR geochronological studies. The amino acids most commonly used for geochronology include, aspartic acid, glutamic acid, leucine, serine, valine and Alloisoleucine. These are introduced below.

Aspartic acid

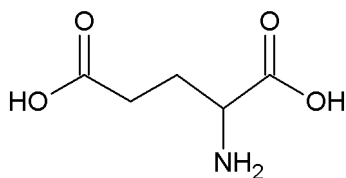


C₄H₇NO₄, molecular weight = 133.10

Aspartic acid is a fast racemising acidic amino acid. The kinetics of Asp racemization are typically non-linear (Goodfriend and Weidman, 2001) with the rate of racemization in molluscs sharply decreasing with higher D/L values. Some of this may be attributed to asparagine being converted to aspartic acid during hydrolysis (Robinson and Rudd, 1974), much of the rest may be attributed to the high concentrations of Asp-rich proteins in molluscs and other invertebrates.

It was suggested that aspartic acid would be of little chronological utility (Lajoie *et al.*, 1980), but it has been found especially useful for Holocene samples (Sloss *et al.*, 2004) in temperate conditions, or for older fossils from sub-arctic conditions e.g. Baffin Island, (Goodfriend *et al.*, 1996). Aspartic acid has been used to estimate the temperature differences between glacial and post-glacial climatic conditions in West Africa and the Mediterranean island of Majorca, for example (Schroeder and Bada, 1973). This is because of the rapid racemization of aspartic acid at higher temperatures (c. 20° C).

Glutamic acid



C₅H₉NO₄, molecular weight = 147.13

Glutamine is converted to glutamic acid during hydrolysis (Robinson and Rudd, 1974). It decomposes by decarboxylation, eventually forming gamma-aminobutyric acid (Vallentyne, 1964). Glutamic acid is one of the more stable amino acids, and has been recently used in

aminostratigraphic studies using non-marine ostracods (Kaufman, 2000, 2005; Kaufman *et al.*, 2001) and Foraminifera (Kaufman, 2006).

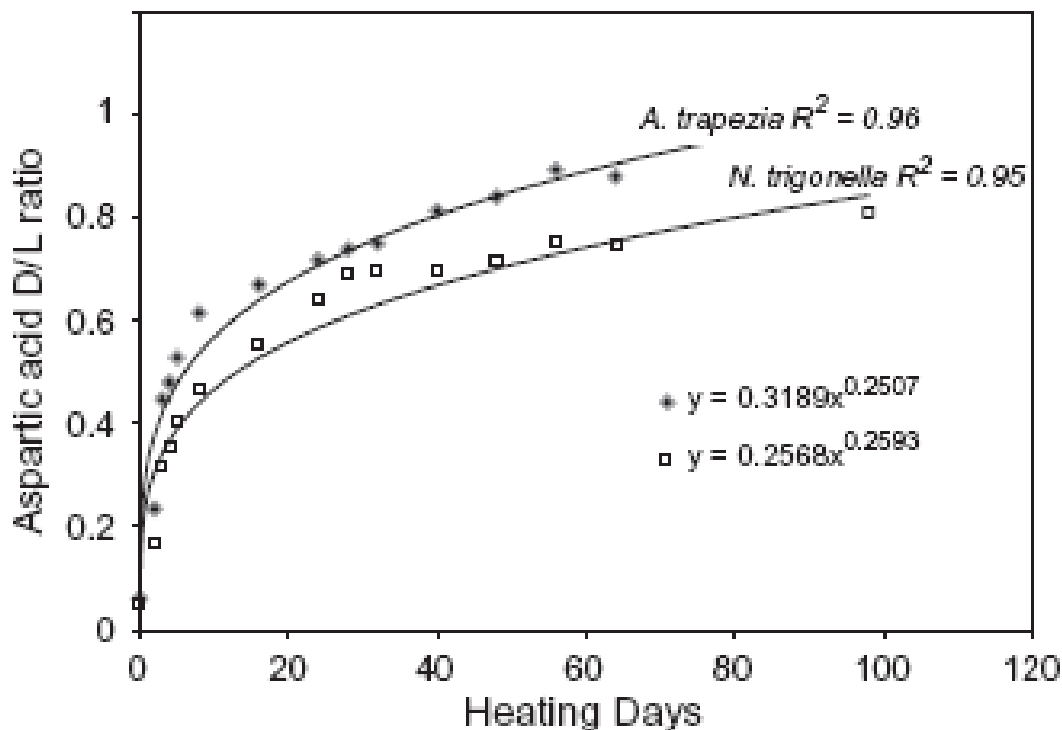
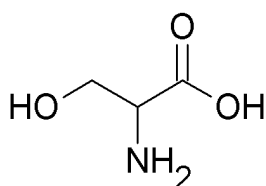


Figure 2.8. Heating studies at constant temperature. Results of controlled kinetic (heating) studies undertaken at constant temperature (110°C) on two bivalve molluscs, *Anadara trapezia* and *Notoisupisula trigonella* (Sloss *et al.*, 2004). The rate of aspartic acid racemization for both species is non-linear, and is modelled above using power law equations. Power law equations have also been applied to aspartic and glutamic acids in similar studies (Kaufman, 2000, 2006) on foraminifers and ostracods.

Serine

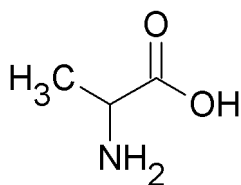


$C_3H_7NO_3$, molecular weight = 105.09

Serine is geochemically and thermally unstable (Lajoie *et al.*, 1980; Bada *et al.*, 1999). The concentration of L-serine relative to that of L-glutamic has been used as a contaminant indicator (e.g. Kaufman, 2006). Peptide-bound serine residues may be preferentially altered to glycine and alanine in a polypeptide chain during diagenesis (Vallentyne, 1964; Akiyama, 1980). Serine is destroyed by acid hydrolysis, and commonly occurs as a contaminant. All

breakdown products of serine have greater stability than the parent material (Vallentyne, 1964).

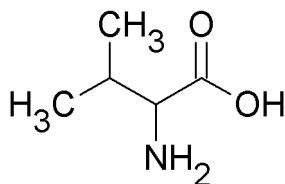
Alanine



C₃H₇NO₂, molecular weight = 88.09

Alanine deaminises to propionic acid (Hoering, 1980), and racemises at rates similar to aspartic acid. Alanine is a major product of serine decomposition (Bada *et al.*, 1999). It appears to be useful in temperate locations for fossils of up to approximately OIS 7, but because of its fast rate of racemization may be useful for Holocene aged samples. However, it is a decomposition product from serine, and therefore its utility in amino acid racemization studies has to be questioned somewhat when using the total hydrolysable amino acid pool, which includes the bulk of amino acids in a sample.

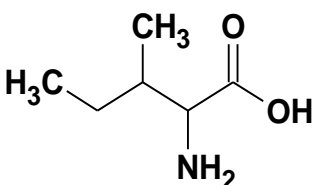
Valine



C₅H₁₁NO₂, molecular weight = 117.15

Valine is one of the most stable amino acids, and has been used with success in South Australian studies (e.g. Murray-Wallace *et al.*, 1991), yet has not been used to a similar extent for geochronological purposes elsewhere. Its rate of racemization is slow, and it is therefore suitable for older Pleistocene samples, compared to the utility of aspartic acid which is more useful for Holocene material for example.

Isoleucine



C₆H₁₃NO₂, molecular weight = 131.18

The ratio of epimers D-alloisoleucine to L-isoleucine has been used with success in bird shells, e.g. *Dromaius novaehollandiae* and *Genyornis newtoni* (Miller *et al.*, 2000) and *Aepyornis* (Clarke *et al.*, 2007). This amino acid has also been used successfully in aminostratigraphic studies on molluscs (e.g. Karrow and Bada, 1980; Hearty and Aharon, 1988) in temperate regions of up to 300,000 yr old.

2.6. The impact of fossil preservation on aminostratigraphic results

2.6.1. Variations in results

An implicit assumption in studies of amino acid racemization geochronology is that, for a given stratum, and with a known temperature history, the rate at which amino acid residues are transferred from internal to terminal to free positions, and the extent to which diagenetic reactions or leaching occurs are a function of time (Kaufman and Sejrup, 1995). The age-resolving power of the method has been described as being a function of the sum of systematic and unsystematic variables involved in obtaining D/L values (Murray-Wallace, 2000, see Figure 2.7 below). Differences in preservation between modern shells is commonly magnified when studied in fossil examples (cf. Robbins *et al.*, 2000), and fossil shells may not be totally closed systems. Whilst systematic (analytical) variation can be estimated by repeat analyses of standards, and relative rates of racemization are known for a range of amino acids and taxa, deviations in results obtained from geological samples provide most of the uncertainty in aminostratigraphic investigations. These issues originate because of the combined impacts of biostratinomic (physical and biological degradation of shell material prior to and during burial) and diagenetic processes on carbonate skeletons.

The passage of organic material from the biosphere into the lithosphere occurs as a result of many interlaced geological and biological phenomena acting upon organic remains (Efremov, 1940). Taphonomy (Efremov, 1940; Martin 1999) refers to the totality of processes, both biostratinomic and diagenetic, that affect pre- and post-mortem (cf. post-depositional) change in skeletal carbonate, but principally refers to the sum of post-depositional processes affecting fossil assemblages. Biostratinomy has been defined as referring to the pre- and syn-burial relationships between skeletal material and their depositional environment (Lawrence, 1968). In the shallow marine environment, biostratinomic processes principally take place within the taphonomically active zone (TAZ) (Table 2.1). This corresponds approximately with the sediment-water interface, but varies, depending in part on the taxa concerned because of niche preferences, and because of variations in depth down profile from the sediment-water interface. Diagenesis refers to the chemical changes incurred by the both non-mineralised (i.e. proteinaceous here) and

mineralised portions of the 'shell' material. Strictly, the diagenetic continuum (i.e. chemical alteration or organic material) begins prior to death and continues through the lithification process, though occurs at significantly reduced rates below the TAZ.

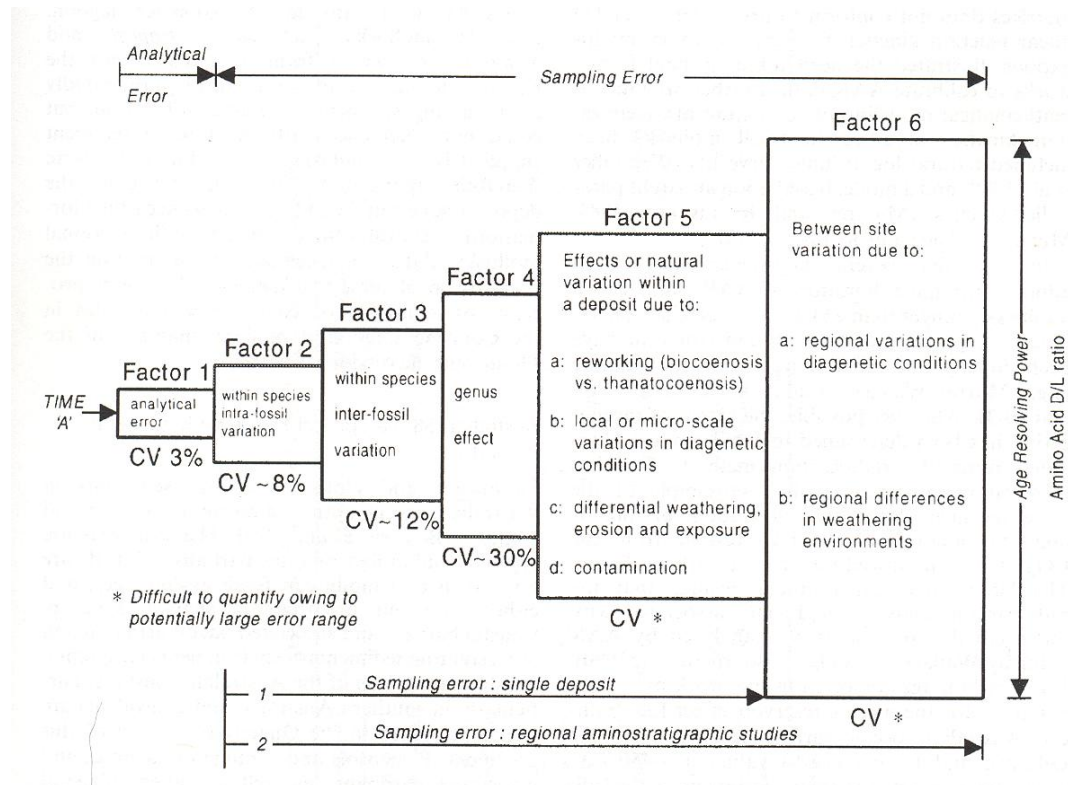


Figure 2.9. Uncertainty in D/L values. Estimates for the variation in uncertainty of D/L values between samples due to systematic and unsystematic analytical and preservational conditions for shallow marine fossils (Murray-Wallace, 2000).

Taphonomic processes affect 'shell' principally through reworking, biological interaction and through interaction with non-biological material, including ground-water and clays. Pre-mortem change refers to, for example, unsuccessful attempts by other organisms to kill molluscs by boring (e.g. by gastropods), nipping (by crabs in stressed environments) etc, mechanical abrasion, and by partial dissolution of valves, particularly the umbone region, as a result of low-pH conditions within the sediment-water interface. Dissolution of valves can also result through release of acidic fluids from within the mollusc mantle, and etching the inner surfaces of shells. These processes can leave shell prone to leaching and further dissolution prior to incorporation within a sediment body. Post mortem processes include transport of the 'shell' as well as physical and chemical breakdown of the skeletal structure and of the associated organic molecules. Preservation is enhanced by rapid burial, especially in fine-grained sediment of low turbulence (Martin, 1999). Taphonomic loss, especially

through dissolution and bioerosion, is typically most severe in shallow-water marine environments. Because of the intimate association of amino acids with biominerals, these processes may result in dissolution, diffusive leaching, and/or contamination of the indigenous amino acids (this study). For aminostratigraphic purposes, these are the principal considerations in the analyses and interpretation of results from fossils.

Despite and the filtering affect of taphonomy on skeletal carbonate (Walker and Goldstein, 1999), and the subsequent post-mortem loss of indigenous proteins (Schroeder and Bada, 1976; Whitelaw *et al.*, 2001), the buffering affect of the calcium carbonate biomineral allows a high degree of preservation of organic matrix and therefore allows racemization-based geochronological studies (Shlyukov *et al.*, 1989).

2.6.2. Biostratinomy and Reworking

Biostratinomic processes, the physical and biological steps involved in the incorporation of skeletal material into the fossil record, may begin prior to death of the organism, and are relevant to AAR studies for two reasons, 1) the results from abraded, worn and/or highly leached skeletons ‘must be viewed with caution’ (Miller and Hare, 1980, p 417; introduced above, and discussed below), and, 2) because reworking creates mixed-age (i.e. time-averaged), assemblages that appear to be ubiquitous in the shallow-marine fossil record: Henderson and Frey, 1986; Goodfriend, 1989. This is because ‘shell’ material is capable of surviving several cycles of reworking and prolonged residence time (average amount of time a particle spends within a single environmental system) in marine environments within the shallow marine sediment-water interface (i.e. the upper part of the TAZ) (Murray-Wallace and Belperio, 1994; Kidwell *et al.*, 2005; Wehmiller *et al.*, 1995; Murray-Wallace *et al.*, 1996; Murray-Wallace *et al.*, 2005). Bioturbation and physical reworking cause time-averaging (temporal mixing) of different fossil communities with the result that temporal mixing commonly goes unrecognised in fossil assemblages (Martin, 1999).

This is therefore problematic because the longer the period of accumulation in any one environment, the greater the number of biological and sedimentary processes that will influence the biomineral supply and preservation within that stratum (Kidwell and Bosence, 1991). Yet, there are also many environments in which fossils are protected and remain well-preserved over significant geological timescales. The use of known life habits, environmental tolerances, post-mortem shell alteration signatures, combined with AAR analyses enable the recognition of reworked organisms, allows differential age-determinations in time-averaged strata, and enables the estimate of temporal scales over which the changes in the depositional environment may have occurred. But, preservational similarities and differences can

complicate these comparisons between fossil samples, environments, their time-averaged assemblages, and AAR-age determinations (Powell and Davies, 1990; Kidwell and Flessa, 1996; Murray-Wallace *et al.*, 2005). Additionally, sampling errors associated with the use of compromised fossil material compound difficulties for obtaining accurate and refined chronologies, and there are no estimates on the uncertainty associated with poorly preserved material (e.g. Murray-Wallace, 2000). Yet, it is necessary to identify and quantify where possible the extent to which age-mixing occurs in order to overcome these issues (Goodfriend and Stanley, 1996) because *neither a fossil's stratigraphic position, nor its taphonomic state, may be a reliable guide to its age*. Therein lies the problem.

The predominant method used to chronologically investigate the reworking phenomena has been the use of paired AAR and ^{14}C dating on bivalve molluscs (Goodfriend, 1989; Murray-Wallace and Belperio, 1994; Wehmiller *et al.*, 1995; Goodfriend and Stanley, 1996; Murray-Wallace *et al.*, 1996; Kowalweski *et al.*, 1998; Carroll, 2001; Barbour Wood *et al.*, 2003). Estimates of the extent of time-averaging in coastal strata vary from 3500 yr in surface sediments to 10,000 yr in deeper shelf settings (Flessa *et al.*, 1993), to scales of time-averaging of $\sim 125,000$ yr on high energy shallow shelves (Martin *et al.*, 1996) and in modern tidal-flat sediments (Murray-Wallace, 1994). Furthermore, shells including those of *Pecten fumatus* having survived several full glacial cycles were reported from the New South Wales continental shelf (Murray-Wallace *et al.*, 2005). The results from these studies suggest that long scales of time-averaging may be more prevalent than previously recognised for molluscs. Apart from one example (Murray-Wallace and Belperio, 1994), reports of reworked foraminifers that have been dated, and from similar environments, are absent in the scientific literature.

2.6.3. Dissolution

Dissolution leads directly to loss of indigenous amino acids and protein residues. This occurs by acid dissolution of the carbonate phase (Grégoire, 1957) and subsequent oxidation and/or leaching of the organic matrix. Abrasion is most effective in conjunction with dissolution of the biomineral, but by itself, abrasive processes appear to have little effect on amino acid preservation (that is, there are no articles available in the published literature which demonstrate that abrasion directly affects amino acid concentrations, and due to this I make the assumption that this is because of the insignificant effect on amino acid preservation by abrasive processes, however it is also likely due to such fossils being deliberately not used).

Calcium carbonate preservation potential is mainly a function of the saturation state of the water with respect to calcium carbonate, biological productivity, oxygenation state and rates of sedimentation (Barbieri *et al.*, 1999). For example, during erosion and/or abrasion,

foraminiferal tests are progressively fragmented, ultimately leading to the release of needle-like calcitic or Mg-calcitic elements and of the anhedral equant crystallites (Debenay *et al.*, 1999). The three forms of calcium carbonate secreted by organisms vary in their solubility in aqueous solution (in Flessa and Brown, 1983, after Chave *et al.*, 1962). Calcitic hard parts with a high MgCO₃ content (e.g. echinoderms) are most soluble; aragonitic skeletal carbonate, typical of most molluscs are less soluble; and calcitic hard parts found for example in brachiopods, oysters, and Foraminifera are least soluble. Calcareous invertebrate skeletons vary significantly in their dissolution rate under experimental and geological conditions (Flessa and Brown, 1983; Clarke II, 1999). Large variation exists between samples having only aragonite biominerals, and the selective dissolution of skeletal carbonate is not regulated by mineralogy alone. The ratio of surface area to weight correlates significantly with the rate of hard part dissolution – high surface area to weight ratio ‘shells’ dissolve more quickly than those of low values. Hard part porosity and calcium carbonate type and structure may also play a role in dissolution rates, as well as surface ornamentation and microstructural variation. Surface textures developed in laboratory experiments include chalky surfaces, thinning of distal margins, etching and hole development of bivalve muscle scars have been found. The rate of dissolution is intimately linked to the microfabric of the shells, leading to differing degrees of preservation between taxa in the same environmental setting (Barbieri *et al.*, 1999).

2.6.4. Diagenesis

Diagenesis refers to the chemical transformations that ultimately give rise to the formation of light hydrocarbons, CO₂, and NH₃ (Collins and Riley, 2001) but also includes processes that may culminate in lithification. As diagenesis proceeds, fossil polypeptides increasingly lose components to for example the nitrogen cycle. Diagenetic alteration of organic matter in mollusc shells increases with age, and is a function of biomineral structure and associated porosity. Organic material is best preserved in environments where temperature and moisture are moderately low (Johnson and Miller, 1997) because higher ambient temperature and hydration states enhance diagenetic change.

In unconsolidated sediments, shell porosity and permeability increase with age and thus fossil shells are not truly closed systems (Robbins *et al.*, 2000). In general, biomineralised protein and amino acids may undergo a variety of chemical post-mortem diagenetic changes (Schroeder and Bada, 1976; Murray-Wallace and Kimber, 1993). These include: 1) hydrolysis of the peptide bond, and release of smaller peptide units and eventually free amino acids, 2) decomposition reactions characteristic of each amino acid, including oxidation, decarboxylation, deamination, 3) destruction or alteration by microorganisms that use the amino acids contained in the detrital remains as a food source, 4) condensation reactions with

other molecules, for example sugars, to produce complex polymers such as humic acids, and, 5) racemization (epimerisation), which may eventually lead to the formation of an equilibrium mixture of equal amounts of the D- and L-enantiomer for each amino acid.

2.6.5. Hydrolysis

Proteins hydrolyse under geochemical conditions by cleavage of an internal peptide bond. This is an internal aminolysis reaction at the N-terminal position, which yields a diketopiperazine (a cyclic dipeptide), and hydrolysis occurs at the C-terminal position (Bada *et al.*, 1999). Diketopiperazine forms when free COOH and free α -NH₂ groups of a dipeptide join to form a cyclic structure (Murray-Wallace, 1993). The rate of hydrolysis is dependent on available water, ambient temperature, and the chemical characteristics of the molecules on either side of the peptide bond (Walton, 1998). Taxonomic variations in polypeptide sequence and structure would be expected to result in generic and species-level differences in hydrolysis, thereby resulting in generic and species-level variation in D/L values. In general, within the biomineral, proteins are nearly completely hydrolysed to smaller peptides and free amino acids in 10⁶ years on the ocean floor, and in 10⁵ years or less in surface environments, though much of this depends on the diagenetic temperature regime (Bada *et al.*, 1999). In comparison, Asparagine (Asn) and Glutamine (Gln) are deaminated quickly during preparative hydrolysis to aspartic acid (Asp) and glutamic acid (Glu) respectively (Hill, 1965; Robinson and Rudd, 1974).

2.6.6. Decomposition reactions

These include oxidation, decarboxylation, deamination, and the interconversion of amino acids to a more stable form. Several thermodynamically unstable amino acids have half-lives too short for geochronological applications (Miller and Clarke, 2007). For example, serine, having the lowest thermal stability (Vallentyne, 1969) decomposes to glycine and alanine (Kvenvolden, 1975). Decomposition of the amino acids serine, threonine and glutamic acid yields water, which would be available for further degradation/hydrolysis reactions (Walton, 1998).

2.6.7. Destruction or alteration by microorganisms

Breakdown of skeletal carbonate generally occurs through dissolution processes, and may involve incorporation of non-indigenous material into the biomineralised structure. This topic is discussed in Section 2.6.3

2.6.8. Condensation reactions

These are the opposite of hydrolysis, and typically occur during the breakdown of original amino acid constituents and their transformation into diagenetic products. For example, amino acids and sugars can covalently bond through non-enzymatic spontaneous glycation condensation reactions to produce brown, partly insoluble melanoidins (Collins *et al.*, 1992). These are high molecular weight heterogeneous polymers formed by way of Maillard reactions (reactions favoured by alkaline conditions, and are where the carbonyl group of the sugar reacts with the amino group of the amino acid to produce N-substituted glycosylamine and H₂O). The products of the Maillard reaction are unstable and are likely to form ketosamines and further breakdown products.

2.6.9. Contamination

Calcium carbonate can adsorb organic matter onto its surface, in addition to incorporating organic matter during biomineralisation (Ingalls *et al.*, 2004). These organics may originate from the surrounding environment, pore waters, or from organic matter associated with the original organism that precipitated the carbonate. Calcium carbonate has a high affinity for organic molecules and preferentially adsorbs more acidic organic compounds when compared with other minerals; these are usually rich in aspartic acid residues (Ingalls *et al.*, 2004). Processes which might introduce amino acids into the biomineral (Bada, 1972, referring to fossil bone) include: a) microbial decomposition of the flesh and other tissues surrounding the bone; b) percolation through the bone of ground-waters containing recent amino acids; c) excessive handling during excavation. Contaminated samples usually have high concentrations of serine, and D/L values much lower than in uncontaminated samples of the same age (Lajoie *et al.*, 1980).

2.6.10. Diffusive leaching of indigenous amino acids

Leaching refers to the physical transport by an aqueous phase, of relatively low molecular weight organic molecules including amino acids and peptides out of skeletal carbonate. Leaching of amino acids from 'shell' implies removal by an external percolating fluid (Collins and Riley, 2000). Permeability in 'shell' is greater in fossils than in modern examples (Robbins *et al.*, 2000) and thus the possibility of transport of molecules both into and out of the 'shell' is greater in fossil material than for modern examples. Leaching of free amino acids from shells results in an apparent lower racemization rate for the shell (Goodfriend *et al.*, 1997). This is because smaller molecules including free amino acids with apparent higher

extents of racemization are preferentially lost through leaching (diffusion), leaving the less racemised and larger molecules within the carbonate matrix.

Protein leaches from powdered shell suspended in water (Pereira-Mouries *et al.*, 2002; Addadi *et al.*, 2006). The most recent model of nacre formation, based on cryo-transmission electron microscopy studies, where H₂O was used as the solvent for EDTA-, HCl-, and ion-exchange resin-demineralised shell of *Atrina serrata* (Levi-Kalisman *et al.*, 2001) suggest that all protein is soluble; that is, protein solubility is dependent on the solvent used. Therefore the use of the term ‘insoluble proteinaceous matrix’ requires care because insolubility is dependent on the ‘decalcifying solution’ (Marin *et al.*, 2007, p 2375). This contradicts many previous observations, but has been quickly accepted by those working in the field of biomineralisation. For example, amorphous calcium carbonate has been shown to be present in larval shells (Weiss *et al.*, 2002; Hasse *et al.*, 2000), and EDTA-etched and critical point-dried (CPD) aragonite tablets have been shown to exhibit a texture of colloidal particles, typical of crystals grown from amorphous calcium carbonate precursors (Addadi *et al.*, 2006). Within the body of literature discussing AAR procedures and results on fossils, as elsewhere, proteinaceous material has been differentiated on the basis of its solubility i.e. insoluble or soluble. The above studies indicate that all of the ‘shell’ is soluble, and it may be that in an aqueous environment the possible extent of solubility of amino acids over time is significantly greater than previously realised.

Rapid loss in total amino acid concentration occurs during the initial phase of diagenesis. This is concomitant with a rise in free amino acid concentrations. At later stages of diagenesis an amino acid concentration plateau exists, and loss after this stage is slow (Wehmiller, 1980; Collins and Riley, 2000; Whitelaw *et al.*, 2001). Hot and alternately dry and wet environments are most conducive to leaching (Miller and Clarke, 2007).

2.7. Chapter summary

For a specific amino acid undergoing racemization, the most important factors are time, temperature and taxonomy (Brigham, 1983; Miller and Mangerud, 1986; Kaufman, 2003). The principal factors affecting racemization for individual taxa, are temperature, and taphonomy. These processes act over time. The incorporation of amino acids in the form of protein is, in the first instance, taxonomically determined. In addition to taxonomy, the process of biomineralisation is further influenced by environmental conditions. Both taphonomic and environmental conditions play a significant role in the fossilisation potential of skeletal-bound proteinaceous matter on which the AAR geochronological studies are ultimately based. Whilst taphonomic filters such as biostratigraphic processes, dissolution, and predation will determine whether a ‘shell’ enters the fossil record, these processes operate on

a range of taxonomic variability, and over a range of timescales. Therefore, the identification and quantification of mixed-age assemblages are necessary (Goodfriend and Stanley, 1996).

2.8. The analytical approach used in this thesis

This thesis aimed to date some strata in three important sedimentary environments in order to solve some major questions related to sea-level change. It is an exploration into several aspects of amino acid racemization dating methods. A conservative approach was taken in that the total hydrolysable amino acid content in fossils was the principal subject matter used for obtaining D/L values for aminostratigraphy and, where calibrated, for chronology. This approach was taken because the majority of racemization based geochronological investigations previously undertaken on molluscs, foraminifers, ostracods and marine sediment samples have predominantly used the total organic pool as the source of amino acids (e.g. Vallentyne, 1969; Kvenvolden *et al.*, 1973; Wehmiller, 1980; Hearty and Aharon, 1988; Murray-Wallace and Bourman, 1990; Goodfriend and Meyer, 1991; Goodfriend *et al.*, 1997; Hearty and Kaufman, 2000; Kaufman *et al.*, 2001; Oches and McCoy, 2001; Sloss *et al.*, 2004; Kaufman, 2005). Therefore this project followed the approach of the majority of studies. However, intracrystalline amino acids were also used here. The intracrystalline amino acid fraction was used initially in a limited investigative role, but for example, in the Gulf of Carpentaria and Kerch Strait, intracrystalline amino acids were brought into use because they gave better results than the THAA fraction, and enabled better understanding of the environments of interest.

Chapter 3

Methods

3.1. Outline

This thesis is presented as a compilation of individual research chapters focusing on a common theme, aminostratigraphy and the recognition of reworked fossils where they exist in the sedimentary record in each of these locations. This chapter presents the details of the amino acid racemization analytical methods used for this project. Subsequent chapters are each written based on the results from a single sub-project, with accompanying methods section detailing the particular approach used for each study.

The principal laboratory method used in this project is Reverse-Phase High Performance Liquid Chromatography (RP-HPLC) (Chapter 2). RP-HPLC is used in this study in conjunction with radiocarbon and uranium-series dating methods. These additional methods allow calibration, and independent checks on the AAR data.

3.2. Field work and sample collection

Fieldwork was conducted at locations on Kangaroo Island, South Australia, in Gulf St Vincent, South Australia, at and around Karumba, Gulf of Carpentaria, northern Australia and at locations in the Black Sea region. These locations are tabulated in Appendix 2. Sample collection was dictated to a large extent by the conditions unique to each study site. This was especially so for locations in the Black Sea region.

Of concern in amino acid racemization studies is that fossils are buried throughout their existence since the time of death. Therefore surface samples were, wherever possible avoided, though this was not always feasible, especially at Kingscote, and at the location of Beach Ridges on Karumba foreshore, Gulf of Carpentaria (Fig. 3.1). Samples recovered from the beach ridge at Karumba were removed from the centre of an 10 cm³ block hammered from the lower portion of *in situ* stratum, about 30 cm below the top. Similarly, samples from the indurated Kingscote cobble beach were also removed from within individual blocks that been buried. However, the principal Kingscote study site is a protected geological monument, therefore minimal destructive sampling was done. Three bivalve shells were recovered from this study site. In contrast conditions at the study locations in Kerch Strait, northwestern Black Sea, allowed in most cases shell samples to be recovered either from outcrop that is presently eroding, or had been. At these locations there is a strong degree of confidence that samples have been buried since initially deposited. All Holocene samples, wherever

collected, were buried shallowly, but the comparatively short time-period since deposition is unlikely to have led to significant extra racemization over this length of time (< 10,000 a).



Figure 3.1. Beach ridges at Karumba, Gulf of Carpentaria. North-facing, indurated and eroding Holocene shell-rich beach ridge at low-tide, Karumba, Gulf of Carpentaria. The burial (i.e. thermal) history of these and similar outcrops are likely to have varied to a greater extent than cores recovered from shallow-water locations continually below water-level. Photograph by A. R. Chivas.

3.3. Sample preparation and Chromatography (RP-HPLC)

3.3.1. Chromatography

Chromatography refers to the separation of molecules by their transport in a mobile phase through a stationary phase. A gaseous mobile phase is used in gas chromatography, while in contrast, for liquid chromatography the mobile phase is a fluid. Reverse-Phase liquid chromatography is one of several types of liquid chromatography. These include affinity, adsorption, partition, ion-exchange, and size-exclusion chromatography (also called gel filtration chromatography). Gas (Lajoie *et al.*, 1980; Murray-Wallace, 1995; Goodfriend *et al.*, 1996; Sloss *et al.*, 2004; Buch *et al.*, 2006), ion-exchange (Hare, 1963; Bada *et al.*, 1978), paired gas-liquid chromatography (Dungworth, 1976; Wehmiller, 1984), and reverse-phase liquid chromatography (Kaufman and Manley, 1998; Hearty *et al.*, 2004) have been used for the analysis of the extent of amino acid racemization in modern and fossil mollusc, foraminifer and ostracod samples.

In normal phase chromatography the stationary bed is strongly polar in nature (e.g. silica) and the mobile phase is non polar. This results in polar samples being retained on the column

longer than those less-polar samples. During Reverse-phase liquid chromatography (RPLC) the opposite occurs, in that the stationary phase is non-polar (e.g. carbon) and the mobile phase is polar. These mobile phases for RPLC are commonly water or alcohol based. Solvent strength becomes stronger with lowered polarity, and the most polar solutes elute first.

High-performance liquid chromatography (HPLC) is the most frequently used method for the resolution of enantiomeric compounds (Bassesteros *et al.*, 1996). It is also, and perhaps more correctly, termed high pressure liquid chromatography. In classical column chromatography columns were open tubes with internal diameters of perhaps 1-4 cm, and mobile phase flow was gravity driven. In contrast, high pressure liquid chromatography is characterized by small diameter closed columns packed tightly with very small diameter column particles, and high pressure is needed to push eluent through the column. Chromatographic systems, such as the Agilent 1100 used here, are automated and standardized so that, compared with older systems, analyses are performed rapidly, and with increased resolution of peaks. The efficiency of a packed column increases as the size of the stationary-phase particles decreases, in part because they allow increasingly uniform (i.e. less turbulent) flow through the column. Smaller particles result in higher resolution and shorter run times (Harris, 2003), hence the term high-performance, but this performance is ultimately pressure dependent (i.e. correct flow rate).

Reverse-phase liquid chromatography is a type of affinity chromatography, where individual compounds are separated from complex mixtures because of the affinity of some molecules for the column packing. The affinity of organic compounds for the column packing material can be changed with changing pH conditions of the eluent and with changing the polarity of the solvent. In this case, this allows the separation of hydrophilic from hydrophobic, and acidic from more basic, amino acid isomers.

3.3.2. HPLC equipment

Two Agilent 1100 HPLC (Fig. 3.2) systems with Chemstation software (Fig. 3.3, 3.4) were used for chromatographic separation of L- and D- amino acid enantiomers during this project. These were designated HPLC1, and HPLC2, operated respectively in the Amino Acid Racemization Laboratory, and in the Geochemistry Laboratories, School of Earth & Environmental Sciences, University of Wollongong. Each system consists of a series of individual elements assembled in a stack as required (Fig. 3.1). The modules used here were a Quaternary Pump, Column compartment, Fluorescence detector, and Autosampler and injection modules. The early analyses were run primarily on HPLC1, before HPLC2 was operable. HPLC 2 was first used by this author, during this study, and required transferring

the methods and settings used on HPLC 1. All sample preparation was undertaken in the AAR Geochronological Laboratory. Routine maintenance including all column changes and consumable part replacement for both HPLC's during this period of work (2005-2009) was undertaken by this author after initial instruction from Agilent staff.

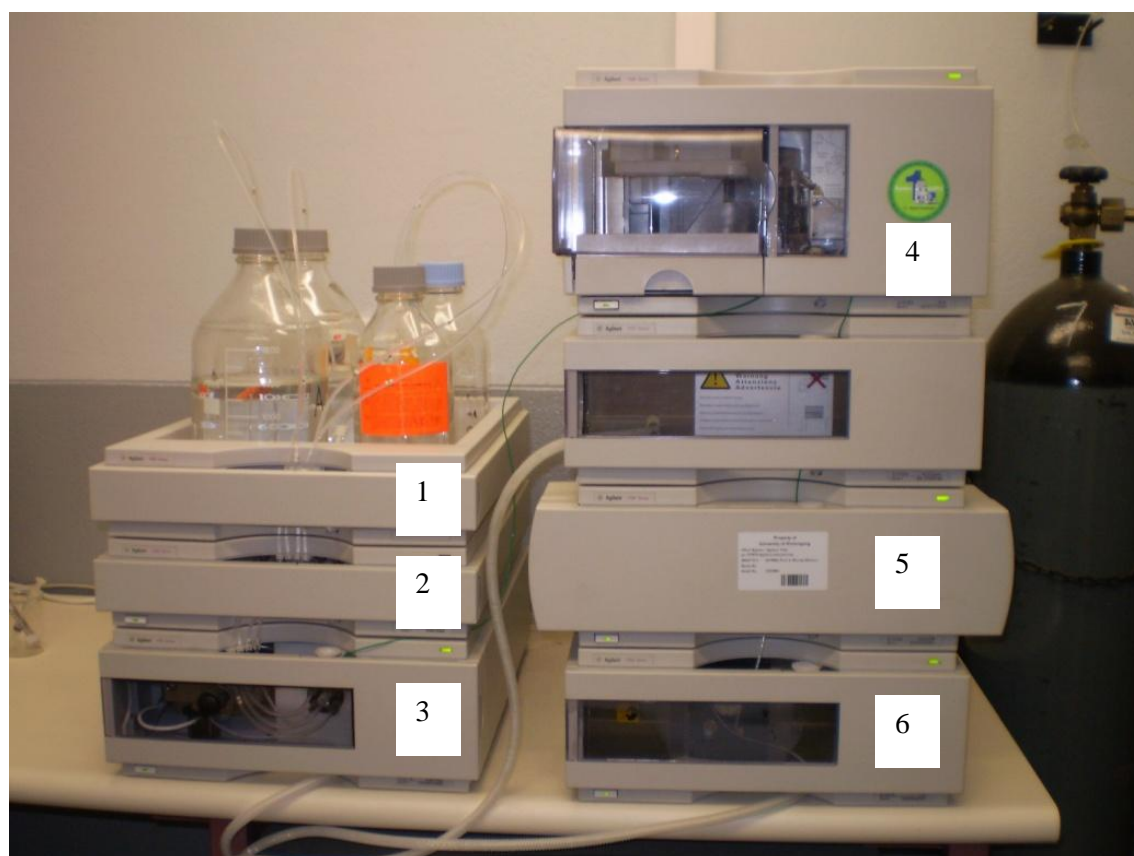


Figure 3.2. Agilent 1100 HPLC system, AAR Geochronology Laboratory, School of Earth and Environmental Science, University of Wollongong. 1 = Eluent tray with mobile phases 2 = Degasser module 3 = Pump module 4 = Vial tray and autosampler module 5 = Column compartment 6 = Fluorescence detector

3.3.3. *Sample selection*

Samples of individual bivalve molluscs and individual and multiple foraminifers were selected according to the requirements of each investigation, detailed in chapters 4 to 8.

3.3.4. *Sample preparation*

All AAR methods used here are based on Kaufman & Manley (1998) with minor modification by the use of bleach. Whole rock preparatory methods are based on Hearty *et al.*, (1992; 2006), Hearty and Kaufman, (2000). Samples were prepared principally according to their mass (size), i.e., whether they were as microfossils, macrofossils, or as whole rock samples. The general procedure, and specific preparation techniques used, their purpose, advantages and drawbacks are presented here. A sample preparation sheet (Appendix 3) was used to systematically prepare samples and assist in record keeping.

3.3.5. *Sample types*

Whole rock samples consisting of sediment with relatively high carbonate content, whole shells, shell fragments, individual foraminifers and ostracods, and bulk samples of foraminifera and ostracods were used in this study.

3.3.6. *Cleaning and cutting of shell samples*

Abrasive cleaning and cutting of shell samples with a dental tool was performed to remove altered shell material and encrusting sediment. Abrasion was undertaken with a dental tool set at as low a speed as possible so as not to raise the temperature of the shell material. This is because of the need to minimize additional racemization induced in the preparation procedures. Abrasion was done 'wet', that is, shell samples were repeatedly immersed in water to reduce the affects of heat produced. This also reduced the significant amount of dust created during this cutting phase. These precautions were also undertaken for cutting samples into the required mass of approximately 0.05-0.1 g for further handling. All shell samples were weighed at this point after cutting.

3.3.7. *Carbonate content in whole-rock samples*

The percentage mass of carbonate was measured in all whole rock samples. This was undertaken so that sufficient concentration of calcium carbonate (and therefore of amino acids) was present in the pre-hydrolysate sample to ensure post hydrolysis concentrations were high enough for RP-HPLC analysis of D and L amino acid enantiomers. Whole Rock samples used here consisted of sieved 250-500 µm diameter shelly material and enclosing

sediment. A single aliquot of 1 g was weighed prior to carbonate removal by acid digestion. The 'shell' content was digested in 8 M HCl until effervescence ceased. Samples were flushed 5 times in double distilled and filtered water, dried in an oven overnight at 110° C, and reweighed when dry, with no carbonate remaining. The percentage carbonate was calculated and a multiplication factor was used for samples having less than 90% CaCO₃ to elevate those levels to an equivalent level of concentration of calcium carbonate to those with higher contents.

3.3.8. Ultrasonic cleaning

After initial cleaning and cutting all samples were cleaned ultrasonically in water. This process utilizes energy released from the creation and collapse of ultrasonically produced microscopic cavitation bubbles. These break up and lift off adhering sediment from the skeletal surface. These bubbles are produced by electronically activated sound waves, and relatively large amounts of energy, primarily in the form of heat, are released in the cavitation implosion shock waves. Cavitation accelerates reactions (Buch *et al.*, 2006) and the ultrasonication process in water has been reported to produce H₂O₂ (Schumb *et al.*, 1955).

Amino acid racemization is a thermally dependent reaction, as determined by the Arrhenius equation (Chapter 2, section 2.3.2). Sufficient energy is produced during the ultrasonication process to reduce the amino acid content of foraminifera (Katz and Mann, 1980). Extended periods of ultrasonic irradiation may produce deamination, decarboxylation and interconversion of amino acids in water (Staas and Spurlock, 1975). This may be attributable to (increased) hydrolysis (and pyrolysis) in the presence of aqueous OH radicals formed through the ultrasonic irradiation and breakdown of H₂O (Naddeo *et al.*, 2007; Jian *et al.*, 2007). Ultrasonication was therefore undertaken in all cases for 10 minutes – this is much less than that recommended by Katz & Man (1980), and a time period of 10 minutes ensured that all samples were equally treated.

3.3.9. Etching of shell

Etching of shell material with dilute HCl is a standard procedure in AAR geochronological studies (e.g., Kvenvolden and Blunt, 1980; Wehmiller *et al.*, 1995; Miller *et al.*, 2000). Cleaning with a rotary dental tool removes most, but not all altered shell material from samples. This is especially so where samples are shell fragments, and excess abrasion would result in their loss. Etching is an additional step to ensure only the best preserved carbonate is used for analysis. A 33% stoichiometric 2M HCl etch (3.3 µL of 2M HCl per mg shell) was used on all shell samples, including those subsequently bleached to isolate the intracrystalline amino acid pool.

3.3.10. Bleach treatment: contaminant removal

A 2 hour 3% hydrogen peroxide soak was initially used as the final pretreatment process for microfossils because they are too small to etch and use individually, recommended by D. Kaufman, and P. Hearty (personal comments 2005; see also Hearty *et al.*, 2004). Routine strong bleaching of all samples using 12.5% NaOCl for one hour was begun during this work because using a 2 hour 3% hydrogen peroxide soak did not remove contaminating amino acids from samples recovered from Gulf of Carpentaria cores (see Chivas *et al.*, 2001; Chapter 8, this study) and this procedure resulted in significant loss by dissolution, of foraminifers from the Gulf of Carpentaria such as *Ammonia sp.* and *Elphidium sp.*, and ostracods including the large marine ostracod *Paranesidea onslowensis*. This is because peroxide provides an additional acid etch (Pingitore *et al.*, 1993) – this may not be significant for shell samples or foraminifer and ostracods with thicker more resistant skeletons but results here indicate this procedure can be fatal for microfossils where they are thin-walled. It was concluded that H₂O₂ causes distinct dissolution of microfossils (cf. Gaffey and Bronnimann, 1993). Thereafter strong bleach (12.5% NaOCl) was used for two purposes –to remove contaminants, and to isolate the intracrystalline amino acid pool. The objective of this first treatment was to remove foreign contaminating amino acids and peptides without destroying the individual sample (test or shell piece).

In contrast to Hydrogen Peroxide, sodium hypochlorite is commonly used for the isolation of intracrystalline amino acids in skeletal carbonate (e.g. Walton and Curry, 1994; Penkman *et al.*, 2007), is basic (pH ~ 11.4) and provided water is not present (Gaffey and Bronnimann, 1993), does not provide an extra unquantified acid etch. Sodium Hypochlorite neutralises amino acids to form salt and water (Estrela *et al.*, 2002). It quickly removes labile, contaminating amino acids by oxidation, and ultimately removes all organic material not incorporated within the intracrystalline-bound organic fraction. This is especially so for microfossils and powdered shell samples. This one hour bleach procedure was adapted for foraminifers, and subsequently employed for all samples in this thesis. This was to ensure consistency in method throughout this project.

3.3.11. Isolation of the intracrystalline amino acid pool

This method was adapted from that of Walton and Curry (1994) and Penkman (*in*: Parfitt *et al.*, 2006; Penkman *et al.*, 2007, 2008). After etching, rinsing five times in double distilled and filtered water, and drying, shell samples were crushed to between 0.25 and 0.5 mm diameter powder. Whole foraminifers, ostracods and powdered shell samples were soaked in 12.5% NaOCl for 48 hours. Upon completion of the required period of bleaching, samples were subjected to rinsing 10 times (i.e. double that of unbleached samples).

3.3.12. Demineralisation

Samples were then weighed for removal of the calcium carbonate by 8M HCl dissolution, and subsequent hydrolysis, and placed in sterile vials. All glassware was cleaned in a high-temperature oven. Glassware was first rinsed clean with double distilled and filtered water to make sure all sediment particles were removed, and placed in an oven for 6 hours or more at 450°C.

Demineralization, hydrolysis, derivatisation and injection of samples were completed using a single clean vial per sample. 1 and 4 mL reaction vials were used for demineralization and hydrolysis. Shell samples and bulk foraminifer samples were demineralised in 8M HCl using a ratio of 20µL of acid per mg of skeletal carbonate. Single foraminifers and ostracods were demineralised and rehydrated using 5µL of 8M HCl, and of rehydration solution. Following demineralization, all samples were sealed in the reaction vials under an N₂ atmosphere for hydrolysis.

3.3.13. Hydrolysis

Hydrolysis is the chemical decomposition or ionic dissociation of a chemical compound caused by the presence of water. The process is speeded up at high temperatures, and by variations in pH. Hydrolysis is used in amino acid racemization studies to release individual amino acids from peptides, so that they may be derivatised prior to injection. Acid hydrolysis is the most common method for protein disassociation to amino acids. Modification of, and complete or partial destruction of several amino acids can occur during this process, especially under oxidizing conditions. Asparagine and glutamine are converted to aspartic acid and glutamic acid respectively during hydrolysis. Acid hydrolysis destroys cysteine and tryptophan. Serine and threonine are partially destroyed, while isoleucine and valine residues may be only partly cleaved.

Hydrolysis was undertaken in all cases for 22 hours at 110°C in a dedicated oven. Approximately 20 minutes after placing the sealed vials in the oven, the vial caps were checked for tightness, and retightened as needed. Upon completion of the hydrolysis period vials were removed from the oven and the hydrolysates vacuum dried in a dessicant drier to which a vacuum pump was attached. HCl hydrolysis results in the production of amino acid chlorides (Hare, 1988). Dried hydrolysates were rehydrated with 0.01M rehydration fluid (0.01M HCl with 0.03mM L-Homo-Arginine and 0.77mM Sodium Azide) and stored in a dedicated fridge until needed.

3.3.14. Derivatisation

Derivatisation describes the covalent process of attaching fluorescent groups to the (nonvolatile) amino acids to enable their detection with a fluorescence detector. *O*-phthaldialdehyde is a non-chiral reagent (Hare, 1988) that reacts with amino acids in alkaline solution giving rise to strongly fluorescent compounds (Roth, 1971). *O*-phthaldialdehyde allows a high degree of sensitivity of fluorescence, but can suffer from instability over short time periods if not used or stored correctly (Heinrikson and Meredith, 1984; Kaufman and Manley, 1998). The advantage of using *o*-phthaldialdehyde is that secondary amines are not derivatised and therefore only primary amino acids will be detected. Derivatisation of DL amino acids with *o*-phthaldialdehyde (OPA) and *N*-acetyl-L-cysteine (IBLC) has been shown to yield diastereomeric isoindole derivatives including D- and L-aspartate, that are separable by RPLC (Aswad, 1984; Bruckner *et al.*, 1991).

During this study aliquots of each sample were derivatised using OPA and IBLC online prior to injection onto the column. The pre-column derivatisation process is fully automated, following a sequence programed into the sample method of Chemstation as an injector program (see table 1), and adapted for either 2 or 4 μ l sample injection volumes. The derivatising agents (OPA and IBLC) are drawn from vial 82, into the off-line sample loop before and after the sample solution as outlined in table 1, and mixed using a motorized plunger. Before and after sample pickup, the needle is dipped into vials 83 and 84 containing a water rinse. These rinsing procedures help to reduce cross contamination, but does not clean the needle internally. However, the HPLC 1100 system is designed with a continuous solvent flow-through process, and this ensures that all internal parts of the autosampler to column components, (needle, capillaries, injector pump, and column) are continuously flushed. This minimizes cross-over between samples. Prior to injection the system switches from the off-line to the on-line loop, and the sample is injected at the beginning of this process. This ensures that all solvents flow through the needle and injector pump. When the flush at the end of each sample injection commences it flushes all of the system in the on-line mode, including the needle, capillaries and column. The system only switches to the off-line mode for the sample pickup, derivatisation and injection process.

Sample hydrolysates have been reported to be stable in vials with punctured septa at room temperature for over one month (Kaufman and Manley, 1998). However, all samples used in this study have only been stored in a dedicated refrigerator. Samples left out at room temperature for more than a few hours have deliberately not been used.

OPA/IBLC reagent is stable for several months when frozen. It is stable for no more than one week at room temperature, and resolution of D- and L-amino acids begins to be reduced after two days (Kaufman and Manley, 1998). During this study fresh OPA/IBLC was

introduced each 3-4 days. This was generally done when changing the Mobile phase A (see below).

3.3.15. *Guard column*

A guard column was not employed on either HPLC because of reports of reduced reliability in results (D. Kaufman, personal comment 2005), and because of the small sample volume used here (i.e. 2 and 4 μ L injection volumes).

3.3.16. *D/L Area and Height measurements*

Results are reported for D/L values based on peak area measurements. These were found to provide better consistency for results from multiple injections of a single (standard) sample (Kaufman and Manley, 1998; this study). Peak heights vary to a greater extent than peak areas with changing chromatographic conditions. Additionally, the amount or concentration of a sample is directly proportional to the peak area, and therefore has more value in *this* study. Manual integration of peak areas introduced greater uncertainties in measurement than when the automated integrator was used, and therefore this was done as little as possible.

3.3.17. *Gradient program*

A programmed linear gradient using three mobile-phase channels was employed. Gradient elution is used because the amino acids in each sample have different polarities, and a change in the polarity (reducing polarity with time) of the mobile phase is required to allow and improve the separation of later eluting compounds such as valine.

Mobile (eluent) A is 23mM sodium acetate with 1.5mM sodium azide adjusted to pH 6.00 with 10% acetic acid. Sodium azide is used to inhibit bacterial growth. Eluent B is 100% HPLC grade methanol. Eluent C is 100% HPLC grade acetonitrile. Mobile A is stable for approximately one week. However, samples are run on the HPLC continuously. The bottles used for Eluents have a maximum capacity of 2L. The HPLC requires approximately 0.5 l per day of Mobile A, and therefore fresh mobile A was generally introduced every four days. Mobile A over five days old was not re-used.

The linear gradient is illustrated in Fig. 3.5. Gradient conditions for each sample change with time to give less polar eluents, thereby giving an increased strength to remove the more hydrophilic amino acids and other organic solutes from the column.

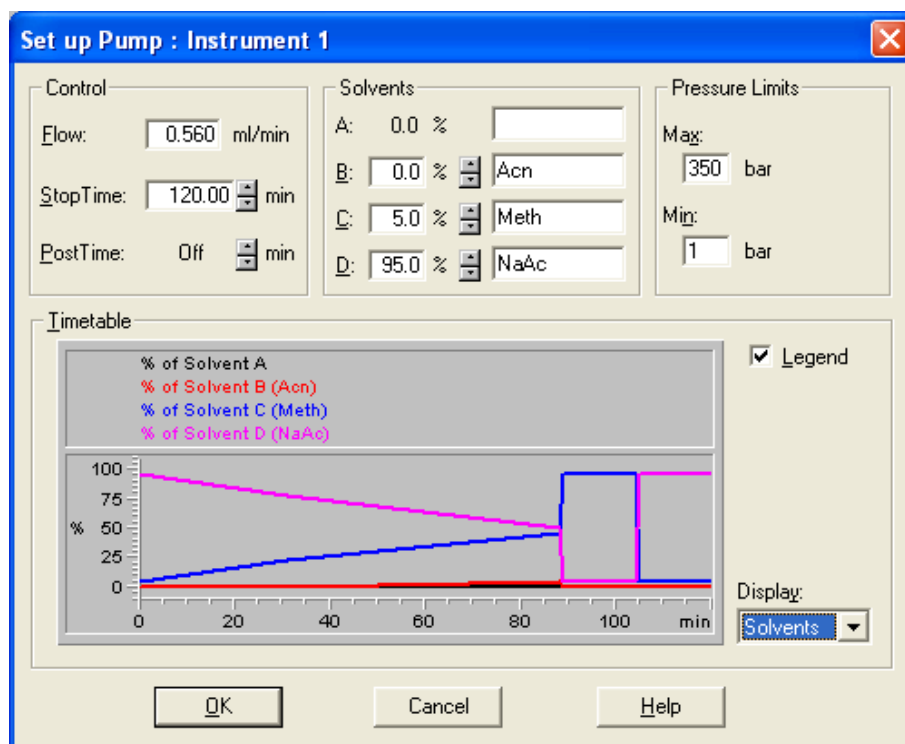


Figure 3.5. Screenshot of solvent gradient used in HPLC 2.

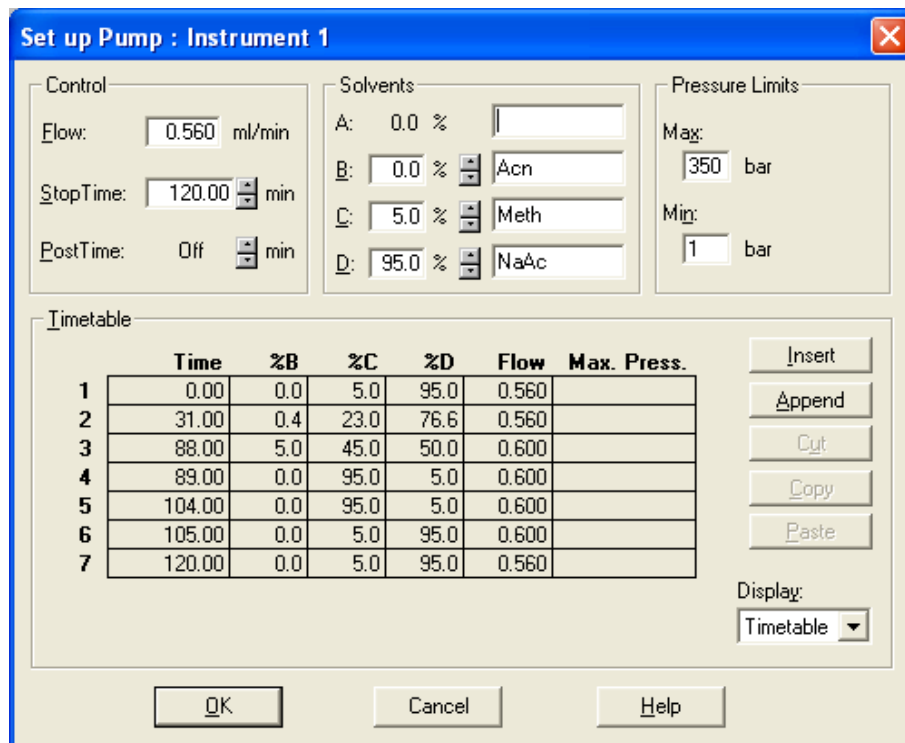


Figure 3.6. Timetable of flow rates for eluents in Figure 3.5, used in HPLC 2.

3.3.18. Column

For most of this project, reverse-phase separation of D and L enantiomers was carried out using a Hypersil BDS C18 column having a 3 mm internal diameter and 5 μm particle size diameter. The present column is a Supelcosil C18 column, also of 3 mm internal diameter and 5 μm particle size diameter. Column temperature during analyses was set at 30°C. This is the temperature originally set by D. Kaufman (16/02/2005). This temperature is higher than that of Bruckner *et al.*, (1991) (25°C), Kaufman and Manley (1998) ($\sim 24 \pm 1^\circ\text{C}$), or than that of the HPLC used in the NEAAR laboratory, York, England (25°C) for the same purpose. Column temperature was set at 30°C because of higher ambient temperatures in the Wollongong laboratory compared to those of Arizona or England. The column in HPLC2 was also set at this temperature so that samples would have been analysed under equivalent conditions. The alkaline mobile phase A ultimately destroys the stationary phase within the column (Hess *et al.*, 2004).

3.3.19. Manipulation of chromatographic data

Results were printed from the HPLC-dedicated desktop computer, and manually transferred to a Microsoft 2007 Access database. Initially all amino acid D/L results were put into the database, but as work progressed and standards were analysed it became apparent that results for phenylalanine, isoleucine and leucine were highly variable and unreliable, and therefore not recorded any further. An initial attempt was made to include glycine results in the dataset because glycine can be found in bacterial contaminants, but there appeared to be no advantage to spending time doing this, and this was also discontinued. The use of a macro which calculates D/L values from peak area and height values, developed by D. Kaufman for use with Chemstation (Kaufman and Manley, 1998, p 999) and used routinely in other studies in the AAR laboratory was not used for this project. Instead peak height and area data were transferred into the database manually by using a data entry form (Fig. 3.3). A macro was used within the database to calculate the D/L values.

Figure 3.7. Data entry form used for data input to database (Microsoft Access). This allowed checking of all chromatograms and data as the peak areas were inputted into the database.

3.4. Testing uncertainties and reproducibility

3.4.1. Evaluating the repeatability of amino acid D/L results

To test the reproducibility of measurements using each of the HPLC units, and between these units, two sets of amino acid standards were used in this work. A synthetic set of DL amino acid standards (Table 3.1) was made from individual L- and D- amino acids obtained from Sigma-Aldrich, to give a near racemic ratio of amino acid enantiomers. These were supplemented by the use of a powdered modern live collected mollusc, *Anadara trapezia*, obtained from shallow water at Oak Flats, Lake Illawarra (Table 3.2). The interlaboratory comparison (ILC) standards are commonly used in laboratories undertaking amino acid racemization studies (Wehmiller, 1984; Kaufman and Manley, 1998; Hearty *et al*, 2004). The results from ILC analyses are illustrated in table 3.3 below.

3.4.2. Repeatability of results for a near-racemic amino acid mixture

Approximately 0.1 g of L and D amino acid standard powders were weighed and mixed in 0.1 L of Milli-Q water, and once dissolved the volume was increased to 1.0 litre by the addition of 0.9 litres of Milli-Q water. These samples were not hydrolysed, but were dried as though they

were hydrolysed, and rehydrated as discussed above to include an internal standard of L-homo-arginine. A comparison of the results for HPLC1 between injection volumes (table 4) shows that overall there is less variation in results for the area D/L values, especially for 2 μ L injections. Apart from the serine 4 μ L injection results, these data are in accord with the estimates of Murray-Wallace (2000) with analytical errors (CV) generally less than 3%, and are similar to those reported by Kaufman and Manley (1998) for inter laboratory comparison standards.

Table 3.1. 2 and 4 μ L injection volumes of a synthetic racemic amino acid mixture. The mean value for standard deviation and coefficient of variation for 4 μ L injections are the estimates for analytical uncertainties used in this thesis.

Amino Acid (D/L values based on area measurements)		4 μ L injection			2 μ L injection		
		Mean	Stdv	CV (%)	Mean	STDV	CV (%)
Asx D/L	HPLC 1	1.064	0.003	0.312	1.066	0.009	0.828
	HPLC 2	0.997	0.046	4.574	1.094	0.006	0.564
	MEAN	1.031	0.025	2.443	1.080	0.008	0.696
Glx D/L	HPLC 1	1.044	0.014	1.367	1.033	0.003	0.321
	HPLC 2	1.024	0.006	1.024	1.023	0.004	0.412
	MEAN	1.034	0.010	1.196	1.028	0.004	0.367
Ser D/L	HPLC 1	1.131	0.077	6.777	1.113	0.003	0.284
	HPLC 2	1.086	0.011	1.038	1.077	0.002	0.172
	MEAN	1.109	0.044	3.908	1.095	0.003	0.228
Ala D/L	HPLC 1	1.098	0.003	0.268	1.091	0.009	0.869
	HPLC 2	1.101	0.007	0.630	1.079	0.005	0.463
	MEAN	1.100	0.005	0.449	1.085	0.007	0.666
Val D/L	HPLC 1	1.104	0.002	0.157	1.105	0.001	0.117
	HPLC 2	1.102	0.005	0.453	1.078	0.011	1.055
	MEAN	1.103	0.004	0.305	1.092	0.006	0.586
Phe D/L	HPLC 1	1.211	0.006	0.474	1.263	0.012	0.956
	HPLC 2	1.017	0.298	29.288	0.981	0.024	2.442
	MEAN	1.114	0.152	14.881	1.122	0.018	1.699
Aile D/L	HPLC 1	1.346	0.009	0.698	1.355	0.015	1.112
	HPLC 2	1.154	0.022	1.912	1.243	0.177	14.267
	MEAN	1.250	0.016	1.310	1.299	0.096	7.690

Despite the coefficient of variation for 2 μ L injections being slightly better than those of 4 μ L injections, 4 μ L injections were used for all subsequent analyses. This was because of two issues – the first was because of the small sample size and low concentration of amino acids in single foraminifers older than Holocene, and the second was because of the need to compare like with like – i.e. injection volumes (and therefore analytical errors). Because the earliest

work in this study was undertaken using 4 μ L injections all subsequent work was done using this injection volume with the intention that all data would be immediately comparable.

3.4.3. Repeatability of 2 and 4 μ L injections of modern geological samples

For comparison with the synthetic amino acids, live articulated bivalves (*Anadara trapezia*) were collected from the western side of the jetty at Balarang, Oak Flats, on the shoreline of Lake Illawarra, New South Wales, in about 0.8 m water depth. These were immediately brought to the AAR lab at the University of Wollongong where they were shucked and cleaned with a dental tool to remove the external surfaces and adhering organic material. Of the shells collected, none were in perfect condition. All had at least one boring, and many umbones had slight dissolution where the shell sat in the sediment, umbo pointing down.

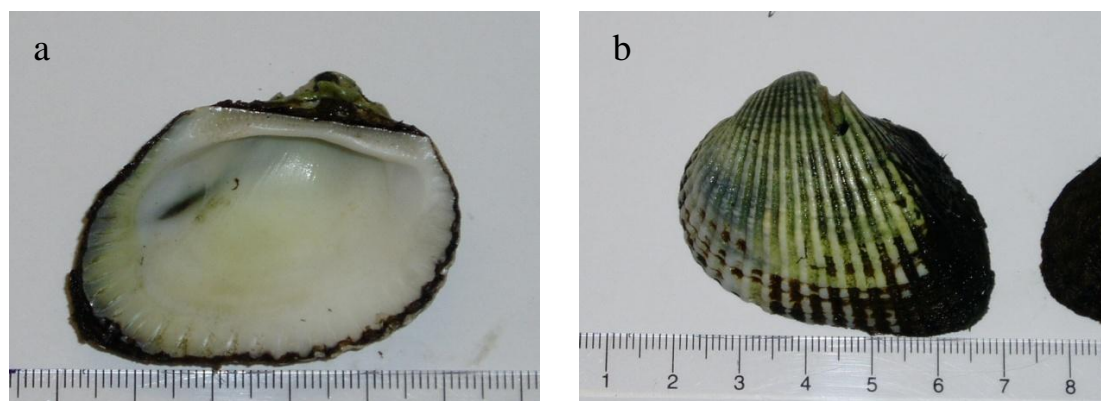


Figure 3.8. Two examples of the bivalve mollusc *Anadara trapezia*, alive at the time of collection, recovered from water depths of 70 cm at Oak Flats, Lake Illawarra. Scale in centimetres. Note the borings (bioerosion) in these examples.

Sections of shell were etched with a stoichiometric 33% 2M HCl acid bath, rinsed five times in double distilled and filtered water and vacuum dried prior to crushing. Crushing was done with a mortar and pestle. The powder was sieved and the 0.25 to 0.5 mm diameter fraction used. This size fraction is the same size as the diameter of individual *Elphidium* foraminifers used in this project from Gulf St Vincent (Chapters 4 and 5). Ideally the use of a homogenised powder should eliminate the problem of inter-shell variation in D/L values (Lajoie *et al.*, 1980; Murray-Wallace, 2000).

Approximately 0.1 to 0.15 g of powder was weighed out and placed into 4 mL reaction vials, and demineralised with 8M HCl using a ratio of 0.2 mL acid per mg of shell powder. Samples were then sealed under N₂ and hydrolysed for 22 hours at 110°C. At the completion of hydrolysis the samples were dried under vacuum in a combined vacuum-dessiccant

apparatus, and rehydrated at the same ratio as for hydrolysis. Analyses were undertaken on both HPLC's.

These results on powdered shell, and those of the near-racemic amino acid standards allow comparison with the results from samples collected for aminostratigraphic purposes. It would be expected that fossil geological samples with values of D- to L-amino acids greater than for samples collected live, and not racemic, would have coefficients of variation intermediate between the values found in these tests.

3.4.4. Repeat analysis of interlaboratory standards

Interlaboratory standards (ILC's) are routinely reported alongside fossil D/L values to ensure the results are comparable with those previously obtained. Four standards, ILCA, ILCB, ILCC and ILCZ were utilized (Figure 3.8).

Several comments are necessary. First, as for the near-racemic amino acid mixture, and the powdered shell, a visual inspection of D/L values for the individual ILC's indicates that aspartic and glutamic acids have the lowest coefficient of variation in D/L values. These results indicate the ILC's have occasional 'odd' amino acid D/L values, and thus anomalous peak areas, that do not appear to affect other amino acid values in a single sample. These occurred primarily in the amino acids serine, alanine, and valine. Retaining these D/L values in a table of results will raise significantly the CV for each amino acid among the ILC's. Removing them however, results in data that does not represent the true variation in data over the duration of time in which these samples were analysed. Table 3.3 below presents the mean data for the ILC's analysed during the duration of this study, and these values represent the mean for all results.

Table 3.2. AAR D/L values from modern *Andara trapezia*, Lake Illawarra, New South Wales (Appendix 2). Results from 2 and 4 μL injections of acid hydrolysate samples from powdered (i.e. homogenised) *Anadara trapezia* alive at the time of collection.

Amino Acid (D/L values based on area measurements)		4 μL injection			2 μL injection		
		MEAN	STDV	CV (%)	MEAN	STDV	CV (%)
Asx D/L	HPLC 1	0.090	0.007	7.674	0.086	0.007	7.786
	HPLC 2	0.088	0.006	7.097	0.088	0.005	6.125
	MEAN	0.089	0.007	7.386	0.087	0.006	6.956
Glx D/L	HPLC 1	0.041	0.003	8.085	0.038	0.003	7.013
	HPLC 2	0.040	0.003	8.046	0.040	0.003	8.016
	MEAN	0.041	0.003	8.066	0.039	0.003	7.515
Ser D/L	HPLC 1	0.085	0.010	11.941	0.080	0.005	5.791
	HPLC 2	0.090	0.010	11.108	0.088	0.010	11.178
	MEAN	0.088	0.010	11.525	0.084	0.008	8.485
Ala D/L	HPLC 1	0.042	0.005	11.871	0.044	0.007	15.811
	HPLC 2	0.045	0.020	44.702	0.040	0.025	62.337
	MEAN	0.044	0.013	28.287	0.042	0.016	39.074
Val D/L	HPLC 1	0.015	0.003	19.956	0.019	0.005	26.065
	HPLC 2	0.014	0.001	7.016	0.016	0.002	7.742
	MEAN	0.015	0.002	13.486	0.018	0.004	16.904
Phe D/L	HPLC 1	0.038	0.011	28.591	0.041	0.009	23.087
	HPLC 2	0.034	0.002	7.038	0.032	0.002	7.742
	MEAN	0.036	0.007	17.815	0.037	0.006	15.415
Aile D/L	HPLC 1	0.035	0.018	50.544	0.047	0.039	83.093
	HPLC 2	0.028	0.032	113.019	0.055	0.024	43.501
	MEAN	0.032	0.025	81.782	0.051	0.032	63.297

Table 3.3. Mean D/L values for Interlaboratory Comparison samples. Results from the analyses of 35 ILCA, 36 ILCB, 41 ILCC, and 35 ILCZ samples for both HPLC1 and HPLC2.

Sample		Aspartic	Glutamic	Serine	Alanine	Valine	L-Ser/L-Glx
ILCA	Mean	0.399611	0.217278	0.492861	0.422306	0.161528	0.226
ILCA	Stdv	0.014141	0.010227	0.04635	0.049394	0.017335	0.015824
ILCA	CV (%)	3.538729	4.706664	9.404284	11.69631	10.7321	7.001869
ILCB	Mean	0.695297	0.433865	0.491081	0.770405	0.409865	0.120486
ILCB	Stdv	0.016042	0.009075	0.05809	0.060614	0.029413	0.007958
ILCB	CV (%)	2.307271	2.091584	11.82891	7.867762	7.17636	6.605283
ILCC	Mean	0.840452	0.837548	0.266833	1.00981	0.902786	0.0885
ILCC	Stdv	0.039644	0.023507	0.202791	0.065065	0.04056	0.079135
ILCC	CV (%)	4.717016	2.806688	75.99904	6.443273	4.492808	89.41847
ILCZ	Mean	0.213528	0.046889	0.146943	0.058629	0.024143	0.77225
ILCZ	Stdv	0.035278	0.010054	0.148486	0.019943	0.009017	0.152345
ILCZ	CV (%)	16.52154	21.44113	101.0499	34.01531	37.34766	19.72737

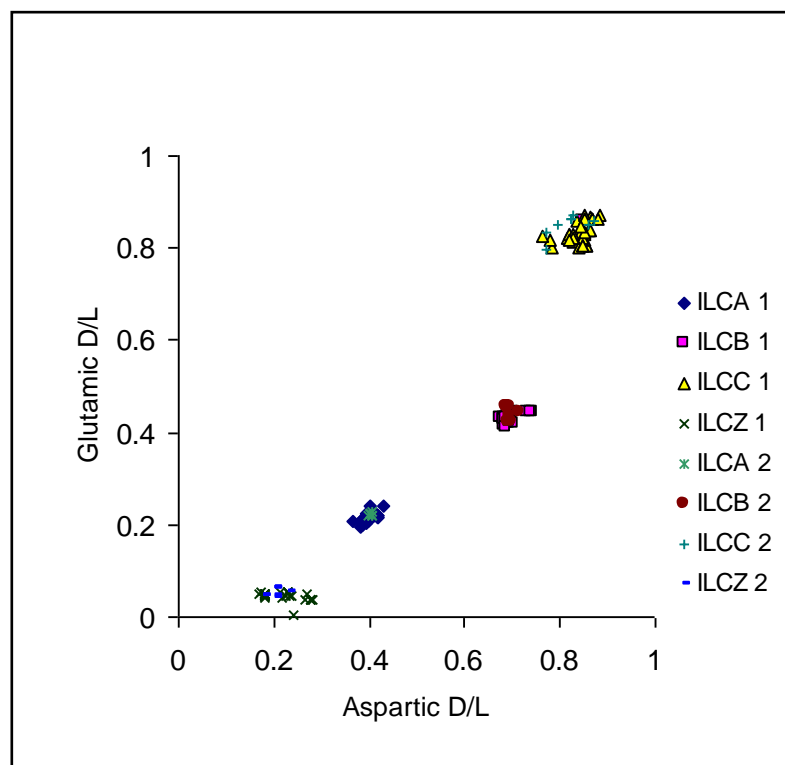


Figure 3.9. Corresponding pairs of amino acid D/L values for aspartic and glutamic acids, from ILC standards. ILCA etc 1, refers to standards analysed on HPLC 1, while ILCA etc 2, refers to results obtained using HPLC 2.

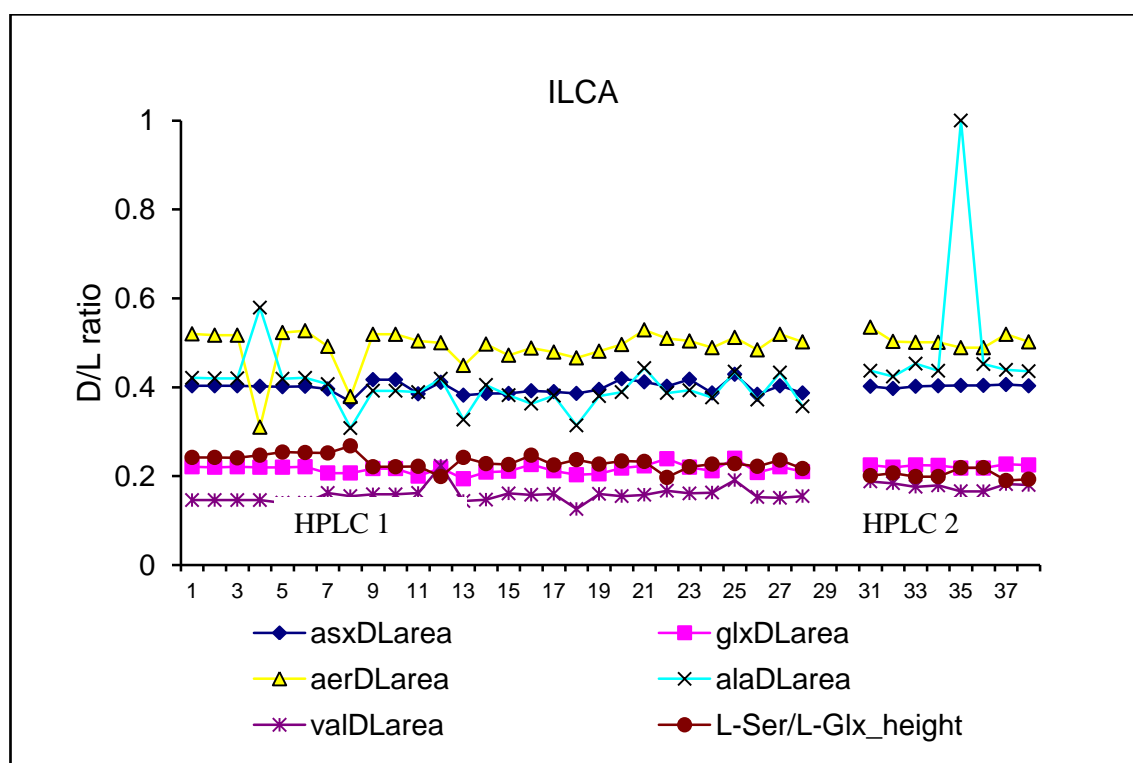


Figure 3.10. All results for ILC A amino acid interlaboratory comparisons

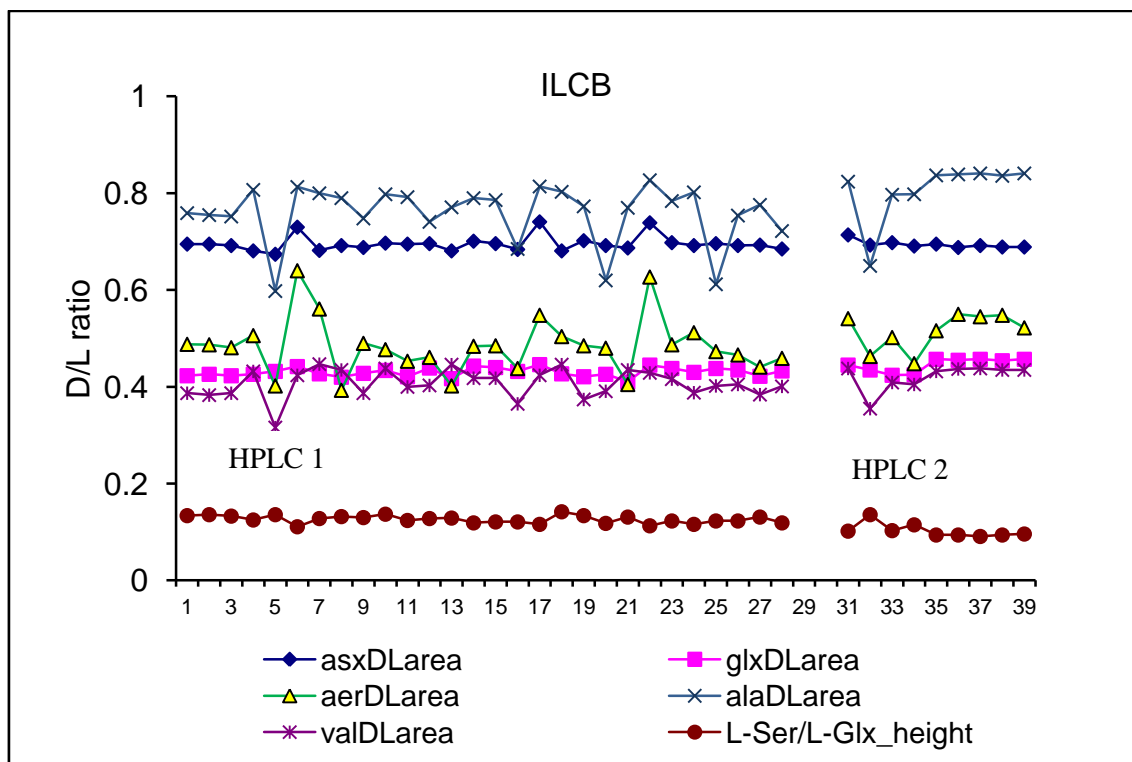


Figure 3.11. All results for ILC B, amino acid interlaboratory comparisons.

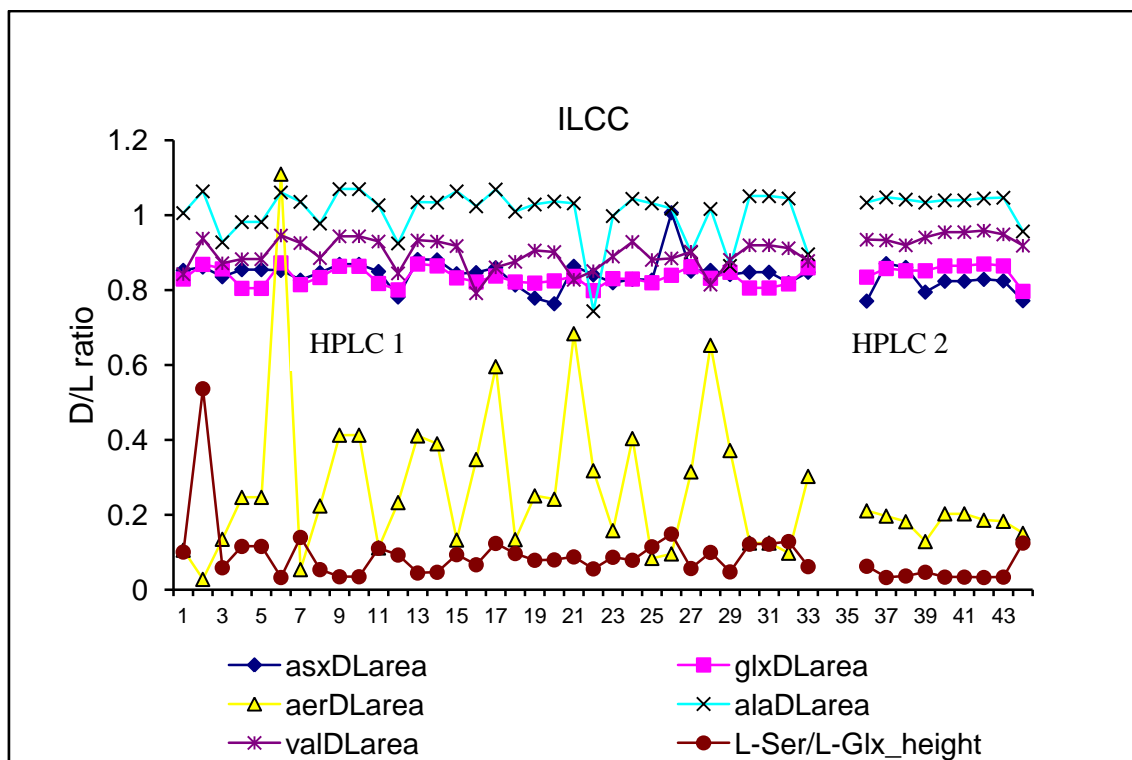


Figure 3.12. All results for ILC C, amino acid interlaboratory comparisons.

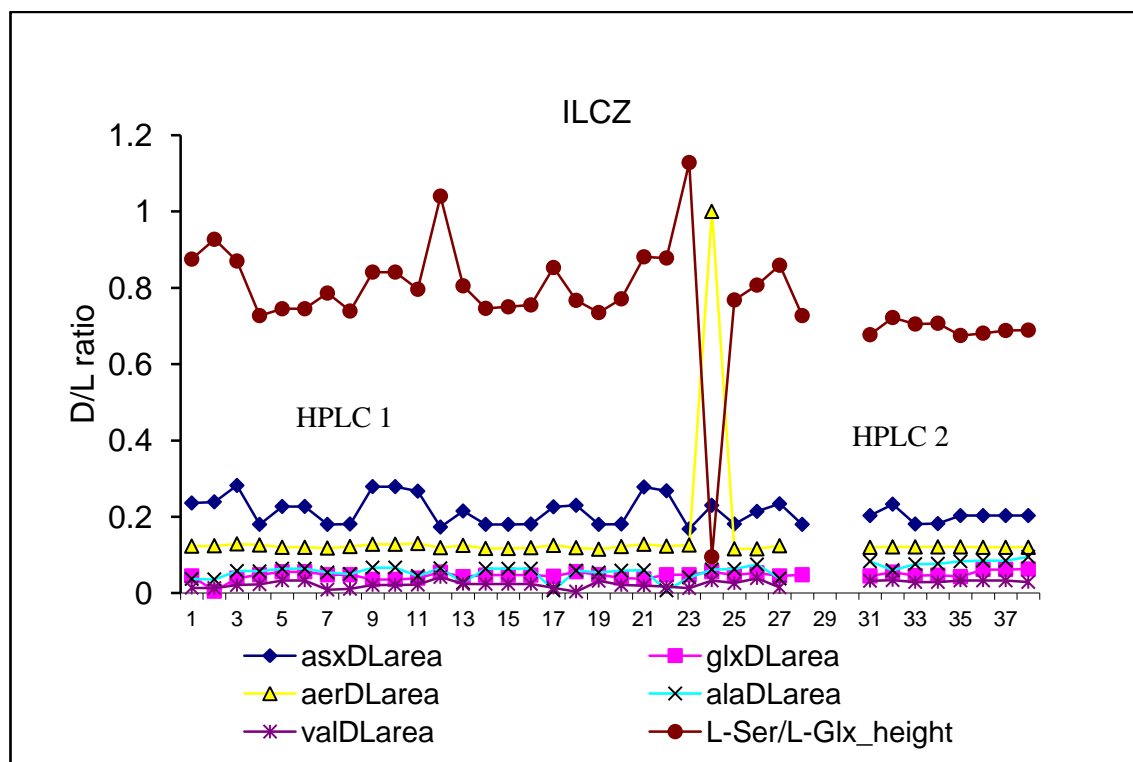


Figure 3.13. All results for ILC Z, amino acid interlaboratory comparisons.

3.5. Taphonomic analysis

3.5.1. Previous taphonomic analyses

The progressive decay of skeletal carbonate in differing marine taphonomic systems has allowed workers to highlight the utility of taphonomic signature analysis. Semi-quantitative scales have been used to illustrate relative changes in taphonomic attributes for molluscs (Powell et al., 2002; Davies et al, 1989), and ostracods (Swanson & van der Lingen, 1997). There does not appear to have been similarly structured semi-quantitative studies undertaken on forams, though many workers have described foraminiferal taphonomy in detail (e.g., Martin, 1999; Barbieri, 2001). Studies of ostracod dissolution indices (Swanson & van der Lingen, 1997) have provided evidence that semi-quantitative scales using low resolution stereomicroscopes are comparable to those using scanning electron microscopes. Similarly, aragonite dissolution in Pteropoda has been studied using dissolution indices compared to the percentage of CO_3^{2-} in marine water columns (Gerhardt and Henrich, 2001). Taphonomy was utilized here in two studies – to differentiate between Holocene and older shells at Kingscote (Chapter 5) and to investigate the extent to which D/L values from foraminifers are affected by preservation (Chapter 6, Gulf St Vincent).

The same taphonomic indices (grades) may be found in differing depositional environments (i.e. similar signatures of and produced from discolouration and dissolution for example, may be found in similar aged deposits, but formed through a variety of processes. The ability to

discriminate between strata which show strong changes in taphonomic attributes is necessary in order to comprehend changes in environment through time.

A general taphonomic index (Table 3.4) was developed in order to compare the preservational state between samples whether they were ostracod, mollusc or foraminifer and whether they were complete or fragmentary. The prime consideration was to use taphonomic signatures which would have in the course of their imprinting on the shell etc, have affected the preservation of peptides and amino acids within the shell matrix to any degree. In reviewing the literature for this and the previous chapter it was found that three taphonomic signatures in particular were critical in estimating the extent of modification of skeletal carbonate due to biostratinomic and diagenetic processes. These were corrosion, completeness, and discolouration. These were the headings under which observations were made in this study.

3.5.2. Corrasion

Corrasion refers to the combined effects of corrosion, abrasion, breakage and dissolution on a specimen. These processes are strongly dependent on the extent of dissolution of the biomineral. For example, there are no reports of abrasion directly affecting amino acid concentrations, whereas loss of indigenous amino acids is consistently reported as being a product of dissolution and subsequent diffusive leaching. Grainy surfaces and chalky textures on shell surfaces are commonly used as evidence of dissolution or leaching of shells, but a chalky luster can have other origins (Cutler, 1995), as shell interiors, confined to the areas inside the pallial line, often acquire a chalky luster during life due to shell dissolution by metabolic acids during periods of shell closure. Dissolution textures are commonly overprinted by abrasive action and by borings, or vice versa. Dissolution bands are common on partially buried shells living in the upper few centimeters of sediment (e.g. live collected *Anadara trapezia* in Lake Illawarra, New South Wales, this study; cf. Cutler, 1995). Given that these shells are not long lived, dissolution can develop relatively quickly, and occurs within the top of the taphonomically active zone. It is difficult to determine such *pre-mortem* dissolution from *post-mortem* dissolution, except that *post-mortem* dissolution is likely to occur also in the region outside of the pallial line in molluscs, and that was the area used here originally for luster examination, but no longer done. Frosting and pitting of surfaces on field-collected shells can be the work of microborers rather than the result of abrasion, while bioerosion can round surfaces and destroy ornamentation, and these actions commonly exist as overprints on the dissolved surface, and therefore can be difficult to differentiate. Therefore the term corrasion was used to cover the multiple processes that collectively remove 'shell' carbonate.

Table 3.4. A general visual preservation index for molluscs, foraminifers and ostracods used in this thesis (Chapters 4 and 5 principally).

Diagnostic feature examined	Grade	Description
Degree of completeness	0	> 90% complete
	1	< 90% complete, identifiable to species level
	2	< 90% complete, identifiable to genus level
	3	< 90% complete, unidentifiable to genus level
Articulation	00	Collected alive, articulated
	0	Articulated, unfilled
	1	Articulated, filled
	2	Disarticulated
Extent of discolouration	0	None, strong original colours present, or transparent
	1	Slight fading of original colour, or translucent
	2	Very strong fading of original colour, nearly totally white
	3	White, no other colour visible anywhere
	4	Lightly discoloured, e.g. light grey, light brown, patchily discoloured
	5	Strongly discoloured, e.g. black, dark grey
Extent of corrasion (= dissolution, abrasion and recrystallisation)	0	None, may be transparent
	1	Translucent generally, beginning of dissolution
	2	White surfaces, none to slight abrasion, retains structural strength
	3	White, pores enlarged, strong abrasion of sculpture, minor delamination, and/or minor pitting, minor loss of structural strength
	4	Chalky, sculpture gone, strong delamination, substantial loss of structural integrity, internal structure of foraminifers visible
Presence of bioerosion	0	None
	1	Single small hole (< 1mm diameter)
	2	Single large hole (> 1 mm diameter)
	3	Multiple small holes
	4	Multiple large holes
Preservation of luster	0	Original pearly luster present
	1	Slight fading yet retains gloss or oily state
	2	Earthy, faded and no gloss
	3	Chalky
Evidence for encrustation	0	None
	1	Minor, localized (< 30% of area)
	2	Moderate (30-90% of area)
	3	Total (> 90% of area)

3.5.3. Completeness

Completeness refers to the percentage of the original fossil remaining – and the extent to which that fossil can be identified. This provides a semi-independent check on the scale of corrasion given to the same sample as greater corrosion will increase the likelihood that the

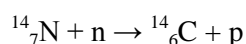
sample cannot be identified to the species level, but perhaps only to the genus level, invariably because of chalky textures and abrasion.

3.5.4. Discolouration

Discolouration refers to the change in colour of the shell from its original state, taken as the colour of a live example. Over time shells may lose their original colour, due primarily to bleaching by sunlight, but this is not always the case because leaching by acids can also produce a similar effect. Discolouration may lead to unnatural colours in the fossil, including orange, grey and black. These result from the incorporation of, for example, microscopic pyrite, or oxidation of incorporated iron compounds during burial processes.

3.6 ^{14}C dating

There are three isotopes of carbon found in nature (Head, 1999). These are the stable isotopes ^{12}C and ^{13}C , and the radioactive isotope ^{14}C . The natural abundances are 98.99% ^{12}C , 1.108 % ^{13}C , and 1×10^{-12} % ^{14}C . Libby was the first person to measure the activity of the ^{14}C isotope for use as a dating method (Zhou et al., 2000). ^{14}C is produced primarily within the atmosphere, but a minor proportion is also produced *in situ* on the surface of the Earth, by radiogenic decay of uranium and thorium, and by way of nuclear weapons testing. In the upper stratosphere and lower troposphere cosmic ray bombardment of Nitrogen with cosmic ray generated neutrons results in the production of radiocarbon by the following reaction:



Oxidation to carbon dioxide quickly follows, with the result that radioactive CO_2 joins the carbon cycle (Dickin, 2005). Dissolved carbonate in the oceans includes CO_2 incorporated from the atmosphere as a result of exchange reactions between these reservoirs. Without mixing of seawater, surface marine water is at equilibrium with the atmosphere with respect to ^{14}C . However, where vertical and horizontal mixing occurs between oceanic masses, such as commonly occurs in oceanic settings, carbonate-secreting organisms will incorporate different amounts of ^{14}C depending on the concentration in the surrounding water.

Living plants and animals incorporate ^{14}C during growth, and once fixed in the relevant tissue or in the biomineral, ^{14}C will only disappear by radioactive decay at a known rate. Therefore the age of the organic material can be determined by measuring the amount of ^{14}C at the present-day. Ages are normally given in years BP, generally referring to years before 1950 because of the bomb spike due to nuclear testing.

Two significant error sources are associated with ^{14}C dating (Drysdales & Head, 1994). These are the incorporation of ‘dead’ carbon into the material of interest, and contamination by modern carbon. Both of these problems are of concern when attempting to date carbonate (molluscs and foraminifers) from shallow marine settings. The age limit for this method is approximately 50 ka (Litherland and Beukans, 1995).

Radiocarbon dating was conducted at ANSTO, Lucas Heights, Sydney, to analyse the extent of radioactive decay of ^{14}C using accelerator mass spectrometry (AMS). AMS methods combine the marriage of middle energy physics with mass spectrometry (McNichol and Aluwihare, 2007), allowing the number of ^{14}C atoms in a sample to be counted (as ions), and thereby shortening the time required for each sample to be analysed. As for conventional beta counting, sample size is determined in the first case by the amount of carbon in the carbonate, and is approximately 12% for CaCO_3 . The advantage of the AMS method over conventional ^{14}C methods is that the minimum sample mass is reduced from approximately several g of carbon for beta counting to less than 200 μg of carbon (Hua *et al.* 2001) for AMS.

The methods used at ANTARES for small samples routinely analysed for Quaternary studies including sediment, peat, coral, foraminifera and shells (Hua *et al.*, 2001), involve sample pretreatment, CO_2 extraction, and graphitization. On completion of the graphitization reaction the graphite is inserted into an aluminium cathode for ^{14}C analysis using the ANTARES accelerator mass spectrometry facility (Lawson *et al.*, 2000; Fink *et al.*, 2001; Hua *et al.*, 2001).

3.7 Uranium-series dating

Marine organisms incorporate substantial seawater uranium and negligible thorium into their skeletons during growth (Thompson *et al.*, 2003). In general, this ‘system’ remains essentially closed since that time, and an assumption is made that the exchange of parent or daughter isotopes with the external environment outside the coral skeleton has not occurred. In theory, closed system behaviour is governed solely by the laws of radioactive decay (van Calsteren and Thomas, 2006) and therefore the age of the sample can be calculated using decay equations. However, this is unlikely to be true for every fossil because processes such as hydrothermal alteration, diagenesis and/or weathering can produce open system behaviour with exchange of isotopes between the external environment and the skeleton. Therefore fossil coral and mollusc samples commonly do not reflect closed system behaviour and differentiates from modern seawater $^{234}\text{U}/^{238}\text{U}$

3.7.1. Uranium-series sample preparation and measurement of isotopic activities

Thermal ionization mass spectrometry (TIMS) measurement of uranium and thorium isotopes was undertaken at the Radiogenic Isotope Laboratory, Centre for Microscopy and Microanalysis, University of Queensland. This method gives the time of element fractionation associated with the incorporation of calcite into the coral skeleton (i.e. time of growth) (van Calsteren and Thomas, 2006).

Samples were hand-picked, cleaned ultrasonically, and spiked with a ^{229}Th – ^{233}U – ^{236}U mixed tracer. The ^{233}U – ^{236}U double spike with precisely known $^{233}\text{U}/^{236}\text{U}$ ratio was used to monitor and correct for U mass-fractionation to improve the analytical precision of U isotope ratio measurements. After total dissolution in nitric acid, concentrated hydrogen peroxide was added to decompose any organic matter and to ensure complete mixing between the spike and the sample. U and Th were co-precipitated with iron hydroxide, and then redissolved in nitric acid prior to purification using standard anion-exchange methods.

U and Th fractions were loaded onto individual pre-degassed, zone-refined rhenium filaments and sandwiched between two graphite layers. Uranium and thorium isotopic signals were measured on a Daly ion counter as $^{232}\text{Th}/^{229}\text{Th}$, $^{229}\text{Th}/^{230}\text{Th}$, $^{233}\text{U}/^{235}\text{U}$, $^{234}\text{U}/^{235}\text{U}$ and $^{233}\text{U}/^{236}\text{U}$ values in peak jumping mode by thermal ionisation mass spectrometry (TIMS) at the University of Queensland. U and Th concentrations, and $^{230}\text{Th}/^{238}\text{U}$ and $^{234}\text{U}/^{238}\text{U}$ values were calculated based on the measured isotope values, tracer and sample weights, as well as isotope concentrations and values of the mixed tracer. Activity values ($^{230}\text{Th}/^{238}\text{U}$ and $^{234}\text{U}/^{238}\text{U}$) were calculated by normalizing to the corresponding values obtained from repeat analyses of the international secular-equilibrium HU-1 uraninite standard (Ludwig *et al.*, 1992). Conventional and open-system $^{230}\text{Th}/^{234}\text{U}$ ages were calculated using the method described in Thompson *et al.* (2003). Details on analytical procedures and instrumentation at University of Queensland are given in Zhao *et al.* (2001) with further modifications described in Yu *et al.* (2006).

Amino acid racemization dating of a raised gravel beach at Kingscote, Kangaroo Island, South Australia

4.1. Outline

Chapter 4 and 5 of this thesis focus on Gulf St Vincent, South Australia. This research was initiated because of uncertainties in the age of and water-depth present during the formation of a last interstadial carbonate unit within the central Gulf St Vincent basin, and its relationship to the global sea-level record. The purpose of this particular work was to obtain fresh AAR data independent of that previously published on the southern Australian margin, and then to use that data to compare and contrast with data obtained on shells and foraminifera from cores and surface samples recovered from central Gulf St Vincent. This latter data was to form the main focus of the work. However, the serendipitous discovery of well preserved coral at Kingscote led to the work on the Kingscote study site being presented here as a separate chapter.

This chapter therefore presents the results of amino acid racemization analyses undertaken on both intra- (THAA) and inter-crystalline (HIAA) amino acids from bivalve molluscs at Kingscote, Kangaroo Island. A limited number of single *Elphidium* were analysed for the extent of racemization in the THAA fraction. Uranium-series dating was undertaken on a single coral specimen, *Goniopora lobata* recovered from Kingscote at the laboratories of the University of Queensland. The discussion focuses on sea-level and the implications of the presence of coral at this location.

4.2. Introduction

The presence of species common to present-day warm and tropical environments, recovered from last interglacial (MIS 5e) (MIS 5e, 125 ka) sedimentary sequences in southern and south-western Australia have long intrigued workers (Howchin, 1909; Ludbrook, 1984; Cann & Clarke, 1993; Murray-Wallace *et al.*, 2000) because they suggest that the coastal regions of southern Australia were warmer than at present. The inference of warmer climatic conditions during MIS 5e have been based on the presence of large concentrations of a small number of indicator species, which include the bivalves, *Anadara trapezia* and *Pinctada charchariarum*, and the megascopic foraminifer *Marginopora vertebralis* (Cann, 1978; Cann & Clarke, 1993). In South Australia, last interglacial (MIS 5e) peritidal and backbarrier lagoonal sediments have been termed the Glanville Formation (Firman, 1966; Ludbrook, 1976; Cann, 1978;

Ludbrook, 1984), and have been mapped on Eyre Peninsula, the central gulfs region, on Kangaroo Island, and in the Coorong (Fig. 1). Glanville age equivalents are found in southwestern and western Australia, a region where last interglacial (MIS 5e) age coral reefs have been found several hundred kilometres south of their present-day extent (Veron & Marsh, 1988), and dated using uranium-series methods (Szabo, 1979; Stirling *et al.*, 1995).

Hermatypic corals (e.g. *Plesiastrea versipora*) live today in Gulf St Vincent (Howchin, 1909; Burgess *et al.*, 2006), yet identifiable corals from the last interglacial (MIS 5e) sedimentary record in South Australia are scarce. As a result, sea-level studies in this region have relied heavily on aminostratigraphic (Kimber & Milnes, 1984; Murray-Wallace & Kimber, 1987; Murray-Wallace, 1995) and luminescence (Huntley *et al.*, 1993; Huntley *et al.*, 1994; Huntley & Prescott, 2001) methods for assigning ages to strata rather than utilising U-series dating. Previous aminostratigraphic investigations in this region have been undertaken with gas chromatography, and employed with success to elucidate the Quaternary stratigraphy and general neotectonic characteristics of this region (Von Der Borch *et al.*, 1980; Murray-Wallace *et al.*, 1995; Murray-Wallace, 2002). These investigations have focused on the central gulfs region of Spencer Gulf and Gulf St Vincent, the Coorong Coastal Plain, and Eyre Peninsula, with a limited number of studies having been undertaken on Kangaroo Island.

Kangaroo Island is situated between the high-energy southern ocean and the restricted marine environment of semi-arid Gulf St Vincent (Fig. 1). The island exists within the southern Australian cool-water temperate carbonate province, dividing the Lincoln from the Lacepede Shelf, and blocking the southeasterly flowing Lincoln Shelf current (Great Australian Bight Current; Li *et al.*, 1998). Thick aeolianite sequences forming coastal cliffs along the south coast have recorded the extremes of southern ocean climate during the Quaternary. In contrast, similar sedimentary strata at Kingscote, on the northern coastline of Kangaroo Island are situated within the southern margin to the protected, and semi-enclosed Gulf St Vincent.

Kingscote is located between the neotectonically uplifted MIS 5e deposits at Sellicks Beach and Normanville on Fleurieu Peninsula to the east, and the tectonically more stable Eyre Peninsula to the west (Bourman *et al.*, 1999; Murray-Wallace, 2002; Murray-Wallace & Bourman, 2002; Sandiford, 2002). A shingle beach facies at Kingscote, Nepean Bay (Fig. 3, 4), with its base raised from present-day sea-level by approximately 2 m, was previously described as last interglacial (MIS 5e) in age (Milnes *et al.*, 1983) based on the presence of the megascopic foraminifer, *Marginopora vertebralis*, and typical Glanville Formation molluscs (Ludbrook, 1984). The faunal elements were described as a thanatocoenose, with most of the shells having been reworked from more than one environment (Milnes *et al.*, 1983). The assemblage was considered to be the conglomeratic equivalent of the Glanville Formation of

Gulf St Vincent. This region is in the far-field of glacial and ice-sheet influence and, therefore, the present position of the Glanville Formation at about sea-level is principally a function of changes in elevation of these palaeo-shorelines by neotectonism (Murray-Wallace, 2002). Hydroisostatic adjustment appears not to have affected this location (Belperio *et al.*, 2002). Numerical dating methods have not previously been applied to these coastal deposits at Kingscote. This study examines the aminostratigraphic and neotectonic relationship of the raised beach deposit at Kingscote to MIS 5e sediments reported from mainland outcrops on the present-day Gulf St Vincent coastline, and to the regional last interglacial (MIS 5e) datum on Eyre Peninsula (+ 2 m APSL, Murray-Wallace & Belperio, 1991).

In contrast to previous work based on gas chromatography in this region (e.g., Murray-Wallace & Kimber, 1987; Murray-Wallace, 1995) this study employs Reverse-Phase High Performance Liquid Chromatography (RP-HPLC) to determine the extent of amino acid racemization (AAR) on bivalve molluscs (*Katelysia*, *Anapella* and *Mactra*) and on single foraminifers (*Elphidium* and *Marginopora*). Independent chronological control was obtained by U-series dating on the coral *Goniopora lobata*.

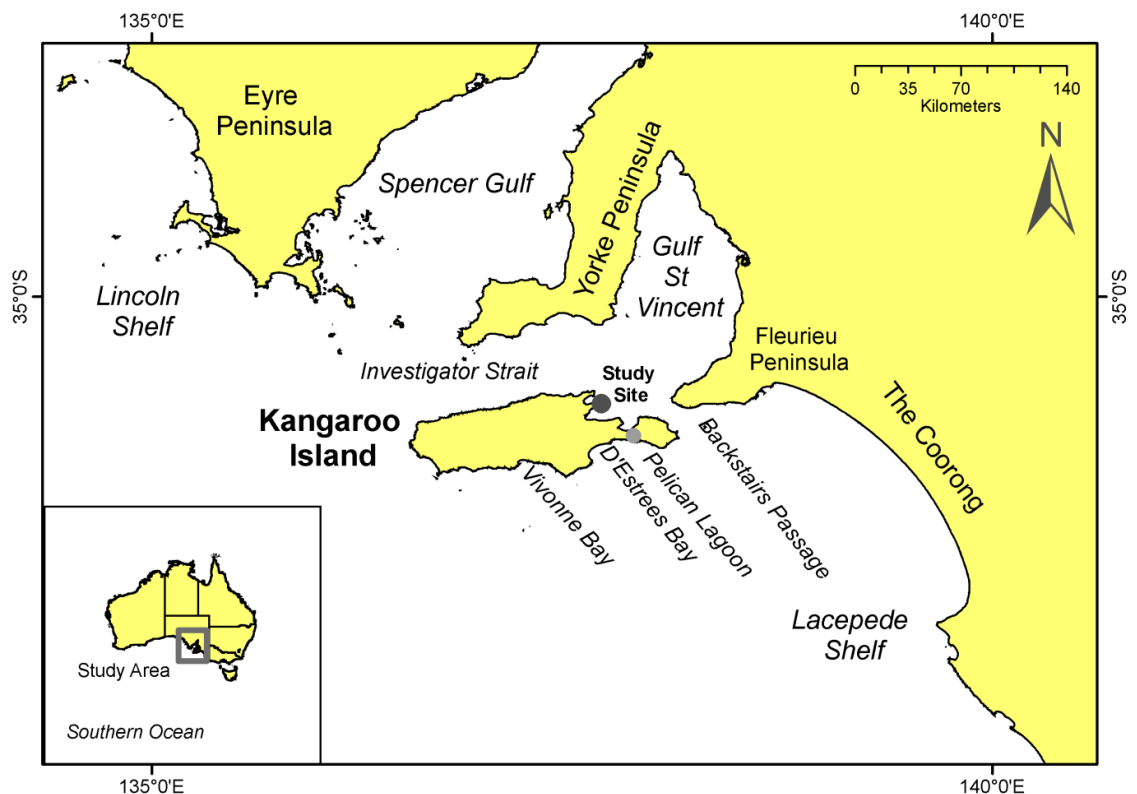


Figure 4.1. Location of Kangaroo Island, South Australia. Kingscote is positioned on the southern margin of Gulf St Vincent, and protected from the Southern Ocean.

4.3. Methods

Field locations were recorded using a Magellan Mobile Mapper, a GIS-enabled GPS system (Fig. 2). Identification of fossil marine molluscs followed Ludbrook (1984), and coral was identified using Veron (1986). Samples for AAR analyses were recovered from the northern, northeastern and southern coastal sections of Kingscote (Fig. 2). RP-HPLC was used to analyse the extent of AAR within bivalve molluscs following the method of Kaufman & Manley (1998) for the total hydrolysable amino acid fraction (THAA), and following the method of Penkman (in Parfitt *et al.*, 2006), for the hydrolysable intracrystalline amino acid fraction (HIAA).

A taphonomic index (Chapter 2) was employed to highlight contrasts in preservation between fossil molluscs. These concepts were derived primarily from the work of Davies *et al.* (1989) Swanson & van der Lingen (1997), Powell *et al.* (2002) Zuschin *et al.* (2003) and from field and laboratory studies. The taphonomic index was used to assist in identifying reworked shells, but also because of the relevance of preservation to processes of protein and amino acid degradation, diffusion (leaching) and contamination. Taphonomic indices were compared with contamination indices (L-Ser (peak height)/L-Glx (peak height)) and valine D/L values. The bivalve mollusc *Katelysia* was the preferred subject because this genus was common to all of this coastal succession, and because it is a robust, stout mollusc, and tends to retain indigenous protein residues over interglacial timescales. Furthermore, previous work in this region utilised this genus, and there is a regional dataset with which to compare results. There is no significant species-effect for racemization in this genus (Murray-Wallace & Kimber, 1989). There are no previous reports on AAR studies of the intertidal foraminifer *Elphidium*. This genus was chosen because it is robust, and ubiquitous in last interglacial (MIS 5e), interstadial MIS 3 and Holocene sedimentary sequences in Gulf St Vincent. A limited number of individuals of the foraminifer *Marginopora vertebralis* were also analysed for the extent of racemization.

Here, the amino acid valine is selected for molluscan aminostratigraphic purposes because it is suited to the analysis of Pleistocene fossils, and thus allows comparison with results from previous AAR studies in this region.

A single coral specimen was recovered from Kingscote and cut into three equal sized pieces for U-series dating, XRD and thin-section analysis. Uranium-series dating ($^{230}\text{Th} - ^{238}\text{U}$) was undertaken at the Radiogenic Isotope Laboratory, Centre for Microscopy and Microanalysis, University of Queensland, following the methods of Zhao *et al.* (2001). Age determination was made using the open-system method of Thompson *et al.* (2003), and decay constants were obtained from Cheng *et al.* (2000).

4.3. Regional setting

Kingscote is situated on the western margin of Nepean Bay, a sheltered marine embayment on the northeast coast of Kangaroo Island, forming part of the southern-most coastline of Gulf St Vincent (Fig. 1, 2). Climate in this location is similar to that of mid Gulf St Vincent, with evaporation greater than precipitation, and rainfall of $< 500 \text{ mm a}^{-1}$, similar to that of Port Gawler (420 mm a^{-1} ; Burrows, 1979; Cann & Gostin, 1985). Current mean annual temperature (CMAT), a relevant consideration for AAR analysis, is 15.4°C . These coastlines are micro-tidal and wave-dominated, despite being sheltered from the southern ocean climate. The Cygnet River discharges into the southwest corner of Nepean Bay, south of Kingscote. The present-day coastal setting at Kingscote is compartmentalised into sandy and rocky intertidal zones within shallow, low energy, coastal waters dominated by shallow seagrass meadows of *Posidonia* sp. and *Halophila australis* to the north and south of Kingscote. Unvegetated sand and sections of reef exist to the east (Bryars *et al.*, 2003). Cliffs are actively eroding, particularly on the northeast of Kingscote, south of Beatrice Point. A Holocene intertidal rock platform is cut into the Kingscote Limestone between Rolls Point and the coastal swimming pool (Fig. 2). Large numbers of *Kataysia* sp valves, some articulated, occur on the sandy shoreline along with a number of gastropod species including *Nerita* that commonly inhabit the adjacent rocky section. At Beatrice Islet, Bay of Shoals (Fig. 2), subaerial sandy gravel sediments are present in the supratidal zone, and are suggestive of a pre-existing shingle/gravel deposit within the Bay of Shoals (Short & Fotheringham, 1986). A competent cobble beach calcarenite also exists at Boxing Bay, on the northern coast of Kangaroo Island (Short & Fotheringham, 1986).

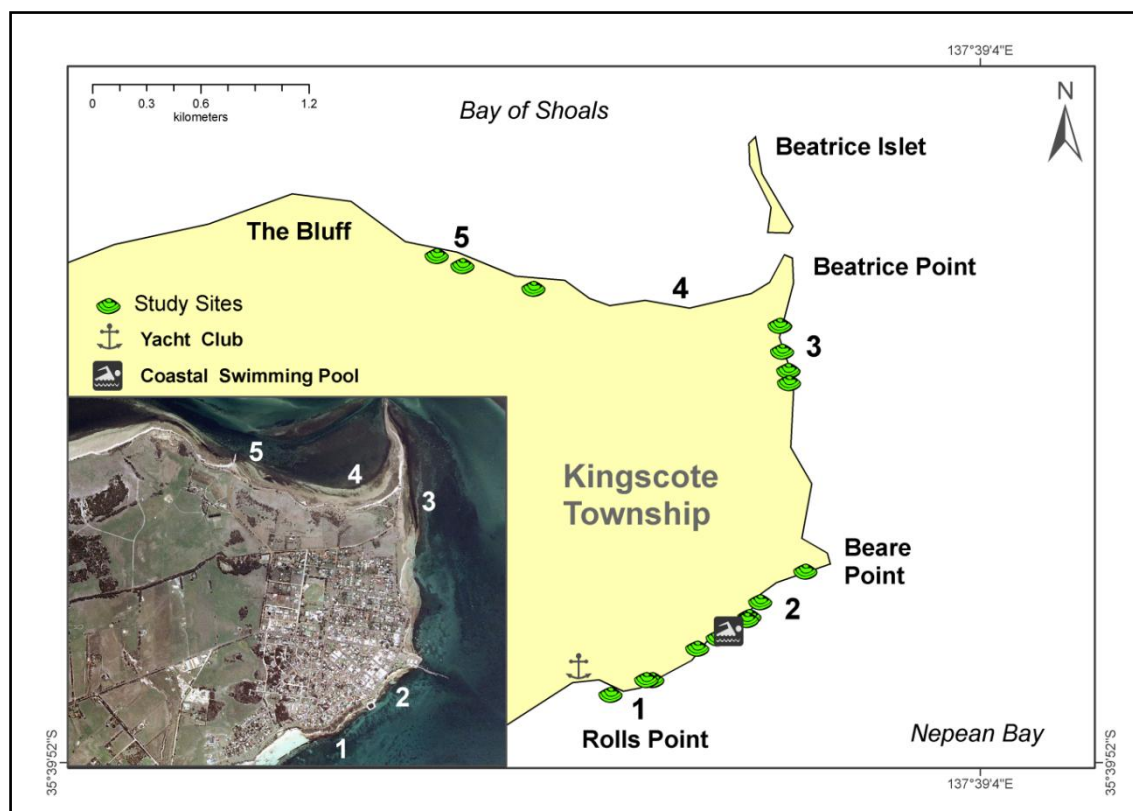


Figure 4.2. Sampling locations at Kingscote. The coastline is divided for descriptive purposes into five subdivisions. Location 1: the southern coastal section centered on Rolls Point. Location 2: Outcrop adjacent to the northern and southern margins of the coastal swimming pool. Location 3: the northeastern cliff section approximately 1.5 km south of Beatrice Point. Location 4: road cuttings along the Bluff to Beatrice Point Road. Location 5: northern carpark. The shingle beach deposit of Milnes *et al.* (1983) is at location 1. Orthophoto (inset) courtesy of the Department of Environment and Heritage, South Australia, 2006.

Table 4.1. Assessed indicators of physical preservation

Taphonomic indicator	Value	Description
Extent of Fragmentation	0	> 90% complete, identifiable to species level
	1	< 90% complete, identifiable to species level
	2	< 90% complete, unidentifiable to species level
	3	< 90% complete, unidentifiable to genus
Degree of Discolouration	0	None, original colour present,
	1	Slight fading of original colour,
	2	Very strong fading of original colour, nearly totally white
	3	White, no original colour visible anywhere,
	4	Lightly discoloured, e.g., light brown, light orange, light grey
Extent of Corrasion (dissolution, abrasion, and recrystallisation)	5	Strongly discoloured, e.g. black, dark grey
	0	None
	1	Beginning of dissolution, and/or slight abrasion
	2	White surfaces, abraded yet retains structural strength
	3	White, strong abrasion of sculpture, minor delamination and/or minor pitting, minor loss of structural strength
	4	Chalky, sculpture gone, strong delamination, substantial loss of structural integrity

4.4. Field observations

4.4.1. Kingscote cobble beach

The cobble beach type section at Rolls Point (Milnes *et al.*, 1983; Location 1, 35.660618° S, 137.633082° E) exists between the Kingscote Yacht Club and the coastal swimming pool on the southeastern coast of Kingscote (Fig. 4.2, 4.3). It overlies gently folded Paleogene Kingscote Limestone. This shingle beach facies consists primarily of sub-rounded to rounded, low to moderate sphericity cobbles of Wisanger Basalt (Jurassic age) within a generally competent, calcretised sandy carbonate matrix. This unit is 1.2 m thick, with modal clast size of 4 – 10 cm, of which approximately 95% is basalt. Basalt clasts of up to 25 cm diameter are present. The remaining 5% consists of limestone and quartz clasts. Limestone blocks of up to 70 cm length occur within the basal portion of this unit. The basal disconformity at this location is approximately 2 m above present sea level, with the cobble unit directly overlying the limestone. The more westerly portion at location 1 is clast-supported, whilst the more easterly sections are matrix-supported.

The shingle blankets the underlying karst, the associated infilled vertical solution pipes and horizontal solution cavities (Fig. 4.3). Flowstone is presently forming on vertical limestone surfaces, and is commonly iron stained (Fig. 4.3, 4.4). The shingle matrix is similarly discoloured. The infilled solution pipes have no such discolouration, indicating they are less permeable, and have formed through different processes. These are capped by horizontal flowstone, visible in thin section as a laminar arrangement of alternating layers of micrite and sparite with similarly arranged quartz grains. For most of the distance between Rolls Point and the coastal swimming pool the most seaward expression of the shingle beach facies and underlying limestone has been removed by erosion and weathering, with the limestone having been weakened significantly by fracture and dissolution. A large section is devoid of shingle.



Figure 4.3. Location1, Rolls Point, 35.660618° S, 137.633082° E. Mollusc shells including an articulated *Katelsia* were recovered from the base of the overhang (line feature). The base of the shingle unit is 2 m apsl. Hammer is 35 cm long.

The basal contact with the underlying Kingscote Limestone at the southern margin to the pool (Location 2, 35.658352° S, 137.638093° E) is approximately +1.8 m above present sea-level, similar to that of Rolls Point (+ 2 m apsl). In contrast, an equivalent shingle exists at between 3.5 - 5 m above present sea-level within the coastal cliffs at the northern side of the coastal swimming pool (location 2, 35.656554° S, 137.64023° E, Figure 4.4). No post- sea-level highstand neotectonic deformation of these cliffs is visible because *in situ* flowstone associated with the shingle masks the fractured and folded Kingscote Limestone. These variations in height at which the shingle unit has been observed must therefore be due to the original altitude of the stranded shoreline and because of geomorphological variations in the pre-existing and underlying limestone.



Figure 4.4. Location 2. 35.656554° S, 137.64023° E. Kingscote Limestone (dipping 24° towards 160°) masked by flowstone. Remnant matrix-supported pebble conglomerate occurs above + 3.6 m apsl (marked by the line). Beneath this is calcarenite with by comparison a larger proportion of angular material and few cobbles.

4.4.2. Location 3, northeastern Kingscote coast

To the south of Beatrice Point (location 3, 35.645061° S, 137.641606° E, Figure 5) a matrix-supported boulder conglomerate overlies calccrete that in turn, overlies cross-bedded and kaolinised Permian fluvialite sediments (see Milnes *et al.*, 1985). Overlying the conglomerate are dune sands with rhizomorphs, and basalt cobbles exist in the upper cliff section. The basal unconformity to the conglomerate is approximately 1 m above mean sea level, and the vertical thickness of this deposit is approximately 4 m in total. At the northernmost extent of the Permian sediments, the highstand deposit is 0.75 m thick. This is overlain in turn by red-brown sand and basalt cobbles. This red-brown sand is the same as that found in road cuttings along the Bluff Road, and is similar to the dune sands overlying this boulder conglomerate. Fossils recovered from this cliff section include a solitary hermatypic scleractinian coral *Goniopora lobata*, the warm water foraminifer *Marginopora vertebralis*, and examples of the foraminifer *Elphidium*.

The coral specimen was recovered (undamaged) from the boulder conglomerate, surprising considering the energy required to move boulders of this size (up to 75 cm diameter). It is unlikely therefore that the coral, nor the enclosing sediment has been transported any

significant distance. The unsorted nature of the conglomerate, with large boulders set in a continuum of angular and rounded grains, clasts and micritic matrix, and evidence for algae and bryozoa in thin section, suggests that this material was deposited over a short period of time, with onshore reworking of sediment during this period. As at locations 1 and 2, the most seaward expression of this sedimentary sequence has not been preserved.



Figure 4.5. Location 3. 35.645061° S, 137.641606° E. Basalt cobble to boulder conglomerate present within, and overlying, calcrete (horizontal arrow) that in turn overlies kaolinised fluvatile sands and silts of Permian age, northeastern Kingscote shoreline, south of Beatrice Point. Dune sands with rhizomorphs overlie the boulder conglomerate. Basalt cobbles (horizontal arrow) occur within the cliff face up to approximately 2-3 m above the unconformity between the conglomerate and underlying units. The coral *Goniopora lobata* was recovered from the circled location.

4.4.3. Bluff Road and northern carpark

At similar heights to the dune sands at location 3, thin lenses of fossils set in a clay and sandy matrix, occur in road cuttings along the Bluff to Beatrice Point Road (Location 4, 35.640970° S, 137.628891° E). In some places these overlie Wisanger Basalt and kaolinised Permian glaciogene sediments. The continuous nature of these fossiliferous sediments, and their relative position with reference to the sediments at locations 3 and 5 suggest that these are *in situ*, and are part of the same stratum. For most of the road's length basalt cobbles are absent. Where they do exist, in the vicinity of the northern the carpark (Location 5, 35.639340° S,

137.641606° E) , the shingle is 2-3 m in height, giving a total height above sea level, in places, of approximately 4 - 5 m. This is consistent with observations at Location 1, 2 and 3. These roadside shell deposits have been previously described as Holocene (Ludbrook, 1984; Milnes *et al.*, 1983). However, the presence of typical Glanville Formation molluscs not found in Holocene sedimentary sequences (Ludbrook, 1984), and recovered from this location points to a last interglacial (MIS 5e) age for these strata. These molluscs include *Callucina lacteola*, *Cassis (Hypocassis) fimbriata*, *Conus (Floraconus) anemone* and *Sinum (Ectosinum) zonale* (Ludbrook, 1984).

Remnant unlithified mollusc- and foraminifer- rich gravel and dune sand overlie calcrete deposited on Triassic fluvial breccia at the carpark, northern coast of Kingscote, (Location 5, Fig. 4.6, 35.63934° S, 137.641606° E). There are no similar deposits to the west of this point. The lower section of these sediments occur at approximately 3 m above present sea-level. These sands have minor amounts of reworked and strongly corroded foraminifera, including *Elphidium* and *Marginopora vertebralis*.

4.4.4. Summary of field and sedimentological evidence

The similar orientation, height above present sea level, presence of an underlying calcrete unit, and unlithified nature of sediments overlying the shingle-conglomerate unit indicate that the boulder conglomerate, dune sands and shingle observed at locations 3, 4 and 5 are of the same sedimentary succession, and are a continuation of the shingle beach facies at Rolls Point. The morphology of this unit is broadly lensoid (Fig. 4.7), with the central section now removed from the easterly portion of the Kingscote coastline by subsequent erosion. At each of the locations studied similar faunal assemblages have been found, and includes warm water species not found at present in this area. The shingle beach and dune succession was the product of onshore reworking of locally derived sediment and biologic material during a previous sea-level highstand. Based on the present-day distribution of the coral *Goniopora lobata*, the presence of the this coral at this location is suggestive of mean sea surface temperatures of 20° C during this highstand phase (Bryant *et al.*, 1992).



Figure 4.6. Location 5, northern carpark, Kingscote. 35.63934° S, 137.641606° E. Shelly gravel and overlying sand with foraminifera *Marginopora vertebralis* and *Elphidium* recovered at this point (arrowed). Calcrete occurs underneath. Approximately 3 m apsl.

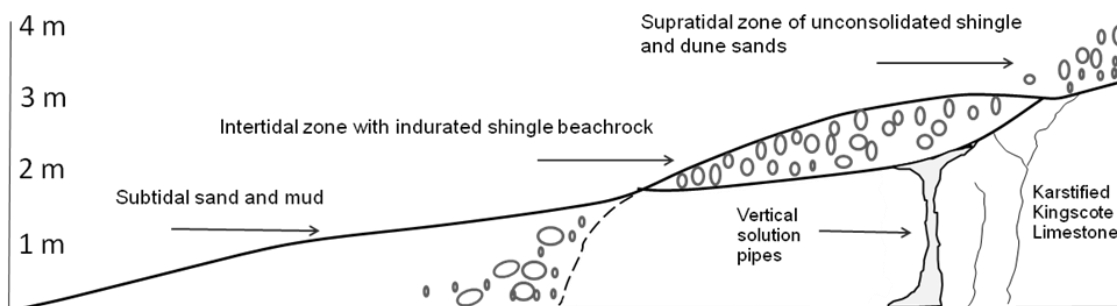


Figure 4.7. Schematic cross section of last interglacial (MIS 5e) shoreline, Kingscote. Competent shingle exists today between approximately 2 and 3 m above mean sea-level. This beachrock must have been formed within the intertidal zone. Unconsolidated shingle and sand found within low-lying cliffs represent the palaeo- supra-tidal zone. The boulder conglomerate at location 3 was emplaced at the base of the present-day cliffs within the subtidal zone.

4.5. Results

4.5.1. Amino acid racemization data

D/L ratio values were obtained from analyses of one articulated bivalve mollusc (*Katelysia*), single valves of *Katelysia*, *Mactra*, and *Anapella cycladea*, and from single foraminifers (*Elphidium* and *Marginopora*). Results are reported for the amino acids aspartic acid (Asx), glutamic acid (Glx), serine (Ser), alanine (Ala), valine (Val) and for the ratio of L-Ser/L-Glx (Tables 1, 2, 3). The latter ratio of L-Ser (peak height) to L-Glx (peak height) is used as an indicator of modern contamination (see Kaufman, 2000, 2006). The relative extent of racemization between amino acids in the bivalves is in general accord with previous studies (Lajoie *et al.*, 1980) with $Asx > Glx > Val$. The coefficient of variation ($CV (\%) = STDV/MEAN*100$) for Asx and Glx show greater consistency than the results for Ser, Ala or Val in either the THAA or HIAA data. However, valine (THAA) has been used with success in studies of Late Quaternary coastal sediments from South Australia (e.g. Murray-Wallace, 1995; Bourman *et al.*, 1999) and therefore AAR age estimates for these molluscs are based on valine D/L results.

THAA D/L values obtained from *Katelysia* recovered from locations 1, 3, 4 and 5 are similar, and therefore suggest a common age. For example, $Asx = 0.563 \pm 0.003$ (location 1), 0.567 ± 0.009 (location 3), 0.621 ± 0.008 (location 4), and 0.578 ± 0.002 (location 5). Similarly, $Val = 0.311 \pm 0.026$, 0.294 ± 0.001 , 0.291 ± 0.041 , and 0.322 ± 0.071 , respectively, for those same samples. Additionally the similarity in THAA D/L values (Table 1) for the bivalve mollusc *Anapella cycladea* from locations 1 and 3 indicate that these shells are of the same age, and therefore the sedimentary units are similar in age. This supports the results from *Katelysia* above.

The mean THAA D/L values for *Katelysia* (Table 3, $Val = 0.296$, $Asx = 0.582$) suggest that these molluscs are older than those recovered from MIS 3 sediments from marine cores in Gulf St Vincent (Cann *et al.*, 1988; Murray-Wallace *et al.*, 1993). These values are similar, but lower, than those of the last interglacial (MIS 5e) Glanville Formation samples from Port Wakefield, Gulf St Vincent and lower than those of the “Older Pleistocene marine beds” of Redcliff, Spencer Gulf, South Australia (Murray-Wallace *et al.*, 1993). This is as expected because the higher mean annual temperature at those locations would result in higher D/L values in similar genera (e.g. Port Wakefield CMAT = $17.0^{\circ}C$, Murray-Wallace *et al.*, 1991). Many of these samples, especially those from Location 4, were recovered from shallow (0-30 cm depth) subsurface environments. It would be expected that such samples would have higher D/L values than those buried since their original deposition to a depth of $\geq 1m$. Samples recovered from locations 1, 2, and 3 were recovered from cliffs that are currently

actively eroding. These samples would likely have been buried continuously since their original deposition. The consistency in D/L values between all of these locations indicate that the samples recovered from along the Bluff Road and from the northern carpark have only recently been subaerially exposed. This probably occurred during road construction.

Results from the HIAA fraction are in accord with those from the THAA fraction, but D/L values are generally higher e. g. Val = 0.359 ± 0.05 (Table 2). This is as expected for intracrystalline amino acid values as the intracrystalline amino acid pool consists of free and peptide-bound amino acids enclosed within single crystallites of calcium carbonate isolated from chemical degradation such as by strong oxidation (Stathoplos & Hare, 1993; Sykes *et al.*, 1995). Free amino acids generally have a higher extent of racemization than peptide bound amino acids and the D/L values obtained on the intracrystalline fraction are the integrated results of these two components. D/L values of intra-crystalline amino acids would therefore be expected to be higher than for the intercrystalline amino acid pool, which is open to leaching and other modifications, and this is what was observed in this study. The general concordance between results from the total and intracrystalline amino acid fractions for *Katelsia* suggest that these results are reliable. Coefficients of variation (CV) for Asx and Glx were higher in HIAA samples than for THAA results. Conversely, CVs for Ser, Ala Val and contaminant index were lower in the intracrystalline data than for the THAA results.

Mean D/L values from the analyses of single *Elphidium* have also demonstrated the age equivalence of the stranded shoreline sediments from the northern and northeastern outcrops with, for example, mean glutamic acid D/L values (THAA) of 0.350 ± 0.054 (Location 3) and 0.330 ± 0.046 (Location 5, Table 1). Valine D/L values from the above study sites are 0.290 ± 0.048 and 0.240 ± 0.008 respectively. These data suggest an age equivalence for the non-indurated sand at these two locations. Mean valine D/L values from individual *Marginopora vertebralis* ($n = 3$) (Table 4.2) recovered from the boulder conglomerate at Location 3 are 0.245 ± 0.194 , and for glutamic these are 0.249 ± 0.014 .

4.5.2. Summary of AAR data

Analyses of the THAA, and HIAA fractions from bivalve molluscs and single foraminifers indicate that the individually preserved shingle-conglomerate units are of the same aminostratigraphic age. The mean valine D/L ratio from *Katelsia* of $0.296, \pm 0.050$ (Table 3) fits the regional trend based on comparisons of CMAT with D/L ratio (Fig. 8). Comparison of these results with the regional data comprising mean D/L values for valine from bivalve molluscs *Anadara trapezia* and *Katelsia* (Murray-Wallace, 1995), this dataset points to a last interglacial (MIS 5e) age for this unit. The range of uncertainty of these data is

not significantly greater than that of the analytical errors produced from comparisons of D/L values between shells of a single genus during laboratory studies, and indicates that there has not been reworking of pre-existing older molluscs into this unit. Exposure of material at locations 4 and 5 is very recent.

Table 4.2. Amino acid racemization D/L ratio results for the Hydrolysable Intracrystalline Amino Acid pool in bivalve molluscs from Kingscote.

Location	Genus	Asx D/L ratio	Glx D/L ratio	Ser D/L ratio	Ala D/L ratio	Val D/L ratio	L-Ser/L- Glx
1 Live collected	<i>Katelysia sp</i> (n = 2)	0.093 ± 0.016	0.036 ± 0.002	0.067 ± 0.023	0.085 ± 0.134	0.013 ± 0.001	1.269 ± 0.098
3 Holocene Beach Ridge	<i>Katelysia sp</i> (n = 7)	0.158 ± 0.009	0.077 ± 0.015	0.326 ± 0.101	0.095 ± 0.002	0.039 ± 0.015	0.800 ± 0.050
1 Cobble beach facies	<i>Katelysia sp</i> (n = 2)	0.563 ± 0.003	0.375 ± 0.021	0.596 ± 0.078	0.736 ± 0.009	0.311 ± 0.026	0.106 ± 0.013
1 Cobble beach facies	<i>Annapella cycladea</i> (n = 2)	0.643 ± 0.009	0.512 ± 0.066	0.111 ± 0.045	0.828 ± 0.004	0.464 ± 0.011	0.282 ± 0.146
3 Northeastern outcrop	<i>Katelysia sp</i> (n = 2)	0.567 ± 0.009	0.364 ± 0.007	0.319 ± 0.022	0.726 ± 0.006	0.294 ± 0.001	0.220 ± 0.015
3 Northeastern outcrop	<i>Annapella cycladea</i> (n = 1)	0.628	0.537	0.298	0.852	0.447	0.091
3 Northeastern outcrop	<i>Elphidium sp</i> (n = 8)	0.621 ± 0.064	0.347 ± 0.054	0.270 ± 0.109	0.583 ± 0.065	0.288 ± 0.048	0.226 ± 0.119
3 Northeastern outcrop	<i>Marginopora Vertebris</i> (n = 3)	0.429 ± 0.012	0.249 ± 0.014	0.364 ± 0.043	0.413 ± 0.121	0.245 ± 0.194	0.270 ± 0.035
4 Bluff Road	<i>Katelysia sp</i> (n = 5)	0.621 ± 0.008	0.406 ± 0.030	0.258 ± 0.068	0.611 ± 0.306	0.291 ± 0.041	0.251 ± 0.119
5 Northern outcrop	<i>Katelysia sp</i> (n = 6)	0.578 ± 0.002	0.415 ± 0.054	0.396 ± 0.082	0.770 ± 0.069	0.322 ± 0.071	0.179 ± 0.046
5 Northern outcrop	<i>Elphidium sp</i> (n = 2)	0.579 ± 0.023	0.332 ± 0.046	0.239 ± 0.023	0.564 ± 0.085	0.244 ± 0.008	0.264 ± 0.073

Table 4.3. Mean D/L ratio results for the total hydrolysable and hydrolysable intracrystalline amino acid fraction for all *Katelsysia*, Kingscote, Kangaroo Island.

Location	Genus	Asx D/L ratio	Glx D/L ratio	Ser D/L ratio	Ala D/L ratio	Val D/L ratio	L-Ser/L- Glx
1 Live collected	<i>Katelsysia sp</i> (n = 3)	0.113 ± 0.012	0.061 ± 0.013	0.181 ± 0.006	0.088 ± 0.044	0.050 ± 0.017	0.727 ± 0.069
1 Cobble beach facies	<i>Katelsysia sp</i> (n = 1)	0.567 ± 0.016	0.341 ± 0.007	0.680 ± 0.027	0.702 ± 0.009	0.273 ± 0.003	0.106 ± 0.062
1 Cobble beach facies	<i>Mactra pura</i> (n=3)	0.509 ± 0.018	0.429 ± 0.054	0.383 ± 0.015	0.770 ± 0.039	0.462 ± 0.053	0.128 ± 0.028
2 Cobble beach facies	<i>Mactra rufescens</i> (n = 2)	0.578 ± 0.015	0.424 ± 0.008	0.379 ± 0.048	0.765 ± 0.028	0.456 ± 0.076	0.160 ± 0.001
3 Northeastern outcrop	<i>Katelsysia sp</i> (n = 8)	0.595 ± 0.031	0.397 ± 0.037	0.444 ± 0.117	0.743 ± 0.025	0.354 ± 0.037	0.122 ± 0.027
3 Northeastern outcrop	<i>Mactra notospisula trigonella</i> (n = 1)	0.624 ± 0.016	0.567 ± 0.007	0.333 ± 0.027	0.873 ± 0.009	0.489 ± 0.003	0.128 ± 0.062
4 Bluff Road	<i>Katelsysia sp</i> (n = 1)	0.782 ± 0.016	0.515 ± 0.007	0.264 ± 0.027	0.388 ± 0.009	0.415 ± 0.003	0.212 ± 0.062
5 Northern outcrop	<i>Katelsysia sp</i> (n = 9)	0.591 ± 0.021	0.403 ± 0.032	0.555 ± 0.044	0.758 ± 0.048	0.366 ± 0.038	0.109 ± 0.019

Table 4.4. Mean D/L values for all *Katelsysia*, using the total hydrolysable, and hydrolysable intracrystalline amino acids.

	Asx D/L ratio	Glx D/L ratio	Ser D/L ratio	Ala D/L ratio	Val D/L ratio	L-Ser/L-Glx
<i>All Katelsysia sp</i>						
THAA (n = 15)	0.582 ± 0.044	0.387 ± 0.041	0.385 ± 0.120	0.711 ± 0.140	0.296 ± 0.050	0.191 ± 0.072
<i>All Katelsysia sp</i>						
HIAA (n = 21)	0.600 ± 0.048	0.403 ± 0.042	0.503 ± 0.113	0.735 ± 0.088	0.359 ± 0.040	0.121 ± 0.031

4.6. Uranium series dating

The single small (10 cm diameter) coral specimen, *Goniopora lobata* (Fig. 4.8a), recovered from the boulder conglomerate at Location 3 (Fig. 4.5) was relatively well preserved, though minor discolouration was evident. Alteration of the exposed surface, probably by meteoric water, was visible. Calcite content was 1.6%, evaluated by XRD. An open-system age of 111 ± 1 ka was obtained, using an initial $\delta^{234}\text{U}$ value of 147 ‰. (Table 4.5). A corresponding conventional $^{234}\text{U}/^{230}\text{Th}$ age of 122 ± 1 ka was obtained. Because of the close agreement of the open and closed system ages, differing by only 11 ka, and good preservation, these ages are regarded as an acceptable guide to the real age. However, the initial $\delta^{234}\text{U}$ value of 174 ± 2 is significantly higher than that of modern coral from the Huon Peninsula ($148\text{--}149 \pm 2$) and Great Barrier Reef (149 ± 1 ; Stirling et al., 1998), though within the upper range of values reported by Stirling et al. (1998) from the Carnarvon and Perth Basins. Furthermore, the ^{232}Th value of 109.4 ppb for this coral is high, violating the assumption (i.e. model) of Thompson *et al.* (2003), and therefore invalidates the open-system age of 111 ± 1 ka. The real age of the specimen may be nearer to 122 ± 1 ka. This is the age used here.

Table 4.5. Results from U-series analyses of the coral *Goniopora lobata*

^{232}Th (ppb)	U (ppm)	$(^{230}\text{Th}/^{232}\text{Th})$	$(^{234}\text{U}/^{238}\text{U})$	$(^{230}\text{Th}/^{238}\text{U})$	Open- system ^{230}Th age	Conventional ^{230}Th Age (ka)	Initial $\delta^{234}\text{U}$
109.4 ± 1.2	3.7167 ± 0.0031	79.55	1.1233 ± 0.0017	0.7701 ± 0.0025	111 ± 1	122 ± 1	174 ± 2

4.7. Fossil preservation

Based on preservation of the sampled shells, three groups of shells are distinguishable. These are; 1) very well preserved shells without encrusting carbonate, and include articulated shells live at the time of collection (*Katelsia*), and valves from modern (Holocene) shoreface environments, 2) carbonate encrusted shells that have slight fading of original colour and occasionally display moderate abrasion of umbone regions (Fig.4.8d, e), and 3) fragments of strongly abraded shells that have no original colour and are almost white, commonly with remnant sedimentary encrustation. These encrusted and abraded shells were all associated with the raised shingle and associated sediments of Locations 1, 2, 3, 4 and 5. The latter group, being strongly abraded, were not analysed for AAR because their degradation may have led to diffusive loss of indigenous amino acids, and thus have resulted in substantially lowered D/L values than those better preserved of similar age.

Many of the *Elphidium* foraminifers, recovered from unconsolidated sand and gravel, were incomplete (Fig. 4.8b, c), discoloured grey and black, and several had single root holes. Most of the discolouration occurred at the location of these holes. Samples of *Marginopora* (Fig. 4.8f) whether recovered from unconsolidated sand at Location 5 or from the boulder conglomerate at Location 3 were on the other hand, generally in good condition, though had very rounded margins.

Contaminant indices (Table 4.1, 4.2, Fig. 4.9) were used to assess the extent to which non-indigenous amino acids may have been incorporated into the biomineralised structure during diagenetic processes. L-serine (peak height) is used as the contaminant indicator species. Its concentration is compared with L-glutamic acid (peak height), because during diagenesis serine quickly breaks down and may be preferentially altered to glycine and alanine during diagenesis (Akiyama, 1980). *Katelsysia* shells live at the time of collection had the highest contamination values (L-Ser/L-Glx = 1.4, THAA), whilst the lowest contamination values were those of the *Katelsysia* samples recovered from location 1 (L-Ser/L-Glx = 0.1, THAA). This is as expected for the total amino acid pool because modern shells tend to have much greater concentrations of serine over that of older examples, having not undergone significant diagenetic alteration, or leaching. One last interglacial (MIS 5e) age *Katelsysia* valve from location 3 had an anomalously high contaminant index of 0.725, a low valine D/L ratio of 0.198 (THAA), and corresponding low serine D/L of 0.18 (THAA), - substantially lower than the mean obtained for the other last interglacial (MIS 5e) *Katelsysia* samples (approximately 0.5). This shell had a moderately high mean taphonomic value of 0.5. In contrast, contaminant indices for the samples analysed for the HIAA fraction were lower in all cases (Fig. 4.9) and no aberrant D/L ratio values were noted. There is a tighter grouping of valine D/L values in results from the intra-crystalline amino acids over that of the total hydrolysable amino acid pool.

4.8. Discussion

4.8.1. AAR results

Aragonitic molluscs have been the most common subject for AAR investigations utilising the THAA fraction in southern Australian studies. There is no previous work detailing results from the analyses of intracrystalline molluscan D/L values from these locations, therefore the results from this study are discussed using the THAA data presented here. However, lower contamination indices and generally higher D/L values in the HIAA fractions from the genera utilised here are in accord with previous claims for the intra-crystalline amino acid pool (e.g.

Penkman *et al.*, 2007). The concordance between the results from the intra- and inter-crystalline amino acid fractions in *Katelsysia* point to their reliability.

A mean THAA valine D/L value of 0.303 ± 0.02 ($n = 15$) from *Katelsysia* sp. indicates a correlation with marine isotopic substage 5e age for the stranded cobble beach facies at Kingscote, Kangaroo Island, based on comparison with results from previous studies southern Australia (e.g. Belperio *et al.*, 1995). This ratio is slightly high for this CMAT (15.4°C; Fig. 10), but is likely related to shallow burial depth and the warmer temperatures experienced at Kingscote when compared with other locations on Kangaroo Island. The uranium-series dating of the coral *Goniopora lobata*, and the presence of typical Glanville Formation fauna including *Marginopora vertebralis*, recovered from the stranded shoreline at Kingscote, provide unambiguous evidence for a previous sea level highstand associated with the last interglacial (MIS 5e) period (MIS 5e) independent of the AAR data. This last interglacial (MIS 5e) faunal assemblage contains fauna from sandy and rocky, intertidal and subtidal habitats.

There are no previously published results from AAR analyses on individual *Elphidium*, nor for single *Marginopora vertebralis*, and less is known about the rates and extent of racemization in foraminifera than for molluscs (Murray-Wallace and Belperio, 1994). A range of preservation states were noted for individual *Elphidium*, none of which were perfectly preserved (Fig. 8b, c). This variation most likely resulted in leaching of the more racemised amino acids in several of these individuals, thereby lowering the apparent D/L values by removing the more highly racemised free amino acids. Yet, the range of uncertainties (to one standard deviation) for this genus at Kingscote is not greater than for the molluscs analysed (Table 1). It is noteworthy that the extent of racemization for *Elphidium* and *Katelsysia* appear broadly similar based on their mean values (Fig. 11).

Results from AAR analyses of individual *Marginopora* indicate a slower rate of racemization for this foraminifer than for *Elphidium* or for the mollusc genera *Katelsysia*, *Annapella* and *Mactra*. D/L values for individual *Marginopora* are, however, similar (e.g. UWGA 7238c, having the lowest D/L values for *Marginopora* in this study, Asx = 0.421 Glx = 0.253 Ser = 0.317 Ala = 0.297 Val = 0.116), though slightly higher than those presented by Murray-Wallace and Belperio (1994, their table 2, row 1, recovered from Glanville Formation sediments) who used approximately 50 individuals per single sample for gas chromatography. This is perhaps in part the result of differing preparatory methods and may reflect contrasts in measurement between GC and HPLC (see Murray-Wallace *et al.*, 2010 for comparison of D/L values from whole-rock samples in southern Australia). Those samples used by Murray-Wallace and Belperio (1994) were etched with 1M HCl to remove the altered and perhaps contaminated exterior portion of foraminifers. In contrast, the individual foraminifers used

here were not etched because of their size, but were instead bleached for 1 h with 12.5% NaOCl.

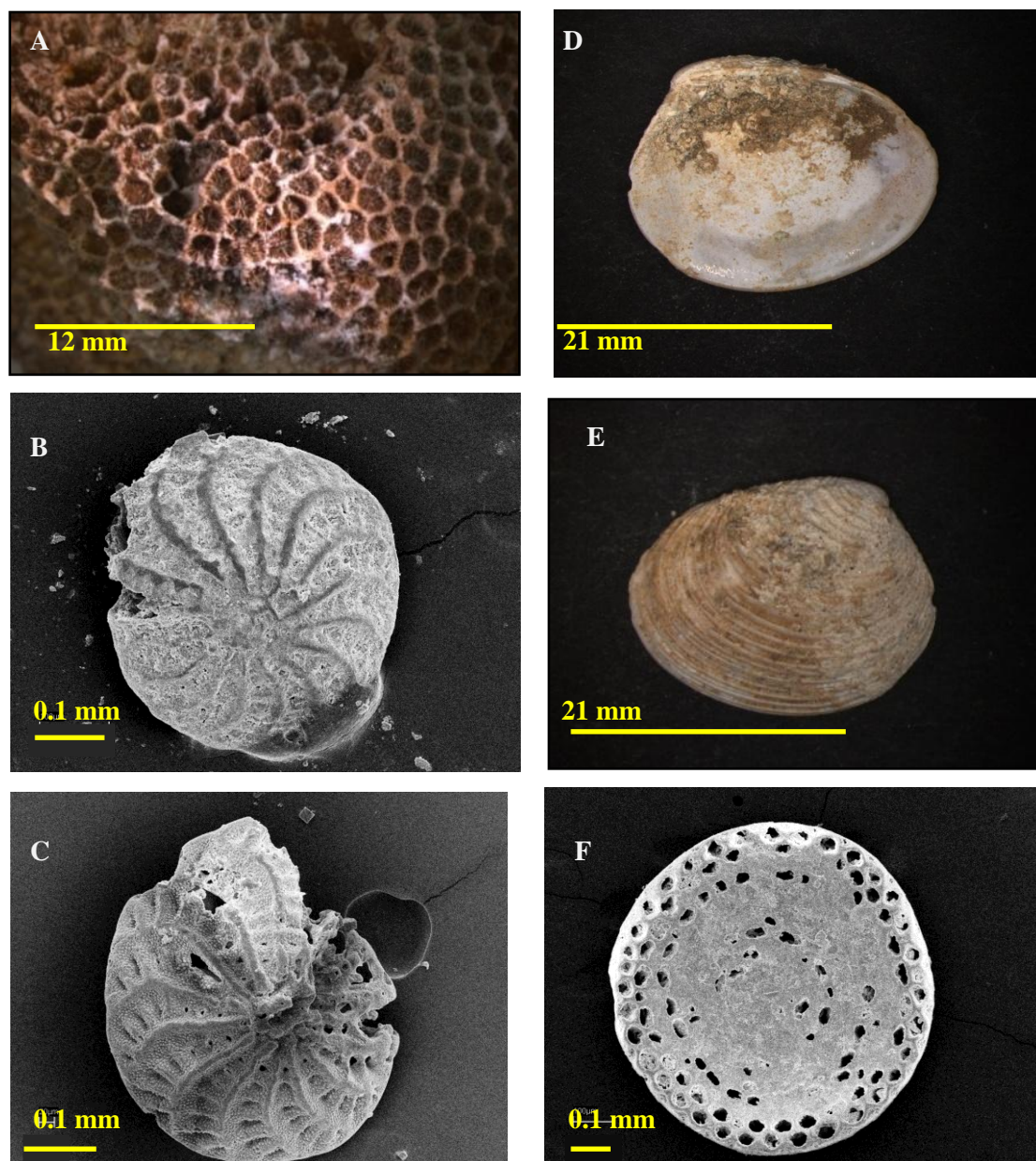


Figure 4.8. Representative examples of taphonomic variation in samples recovered from the raised beach facies, Kingscote, Kangaroo Island. 1. Moderately well preserved *Goniopora lobata*, location 3, 1.5 km south of Beatrice Point, with clay infilled corralites, 2, 3, Examples of *Elphidium* from location 3. 4, 5, *Kataysia scalarina* with carbonate encrustation from the Bluff coastal road. 6. *Marginopora vertebralis*, recovered from location 5, northern carpark.

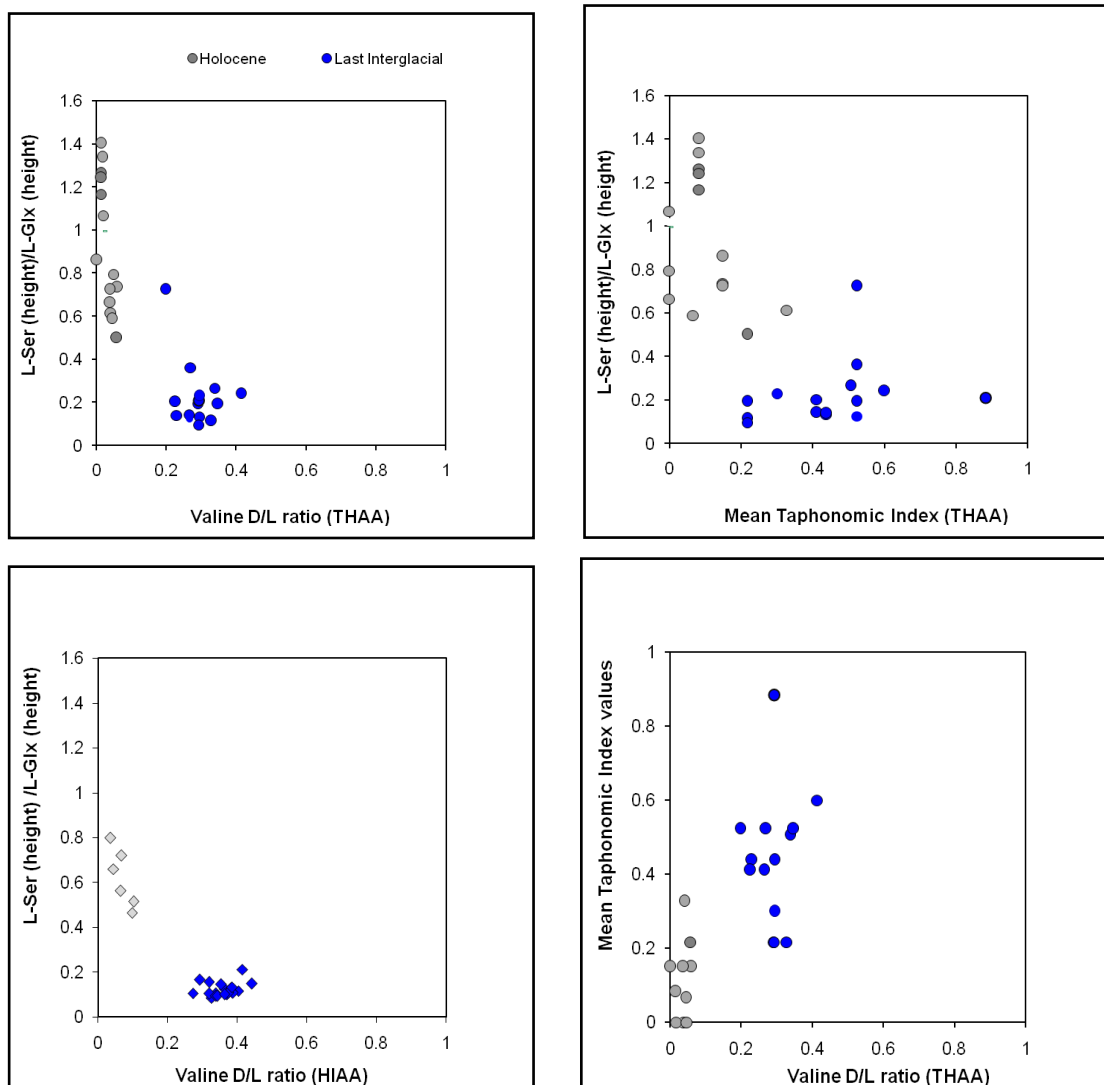


Figure 4.9. Scatter plots of contamination indices, mean taphonomic values and valine D/L values for the total hydrolysable amino acid results. For comparison valine D/L ratio results from the hydrolysable intracrystalline amino acid pool are plotted against the ratio of L-Ser/L-Glx. Note the tighter clustering of data for this latter example compared with that of the THAA results.

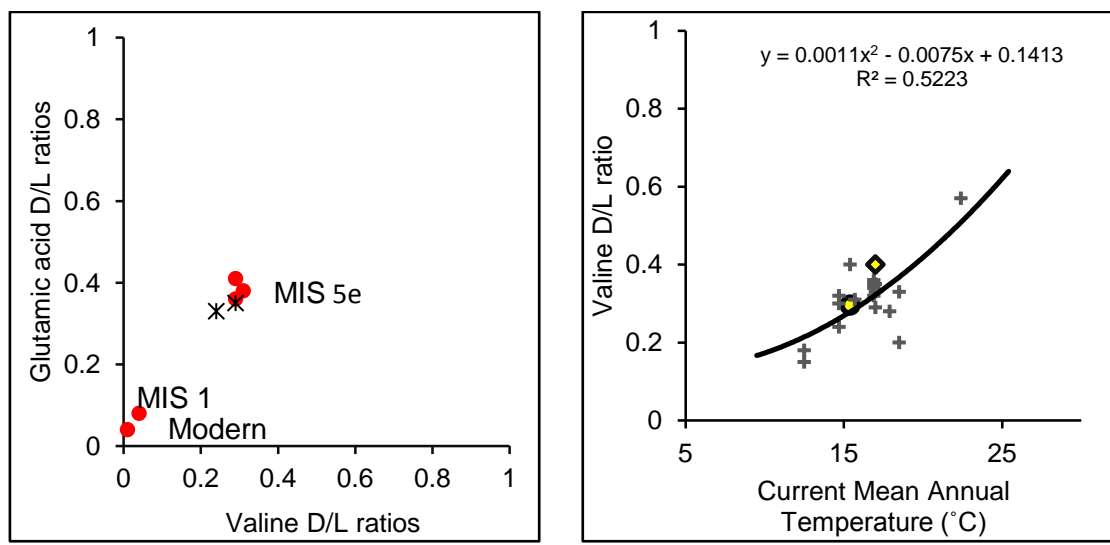


Figure 4.10. a) Mean valine vs glutamic acid D/L values using the THAA fraction, for *Katelsysia* and *Elphidium* (filled red circles) samples recovered from the last interglacial (MIS 5e) sediments at Kingscote, Kangaroo Island. b) CMAT vs valine D/L values for south Australian molluscs *Katelsysia* and *Anadara trapezia* (crosses, Murray-Wallace, 1995) compared to the mean *Katelsysia* D/L from Kingscote (circle, this study), and from a single *Katelsysia* sample from the last interglacial (MIS 5e) site at Port Wakefield, Gulf St Vincent (diamond, this study). The curve was obtained on the data from Murray-Wallace (1995).

4.8.2. Palaeo- Sea-levels

The height of the last interglacial (MIS 5e) sea-level at Kingscote cannot be precisely inferred from the elevation of the stranded shoreline deposits because sections of this stratum are missing, having been removed by cliff erosion, a process continuing today. However, the height of the base of the shingle at Rolls Point is suggestive of a mean sea level height approximately 2.5 m above present values, and this is also suggested by evidence from the northern Kingscote locations (Locations 3, 4, 5). There is no evidence of neotectonic displacement between these sections of coast, suggesting that the height of the indurated shingle is related to the palaeo- wave-climate. Given this, a mean sea-level height of approximately 2.5 m above present sea-level (APSL) appears reasonable (Fig. 4.11). The sea-level heights inferred here are similar to, but less precisely defined, than those of tectonically stable Eyre Peninsula where the terrestrial feather-edge of last interglacial (MIS 5e) age intertidal (back-barrier lagoonal) sediments crop out for over 500 km at a height of + 2 m APSL (Murray-Wallace and Belperio, 1991). This appears to limit the field of neo-tectonic deformation within the southern Gulf St Vincent region to southern Fleurieu Peninsula and surrounds. However, further work on Kangaroo Island to the east of Kingscote is required to confirm this.

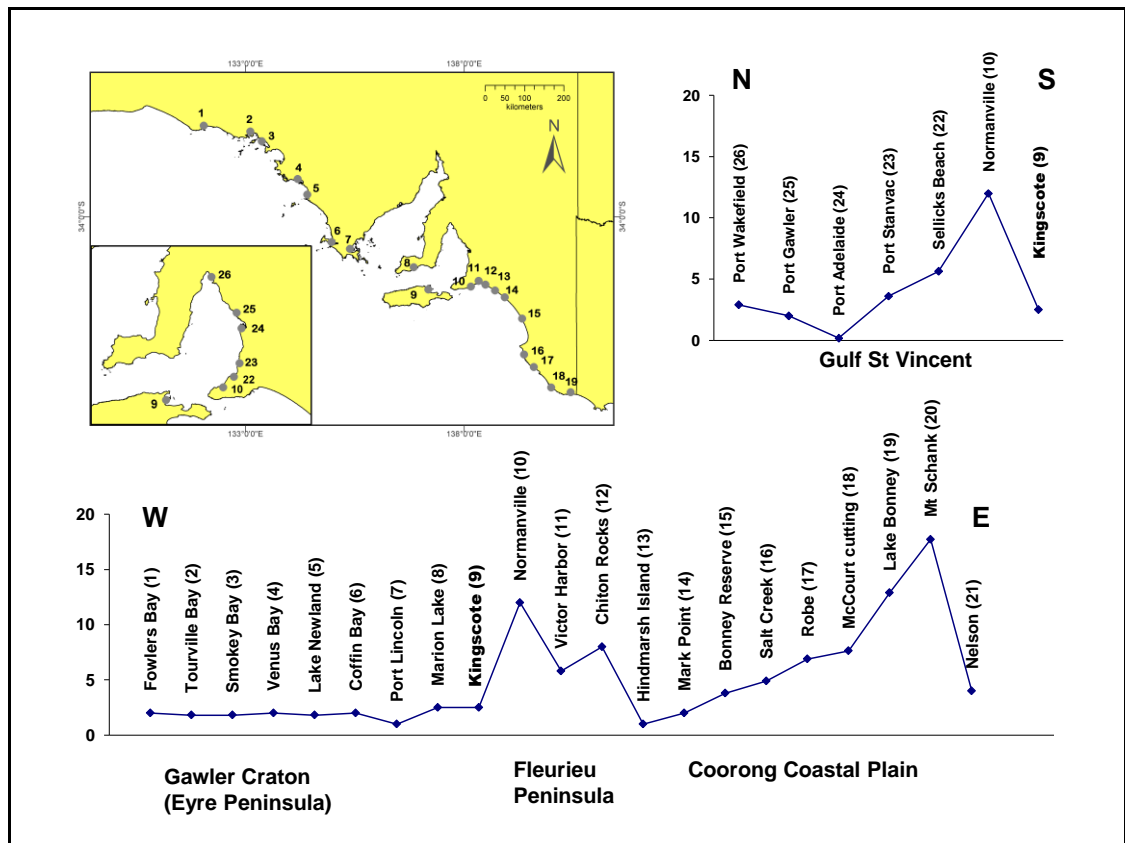


Figure 4.11. Last interglacial (MIS 5e) sea-level heights for South Australia (adapted and modified from Murray-Wallace, 2002) including that inferred here for Kingscote, Kangaroo Island. Within the Gulf St Vincent region the area centred on Port Adelaide is subsiding (Belperio *et al.*, 2002) whilst up to 12 m of uplift has occurred over the past 122 ka on the Fleurieu Peninsula (Bourman *et al.*, 1999).

4.7.3. Sea surface temperatures, the Leeuwin current, and palaeoenvironments

Higher ambient temperatures than at present are indicated for the MIS 5e interval at Kingscote by the presence of last interglacial (MIS 5e) mollusc species typical of warmer coastal waters in South Australia, and found today for example in the upper reaches of Gulf St Vincent, Spencer Gulf and at Fowlers Bay (see Ludbrook, 1984). These include *Conus (Floraconus) anemone*, *Cassis (Hypocassis) fimbriata*, *Sinum (Ectosinum) zonale* and *Bittum (Sembittum) granarium*. The Kingscote assemblage is broadly similar to those currently found in, for example, northern Spencer Gulf, South Australia (Ainslie *et al.*, 1989). A similar conclusion for higher sea surface temperatures at Kingscote can be inferred from the presence of the sub-tropical foraminifer, *Marginopora vertebralis* (Köhler-Rink and Kühl, 2000), and the sub-tropical coral, *Goniopora lobata* (Veron 1986).

The single coral specimen, a scleractinian Poritid coral, *Goniopora lobata*, found at Kingscote is a shallow water (intertidal to 6 m water depth), occasionally lagoonal, coral

(Veron & Marsh, 1988) and tends to grow to the exclusion of other corals, on reef faces in turbid water protected from strong wave action (Bryant *et al.*, 1992; Veron 1986; Veron & Marsh, 1988). *Goniopora lobata*, typically inhabits higher energy shallow environments in sub-tropical to tropical conditions. The current southern limit of this species offshore is Dirk Hartog Island, Western Australia (26° S), and Elizabeth Reef, Eastern Australia (29°55' S). Onshore it has been found on the northern New South Wales coast at Wilgoolga and Tree Point (Bryant *et al.*, 1992), and in Freycinet Reach, Shark Bay (O'Leary *et al.*, 2007). A minimum monthly average water temperature for the northern New South Wales locations (Bryant *et al.*, 1992) is 20°C, similar to that at Shark Bay.

This suggests that the mean sea-surface temperature during the last interglacial (MIS 5e) at Kingscote was significantly higher than at present, and implies that this region may have experienced the trailing edge effects of the Leeuwin Current at that time.

Determining the sea-surface temperature for the nearshore water regions such as at Kingscote is problematic because of the effect of thermal radiation from the land on satellite infrared imagery (CSIRO Marine and Atmospheric Research – Remote Sensing Facility staff). Mean yearly SST for Kingscote is 18.09°C averaged over 2 years, within a 1° radius of Kingscote (Directorate of Oceanography and Meteorology, Australia). Data from CSIRO for the years 1990 to 2002 indicates a mean SST of 16.7 to 17.2°C for the coastal waters around Kangaroo Island (CSIRO Marine and Atmospheric Research – Remote Sensing Facility).

Based on the faunal evidence presented here, approximate present day sea surface temperatures, and the present geographical range of *Goniopora lobata*, a minimum increase in mean annual sea surface temperatures of 2-3°C over present-day values would have allowed this species of coral and the foraminifer *Marginopora vertebralis* to live at Kingscote. This estimate is slightly higher, but in the same range as previous studies (e.g. + 2°C Murray-Wallace *et al.*, 2000).

A southwards expansion of warmer upper and central Gulf St. Vincent waters into the Kingscote region during the last interglacial (MIS 5e) would have enabled coral growth by raising SST's. However, coral seeding could only have occurred with the assistance of warm currents. An enhanced Leeuwin Current, a warm tropically sourced current that flows south along the western Australian coast, would have provided the transport mechanism. This may have also assisted for example, in the colonisation of Vivonne Bay on the southern Kangaroo Island coast by *Anadara trapezia*. Furthermore, additional hermatypic coral fragments have been found at Vivonne Bay on the south coast of Kangaroo Island (this study). This evidence, along with previous reports of *Anadara trapezia* at this location (Ludbrook, 1984), is additionally suggestive of warmer water existing on the southern coastline of Kangaroo Island at that time. The coral age of 122 ± 1 ka places the approximate timing of coral growth at

Kingscote at or near the termination of the major period of reef growth in Western Australia during the last interglacial (MIS 5e) (Stirling et al., 1998). This appears to have been the period when the Leeuwin Current had its maximum influence on the southern Australian coastal environments given the presence of coral on Kangaroo Island coasts. At the present time the Leeuwin Current is warmest when the West Pacific Warm Pool is also at its warmest (McCullough and Esat, 2000). This suggests that the presence of *Goniopora lobata* at Kingscote may be directly related to higher global SST's during the last interglacial (MIS 5e) and larger volumes of warm water distributed out of the West Pacific Warm Pool. It appears highly likely that these temperatures may have resulted in large-scale shifts in biogeographic provinces (in this case, coral) southward due to those higher temperatures. Coral reefs have extended beyond their current latitudinal limits during the Holocene and in previous interglacials (Woodroffe et al., 2010). The presence of last interglacial (MIS 5e) *Goniopora lobata* at Kingscote, the result of an enhanced Leeuwin current driven by higher global sea temperatures suggests that a southward reef expansion may occur due to higher sea surface temperatures around Australia (Woodroffe et al., 2010), higher temperatures which will be the result of current anthropogenic forcing of climate.

4.9. Chapter summary

A shingle to boulder conglomerate of Last interglacial (MIS 5e) age (122 ± 1 ka) was deposited at Kingscote, Kangaroo Island, at a similar height (+ 2-3 m) above present sea level as the regional MIS 5e datum on Eyre Peninsula (+ 2 m above sea level), during an interval in which environmental conditions were warmer and more humid than at present.

During the Last interglacial (MIS 5e) an enhanced Leeuwin current and an expansion of warm central and upper Gulf St Vincent waters (less saline than at present because of increased precipitation compared with today), into the Kingscote coastal region enabled colonisation by a number of warmer-water species including, *Marginopora vertebralis* and *Goniopora lobata*. The presence of coral within last interglacial (MIS 5e) outcrops on the southern and northern coast of Kangaroo Island and an open seaway through Pelican Lagoon are suggestive of less restricted interaction between Gulf St Vincent and the open coastal areas of southern Australia during the latter stages of the last interglacial (MIS 5e) than that occurring at the present-day.

ACKNOWLEDGEMENTS

Financial support for fieldwork was from an Australian Research Council Discovery grant (DP0558042) to Colin Murray-Wallace. Gilbert Price dated the coral at the University of Queensland. Assoc Prof. Brian Jones provided useful comments. Heidi Brown assisted with

obtaining spatial data. I am grateful also to David Griffin, Chris Rathbone and Glen Smith, Centre for Marine and Atmospheric Research, CSIRO, Hobart for discussions and assistance with SST data.

Chapter 5

Amino acid racemization dating of single *Elphidium*, Gulf St Vincent, South Australia: preservation and age-mixing in a shallow semi-enclosed temperate carbonate basin

5.1. Outline

This project set out to determine the aminostratigraphic relationships among sedimentary strata in Late Quaternary Gulf St Vincent, South Australia. Previous work had recognised and determined the age of a last interstadial unit in cores from the central basin, but the age and hypothesised water-level for Gulf St Vincent contrasted with, for example, the sea-level record from Huon Peninsula, Papua New Guinea.

This study focused on the use of single foraminifers, *Elphidium* sp, as aminostratigraphic tools. Samples from several cores were used to determine the spatial extent of last interstadial age *Elphidium* tests in this shallow semi-enclosed basin. Observations are made on the extent of reworking of bioclasts, and the reliability of using modern foraminifer samples for deducing palaeo-environmental conditions such as sea-level are discussed.

5.2. Introduction

The amino acid racemization (AAR) geochronological method has become a useful tool for identifying reworked fossils in marine environments (Goodfriend, 1989 ; Murray-Wallace and Belperio, 1994; Wehmiller *et al.*, 1995; Goodfriend and Stanley, 1996; Murray-Wallace *et al.*, 1996; Kowalweski *et al.*, 1998; Carroll, 2001; Barbour Wood, *et al.*, 2003). Until recently these studies have predominantly employed bivalve molluscs as the subject matter because using the technology available, an initial mass of 1-2 g of shell was required to yield sufficient concentrations of amino acids from fossils. A lesser number of studies used large numbers of individual foraminifer tests within a single sample for aminostratigraphic purposes (Cann and Murray-Wallace, 1986). With the development of the most recent reverse-phase high performance liquid chromatography (RP HPLC) system (Agilent 1100) and an injection volume of as little as 2µL (Kaufman and Manley, 1998), it has become possible to assign ages to individual foraminifera (Hearty *et al.*, 2004; Kaufman, 2006) and ostracods (Kaufman, 2000, 2005) from ¹⁴C or U-series calibration of amino acid D/L values (Clarke and Murray-Wallace, 2006).

Many studies on foraminifera have relied on bulk samples consisting of hundreds to thousands of individual tests to obtain data for palaeoenvironmental reconstructions. However, foraminifera populations in surface sediments may become enriched by sorting, diluted by transport and dissolution and/or mixed by biologic and physical processes. Thus strata in shallow coastal environments, and their associated microfossils, may become homogenized over the duration of their formation (Berkeley *et al.*, 2007). Such samples are therefore invariably time-averaged populations where the age of individual elements may be effectively ignored but this really is a question of magnitude and scale. To understand these records at fine scales of resolution the ages of individual foraminifera must be taken into account. The advantage of employing calcareous foraminifera is that they are composed of stable calcite, in contrast to for example bivalve molluscs which quite often are completely composed of metastable aragonite and perhaps less likely to be as well preserved over long timescales. While some recent AAR studies have utilized brachiopods or gastropod opercula (both calcite) in chronological studies, (Walton and Curry, 1994; Walton, 1998; Parfitt *et al.*, 2005; Penkman *et al.*, 2007, 2008) calcareous foraminifera from shallow marine environments have received little attention until recently.

The late Quaternary sediments of semi-enclosed Gulf St Vincent (Fig. 5.1) have been the subject of several studies aimed at investigating changes in sea level primarily attributed to eustatic oscillations over last interglacial (MIS 5e) to Holocene time-scales (Cann *et al.*, 1988, 1993; Murray-Wallace *et al.*, 1993). Being in the far field of glacial influence, this region was neither affected by glacio-isostatic adjustment nor by glacial sediments, and therefore provides a record of sedimentation for the late Quaternary that is only affected by neotectonics (e.g. Sandiford, 2002; Murray-Wallace, 2002) and hydroisostasy in the upper reaches (Belperio *et al.*, 2002) with hydroisostatic adjustment occurring after the Holocene transgression (Belperio *et al.*, 2002). The spatial and environmental variability of foraminiferal assemblages within the modern sediments of Gulf St Vincent have been used to elucidate palaeo-environmental change, and inferred from Holocene and late Pleistocene sediments (Cann *et al.*, 1988, 1993; Murray-Wallace *et al.*, 1993).

Previously, attempts were made to compare variations in water depth in the Gulf during marine isotope stage 3 to estimates of sea level recorded in sections of the uplifted coral record of Huon Peninsula (Cann *et al.*, 1988). A significant discrepancy exists in the inferred palaeo sea-level record as deduced from the study of benthic foraminifera from Gulf St Vincent (Cann *et al.*, 1988, 1993; Murray-Wallace *et al.*, 1993), with that of the marine isotopic record (see Chappell *et al.*, 1996; Murray-Wallace, 2002; Waelbroek *et al.*, 2002) and recent studies of the Murray Canyons region of the continental shelf that indicate a highest sea-level for MIS 3 of c. -50 m (Gingele *et al.*, 2004; Hill *et al.*, 2009). In

comparison, the inferred palaeo sea-level record based on the logarithmic ratio of the benthic foraminifers, *Elphidium crispum* to *Elphidium macelliforme* in surficial sediments and their distribution in cores from Gulf St Vincent and Spencer Gulf suggested water depths within Gulf St Vincent of between -22 and -28 m for the time period 30-45 ka BP - though the R^2 values for those data only indicate moderate levels of correlation (Cann *et al.*, 1988, 1993; Murray-Wallace *et al.*, 1993).

5.3. Aims

The aim of this project was to investigate, using amino acid racemization methods, the utility of single *Elphidium* (Foraminifera) as a chronological and aminostratigraphic tool for late Pleistocene and Holocene studies. An attempt was made to recognize reworked *Elphidium* tests based on D/L ratio results. The term reworked is used here to refer to populations of either Foraminifera or molluscs where two or more distinct age populations are found, using the extent of amino acid racemization in replicate samples (Wehmiller *et al.*, 1995). In this sense, this term does not directly imply out of habitat reworking of individual *Elphidium*. Rather, within this semi-enclosed environment reworking refers to the mixing of foraminifera and similar taxa due primarily to the incorporation of older samples in younger strata.

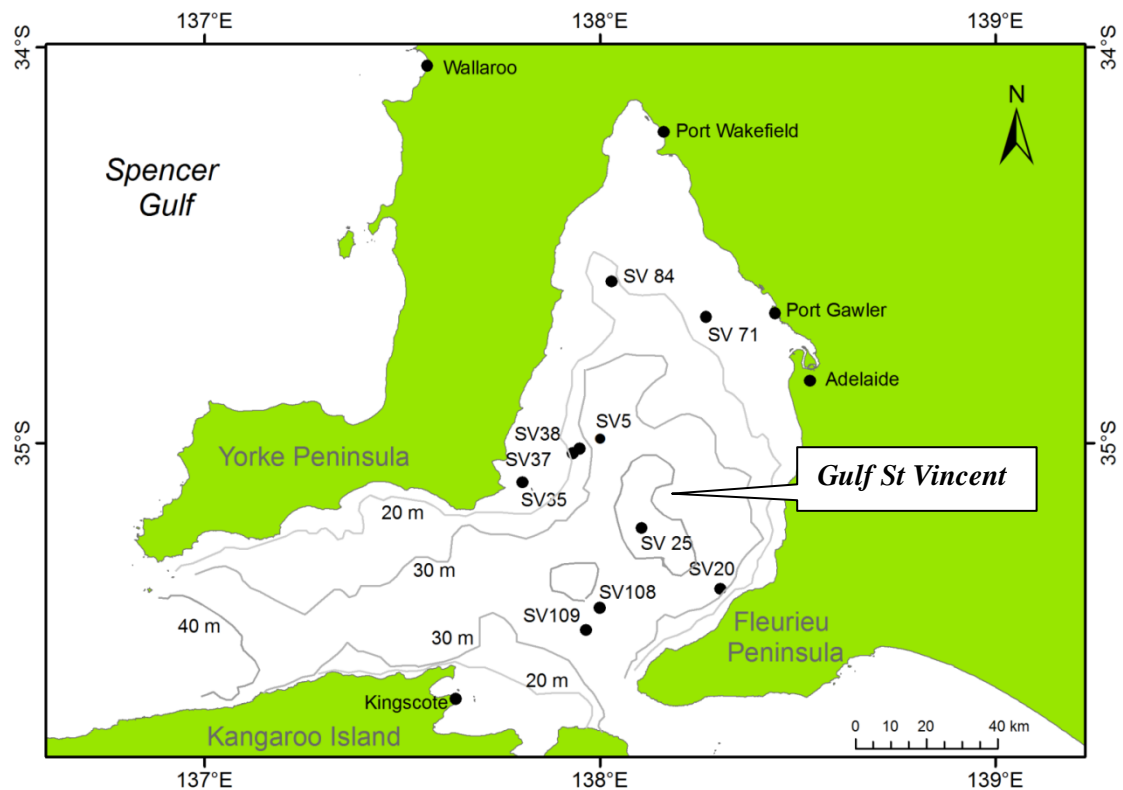


Figure 5.1. Location of core and surface sampling locations, Gulf St Vincent, South Australia.

5.4. Methods

Elphidium tests of 250-500 μm diameter were analysed from 10 cores, 4 grab samples and 2 coastal locations that included modern samples from intertidal Port Gawler and suspected last interglacial (MIS 5e) age sediments from Port Wakefield. This study focused on core SV#5 (Cann *et al.*, 1988) from the central region of Gulf St Vincent, recovered from a water depth of 36.4 m, consisting of carbonate sediments previously dated to MIS 3 overlain by sediments of Holocene age. One half of core SV5, previously sampled (Cann *et al.*, 1988) but generally intact, was obtained from the core library, Adelaide, cut into 1 cm slices, and analysed at the Amino Acid Geochronology Laboratory, University of Wollongong. Additional foraminifer samples were recovered from these additional Gulf St. Vincent cores and selected coastal strata in an attempt to define the spatial limit of latest Pleistocene deposits within this basin. Samples recovered with a grab sampler (sieved $> 250 \mu\text{m}$) were obtained from the locations of cores SV 37 (water depth 18.4 m), and SV 38 (water depth 26.8 m). Surficial samples (sieved $> 250 \mu\text{m}$) of *Elphidium* were recovered from the upper 5 cm of surface sediments at Port Gawler.

Samples were taken from core SV#5, Gulf St. Vincent, from 1 cm slices at intervals of 5 cm. One slice was of 2 cm thickness (15-17 cm depth). Single *Elphidium* from 1 cm slices at 1 cm intervals were picked to investigate the amount and extent of reworking around the disconformity between late Pleistocene and basal Holocene sediments and marked by a colour change at 53 cm in core SV#5. A large portion of the Holocene section of core SV5 had previously been removed for earlier studies (Cann *et al.*, 1988; Murray-Wallace *et al.*, 1993; Riggs, 2002), however there was sufficient sediment left to obtain some Holocene specimens.

^{14}C AMS analyses were undertaken at the facilities of the Australian Nuclear Science and Technology Organisation (ANSTO), Lucas Heights, Sydney, on four bulk samples of well preserved *Elphidium* recovered from three 1 cm slices and one 2 cm section of core SV5. These horizons were 15-17 cm, 95 cm, 180 cm, and 320 cm. An equivalent mass of well preserved *Elphidium* from these same horizons was also analysed for the extent of racemization. AMS ^{14}C ages are reported uncalibrated so that comparisons may be made with previous studies, and because three of the four radiocarbon ages reported here are beyond the age limit of current calibration curves.

Individual foraminifer samples, each comprising a single *Elphidium* test weighing approximately 0.00003g, generally *Elphidium crispum* or *Elphidium macelliforme*, were analysed with the aim of measuring the extent of racemization of the total hydrolysable amino acid (THAA) fraction using reverse-phase high performance liquid chromatography, a method adapted from that of Kaufman & Manley (1998) and Hearty *et al.*, (2004). All foraminifer tests were used where sufficiently complete or robust. Modification of the methods of

Kaufman & Manley (1998) and Hearty *et al.*, (2004) involved strong bleaching of the skeletal carbonate (12.5% NaOCl) for one hour after ultrasonication. A subset of tests were bleached with 12.5% NaOCl for 48 hours to attempt to isolate and analyse the hydrolysable intracrystalline amino acid (HIAA) pool in single tests. Whole rock analyses on selected 1 cm horizons were undertaken to compare with the bulk and single foraminiferal data. The 250-500 µm sieved fraction was used following the methods of Hearty *et al.*, (2006) with the following alterations: after undergoing a 33% stoichiometric 2M HCl etch, samples were subsequently bleached for one hour with 12.5% NaOCl prior to digestion and hydrolysis.

Observations on the variation in preservation of *Elphidium* tests was accomplished using a semi-quantitative visual inspection (Table 5.1). The extents of corrosion, discolouration and completeness were employed with D/L ratio results to assess the extent to which preservation affects results from this genus. This was undertaken once it was realised from the initial results that the portion of core SV5 between 54 cm and the base of the core at 390 cm was of one aminostratigraphic age and therefore it was possible to investigate the extent to which preservation may affect results for these foraminifera from a single deposit.

The ages of single *Elphidium* were calibrated using a parabolic equation based on glutamic acid D/L values calibrated with the square-root of ^{14}C ages.

Table 5.1. Preservation features examined in *Elphidium* tests from Gulf St Vincent.

Diagnostic feature examined	Grade	Description
Degree of completeness	0	> 90% complete
	1	< 90% complete, identifiable to species level
	2	< 90% complete, identifiable to genus level
	3	< 90% complete, unidentifiable to genus level
Extent of discolouration	0	None, strong original colours present, or transparent
	1	Slight fading of original colour, or translucent
	2	Very strong fading of original colour, nearly totally white
	3	White, no other colour visible anywhere
	4	Lightly discoloured, e.g. light grey, light brown, patchily discoloured
	5	Strongly discoloured, e.g. black, dark grey
Extent of corrosion (= dissolution, abrasion and recrystallisation)	0	None, may be transparent
	1	Translucent generally, beginning of dissolution
	2	White surfaces, none to slight abrasion, retains structural strength
	3	White, pores enlarged, strong abrasion of sculpture, minor delamination, and/or minor pitting, minor loss of structural strength
	4	Chalky, sculpture gone, strong delamination, substantial loss of structural integrity, internal structure of foraminifers visible

5.5. Regional setting

Semi-enclosed Gulf St Vincent and its associated coastlines lie within the larger and pre-existing St Vincent Basin (Parkin, 1969). This basin contains an extensive suite of Tertiary and Quaternary strata (Murray-Wallace *et al.*, 1995; Murray-Wallace, 2002). Gulf St Vincent

contains sedimentary records of late Quaternary sea-level changes in a far-field, relatively stable intraplate setting with minimal glacio-isostatic re-adjustment. However, significant neo-tectonic deformation is evident on Fleurieu Peninsula, and hydro-isostatic flexure has occurred during the Holocene in the northern gulf region. The Gulf is set within the southern Australian cool-water temperate carbonate province, and has a semi-arid climate (Short, 1988; Belperio *et al.*, 2002) that is dependent on the seasonal position of subtropical highs and mid-latitude lows (Short, 2004). Because of the regional aridity there is today little fluvial transport of terrigenous sediment into the gulf (Short, 1988; Belperio *et al.*, 2002). Except for the Onkaparinga river, no perennial rivers discharge into the gulf (de Silva Samarasinghe *et al.*, 2003; Wilkinson *et al.*, 2005). The remaining rivers are generally narrow creeks, vary seasonally in their flow, several are dammed, and little outflow enters the gulf. Indeed, even when they do flow, the waters do not always reach the gulf.

The sediments of the gulf are derived primarily from marine invertebrates, and are dominated by species of foraminifers, molluscs and algae that are characteristic of cool-water, higher salinity foramol provinces (Lees & Buller, 1972; Burne & Colwell, 1982; Gostin *et al.*, 1988). Preservation of skeletal elements ranges between poor and good (Nelson, 1988; this study) and appears typical of shallow-water, semi-enclosed, cool-water temperate-carbonate systems. Reworking of sub-tidal sediment occurs at the present time due to the large numbers of prawns, crabs and holothurians within the gulf (Shepherd & Sprigg, 1976). Though semi-enclosed, the Southern Ocean also continues to influence sediment distribution within the entrances and lower to mid-gulf region through storm-generated waves in the shallow waters. Two predominant seagrass species inhabit the gulf, with the shorter *Zostera* sp. growing between mean sea level and low tide, and *Posidonia* sp. occurring from below low tide to a few metres depth. Biogenic carbonate is produced principally in these vast seagrass meadows, and is commonly reworked shoreward to form wide intertidal sand flats and associated shelly beach ridge plains (Belperio *et al.*, 1984; Short, 2002). The in-situ vertical accretion of seagrass meadows results in sea-grass banks, which ultimately change laterally to mud-flat environments.

Current mean annual temperature (CMAT) for Adelaide (Adelaide Airport, years 1955-2007) is 16.4° C. For Troubridge Lighthouse it is 16.7° C (years 1969-1980), and for Kingscote CMAT is 15.4° C (years 1877-2002) (all data from Bureau of Meteorology). CMAT for Wallaroo is estimated at 16.75°C based on data from nearby Kadina (Beureau of Meteorology). Maximum summer temperatures around Adelaide and Port Gawler can exceed 40° C, while in winter minimum temperatures rarely fall to 0° C (Cann & Gostin, 1985). CMAT for SV5 is approximately 17°C (Murray-Wallace *et al.*, 1993).

5.5.1. Core SV#5 and adjacent sampling locations, Gulf St Vincent

Core SV5 is one of a suite of cores recovered from Gulf St Vincent. The site of vibrocore SV5 (34.59.30° S, 138.00.05° E, 36.4 m water depth), lies at the northern end of a central, flat elongate sea floor, adjacent to the deepest (c. 40 m water depth) and central section of Gulf St. Vincent (Cann *et al.*, 1988; Murray-Wallace *et al.*, 1993). In core SV5 the boundary at 53 cm depth, between the Holocene and MIS 3 strata appeared to be indicated by a distinct colour change from the overlying light greenish grey (Munsell colour 5GY7/1) bioclastic sands to a pinkish grey shell fragment rich bioclastic sand. This was visible in the dried out core collected from the core library, Glenside, Adelaide (18/05/2006).

A limited number of additional samples were used, recovered from a selection of cores, principally taken from the central and deeper sections of Gulf St Vincent. To obtain modern samples for comparison surficial samples were additionally chosen from Port Gawler tidal flats, from last interglacial (MIS 5e) beach ridges at Port Wakefield and from the locations of cores SV37 and SV38. These latter locations are in close proximity to that of SV5, but in shallower water. Stratigraphic logs and additional details of these cores are published in Cann *et al.* (1988, 1993) and Murray-Wallace *et al.* (1993).

Coastal sediments of last interglacial (MIS 5e) age and mapped as the Glanville Formation, are dominated by carbonate sands and have fossils indicating warmer water than at present during that period of time. These outcrop extensively on the southern Australian coastline (Murray-Wallace and Belperio, 1991; Murray-Wallace, 1995). Uranium-series dating has established beyond doubt the last interglacial (MIS 5e) age of these strata (Zhu *et al.*, 1993; Murray-Wallace, 1995), and thus the outcrops of last interglacial (MIS 5e) age beach ridges at Port Wakefield, occur on the landward margin of the limits of the present-day supratidal zone, provide a benchmark in this study with which to compare the data from core SV#5, the adjacent cores and grab samples.

5.6. Results

5.6.1. Paired AAR and AMS ^{14}C dating of bulk samples of *Elphidium*

Two distinct age populations are indicated from AMS ^{14}C analyses on bulk foraminifer samples from 15-17, 95, 180 and 320 cm depth in core SV 5 (Table 5.2). These populations are dated to the Holocene ($3,750 \pm 70$ a for the horizon at 15-17 cm), and MIS 3 ($41,800 \pm 1,300$ a, $45,895 \pm 2,500$ a and $> 47,000$ a BP) for the remainder of the core. It is worthwhile to note these determinations were undertaken on stable calcite, the age range of this method at ANSTO is c. 50 ka, and the similarity of these ages to those previously obtained on molluscs in this same core ($37,600 \pm 1450$, -1400 a, on *Katelsia rhytiphora*, 140 cm depth; to $45,100 \pm 5,100$, - 3,100 a, on *Ostrea angasi*, 370 cm depth).

The core section from 95 cm to 320 cm is of one aminostratigraphic age based upon the extent of racemization in the amino acids aspartic, glutamic, alanine and valine, in equivalent bulk *Elphidium* samples. There are apparent downcore reversals (Fig. 5.2) in D/L values for Asx between 180 cm ($Asx = 0.575 \pm 0.002$) and 320 cm ($Asx = 0.556 \pm 0.004$). Similarly, the amino acid values for Glx (0.298 ± 0.008), Ser (0.386 ± 0.045) and Ala (0.516 ± 0.003) are higher in the 180 cm horizon samples than those from the horizon at 320 cm (Glx = 0.297 ± 0.002 , Ser = 0.310 ± 0.078 , Ala = 0.495 ± 0.014). D/L values for valine from these latter two horizons are the same (Val = 0.266 ± 0.010 , 180 cm, and Val = 0.266 ± 0.003 , 320 cm).

There are several factors that may account for the apparent reversals. These include the degree to which the sediment is homogenised, the extent of leaching occurring at each of these horizons, as well as differential preservation of foraminifer tests between horizons. However, when these data are considered together with the single foraminifer data below, these apparent reversals are not significant and represent natural D/L variations within a single population. The extent of variation between these results is much less than that found in sampled individual one centimetre horizons. The results from whole rock analyses of the same horizons also indicate this reversal (Fig. 5.2). The inference gained from this is that the AAR data on bulk foraminifera is representative of the sediment as a whole.

Results from whole rock analyses using sediment from the same horizons as that of the paired AMS C-14 and AAR analyses on bulk forams, depicted the same apparent reversal in D/L values. D/L values in whole-rock samples were slightly higher than for bulk foraminifer results. This is because whole-rock samples consist of sediments that are comprised of a mixed assemblage of molluscs, forams, ostracods, and bryozoa. *Elphidium* foraminifers comprise a small fraction of the total population of skeletal material, and appear to racemise at slightly lower rates, similar to the bivalve mollusc *Katelysia*.

Table 5.2. AMS ^{14}C and AAR data from bulk samples of *Elphidium*. Results from paired *Elphidium* AAR/C-14 analyses, core SV5, Gulf St. Vincent. AAR results given as D/L ratio \pm 1stdv. The corresponding coefficient of variation ($= \text{STDV}/\text{Mean} \times 100$) is in brackets. AAR analyses were in triplicate undertaken by repeat injections of the same acid hydrolysate sample.

Depth (cm)	Asx D/L ratio	Glx D/L ratio	Ser D/L ratio	Ala D/L ratio	Val D/L ratio	^{14}C age uncalibrated	ANSTO code
15-17 (n = 3)	0.278 \pm 0.01 (3.941 %)	0.101 \pm 0.002 (1.980 %)	0.240 \pm 0.002 (0.722 %)	0.148 \pm 0.002 (1.030 %)	0.083 \pm 0.001 (0.693 %)	3,750 \pm 70	OZJ420
95 (n = 3)	0.508 \pm 0.002 (0.410 %)	0.277 \pm 0.001 (0.361 %)	0.277 \pm 0.001 (0.209 %)	0.491 \pm 0.002 (0.471 %)	0.244 \pm 0.001 (0.410 %)	41,800 \pm 1300	OZJ421
180 (n = 3)	0.575 \pm 0.004 (0.696 %)	0.298 \pm 0.008 (2.521 %)	0.386 \pm 0.045 (11.758 %)	0.516 \pm 0.003 (0.623 %)	0.266 \pm 0.010 (3.608 %)	45,895 \pm 2500	OZJ422
320 (n = 3)	0.556 \pm 0.004 (0.681 %)	0.297 \pm 0.002 (0.700 %)	0.310 \pm 0.078 (25.161 %)	0.495 \pm 0.014 (2.872 %)	0.266 \pm 0.003 (1.210 %)	> 47,000	OZJ423

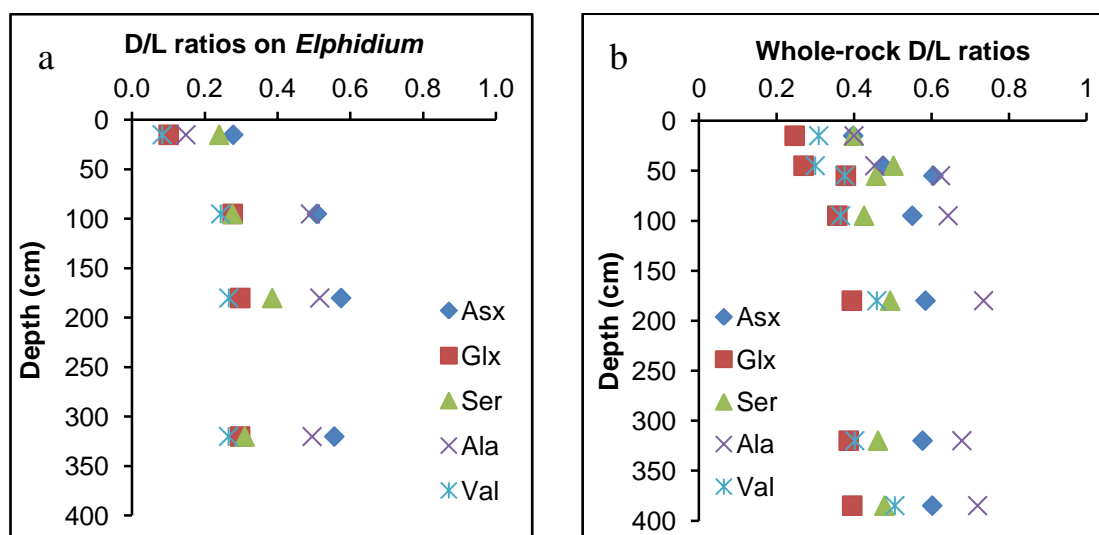


Figure 5.2. Variation in D/L values from bulk foraminifer samples, core SV5. 5.2a) Variation of mean D/L ratio on bulk foraminifers with depth for the amino acids glutamic, aspartic, serine, alanine and valine. An equivalent set of bulk foraminifer samples from these horizons were dated by AMS ^{14}C at ANSTO. Note the slight reversal in D/L values downcore from 180 cm to 320 cm. 5.2b) Whole-rock mean D/L values for core SV5 broadly exhibiting the same down-core distribution of D/L values.

5.6.2. Single foraminifer data, SV#5: Sample Screening

Screening was undertaken to rule out contamination by exogenous amino acids, and to rule out the use of results from individual foraminifers in which partial recrystallisation had occurred. Screening was not undertaken specifically to remove results that did not fit expected or known ages because this study required the identification of reworked tests. However, these latter results were removed from the final data set to obtain mean ages for the individual horizons concerned that were not time-averaged.

Screening was subsequently undertaken by removing sample results with Ser D/L values of ≤ 0.1 and those with values of L-Ser/L-Glx ≥ 0.5 in foraminifers from the core section 54-385 cm. Serine is highly mobile, yet racemises initially at a fast rate. If the amino acids in the skeletal carbonate are fully isolated from the external environment, serine D/L values should be similar to the other amino acid results in these samples, and within the sample population as a whole. These low Ser D/L values of ≤ 0.1 commonly corresponded with anomalously low D/L values for Asx and Glx, and very high L-Ser peak heights and areas, and therefore resulted in high contaminant indices (i.e. high values of L-Ser (peak height)/L-Glx (peak height)). 54% of rejected results demonstrated this relationship. For tests recovered from the 0-53 cm section of core SV5, a contaminant index of < 1.0 was deemed acceptable because there will normally be moderately high concentrations of L-serine in samples of Holocene age, and two samples were rejected.

The second stage in screening was undertaken after analysing the relationship between preservation and D/L values, the results of which are presented in section 5.5.3.

5.6.3. *Preservation and D/L values*

The graphical relationship between preservation and D/L values are illustrated below (Figs. 5.2 to 5.5) for 434 single *Elphidium* tests recovered from horizons between 54 and 385 cm. These foraminifera in this section of core were used for this purpose because they appeared to be of a single aminostragaphic age. Best preserved tests (Fig. 5.2) generally have lower D/L values than for those tests less well preserved, and worst preserved have highest D/L values. These latter, less well preserved *Elphidium* tests may simply be of an older age. However, for all preservation values between worst and best, this relationship is not clear with the positions of these mean values being mixed (Fig. 5.2). D/L values for the mean values of worst preserved tests were 15% (aspartic) and 18% (glutamic) greater than for the best preserved. Complete tests have lower D/L values, incomplete the highest (Fig. 5.3). The mean aspartic D/L value for worst preserved (i.e. incomplete and broken) tests was 10% greater than for best preserved, and for glutamic this value was 9% greater. For discolouration (Fig. 5.4) chalky white tests have slightly lowered D/L values and the resulting differences between best preserved and chalky tests was 6% lower for aspartic and 2% lower for glutamic. In contrast, highly corroded tests have the highest D/L values, approximately 8% greater than for best preserved tests in both these amino acids (Fig. 5.5). These corroded tests were also chalky.

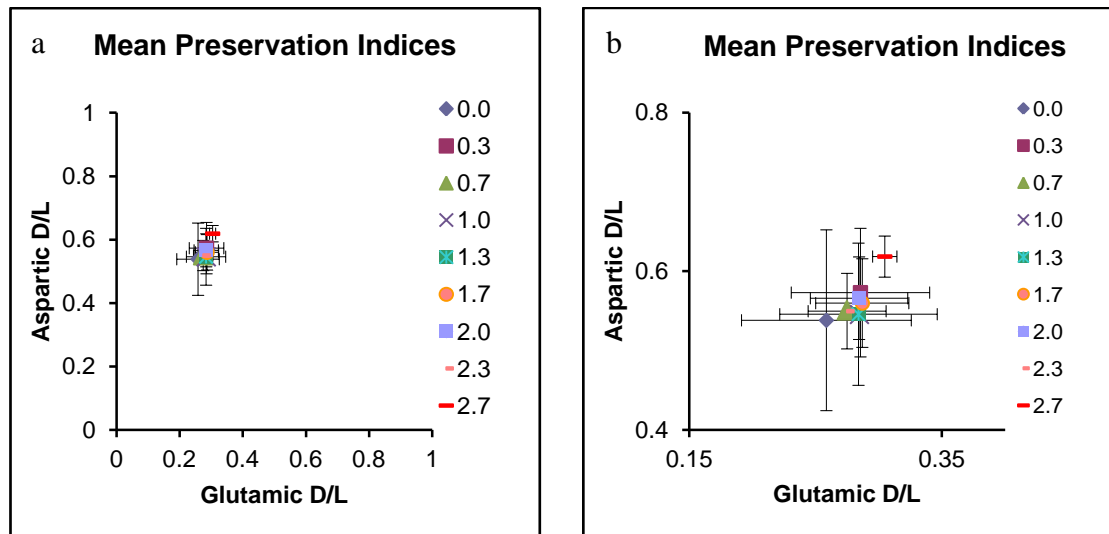


Figure 5.3. a) and b) Mean preservation grades for individual *Elphidium* tests from 54 to 385 cm depth in core SV5. Best preserved tests (mean grade = 0) have lowest D/L values while worst preserved (mean grade = 2.7) have highest D/L values. However, there is no clear correspondence between grade and D/L ratio for the other preservation grades, except for being intermediate between best and worst preserved. All results for all grades fit within the envelope for one standard deviation of the mean for best preserved tests. This increasing D/L ratio with decreasing state of preservation may simply be due to the older age of the less well preserved tests.

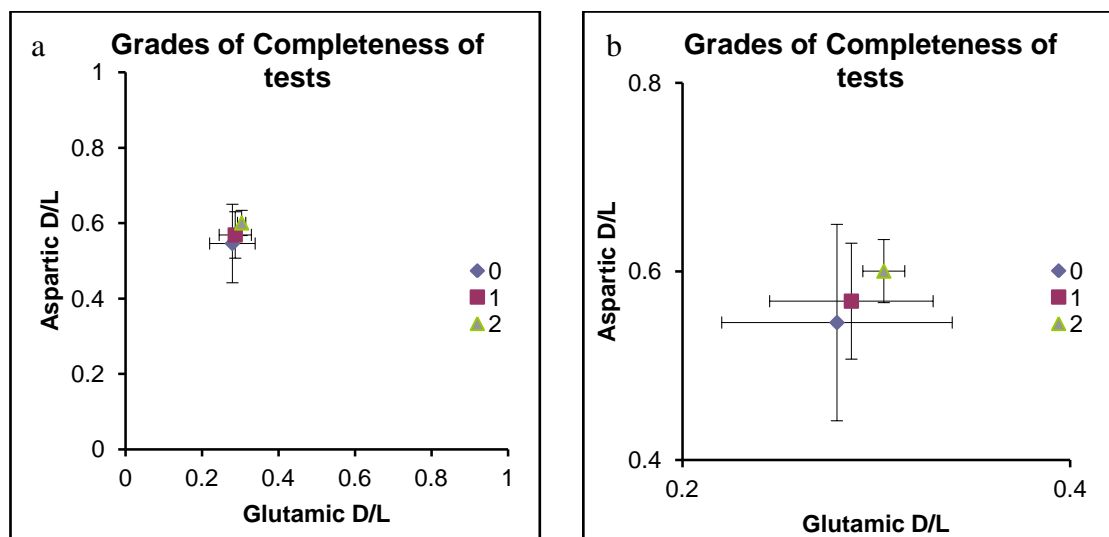


Figure 5.4. a) and b) Correspondence of aspartic and glutamic D/L values with variation in completeness of *Elphidium* tests. Best preserved tests (grade = 0) had lower aspartic and glutamic acid D/L values, and worst preserved had higher D/L values.

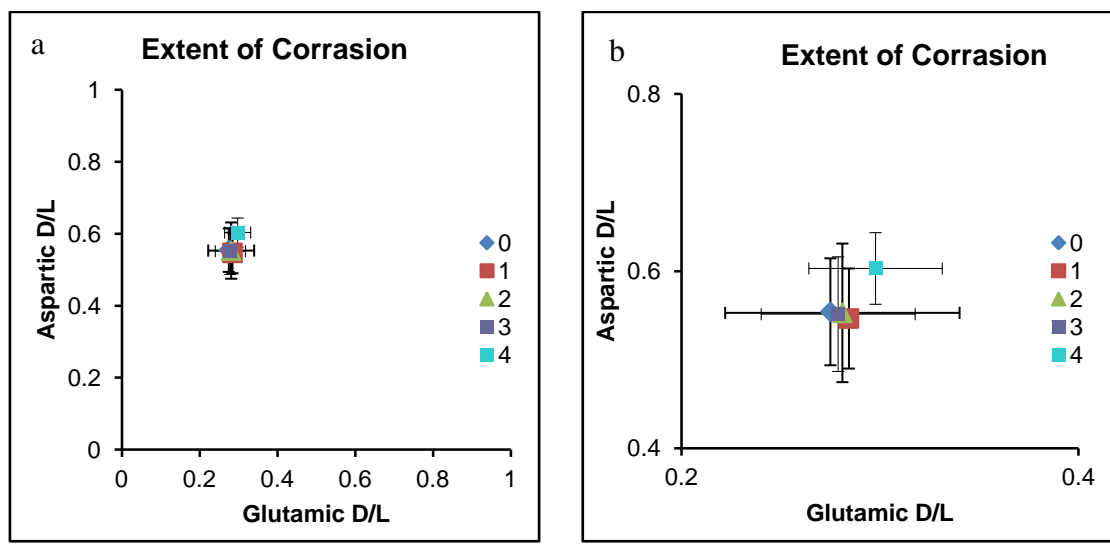


Figure 5.5. a) and b) Extent of corrasion of *Elphidium* tests. All grades of corrasion gave more or less the same D/L values except for those tests with corrasion grade = 4. These tests were chalky, indicating slight dissolution and likely diffusive loss of amino acids from the tests. Diffusive loss of amino acids commonly results in lower D/L values because of the loss of the more highly racemised free amino acids, leaving behind a greater proportion of peptide-bound amino acids, generally at terminal positions. Overall, discoloration dissolution appear to only have slight influence on the observed extent of amino acid racemization in these tests.

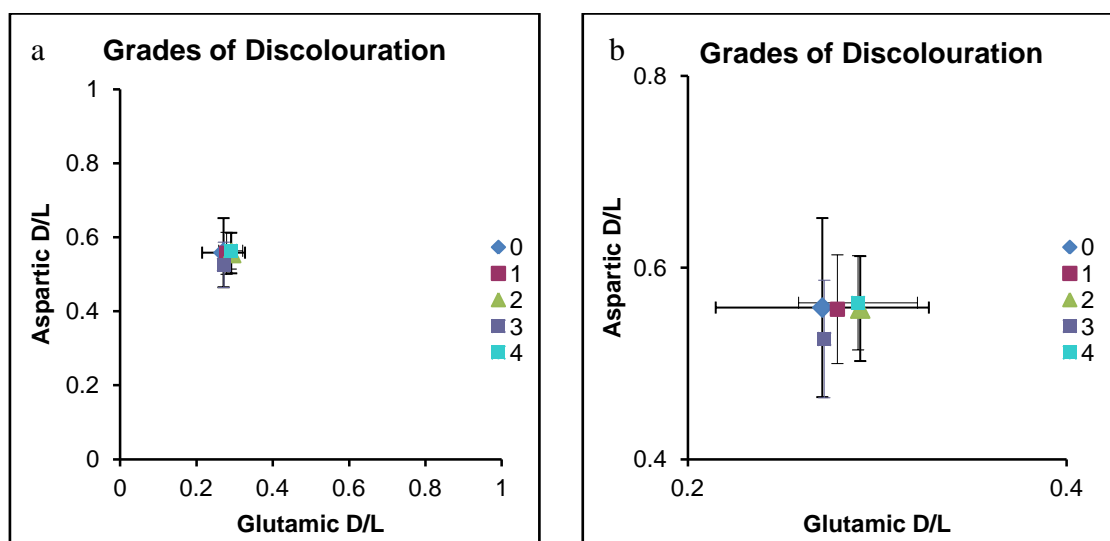


Figure 5.6. a) and b) Variation in Asx and Glx D/L values with variation in the extent of discolouration of *Elphidium* tests. In general all grades of test plotted close together especially for aspartic D/L values, with only results from chalky tests (grade = 3) having slightly lowered D/L values.

5.6.4. Single *Elphidium* results (SV#5) and ^{14}C calibration of ages

The results from AAR analyses of 554 single *Elphidium* tests recovered from core SV5 were obtained for the amino acids, aspartic, glutamic, and serine. 63 results (11.4 %) were rejected because either concentrations were too low or because of high contamination index values as

outlined above. The results from 294 best preserved tests were compared with 472 results from all *Elphidium* tests not previously rejected (Fig. 5.8, 5.9). Using the results from only the best preserved *Elphidium* does not alter the final dataset of D/L values and calibrated ages from that of all results, except to leave gaps downcore where in a single horizon were obtained on less than best preserved foraminifers (Fig. 5.8, 5.9). Sidereal ages, calculated using a parabolic equation (Fig. 5.10) are based on the glutamic acid D/L values of all preservation grades, recovered from 50 1 cm, and one 2 cm horizons in core SV5. This is an average of approximately 6 *Elphidium* tests per one centimetre horizon. Two populations of *Elphidium* were present in the results, with a significant step in mean D/L values across the 53-54 cm interval (Fig. 5.9).

Table 5.3. Mean D/L values downcore SV5 for single tests of the foraminifer, *Elphidium* sp. *Elphidium* tests were analysed using both long and short analytical times (long run, short run), and therefore there are some apparent gaps in the table where only short runs were employed, and the results from alanine and valine are not reported. This was done because it reduced time using the HPLC during a period when the laboratory was extremely busy, but more importantly it was done because only the results from glutamic acid, when calibrated, replicated the ages obtained on the bulk samples of *Elphidium* by radiocarbon dating during the initial stage of this investigation. These data below are the final data whereby samples that appear out of stratigraphic order have been removed. These removed data and ages are in Table 5.2.

SV#5 DEPTH	n =	Asx D/L	Glx D/L	Ser D/L	Ala D/L	Val D/L	L-Ser/L- Glx	calibrated parabolic Glx age
15	10	0.252	0.092	0.182	0.172	0.023	0.579	2,320
33	11	0.279	0.093	0.172	0.186	0.129	0.543	2,417
45	2	0.327	0.112	0.142			0.730	4,225
46	3	0.346	0.128	0.062	0.297	0.179	0.791	6,136
47	14	0.344	0.123	0.224	0.218	0.089	0.510	5,474
48	3	0.358	0.124	0.302	0.200	0.098	0.337	5,667
49	4	0.354	0.121	0.278	0.202	0.080	0.441	5,256
50	5	0.396	0.139	0.272	0.236	0.084	0.389	7,685
51	3	0.329	0.115	0.193			0.610	4,519
53	7	0.277	0.101	0.203	0.187	0.099	0.616	3,078
54	10	0.599	0.343	0.327	0.572	0.297	0.190	66,392
57	3	0.534	0.281	0.244	0.477	0.244	0.215	42,367
60	8	0.556	0.303	0.225	0.508	0.267	0.244	50,344
65	6	0.568	0.312	0.215	0.502	0.270	0.236	53,541
75	2	0.552	0.303	0.238	0.481	0.263	0.218	50,064
90	8	0.582	0.280	0.235	0.435	0.230	0.358	41,940
95	7	0.558	0.293	0.208			0.242	46,533
100	9	0.547	0.271	0.209	0.425	0.213	0.273	39,116
105	4	0.575	0.271	0.231	0.467		0.272	39,089
115	1	0.573	0.279	0.106	0.533	0.251	0.423	41,684
120	6	0.620	0.317	0.334	0.520	0.300	0.230	55,421
125	8	0.586	0.311	0.315	0.542	0.291	0.210	53,236
145	9	0.572	0.302	0.250	0.518	0.250	0.256	49,961
150	7	0.591	0.283	0.240	0.468	0.271	0.293	43,106
155	8	0.516	0.311	0.270	0.534	0.275	0.246	53,140
160	9	0.621	0.303	0.279	0.516	0.303	0.256	50,375
165	4	0.501	0.266	0.182	0.438	0.221	0.278	37,378
175	7	0.546	0.279	0.220	0.473	0.254	0.250	41,733
180	7	0.592	0.293	0.226	0.572	0.279	0.298	46,533
185	6	0.573	0.275	0.218	0.537	0.247	0.243	40,390
195	2	0.609	0.287	0.283	1.058		0.199	44,451
200	5	0.588	0.299	0.259	0.490	0.265	0.246	48,841
205	9	0.605	0.296	0.293	0.519	0.526	0.198	47,669
215	6	0.613	0.297	0.253	0.508	0.317	0.260	47,912
220	7	0.542	0.296	0.223	0.495	0.231	0.286	47,773
225	6	0.597	0.303	0.244	0.356	0.278	0.228	50,188
230	8	0.608	0.309	0.259	0.570	0.285	0.252	52,327
235	5	0.565	0.275	0.220	0.693	1.000	0.225	40,468
240	8	0.560	0.293	0.238	0.461	0.255	0.260	46,719
250	4	0.546	0.317	0.221	0.547	0.257	0.297	55,519
265	8	0.584	0.316	0.274	0.530	0.276	0.226	55,029
270	5	0.615	0.336	0.260	0.530	0.318	0.320	63,420
275	4	0.548	0.306	0.217	0.465	0.277	0.258	51,378
280	9	0.607	0.311	0.312	0.495	0.277	0.179	53,199
285	24	0.577	0.306	0.264	0.527	0.262	0.212	51,315

290	8	0.564	0.294	0.263	0.504	0.227	0.207	47,035
295	10	0.565	0.313	0.255	0.499	0.267	0.210	53,979
300	10	0.596	0.296	0.207	0.477	0.307	0.289	47,560
320	8	0.594	0.297	0.272	0.464	0.293	0.249	48,034
325	9	0.563	0.312	0.287	0.520	0.300	0.214	53,669
330	6	0.596	0.303	0.336	0.508	0.277	0.175	50,251
340	6	0.564	0.314	0.216	0.529	0.247	0.251	54,315
345	6	0.571	0.291	0.192			0.304	45,748
350	9	0.601	0.288	0.280	0.450	0.285	0.227	44,960
355	14	0.592	0.302	0.285	0.541	0.222	0.203	49,984
380	4	0.615	0.308	0.276	0.490	0.299	0.197	52,231
385	9	0.568	0.297	0.205	0.502	0.249	0.320	47,872

57	400							
horizons	count							
							Mean	48,813
							Median	48,841
							Max	66,392
							Min	37,378
							stdv	5,916

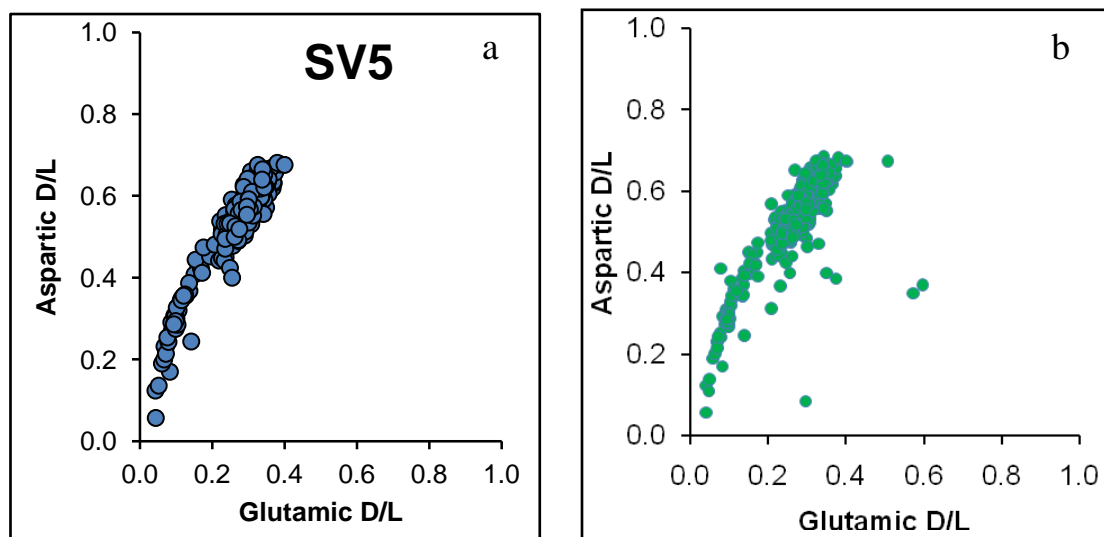


Figure 5.7. Comparison of the covariance of D/L values in best preserved (a, blue circles) and all (b, green circles) single *Elphidium* tests from 15 cm to 385 cm depth in core SV5, Gulf St Vincent.

Table 5.4. D/L values and calculated parabolic ages removed from the dataset in Table 5.1 because they have apparent ages that are out of stratigraphic order. For the Holocene portion of SV5 these are interpreted as being indicative of reworking. The subset of samples from the last interstadial section of core SV5 are problematic because they generally indicate ages of MIS2 (see Fig. 5.13 and caption). These ages were found also in using a power-law equation (Fig. 5.10). These removed data were chosen on the basis of their calibrated age, and 30 ka or less was chosen as the cutoff age for the sediments in the 54-385 cm portion of SV5, and are discussed further in section 5.6.3.

SV#5 DEPTH	Asx D/L	Glx D/L	Ser D/L	Ala D/L	Val D/L	L-Ser/L- Glx	calibrated parabolic Glx age
15	0.499	0.254	0.174	0.466		0.372	34,102
15	0.519	0.304	0.249	0.597	0.534	0.277	51,227
15	0.523	0.281	0.19			0.286	42,918
15	0.488	0.294	0.309			0.284	47,524
33	0.548	0.29	0.23	0.537	0.352	0.217	46,082
46	0.557	0.258	0.138	0.543	0.263	0.418	35,344
46	0.529	0.216	0.144	0.463	0.308	0.457	23,409
46	0.554	0.298	0.196	0.494	0.247	0.254	48,988
46	0.551	0.353	0.173	0.609	0.669	0.322	71,378
47	0.566	0.297	0.217	0.550	0.225	0.390	48,620
47	0.400	0.353	0.235	0.264	0.104	0.362	71,378
47	0.582	0.297	0.290	0.549	0.421	0.255	48,620
47	0.587	0.299	0.252	0.559	0.365	0.308	49,358
47	0.595	0.306	0.255	0.595	0.339	0.264	51,984
48	0.600	0.313	0.453	0.570	0.315	0.161	54,678
48	0.532	0.264	0.152	0.480	0.256	0.314	37,249
48	0.496	0.211	0.343	0.331	0.173	0.253	22,151
48	0.674	0.405	0.385	0.620	0.357	0.126	96,410
48	0.500	0.254	0.416	0.363	0.295	0.325	34,102
48	0.539	0.262	0.295	0.540	0.509	0.258	36,608
48	0.521	0.241	0.073	0.451	0.279	0.535	30,218
48	0.527	0.233	0.088	0.489	0.341	0.501	27,945
48	0.486	0.299	0.222	0.828	0.076	0.289	49,358
48	0.606	0.333	0.287	0.576	0.418	0.207	62,750
49	0.525	0.308	0.147	0.477	0.190	0.433	52,747
49	0.365	0.234	0.166	0.264	0.086	0.613	28,224
49	0.541	0.301	0.159	0.499	0.226	0.414	50,101
49	0.511	0.267	0.343	0.359	0.294	0.232	38,220
49	0.586	0.309	0.105	0.525	0.259	0.813	53,130
49	0.386	0.374	0.269	0.253	0.077	0.874	81,035
49	0.532	0.276	0.112	0.474	0.126	0.524	41,209
50	0.517	0.249	0.226	0.398	0.170	0.253	32,580
50	0.517	0.252	0.189	0.374	0.174	0.420	33,489
50	0.432	0.209	0.168	0.394	0.237	0.441	21,658
50	0.517	0.226	0.096	0.389	0.240	0.559	26,028
50	0.567	0.266	0.184	0.432	0.241	0.273	37,895
51	0.499	0.263	0.120			0.412	36,928
51	0.368	0.597	0.105			0.541	221,370
53	0.549	0.284	0.166	0.492	0.284	0.312	43,960
53	0.587	0.319	0.249	0.53	0.329	0.221	57,041
53	0.562	0.299	0.247	0.485	0.26	0.178	49,358
53	0.514	0.293	0.349	0.486	0.267	0.154	47,161
53	0.558	0.303	0.275	0.524	0.3	0.174	50,850
53	0.609	0.347	0.375	0.592	0.343	0.138	68,731
53	0.487	0.246	0.210			0.214	31,684
75	0.672	0.507	0.178	0.625	0.384	0.254	156,420
105	0.470	0.209	0.119			0.350	21,658

105	0.533	0.228	0.113	0.468		0.495	26,569
115	0.465	0.215	0.132	0.381	0.171	0.291	23,155
115	0.495	0.239	0.100	0.481	0.213	0.611	29,641
125	0.515	0.231	0.130	0.459	0.239	0.385	27,390
145	0.518	0.227	0.124	0.416	0.217	0.356	26,298
160	0.538	0.222	0.135	0.452	0.247	0.391	24,964
175	0.442	0.219	0.123	0.367	0.185	0.344	24,180
180	0.442	0.234	0.132	0.575	0.154	0.433	28,224
185	0.553	0.237	0.121	0.485	0.123	0.458	29,070
185	0.474	0.176	0.134	0.264	0.195	0.388	14,320
195	0.481	0.207	0.104			0.427	21,170
215	0.568	0.211	0.171	0.266	0.230	0.282	22,151
225	0.500	0.232	0.122			0.355	27,667
230	0.490	0.227	0.196	0.567	0.232	0.368	26,298
265	0.503	0.235	0.148	0.440	0.204	0.303	28,505
345	0.506	0.240	0.117			0.351	29,929
345	0.471	0.236	0.175			0.282	28,787
380	0.495	0.236	0.216	0.375	0.191	0.229	28,787
165	0.452	0.194	0.094	0.451	0.184	0.487	18,135
165	0.412	0.172	0.057	0.409	0.174	0.491	13,533
95	0.467	0.228	0.123			0.328	26,569
75	0.464	0.230	0.148	0.380	0.176	0.405	27,115
175	0.448	0.227	0.135	0.39	0.179	0.435	26,298
285	0.532	0.234	0.201	0.500	0.247	0.453	28,224
345	0.532	0.242	0.108			0.371	30,508

Parabolic and power-law curve fitting was undertaken using D/L values from the bulk foraminifer analyses, and the mean Glx D/L ratio (0.450) from SV84 131 cm depth, a last interglacial (MIS 5e) deposit. The site from which core SV84 was recovered is 35.9 km from that of SV5 and it is probable that these locations have experienced similar effective diagenetic temperature regimes.

D/L values, lithology and faunal evidence (the presence of *Marginopora vertebralis*, this study; and *Callucina lacteola*, core logs) indicate that the horizon 131 cm in core SV84 is of last interglacial (MIS 5e) age. Additionally, the mean D/L ratio of *Elphidium* tests from 131 cm depth in core SV84 is similar to that for *Elphidium* from the Anadara Beds (Glanville Formation), Port Wakefield, known to be of last interglacial (MIS 5e) age (Murray-Wallace, 1995). It could be possible these samples are reworked from the Glanville Formation into a younger late Pleistocene unit – but all of these data in this study support a last interglacial (MIS 5e) age, and there is no evidence of younger samples in this unit. This appears to be the first description of *Marginopora vertebralis*, a large benthic foraminifer that inhabits warm water associated with the Leeuwin Current on the western coastal margin of Australia. Within the southern Australian region it is associated with coastal deposits of last interglacial (MIS 5e) age, and thus its presence in core SV84, is strongly suggestive of this last Interglacial age, and is consistent with the description from the core logs that the sedimentary unit within which it was located was of the Glanville Formation – the confirmed last interglacial (MIS 5e) coastal unit in southern Australia (Murray-Wallace, 1995).

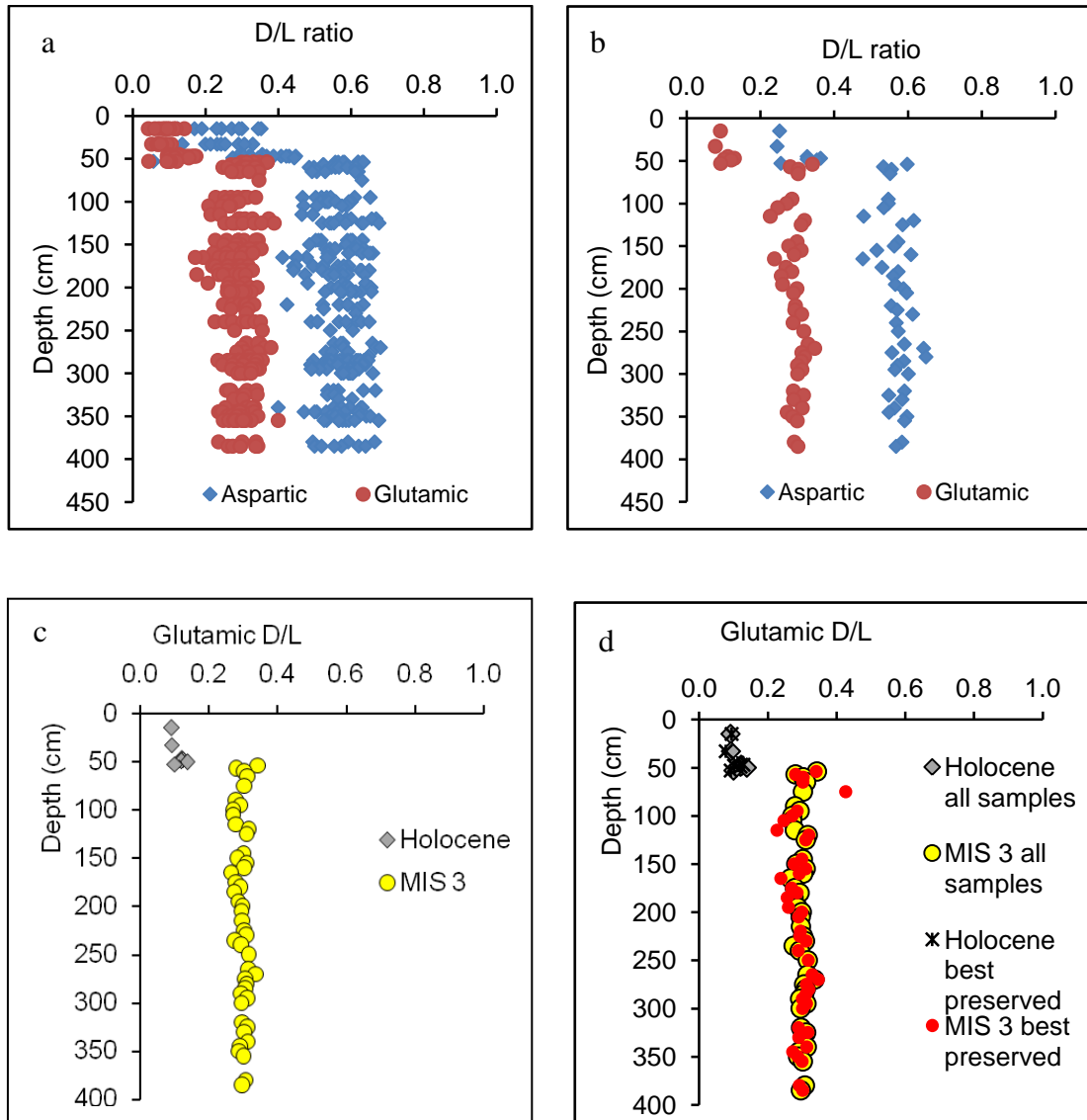


Figure 5.8. Variation in D/L values for single *Elphidium* in core SV#5. a) Aspartic and glutamic D/L values for best preserved samples from one-centimetre horizons, b) mean D/L values for each horizon, c) downcore variation in mean glutamic D/L values for all samples, d) downcore mean D/L values for all samples with the results for best preserved tests. Removal of D/L values obtained on less well preserved *Elphidium* left gaps in the downcore record, and ultimately did nothing to improve chronology, especially in light of the relationship between preservation and D/L values illustrated above (Fig. 5.4 – 5.8 inclusive).

Using both the power-law and the parabolic method of obtaining calibrated ages it was found that only D/L values from glutamic acid transformed into numeric ages similar to the AMS ^{14}C dated samples (Fig. 5.7). Therefore only Glx based ages were used thereafter for age estimation within this study. However, it must be recognised this simplifies the problem of calibrating D/L values and translating those values into meaningful ages.

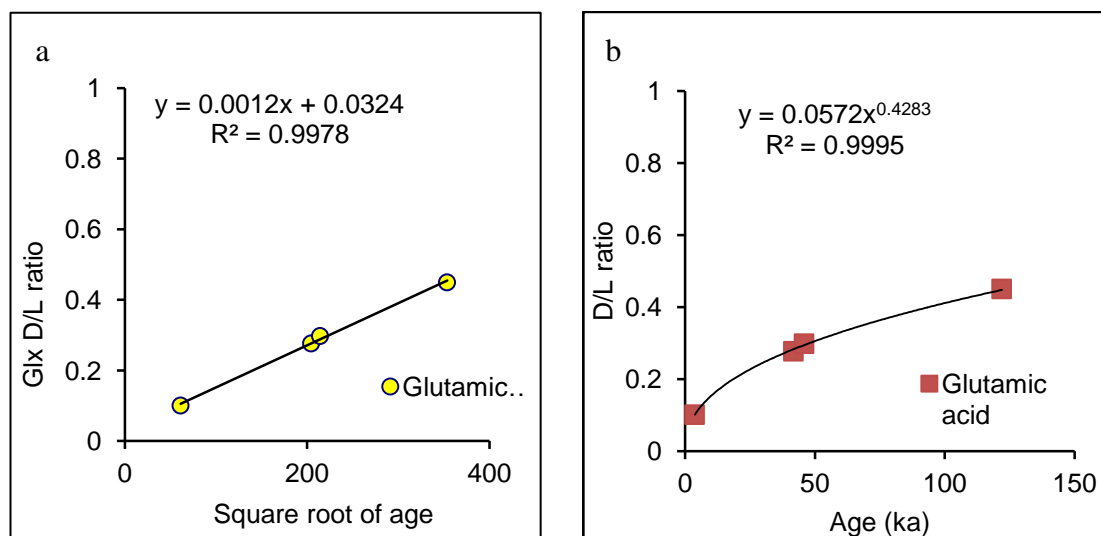


Figure 5.9. Parabolic (a) and power-law (b) curve fitting for glutamic acid D/L values from calibration samples. Only glutamic D/L values were used for obtaining ages on individual tests because the ages from this dataset were closest to matching the AMS radiocarbon ages on the calibration samples. Of these two methods of calibration, the ages obtained using the parabolic equation $y = 0.0012x + 0.0324$ were used to discuss ages. This is because the ages obtained using the parabolic equation on the calibration samples in two (AMS dated bulk *Elphidium*, at 15 and 180 cm depth) out of three occasions were closer to the AMS ages on those same samples than the power-law derived ages.

A close agreement was observed between the Glx D/L values of bulk foraminifers and mean Glx D/L values from individual foraminifers from the core slices at 95 cm and 180 cm. The results for the 320 cm horizon are exactly the same for bulk and mean individual foraminifer analyses (Glx = 0.297). It is concluded therefore that the mean D/L values from individual foraminifer tests can be used in investigations in this basin with approximately equal weight as that of the bulk foraminiferal results, because they are both representative of the total sediment population. This therefore allows the extent of reworking in this sedimentary basin to be examined with a degree of confidence.

The section of core SV5 between 0.54 and 3.85 m depth is of last interstadial age (Marine Isotopic Stage 3), based on ^{14}C -calibrated D/L values using the parabolic equation $y = 0.0012x + 0.034$ (Fig. 5.12), with a minimum calibrated age of 37,378 a, maximum of 66,392 a, and a mean age of $48,813 \pm 5,916$ a. The median age is 48,841 a. Mean aspartic and glutamic acid D/L values are similar in all portions of this pre-Holocene section of SV5 with a grand mean for coefficients of variation of 5.7% (Asx) and 7.9% (Glx). However, the ages obtained on aspartic and valine varied substantially in some cases from that of glutamic acid, and were therefore not used further. Single foraminifer D/L values coupled with the whole rock and bulk AAR results indicate that this portion of core SV5, from 53-390 cm depth, is either mixed, time-averaged over some part or all of the range of MIS 3 timescales (i.e. approximately 38,000 to 66,000 years), or deposited over a relatively short period of time given the minimal change in D/L values downcore from 54 cm to 385 cm depth. It is likely

that both of these processes have contributed to the distribution of D/L values in the *Elphidium* tests, downcore in SV5. A significant proportion of the sediments within the Holocene section of SV5 include reworked tests of MIS 3 age (Fig. 5.12).

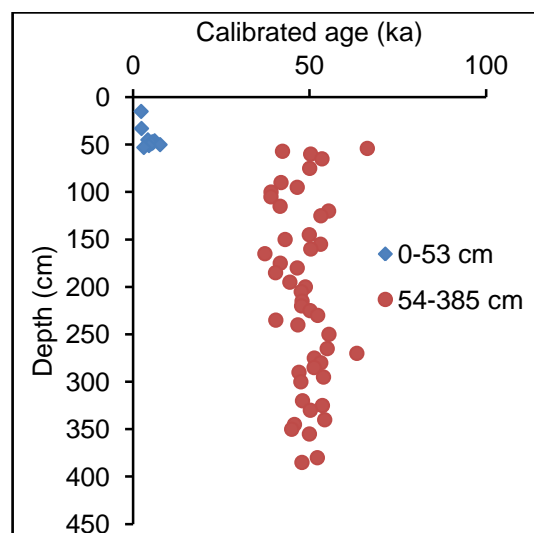


Figure 5.10. Variations in ^{14}C -calibrated AAR ages in sidereal years, for core SV5 based on mean D/L values for glutamic acid in single *Elphidium* tests from one-centimetre slices. Calibrated ages were obtained using the parabolic equation $y = 0.0012x + 0.0342$.

5.6.5. Modern and surface samples

In addition to foraminifera tests and whole-rock samples analysed from core SV5, a total of 21 additional samples of *Elphidium* tests were analysed from 9 cores samples, 2 submarine surface samples from the locations of cores SV37 and SV38, 2 samples from intertidal sediment surfaces at Port Gawler, and a single sample from a last interglacial (MIS 5e) coastal deposit at Port Wakefield. The distribution of D/L values for the amino acids aspartic and glutamic in these additional samples are similar to those from SV5, allowing the calibration to sidereal years of these D/L values with the parabolic equation presented above (Fig. 5.10).

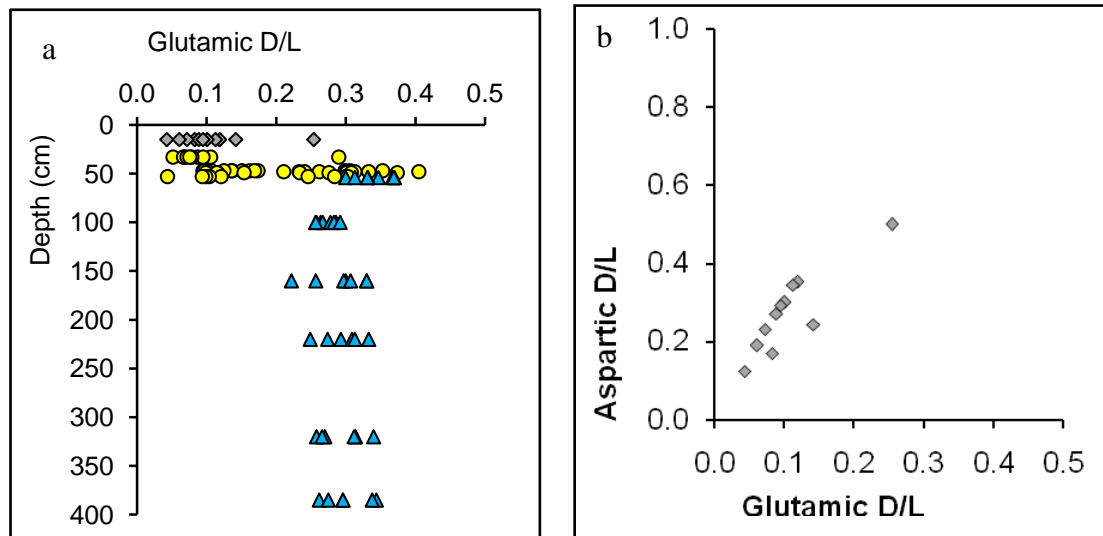


Figure 5.11. a) Results from (randomly chosen) one centimeter horizons illustrating that mixed-age *Elphidium* populations that were present above 53 cm in core SV5 are notably absent from horizons below this boundary. b) Grey diamonds represent D/L values from single *Elphidium* recovered from the 15 cm horizon, SV5. These results are from best preserved samples. Of note are the presence of glutamic D/L values between approximately 0.15 and 0.24 that are indicative of MIS 2 ages.

These foraminifers range in age from a few years to approximately 125,000 years. The youngest *Elphidium* were located in core SV35, 30-34 cm depth, with a mean age of 48 years. Mixed-age assemblages, consisting predominantly of Holocene and MIS 3 age foraminifers were found in SV109, SV25, SV108 and SV11. It is notable that the locations of cores in which *Elphidium* tests of MIS 3 age exist are within the deeper and central section of Gulf St Vincent in water depths of -30 -40 m, and distal from shallow coastal waters. These water depths contrast with the -22 to -28 m palaeo water depth deduced for these MIS3 sediments from the ratio of benthic foraminifera in present-day surficial and core sediments within Gulf St Vincent and Spencer Gulf (Cann *et al.*, 1988, 1993; Murray-Wallace, 1993)

Results from grab samples (SV37, 38, and intertidal surface samples Port Gawler 2A and 5F) indicate Holocene ages for *Elphidium* at these locations.

The oldest mean ages, equating with marine isotopic stage 5e were obtained from core SV84 131 cm (Glx D/L = 0.446 ± 0.055), and from the Anadara Beds at Port Wakefield (Glx D/L = 0.420 ± 0.035)

MIS 3 results, oldest first are SV20 282 cm (Glx D/L = 0.331 ± 0.024), SV5 57-385 cm (Glx D/L = 0.293 ± 0.037), SV25 232 cm (Glx D/L = 0.312 ± 0.120), SV25 242 cm (Glx D/L = 0.248 ± 0.061). Holocene results may be divided into those core horizons with reworked MIS 3 forams and those without.

Significantly, the youngest mean calibrated age was obtained on samples from SV35 30-34 cm depth (Glx D/L = 0.045 ± 0.003) having a mean age of 82 a. Surface samples from Port Gawler were the next oldest, - sample 5F recovered from the vicinity of an intertidal ebb tide

delta set within an intertidal *Zostera* – *Katylsia* zone, had a mean age of 499 a (Glx D/L = 0.054 ± 0.019), while those of sample 2A, obtained from a flood tide delta sand bar at Port Wakefield had a mean age of 2,564 a (Glx D/L = 0.088 ± 0.031).

The lowest age on a single *Elphidium* test was from Port Gawler, (surface sample 5F) with a calibrated age of 2 a. The oldest test in this sample had a calibrated age of 2,652 a.

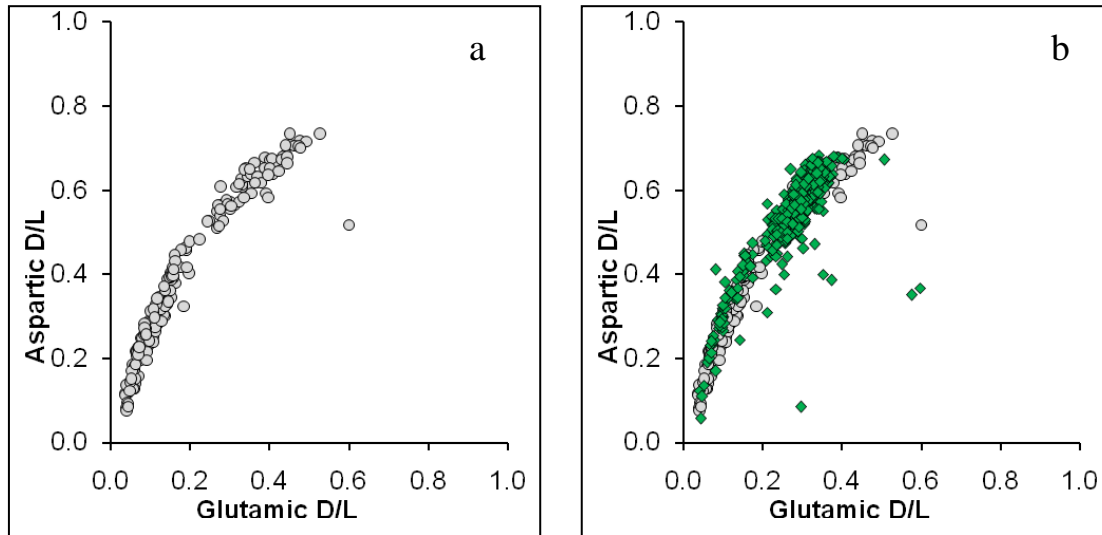


Figure 5.12. Covariance of aspartic and glutamic D/L values for a) data other than that from core SV5, and b) both sets of data, with the results from all preservation grades (green diamonds) from core SV5 overlying the data from other core and surface samples. It is evident from a) that racemization in these tests is non-linear, and that the apparent break in slope occurs approximately at a glutamic D/L of 0.2 (equivalent to MIS 2 age, c. 20 ka).

5.7. Discussion

5.7.1. Previous ^{14}C dating of molluscs from central Gulf St Vincent

AMS radiocarbon ages obtained here on bulk foraminifer test samples are generally older than those previously obtained by conventional β -counting on molluscs for similar depths in core SV5 (Table 5.3, Fig. 5.14), (Cann *et al.*, 1988; Murray-Wallace *et al.*, 1993). Additional radiocarbon ages, also undertaken by conventional β -counting, on bivalve molluscs from core SV23 (Cann *et al.*, 1993) are similar to and therefore support the earlier determinations (Cann *et al.*, 1988; Murray-Wallace *et al.*, 1993). The bivalve mollusc *Ostrea* precipitates calcite (Murray-Wallace *et al.*, 1993), as does the foraminifer *Elphidium*, and therefore this is unlikely to be the source of the discrepancy in ages because there is no metastable aragonite in these samples.

Table 5.5. Previous ^{14}C dating (after Cann *et al.*, 1988, 1993)

Lab code	Core and depth (cm)	Altitude relative to present mean sea level (m)	$\delta^{13}\text{C}$ PDB	Conventional ^{14}C age yr B.P.	Material dated
CS-545	SV5-25	-36.7	1.4	1940 \pm 90	<i>Chlamys (Equichlamys) bifrons</i>
CS-546	SV5-140	-37.8	1.4	37,600 (+ 1700 - 1400)	<i>Katelysia rhytiphora</i>
CS-547	SV5-161	-38.0	0.9	> 40,000	<i>Ostrea angasi</i>
CS-662	SV5-196	-38.4	2.72	37,700 (+ 3000 - 2200)	<i>Ostrea angasi</i>
CS-548	SV5-370	-40.1	1.0	45,100 (+ 5100 - 3100)	<i>Ostrea angasi</i>

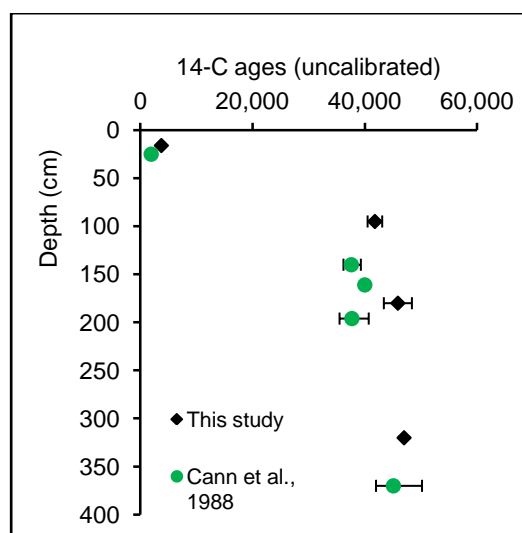


Figure 5.13. Similarities in radiocarbon ages among samples of bulk *Elphidium* tests, and previously dated bivalve molluscs in core SV5 (Cann *et al.*, 1988; Murray-Wallace, *et al.*, 1993). The data are in broad agreement, but some of the potential differences may relate to improvements in radiocarbon sample pretreatment and improvements in ‘background’ values.

5.7.2 Relative extents of racemization and comparison with previous AAR data

D/L values obtained from the analyses of single *Elphidium* tests were slightly lower than for the bivalve mollusc, *Katelysia* at similar horizons in core SV5. This relationship was also observed between these taxa recovered from the ‘Anadara Beds’ Port Wakefield, northern Gulf St Vincent, and also from Wallaroo, mid Spencer Gulf, both of which are last interglacial (MIS 5e) age. In general, the extent of racemization between these taxa determined for aspartic acid were similar, but glutamic D/L values were higher in these molluscs than for the foraminifer tests.

Based on the extent of amino acid racemization in the amino acid valine, D/L values measured in this study from specimens of the bivalve mollusc *Katelsysia* (Fig. 5.10) are generally higher than that previously reported for this genus, and higher in general than for other molluscs in southern Australian last interglacial (MIS 5e) and last interstadial strata (Cann *et al.*, 1988; Murray-Wallace *et al.*, 1993; Murray-Wallace, 1995, 2000). These data appear to indicate systematically higher D/L values for these molluscs over previous studies in this region using gas chromatography (Murray-Wallace, 1995, 2000).

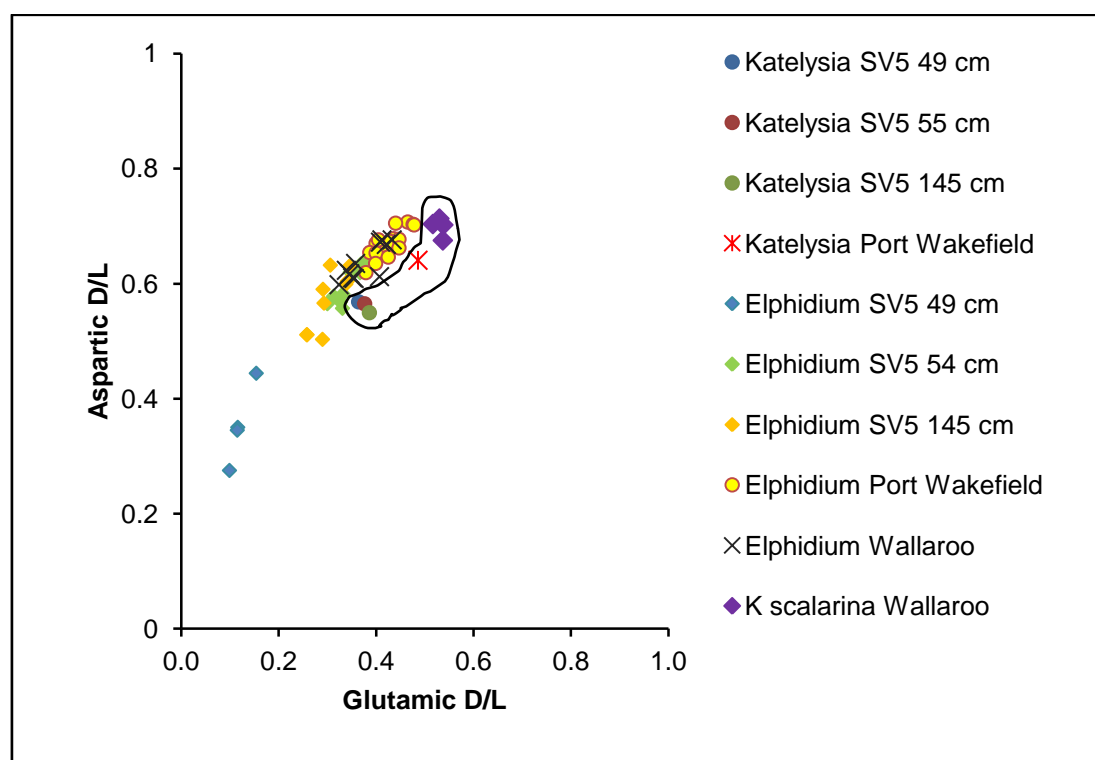


Figure 5.14. D/L values for *Elphidium* and the shallow-water bivalve mollusc *Katelsysia* (circled) obtained using RP-HPLC (this study). The specimen of *Katelsysia* at 49 cm depth in SV5 has been reworked from the underlying unit determined here (and previously) to be of MIS 3 age (Cann *et al.*, 1988; Murray-Wallace, 1993). The presence of reworked tests of the Foraminifer *Elphidium* was also noted in all Holocene sections of core SV5 during this study.

Murray-Wallace *et al.* (2010) note a similar phenomenon using *Katelsysia rhytiphora* from the Woakwine Range (125 ka, MIS 5e) with mean valine D/L values of 0.223 ± 0.08 from RP-HPLC and a higher mean valine D/L value of 0.248 ± 0.026 using GC. The sample size required for gas chromatography is significantly greater (1-2 g, commonly a whole shell) than that for this reverse-phase liquid chromatography (here between 0.01 and 0.005 g was used). Recent work by Wehmiller (unpublished) has also highlighted this issue in an interlaboratory comparison study. These differences appear to be related to the different methods used for GC and RP-HPLC. This is because the preparatory procedures for both GC and RP-HPLC of

the sample are the same, therefore the difference must lie in the chromatographic system, including for example in the derivatizing reagent and column stationary phase used.

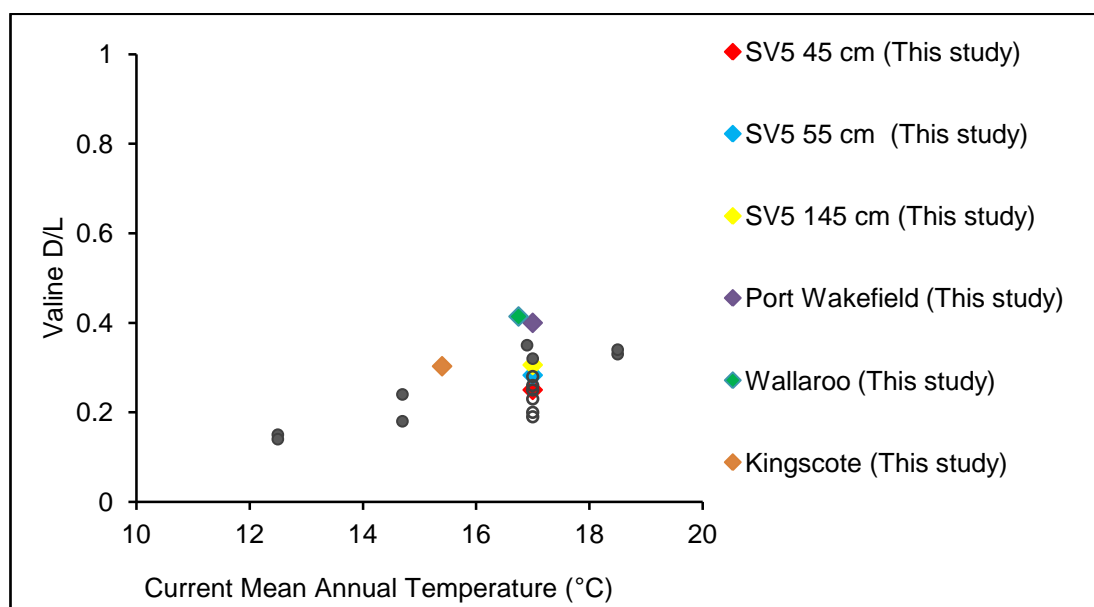


Figure 5.15. Comparison among valine AAR data for the bivalve mollusc *Katelysia* from South Australian study sites (Murray-Wallace 1995, 2000). The amino acid Valine is used here because there are no data for glutamic acid. The samples of *Katelysia* from SV5 are of MIS 3 age, the samples from Port Wakefield are from the last interglacial (MIS 5e) highstand coastal deposit, and those shells from Wallaroo, are also of last interglacial (MIS 5e) age, based on the comparison of their D/L values with those of core SV5 and Port Wakefield.

5.7.3 Age mixing

Based solely on the extent of amino acid racemization of single *Elphidium* from one-centimetre slices of core SV5, and subsequent calibration using ^{14}C ages on bulk foraminifer samples, it appears that the MIS 3 portion of this core from 54 to 385 cm is time-averaged over the range of ages of marine isotope stage 3. However because the age resolving power of the amino acid racemization dating method is lower than for example that of radiocarbon dating, it could also be inferred that the similarity of ages in this unit are the result of the rapid deposition of skeletal carbonate within Gulf St Vincent at some point around 48 ± 6 ka BP. However, this is dependent on the scale of observation, with deposition over a time slice of perhaps 1-2 ka while not being particularly rapid (see chapter 6) is short when compared to the length of time *since* deposition.

The absence of foraminifers of last interglacial (MIS 5e) age in these sediments suggests that very little sediment within the present day central Gulf St Vincent basin has been derived from a pre-existing Late Pleistocene source. In contrast with the indurated sediments of the

Late Pleistocene Glanville Formation, MIS 3 sediments must have been unconsolidated at the time of the ingress of marine water during and after the Holocene transgression for them to be incorporated into the Holocene section of core SV5. This may suggest little sediment was deposited during MIS 2 in Gulf St Vincent, where cooler and perhaps even drier conditions may have prevailed.

Reworked bioclasts included both molluscs and microfossils. Indeed, age-mixing of single *Elphidium* was evident in all one-centimetre slices from 15 to 53 cm depth. It is unlikely that mixing to this extent was solely caused by the post-glacial marine transgression. Bioturbation and reworking of shallow-water sediment into the deeper parts of the Gulf St Vincent basin are perhaps also responsible for this. Storm-driven disturbance including resuspension of bottom sediments may also contribute to the stratigraphic disorder in these sediments. Similar conclusions were drawn on shells in cores to a depth of 50 cm from tidal flats in Choya Bay, Gulf of California (Flessa *et al.* 1993). Shrimp and polychaete worms have been reported to bury bioclastic sediments to at least 60 cm depth (Martin *et al.*, 1995). It is likely that the depth of reworking in Gulf St Vincent is similar because similar taxa are present. Thus the taphonomically active zone extends to this depth in Gulf St Vincent.

Coefficients of variation among the additional samples (Table 5. 4) from Gulf St Vincent are similar to the values obtained from the Holocene section of SV5, are similarly higher than would be expected for homogenous samples, and also indicate that these data are time-averaged and mixed. These basin-wide data appear to support observations (Shepard and Sprigg, 1976) describing sediments being physically and biologically reworked within the Gulf. It is highly likely that similar processes were also occurring during the Last Interstadial.

The results presented here raise some questions concerning Cann *et al.*'s, (1988) *Elphidium* species/depth ratio for Gulf St Vincent. Those values were built on empirical data collected from the analysis of 'modern' grab samples across the gulf. However, the evidence presented here suggests that the present distribution of *Elphidium* tests within Gulf St Vincent may not actually represent the spatial distribution of living *Elphidium* in the gulf. An example is the samples of *Elphidium* from Port Gawler, which were recovered from a tidally-dominated intertidal zone in which dead articulated *Katelsia* are commonly transported shorewards over a distance of ~ 2 km or more by wave action produced by onshore winds, and currents (this study, based on the observation of this phenomenon at Port Gawler). The sediments in which those shells lived are also being transported and thus also any living or dead *Elphidium* will be reworked. There are no live-dead studies on foraminifera from this location to base a hypothesis that indicates the species found in grab samples are representative of those locations, and therefore the *Elphidium* ratio only refers to dead, and probably transported specimens. The reworking of foraminifera and molluscs within shallow tidal and subtidal

environments of Gulf St Vincent is occurring at the present-day (this study, based on observation at Port Gawler). This conclusion is supported by the data from Holocene samples noted here, with significant age-mixing of Late Pleistocene and Holocene foraminifera in these sediments. In particular, all of the samples within the post-glacial (i.e. Holocene) sediments analysed in this study display some degree of age-mixing, and in surficial samples there were few perfectly preserved tests likely to represent most-recently deceased specimens. The young ages obtained on foraminifera, from Core SV35, 30-34 cm depth, suggest either reworking of sediment, or, *Elphidium* may have lived at shallow depths within the relatively porous sediment. If reworking is the cause of the presence of such young tests within the core, then this supports the argument for significant reworking. On the other hand, if some of these samples actually were live recently at 30-34 cm depth in the sediment, this suggests that a) it probably happens elsewhere in this basin, and b) the presence of unrecognised infauna may partially explain the apparent age mixing of Holocene sediments in this location. D/L values alone will not solve this issue – only studies of live/dead foraminifera within Gulf St Vincent will answer this question.

One of the major issues in this study was the presence of possible MIS 2 age tests (i.e. last glacial) in MIS 3 and Holocene sediments. Reworked tests in the Holocene portion of core SV5 and the additional cores were of MIS 3 age, present in Holocene sediments. A small population of *Elphidium* tests had Glx D/L values ranging between approximately, 0.150 to 0.235 and calibrated ages of 17 to 24 ka. These ages were calculated using the equation in Fig. 5.10, $y = 0.0012x + 0.0324$. The intercept, $c = 0.0324$, is less than, but close to, the lowest glutamic D/L ratio ($glx = 0.036$) measured in this study, obtained on a single *Elphidium* test from a surface sample of the present-day tidal flats at Port Gawler.

These results were removed from the population of results for chronology, but their presence requires explanation. MIS 2 is the period of the LGM with regressive sea-levels of up to c. - 120 m compared to present-day (e.g. Waelbroek et al., 2002).

Table 5.6. Mean D/L values from samples in adjacent cores, and surface samples from Gulf St Vincent. Ages were obtained using the same equation as for SV5 (Fig. 5.10).

Sample source	Depth (cm)	N =	Glu D/L	Stdv	CV (%)	Calibrated parabolic age (yrs)
SV35	30-34	6	0.045	0.003	7.31	48
5F	0	8	0.054	0.019	36.12	441
SV109	19-22	9	0.072	0.022	30.30	1180
SV107	10-13	11	0.079	0.039	49.6	2298
SV 37	0	8	0.086	0.022	25.214	2266
2A	0	6	0.088	0.031	35.61	2438
SV71	51-54	7	0.091	0.020	21.59	2351
SV25	22	7	0.098	0.025	25.07	3026
SV71	29-31	6	0.111	0.022	19.64	4157
SV 38	0	6	0.115	0.034	30.87	4691
SV109	6-8	4	0.107	0.024	22.58	3802
SV111	79-83	3	0.146	0.007	5.06	8503
SV109	49-52	4	0.132	0.026	19.78	6881
SV109	58	4	0.137	0.016	11.96	7323
SV108	28-31	3	0.119	0.024	20.53	5111
SV25	242-244	5	0.273	0.015	5.60	40020
SV25	232-234	6	0.279	0.027	9.83	42552
SV20	282-287	10	0.331	0.024	7.22	62363
SV84	131-134	2	0.450	0.008	1.73	122334
Port Wakefield		8	0.452	0.018	4.05	124236

These values may be the result of leaching of indigenous amino acids from foraminifers of MIS 3, or older, age. However, the results of the study undertaken here comparing preservation with D/L values, in this case, suggests that leaching has not been a significant problem for these tests composed of stable calcite. Indeed, removal of the results measured on less well preserved tests did not change the results significantly (Fig. 5.14). It would be expected that D/L values would be lowered in less well preserved tests if there were significant diffusive leaching of amino acids from these samples. Yet this was not found here – graphical evidence (Fig. 5.14) suggests that there has been no diffusive leaching of amino acids and subsequent lowering of D/L values in less well-preserved tests because both datasets plot together. In contrast, removal of results that were anomalous on the basis of low serine D/L values and high contamination indices resulted in a subset of data clearly different from those of both the best preserved samples (Fig. 5.15), and based on the downcore distribution in D/L values for all tests (Fig. 5.14) these rejected results were also different from the results of all other tests in core SV5.

Elphidium is an intertidal to shallow-water foraminifer, and requires the presence of marine or saline estuarine (i.e. brackish) waters to live. If there was a saline lake facies present above the MIS 3 sediments it would be quite feasible for MIS 2 ages to be obtained on foraminifera in the Holocene section of core SV5. The semi-consolidated nature of the MIS 3 section of core SV5 would possibly make the reworking of *Elphidium* tests downcore (to 3 m depth in the core) extremely unlikely. This is unless these sediments only became somewhat consolidated later. It is possible that the parabolic and power-law curve fitting does not allow for these lower D/L values to be calculated as ages that are representative of the true age of these tests. The linear nature of the aspartic-glutamic D/L pairs for low and moderate D/L values, and the non-linear aspect of parabolic curve fitting may be partly responsible for these data.

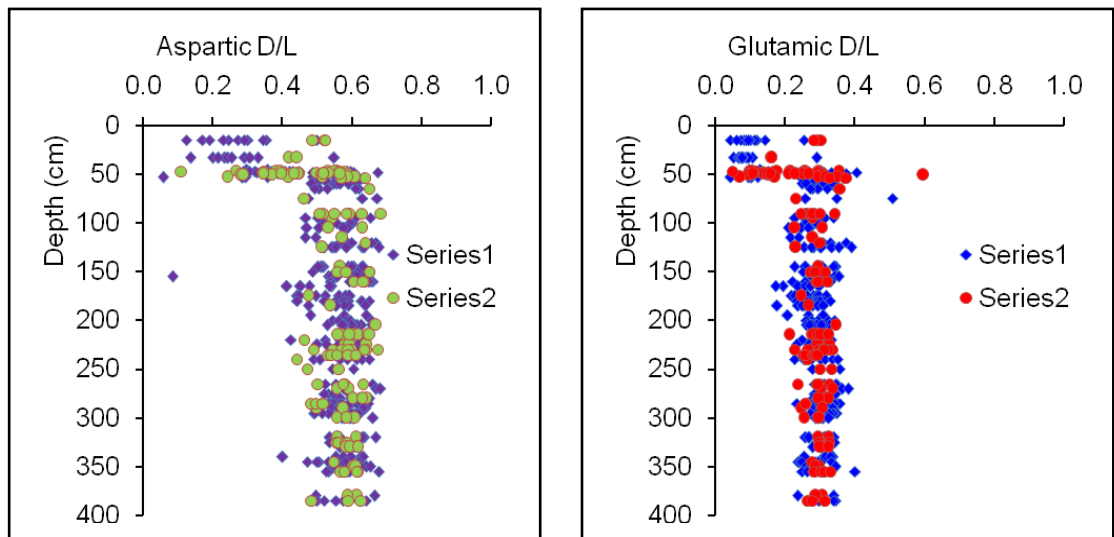


Figure 5.16. Screening of D/L values in SV5. Series 1 samples retained, Series 2 samples removed because they were less well preserved, and in the Holocene section of SV5 tests were removed to get a mean age for each horizon that did not include reworked *Elphidium*. *Elphidium* tests removed because of poor preservation did not have (overall) abnormally different D/L values. It was concluded that visual preservation discrimination does not provide the best method of differentiating between ‘good’ and ‘bad’ *Elphidium* tests for AAR.

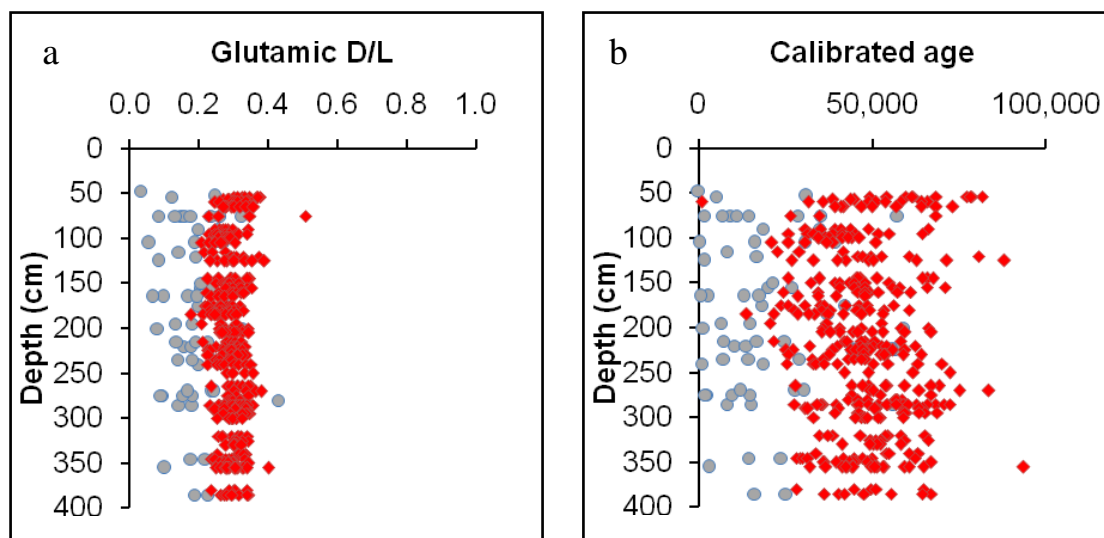


Figure 5.17. a) D/L values and b) calibrated ages calculated for single *Elphidium* tests in core SV5. Differentiation of D/L values and calibrated ages between the results from individual rejected tests (grey circles) and those of the best preserved tests (red diamonds). Using the formula in Fig. 5.10a ($y = 0.0012x + 0.0324$, where $y = mx + c$) a glutamic D/L value of 0.2 will give a calibrated age of 19,506 a, while a glutamic D/L of 0.35 will give a calibrated age of 70,050 a. A similar distribution of ages was found using the power law equation in Fig. 10b. This parabolic equation results in an age of 650 ka for a racemic glutamic D/L value.

The concentration of the amino acids, aspartic, glutamic and serine, in all samples consisting of single tests (bleached for one hour) were equivalent, being in the range of $1\text{--}7 \times 10^{-11}$ mol (10–70 pico-moles) per 1g mass of *Elphidium* tests (Fig. 5.19a). In addition, broken and degraded *Elphidium* tests of last interglacial (MIS 5e) age from Kingscote, Kangaroo Island, and modern *Elphidium* tests from the estuary of the Minnamurra River, New South Wales, also had similar concentrations of these amino acids. The results from tests removed during the initial screening of results also indicate concentrations of these amino acids of approximately 6×10^{-11} mol per 1g mass of *Elphidium* tests. This evidence suggests strongly that there has been insignificant diffusive leaching of amino acids from the rejected samples (Fig. 5.19a). Given this, it is possible that the anomalous results in these tests are a product of contamination by younger amino acids.

The extent of racemization varies for a single amino acid in tests of comparable age, even where the same D/L ratio is recorded for one amino acid from several tests (Table 5.2). Aspartic and glutamic acid D/L values tend to have less variation than alanine and/or valine between samples. For a fixed Asx or Glx value the coefficients of variation for the corresponding Glx or Asx data are approximately 5%. This is less than mean Glx values from a number of the individual core slices between 54 cm and 385 cm depth, and is generally significantly lower than for Holocene coefficients of variation for these amino acids. This therefore is unlikely to be the reason for the significant variation in those aberrant Glx D/L values for the core section between 54 cm and 385 cm depth. It is therefore argued that the

incorporation of contaminating organic acids is the reason for the presence of apparent MIS 2 age foraminifers in both Holocene and MIS 3 sediments within Gulf St Vincent because there is no evidence to suggest diffusive loss of amino acids, and the downcore mixing of *Elphidium* tests younger than MIS 3 seems unlikely.

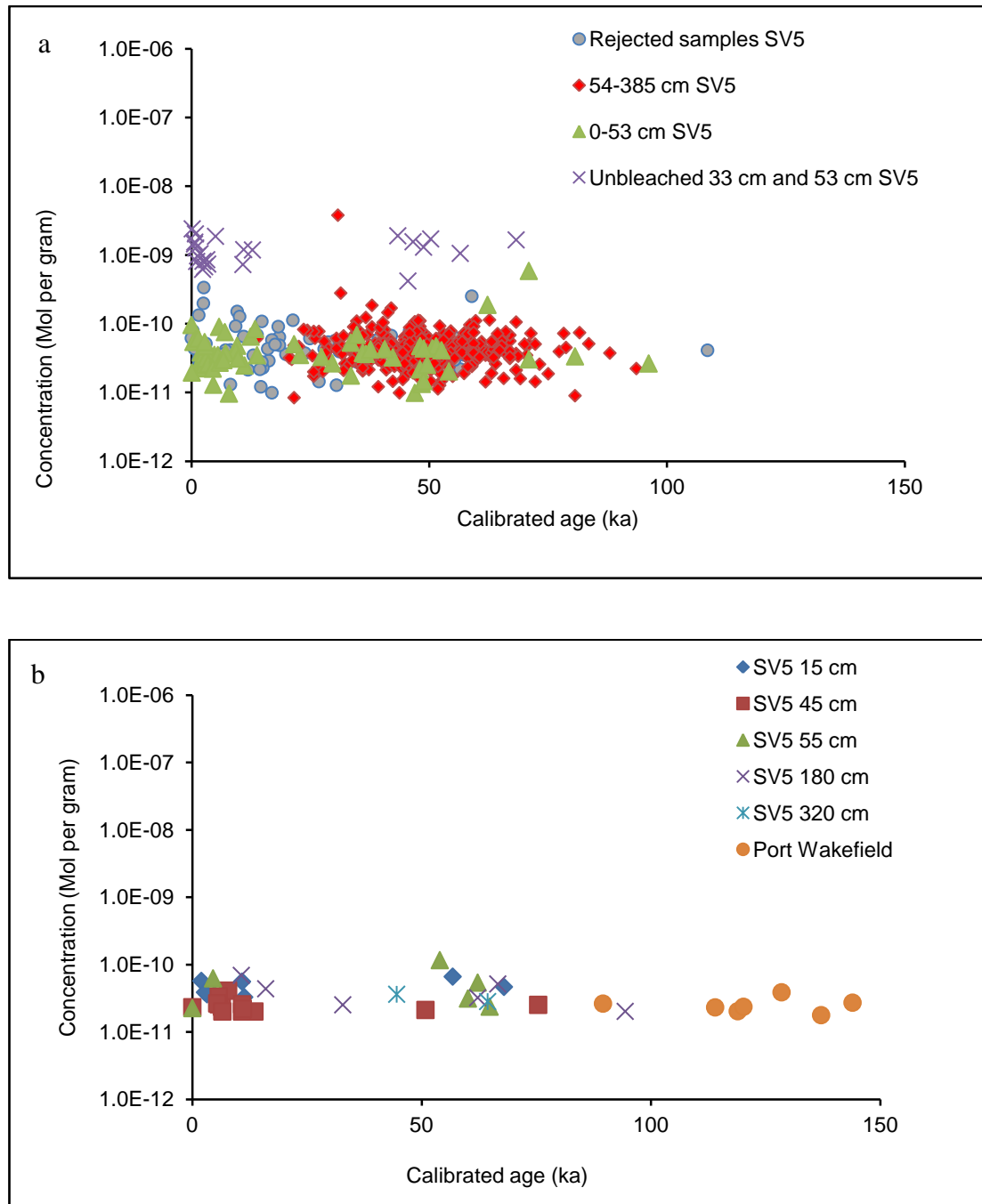


Figure 5.18. a) Concentration summed for the amino acids aspartic, glutamic and serine in single *Elphidium* tests from core SV5, Gulf St Vincent bleached for one hour using 12.5% NaOCl. b) total concentration of the amino acids aspartic, glutamic and serine in individual tests of the foraminifera *Elphidium*, bleached for 48 hours with 12.5% NaOCl. This suggests that intercrystalline amino acids within these foraminifera may be lost rather quickly by oxidative processes, to leave behind a higher proportion of intracrystalline amino acids.

Table 5.7. Variations in D/L values among *Elphidium* tests with one fixed D/L value – here either glutamic is fixed, or aspartic acid.

Depth	Asx	Glx	Ser	Ala	Val	L-Ser/L-Glx	Calibrated Asx age	Calibrated Glx age
150	0.617	0.297	0.241	0.456	0.26	0.331	58,859	48,579
160	0.593	0.297	0.308	0.517	0.29	0.228	53,411	48,579
160	0.635	0.297	0.192	0.531	0.312	0.333	63,118	48,579
165	0.534	0.297	0.19	0.426	0.239	0.289	41,144	48,579
215	0.616	0.297	0.201	0.469	0.299	0.267	58,627	48,579
235	0.586	0.297		0.515	0.267	0.141	51,872	48,579
300	0.609	0.297	0.167	0.461	0.311	0.331	57,014	48,579
300	0.583	0.297	0.234	0.512	0.313	0.251	51,220	48,579
Mean	0.597	0.297	0.217	0.488	0.282	0.272	48,675	48,579
STDV	0.0308	0	0.044	0.036	0.0291	0.062	18,304	0
CV (%)	5.166	0	20.270	7.379	10.311	22.713	37.60	0.00
205	0.577	0.276	0.33	0.509	0.335	0.138	49,927	41,046
185	0.577	0.279	0.231	0.687	0.19	0.192	49,927	42,083
355	0.577	0.287	0.264	0.514	0.261	0.178	49,927	44,913
355	0.577	0.306	0.195			0.243	49,927	52,002
325	0.577	0.309	0.302	0.535	0.278	0.208	49,927	53,169
Mean	0.577	0.291	0.264	0.561	0.266	0.192	49,927	46,643
STDV	0.000	0.015	0.054	0.085	0.060	0.039	0	5,622
CV (%)	0.00	5.24	20.41	15.07	22.46	20.14	0.00	12.05

5.7.4 MIS 3 Bathymetry

The distribution of last interstadial tests within the samples recovered from Gulf St Vincent indicate a spatial distribution of last interstadial sediment that is restricted to bathymetric depths of -30 m or below (Fig. 5.17). Evidence for MIS 3 sediments in shallower present-day environments was not found in this study, nor are these described in the core logs for Gulf St Vincent. Based on the present-day bathymetry this distribution appears to indicate a water depth within the gulf of c. 10 m during the latter part of the last interstadial, and therefore indicates sea-levels of c. -30 m compared to present-day values. The spatial distribution is restricted to the mid-gulf area, stretching from the locations of cores SV4 and 5, to SV20 (Fig. 5.17).

This estimate of the maximum sea-level of -30 m and minimum of -43 m is based on the depth distribution of MIS 3 aged sediments in Gulf St Vincent (this study; core logs; data in Cann *et al.*, 2006). These estimates for sea-level are approximately 8 (maximum) and 13 m

(minimum) below the estimate of Cann *et al.*, (1988) and Murray-Wallace *et al.*, (1993) for palaeo- sea-levels at -22 to -30 m during the latter part of MIS 3, and differ somewhat to the values proposed by Chappell *et al.*, (1996), ranging between -53 and -37 m for the peak of MIS 3 at 45.8 ± 0.7 ka (Holland and Murray-Wallace, 2003), though the value of -37 m is within the height range proposed here.

An alternative estimate for sea-level during MIS 3 (Fig. 5.21) is of -30 to -60 m for the time period 45,000 – 50,000 a BP (Cabioch and Ayliffe, 2001). This is close to the results of this study, as is the estimate of Shackleton (2000) at 50,000 a BP. It is probable that these three estimates are on the same high-stand of sea-level, with variations in ages due to differences in dating methods.

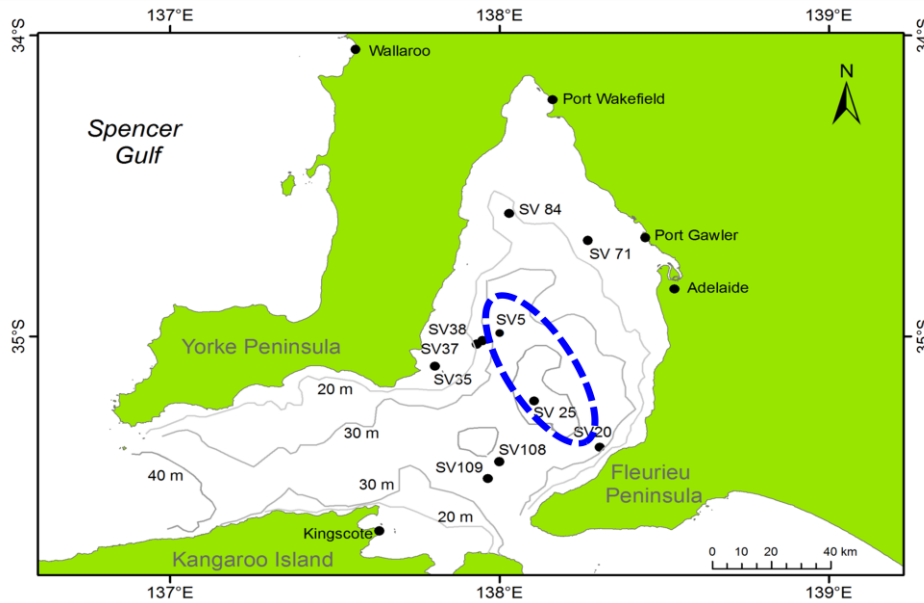


Figure 5.19. The spatial distribution of Marine Isotope Stage 3 sediments within Gulf St Vincent are restricted to the central basin, approximately centered on the location of core SV25. This area exists below the -30 m isobath, suggesting that there was no more than 13 m of water within the Gulf at that time from the intertidal zone to the deepest sections of the basin.

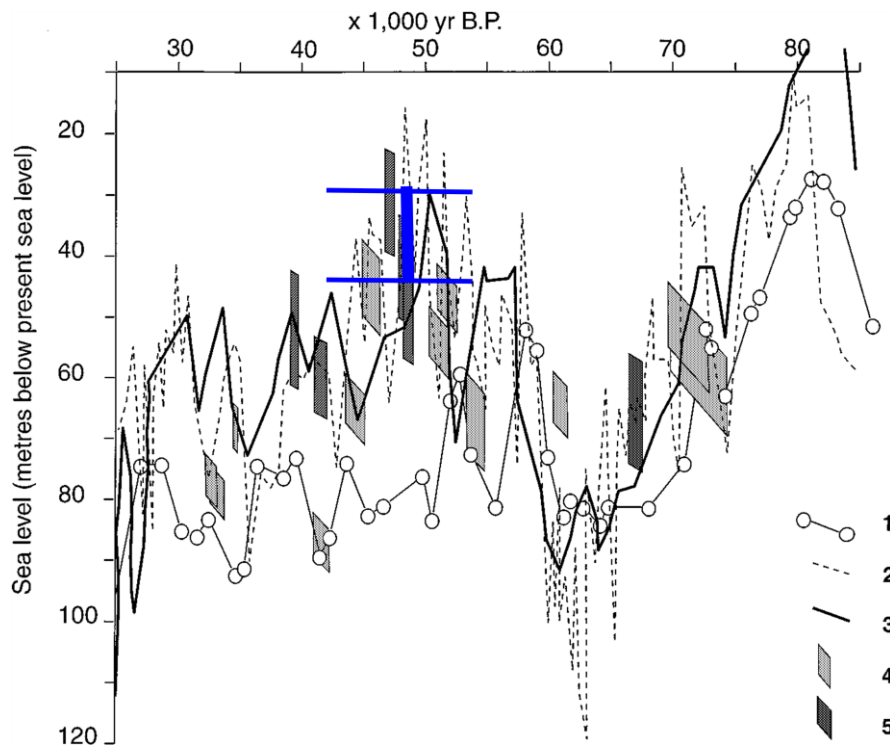


Figure 5.20. Estimates for the height of sea-level derived in previous studies, adapted from Cabioch and Ayliff, 2001, compared with the estimate obtained in this work (blue line and estimates of uncertainty for the upper and lower sea-level estimates) of between -30 and -43 m, dated to $48,800 \pm 6,000$ a. Sea-level curves: 1, Shackleton, 1987, after Chappell *et al.*, 1996; 2, Sulu Sea (Linsley, 1996); 3, Shackleton, 2000; 4, PNG coral terraces (Chappell *et al.*, 1996); 5, Malakula coral terraces, Vanuatu (Cabioch and Ayliffe, 2001).

5.8 Chapter summary

- Based on AMS ^{14}C calibration of single *Elphidium* glutamic acid D/L values using a parabolic age model, it has been found that core SV5 is composed of two sedimentary units. These are an interstadial unit of approximately 49 ± 6 ka age for the sedimentary package between 54 and 390 cm depth, and the sediment from between 0 and 53 cm depth is of Holocene age ($< 7,700$ a BP).
- Both of these strata are composed of mixed-age foraminifer tests and molluscs.
- Whereas the last interstadial portion of SV5 is mixed interformationally with no significant evidence for the incorporation of pre-existing sediments, the sediments of the Holocene section of SV5 incorporate to a large extent Last Interstadial age *Elphidium* tests.
- The distribution of Last Interstadial tests within Gulf St Vincent is restricted to present-day bathymetric values of -30 m to -43 m, and indicates water depths for the Last Interstadial, corresponding with mid-late MIS 3, of c. 10 m above the present lowest gulf floor.
- This study differs from Cann *et al.*'s (1988) estimate for sea-levels of -22 to -30 m in Gulf St Vincent during MIS 3, indicating sea-levels closer to that of Cabioch and Ayliff (2001) and Shackleton (2000). Furthermore, the age-mixing of foraminifer tests in core SV5 does not support the previous hypothesis (Cann *et al.*, 1988) that *Elphidium* values are directly related to water depth in the last interstadial Gulf St Vincent.

Acknowledgements

Grateful thanks go to Mary-Anne Binnie for the samples from Port Gawler, and to John Cann for grab samples from the locations of cores SV37 and SV38, and to both for subsequent discussions on this topic. ^{14}C AMS ages were obtained under grant no. 06/134 from AINSE to Prof. Colin Murray-Wallace.

Chapter 6

Prompt transgression and gradual salinisation of the early Holocene Black Sea constrained by amino acid racemization and accelerator mass spectrometry dating

Published as: Nicholas, W. A., Chivas, A. R., Murray-Wallace, C. V., Fink, D., 2011. Prompt transgression and gradual salinisation of the early Holocene Black Sea constrained by amino acid racemization and accelerator mass spectrometry dating. *Quaternary Science Reviews* 30, 3769-3790.

6.1 Outline

This chapter and the next are based on the application of AAR methods to the topic of the timing of sea-level change in the Black Sea. Though originally planned as part of one project on the Black Sea, the stratigraphy and location of the study sites investigated required this work to be investigated as two discrete studies rather than one. This chapter presents the results on the post-glacial Black Sea, while Chapter 7 presents the results from older, last interglacial (MIS 5e) age strata.

6.2 Introduction

Many studies have attempted to confirm or refute the Ryan *et al.* (1997) hypothesis of an early Holocene catastrophic flood into the Black Sea basin (Fig. 6.1), using data from both conventional (β , or scintillation counting) and accelerator mass spectrometry (AMS) radiocarbon methods (e.g. Uchupi and Ross, 2000; Görür *et al.*, 2001; Aksu *et al.*, 2002; Ryan *et al.*, 2003; Bahr *et al.*, 2006; Giosan *et al.*, 2006; Major *et al.*, 2006; Hiscott *et al.*, 2007; Ivanova *et al.*, 2007; Konikov *et al.*, 2007; Ryan, 2007; Sorokin and Kuprin, 2007; Yanko-Hombach, 2007; Dolukhanov *et al.*, 2009; Giosan *et al.*, 2009; Lericolais *et al.*, 2009; Marret *et al.*, 2009). Shcherbakov (1991), who first proposed an “instantaneous flooding” of Crimean shelves (i.e. the Black Sea), described a late Pleistocene to Holocene transgression without evidence for reworking of previously exposed ‘plains and lagoons’. This hypothesis was derived in part from conventional (β -counting) radiocarbon dating of bulk samples of mollusc shells. The growing number of samples now dated using AMS methods has effectively resulted in two radiocarbon-based chronologies being used in the Black Sea

region. The results from these two methods have at times been utilised together, resulting in contrasting hypotheses on the post-glacial history of the Black Sea.

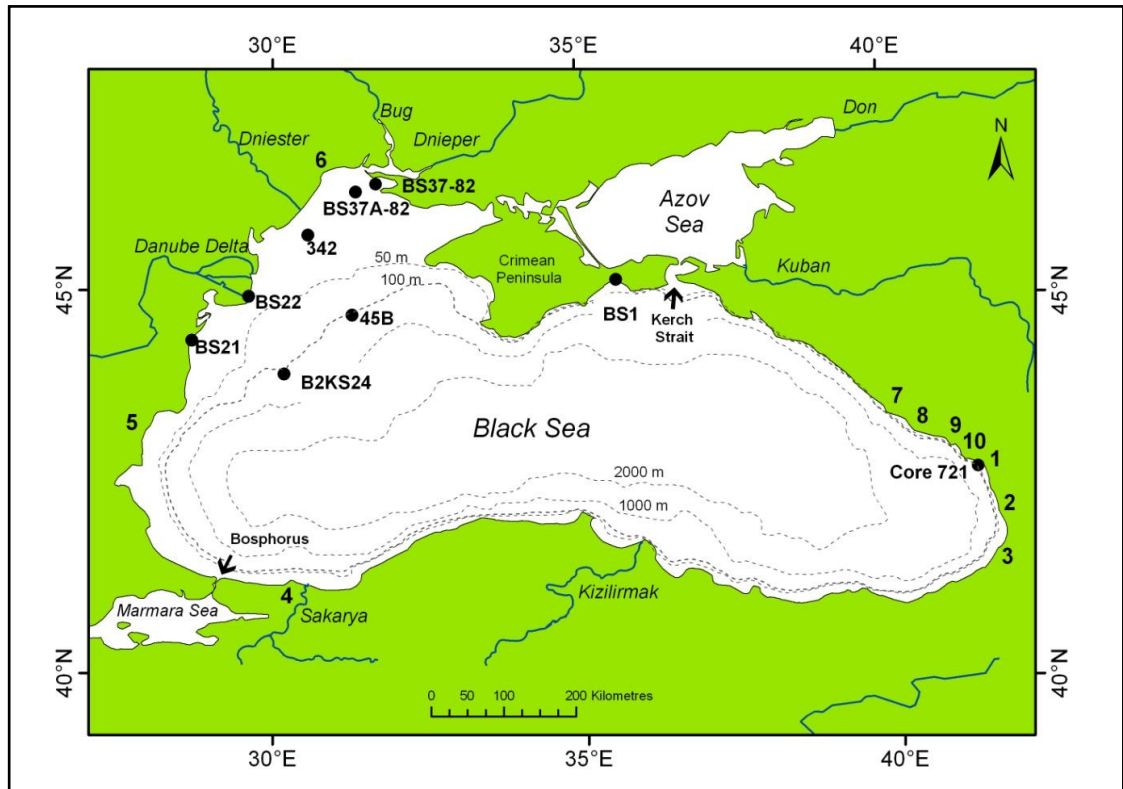


Figure 6.1. The Black Sea, showing principal rivers, general bathymetry, coastal study sites, and sediment-core locations. The location of core B2KS24 is also included for reference (Lericolais *et al.*, 2009). Locations at which radiocarbon-dated peat samples have previously been recovered are numbered 1-10: 1, Sukhumi Bay; 2, Colchis coast; 3, Kobuleti coast; 4, Sakarya delta; 5, Bulgarian coast; 6, Ukrainian coast including Odessa Bay; 7, Adler coast; 8, Gagra coast; 9, Pitsunda Peninsula; 10, Gudauta coast. Bathymetry based on Sur *et al.* (1996).

6.3 The problem of radiocarbon ages and sea-level curves in the Black Sea

There are no fixed sea-level indicators in the Black Sea. Therefore deriving an historical sea-level for this basin is not a trivial task, and this has led to debate on the Ryan *et al.* (1997) ‘Flood’ hypothesis which proposed a catastrophic early Holocene transgression of the previously isolated lake by Mediterranean-sourced water, and formation of the present semi-enclosed basin. Outflow hypotheses (Aksu *et al.*, 2002; Hiscott *et al.*, 2007; Yanko-Hombach *et al.*, 2007) argue the converse. The traditional biostratigraphic interpretation of Black Sea sedimentation relies on marker Mediterranean or Caspian taxa (Nevesskaya, 1974), dated using conventional (β -counting) radiocarbon methods. The flood hypothesis is not, however, unambiguously supported by the previously derived conventional ^{14}C measurements on multiple mollusc specimens (Shcherbakov and Babak, 1979; Panin *et al.*, 1983; Balabanov,

2007), and hence possible mixed age populations, but is derived by using ages on molluscs, commonly from individual shells, and dated by accelerator mass spectrometry (AMS) methods (Ryan *et al.*, 1997; Ryan *et al.*, 2003; Major *et al.*, 2006; Lericolais *et al.*, 2009, 2010; Soulet *et al.*, 2011a, b).

A number of sea-level curves, including those derived from computer models, have been produced from radiocarbon-based chronology for the post-glacial Black Sea (e.g. Chepalyga, 1984; Aksu *et al.*, 2002; Balabanov, 2007; de Klerk *et al.*, 2009; Thom, 2010). However, the use of radiocarbon chronology to derive sea-levels has been problematic with conventional ^{14}C ages, derived from bulk samples, on occasion being composed of marine and terrestrial shells (Noakes and Herz, 1983; Balabanov, 2007). This is despite the obvious complication of attempting to associate one specific environment to the age obtained, and the likely probability of variation in reservoir ages among individual components of these samples.

An apparent difference exists between age-depth distribution of the radiocarbon data from AMS-based ages on mollusc samples and those ages obtained using scintillation-counting methods (cf. Yanko-Hombach, 2007). Many ages (Fig. 6.2) obtained using scintillation-counting methods were determined from bulk shell samples recovered from locations high on the present shelf – commonly at or near sea-level. In contrast, most AMS ages have been obtained on shells (molluscs and ostracods) from the mid to outer shelves, slope and basin. It seems likely that evidence from these two radiocarbon datasets, to a large extent, give rise to the contrasting hypotheses debated; the evidence from conventional radiocarbon ages on bulk samples of individual shells from the inner shelf, may indicate that water-levels in the post-glacial Black Sea did not fall significantly below the level of the Bosphorus sill in the earliest Holocene or, based on the distribution and ages of mollusc species dated by AMS methods obtained from locations in deeper water on the shelf, that a significant drop in water-level occurred following the Younger Dryas, and which was followed by a prompt incursion of ultimately Mediterranean-sourced marine water.

Conventional radiocarbon dating on bulk (i.e. multiple) mollusc samples from the Black Sea, occasionally using all shell from 1 m or more of core (indicated by Brückner *et al.*, 2010) results in time-averaged dates that are always older than the depositional event in question (Kowalewski *et al.*, 1998), and commonly older than AMS dates on individual shells from the same strata (Buynevich *et al.*, 2011). Therefore, results from bulk samples composed of multiple individual shells may not most accurately represent the chronology of events in the Black Sea. AMS ages, commonly on single molluscs, offer the advantage of enabling the dating of individual components of a stratum (Chivas *et al.*, 1986), thereby reducing or eliminating to a large extent the degree of time-averaging in dates, results in considerably

smaller errors (Buynevich *et al.*, 2011) and allows the recognition of mixed-age assemblages where they exist.

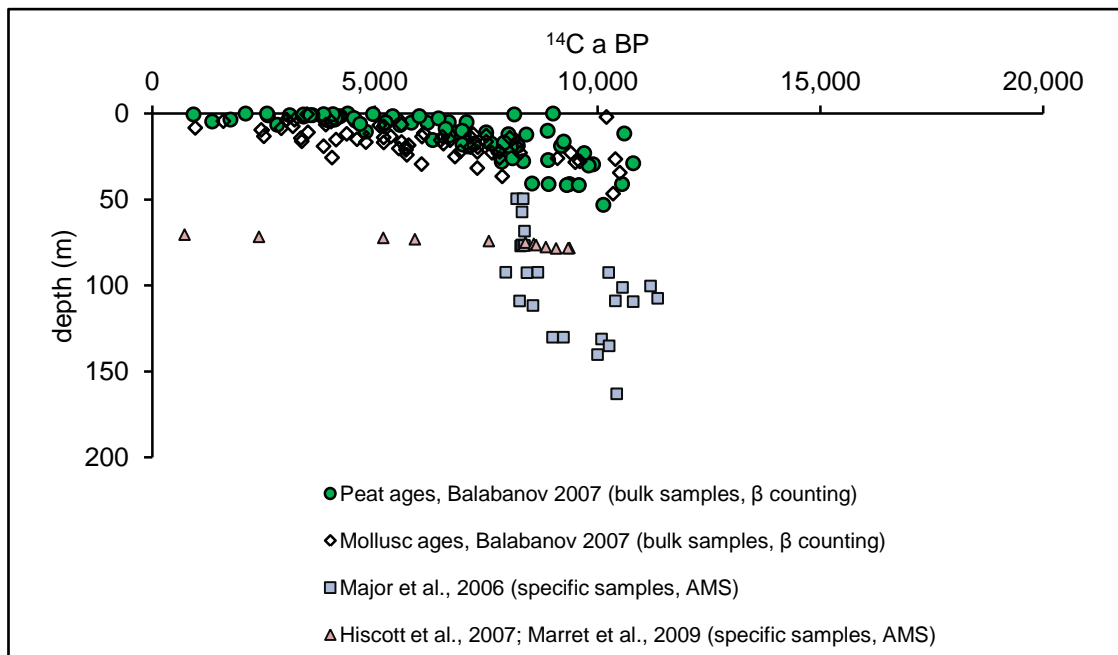


Figure 6.2. Difference in age-depth distribution among conventional radiocarbon-dated bulk mollusc samples (blue squares), conventional radiocarbon-dated bulk peat samples (green dots) and AMS ages on molluscs and ostracods. While it is relatively easy to assign a terrestrial association (i.e. non-marine) to the peat ages, such an approach for the conventionally-dated bulk mollusc samples is difficult because in some cases no mollusc type is clearly recorded (Balabanov, 2007), and thus an environmental association is not clearly definable.

The continuing use of conventional radiocarbon data from bulk mollusc samples in the same context as AMS ages has clouded a number of other issues that have, in turn, continued to hamper the understanding of the early Holocene sea-level history of this basin. These topics include the unresolved issue of neotectonics (e.g. Devdariani and Novikova, 1978; Fouache *et al.*, 2003; Koral, 2007; Brückner *et al.*, 2010), the appropriate application of radiocarbon reservoir ages (Jones and Gagnon, 1994; Siani *et al.* 2000; Kwiecen *et al.*, 2008; Lericolais *et al.*, 2009; Soulet *et al.*, 2011a, b), and the extent to which reworked fossils have been used for chronological and environmental considerations (Giosan *et al.*, 2009; Brückner *et al.*, 2010). Reference has been made in several studies to the presence and radiocarbon dating of shell hash (e.g. multishell samples – Giosan *et al.*, 2005), yet there are few direct observations or descriptions of ages obtained on individual articulated and *in situ* molluscs (e.g. Giosan *et al.*, 2006, 2009; Ongan *et al.*, 2009). This may be simply an issue of reporting, but it is however problematic for defining reliable chronologies because age-mixing may complicate

biostratigraphical or geochronological interpretations, and leads to significantly reduced temporal resolution (Crusius *et al.*, 2004).

The principal method used to determine the extent of age-mixing in coastal sedimentary sequences is the amino acid racemization (AAR) analytical technique, calibrated with AMS ^{14}C ages on the same individual fossils (Goodfriend, 1989; Murray-Wallace and Belperio, 1994; Wehmiller *et al.*, 1995; Goodfriend and Stanley, 1996; Murray-Wallace *et al.*, 1996; Kowalweski *et al.*, 1998; Carroll, 2001; Barbour Wood *et al.*, 2003). Amino Acid Racemization (AAR) methods, reliant on the relative proportions of amino acid D- and L-enantiomers in fossils, have been applied to a wide range of environmental studies, but particularly those focusing on environmental change associated with late Pleistocene and Holocene oscillations in sea-level. For example, aminostratigraphic methods have been applied to fossil bivalve mollusc shells, *Dreissenia* sp. and *Didacna* sp., from the Caspian Sea collected from the Lower Volga and Dagestan coastal areas (Shlyukov *et al.*, 1989). Similarly, marine terraces from Baja California (Keenan *et al.*, 1987), South Carolina (Hollin and Hearty, 1990), and South Australia (Murray-Wallace, 2002) have been successfully investigated using this method.

6.4 The modern environment

The Black Sea is a semi-enclosed, restricted, estuarine sea, having a variable salinity of approximately 18‰ in surface waters distant from fluvial discharge (Popescu *et al.*, 2006). It is connected to the Mediterranean Sea (i.e. the global ocean) only by the Sea of Marmara and narrow Bosphorus Strait, (Fig. 6.1). As a result, interaction with the oceanic marine reservoir is limited, and the only other major flux of water is from the large rivers, of which the Danube contributes 53% (Major *et al.*, 2006). The largest rivers, the Danube, Dnieper, Dniester and Don, enter the Black Sea on the northwestern and northern coasts, flowing over the relatively broad Ukrainian and Romanian shelves prior to discharging in the central basin. Sediments rich in organic-carbon accumulating in the Black Sea are strongly influenced by these terrigenous inputs – sediments that include old radiocarbon sourced from the surrounding hinterland (Eglinton, 1997). Numerous, and comparatively shorter, fluvial systems discharge onto the narrow shelves on the coasts of Georgia, and Turkey, locations where coastal peat is forming at present (Connor *et al.*, 2007), commonly at the foot of the steep cliff-backed southeastern coasts. The present Black Sea basin is a modern example of the classical euxinic basin (Ogawa *et al.*, 2009), having restricted circulation, and anaerobic conditions in 99% of the water column. A permanent halocline at 100-150 m water depth differentiates the

oxygenated surface waters from the anoxic-sulfide basinal waters. This differentiation leads to oxygenated shelves, suboxic water at or just below shelf break, and anoxic water from the upper slope below the 200 m isobath to the abyssal plain. These conditions are the result of elevated primary production, strong density stratification and weak ventilation. The resultant water column in the Black Sea is divided into three water masses (0-150 m, 150-1,700 m, 1,700-2,200 m; Oguz *et al.*, 2004), of which an estuarine-brackish water mass (distal to estuaries and deltas) with salinity of 17-18‰ occupies the upper 150 m. Water below 150 m is sulfide-rich. Salinity in close proximity to deltas can be 1-5‰ (Stanev *et al.*, 2002). However, the upper water mass (0-150 m) is seasonally variable with respect to salinity and temperature. Ventilation through density stratification only occurs in the upper 60 m (Oguz *et al.*, 2002). Shelf systems in the Black Sea are thus dominated, at present, by brackish, Mediterranean-derived estuarine taxa, suited to nutrient-rich conditions, fed by numerous discharging rivers sourced from central Europe or Eurasia. These ecosystems are limited to the upper 150 m of the water column. Remnant Caspian fauna inhabit lagoons (limans), rivers and lakes in the northwest and north.

Methane and other products within the Black Sea, and originating from numerous cold-water seeps, mud volcanoes, and methane clathrates are not dissipated quickly, but rather remain in the water column and become heavily oxidised and fractionated (Reeburgh *et al.*, 2006). At present, methane is being added to the Black Sea water-column approximately as fast as it is being oxidized, a proportion of which consists of old radiocarbon (Gulin *et al.*, 2003; Reeburgh *et al.*, 2006), and originates in source rocks of a variety of ages (Slack *et al.*, 1998; Dimitrov 2002; Kessler *et al.*, 2006; Naudts *et al.*, 2008; Stadnitskaia *et al.*, 2008). ^{14}C - CH_4 from seeps in the Black Sea were found to have a radiocarbon ages between 18.2 ka ^{14}C BP (Guilin *et al.*, 2003) and 24 ka ^{14}C BP (Kessler *et al.*, 2006). Ventilation of deep water layers is extremely limited, and residence time in the deep water is ~ 300 a (Murray *et al.*, 2007). Molluscs that grow adjacent to seeps at a number of locations within the Black Sea basin; (e.g. *Mytilus galloprovincialis* growing at Zelenka gas seepage, 200-250 m from Cape Kaliakra, Bulgaria, Dimitrov 2002), incorporate a portion of old ^{14}C (Hovland and Risk, 2003; Reeburgh, 2007). This is likely to lead to a spatial variation in reservoir age across the Black Sea between taxa that inhabit seep communities and those that do not, and complicates attempts to estimate modern reservoir ages for the Black Sea (Siani *et al.*, 2000; Kwiecien *et al.*, 2008). These reservoir age values will also have changed over time. These issues make the Black Sea sediments particularly problematic for radiocarbon dating.

6.5 Methods

The AAR results presented herein are the first from the Black Sea, and are presented for comparison with, and to give context to, the results from ^{14}C dating. However, the focus of this paper is the radiocarbon chronology.

Cores were collected using Russian coring methods, and sampled in Odessa, Ukraine. Sediment samples (Table 6.1) were recovered during fieldwork on the Crimean (2007), Romanian and Bulgarian coasts (2008). Four peat and 66 shell samples were analysed from five cores from the Ukrainian and Georgian shelves (Tables 6.1, 6.2, 6.3). Four shell samples consisted of bulk samples of micro-molluscs. The remaining samples were of single valves, primarily of either *Cardium*, *Dreissena*, or *Mytilus*. Reverse-Phase High Performance Liquid Chromatography (RP-HPLC) was used to examine the extent of AAR in the total hydrolysable amino acid fraction in bivalve molluscs *Dreissena*, *Cardium*, *Chione* and *Mytilus* (Table 3). The AAR method used here is based on Kaufman and Manley (1998). D/L values obtained on aspartic (asx) and glutamic (glx) acids were used for comparative chronology, and AAR-based numeric ages are presented for the mean value determined from individually calibrated aspartic acid and glutamic acid calibration curves. These AMS-calibrated amino acid racemization calibration curves were derived using a parabolic method of estimating ages. Radiocarbon ages on peat and *Dreissena* were calibrated using Calib Rev 5.0.1 and the Intcal09 calibration curve (Reimer *et al.*, 2009).

Basal peat at 26.7 m depth in core 721 (water depth 14.9 m) was previously dated using conventional radiocarbon dating. The dates obtained were $9,310 \pm 80$ ^{14}C a BP (code TB-346) (Apakidze *et al.*, 1987) and $9,580 \pm 80$ ^{14}C a BP for the same horizon (Yanko and Troitskaya, 1987; Yanko-Hombach, 2007; Yanko-Hombach *et al.* 2007). Apart from these dates on peat there are no other dates previously obtained from core 721.

6.6. AMS ^{14}C ages, and observations on chronology

6.6.1 Cores BS37-82 and BS37A-82

Seven radiocarbon ages (Figs. 6.3 and 6.4, Tables 6.1, 6.2) were obtained from individual pieces of the bivalve mollusc *Cardium edule*, recovered from cores BS37-82 and BS37A-82 (water depths 17.7 and 19.6 m respectively) approximately 5 km apart. These ages indicate that an environment suitable for *Cardium edule* existed on the shallow inshore Ukrainian shelf since approximately 7,150 ^{14}C a BP. The age-depth distribution of AMS dates from these samples are in stratigraphic order within each core (Fig. 6.3a), but indicate some degree of

stratigraphic offset between the cores (Fig. 6.3b). Five of these ages were used to calibrate amino acid D/L values. These are discussed further in Section 6.1.

Table 6.1. Locations of core and coastal sampling stations.

Core/Outcrop	Location	Latitude	Longitude	Water Depth (m)	Length of core	Reference/Recovered by
BS 37-82	Ukrainian shelf			17.7	3.08	Konikov, (2007)
BS 37A-82	Ukrainian shelf	46°17'30" N,	31°21'45" E,	19.6	3.07	Konikov, (2007)
721	Sukhumi Bay, Georgia.	42°59'35.5" N 0.8 km southeast of Basla River	41°2'9.79" E Estimated using ArcGis 9.2, (WGS 84)	14.9	27.2	Apakidze <i>et al.</i> 1987 Yanko and Troitskaya, 1987 Yanko-Hombach <i>et al.</i> 2007
342	Ukrainian shelf	45°43'09" N,	30°34'28" E,	30	1.7	Unpublished Core collected by Prichernomorgeologiya (Ukrainian Geological survey of Black sea region)
45B	Ukrainian shelf edge	44°40'16" N,	31°17'30" E,	107	0.75	Unpublished Core collected during Ukrainian HERMES cruise
Feodeosia Foreshore BS-1						
Constanta Foreshore BS-21	Romanian coast	45.09978 N	29.39560 E	0	0	This study
Danube Delta, at St George Distributory Coast BS-22	Danube Delta foreshore	44.8912 N	29.6259 E	0	0	This study

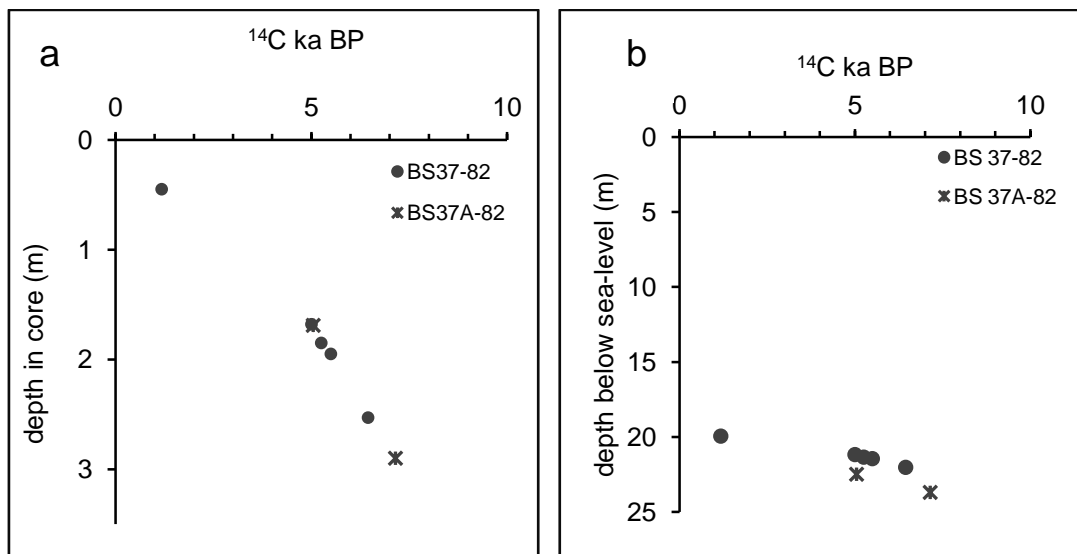


Figure 6.3. AMS ^{14}C ages derived during this study on individual shell fragments of the bivalve mollusc *Cardium edule*, from the two adjacent cores BS-37-82 and BS37A-82 (Konikov *et al.*, 2007), northwestern Black Sea. AMS ages are uncorrected for marine reservoir effect, and uncalibrated.

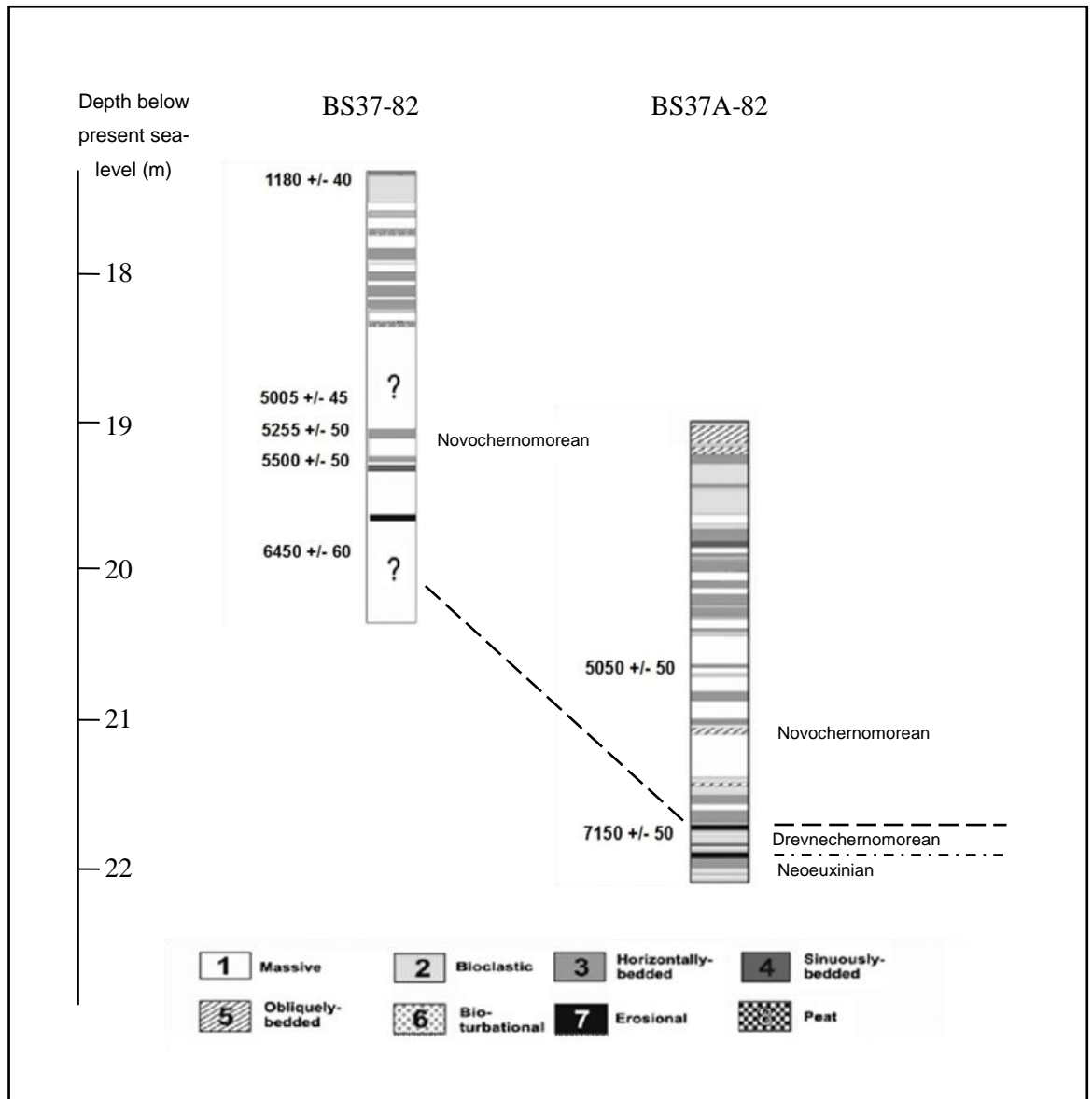


Figure 6.4. AMS ^{14}C chronology obtained during this study on cores BS37-82 and BS37A-82, and redrawn from Konikov *et al.* (2007). The ‘massive’ sedimentary units in these cores, lacking sedimentary structures may indicate rapid sedimentation, with sediments derived proximal to the location of the cores on the innermost shelf. Prolonged transport, by contrast, would induce some stratification. Erosional horizons we suggest relate to submarine, rather than subaerial erosion. The differentiation into the classical Black Sea stratigraphic units (Konikov *et al.*, 2007) is illustrated for comparison.

Table 6.2 AMS ¹⁴C ages obtained on bivalve molluscs and peat during this study

Core	Depth in core (m)	material	¹⁴ C age,	1σ	δ (¹³ C) ^{a,b}	1σ	PMC ^c	1σ	ANSTO code	UWG A no.
BS 37-82	19.95	<i>Cardium edule</i> single fragment	1180	40	0.0		86.33	0.37	OZL300	7229
BS 37-82	21.18	<i>Cardium edule</i> single fragment	5005	45	-1.0	0.1	53.62	0.29	OZM334	7221
BS 37-82	21.35	<i>Cardium edule</i> single fragment	5255	50	-0.3	0.1	51.98	0.29	OZM335	7220
BS 37-82	21.45	<i>Cardium edule</i> single fragment	5500	50	-0.2	0.1	50.42	0.29	OZM336	7224
BS 37-82	22.03	<i>Cardium edule</i> single fragment	6450	60	0.0		44.82	0.31	OZL301	
BS 37A-82	22.49	<i>Cardium edule</i> single fragment	5050	50	0.0		53.3	0.28	OZL302	7228
BS 37A-82	23.7	<i>Cardium edule</i> single fragment	7150	50	0.0		41.07	0.23	OZL303	
721	2.0	micromolluscs	1790	90	0.0		80.06	0.81	OZL304	
721	8.0	micromolluscs	2530	80	0.0		73.02	0.72	OZL305	
721	15	micromolluscs	3190	90	0.1		67.24	0.75	OZL306	
721	22	micromolluscs	8210	120	0.0		36	0.52	OZL307	
721	26.2	Peat	8530	70	-25	0	34.58	0.47	OZK766	
721	26.5	Peat	9370	70	-29.1	0.1	31.15	0.24	OZK767	
342	0.85	<i>Cardium edule</i> single valve	9140	60	-4.4	0.1	32.04	0.22	OZL582	8026
342	1.15	<i>Dreissena polymorpha</i> single valve	9620	60	-8.7	0.2	30.19	0.2	OZL579	8025
342	1.15	Peat	9020	70	-24.9	0.3	32.55	0.28	OZL577	
342	1.65	Peat	8920	60	-28.1	0	32.94	0.23	OZL581	
342	0.85	<i>Mytilus</i> (A) single valve	5765	35	0.1	0.1	48.78	0.2	OZM332	8059
342	0.85	<i>Mytilus</i> (B) single valve	4365	30	-1.2	0.1	58.09	0.21	OZM333	8058
45B	0.31	<i>Mytilus</i> single valve	6530	45	-0.7	0.1	44.36	0.24	OZL583	8027
45B	0.44	<i>Dreissena rostriformis</i> (A) single valve	8820	70	0.4	0.1	33.37	0.25	OZL580	8024
45B	0.44	<i>Dreissena rostriformis</i> (B) single valve	8695	50	0.4	0.1	33.88	0.2	OZL578	8023
45B	0.44	<i>Dreissena rostriformis</i> (C) single valve	8170	60	-0.2	0.2	36.19	0.26	OZM331	

^a δ (¹³C) values relate solely to the graphite derived from the fraction used for the radiocarbon measurement. It may be the case that the value obtained from the graphite is not the same as that of the original bulk material.

^b δ (¹³C) values of 0.0 are assumed. Measured values are not available.

^c PMC = per cent modern carbon

6.6.2 Core 721, Sukhumi Bay, Georgia

Seven AMS radiocarbon ages were obtained on samples from core 721 (Fig. 6. 5, Tables 6.1, 6.2). These include five dates on bulk samples of micromolluscs consisting primarily of *Cardium* sp. and two on peat. Peat recovered from 26.2 m depth was dated as $8,530 \pm 110$ ^{14}C a BP, and the sample from 26.5 m depth was dated at $9,370 \pm 70$ ^{14}C a BP. This older value is similar to those previously published using conventional radiocarbon dating methods (Apakidze *et al.*, 1987; Yanko and Troitskaya, 1987; Yanko-Hombach, 2007; Yanko-Hombach *et al.* 2007). Using these data, and extrapolating, an estimated age of $8,250$ ^{14}C a BP is obtained for the top of the peat at 26.1 m. The gravel unit immediately above the peat between approximately 19.2 and 26.1 m contains mollusc remains including those of *Dreissenia polymorpha* and *Cardium edule* (Fig. 9 of Yanko-Hombach *et al.*, 2007). Micromolluscs from 22.0 m depth were dated at $8,210 \pm 120$ ^{14}C a BP.

Micromolluscs recovered from 15.0 m depth in core 721 (water depth 14.9 m) were dated to $3,190 \pm 90$ ^{14}C a BP. Those from 8 m depth were dated to $2,530 \pm 80$, and samples from 2.0 m were dated to $1,790 \pm 90$ ^{14}C a BP. The boundary between the peat and silt is erosive, and therefore the transition between these units and the underlying peat is abrupt, and unconformable – there is a time gap between formation of the peat in a non-marine environment and the deposition of the marine gravel unit directly above it (marine influence is indicated by the presence of the Mediterranean-derived bivalve mollusc, *Cardium edule*). This is suggestive of some metres of water at the time of deposition of the sediment above the peat, and indicates a transgressive event at this location just after $8,530$ ^{14}C a BP.

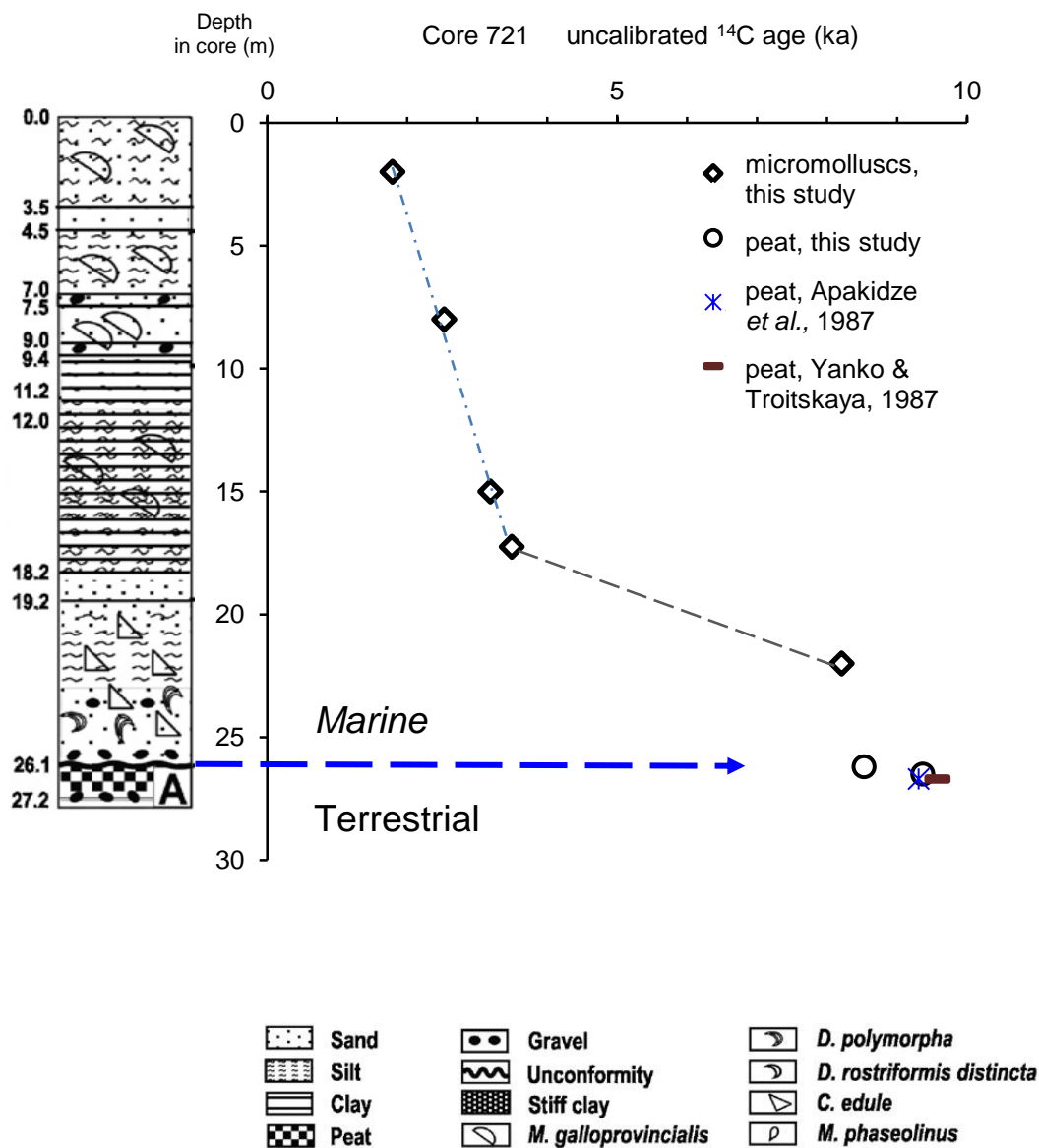


Figure 6.5. Radiocarbon ages for core 721, Sukhumi Bay, Georgian shelf. Stratigraphic log and associated legend adapted from Yanko-Hombach *et al.* (2007). Circles represent ages of peat obtained in this study (see Table 2). Note the significant decrease in sedimentation rate between 17.25 m and 22.0 m. We note the similarity of previous ages on peat (Apakidze *et al.*, 1987 and Yanko and Troitskaya, 1987, from Balabanov, 2007) and those obtained here.

6.6.3 Core 342 Ukrainian Shelf

The sediments within core 342 (Fig. 6.6) comprise the upper section of a 40 m long core recovered from 30 m water depth. These sediments and fossils indicate a transition, from alluvial sedimentation at the base (sample 342/5, 1.6-1.7 m) to lacustrine conditions (sample 342/4, 1.1-1.2 m) followed by deposition in a marine setting. Sediments in samples 342/3

(0.8-0.9 m depth) and 342/2 (0.55-0.60 m depth) are of mixed assemblages, marine and non-marine, and these sediments must be considered reworked. This is because the principal species in samples 342/3 and 342/2, *Dreissena polymorpha*, is indicative of non-marine conditions, while the presence in the same samples of small numbers of well preserved broken fragments of the bivalve mollusc, *Mytilus*, indicates the presence of Mediterranean-sourced marine water. These latter shell fragments have excellent to good internal lustre, none or minor loss of colour, no dissolution and no borings. Non-marine conditions (i.e. very low salinity brackish to freshwater) are indicated by the presence of *Dreissena polymorpha* and also *Monodacna* sp.. A very small number of *Dreissena polymorpha* were moderately well preserved with original colouration, and no loss of lustre, or only slightly dissolved with internal lustre being chalky. However, most were bleached, and had varying degrees of dissolution. Along with the known habitat of *Dreissena polymorpha* and *Monodacna colorata*, together these variations in preservation suggest shallow water conditions for the original depositional environment. The lack of bleaching and dissolution indicates the *Mytilus* in these samples were mixed with the less well preserved *Dreissena* and *Monodacna* when water was at least some metres deep, and the *Mytilus* had not been exposed to sub-aerial or near sub-aerial conditions for any significant length of time.

Two radiocarbon age determinations were undertaken, each on a single peat sample (Table 6.2; Fig. 6.6). The older, and uppermost peat ($9,020 \pm 70$ ^{14}C a BP, sample 342/4, 1.15 m depth) had an incorporated single, and complete *Dreissena polymorpha* valve. Several unidentified gastropods and numerous shell fragments, were also recovered from this latter sample. Of those identifiable shells, *Dreissena polymorpha* was the dominant shell component, and a large proportion of these *Dreissena* retained original colouration, suggesting incorporation into the peat sediment soon after death because bleaching did not occur. The single *Dreissena polymorpha* valve ($9,620 \pm 60$ ^{14}C a BP) recovered from within the peat has an apparent age 600 years older than the peat. The $\delta^{13}\text{C}$ value (-8.7 ± 0.2) (suggestive of a fluvial, i.e. freshwater) environment was measured on the graphite used for AMS and not on the carbonate, therefore these (and similarly produced) $\delta^{13}\text{C}$ values in this study are not discussed further. A single *Cardium* valve ($9,140 \pm 60$ ^{14}C a BP) from sample 342/3 (Fig. 6.6) overlying the peat is older than the peat from the lower horizon (342/4) by 120 ^{14}C a. In contrast, the lower peat sample from 1.55 m depth (342/5) had an age ($8,920 \pm 60$ ^{14}C a BP) younger than the peat at 1.15 m. Because there is no marine reservoir age on peat, these ages allow us to constrain the deposition of sediments within this core to after (i.e. younger than) 8,900 ^{14}C a BP.

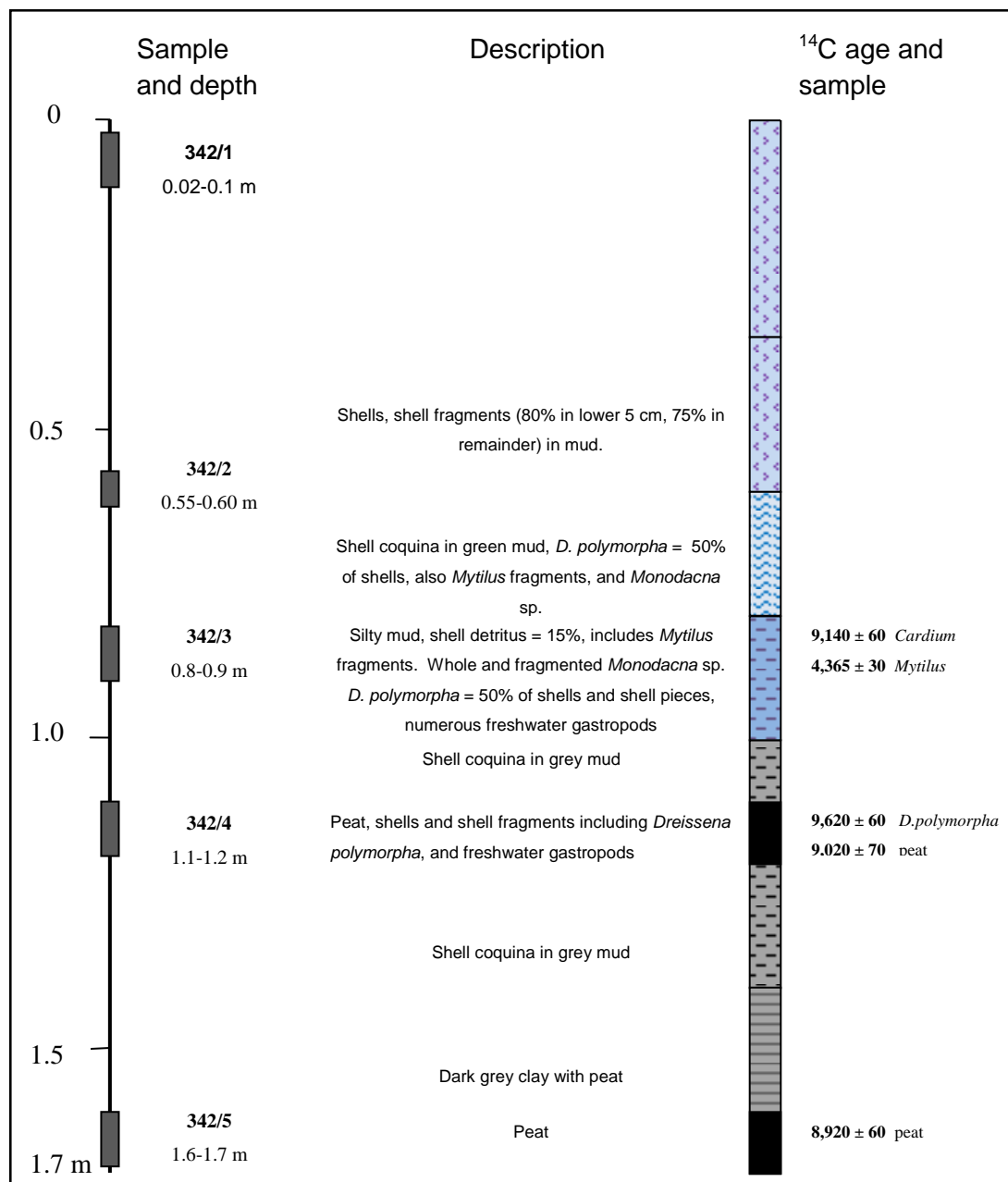


Figure 6.6. Stratigraphic log and description of core 342, recovered from the inner Ukrainian shelf by Prichernomorgeologiya (Ukrainian Geological Survey of Black Sea Region). The description offered here is based on the original description given by Sergei Kadurin to Nicholas and Chivas, and additional data obtained during this study.

6.6.4 Core 45B Ukrainian Shelf

Core 45B from 107 metres below sea-level (mbsl) on the outer Ukrainian shelf, consists of three strata (Fig. 6.7, Tables 6.1, 6.2), each composed of shell-rich fine-grained sediment. The lowermost unit from 0.45 m depth in core 45B records a period of shallow-water sedimentation, indicated by bleached and partially to highly dissolved valves and fragments of the bivalve *Dreissena rostriformis* (mean age 8,562 ¹⁴C a BP; individually, 8,170 ± 60, 8,695 ± 50, and 8,820 ± 70 ¹⁴C a BP; Table 2; Fig. 6. 7). Examples of the gastropod *Turricaspiia caspia*

present in this sample are, by contrast, significantly better preserved, though commonly broken. This shell coquina is directly overlain by numerous unbleached, yet broken fragments of *Mytilus* in a mud matrix ($6,530 \pm 45$ ^{14}C a BP), indicating estuarine to marine conditions similar to the modern Black Sea. Unsourced here, and overlying the *Mytilus* layer is the uppermost mud unit rich in the marine mollusc *Modiolus*. Notably, the *Mytilus* fragments were unbleached and without dissolution, indicating deposition at depth beneath the bleaching influence of the sun. Comparatively moderate energy conditions are required to have broken these valves, yet they are likely to have been deposited below storm wave-base in quiet conditions, as evidenced by the high mud content. These storm-derived deposits contrast strongly with the underlying *Dreissena* coquina because many of the much more fragile *Dreissena* valves are complete. This suggests lower-energy conditions during deposition of the *Dreissena*, and perhaps comparatively little transport. The *Dreissena* coquina also contrasts with the *Mytilus* by being very well sorted, with minimal mud present, (only carbonate mud exists, and which is derived from the breakdown of shells). This and the bleached condition suggests a protected shallow, nearshore (e.g. beach ridge, or shallow inshore) deposit with shells forming a concentration deposit because of wave action in shallow-water conditions. The lack of terrestrial sediments, particularly clay, indicates a reduced fluvial influence at the location of deposition. This coquina represents, or was in close proximity to, a palaeo-shoreline. The contact between these the *Mytilus*- and *Dreissena* *rostiformis*-rich units is sharp, and the time-gap between these individual events is approximately 2,100 ^{14}C a. Both these ages, and the time-gap between these units are similar to those in core B2KS24, for example, located in 96 m of water, and a further 130 km to the southwest (Lericolais *et al.*, 2009) (Figs. 6.1, 6.7).

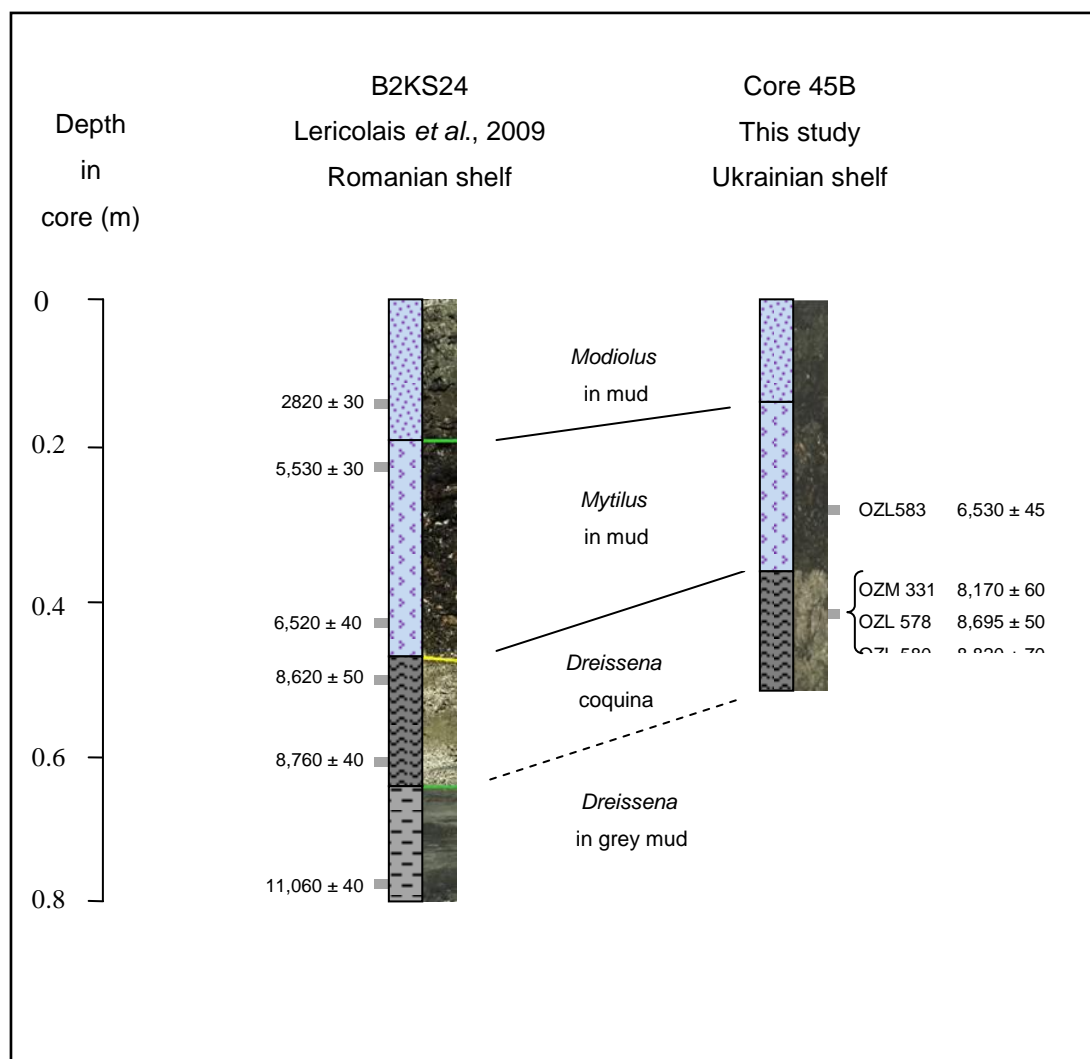


Figure 6.7. Chronological and lithological correlation between cores from Ukrainian (45B, this study) and Romanian (B2KS24, Lericolais *et al.*, 2009) shelves, Photograph of core 45B courtesy of Sergei Kadurin. ANSTO lab codes are presented above, to the left of sample ages. OZL 578, OZL 580 and OZM 331 were all from the same sample, 43-45 cm depth in core 45B (arrowed). To measure the extent of time-averaging in the *Dreissena coquina* three single *Dreissena rostriformis* shells were dated by ^{14}C AMS methods from this same sample.

6.7 Amino acid racemization data and implications

6.6.1 Cores BS37-82, and BS37A-82, Ukrainian shelf

Radiocarbon age determinations were made on seven samples of the bivalve mollusc *Cardium edule* (Fig. 6.8). Five of these were from core BS37-82 and two from BS37A-82 (Table 6.3). Of these, sufficient sample was retained from five fragments of *Cardium edule* for amino acid racemization analyses, and these were used to calibrate D/L values using the parabolic method of calculating numeric ages (Mitterer and Kriausakul, 1989; Murray-Wallace and Kimber, 1993).

The extent of racemization was measured in 11 shell pieces, 10 of which were from core BS37A-82, and one from core BS37-82. While radiocarbon dates increase with depth, D/L values are not in agreement with this (Table 6.3), with for example, an aspartic (asx) D/L value of 0.196 for the sample at 1.59 m in core BS37-82, while the asx D/L value for the sample at 1.55 m was 0.227. Furthermore the highest asx D/L value (0.275) was obtained on the shell piece from 1.95 m depth, yet the lowest extent of racemization for aspartic acid in this core was from the sample at 1.93 m (asx = 0.181). Similar results were found using glutamic acid in these samples. These differences in D/L values are attributed to both age and to intrashell variability. These samples were from individual pieces of broken, disarticulated shell, and it was therefore not possible to use the same sampling location (e.g. the umbo) for each piece. Furthermore, the depositonal event (stratum) in which these shells were deposited occurred after their disarticulation and fragmentation. The radiocarbon dates indicate when the shells were growing, while, in contrast, the AAR D/L values represent the integrated time since death, and include the effects of taphonomic and diagenetic processes that have acted on the shell since that time.

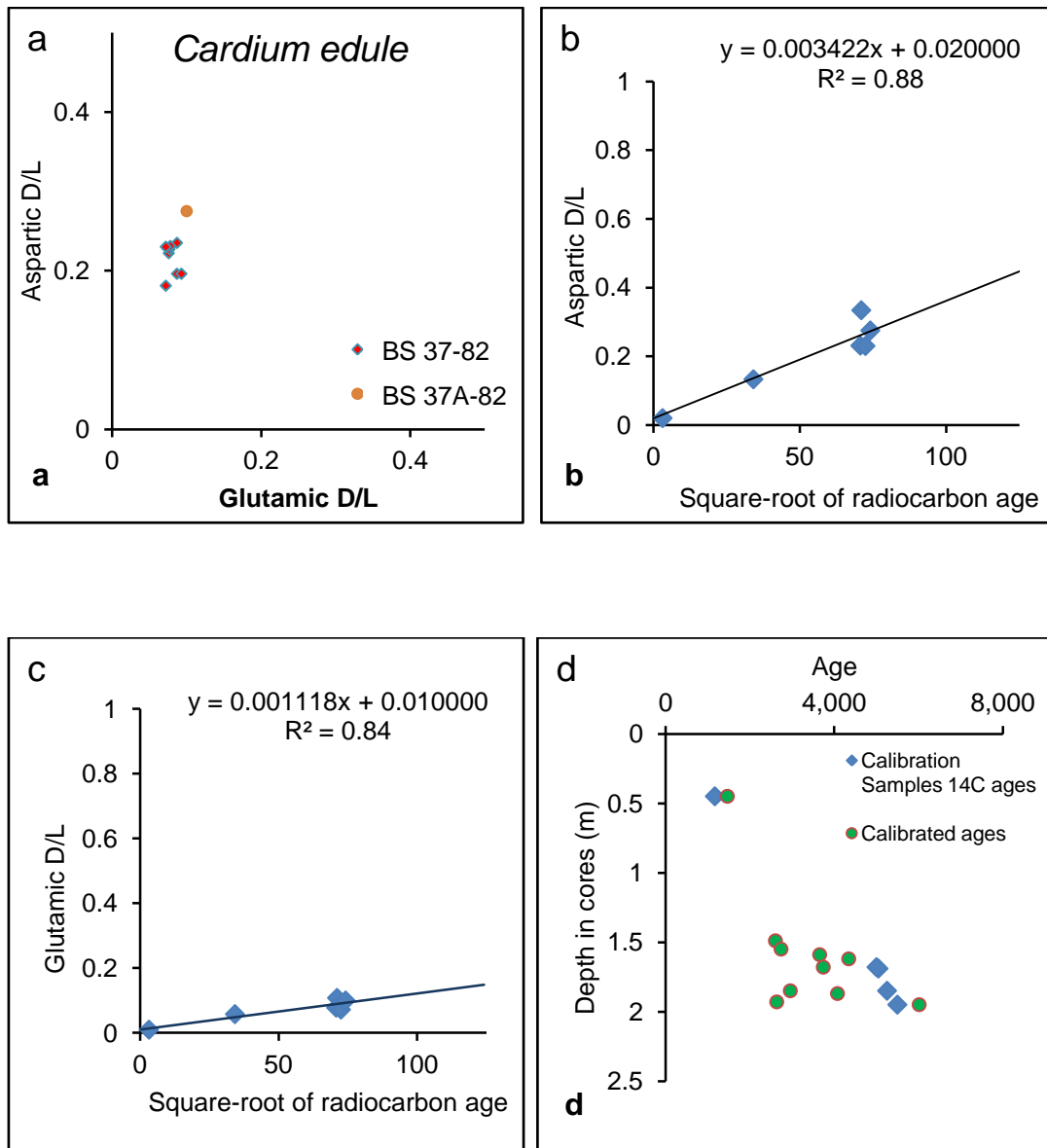


Figure 6.8. D/L values and concordance of results for aspartic and glutamic D/L values for *Cardium edule* from cores BS37-82 analysed for the extent of amino acid racemization. b) and c) Parabolic curves and associated equations for aspartic and glutamic acids. d) Age-depth relationship for calibrated ages on these mollusc valves.

Table 6. 3. Aspartic and Glutamic D/L values derived by RP-HPLC analyses on bivalve molluscs, *Cardium edule*, *Chione gallina*, *Mytilus* sp., *Dreissena polymorpha*, *Dreissena rostriformis*, post-glacial Black Sea, and on interlaboratory comparison standards.

Core	Genus	¹⁴ C age	Depth in core (m)	Asx	± 1σ	Glx	± 1σ	UWGA number	ANSTO code
BS 37-82	<i>Cardium</i>		1.49	0.222	0.016	0.076	0	7226	
BS 37-82	<i>Cardium</i>		1.55	0.227	0.028	0.077	0.006	7219	
BS 37-82	<i>Cardium</i>		1.59	0.196	0.021	0.087	0.006	7227	
BS 37-82	<i>Cardium</i>		1.62	0.235	0.052	0.087	0.011	7222	
BS 37-82	<i>Cardium</i>		1.68	0.231	0.009	0.078	0.003	7221	
BS 37-82	<i>Cardium</i>		1.85	0.23	0.018	0.072	0.007	7220	
BS 37-82	<i>Cardium</i>		1.87	0.196	0.021	0.093	0.001	7225	
BS 37-82	<i>Cardium</i>		1.93	0.181	0.012	0.072	0.003	7223	
BS 37-82	<i>Cardium</i>		1.95	0.275	0.048	0.1	0.001	7224	
BS 37A-82	<i>Cardium</i>	5050 ± 50	1.69	0.334	.	0.108	0.003	7228	OZL302
BS-21	<i>Cardium</i>		0	0.163		0.074		8007	
BS-21	<i>Cardium</i>		0	0.162		0.073		8008	
BS-21	<i>Cardium</i>		0	0.095		0.049		8009	
BS-21	<i>Cardium</i>		0	0.158		0.074		8010	
BS-21	<i>Cardium</i>		0	0.108		0.051		8011	
BS-22	<i>Cardium</i>		0	0.087		0.039		8012	
BS-22	<i>Cardium</i>		0	0.087		0.039		8013	
BS-22	<i>Cardium</i>		0	0.088		0.046		8014	
BS-22	<i>Cardium</i>		0	0.067		0.033		8015	
BS-22	<i>Cardium</i>		0	0.081		0.077		8016	
45B/30	<i>Mytilus</i>	6530 ± 45	0.31	0.237	0.117	0.094	0.035	8027	OZL583
45B/30	<i>Mytilus</i>		0.31	0.266	0.036	0.111	0.021	8028	
45B/30	<i>Mytilus</i>		0.31	0.211	0.043	0.106	0.006	8029	
45B/30	<i>Mytilus</i>		0.31	0.212	0.103	0.099	0.033	8030	
45B/30	<i>Mytilus</i>		0.31	0.173	0.078	0.087	0.029	8031	
45B/30	<i>Mytilus</i>		0.31	0.324	0.008	0.129	0.003	8032	
45B/40 B	<i>Dreissena rostriformis</i>	8695 ± 50	0.44	0.279	0.011	0.115	0.021	8023	OZL578
45B/40 A	<i>Dreissena rostriformis</i>	8820 ± 70	0.44	0.349	0.028	0.128	0.013	8024	OZL580
45B/40	<i>Dreissena rostriformis</i>		0.44	0.313	0.035	0.117	0.008	8033	
45B/40	<i>Dreissena rostriformis</i>		0.44	0.302	0.03	0.116	0.001	8034	
45B/40	<i>Dreissena rostriformis</i>		0.44	0.28	0.045	0.117	0.003	8035	
45B/40	<i>Dreissena rostriformis</i>		0.44	0.288	0.002	0.103	0.004	8036	
45B/40	<i>Dreissena rostriformis</i>		0.44	0.327	0.033	0.107	0.005	8037	
342/4	<i>Dreissena polymorpha</i>	9620 ± 70	0.85	0.2885	0.039	0.093	0.004	8025	OZL579
			0.85						
342/3	<i>Dreissena polymorpha</i>		0.85	0.318		0.125		8038	
342/3	<i>Dreissena polymorpha</i>		0.85	0.363		0.13		8039	

342/3	<i>Dreissena polymorpha</i>		0.85	0.348		0.099		8040	
342/3	<i>Dreissena polymorpha</i>		0.85	0.344		0.129		8041	
342/2	<i>Dreissena polymorpha</i>		0.58	0.363		0.128		8042	
342/2	<i>Dreissena polymorpha</i>		0.58	Nil		Nil		8043	
342/2	<i>Dreissena polymorpha</i>		0.58	0.348		0.175		8044	
342/2	<i>Dreissena polymorpha</i>		0.58	0.341		0.118		8045	
342/2	<i>Dreissena polymorpha</i>		0.58	0.342		0.133		8046	
342/3	<i>Cardium</i>		0.85	0.345		0.13		8047	
342/3	<i>Cardium</i>		0.85	0.219		0.117		8048	
342/3	<i>Cardium</i>		0.85	0.281		0.134		8049	
342/3	<i>Cardium</i>		0.85	0.253		0.131		8050	
342/3	<i>Cardium</i>		0.85	0.244		0.122		8051	
342/3	<i>Cardium</i>	9140 ± 60	0.85	0.297		0.113		8052	
342/2	<i>Cardium</i>		0.58	0.233	0.029	0.085	0.012	8053	
342/2	<i>Cardium</i>		0.58	0.291	0.041	0.126	0.013	8054	
342/2	<i>Cardium</i>		0.58	0.32	0.047	0.127	0.002	8055	
342/2	<i>Mytilus</i>		0.58	0.257	0.024	0.113	0.013	8056	
342/2	<i>Mytilus</i>		0.58	0.245	0.012	0.107	0.005	8057	
342/3	<i>Mytilus</i>	4365 ± 30	0.85	0.226	0	0.09	0.003	8058	OZM333
342/3	<i>Mytilus</i>	5765 ± 35	0.85	0.245	0	0.11	0.003	8059	OZM332
342/3	<i>Mytilus</i>		0.85	0.217	0.001	0.094	0	8060	
342/3	<i>Mytilus</i>		0.85	0.381	0.001	0.101	0.008	8061	
342/3	<i>Mytilus</i>		0.85	0.196	0.001	0.086	0.001	8062	
	ILCA			0.385		0.218			
	ILCB			0.700		0.434			
	ILCC			0.904		0.859			
	ILCZ			0.167		0.052			

6.7.2 Core 342, Ukrainian Shelf

Mytilus, *Cardium edule* and *Dreissena polymorpha* were the species analysed from core 342 (Fig. 6.9). The presence of wholly and partially bleached, broken and complete single valves of the Ponto-Caspian species, *Monodacna* sp. and *Dreissena polymorpha* with unbleached fragments of the Mediterranean-derived species, *Mytilus*, in the same sediment layer indicates mixing of sediment because these shells have significantly different environmental tolerances, and their habitats do not overlap. Furthermore, the extent of physical and chemical alteration including removal of pigment by bleaching (oxidation) of the two Ponto-Caspian species is significantly greater than that for *Mytilus* in these

samples, indicating different taphonomic pathways. Overall, *Mytilus* had the lowest D/L values while *Dreissena polymorpha* had the highest. The D/L values for *Cardium edule* (asx = 0.345 to 0.233; glx = 0.134 to 0.085) overlapped to some extent with *Mytilus* (asx = 0.381 to 0.196; glx = 0.113 to 0.086), but do not overlap (Fig. 6.9) those of *Dreissena polymorpha* (asx = 0.363 to 0.318; glx = 0.175 to 0.099). This distribution of D/L values appears consistent with a transition from non-marine to marine environments.

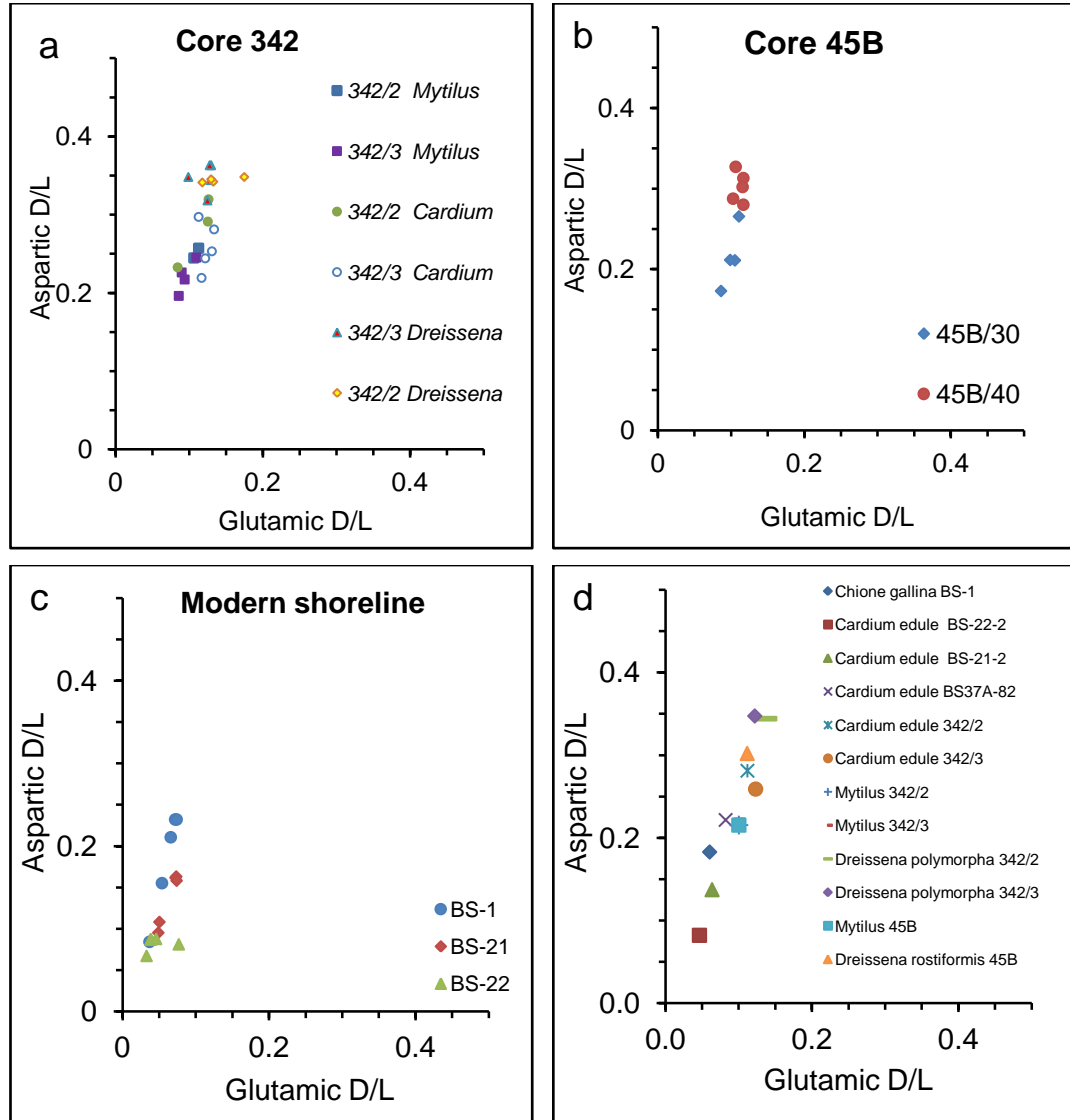


Figure 6.9. D/L values in a) core 342, b) 45B, c) modern samples and d) mean D/L for each stratum sampled. Data from Kerch Strait (unpublished) suggests that the racemization rate of *Mytilus* is faster than that for *Cardium* over the last 125 ka, however comparative rates of racemization are not certain for Holocene timescales and thus the values offered here are conservatively taken at face value. Thus, in core 342, *Dreissena polymorpha* are older than *Cardium* which are in turn older than *Mytilus*. Overall, *D. polymorpha* are older than *D. rostriformis*, with *Mytilus* in 342 and 45B having an apparently similar age. D/L values indicate that *Chione*, and collected at Feodeosia beach, are older than those collected on the western shoreline. Mean annual temperatures (MAT) for Feodeosia and the Danube coast are similar (11° C), and suggest that the higher extent of racemization in *Chione* shells is not temperature-related.

6.7.3 Core 45B, Ukrainian Shelf

Dreissena rostiformis and *Mytilus* were analyzed from core 45B (Fig. 6.9b) because their apparent stratigraphic relationship, and radiocarbon ages on a limited number of shells (Lericolais *et al.*, 2009; this study) suggested a significant time-gap between the deposition of the *Dreissena* and the *Mytilus* fragments. D/L values for *Dreissena rostiformis* in core 45B (asx = 0.349 to 0.280; glx = 0.128 to 0.103) are higher than those for *Mytilus* (asx = 0.324 to 0.173; glx = 0.129 to 0.094), and when included with the stratigraphic relationship of these shell pieces, these results support a transition from non-marine to marine conditions in a geologically short time. The extent of racemization of aspartic and glutamic acids in 45B are broadly equivalent with the results from Core 342.

Because of the bleached and partially dissolved nature of the *Dreissena polymorpha* samples in core 342, and similarly for those *Dreissena rostiformis* from the coquina in core 45B, it would be expected that some degree of loss of the more highly racemised free amino acid pool may have occurred, and have resulted in D/L values that were slightly lower than for unbleached samples of the same genus. If better preserved examples (not available in these samples) of *Dreissena* had been analysed it would be expected that there would be a greater difference in the extents of racemization than found here between *Mytilus* and *Dreissana*. Thus, despite the mixed nature of the taxa in core 342, these amino acid D/L values indicate mixing of older *Dreissena* with younger *Cardium* and *Mytilus* fragments.

6.7.4 Modern shoreline deposits

Articulated shells were recovered from three locations, Feodosia, western Kerch Peninsula; Constanta beach, Romania; and the southernmost Danube Delta coast 200 m north of the St George distributary (Table 6.3, Fig. 6. 9c). The lowest D/L values (mean asx D/L = 0.082, mean glx D/L = 0.047, in sample BS-22) were found from examples of the bivalve mollusc *Cardium edule* from the Danube Delta, and the highest extent of racemization (~ oldest) in 'modern' shells were from samples of the bivalve mollusc *Chione gallina* from Feodosia (mean asx D/L = 0.183, mean glx D/L = 0.061). Data from last interglacial (MIS 5e) deposits in Kerch Strait (unpublished, Chapter 7) indicate that *Chione* and *Cardium* are likely to have similar racemization rates (similar extents of racemization in the same deposit). Accepting this, it would seem that the shells at Feodosia are significantly older than those from Constanta and from the Danube Delta. The youngest AAR-based ages, determined to be from the samples from the Danube Delta, are consistent with the nature of this environment. The extent of time-averaging for these samples is over several hundred years, compared with some thousands for all other locations. This scale of time-averaging for the Danube Delta is similar

to the AMS dated *Dreissena coquina* from core 45B. Taken together, the amino acid racemization data are consistent with the stratigraphy in, and among the sampled horizons, with *Dreissena* consistently the oldest (Fig. 6.9d) and the youngest are the *Cardium* valves from the modern Danube Delta.

6.7.5 Amino Acid Racemization data, age-mixing of molluscs, and implications for chronology

Radiocarbon-calibrated amino acid racemization ages indicate that, in general, the extent of mixing of sub-fossil shells from the material examined is not significant (i.e. not over for example interglacial-interglacial timescales) and suggests a short period of time in which the environment underwent profound change from non-marine (lacustrine) conditions to marine (Figure 6.10). The extent of time-averaging in adjacent horizons in core BS-37-82 was found to be up to 3,400 yr based on aspartic and glutamic acid D/L values calibrated with AMS ^{14}C dates. The extent of age-mixing among mollusc shells in samples 342/2, and 342/3, was approximately of the same magnitude, bearing in mind the restrictions on the comparison of mollusc ages from species that inhabit different environments where reservoir ages are uncertain. Based on these results, it is clear therefore that there will be a significant inaccuracy in using bulk samples consisting of multiple individual shells from these cores for detailed chronology, especially where those samples were composed of mixed species. Here, the age of the sedimentary event in question will invariably be younger than the age of the single, and commonly fragmented, valves. Attempts to date horizons with single reworked valves are therefore prone to overestimating the age of the sedimentation event in question, and as a result any interpretation of dates from such analyses are questionable except at the broad scale. The exception to this may be where the difference in ages of shells from individual horizons reflects the actual age difference between successive sedimentary events. Furthermore, where mollusc shells are reworked, the associated and enclosing sediments in which they are encapsulated and which include pollen, dinoflagellate cysts, foraminifers and ostracods, will also have been reworked. The implication is that palaeoenvironmental studies undertaken on reworked shallow water sediments such as those from the Black Sea shelves may, in many cases, be unreliable at scales of resolution finer than the major depositional units commonly described (e.g. unit 1, 2 or 3 etc of Ryan *et al.*, 1997; Mudie *et al.*, 2002, or units A, B, C or Hiscott *et al.*, 2007). This will be exacerbated by proximity to fluvial systems (e.g. core 721), and faunal records from many cores are too limited to make meaningful environmental interpretation (Boomer *et al.*, 2010). Therefore, to overcome this complexity, other palaeoenvironmental records are required.

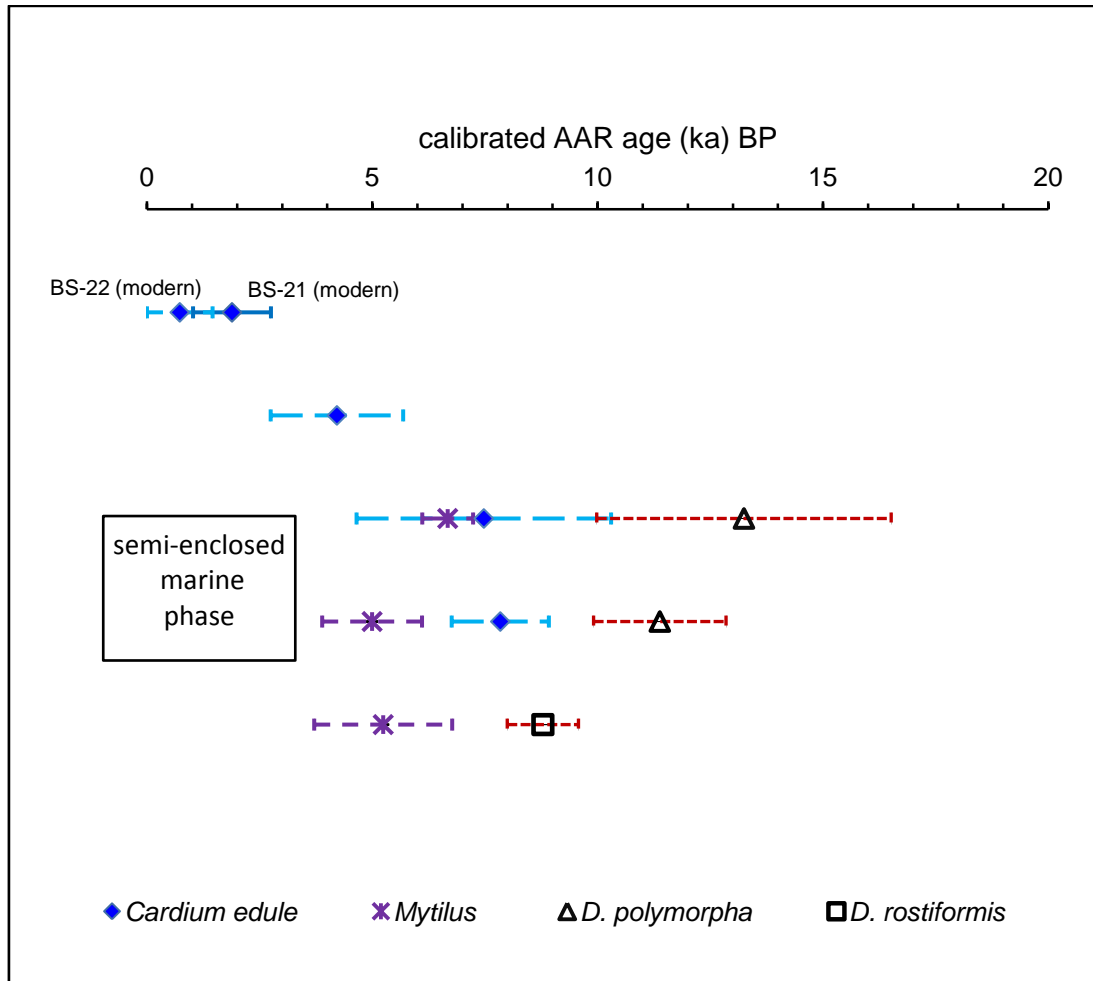


Figure 6.10. Mean ^{14}C -calibrated AAR ages and error bars (1σ uncertainties), on Black Sea molluscs. While there is a clear differentiation between the mean ages of the shells analysed, and the range (1σ) of ages overlap in several instances, there is little if any overlap between the marine shells *Cardium* and *Mytilus*, and the non-marine shells *Dreissena*. This reflects a sharp rather than gradual transition between the pre-existing lacustrine environment, and that of the Mediterranean-influenced transgressive waters. Any overlap likely reflects several processes, including age-mixing, processes associated with poorly preserved shells such as diffusive loss of amino acids and resultant lowered D/L values, as well as sampling on different parts of valves because of their fragmented state.

6.8 Revisiting the radiocarbon data

6.8.1 AMS dating and age-depth relationships of coastal peat deposits

Ages on small bulk samples of bivalve micro-molluscs from the upper sections of core 721 (Fig. 6. 5) indicate a mean sedimentation rate of 0.9 cm per annum for the strata between 2.0 m ($1,790 \pm 90$ ^{14}C a) and 17.25 m ($3,495 \pm 50$ ^{14}C a). This rate is high, yet given the proximity of the core site to the mouth of the Basla River, Sukhumi Bay (0.8 km distant, Balabanov 2007), this is not surprising. It does however appear to indicate more or less constant sedimentation over the past 3,500 ^{14}C a, and therefore is suggestive of a stable climatic regime at this location over that time, with moderately high rates of precipitation. Between 17.25 and

22.0 m in the core, the sedimentation rate is 0.1 cm a^{-1} . This is a significantly lower sedimentation rate than for the bulk of core 721, and may suggest a relative hiatus in sedimentation, low precipitation, or a higher extent of sediment reworking and/or perhaps erosion. However, data from this, or any other single core, is insufficient to base any basin-wide hypothesis, and other data therefore require consideration. In this case, we note the similarity of radiocarbon age-depth relationships between shallow-marine sediments in core 721 with that of the pollen record from Lake Aligol, Tsalka Plateau, Georgia (Connor, 2006). These data indicate a period of reduced sedimentation for broadly similar time (Fig. 6.11), and are suggestive of a regional climatic signature driven by low precipitation. Conditions on the Tsalka Plateau during the early Holocene were seasonally drier, cooler and cloudier than at present (Connor, 2006; Connor and Kvavadze, 2008). This is important because Sukhumi is situated on a narrow coastal strip backed by high mountains whose runoff flows directly into the Black Sea. The exact timing of the change in this regime to a more moist precipitation regime is uncertain, but lies between 3,500 and 8,200 ^{14}C a BP (core 721, uncorrected and uncalibrated ^{14}C a on molluscs). The regional climate in Georgia remained dry enough to prevent forests covering a wide area until 5-6,000 Cal a BP (Connor, 2006; Connor and Kvavadze, 2008).

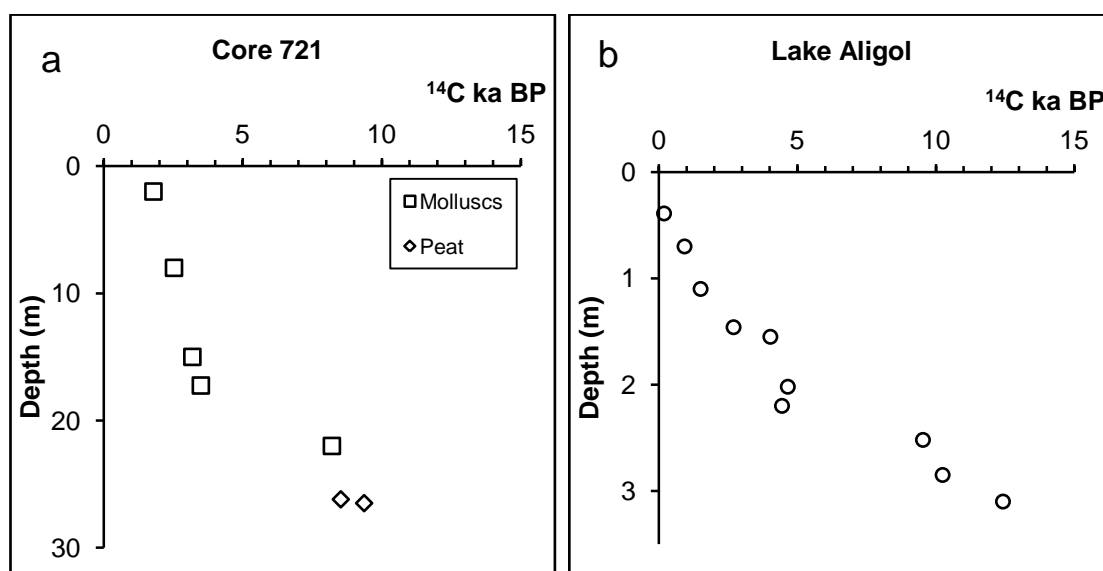


Figure 6.11. Similarity in age-depth relationship for AMS-dated radiocarbon samples between core 721 (this study) and a 3.1 m core from Lake Aligol, Georgia (Connor, 2006). Between 4,450 and 9,540 ^{14}C a BP there appears to be a significantly lowered sedimentation rate in the Georgian Mountains compared to more recent millenia. This period of lowered sedimentation is similar to that in core 721 between 3,495 and 8,210 ^{14}C a BP, and is suggestive of a regional period of lowered precipitation in Georgia compared to more recent trends.

Between approximately 9,580 and 8,530 ^{14}C a BP (Figure 6.5), organic matter was accumulating close to the modern shoreline at Sukhumi in a non-marine environment at depths of 42.1-41.0 m below present sea-level, and below the level of the Bosphorus Sill (Algan *et al.*, 2001). This was followed by a prompt transgression of marine water prior to approximately 8.21 ^{14}C ka BP (micromolluscs). At the basin-wide scale, sea-level curves based on mollusc ages alone may not clearly indicate if a significant transgressive event took place, but do indicate that a change from Caspian to Mediterranean fauna occurred during the early Holocene. This is because most AMS ages on molluscs from the Black Sea have been obtained from single valves, or fragments not in original life position, and these must therefore be indicative of some degree of reworking. Because the reworking of fossil molluscs can result in transport onshore, or downslope, any sea-level curve based on mollusc age-depth relationships is unlikely to be representative of the actual sea-level for the Black Sea, particularly in the absence of ages from articulated and *in-situ* molluscs. The exception to this is where bleached shell coquina is present at similar depths across a broad expanse of shelf in the Black Sea, marking the approximate position of palaeoshorelines.

6.8.2 Evidence from the Northwestern shelf of the Black Sea

The spatial and stratigraphic distribution of sub-fossil shells and alluvial sediments is similar for both the Ukrainian and Romanian sections of the northwest shelf (Figs. 6.7, 6.12; Popescu, 2004; Strechie-Sliwinski, 2007) with alluvial deposits occurring up to 85 to 90 m depth below present sea-level. A similar distribution of molluscs and shelf morphology has been noted also from the Bulgarian shelf (Ionin *et al.*, 1978). This suggests that environmental conditions on the mid and outer northwestern and western shelf, as indicated by the vertical and horizontal distribution of mollusc species, are representative for the Black Sea as a whole.

The presence of coquina consisting of *Dreissena rostriformis* at 107 m depth (core 45B) on the Ukrainian shelf is indicative of very shallow water conditions at the time of deposition, and are probably representative of, or indicate immediate proximity to, a palaeo-shoreline. Oxidation is required to remove original organic pigment from mollusc shell. The bleached and dissolved shells from the *Dreissena* coquina were either subaerially exposed, or bleached by sunlight in shallow water to result in loss of pigment. Exposure of these shells to the low salinity (alkaline) water column is unlikely to have led to acid digestion. These and similar deposits (e.g. B2KS24) are likely to represent a palaeoshoreline extending from the Romanian shelf to the south of the palaeo-Danube, trending approximately parallel to the 100 m isobath on the Ukrainian shelf, and are also present on the Crimean shelf at similar depths (Shcherbakov and Babak, 1979; Shcherbakov, 1991; Major *et al.*, 2006).

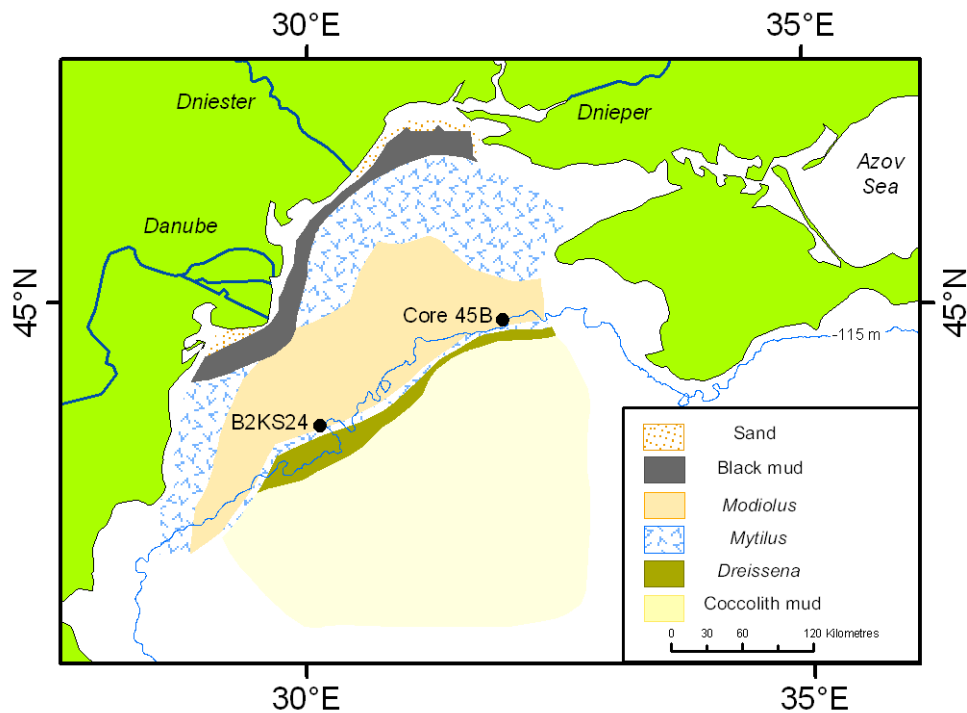


Figure 6.12. Spatial distribution of bivalve molluscs on the present northwestern shelf (Redrawn from Popescu, 2007 and Lericolais *et al.*, 2010). The locations from which core 45B and B2KS24 were recovered are near the southern margin of the *Modiolus* zone close to shelf break. At these locations *Modiolus* shells overlie *Mytilus* which in turn unconformably overlie *Dreissena* coquina.

6.8.3 Radiocarbon ages on peat deposits

The dates on peat obtained in this study on core 721 are in broad stratigraphic order (Figs. 6.5, 6.13). That is, the age of $8,530 \pm 110$ ^{14}C a BP at 26.2 m is younger than that of $9,370 \pm 70$ ^{14}C a BP at 26.5 m. The similarity of the previously published peat dates to the date presented here for the sample from 26.5 m in core 721 (40.4 mbsl) suggests that Apakidze *et al.*'s (1987) earlier data on peat deposits from Sukhumi Bay and other coastal locations within the Black Sea is equivalent. Thus, we use previously published radiocarbon dates on peat, including those from conventional β -counting, from the Black Sea region to investigate sea-level. The assumption is made here that the ^{14}C ages obtained from these peat deposits are representative of periods of time during which these deposits formed in coastal (terrestrial) settings above, or adjacent to, sea-level, and therefore changes in the age-depth positions of the peat deposits on the coast at Sukhumi over time demonstrate a response to changes in sea-level (Allan, 1990, 1995; Jordan and Mason, 1999; Nyman *et al.*, 2006; Connor *et al.* 2007; Brückner *et al.*, 2010). The general form of the sea-level curve produced (Fig. 6.13), without taking into account the extent of neotectonic uplift nor subsidence, appears to indicate a rising sea-level

in the early to mid Holocene, between approximately 9,400 ^{14}C a (basal peat, core 721) BP and 6,600 ^{14}C a BP (core 100, 8.8 m water depth; Balabanov, 2007), on the Sukhumi coast.

Holocene peat development in Sukhumi Bay is likely to reflect more closely the changes in sea-level than those peat records from the gently sloping western coasts of the Black Sea because of the distal position of the latter from any palaeo shore-line during the lake phase. For this reason the data from core 721 together with previously published (Görür *et al.*, 2001; Balabanov, 2007; Filipova-Marinova, 2007) conventional ages on peat were used to constrain the sea-level curve for the Black Sea during the Holocene. Coastal peat records (Figs. 6.1, 6.14) from present-day Bulgaria, Turkey (Sakarya Delta), and Ukraine, distal from the coast of Georgia and thus from Sukhumi Bay, show a simultaneous rise in water-level beginning below the level of the Bosphorus Sill (35 m depth). These data indicate this transgressive event was recorded basin-wide. This nullifies any outflow hypothesis (Aksu *et al.*, 1999) for the early Holocene because water-level would have had to be above the level of the sill at that time for outflow to occur. This peat-based sea-level curve is broadly contiguous with an age-depth curve based on *Dreissena* shell hash (i.e. coquina) ages, uncorrected for reservoir effect (Fig. 6.15), and together indicate a sea-level curve for the Holocene Black Sea. This evidence indicates an early Holocene transgression of the Black Sea, and a rising water-level that begins within the lake from below the depth of the Bosphorus sill at or below water depths of 107-112 m.

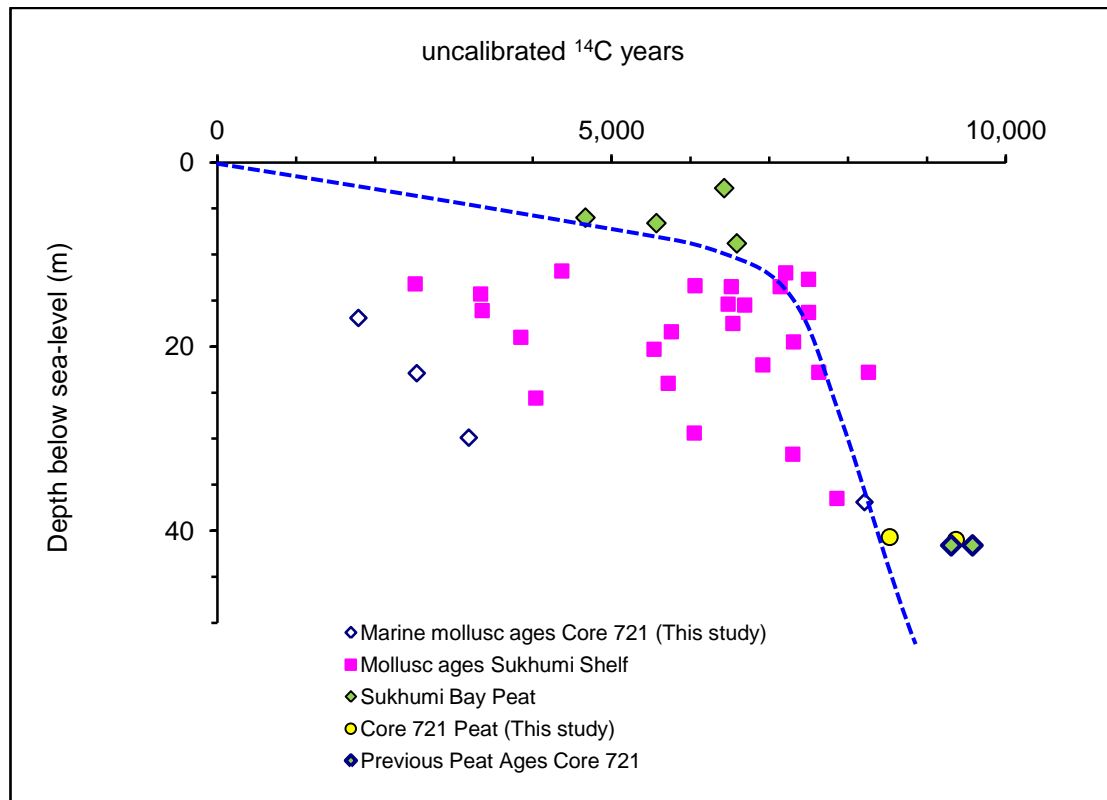


Figure 6.13. Sea-level curve (dashed line) and age-depth distribution of molluscs (filled squares, Balabanov, 2007), micromolluscs (this study; unfilled diamonds), and peat (filled diamonds) in Sukhumi Bay sediments based on conventional radiocarbon dating presented in Balabanov (2007), and the AMS radiocarbon ages obtained during this study on peat (filled circles). All of the mollusc samples from Sukhumi shelf dated by conventional methods are on bulk samples of shells, commonly with mixed marine and freshwater species together. These data are therefore problematic because assigning a specific environment to these ages is not possible. We therefore only consider the AMS data on identifiable individual molluscs as useful in this regard in the Black Sea.

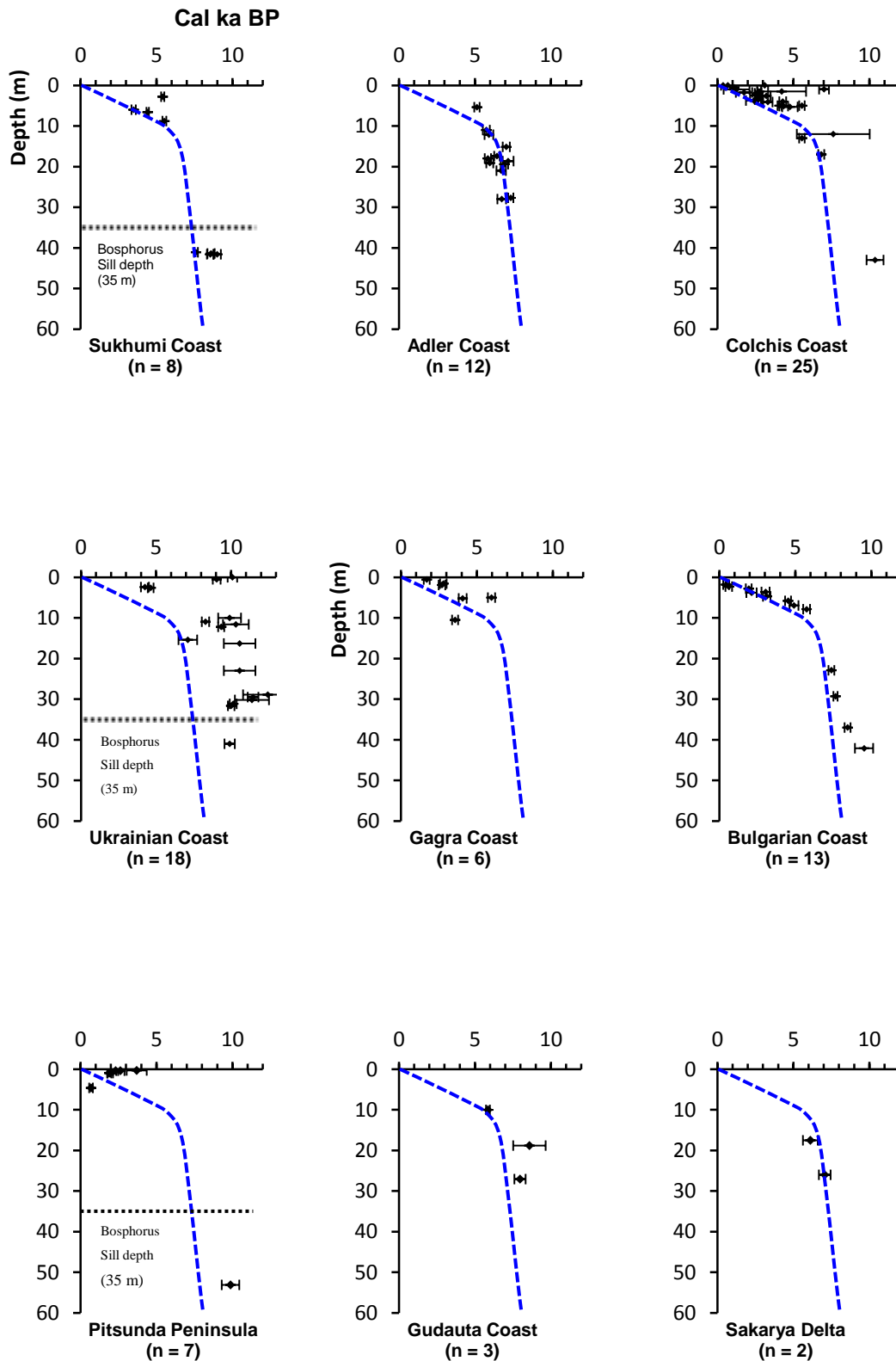


Figure 6.14. Sukhumi sea-level curve (dashed line) applied to peat ages from basin-wide locations in the Black Sea. These diagrams indicate an apparent similarity in age-depth distribution of peat samples among the individual locations (Fig. 1). Notably at four of these locations (Pitsunda Peninsula, Ukrainian coast, Colchis coast and Bulgaria; Fig. 1), peat was collected from below the level of the Bosphorus Sill, just as at Sukhumi Bay. In other words, this transgression was initiated from below the level of the Bosphorus Sill.

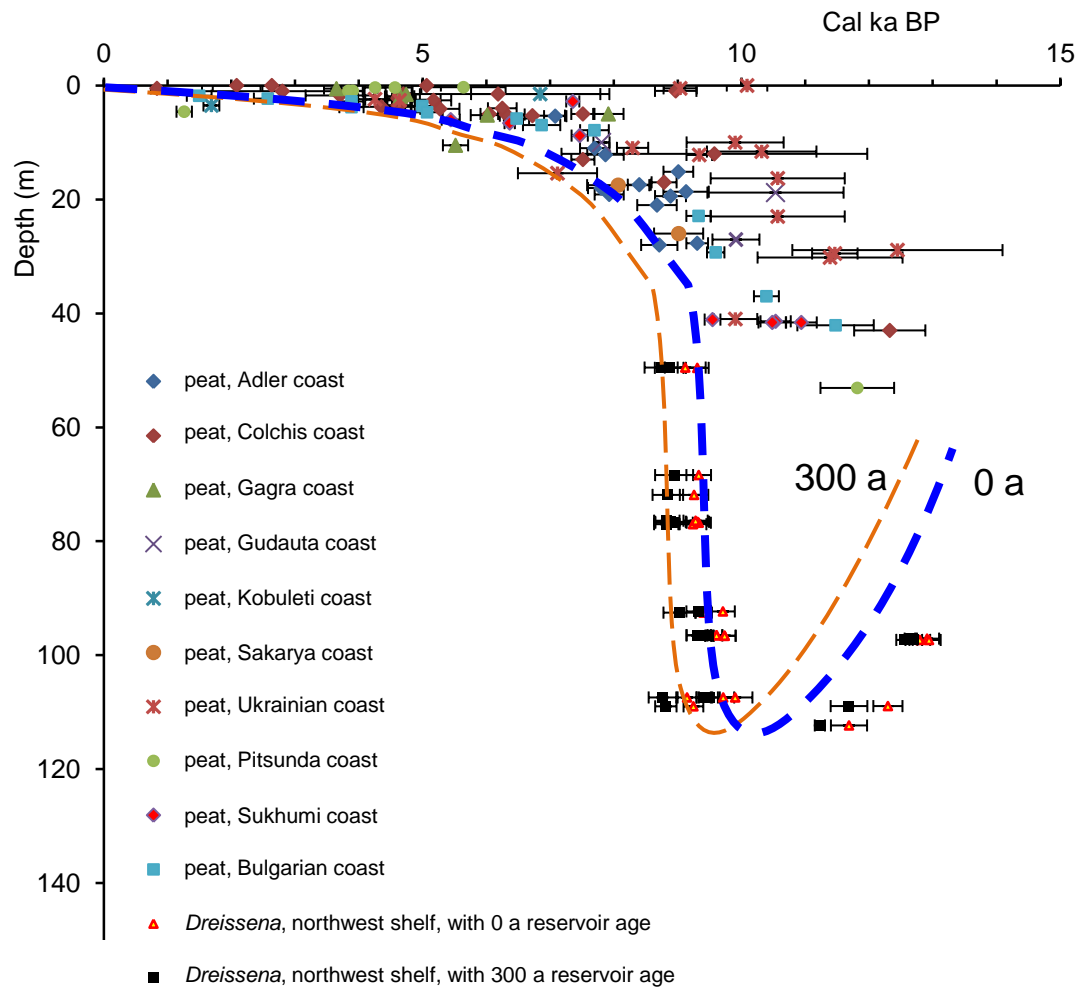


Figure 6.15. Sea-level curve for the post-glacial Black Sea from the initiation of the Younger Dryas to the present based on calibrated radiocarbon ages on peat, and *Dreissena coquina*. *Dreissena* from the northwest shelf was calibrated with 0 a (Kwiecien *et al.*, 2008), and 300 a (Soulet *et al.*, 2011a) reservoir age estimates. The oldest section of the sea-level curve is based on the age-depth relationship of *Dreissena* shells in mud, common in cores below the *Dreissena coquina* (e.g. Lericolais *et al.*, 2009). Based on these calibrated data, a near zero reservoir correction is suggested for the initial period of marine ingress (cf. Kwiecien *et al.*, 2008). However, additional radiocarbon ages on molluscs have not been calibrated because of the uncertainty in estimates of the reservoir effect. The 8.2 ka event occurred some 1100 yr after the water-level in this basin reached the Bosphorus Sill, and connection with the distal Mediterranean Sea had been re-established; however, evidence for that event is not present here.

This sea-level curve (Fig. 6.16a, b) indicates a transgressive event and change from fresh or slightly brackish lacustrine conditions, indicated by the presence of *Dreissena rostriformis* (Orlova *et al.*, 2005) to semi-enclosed marine conditions during the early Holocene Black Sea. The proliferation of large numbers of the bivalve mollusc *Dreissena rostriformis* on the outer and mid northwestern shelf marking a transgressing shoreline are likely to have been a response to changing and perhaps initially favourable water conditions prior to and during the

transgressive event. This was followed by a continuing rise in salinity enabling marine molluscs to proliferate during the mid to late Holocene. Despite the possible extent of time-averaging for molluscs on shelves in the Black Sea, differences in reporting ^{14}C ages, and the likelihood of variations in reservoir ages between mollusc samples, these basinwide data indicate that the first Mediterranean molluscs appeared in the Pontic Basin during the early Holocene.

This composite sea-level curve (Fig 6.16), which is constrained by the presence of coastal peat (giving the upper boundary for sea-level), enables us to make some observations on possible reservoir ages for the early Black Sea, and the preceding lacustrine phase. The fit of calibrated peat and *Dreissena* ages (Fig. 6.15; using a zero reservoir correction), suggest that since the end of the Younger Dryas the surface waters of the latest lacustrine phase in which *Dreissena* lived were in equilibrium with the atmosphere (Major *et al.*, 2002; Kwiecien *et al.*, 2008). We suggest a near-0 yearr reservoir age for the upper water column of the post Younger Dryas lake, a conclusion requiring a stratified palaeo-lake and ventilated upper water column in coastal regions on the northwestern shelf. This requires separation of the uppermost water in the Black Sea from the main body of water in the ~ 2 km deep basin, and suggests an influx of ventilated less dense water (low or nil salinity) from an external, most probably fluvial, source. Similar processes occur on the inner shelf in front of the Danube Delta at present. This stratification existed through 9.6-9.2 ka Cal a BP when some mixing (homogenisation) of the water column must have occurred due to the comparatively large influx of saline transgressing water (Bahr *et al.*, 2006). Once the stratified water column became re-established the reservoir age approached more recent estimates in locations more distal to large fluvial input. The age of a single *Dreissena polymorpha*, uncorrected for reservoir effect ($9,620 \pm 60$ ^{14}C a BP) and recovered from within a peat sample at 1.15 m depth in core 342 is 600 radiocarbon years older than the enclosing peat ($9,020 \pm 70$ ^{14}C a BP). A second peat sample at 1.65 m is younger ($8,920 \pm 60$ ^{14}C a BP) indicating reworked sediment. Although the number of radiocarbon determinations on *Dreissena* are few, the amino acid racemization data independently indicate that the *D. polymorpha* in core 342 are slightly older than *D. rostiformis* in core 45B. We suggest a low (near-zero) reservoir correction for this, and similar *D. polymorpha* from core 342.

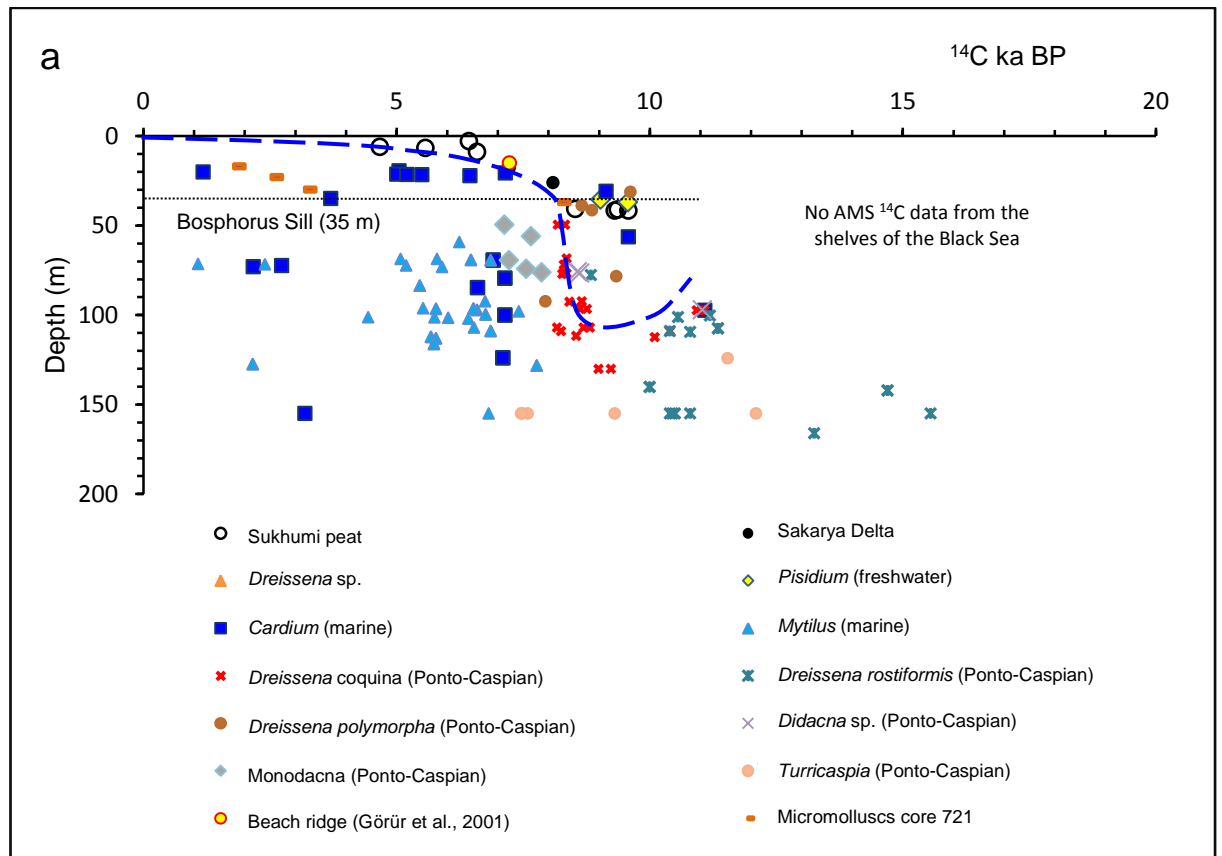


Figure 6.16a. Composite sea-level curve, and radiocarbon age-depth relationship among marine, brackish, and freshwater molluscs and reference peat samples (Sukhumi Bay and Sakarya delta) from the Black Sea. It is notable that most reports of *Dreissena polymorpha* are from levels higher on the shelf than *Dreissena rostriformis*. It is suggested here that this distribution is because the *D. polymorpha* inhabited generally freshwater environments on the shelves while *D. rostriformis* principally inhabited the low salinity coastal regions in the brackish lake.

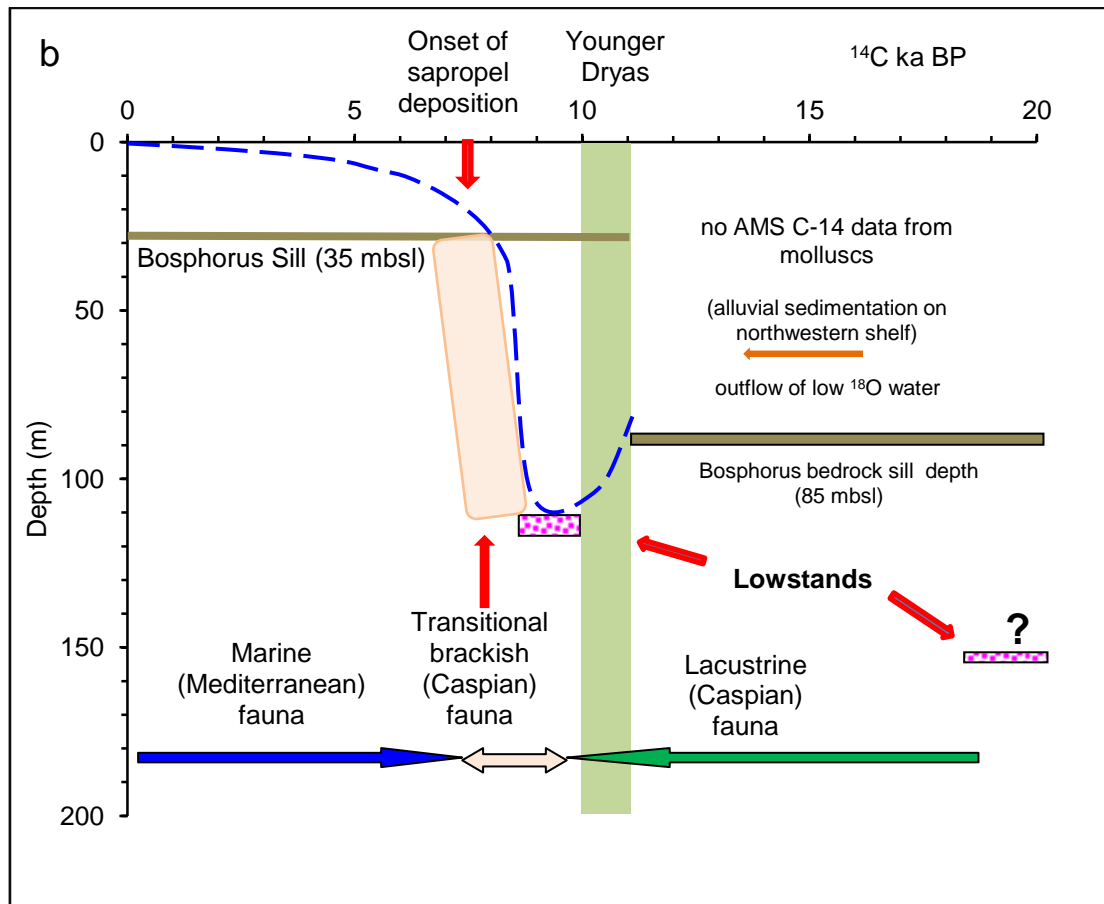


Figure 6.16b. Summary figure of the major phases of the development of the lacustrine to marine Black Sea during the Younger Dryas to late Holocene. There are no AMS ^{14}C ages older than 13 ^{14}C ka BP on fossil shells from the shelves of the Black Sea, despite such ages from conventional radiocarbon dating being used in a number of studies. This is likely to reflect, to a large extent, subaerial exposure and weathering of the outer and mid shelf sediments above the shelf break since the Last Glacial Maximum. The depth of the LGM lake level is estimated, and drawn here at -150 m because there is no evidence based on the dating of individual shells by AMS methods that a LGM shoreline exists above the early Holocene *Dreissena coquina*, and a LGM shoreline may therefore exist below these levels. Any glacial outflow from the lake is limited by the depth of bedrock in the Bosphorus Strait, and must have occurred when lake levels were between 35 and 85 m depth.

6.9 Palaeoclimate: the post Younger Dryas in the Black Sea

The rapid changes in water-level within the Black Sea (Fig. 6.16) cannot be explained without taking into account the regional and global climate (Badertscher *et al.*, 2011). The sea-level curve presented here suggests that water-level in the post-glacial lacustrine phase was at 50-60 mbsl prior to drawdown during the Younger Dryas. Sources of water during this time include fluvial meltwater from the Scandinavian and Eurasian ice sheets (Bahr *et al.*, 2005, 2008), and perhaps from the Caspian Sea via the Manych Passage (Svitoch, 2009). However, the chronology on the Manych passage is based on conventional radiocarbon dating of bulk mollusc samples (Chepalyga, 2007) and thus poorly constrained. The absence of AMS radiocarbon ages on molluscs older than 13,000 ^{14}C a BP from the shelves of the lake (Fig.

6.16) suggests the shelves were subaerially exposed prior to the Younger Dryas, and any drawdown may not have been significant. Though the chronology here is different to that based on previous conventional radiocarbon ages, this is consistent with geomorphological evidence (Dolukhanov *et al.*, 2009; Larchenkov and Kadurin, 2011) which indicates alluvial sedimentation on the northwest (Ukrainian) shelf. AMS dates on *Dreissena* shells from sediments 8 m above basement within the Bosphorus Strait indicate the presence of fresh to low-salinity brackish water outflowing at $16,600 \pm 280$ ^{14}C a BP. This outflow, prior to the Younger Dryas, can only have been at a lower level than present, but above basement rock (basement sill at 80-85 mbsl, Algan *et al.*, 2001). Low- ^{18}O water was present prior to the Younger Dryas within the lake phase (Bahr *et al.*, 2008). If there were subaerial exposure of the shelves and outflow into the sea of Marmara during this time, it would require either an influx of low- ^{18}O water (Bahr *et al.*, 2008; Badertscher *et al.*, 2011), or perhaps disturbance of the 2 km deep water column of the Black Sea, to maintain this geochemical balance. If the Bosphorus were open during melt-water phases, closure by sedimentation, and/or tectonics to a height < 35 mbsl as indicated by Soulet *et al.* (2011a) must have occurred sometime between the end of outflow at approximately 13.5 ^{14}C a BP and the transgression at 8.6 ^{14}C ka BP. An 'evaporative' drawdown of the lake may never have happened. It seems more likely that a reduction in precipitation occurred, concomitant with the onset of the Younger Dryas.

Terrestrial evidence from the circum Black Sea region suggests cooler conditions than present existed during the earliest Holocene, and prior to the onset of the mid Holocene 'optimum'. Evidence from a number of studies on Holocene sediments from the Black Sea basin suggest that sedimentation rates within regions proximal to coastal areas, were lower during the early to mid Holocene, than for the Mid Holocene - to present (e.g. Fig. 6.11). Terrestrial records from Turkey (Eastwood *et al.*, 1999; Wick *et al.*, 2003), and Romania (Feurdean, 2005; Feurdean *et al.*, 2007) and deep-water data from the western Black Sea (Atanassova, 2005) are suggestive of comparatively dry conditions between approximately 10,000 and 8,000 a BP. This evidence includes significant charcoal deposits, dated to before 8,200 a BP at Lake Van, Turkey (Wick *et al.*, 2003) which may indicate lowered precipitation. Measurements of $\delta^{18}\text{O}$ on travertine in southwestern Turkey indicate warming at $9,000 \pm 600$ a BP (Vermoere *et al.*, 1999) and provide further support for slightly more arid conditions. Drier conditions in Romania (Feurdean *et al.*, 2007) are strongly suggestive of reduced Danube discharge at this time. The climate in Romania became moister after approximately 8,000 cal a BP, and similarly in western Bulgaria (Tonkov, 2003; Tonkov *et al.*, 2008).

Pollen-based evidence (Connor and Kvavadze, 2008) from Georgia indicates a period of lowered precipitation at the time of the initial marine ingress to the isolated lake. This is consistent with the absence of terrestrially-derived sediments from the *Dreissena* layer in core

45B, and the low sedimentation rate in core 721 above the peat layer. The Younger Dryas (YD) cooling is distinct in Georgia (Connor, 2006; Connor and Kvavadze, 2008), and similar to, for example, the evidence from Lake Van, Turkey (Lemke and Sturm, 1997), the European Alps (Ivy-Ochs *et al.*, 2009) and as far afield as Ireland (Diefendorf *et al.*, 2006). The timing of environmental change associated with the Younger Dryas within the circum-Black Sea region, including the European Alps (Magny *et al.*, 2001; Magny and Bégeot, 2004), the eastern Mediterranean (Casford *et al.*, 2001), Turkey (Rossignol-Strick, 1995) and Georgia (Connor and Kvavadze, 2008), indicates therefore a teleconnection with major atmospheric and oceanographic events in the North Atlantic. However, evidence for the 8.2 ka cooling event is not present here, suggesting attenuation of North Atlantic influence occurs, such that the Black Sea basin acts to ameliorate short-term climatic signatures.

During, and until the termination of the YD, alpine and other glaciers advanced repeatedly (Ivy-Ochs *et al.*, 2009), and rapid shrinkage of those glaciers occurred at or slightly before 10.5 cal ka BP. Because the source of the Danube lies in the northern European Alps, the advance of the alpine glaciers during the Younger Dryas can only have reduced, significantly, the volume of water flowing into the Black Sea via the Danube and adjacent rivers. The timing of rapid shrinkage of the alpine glaciers is coincident with the lowstand evident in Fig. 6.16, and also with the rapid uplift of land in south central Sweden that gave rise to (Baltic) Lake Ancylus around 9,500 ¹⁴C a BP (Ojala *et al.*, 2005). Thus, as suggested by Lericolais *et al.* (2009) the presence of Lake Ancylus may have influenced water levels during the isolation phase of the Black Sea by re-routing water from the headwater catchments of rivers entering the northwest shelf. Because of the significant crustal depression due to ice-loading in the Baltic region during the last glacial (Lambeck *et al.*, 1998), the palaeo-fluvial systems of the many catchments draining into Lake Ancylus may have been larger. However, the combined evidence from the Georgian uplands, core 45B and core 721 presented here suggests that there was insufficient precipitation for the major rivers to raise the levels of the Black Sea in the earliest Holocene (Connor, 2006; Connor and Kvavadze, 2008).

6.10 Prompt transgression and gradual salinisation of the Holocene Black Sea

Previously, the work of Hiscott *et al.*, (2007) and Marret *et al.*, (2009) had suggested the presence of marine shells on the shelf at approximately 78 m depth on the southwest shelf when the majority of evidence indicates a lacustrine phase. However, these identifications have been changed to *Dreissena*, *Didacna* and *Theodoxus* (Hiscott *et al.*, 2010; Marret *et al.*, 2010). These latter species are indicative of non-marine, fresh to low-salinity brackish water (mean value ~ 4‰, Orlova *et al.*, 2005). The presence of *Pisidium* (pea clam, indicative of freshwater; Lericolais *et al.*, 2010) and substantial numbers of recovered Ponto-Caspian fauna

(including *Dreissena* and *Didacna*: Hiscott *et al.*, 2010; Marret *et al.*, 2010) at levels substantially below that of the Bosphorus Sill provide significant support for lowered water-level when the marine inundation began, and counter statistically limited evidence ($n = 3$) from reworked euryhaline bivalve molluscs (*Cardium*, this study; Major *et al.*, 2006; Giunta *et al.*, 2007) for a marine presence prior to this phase.

Thus, euryhaline Mediterranean molluscs colonised the Black Sea during a gradual change in salinity following the prompt transgression. The presence of bivalve molluscs *Monodacna caspia* and *Dreissena* (*D. rostriformis*, maximum normal salinity tolerance from 0 to 6-8‰, Orlova *et al.*, 2005) in the Black Sea between 8,600 and 7,130 (age of youngest *Monodacna* on shelf at -49 m, Major *et al.*, 2006) suggests a period of 1,500 ^{14}C a in which conditions changed from that suitable for Ponto-Caspian fauna to that of an environment capable of supporting a Mediterranean-type fauna. At some stage during this time both Caspian-derived and Mediterranean-derived taxa may have co-existed (Fig. 6.16a, b), with the age-depth distribution of *Monodacna* (Fig. 6.16a, b) overlapping with the marine fauna and the pre-existing *Dreissena* population over a 1,000 a period. The end of this period of overlap is contiguous with the earliest deposition of sapropel in the Holocene Black Sea. This appears to indicate a salinity and/or nutrient threshold across which the Ponto-Caspian fauna could not survive.

An unknown quantity in this debate is the extent to which the 2 km deep water column in the lacustrine phase was saline, and the contribution of that water to the surface layer. Even if this volume of water prior to the transgression had a salinity of 6-8 ‰, the volume of transgressing water (35‰ salinity) required to raise water-level to that of the Bosphorus Sill would be insufficient to raise suddenly the salinity of the lake to present values (c. 18-20 ‰) over the duration of the transgression. Only upon reconnection through the Bosphorus would any outflow of less saline water allow a substantial increase in salinity.

6.11 Reservoir ages and water level

There is no universally accepted ^{14}C reservoir correction for marine carbonate from the Black Sea, especially for the period of transition between lacustrine and marine conditions (Jones and Gagnon, 1994; Siani *et al.*, 2000; Kwiecien *et al.*, 2008; Soulet *et al.*, 2011a,b). The use of a single valve (*Cardium*, $9,140 \pm 60$ ^{14}C a BP, this study) is insufficient to attempt to determine a reservoir age for the earliest marine stage of the early Holocene Black Sea. A reservoir age of approximately 1,000 a is required to place this shell to the left of the sea-level curve in Fig. 6.16. This estimate is not outside the limits of previous reservoir age limits for the Black Sea, but contrasts strongly with the evidence from *Dreissena coquina* indicating a

near-zero reservoir age (Fig. 15). It is possible this shell has been misidentified. Data from two other *Cardium* (*Cerastoderma*) have been published (Major *et al.*, 2006; Giunta *et al.*, 2007), with ages that also plot within the area dominated by *Dreissena* (Fig. 6.16a) and therefore require consideration. The oldest date from a *Cardium* sample recovered from the deeper part of the northwest shelf (96 m; Giunta *et al.*, 2007), and the youngest on the shallowest (sample 342/3, this study), and the age-depth spread of these three data points is consistent with a transgression. However, based on Fig. 6.16, the youngest (this study) is located in an age-depth field dominated by peat samples, and is unlikely to represent those environments. Indeed, the polymorphic and euryhaline nature of *Cardium* within the Black Sea reduces its utility in fine-scale environmental identification (Panin, pers Comm., 2010).

The influence of any hardwater effect on molluscs that have populated coastal regions within the sphere of influence of fluvial water is unknown (Major *et al.*, 2006). Attributing reservoir age corrections obtained from marine environments to euryhaline molluscs such as *Cardium* that may inhabit a range of environments is fraught with uncertainty (Keith and Anderson, 1963). There is the likelihood that shells that grew in a fluvial or deltaic environment have undergone several episodes of transport and reworking (Stanley and Hait, 2000; this study), and as a result any environmental significance attributed to the lithologies in which they have been found must be treated with caution. Paired (articulated) valves found *in situ* in *life position* are the only likely reliable dating medium in these environments. There are few such reports for the Black Sea region; exceptions include work by Giosan *et al.* (2009) and Ongan *et al.* (2009).

The 600-year difference between the peat and encapsulated *Dreissena polymorpha* shell in core 342 may be due to reservoir effects on the carbonate, and/or mixing of different aged sedimentary particles. Additionally, the peat may not have been produced in the same environment nor time as the shells. The age on the underlying (sample 342/5) and younger peat sample gives a minimum age for this alluvial section of this core, because it requires no marine reservoir correction. This sedimentary stratum was deposited sometime after 8,920 ¹⁴C a BP (10,068 cal a BP). Thus, just after 10,000 cal a BP, fresh-water conditions, probably fluvial (sample 342/5) and then lagoonal/lacustrine conditions (sample 342/4) existed at the location of core 342 on the inner Ukrainian Shelf, with no evidence for marine conditions found in these two strata.

The evidence from Georgia (core 721) and the inner Ukraine shelf (core 342) is supported by evidence from the Danube Delta (Giosan *et al.*, 2009) with two radiocarbon age determinations on articulated *Dreissena polymorpha* having ages of 8,860 ± 45, and 8,660 ± 45 ¹⁴C a BP (9,590 and 10,102 Cal a BP) recovered from -38.8 and -41.4 m below present sea-level. Thus the Ukrainian and Romanian shelves, to depths of c. 40 m, only had non-marine

environments associated with fluvial or lacustrine systems (limited in size) at the beginning of the Holocene. At the same time, at 41.6 m depth on the inner, and comparatively steeply dipping Georgian shelf at Sukhumi Bay, peat was forming at 11,000 to 10,500 Cal a BP (Figs. 6.5, 6.14). The youngest peat in this core, dated to 9,550 cal a BP at 40.7 m below present sea-level (this study) indicates that, broadly speaking, the same conditions existed in Sukhumi Bay as on the Ukrainian and Romanian shelves at approximately the same depths, and there is no evidence of marine conditions at either of these locations during the earliest Holocene.

The sea-level curve in Fig.6.16 does not focus on a specific study site, but rather attempts to correlate on a basin-wide scale. It cannot account for local neotectonic movements, yet the evidence from coastal peat from the Ukrainian, Turkish, Bulgarian and Georgian coasts suggests a similar sea-level history for the Black Sea over approximately the past 10,000 years. The Danube delta and associated inner to mid shelf is perhaps the most tectonically stable portion of the Black Sea coastal regions at present. This lends itself to suggesting that any depression of shelf here has been minimal, and therefore because similar deposits have been found on the outer Ukrainian, Romanian and Bulgarian shelves, at similar depths, it is reasonable to suggest an initial palaeoshoreline of c. 95-107 m water depth for the time when the lake-level began to rise due to large-scale influx of Mediterranean-derived water.

The age-depth relationship for coastal peat in the Black Sea region indicates that water-level rose from below the level of the shallow Bosphorus Sill, and thus in contrast to Aksu *et al.* (1999) and others, we find no evidence for post Younger Dryas outflow from the Black Sea into the Marmara Sea (prior to approximately 9,000 ¹⁴C a BP. Furthermore, this evidence suggests that though a transgression of Mediterranean water into the Black Sea occurred, the water-level of the Black Sea may not initially have changed catastrophically as suggested by Ryan *et al.* (1997, 2003) during the Early Holocene.

This composite sea-level curve (Figs. 6.15, 6.16) suggests a transgressing sea-level that may have taken ~ 400 a (see also Thom, 2010) to reach the level of the Bosphorus Sill from the time of the initial ingress and depth of 107 m. This is slightly shorter than estimated by Görür *et al.* (2001), however these sea-level curves are broadly similar with water-levels of 20 mbsl at ~ 8.0 ¹⁴C ka BP. After an initial slow inflow, the bulk of Mediterranean water may have ingressed relatively swiftly. This is a rate similar to that suggested by Lericolais *et al.* (2009, 2011), and one substantially lower than that proposed by Ryan *et al.* (1997, 2003) and Siddall *et al.* (2004). The lacustrine low-stand is estimated here to occur immediately prior to 9.6 ¹⁴C ka BP, an age similar to that of Lericolais *et al.* (2011) who describe dunes being formed between 9.7 and 8.5 ¹⁴C ka BP on the desiccated northwestern Black Sea shelf. The length of time estimated for the period of lowered water-level is approximately 1,200 a (Fig. 6.16).

6.12 Synthesis

Peat deposits dated to between 12,500 and 8,300 cal a BP, recovered from the inner Ukrainian shelf (Balabanov, 2007) (Fig. 6.1, location 6) indicate terrestrial conditions at a depth of 41 m or more below present sea-level, a level below that of the Bosphorus Sill (35 m water depth). On the Ukrainian and Romanian shelves these terrestrial deposits are overlain by sediments with marine shells including *Cardium*, and *Mytilus*. In core 721 at Sukhumi Bay, Georgia, peat deposits, overlain by marine molluscs, have been recovered from below the level of the sill at 41 m depth (depth of water = 14.9 m, Fig. 6.5). The change from terrestrial to marine conditions in this core was found to occur between $8,530 \pm 110$ ^{14}C a BP (peat 26.2 m) and $8,210 \pm 120$ ^{14}C a BP (micromolluscs that include Mediterranean species, *Cardium*, 22.0 m). An AMS date obtained here on peat (26.5 m, $9,370 \pm 70$ ^{14}C a BP) is comparable to previous conventional radiocarbon ages at 26.7 m in this core (Balabanov, 2007), the likely difference being the extent of homogeneity of organic sediment. These results indicate prompt transgression by marine water occurred at Sukhumi Bay from below the level of the sill.

The Caspian bivalve mollusc *Dreissena rostriformis*, is commonly indicative of low-salinity brackish water (Therriault *et al.*, 2004; Orlova *et al.*, 2005), and thus restricted lacustrine conditions. On the outer Ukrainian shelf, a 20 cm thick shell coquina largely composed of bleached *Dreissena rostriformis* valves (mean age $8,562$ ^{14}C a BP; individually $8,170 \pm 60$, $8,695 \pm 40$, $8,820 \pm 70$ ^{14}C a BP) is present in core 45 (0.44 m in core, water depth 107 m). These are overlain by relatively unaltered fragments of the marine bivalve *Mytilus*, and in turn by the marine bivalve *Modiolus* (Fig. 6.7). These sediments in core 45 are correlatives of similar deposits from core B2KS24 (Lericolais *et al.*, 2009), located approximately 130 km distant on the southern margin to the Danube canyon. The similarity of these cores in age and composition indicate formation under near identical conditions at very similar times. In both cores the *Dreissena* hash (mean age $8,690$ ^{14}C a BP; individually $8,620 \pm 50$, $8,760 \pm 40$ ^{14}C a BP, core B2KS24) is unconformably overlain by *Mytilus* fragments, dated to $6,530 \pm 45$ ^{14}C yr BP ($6,520 \pm 40$ ^{14}C a BP, core B2KS24). In both cores, there is a time gap of approximately $2,200$ ^{14}C a between the freshwater and marine molluscs. Amino acid racemization data support this conclusion, with a time gap of approximately 2,800 a between ^{14}C -calibrated amino acid D/L values from *Dreissena rostriformis* and *Mytilus* specimens recovered from core 45. Comparison between the two AMS ages on this and similar *Dreissena* coquina (Major *et al.*, 2006; Lericolais *et al.*, 2009) indicate these individual bioclastic units have formed over short durations because the extent of age-mixing of *Dreissena* valves in these individual strata is very low (100s of years). These *Dreissena* coquinas, composed of shallow-water, near-shore species (Shcherbakov and Babak, 1979)

seem indicative of a palaeoshoreline, because the bleached (i.e. oxidised) condition of these shells points to subaerial exposure, or minimal water depths. This palaeo-shoreline extended across the Ukrainian and Romanian shelves between water depths of 95 and 112 m during the initial marine ingress. At this time fluvial input into the lacustrine phase of the Black Sea was lower than present, particularly indicated by the absence of terrestrial sediments in *Dreissena coquina* (core 45B), the reduced sedimentation in the first marine sediments of core 721, and pollen-based evidence from Georgia indicative of lowered precipitation (Connor, 2006; Connor and Kvavadze, 2008).

The age-depth curve indicated by calibrated AMS ages on single *Dreissena* from coquina layers (Fig. 6.15) suggests a rapidly migrating shoreline formed between approximately 9,600 (107 and 112 m water depth) and 9,250 cal a BP (49 m water depth). This age constrains the initial development of the Danube delta, and other deltas at their present locations to after 9,200 cal a BP. Whilst on a geological time-scale this event was quick, this transgression was not catastrophic.

Several processes, driven by Younger Dryas to early Holocene aridity (Connor, 2006; Feurdean *et al.*, 2007; Connor and Kvavadze, 2008) led to a lowered water level in the lacustrine Black Sea by removing large volumes of freshwater from the catchment of the Pontic Basin. However, the extent of drawdown may not have been substantial because the absence of AMS radiocarbon dated shells from the shelves appears to indicate subaerial exposure of the shelves prior to the Younger Dryas and therefore an open Bosphorus seaway. The Younger Dryas cooling event would have particularly affected the catchments of the major rivers (Danube, Dniester, Bug, and Dnieper) entering the Black Sea on the northwestern and western shelves. Processes that would have reduced water flow into the Black Sea include the growth of Alpine glaciers and the post Younger Dryas development of Lake Ancylus (Jensen *et al.*, 1999). Cessation of flow via the Manych depression of Caspian water into the palaeo-lake (Bahr *et al.*, 2005, 2008) would also have contributed significantly, as would early Holocene aridity (Connor and Kvavadze, 2008). Notwithstanding the difficulties in obtaining long cores, the lack of peat deposits recorded from below water depths of 40 m may reflect the climatically driven aridity and rapid change in water table due to the drawdown process which together inhibited the development of coastal peat deposits. The brackish water and post-glacial oscillation of water-level on the shelves of the palaeo-lake may have resulted in an environment largely unfavourable for human habitation until stabilisation of water-level after reconnection with the Mediterranean via the Bosphorus.

6.13 Conclusions

- (1) The AMS ^{14}C record on molluscs from the Black Sea, commonly using single shells, is different to results from conventional radiocarbon methods on bulk mollusc samples consisting of multiple individual shells that commonly inhabited different environments, and may have had different reservoir ages.
- (2) Using the results from amino acid racemization and radiocarbon dating methods on the same samples allowed a new perspective into the history of the Black Sea. Amino acid racemization D/L values calibrated with AMS ^{14}C ages on the same shells indicate a comparatively quick transition from lacustrine to marine conditions in the early Holocene Black Sea.
- (3) Accordingly, we have reassessed previously published ^{14}C ages on peat recovered from locations on the Bulgarian, Ukrainian, Turkish, Russian and Georgian coasts. These data indicate a sea-level rise during the early Holocene from an initial depth below the level of the Bosphorus Sill (35 m water depth).
- (4) On the outer Ukrainian and Romanian shelves at variable water depths of between 96-112 m, lacustrine-deltaic bivalve mollusc coquina (*Dreissena rostriformis*) of Caspian affinity are unconformably overlain by Mediterranean-sourced bivalves (*Mytilus*).
- (5) A sea-level curve constructed using ^{14}C age-depth on basinwide coastal peat deposits and AMS ^{14}C ages from *Dreissena* coquina indicates a prompt transgression that took ~ 400 a to raise water-levels from proximity to a palaeoshoreline (core 45B, 107 m depth) to the level of the Bosphorus Sill (35 m depth). This event was accompanied by a gradual rise in salinity from a maximum of 6-8‰ in the lacustrine phase and a parallel change in fauna from Ponto-Caspian-derived to Mediterranean over the same time period (1,000 a).
- (6) The absence of AMS-based radiocarbon ages on molluscs from the shelves of the Black Sea prior to 13 ka ^{14}C BP suggests the shelves were subaerially exposed from the LGM to the Younger Dryas, and the Bosphorus seaway was open to some extent prior to the Younger Dryas allowing outflow until Alpine and other glaciers advanced. The Bosphorus closed by way of sedimentation and/or tectonics to a height < 35 mbsl at some stage between the Younger Dryas and substantial marine ingress at 8.6 ka ^{14}C BP.

Chapter Seven

An aminostratigraphic study of Kerch Strait, northeastern Black Sea

7.1 Aims and outline

Last interglacial (MIS 5e) (Karangatian) sediments within the Black Sea exist in Kerch Strait, at Eltigen, Kerch Peninsula, Ukraine, and at Cape Tuzla, Taman Peninsula, Krasnodor Territory, Russia. The age of the Karangatian in the Black Sea is poorly constrained, with a number of ages having been previously reported for the coastal terraces of Kerch Strait, raised above present sea-level by several meters in places. This study aimed at deriving an aminostratigraphic chronology for these marine and non-marine sedimentary sequences because some of the previously reported ages and interpretations are out of step with the global sea-level record. D/L values were obtained on the total hydrolysable amino acids (THAA) and hydrolysable intracrystalline amino acids (HIAA) in bivalve molluscs and gastropods, and from the THAA in single foraminifers, *Elphidium* sp. Uranium-series ages on three articulated bivalve molluscs (2 *Cardium edule*, 1 *Chione gallina*) were used to calibrate D/L values and obtain numeric ages.

7.2 Introduction

Shallow marine fauna of Mediterranean affinity have been described from a number of locations within the Black Sea region, distal from their source – the Mediterranean Sea. Colonisation by these taxa prior to the last glacial maximum may have occurred during the Karangatian, a time period in which salinity rose to approximately 30‰ in this restricted sea (Muratov *et al.*, 1974; Dodonov *et al.*, 2000) and the Black Sea existed as a marine environment. In the northern Black Sea region sedimentary units of Karangatian age exist on the Caucasus coast, inner Ukrainian shelf, and Kerch Strait. Karangatian type localities (Salvador, 1994) exist at Eltigen, Kerch Peninsula, Ukraine and at Cape Tuzla, Taman Peninsula, Krasnodor Territory, Russia (Dodonov *et al.*, 2003; Svitoch, 2009).

The age of the Karangatian in the Black Sea is poorly constrained. The age of the last interglacial (MIS 5e) in northern Eurasia, including the northern Black Sea and Sea of Azov region, has been postulated to have lasted for the whole of marine oxygen isotope stage 5 (Molodkov and Bolikhovskays, 2002). It has been proposed to be composed of five marine transgressive-regressive cycles lasting from 245-65 ka (Zubakov, 1988). More recently this multistage event has been estimated to have lasted 50-70 ka (Svitoch *et al.*, 2000). The

stratotype at Eltigen have been described as being composed of three sedimentary cycles that correspond with oscillations in sea-level within the Black Sea (Dodonov *et al.*, 2000). Such fluctuations in sea-level may not conform to the marine oxygen isotopic scheme because of the isolation of this basin from the global ocean (i.e. the Mediterranean Sea). The influence of the marine realm on the Black Sea, being only open to marine influence through the Bosphorous and Dardanelles channels together, is controlled by the depth of the shallowest sill (today at -35 m in the Bosphorous). The extent to which the Black Sea has been in connection with the Mediterranean Sea since MIS 5e is largely uncertain. The exact transport path for any marine incursion into the Black Sea during the last interglacial (MIS 5e) is uncertain. These issues are exacerbated by the extent to which neotectonic movements have raised or lowered Karangatian sedimentary sequences above or below sea-level. Locations in which Karangatian sequences are visible are, to variable extents, tectonically active. As a result stratigraphic relationships are uncertain.

Marine coastal sedimentary sequences of the stratotype at Eltigen in Kerch Strait have been ascribed a last interglacial (MIS 5e), Karangatian age (MIS 5, Eemian, Mikulino) based on U/Th dating techniques (Zubakov, 1988; Arslanov, 1993; Dodonov *et al.*, 2000; Arslanov *et al.*, 2002). The range of ages obtained using U/Th methods on molluscs from Karangatian outcrops within present-day Kerch Strait spans 75 ka (Arslanov *et al.*, 2002). Most of these ages are between 90 and 130 ka, and based on the results of analyses on molluscs only from Eltigen (Dodonov *et al.*, 2000; Arslanov *et al.*, 2002). However, the southernmost section at Eltigen (Fig. 1) has also been dated to MIS 7a and 7c (Bylinsky *et al.*, 1990), and, luminescence- based ages for the southern Eltigenian exposure are from 150-200 ka (Zubakov, 1988). Therefore in this study amino acid racemization geochronological methods were utilised to investigate these sedimentary sequences (Murray-Wallace and Belperio, 1991; Murray-Wallace, 1995; Wehmiller and York, 1995; Sloss *et al.*, 2006; Owen *et al.*, 2007), and where possible attempt to correlate among these strata, located on the eastern and western coasts of Kerch Strait.

Initial work in this study, using the total hydrolysable amino acid content in fossils shells, highlighted inconsistencies in the results among individual shells and therefore in this study a second set of shells were analysed to determine D/L values from both the intra- and inter-crystalline amino acid fractions.

7.3. Regional geology and geomorphology

Kerch Strait is a shallow (~7-15m deep) channel separating the Crimean (Ukrainian) Kerch Peninsula from Krasnodar Territory (Russian Caucasus). During the Late Pleistocene a marine transgression of this region occurred, with subsequent colonisation by euryhaline Mediterranean fauna. This fauna has been described as the most stenohaline and thermophilic of the Black Sea Quaternary period (Nikonov *et al.*, 1992). This, the Karangatian transgression, named for the type section at Cape Karangat, on Kerch Peninsula, penetrated eastward as far as the western part of the Caspian Sea (Dodonov *et al.*, 2000; Svitoch & Yanina, 2001). Karangatian aged sediments (Mikulino Interglaciation, Chepalyga, 1984) have been described from the Crimea, the Caucasus, Bulgaria and Azov Sea region (Dodonov *et al.*, 2000), but only in the faulted, folded and uplifted Kerch-Tamanian block and on the Caucasian coastline do Karangatian-age terraces exist today raised from sea-level. Karangatian sediments in the Sea of Azov are below present sea-level. Several workers have correlated the sedimentary sequence at Eltigen, Kerch Peninsula, to the marine oxygen isotopic time-scale (e.g. Zubakov, 1988) but there is a large degree of uncertainty between the previous dating methods.

The best exposure of Karangatian sediments occurs at Eltigen, on the western Kerch Peninsula, and also at Lake Chokrak (Nikonov *et al.*, 1992). Sedimentary and fossiliferous Karangatian correlatives exist at Maly Kut, Cape Tuzla (Zubakov, 1988) and Cape Ayz-Aul, western Kerch Peninsula. At Eltigen, the outcrop extends for approximately 3.5 km, from the seaward side of the northern margin of Lake Tobechnik (45.18081°N, 36.40532°E) to the southern margin of Eltigen village (45° 12' 51.83" N, 36° 24' 7.86" E). These sediments are composed of basal lagoonal deposits (cf the Sarmation clays of Dodonov *et al.*, 2000), overlain by transgressive, generally northward dipping, mollusc rich sands and gravels. These are in turn overlain by loess and palaeosols. Current Mean Annual Temperature at Kerch is estimated as 11.2° C (Rivas-Martinez, 1996-2005).

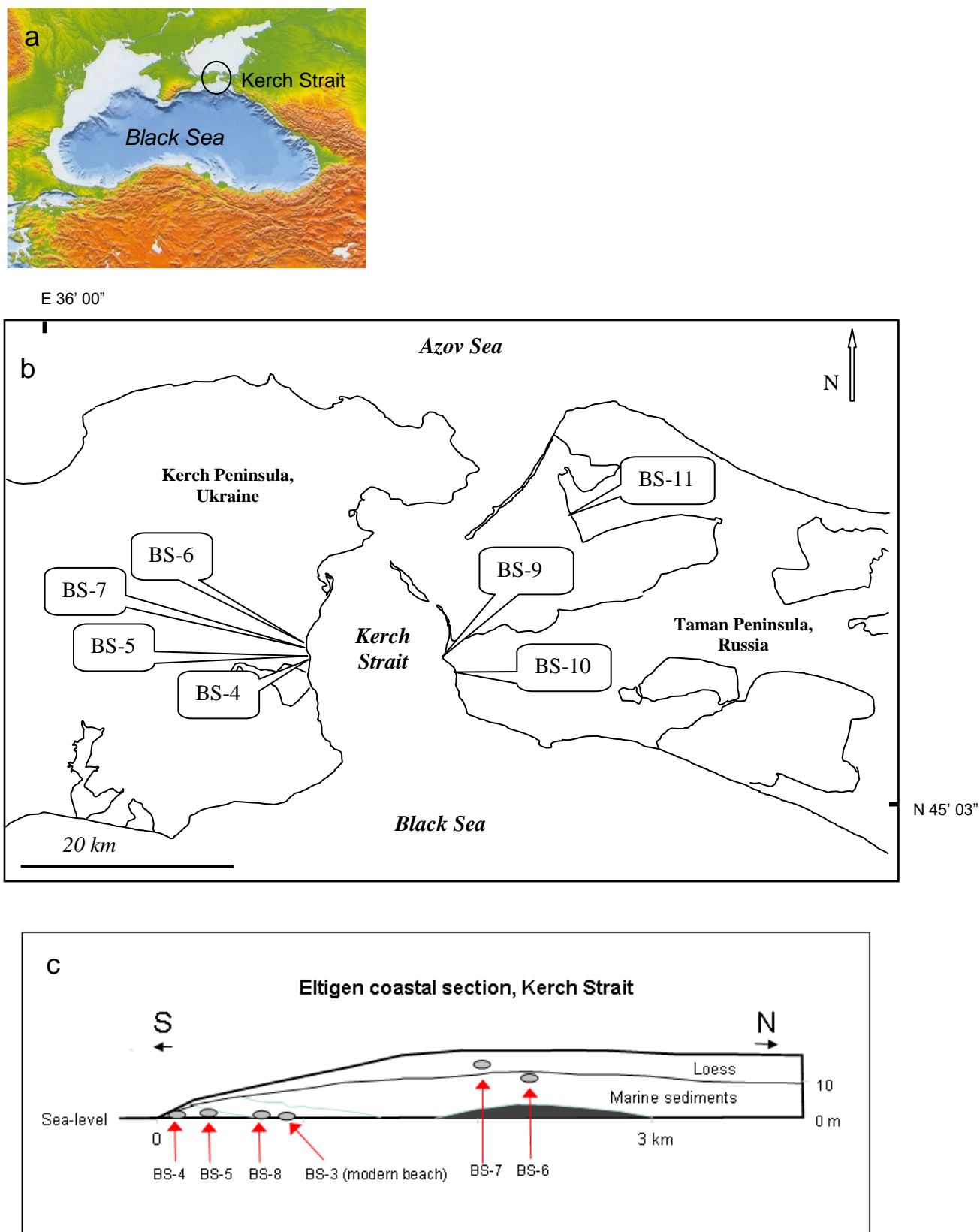


Figure 7.1. Sampling sites, Kerch Strait. a) Location of Kerch Strait, northwestern Black Sea, b) location of study sites, c) profile of Eltigen section with sampling locations. Profile adapted from Dodonov *et al.* (2000).

7.4. Methods

Fieldwork was undertaken in May 2007 at Eltigen, Kerch Peninsula, Ukraine, and Maly Kut, Cape Tuzla and Cape Krotkov on the Taman Peninsula, Krasnodar Territory, Russia. Articulated bivalve molluscs were the preferred subject for analyses, but only few were recovered, with by far the greater proportion being of individual valves. Amino acid racemization analyses were undertaken at the School of Earth and Environmental Sciences, University of Wollongong, Australia. Reverse-Phase High Performance Liquid Chromatography (Kaufman and Manley, 1998; Hearty *et al.*, 2004) was undertaken on bivalve molluscs, foraminifers and whole rock samples.

D/L values in the proteinaceous amino acids from the hydrolysable amino acid pool in aragonite molluscs was determined using methods similar to Penkman (2007, 2008). The hinge region of each mollusc was selected for use, with both the THAA and HIAA investigations, was cleaned with a dental tool, cut into pieces of 0.1-0.5 mg mass, etched with a stoichiometric volume of 2M HCl to remove approximately 33% of the shell exterior.

Uranium-series dating was undertaken at the Radiogenic Isotopic Laboratory, University of Queensland. Details on analytical procedures and instrumentation at University of Queensland are given in Zhao *et al.* (2001). ^{14}C AMS radiocarbon dating was undertaken on two individual juvenile *Helicella*, at the ANSTO facility, Lucas Heights, Sydney following the methods of Hua *et al.*, (2001). Uranium-series dating was undertaken on articulated shells, and these were also the target of the amino acid racemization studies. However, in transport from Russia to Wollongong, many of those shells collected as articulated and whole, were upon inspection found to be broken and disarticulated. Only shells originally collected as articulated samples were used, but these are described here as articulated or disarticulated, this referring to the state of preservation of the samples as received in the laboratory. Samples were also collected for luminescence dating, but are not discussed here.

7.5 Field observations and study site descriptions

7.5.1 Eltigen (BS 3-8 inclusive), Kerch Peninsula, Ukraine

(southern most point (BS-4) 45.18081° N 36.40532° E, northernmost study site, (BS-6), 45.19731° N, 36.40493° E)

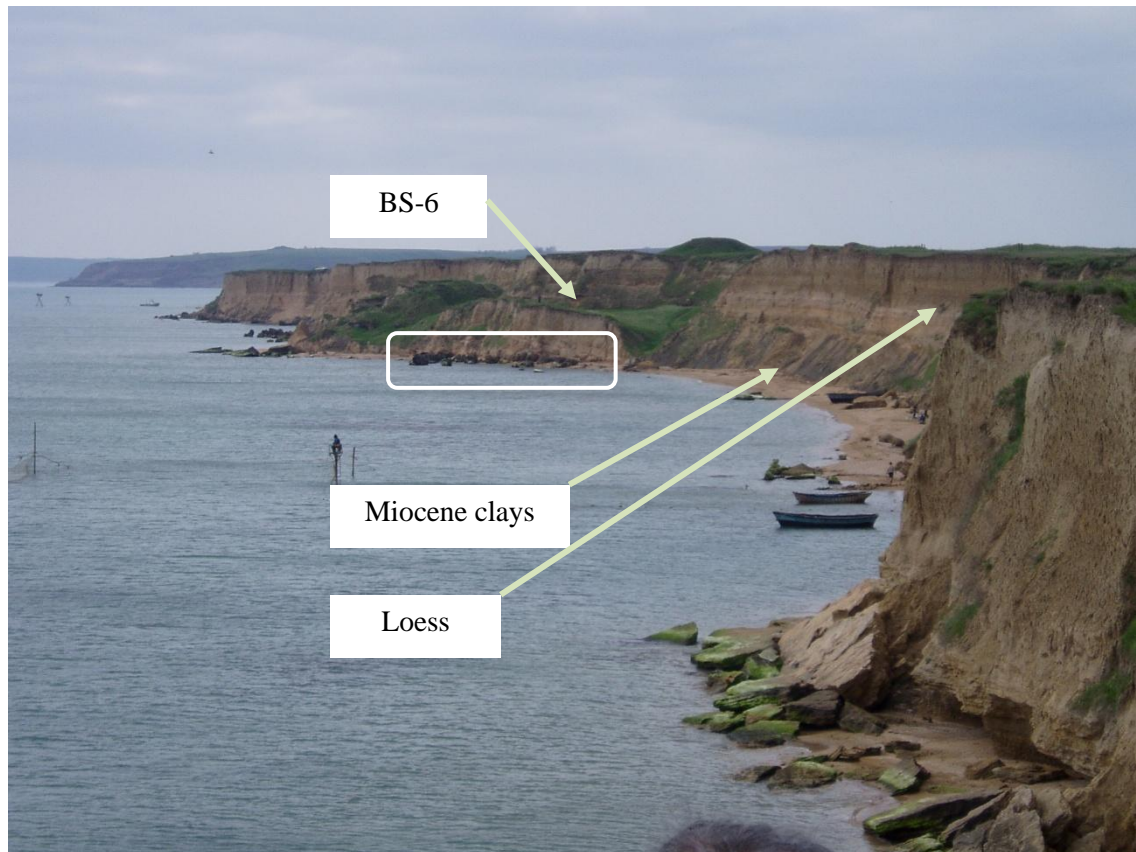


Figure 7.2. Coastal cliffs at Eltigen, Kerch Peninsula, northern Black Sea. View to south. Study site BS-6 is marked above, and is the northern-most study site investigated at Eltigen. To the north of BS-6 (arrowed) the sedimentary sequence of interest is situated above Miocene clays beneath thick loess. Bioherms (in box above) occur above the Miocene strata, and at the base of shell-rich estuarine-marine sediments.

The section of interest at Eltigen is 3.327 km long. The shoreline here is punctuated in places by large (up to 3 m in height) limestone bioherm structures, composed primarily of *Ostrea* shells set in a carbonate and algal matrix. One anticlinal fold, trending approximately east-west, and composed of Miocene clays, was truncated by, and underlies, the sedimentary sequence at Eltigen (grid ref 36.40493° E, 45.19731° N). Together with the overlying Karangatian sands and gravels, these form cliffs up to 25 m high. Here, in places, bioherm structures exist at the base of the Eltigenian sediments above the unconformity between the

Miocene and Late Quaternary sediments. Similar bioherms were located at Cape Krotkov (see below).

7.5.2 *Cape Tuzla (BS 9)*

(36.59803° E, 45.19549° N)

Cape Tuzla is located on the Taman Peninsula, south of Tuzla Promontory (Pilipenko et al., 2006; Svitoch, 2009; this study). The Tuzla section is located at the beginning of the Tuzla barrier spit (Svitoch, 2009). The sediments at this location are composed of Karangatian marine sands and clays overlain by loess and soil horizons. These units overlie Miocene (Neogene) clays and together form cliffs approximately 12 m high at the measured section, but in places are up to 20 m thick (Svitoch, 2009). The basal unconformity separating these strata is erosional and undulatory. Immediately overlying the unconformity is a gravel unit with a thin (1.5 cm thick) manganese layer and incorporated shell fragments. This unit may represent the erosional lag deposit associated with the marine sediments directly above it, yet given the known history of frequent water level oscillation on a geological time-frame within the Black Sea, this has to be viewed with caution. Above the basal conglomerate is approximately 1.4 m of well-sorted sand, micaceous and ferruginous in the upper sections. These sediments are overlain by similar sands rich in shell fragments, a coquina, possibly representing a palaeoshoreline. The top of this coquina grades upwards into dune sands, overlain by a thick sequence of loess.

7.5.3 *Cape Krotkov (BS 10)*

(36.61435° E, 45.17561° N)

This study site, located at a small isolated outcrop on the eastern side of Kerch Strait, consists of a shell rich bioherm layer below fine grained sediments, predominantly of silt grade siliciclastics. A fine-grained lagoonal unit, rich in *Cardium edule*, some of which are articulated, overlies the bioherm and its associated fine-grained sedimentary units. This 0.6 m thick unit is notably lighter in colour than the overlying and lower deposits. The uppermost, third, unit consists of lagoonal sediments with occasional *Cardium edule*, rarely articulated. All three units have varying amounts of bioherm rubble incorporated within them, lesser upwards. That they all have similar material suggests the upper layers have been partly reworked from the lower.

7.5.4. *Maly Kut (BS 11)*

(36.78170° E, 45.33402° N)

The study site at Maly Kut, a low-lying cliff sequence, consists of well sorted sands, (up to 100% sand sized grains), overlaid by thin silt-grade sediments with occasional shells, including *Cardium edule* and *Chione gallina*.

7.6. Results: total hydrolysable amino acids

7.6.1 *Whole-rock samples.*

Data was obtained for five study sites at Eltigen, BS-3, 4, 5, 6 and 8 (Table 7.1, Figure 7.2). The whole-rock method was the first method used in this study because it was thought that it may be the easiest way to differentiate different aged sedimentary units at Eltigen. It was chosen in preference to AAR analysis on individual mollusc shells because of uncertainties in racemization rates among the species found at these locations. These uncertainties are primarily because the taxa found here have not previously been studied using these methods. Whole-rock samples consist of an integrated amalgam of skeletal grains produced during taphonomic alteration and destruction of carbonate shell, foraminifers, ostracods and other carbonate-bearing skeletons. Thus, whole-rock samples consist of reworked skeletal carbonate, but the extent of reworking of the individual components may be variable. In regions where calcrete is present, this diagenetically-produced carbonate commonly is also part of the whole-rock sample. Using the amino acid racemization technique (Kaufman & Manley, 1998; Murray-Wallace *et al.*, 2010) it is possible to examine the extent of racemization in the individual skeletal carbonate elements to differentiate components of the sample which have differing ages. This therefore allows an estimate of the extent of reworking in whole-rock samples.

A modern skeletal carbonate sediment sample, collected from the present-day shell-rich beach at Feodosia, BS-1, approximately 30 cm above sea-level, and 5 cm below the shell-rich surface, yielded D/L values significantly higher (Asp = 0.331, Glx = 0.157, Val = 0.128) than D/L values obtained from articulated *Chione gallina* from the same location point (Asp = 0.189, Glx = 0.062, Val = 0.032). These results suggest that whole-rock samples from this location consist of individual skeletal grains of more than one age, and that much of this sediment must be reworked to varying degrees. However, these results do not imply that whole-rock samples from within Kerch Strait will demonstrate the same degree of

racemization, though the current mean annual temperature at both locations are the same (11° C).

Variations in the proportion of skeletal carbonate grains in a whole-rock sample among differing samples may reflect the source of sediment that make up each of the sedimentary units. Differing sources, their associated fauna, and variations in taphonomic and diagenetic processes are likely to produce whole-rock samples with differing D/L values. Large variations existed in the carbonate content among the individual whole-rock samples taken from this location. These variations may result in differences in D/L values among similar aged strata because where carbonate concentrations are low there may be concentrations of individual taxa, and thus variations among results because of the contained species (i.e. due to the species and genus effect).

With this in mind, it was found that aspartic and glutamic acid D/L values (Table 7.1) are generally similar for samples from BS-4, 5, 6 and 8, and indicates these are of a similar aminostratigraphic age. However, glutamic D/L values for BS-4-15, BS-4-17 and BS-8-8 are higher than for the other samples. These higher values were obtained on samples recovered from stratigraphically higher positions in the sedimentary sequence at each location.

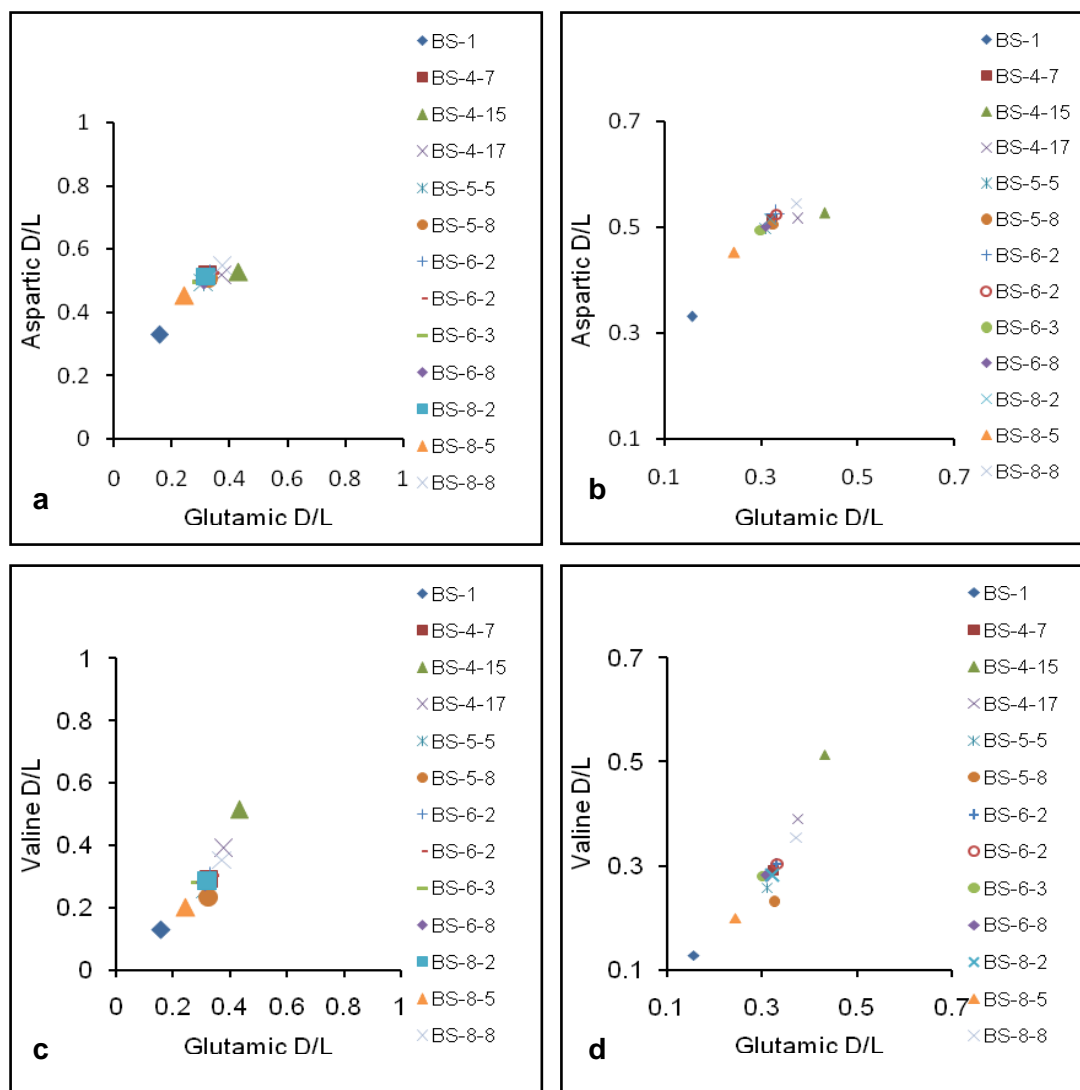


Figure 7.3. Whole-rock data from Eltigen, Kerch Strait. BS-1 is the present-day beach sample from Feodosia, western Kerch Peninsula, northeastern Black Sea. The results from aspartic-glutamic and valine-glutamic D/L pairs indicate the same apparent age relationship between individual horizons. BS-4-15 is the oldest, and BS-8-5 is the youngest. However, these results as graphically portrayed above require a careful interpretation. The sample BS-4-15 overlies BS-4-7 directly. Both are overlain by BS-4-17.

Table 7.1 . AAR data from the total hydrolysable amino acid pool in foraminifer, whole-rock and shell samples recovered from coastal sedimentary sequences in Kerch Strait. Mean D/L values are presented only for samples from the same horizon at each study site.

Study site	Species	Lab (UWGA) code	Asx D/L	Glx D/L	Ser D/L	Ala D/L	Val D/L
BS-5-2	<i>Elphidium</i>	7251 A	0.49	0.499	0.059	0.77	0.934
BS-5-2	<i>Elphidium</i>	7251 B	0.731	0.8	0.086	0.924	1.11
BS-5-2	<i>Elphidium</i>	7251 C	0.511	0.541	0.153	0.648	0.798
BS-5-2	<i>Elphidium</i>	7251 E	0.721	0.769	0.175	0.93	1.164
BS-5-2	<i>Elphidium</i>	7251 F	0.6	0.809	0.087	1.02	1.115
BS-5-2	<i>Elphidium</i>	7251 G	0.678	0.734	0.15	0.821	1.000
BS-5-2	<i>Elphidium</i>	7251 H	0.367	0.5	0.039	0.863	1.015
BS-5-2	<i>Elphidium</i>	7251 H	0.661	0.783	-	0.936	1.457
BS-5-2	<i>Elphidium</i>	7251 I	0.562	0.681	0.156	0.873	0.832
	Mean		0.591	0.68	0.113	0.865	1.047
	Stdv		0.114	0.123	0.048	0.103	0.187
	(%)		19	18	42	12	18
BS-1	Whole-rock	6296 A, B	0.331	0.157	0.366	0.209	0.128
BS-4-7	Whole-rock	6296 Z	0.517	0.323	0.337	0.546	0.292
BS-4-15	Whole-rock	6296 E2	0.527	0.432	0.312	0.672	0.514
BS-4-17	Whole-rock	6296 E, F	0.516	0.375	0.446	0.584	0.39
BS-5-5	Whole-rock	6296 I, J	0.496	0.311	0.328	0.456	0.258
BS-5-8	Whole-rock	6296 A2, G2	0.506	0.326	0.248	0.312	0.23
BS-6-2	Whole-rock	6296 L	0.525	0.331	0.419	0.529	0.304
BS-6-3	Whole-rock	6296 M, N	0.495	0.301	0.387	0.498	0.281
BS-6-8	Whole-rock	6296 C2, I2	0.501	0.31	0.409	0.51	0.282
BS-8-2	Whole-rock	6296 O, P	0.514	0.321	0.3875	0.412	0.283
BS-8-5	Whole-rock	6296 B2, H2	0.452	0.245	0.445	0.357	0.199
BS-8-8	Whole-rock	6296 Q, R	0.546	0.374	0.337	0.565	0.354
BS-4-12	<i>Cardium edule</i> (U/Th)	7253	0.422	0.199	0.394	0.301	0.132
BS-11-3	<i>Cardium edule</i> (U/Th)	7252	0.438	0.239	0.472	0.393	0.176
BS-10-4	<i>Cardium edule</i>	7298	0.398	0.211	0.402	0.304	0.117
BS-10-4	<i>Cardium edule</i>	7299	0.421	0.208	0.443	0.304	0.136
BS-10-4	<i>Cardium edule</i>	8000	0.4	0.175	0.415	0.231	0.11
	Mean		0.406	0.198	0.42	0.28	0.121
	Stdv		0.01	0.016	0.017	0.034	0.011
	(%)		3	8	4	12	9
BS-10-2	<i>Cardium edule</i>	8001	0.358	0.223	0.51	0.337	0.181
BS-10-2	<i>Cardium edule</i>	8002	0.412	0.198	0.396	0.231	0.132
BS-10-2	<i>Cardium edule</i>	8003	0.379	0.248	0.392	0.341	0.185
BS-10-2	<i>Cardium edule</i>	8004	0.367	0.237	0.437	0.388	0.176
BS-10-2	<i>Cardium edule</i>	8005	0.339	0.246	0.441	0.384	0.172
BS-10-2	<i>Cardium edule</i>	8006	0.425	0.239	0.452	0.35	0.169
	Mean		0.38	0.232	0.438	0.339	0.169
	Stdv		0.03	0.017	0.039	0.052	0.017
	(%)		8	7	9	15	10
BS-6-3	<i>Cardium edule</i>	7230	0.454	0.285	0.564	0.58	0.202

BS-6-3	<i>Cardium edule</i>	7230	0.514	0.28	0.557	1.094	0.186
BS-6-3	<i>Cardium edule</i>	7230	0.45	0.291	0.473	0.579	0.181
BS-6-3	<i>Cardium edule</i>	7230	0.432	0.28	0.662	0.565	0.22
	Mean		0.463	0.284	0.564	0.705	0.197
	Stdv		0.031	0.005	0.067	0.225	0.015
	(%)		7	2	12	32	8
BS-6-4	<i>Cardium edule</i>	7232	0.493	0.292	0.645	0.536	0.185
BS-6-4	<i>Cardium edule</i>	7232	0.455	0.29	0.704	0.565	0.192
BS-6-4	<i>Cardium edule</i>	7232	0.439	0.246	0.572	0.506	0.146
BS-6-4	<i>Cardium edule</i>	7232	0.492	0.291	0.574	0.542	0.192
BS-6-4	<i>Cardium edule</i>	7232	0.423	0.275	0.493	0.517	0.17
	Mean		0.46	0.279	0.598	0.533	0.177
	Stdv		0.028	0.018	0.072	0.02	0.017
	(%)		6	6	12	4	10
BS-1	<i>Chione gallina</i>	8017	0.2105	0.066	0.3355	0.0635	0.0325
BS-1	<i>Chione gallina</i>	8018	0.232	0.072	0.3595	0.086	0.0365
BS-1	<i>Chione gallina</i>	8019	0.232	0.074	0.3715	0.073	0.04
BS-1	<i>Chione gallina</i>	8020	0.155	0.054	0.193	0.029	0.0275
BS-1	<i>Chione gallina</i>	8021	0.116	0.0455	0.1295	0.035	0.022
	Mean		0.189	0.062	0.278	0.057	0.032
	Stdv		0.052	0.012	0.110	0.025	0.007
	(%)		27	20	39	43	23
BS-3	<i>Chione gallina</i>	6298	0.071	0.036	0.063	0.035	0.055
BS-3	<i>Chione gallina</i>	6299	0.074	0.038	0.056	0.027	0.057
	Mean		0.073	0.037	0.06	0.031	0.056
	Stdv		0.002	0.001	0.004	0.004	0.001
	(%)		2	3	6	13	2
BS-11-3	<i>Chione gallina</i>	7204	0.442	0.185	0.517	0.349	0.214
BS-11-3	<i>Chione gallina</i>	7208	0.485	0.21	0.548	0.426	0.196
	Mean		0.464	0.198	0.533	0.388	0.205
	Stdv		0.022	0.013	0.016	0.038	0.009
	(%)		5	6	3	10	4
BS-4-16	<i>Chione gallina</i>	7201	0.498	0.241	0.536	0.461	0.231
BS-4-16	<i>Chione gallina</i>	7202	0.507	0.248	0.503	0.506	0.227
BS-4-16	<i>Chione gallina</i>	7203	0.513	0.254	0.56	0.438	0.252
	Mean		0.506	0.248	0.533	0.468	0.237
	Stdv		0.006	0.005	0.023	0.028	0.011
	(%)		1	2	4	6	5
BS-4-17	<i>Chione gallina</i>	6297	0.55	0.276	0.597	0.543	0.265
BS-6-7	<i>Chione gallina</i> (U/Th)	7254	0.498	0.256	0.2975	0.4655	0.219
BS-6-7	<i>Chione gallina</i>	7205	0.486	0.285	0.589	0.59	0.271
BS-6-7	<i>Chione gallina</i>	7210	0.443	0.270	0.437	0.581	0.261
BS-6-7	<i>Chione gallina</i>	7211	0.488	0.295	0.580	0.598	0.280
	Mean		0.521	0.278	0.651	0.572	0.218
	Stdv		0.027	0.017	0.039	0.038	0.033
	(%)		5	6	6	7	15

BS-6-7	<i>Chione gallina</i>	7234	0.5555	0.298	0.7035	0.5645	0.2335
BS-6-7	<i>Chione gallina</i>	7234	0.511	0.2585	0.648	0.5125	0.1765
BS-6-7	<i>Chione gallina</i>	7234	0.5015	0.258	0.634	0.5665	0.1905
BS-6-7	<i>Chione gallina</i>	7234	0.5495	0.2915	0.681	0.6285	0.22
	Mean		0.529	0.277	0.667	0.568	0.205
	Stdv		0.027	0.021	0.032	0.047	0.026
	(%)		5	8	5	8	13
BS-6-4	<i>Chione gallina</i>	7233A	0.514	0.263	0.6505	0.549	0.2
BS-6-4	<i>Chione gallina</i>	7232I	0.5585	0.2875	0.6815	0.538	0.189
	Mean		0.536	0.275	0.666	0.544	0.195
	Stdv		0.022	0.012	0.016	0.006	0.006
	(%)		4	4	2	1	3
BS-9-8	<i>Chione gallina</i>	7206	0.454	0.202	0.507	0.464	0.213
BS-6-3	<i>Mytilus</i>	7231A	0.624	0.366	0.712	0.612	0.308
BS-6-3	<i>Mytilus</i>	7231C	0.633	0.339	0.745	0.602	0.306
BS-6-4	<i>Mytilus</i>	7232C	0.601	0.321	0.6915	0.591	0.2715
	Mean		0.619	0.342	0.716	0.602	0.295
	Stdv		0.013	0.018	0.022	0.009	0.017
	(%)		2	5	3	1	6
BS-4-18	<i>Helicella</i>	7297	0.518	0.288	0.587		
BS-4-20	<i>Helicella</i>	7289	0.531	0.283	0.548	0.326	0.153
BS-4-20	<i>Helicella</i>	7290	0.526	0.282	0.717	0.407	0.125
BS-4-20	<i>Helicella</i>	7282	0.548	0.278	0.529	0.365	0.173
	Mean		0.535	0.281	0.598	0.366	0.15
	Stdv		0.009	0.002	0.085	0.033	0.02
	(%)		2	1	14	9	13
BS-5-10	<i>Helicella</i>	7281	0.54	0.298	0.572	0.336	0.184
BS-5-10	<i>Helicella</i>	7284	0.529	0.268	0.507	0.296	0.146
BS-5-10	<i>Helicella</i>	7285	0.536	0.26	0.645	0.299	0.135
BS-5-10	<i>Helicella</i>	7286	0.633	0.405	0.604	0.442	0.235
BS-5-10	<i>Helicella</i>	7288	0.484	0.296	0.373	0.306	0.176
BS-5-10	<i>Helicella</i>	7290	0.528	0.293	0.678		
	Mean		0.542	0.303	0.563	0.336	0.175
	Stdv		0.045	0.048	0.101	0.055	0.035
	(%)		8	16	18	16	20
BS-10-2	<i>Helicella</i>	7283	0.493	0.284	0.38	0.326	0.182
BS-12-1	<i>Helicella</i>	7291	0.067	0.036	0.028	0.035	0.049
BS-12-1	<i>Helicella</i>	7292	0.061	0.034	0.025	0.054	0.024
BS-12-1	<i>Helicella</i>	7293	0.077	0.039	0.029	0.042	0.045
BS-12-1	<i>Helicella</i>	7294	0.065	0.034	0.027	0.093	0.066
BS-12-1	<i>Helicella</i>	7295	0.08	0.041	0.031	0.045	0.032
	Mean		0.07	0.037	0.028	0.054	0.043
	Stdv		0.007	0.003	0.002	0.021	0.014
	(%)		10	8	7	38	34
BS-7-2	<i>Helicella</i>	8022	0.161	0.069	0.218	0.036	
BS-7-2	<i>Helicella</i>	8022	0.181	0.064	0.264	0.075	0.041
BS-7-2	<i>Helicella</i>	8022	0.187	0.067	0.256	0.077	0.034
	Mean		0.176	0.067	0.246	0.063	0.038

Stdv (%)	0.011 6	0.002 3	0.02 8	0.019 30	0.004 9
ILCA	0.386	0.203	0.466	0.314	0.126
ILCB	0.684	0.432	0.438	0.685	0.365
ILCC	0.847	0.822	0.348	1.024	0.792
ILCZ	0.18	0.048	0.115	0.054	0.032

7.6.2. *Elphidium*

Similar to the results from core 721, Sukhumi Bay, relatively few microfossils were found in sediments recovered from Eltigen compared with Australian marginal marine sedimentary sequences (chapters 4, 5, 6). They were poorly preserved, commonly found as partial and discoloured tests, with iron staining. As a result of their poor preservation it was decided, after working on whole-rock samples, to analyse a limited number of *Elphidium* tests for the extent of racemization. Nine poorly preserved *Elphidium* tests from BS-5-2 were analysed for the extent of amino acid racemization in the total hydrolysable amino acid fraction. The *Elphidium* tests in the sediment sample from BS-5-2 were chosen because they were comparatively more numerous than in other sediment samples from Eltigen.

The fragmented nature, and range of D/L ratio values among the amino acids aspartic, glutamic, serine, alanine and valine in each test suggest a degree of reworking and/or loss of indigenous amino acids from these tests. Of the amino acids used in this study, valine is the most stable, having a relatively slow racemization rate compared to the other amino acids, and its more hydrophilic nature. The mean valine D/L, (whose value is slightly above the theoretical maximum value for this amino acid) in these tests of 1.047 ± 0.187 indicates racemic conditions for this amino acid. In contrast, the mean D/L ratio for aspartic acid of 0.591 ± 0.114 indicates a significantly lower extent of racemization for this amino acid in these tests. Similarly, the mean value for glutamic acid, 0.680 ± 0.123 , indicates a lower degree of racemization than for valine. Also D/L values for serine, mean = 0.113 ± 0.048 , are extremely low when compared with valine. Alanine, which decomposes to serine, had values in some cases (Table 8.1) that were near racemic, with a mean value of 0.865 ± 0.103 . Thus, the relative rates of racemization among these amino acids in these *Elphidium* tests are not in accord with previous studies on foraminifera (Kvenvolden *et al.*, 1973; this study, chapter 5). It is not possible to accurately estimate an age for these samples because the relative rates of racemization do not follow the generally accepted pattern and in several cases D- peak areas were too small to measure. Typically, diffusive leaching of the free, and more highly racemised amino acids in the total hydrolysable amino acid pool results in D/L values that are

lowered when compared with more well preserved examples. This is because the less racemised protein bound amino acids remain after leaching, and thus the D/L values obtained reflect the lower rate of racemization in these N and C-terminal residues. The amino acids in these foraminifera tests having relatively low D/L values are the hydrophylic amino acids, aspartic, glutamic and serine, and are those more prone to diffusive loss from the skeletal carbonate. Valine by comparison appears relatively stable, and much less reactive to hydrous conditions. These valine values suggest ages significantly older than for the whole-rock data. The incorporation of these and similar fossil material into the whole-rock samples will raise the D/L values in the whole-rock samples depending on the proportion of *Elphidium* and other old tests present. No further studies were undertaken on foraminifers from Kerch Strait.

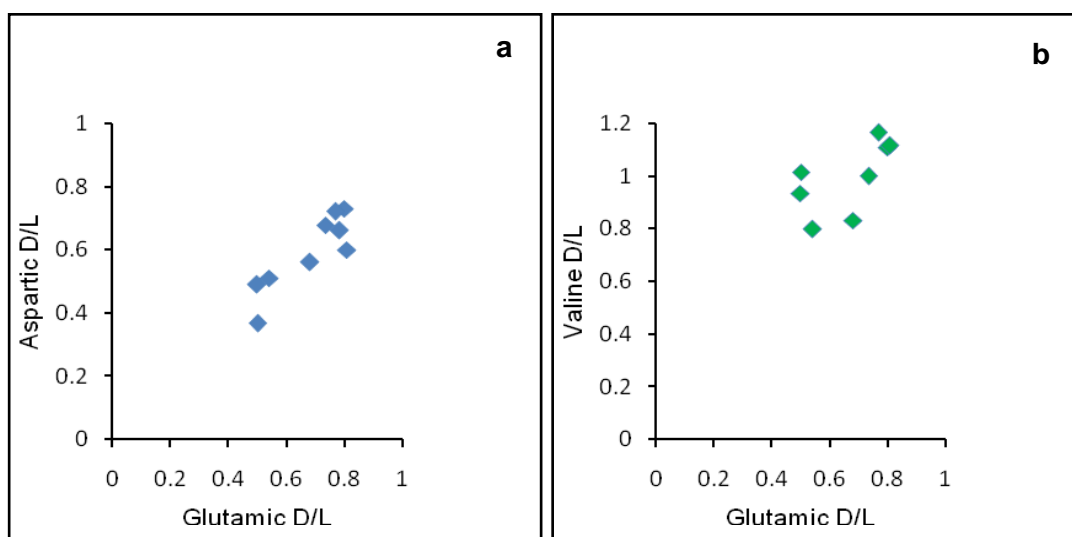


Figure 7.4. D/L values obtained from individual foraminifer tests, *Elphidium*, BS-5-2, Eltigen. Glutamic and Valine D/L values both suggest relatively old ages for these fossil tests, when compared with the results from whole-rock, bivalve molluscs and gastropods.

7.6.3. *Cardium edule*

Articulated and disarticulated *Cardium edule* were recovered from coastal exposures at Eltigen, Cape Krotkov and Maly Kut. Two valves underwent paired AAR and U/Th analyses. The results of this allowed calibration of amino acid racemization values with the uranium-series ages, described in section 7.5.5. The relative rates of racemization among the amino acids in these fossils follow the generally accepted pattern for bivalve molluscs (Lajoie *et al.*, 1980).

The highest D/L values were found in disarticulated samples of *Cardium edule* recovered from BS-6-3 (Asp = 0.463 ± 0.031 , glu = 0.284 ± 0.005 , val = 0.197 ± 0.015), and BS-6-4 (Asp = 0.460 ± 0.028 , glx = 0.279 ± 0.018 , val = 0.177 ± 0.017). Based on these D/L

values, these horizons, BS-6-3 at 3.7 m and BS-6-4 at 4.0 m high from the base of this study site at Eltigen, must be of a similar aminostratigraphic age.

In comparison, articulated *Cardium edule* shells had lower D/L values, with those from BS-4-12 having mean values of $asx = 0.450 \pm 0.038$, $glx = 0.226 \pm 0.038$, and $valine = 0.161 \pm 0.040$. Equivalent shells from BS-11-3a had values of $asx = 0.424 \pm 0.197$, $glx = 0.222 \pm 0.024$, and $valine = 0.155 \pm 0.030$. These data indicate that *Cardium edule* are older at BS-4, being the southern-most study site at Eltigen, while BS-11 located at Maly Kut, Taman Peninsula, would be only slightly older. It may be argued that these are aminostratigraphically similar in age, based on the glutamic and valine D/L values.

7.6.4 *Chione gallina*

The range of glutamic D/L values obtained on *Chione gallina* appear to be similar to that of *Cardium edule*, yet aspartic and valine D/L values are slightly higher for *Chione*. D/L values on samples from Maly Kut (BS-11), $asx = 0.464 \pm 0.022$, $glx = 0.198 \pm 0.013$, $val = 0.205 \pm 0.009$, are lower than those of BS-6 or BS-4. The lower extent of racemization may be due to a younger age for samples from Maly Kut, or may be because there has been a degree of diffusive loss of amino acids from the skeletal carbonate matrix, or because of difference in the integrated burial temperature. A single articulated *Chione gallina* from BS-4-17 ($asx = 0.550$, $glx = 0.276$, $val = 0.265$) has a similar glutamic D/L ratio to those disarticulated specimens from BS-6-7 (mean $asx = 0.529 \pm 0.027$, $glx = 0.277 \pm 0.021$, $val = 0.205 \pm 0.026$), but higher extents of racemization for aspartic and valine. The mean values for *Chione gallina* from BS-4-16 (mean $asx = 0.506 \pm 0.006$, $glx = 0.248 \pm 0.005$, $val = 0.237 \pm 0.011$), are lower than for BS-6-7 for aspartic and glutamic acids but higher for valine. If there was a significant difference in ages between the study site at BS-4 and that of BS-6 it would be expected that there would be some degree of separation of D/L values on a bivariate plot such as that below for these two locations. There is not, and thus it is concluded from the analysis of the total hydrolysable amino acids that the age difference between these two locations is not significantly different using this method, if such an age difference exists. However, the samples from Maly Kut and Cape Tuzla have lower D/L values, and therefore it is suggested that they are likely to be younger than the sedimentary sequence at Eltigen based on the results of the THAA fraction in articulated *Chione gallina*.

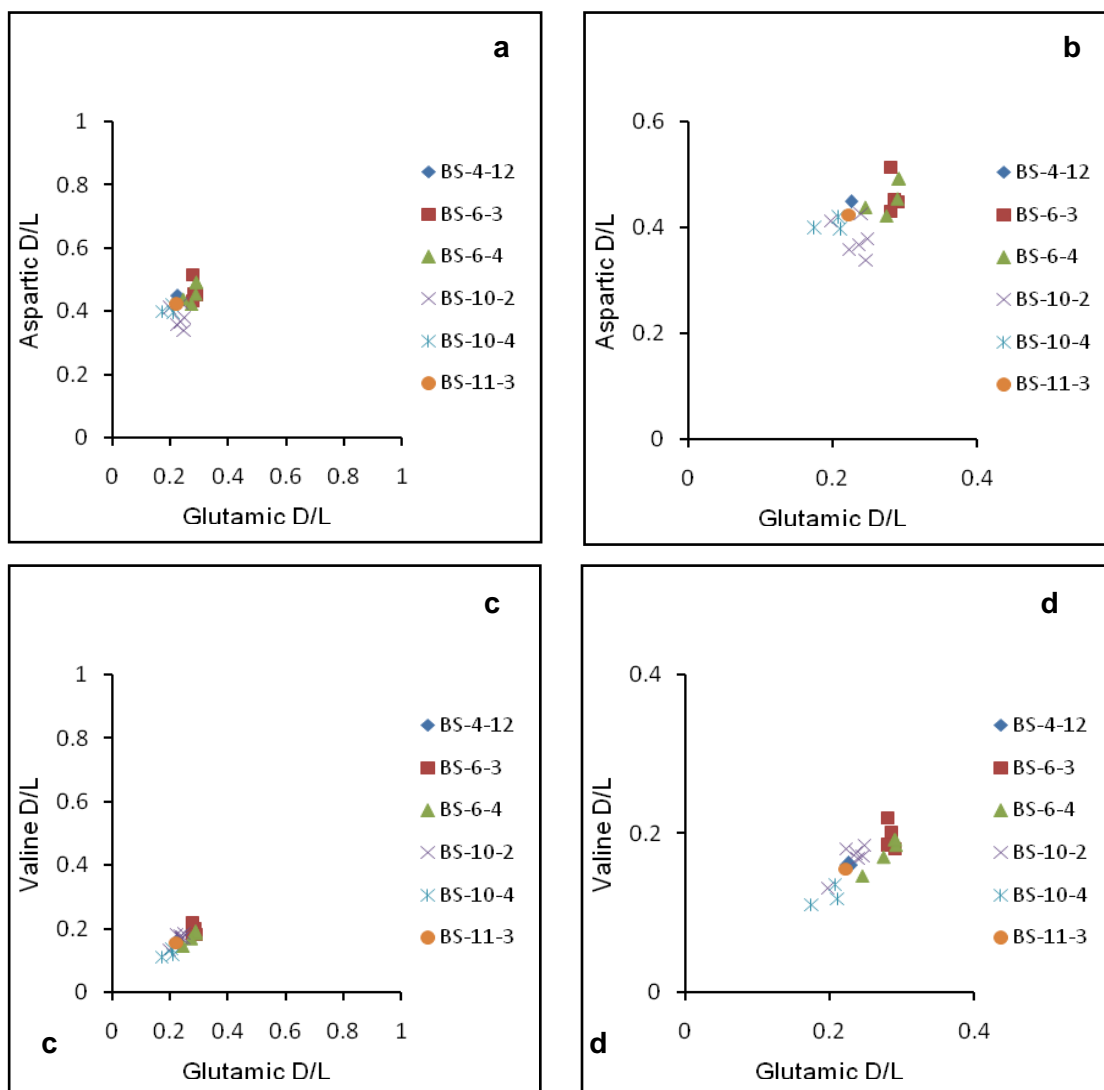


Figure 7.5. Covariance of THAA D/L values for specimens of the bivalve mollusc, *Cardium edule*, Kerch Strait. b) and d) are figures 7.3a, and c blown up for clarity. *Cardium edule* from BS-6-3 and BS-6-4 were disarticulated, all others were articulated.

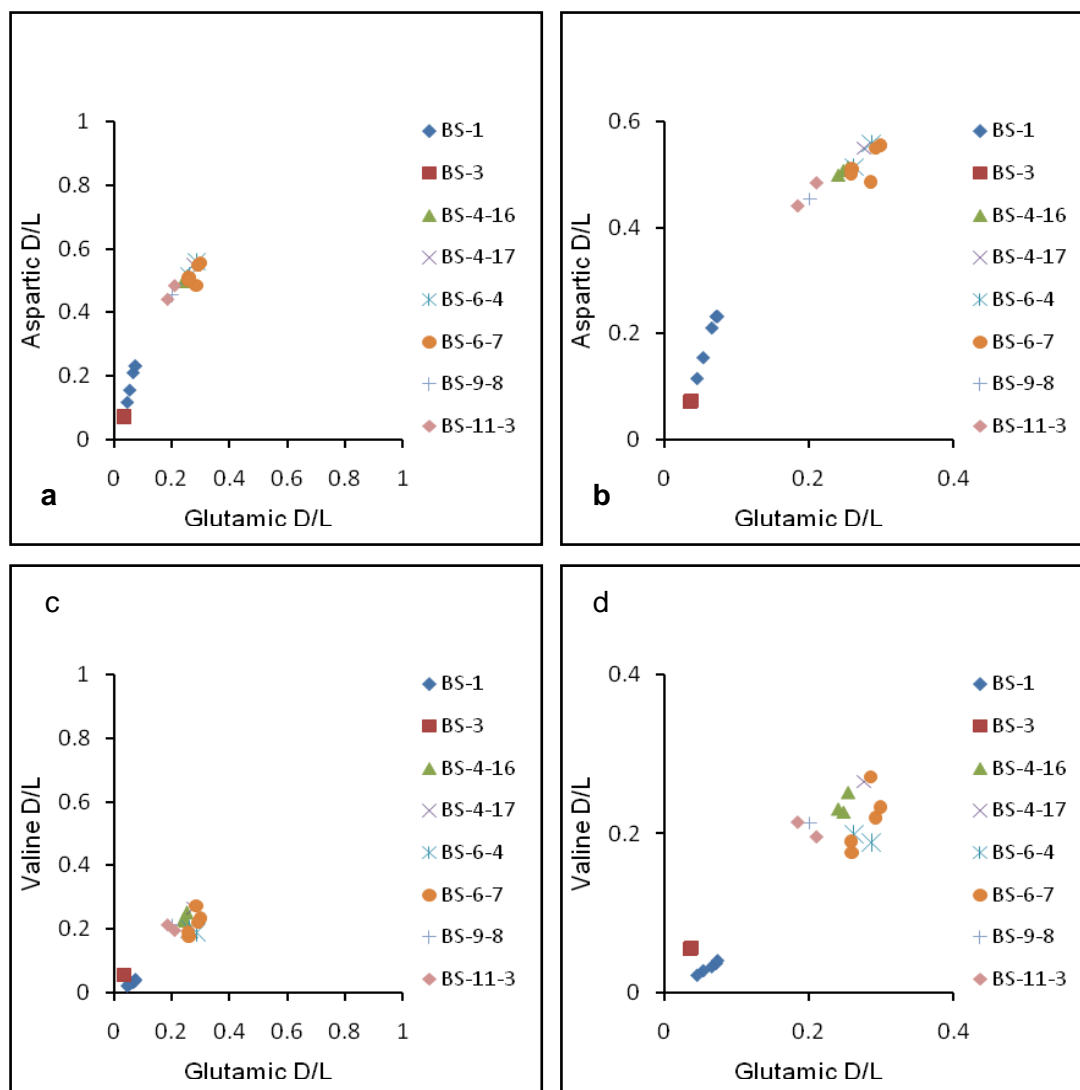


Figure 7.6. D/L values for individual articulated *Chione gallina*, Kerch Strait, northeastern Black Sea. All results, apart from BS-6-7 (D), are based on the analysis of the total hydrolysable amino acids in articulated shells. *Chione gallina* shells from BS-6-7 (D) were disarticulated. Valine D/L values in shells from BS-4-16 and BS-4-17 overlap with those of BS-6-7. D/L values in shells from BS-9-8 and BS-11-3 are slightly lower in comparison.

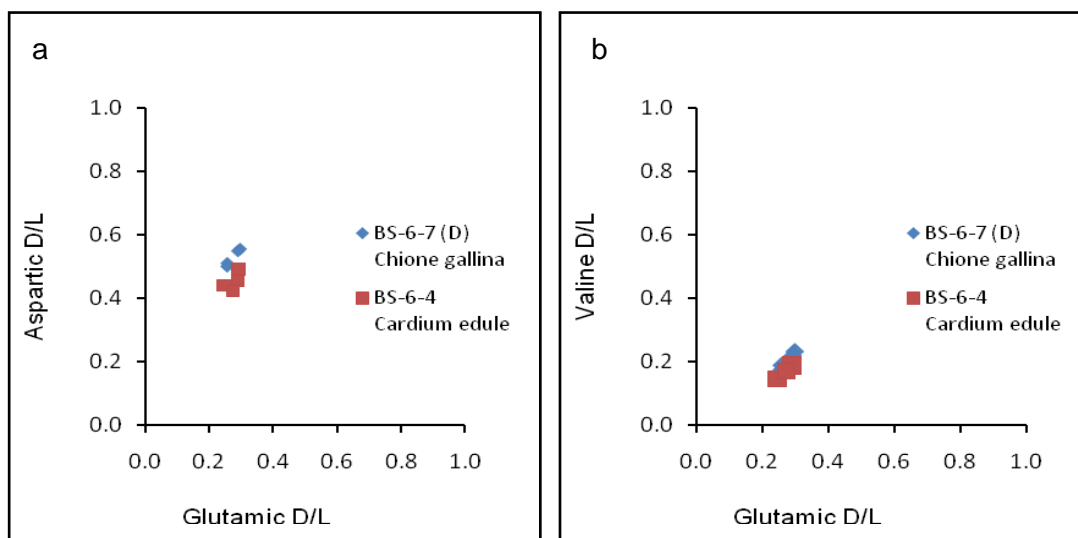


Figure 7.7. Comparison of D/L values among disarticulated *Chione gallina* and *Cardium edule*, all from BS-6-7, appears to indicate that amino acids within *Chione gallina* racemise at a faster rate than those of *Cardium edule*.

The apparent rate of racemization for *Cardium edule* appears lower than that of *Chione gallina*. However, this rate difference (Fig. 7.7) is insufficient to account for the difference in D/L values between these two species at this site. *Cardium edule* (BS-4-12), having substantially lower D/L values than *Chione gallina* at this site, was recovered approximately 1 m below BS-4-17, from where *Chione gallina* were collected. Analysis of the sediments from this, and the other study sites in Kerch Strait, determined that most of the ‘lagoon sediments’ were of silt-grade (calcium carbonate removed by HCl dissolution), and relatively little clay was found to be present. Thus these sediments, and for example, those from Cape Krotkov (Fig. 7f, BS-10), are likely to be relatively porous and permeable, amenable to the flow of ground water. If there was diffusive leaching of amino acids from the skeletal carbonate matrix, it would be feasible that it would happen in this type of environment.

Overall, when one looks at the data comparing study site with study site, it can be seen that the studied strata from BS-4, 5, 6 and 8 at Eltigen are the same aminostratigraphic age. The lower D/L values for *Cardium edule* from BS-4-12 may be due to diffusive leaching of the free amino acid component from the fossil calcium carbonate matrix. However, these values are similar to *Cardium edule* from BS-10-2, Cape Krotkov, Taman Peninsula. This is discussed further in section 8.5.7, where the results from analysis of intracrystalline amino acids in these bivalve molluscs is discussed.

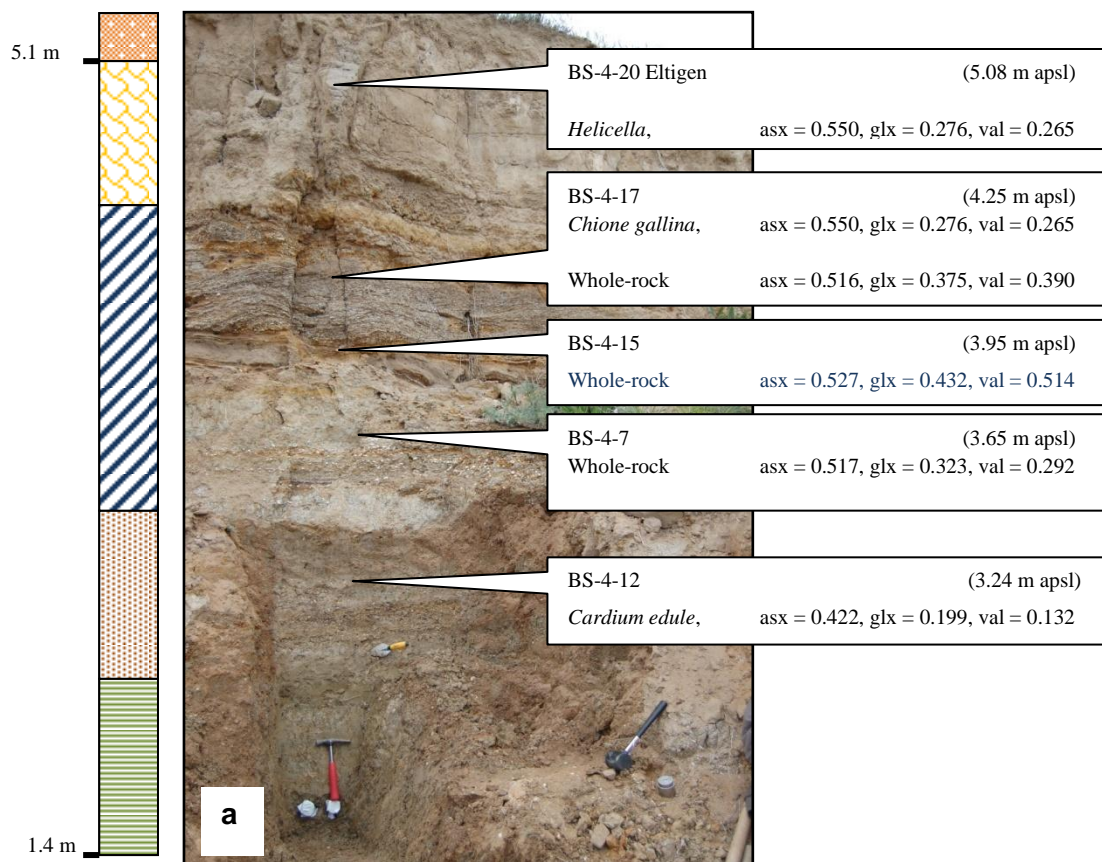
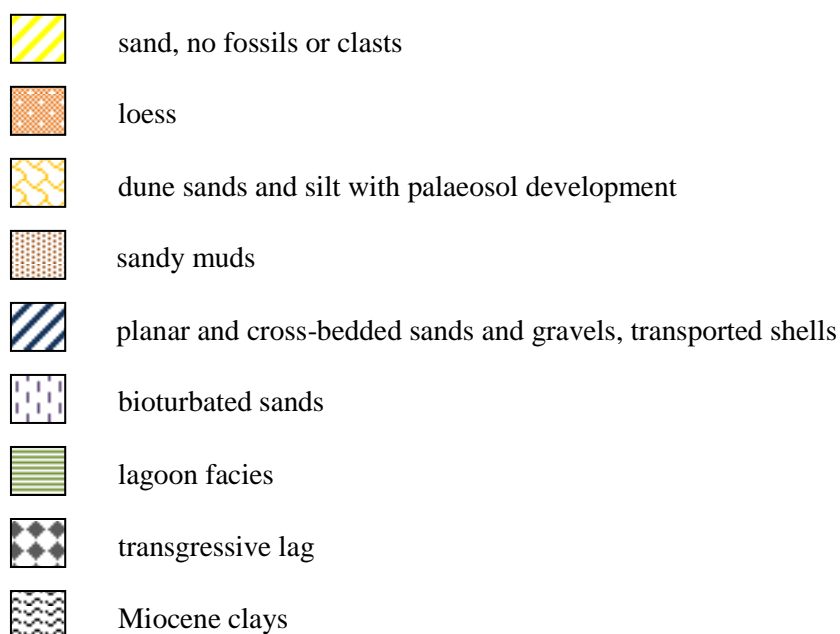
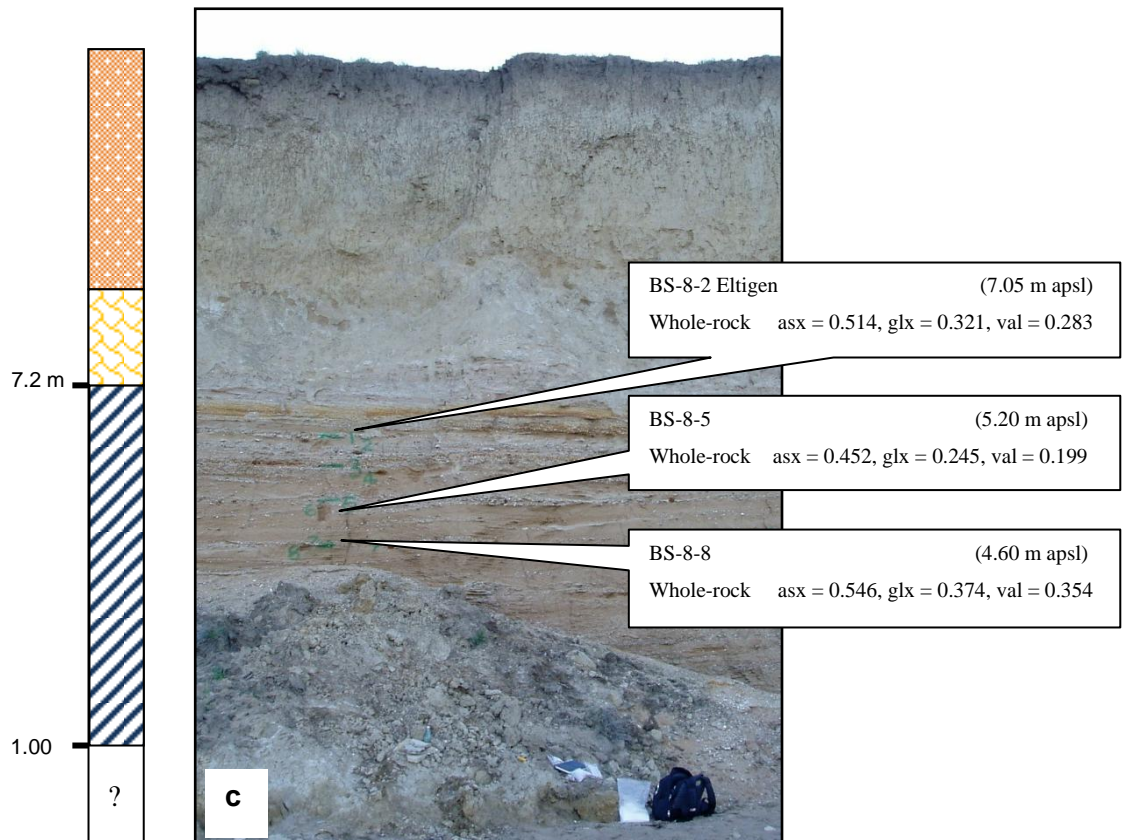
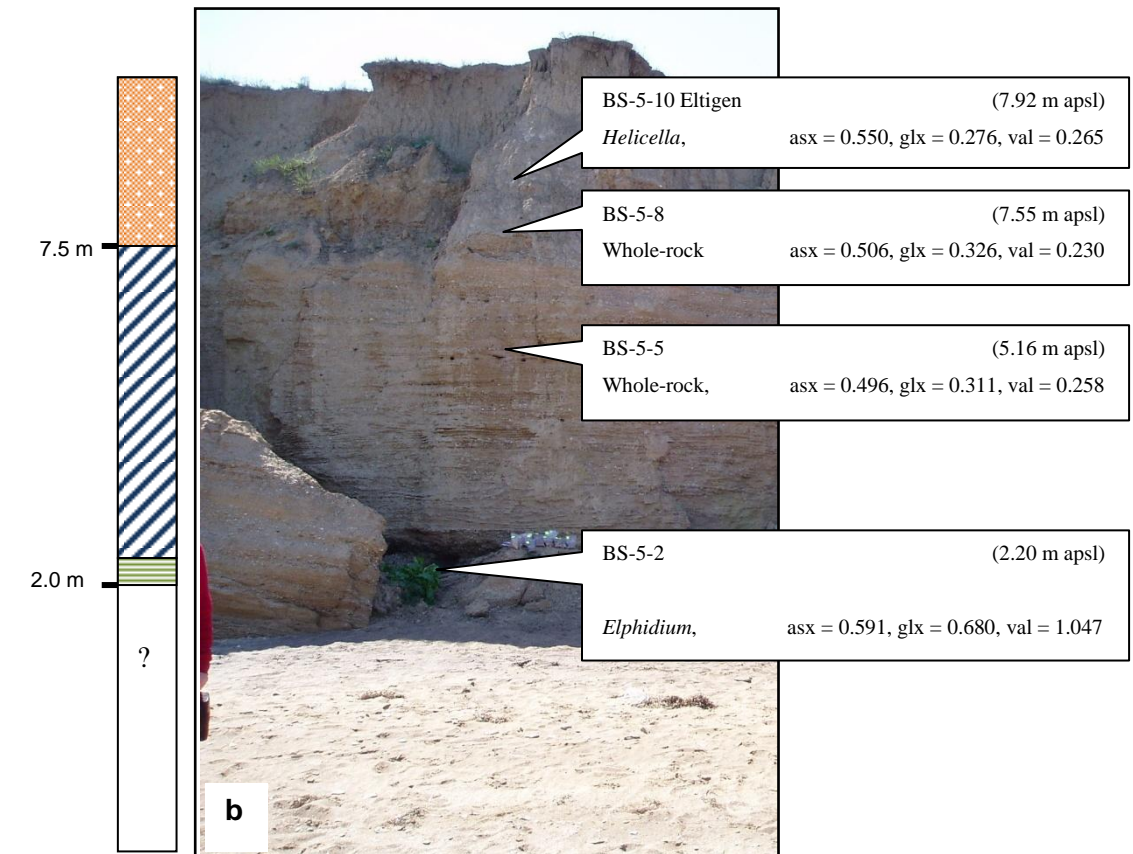
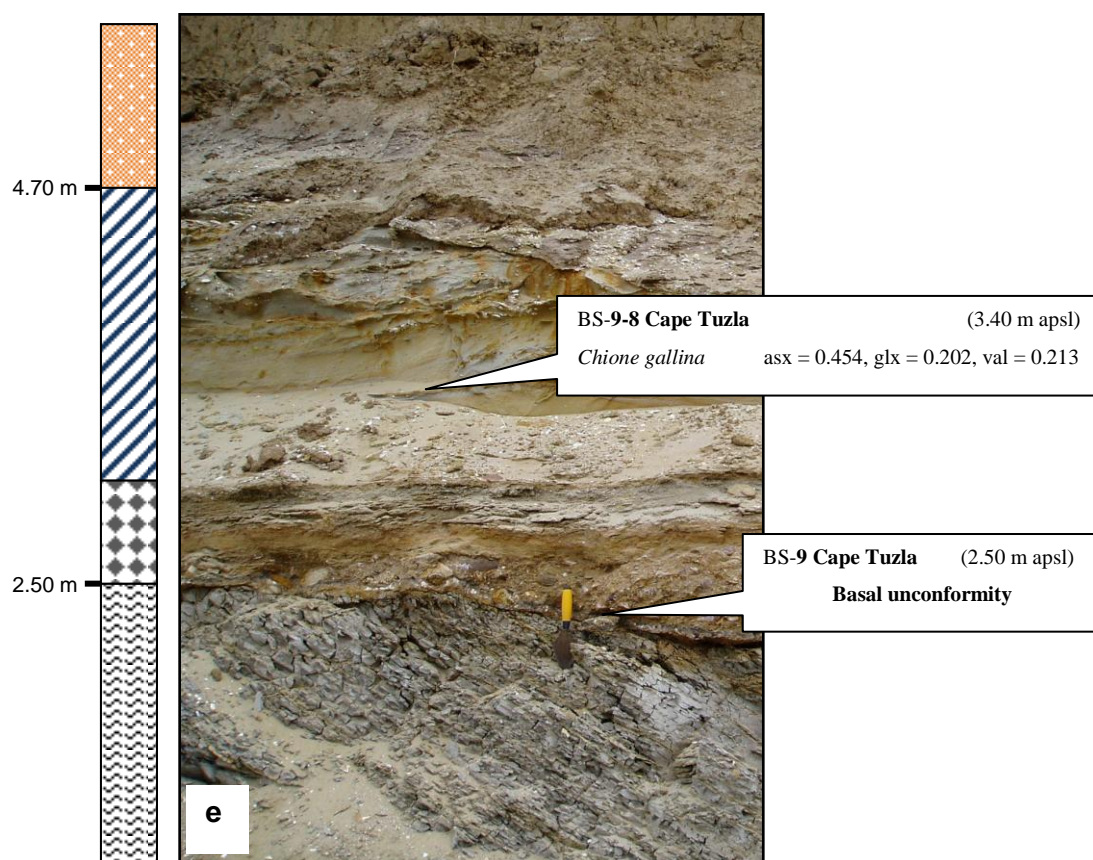
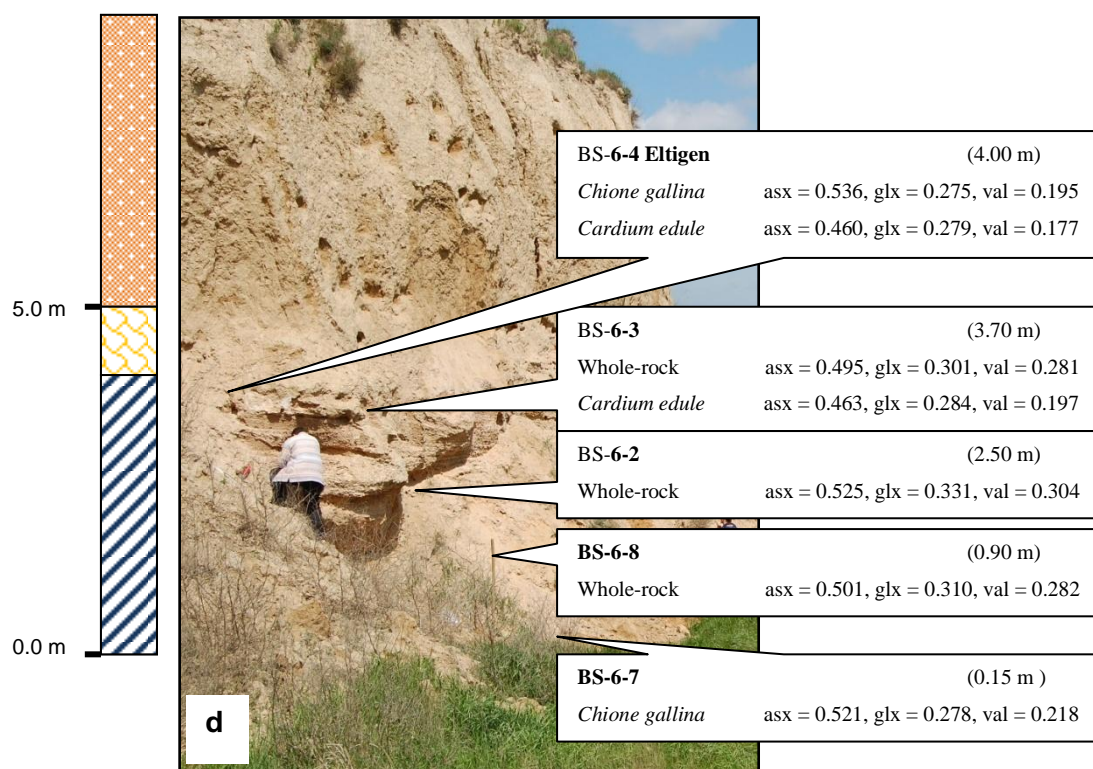
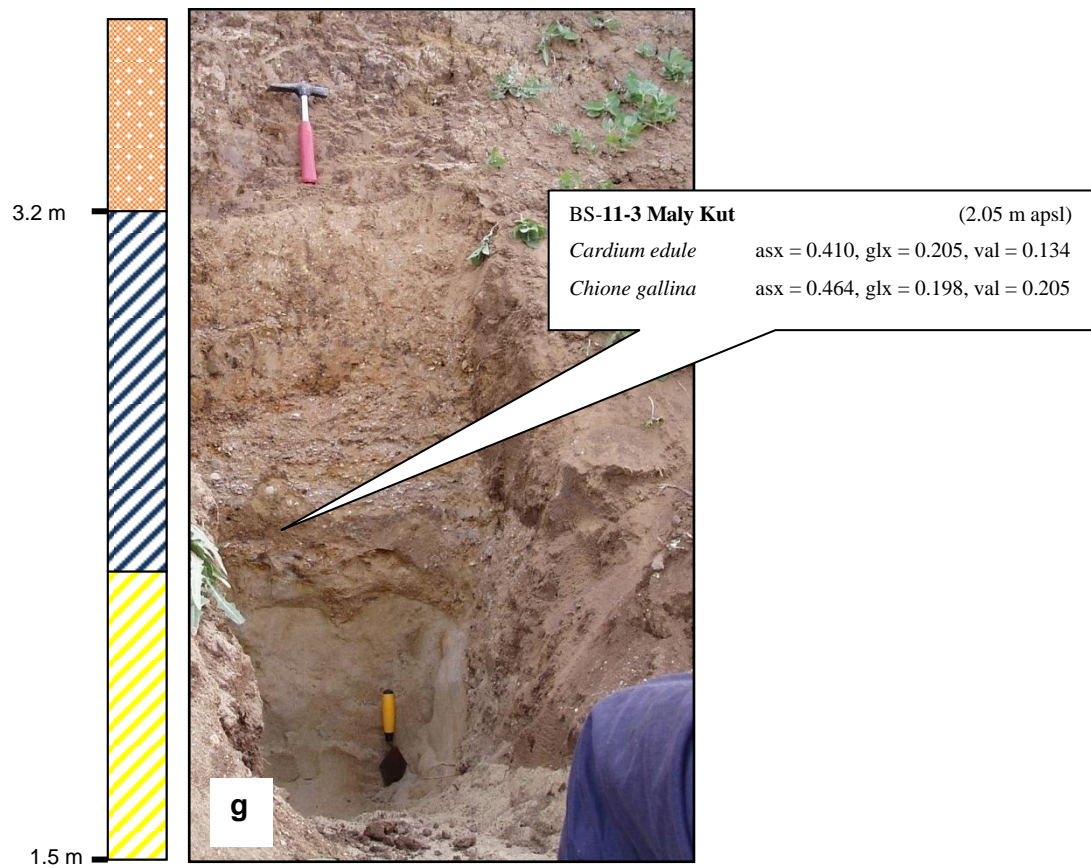
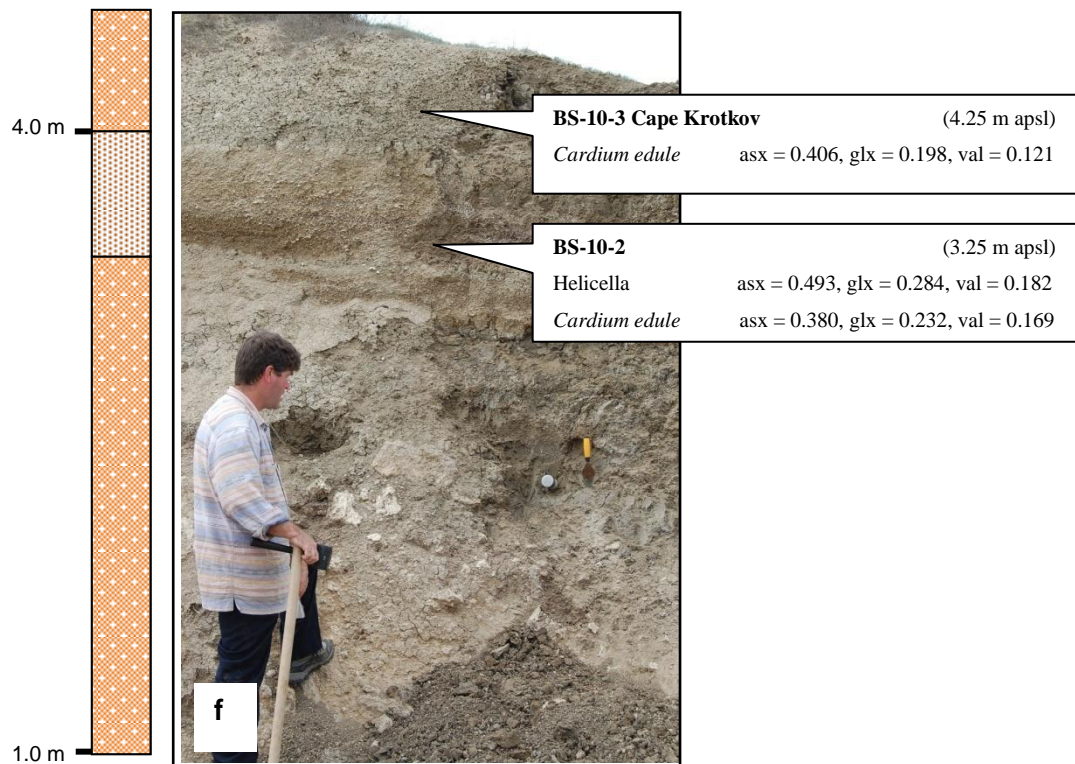


Figure 7.8. D/L values at study sites, with simplified stratigraphic logs, scale, and legend below. a above, and b, c, d, e, f and g below. Except for BS-6, all sampling points measured in meters above present sea-level (m apsl). Measurements at BS-6 refer to meters above the base of section at that sampling station. Photographs 7.8d and 7.8f by A. Chivas.









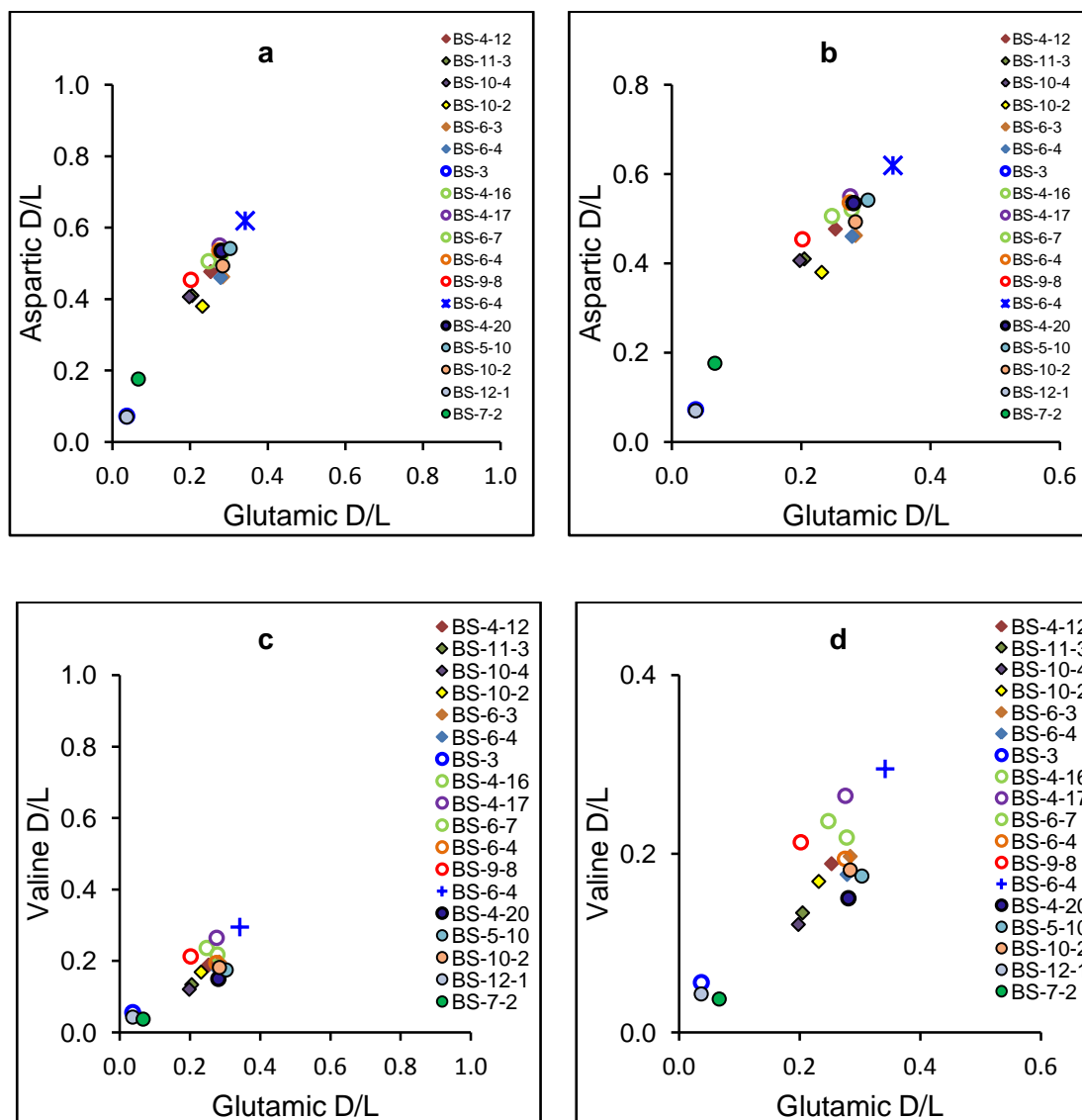


Figure 7.9. Mean D/L values for *Chione* (unfilled circles), *Mytilus* (blue cross), and *Cardium* (filled diamonds), Eltigen, Kerch Strait. Results among articulated and disarticulated *Chione* and *Cardium* are similar. Also illustrated above are the mean values for the coastal gastropod, *Helicella* (closed circles). D/L values for *Mytilus edulis* by comparison with either *Chione* or *Cardium* are significantly higher. This may, in the first instance, be due to a higher rate of racemization for the latter species. Overall, lower D/L values were obtained on samples from the Taman Peninsula than those from Eltigen.

7.6.5. Uranium-series dating and calibration of D/L values

Uranium-series dating was undertaken on bivalves from BS-4-12, BS-6-7, and BS-11-3A. The results are presented in Table 7.2. Two valves from each study site were dated, *Cardium edule* from BS-4-12 and BS-11-3A, and *Chione gallina* from BS-6-7.

Table 7.2. Uranium-series data from bivalves *Cardium edule* and *Chione gallina*, Kerch Strait.

Sample Name	U (ppm)	^{232}Th (ppb)	$(^{230}\text{Th}/^{232}\text{Th})$	$(^{230}\text{Th}/^{238}\text{U})^{1/2}$	$(^{234}\text{U}/^{238}\text{U})$	uncorr. ^{230}Th Age (ka)	$\pm 2\sigma$	corr. ^{230}Th Age (ka)	$\pm 2\sigma$
BS-6-7-4	1.0834	1.7357	1213.1	0.6405	1.1866	82.3	1.0	82.2	1.0
BS-6-7-5	1.1132	1.8831	1118.9	0.6238	1.1920	78.6	0.6	78.6	0.6
BS-11-3a-1	1.5982	2.6617	2128.3	1.1682	1.4745	149.6	1.6	149.5	1.6
BS-11-3a-2	0.6307	0.8842	2476.8	1.1444	1.4675	145.2	1.4	145.2	1.4
BS-4-12-1	1.5472	1.6465	1914.0	0.6713	1.2361	82.6	0.5	82.5	0.5
BS-4-12-2	2.2521	2.1130	2286.7	0.7071	1.2480	87.7	0.8	87.7	0.8

Calibration of D/L values with uranium-series ages resulted in ages tabulated below (Table 8.4). These ages were obtained using the THAA D/L values plotted against the square-root of the uranium-series age to produce parabolic equations, presented below in Figures 7.11, 7.12. The calibrated ages obtained using individual amino acids from the THAA fraction in molluscs from each study site vary to a great extent, ranging from 46 ka (*Chione gallina*, BS-11-3) to 200 ka (*Cardium edule*, BS-6-3). Three of the mean ages are older than last interglacial (MIS 5e) (BS-6-3, *Cardium edule*, 180 ka; BS-6-4, *Cardium edule*, 163 ka; BS-4-12, *Cardium edule*, 162 ka), one is of last interglacial (MIS 5e) age (BS-10-2, *Cardium edule*, 119 ka), and the remainder range from 61 ka (BS-11-3, *Chione gallina*) to 106 ka (BS-4-17, *Chione gallina*) in age. Because of this range of calibrated ages, these are not used here to infer a specific age for the sedimentary sequences at Eltigen, nor for the study sites at Cape Krotkov, Cape Tuzla or Maly Kut. Because of the wide range of ages on shells from adjacent sedimentary strata a number of additional analyses were undertaken on the intracrystalline amino acid fraction in *Cardium edule* and *Chione gallina*, outlined below in section 7.5.15.

However, an alternative method to estimate aminostratigraphic ages is to plot D/L values against current mean annual temperature for the amino acids in question from a number of locations of known age. The objective is to investigate whether there is a visible relationship between the D/L values and mean annual temperature for the study sites when compared with earlier studies. Here, the amino acid valine was used, and based primarily on results obtained in this thesis, these data suggest that the shells from Kerch Strait are of last interglacial (MIS 5e) age (*sensu lato*), with those from BS-4 of MIS 5e age, and those from BS-6 are MIS5c age. For both study sites D/L values from *Cardium edule* are at the lower extent of the last

interglacial (MIS 5e) envelope, while those of *Chione gallina* are at the upper margin of this age correlation.

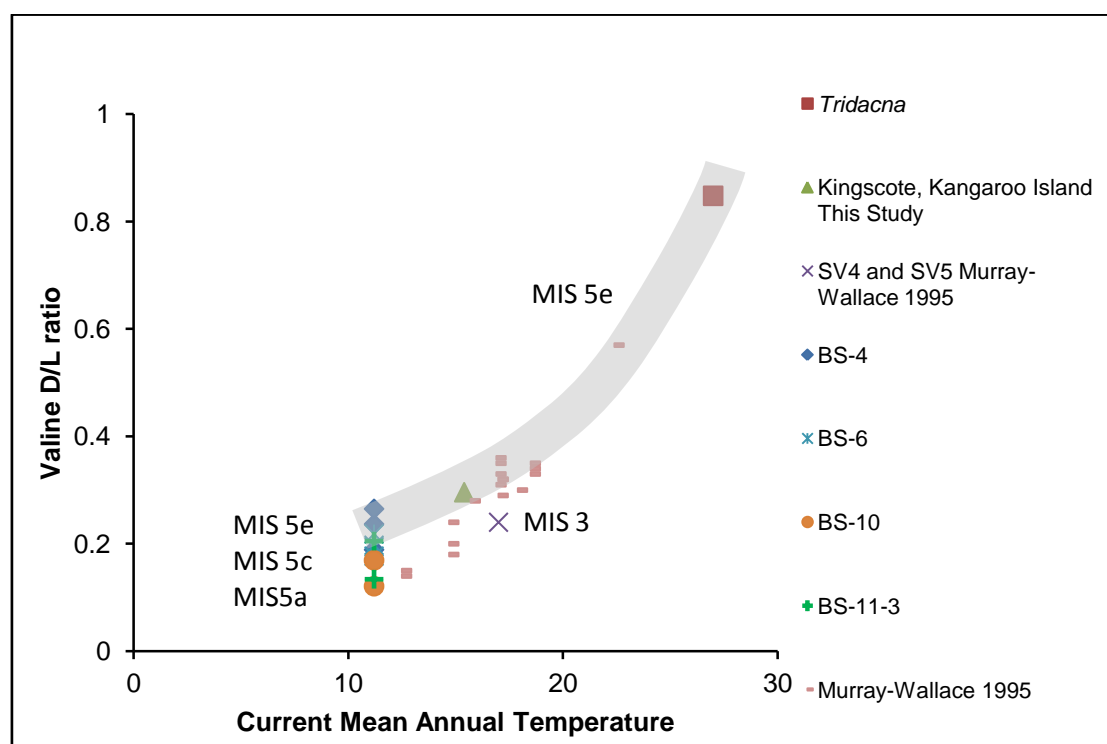


Figure 7.10. Valine D/L values in last interglacial (MIS 5e) age bivalve molluscs, Kerch Strait, northwestern Black Sea (BS-4, MIS5e; BS-6, MIS5c; BS-10, MIS5c and 5a; BS-11, MIS5c or 5a?). For comparison valine D/L values from *Tridacna*, Huon Peninsula (Chapter 8), *Katylsia* from Kingscote, Kangaroo Island (Chapter 4), and *Katylsia* from cores SV4 and SV5 Gulf St Vincent, and additional Australian localities (Murray-Wallace, 1995) are presented. The envelope drawn above represents the approximate relationship between CMAT and valine D/L values for MIS 5e.

Table 7.3. Table of calibrated ages based on D/L values from the total hydrolysable amino acid (THAA) pool in bivalve molluscs *Chione gallina* and *Cardium edule*, recovered from coastal study sites in Kerch Strait.

Sample	Species	<i>n</i> =	calibrated aspartic age	1σ	calibrated glutamic age	1σ	calibrated valine age	1σ	mean age	1σ
BS-3	<i>Chione gallina</i>	2	564	61	343	63	2,270	195	1,059	1,055
BS-4-12	<i>Cardium edule</i>	1	155,549		153,405		175,980		161,645	12,461
BS-4-16	<i>Chione gallina</i>	3	83,178	2,654	74,855	4,304	95,783	12,210	84,605	10,537
BS-4-17	<i>Chione gallina</i>	1	99,378		94,755		122,560		105,564	14,899
BS-6-3	<i>Cardium edule</i>	4	145,601	27,076	199,199	8,258	195,706	40,588	180,169	29,987
BS-6-4	<i>Cardium edule</i>	5	143,913	22,959	192,003	29,016	153,116	37,018	163,011	25,526
BS-6-4	<i>Chione gallina</i>	2	94,341	11,789	94,417	12,874	61,597	5,585	83,452	18,927
BS-6-7	<i>Chione gallina</i>	6	87,309	10,498	94,086	14,209	81,834	27,977	87,743	6,138
BS-10-2	<i>Cardium edule</i>	5	91,350	19,293	126,513	22,395	137,901	33,055	118,588	24,266
BS-10-4	<i>Cardium edule</i>	2	106,541	8,102	87,754	20,042	60,887	17,404	85,061	22,946
BS-9-8	<i>Chione gallina</i>	3	69,070	4,537	61,997	20,323	138,340	88,822	89,802	42,183
BS-11-3	<i>Cardium edule</i>	1	108,760		94,348		77,548		93,552	15,621
BS-11-3	<i>Chione gallina</i>	2	69,044	9,743	45,507	9,108	69,473	9,698	61,341	13,715

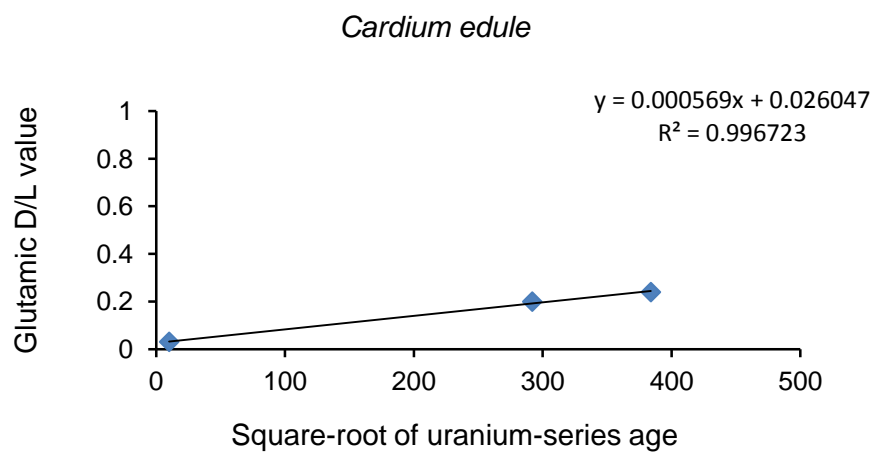
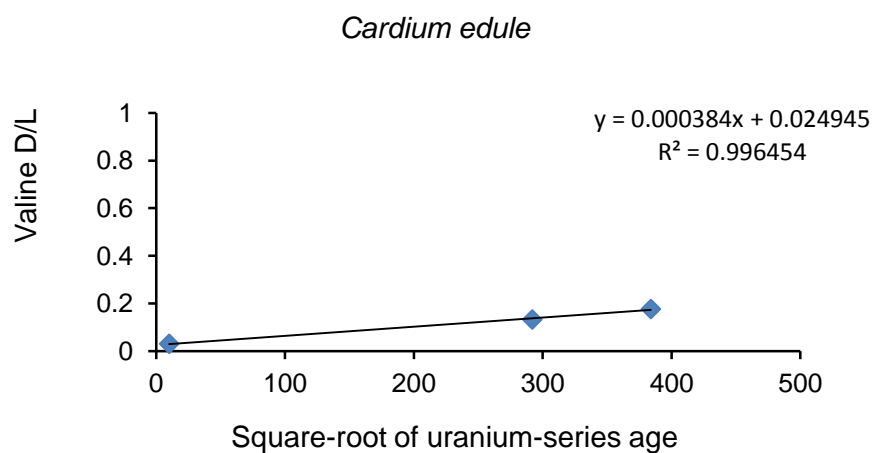


Figure 7.11. Parabolic equations based on D/L ratio against square-root of the age of calibration samples, *Cardium edule*.

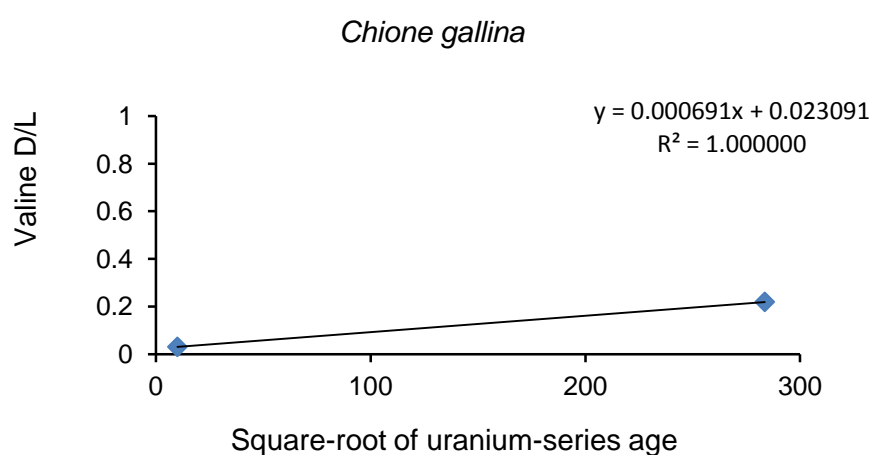
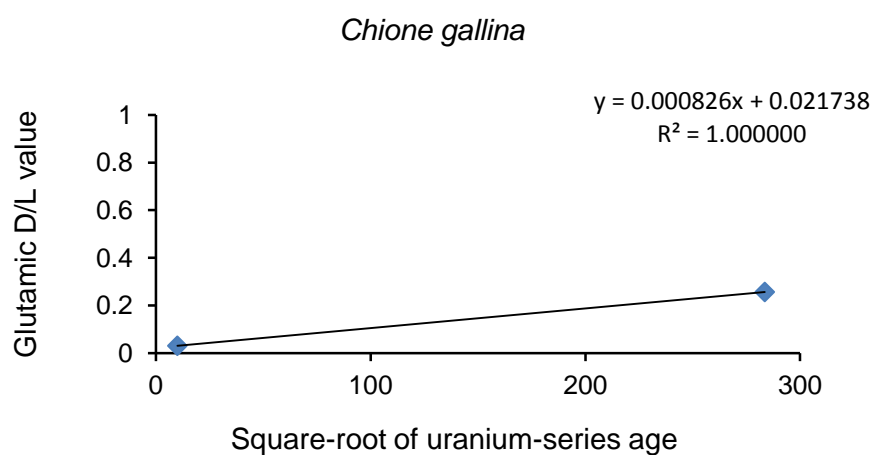


Figure 7.12. Parabolic equations based on the relationship between D/L ratio and square-root of the age of calibration samples for the bivalve mollusc *Chione gallina*, from Kerch Strait.

7.6.6. Terrestrial gastropods

A number of sub-fossil examples of the coastal gastropod, *Helicella* sp., were recovered from sediments at Eltigen and Cape Krotkov. Modern equivalents were collected at BS-12, Taman Peninsula. The results from AAR analyses on these are presented in Table 7.1, and AMS ^{14}C ages are presented in Table 7.4.

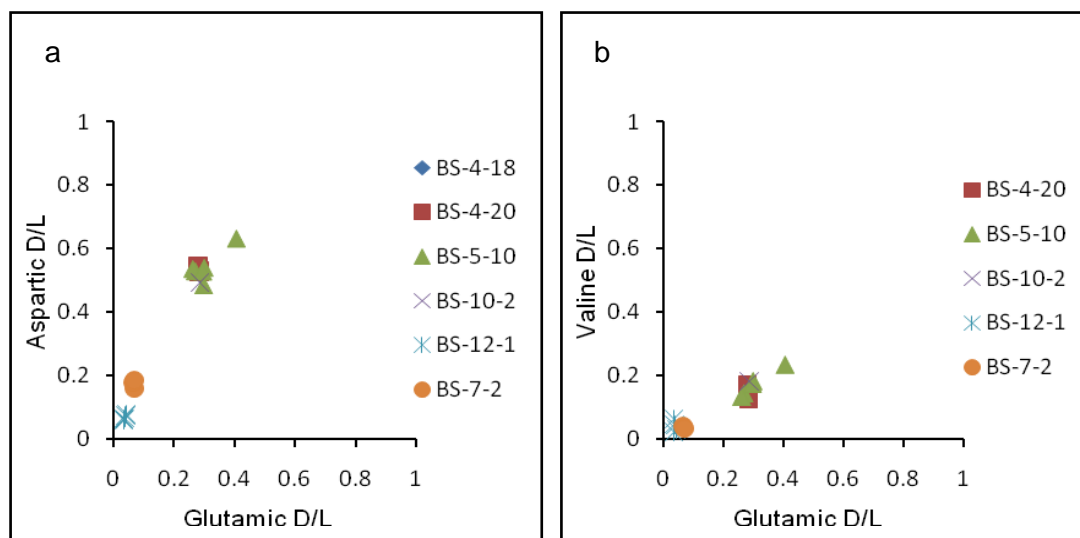


Figure 7.13. D/L values for the terrestrial gastropod *Helicella*, Kerch Strait, northwestern Black Sea.

Table 7.4 AMS ^{14}C ages on individual *Helicella*, Kerch Strait.

ANSTO code	Material	Location	Depth from surface (m)	$\delta^{13}\text{C}$	Percent Carbon pMC	Modern 1σ error	Conventional ^{14}C age Yrs BP	1σ error
OZL400	Terrestrial gastropod <i>Helicella</i>	BS-7-2	5.2	-6.6 ± 0.4	0.50	0.04	42,520	630
OZL401	Terrestrial gastropod <i>Helicella</i>	BS-7-2	5.2	-6.9 ± 0.1	0.58	0.03	41,340	410

Two AMS ^{14}C analyses were undertaken on terrestrial gastropods, *Helicella*, recovered from loess (BS-7-2) overlying shallow marine sediments in coastal exposures at Eltigen. Three equivalent *Helicella* shell samples from the same horizon were analysed for the extent of amino acid racemization (AAR).

At one Eltigen study site, BS-7-2, 5 juvenile examples of *Helicella* were recovered from the base of loess sediments 60cm above the uppermost marine unit, with three being analysed for the extent of AAR. D/L values in these samples are significantly lower than those from the other locations in this study, suggestive of ages of perhaps only few hundred to a few thousand years old based on comparison with the evidence from the *Helicella* from BS-4, 5 and BS-10. Two equivalent shells of *Helicella* were therefore analysed by AMS, and found to have ages of $41,340 \pm 410$, and $42,520 \pm 630$ ^{14}C yr BP. Attempts to calibrate the AAR results with the paired AAR- ^{14}C data from BS-7-2 resulted in calibrated ages significantly older than otherwise expected for those samples with glutamic D/L values of approximately

0.290 resulting in calibrated ages of approximately 10^6 yr. This may be because D/L values obtained on the AMS dated *Helicella* are depressed due to deposition and burial in cold conditions. In contrast, the higher D/L values for the other *Helicella* at Eltigen are a result of their being deposited in much warmer conditions, with higher extents of racemization being reached prior to colder conditions being established later on during MIS 4, or at the end of MIS 3.

7.6.7 Intracrystalline amino acids in *Cardium edule* and *Chione gallina*, and their age calibration

Hydrolysable intracrystalline amino acids include protein-bound and free amino acids, and are generally considered to be protected from oxidation and contamination by their internal, isolated position within individual calcium carbonate crystallites. The nature of the enclosing medium, calcium carbonate, either as aragonite or calcite, provides a measure of stability against, for example, acid ground waters, and protects the intracrystalline organic molecules against contamination by extraneous amino acids in that groundwater, and in the associated diagenetic environment.

Because of the above considerations, and the large variation in calibrated ages for the molluscs from Kerch Strait, a limited number of samples were also analysed for the extent of racemization of the hydrolysable intracrystalline amino acids in the selected fossils. D/L values for the selected fossils are presented below in Table 7.5 and their associated calibrated ages are presented in Table 7.6.

As with the THAA data (Table 7.1), the D/L ratio data obtained from shells of *Cardium edule* was more consistent among the individual amino acids, aspartic, glutamic, alanine and valine within each valve. Similarly, the HIAA D/L ratio-based and calibrated ages was more consistent among amino acids in individual valves, and among valves of this species from each sampled horizon.

In contrast, and as with the total hydrolysable amino acid data in examples of *Chione gallina*, results from the HIAA pool in this species were less consistent among the amino acids and among individual shells. D/L values from the hydrolysable intracrystalline amino acids in *Chione gallina* were similar to those from the THAA results. For both the intracrystalline and intercrystalline based D/L values, higher apparent rates of racemization were evident for *Chione gallina* over that of *Cardium edule*.

Aspartic glutamic and valine D/L values in the single *Cardium edule* from BS-4-12 are indistinguishable from the results obtained on *Cardium edule* from BS-10-2 to one standard

deviation. D/L values obtained from *Cardium edule* from BS-10-4 are marginally lower than those from the same species at BS-10-2. The single sample of this species from BS-11-3 had aspartic and glutamic values (asx = 0.405, glx = 0.265) in line with BS-4-12, though the valine D/L ratio was somewhat lower (val = 0.172), but was within one standard deviation of the mean for BS-10-4. These results, being D/L values from the intra-crystalline amino acid fraction in examples of *Cardium edule*, indicate an equivalent aminostratigraphic age for these sampled strata.

The mean D/L values from *Chione gallina* recovered from BS-4-16 and BS-6-7 are equivalent to one standard deviation. As with the THAA D/L values, results from the sample from BS-4-17 are the highest for this species in Kerch Strait. This is problematic because BS-4-17 and BS-4-16 refer to points within the same stratum, with BS-4-17 being the higher (Fig. 8.). *Chione gallina* from BS-9-8 and BS-11-3 are of an equivalent aminostratigraphic age, but have lower rates of racemization for aspartic and glutamic acids than those samples from Eltigen. One sample from BS-6-7 had a valine D/L ratio (val = 0.248) similar to those from BS-9-8 (mean val = 0.250) and BS-11-3 (mean val = 0.252).

Overall, these results indicate that the shallow marginal marine strata at Eltigen and Cape Krotkov are equivalent in age, but the sampled horizons at Maly Kut and Cape Tuzla may be slightly, but not significantly, younger than Eltigen and Cape Krotkov.

Table 7.5. Hydrolysable intracrystalline amino acids D/L values in bivalve molluscs from Kerch Strait, northeastern Black Sea.

	Study site	Species	Lab (UWGA) code	Asx D/L	Glx D/L	Ser D/L	Ala D/L	Val D/L
1	BS-4-12	<i>Cardium edule</i>	7253	0.429	0.244	0.411	0.4355	0.2015
2	BS-10-2	<i>Cardium edule</i>	8001	0.3955	0.2565	0.451	0.37	0.1945
3	BS-10-2	<i>Cardium edule</i>	8002	0.3825	0.2035	0.504	0.2525	0.132
4	BS-10-2	<i>Cardium edule</i>	8003	0.426	0.2815	0.4035	0.3955	0.1865
5	BS-10-2	<i>Cardium edule</i>	8004	0.389	0.2595	0.378	0.403	0.1955
6	BS-10-2	<i>Cardium edule</i>	8005	0.3445	0.2525	0.3905	0.41	0.1855
7	BS-10-2	<i>Cardium edule</i>	8006	0.4455	0.247	0.3235	0.3975	0.195
			Mean	0.397	0.250	0.408	0.371	0.182
			Stdv	0.035	0.026	0.062	0.060	0.025
			Cv	9	10	15	16	14
8	BS-10-4	<i>Cardium edule</i>	7298	0.388	0.26	0.505	0.4195	0.1915
9	BS-10-4	<i>Cardium edule</i>	7299	0.397	0.2265	0.4775	0.329	0.1655
10	BS-10-4	<i>Cardium edule</i>	8000	0.405	0.249	0.4585	0.367	0.186
			Mean	0.397	0.245	0.480	0.372	0.181
			Stdv	0.009	0.017	0.023	0.045	0.014
			Cv	2	7	5	12	8
11	BS-11-3A	<i>Cardium edule</i>	7252	0.405	0.265	0.541	0.446	0.172
12	BS-3	<i>Chione gallina</i>	6298	0.1155	0.0615	0.278	0.048	0.1375
13	BS-3	<i>Chione gallina</i>	6299	0.15	0.0855	0.2615	0.088	0.139
			Mean	0.133	0.074	0.270	0.068	0.138
			Stdv	0.024	0.017	0.012	0.028	0.001
			Cv	18	23	4	42	1
14	BS-4-16	<i>Chione gallina</i>	7201	0.487	0.26	0.567	0.4315	0.237
15	BS-4-16	<i>Chione gallina</i>	7202	0.519	0.2925	0.6185	0.442	0.2805
16	BS-4-16	<i>Chione gallina</i>	7203	0.52	0.2735	0.62	0.422	0.257
			Mean	0.509	0.275	0.602	0.432	0.258
			Stdv	0.019	0.016	0.030	0.010	0.022
			Cv	4	6	5	2	8
17	BS-4-17	<i>Chione gallina</i>	6297	0.583	0.321	0.718	0.585	0.325
18	BS-6-7	<i>Chione gallina</i>	7210	0.489	0.2775	0.5885	0.4855	0.2655

19	BS-6-7	<i>Chione gallina</i>	7269	0.4955	0.275	0.587	0.4715	0.248
20	BS-6-7	<i>Chione gallina</i>	7269	0.535	0.2895	0.6455	0.5535	0.304
21	BS-6-7	<i>Chione gallina</i>	7269	0.497	0.2735	0.6145	0.4975	0.2795
22	BS-6-7	<i>Chione gallina</i>	7269	0.4975	0.301	0.629	0.497	0.281
23	BS-6-7	<i>Chione gallina</i>	7269	0.511	0.289	0.6005	0.4965	0.267
24	BS-6-7	<i>Chione gallina</i>	BS 6 7	0.4865	0.2895	0.5625	0.4615	0.2695
25	BS-6-7	<i>Chione gallina</i>	7205	0.488	0.2875	0.604	0.4985	0.2645
			Mean	0.500	0.285	0.604	0.495	0.272
			Stdv	0.016	0.009	0.026	0.027	0.016
			Cv	3	3	4	6	6
26	BS-9-8	<i>Chione gallina</i>	7206	0.4645	0.2465	0.523	0.4815	0.2545
27	BS-9-8	<i>Chione gallina</i>	7207	0.481	0.25	0.4025	0.4485	0.2455
			Mean	0.473	0.248	0.463	0.465	0.250
			Stdv	0.012	0.002	0.085	0.023	0.006
			Cv	2	1	18	5	3
28	BS-11-3	<i>Chione gallina</i>	7208	0.467	0.253	0.457	0.405	0.264
29	BS-11-3	<i>Chione gallina</i>	7208b	0.4945	0.2545	0.595	0.411	0.258
30	BS-11-3	<i>Chione gallina</i>	7209	0.4505	0.2315	0.525	0.4055	0.2325
			Mean	0.471	0.246	0.526	0.407	0.252
			Stdv	0.022	0.013	0.069	0.003	0.017
			Cv	5	5	13	1	7

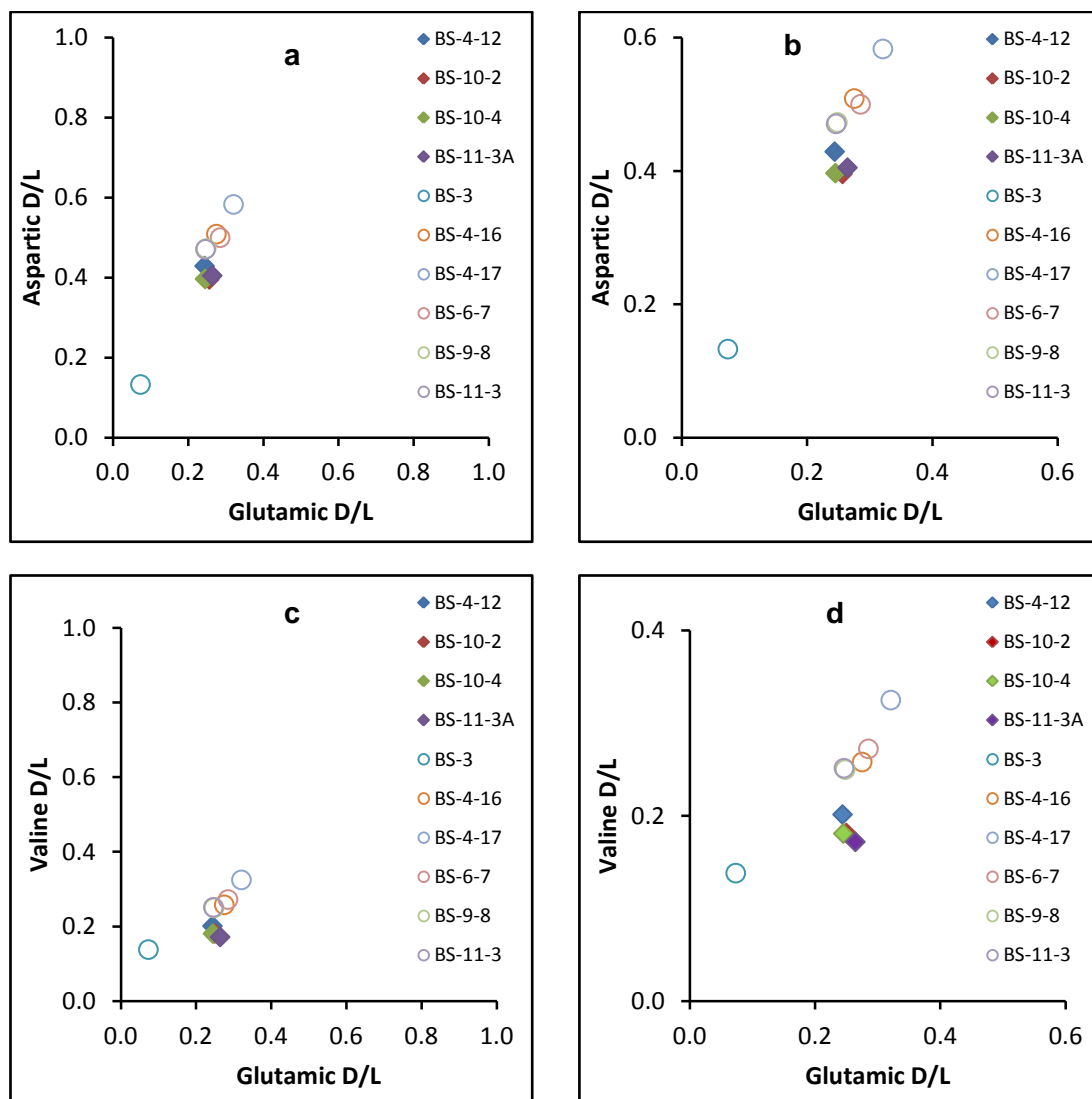


Figure 7.14. D/L values in the intracrystalline amino acids aspartic, glutamic and valine in *Chione gallina* (unfilled circles) and *Cardium edule* (filled diamonds) from Kerch Strait, northeastern Black Sea.

Ages calibrated with uranium-series dates fall into two categories; *Cardium edule*, with mean ages of approximately 100 – 130 ka, and *Chione gallina* with mean ages of 60-74 ka. Despite an apparent higher extent of racemization in *Chione gallina*, the calibrated ages are younger than the dates on the calibration samples. This is a result of a lower slope of the calibration curve, compared to that of *Cardium edule*. This lesser gradient may be because the calibration ages are under estimates of the actual age. A significantly larger number of calibration points are required for accuracy than presented here.

Table 7.6. Table of calibrated ages using the hydrolysable intra-crystalline amino acid (HIAA) pool in bivalve molluscs *Chione gallina* and *Cardium edule*, recovered from coastal study sites in Kerch Strait.

Sample	Species	n =	calibrated aspartic age	1σ	calibrated glutamic age	1σ	calibrated Valine age	1σ	Mean calibrated age	1σ
BS-3	<i>Chione gallina</i>	2	2,135	1,356	2,432	1,763	13,997	274	6,188	6,764
BS-4-12	<i>Cardium edule</i>	1	131,647		106,279		152,616		130,181	23,203
BS-4-16	<i>Chione gallina</i>	3	76,983	6,356	72,103	9,623	62,559	11,918	70,548	7,337
BS-4-17	<i>Chione gallina</i>	1	104,483		101,145		103,945		103,191	1,792
BS-6-7	<i>Chione gallina</i>	8	74,018	5,564	77,948	5,693	70,446	9,640	74,137	3,752
BS-10-2	<i>Cardium edule</i>	6	110,916	22,966	113,896	25,651	121,723	33,996	115,512	5,582
BS-10-4	<i>Cardium edule</i>	3	109,633	5,533	107,942	17,243	118,960	21,012	112,178	5,934
BS-9-8	<i>Chione gallina</i>	2	65,101	3,679	56,898	1,290	57,834	3,345	59,944	4,490
BS-11-3	<i>Cardium edule</i>	1	115,079		128,154		104,628		115,954	11,787
BS-11-3	<i>Chione gallina</i>	3	64,546	7,020	56,031	6,538	58,824	8,685	59,800	4,341

7.7 Discussion

7.7.1 Palaeoenvironment of the Karangatian transgression in Kerch strait.

Neveeskaya (1965) described the first migration of Karangatian-age marine molluscs into the Black Sea Basin as being composed of *Ostrea edulis* and *Paphia senescens*. The second marine wave consisted primarily of *Cardium edule*, *Chione gallina*, *Mytilus galloprovincialis*, *Spisula subtruncata* and *Cerithium vulgatum*. *Ostrea edulis* in the Black Sea has a Mediterranean affinity. It represents a ‘marginal marine’ environment, contrasting strongly with the lower-salinity to non-saline environments represented by Caspian taxa including the Dreissenidae. At Eltigen, *Ostrea*-rich bioherms are overlain by lagoonal sediments with *Cardium edule*, and estuarine facies laden with a mixed assemblage of *Ostrea edulis*, *Paphia senescens*, *Chione gallina*, *Mytilus galloprovincialis* and *Spisula subtruncata*. Individual horizons, or beds commonly have one or two dominant species. For example, at BS-6 the upper portion of the marine sedimentary sequence was dominated by *Mytilus galloprovincialis* (Fig. 8.8d, 8.13), while the bioherms at BS-3 (Fig. 8.13) are monospecific structures consisting of *Ostrea edulis* and algae, and are overlain at this study site by a thick marine sequence dominated by disarticulated *Mytilus galloprovincialis*.

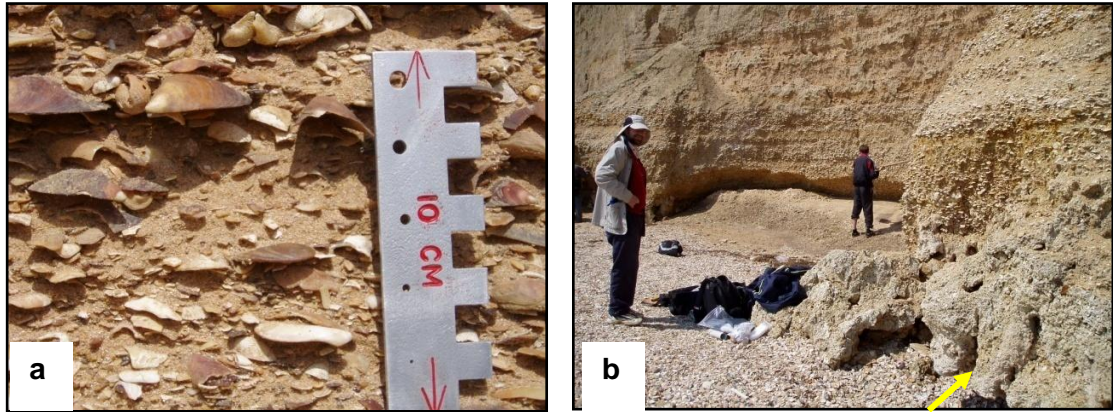


Figure 7.15. *Mytilus* and *Ostrea*-rich strata, Eltigen. a) *Mytilus galloprovincialis* dominated bed at BS-6. These units rich in the marine bivalve mollusc *Mytilus* commonly also had *Ostrea*, *Pecten* and *Cardium edule*. b) At BS-3, *Ostrea*-dominated bioherms are overlain by *Mytilus* and *Ostrea* rich sediments, suggesting that the sediments in the *Mytilus*-rich units at BS-6 and BS-3 represent similar environments, but are distinct from the environments represented by the bioherms (arrowed).

The sedimentary sequence at Eltigen represents three principal depositional environments. These are *Cardium edule* dominated lagoons dominated by silt-grade sediments, near-shore estuarine, and shallow coastal environments dominated by disarticulated shells including *Mytilus galloprovincialis*, and, lesser numbers of *Ostrea*, *Paphia* and rarer *Pecten*. This third environment is represented by bioherms. Though the bioherms at Eltigen are dominated by *Ostrea*, *Mytilus* also commonly are found in similar environments today. Critically, *Ostrea*, *Mytilus* and *Pecten* prefer oxygenated, clear water with low turbidity. This implies formation in quiet water distal from fluvial discharge, which are typically laden with clay sediments, or formation during a period of lowered fluvial activity. This is also implied for all of these sequences at this time, because of the lack of clays in the sediments. This is because the sedimentary sequences at Eltigen and those of Maly Kut, Cape Krotkov and Cape Tuzla are dominated by sediments poor in clays, but predominantly rich in silt, and to a lesser extent sand grade siliciclastics.

The bulk of sediment in the near-shore estuarine sediments consists of shell fragments, with individual horizons varying in the proportion of clasts. The orientation of shells predominantly indicates turbulent conditions. In contrast with these conditions, sediments containing *Cardium edule* are typically fine-grained silts and muds, indicative of relatively quiet conditions in shallow water. However, the lack of clays in these deposits suggests little weathering during this depositional period, and reworking of locally-derived loess sediments. The lack of clays in these sequences may also be the result of higher-energy hydrodynamic conditions during this transgressive regime, with clays in the water column not able to flocculate and be deposited. Prompt transgressions tend to halt, for a time, sedimentation because the depositional environment is rapidly moved landward and transport paths for

sediment laden fluvial water are disrupted. These may be additional reasons for the lack of fines in the Karangatian sediments of Kerch Strait.

The sedimentary sequences in Kerch Strait may have been deposited during a transgression of the Sea of Azov from what is presently termed the Black Sea. The architecture of the deposits can be attributed to deposition within and on the margins of an initially deep palaeovalley, and formation of an estuarine-like channel transporting detritus-rich sediment into the Azov Sea. The general model for deposition in Kerch Strait, as developed here, begins with a relatively high-energy transgressive and erosive episode truncating Sarmatian clays with deposition of a coarse clastic unit (i.e. a transgressive lag deposit). This was followed by formation of the bioherms, in relatively clear water, perhaps 10-20 m depth. On the margins of this water body lagoons would have developed in depressions, perhaps not contiguous with the transgressing marine water-body, but the water-levels in these environments would have been controlled to some extent by proximity to the marine water body. The bioherms were in places overlain by fine-grained lagoonal sediments (e.g. Cape Krotkov), while laterally-equivalent depositional events were estuarine-like (BS-6, Eltigen). These formed the thick shell and gravel-conglomeratic units. Regression following this led to the development of dunes in Kerch Strait. The uplift of the central Eltigenian section must have occurred after MIS 5e accumulation of loess sediments may have begun in MIS 5d, though the bulk of loess in the locations investigated may be of MIS 3 to MIS 2 age. Repeated deposition and erosion of these silt sediments may have occurred between MIS 5d and MIS 2.

Only at BS-4 is a full transgressive-regressive cycle evident: lagoonal sediments are overlain by marine, in turn overlain by dune sands, and loess. The bioherms at BS-10, overlain by fine-grained sediments typical of lagoonal conditions, and inhabited by *Cardium edule*, with rare *Helicella*, indicate a drop in water-level, from the deeper water conditions required by bioherms, to shallow restricted liman-like conditions and brackish water.

The AMS ages on *Helicella* provide a younger bounding age for the older gastropods, and therefore also for the marine sedimentary sequences. These AMS ages appear to indicate that erosion of previously deposited loess of MIS 5d or younger may have occurred at this location, because at BS-7-2 this loess appears to directly overlie the last interglacial (MIS 5e) marine sequences. Given that at this location, and at BS-6, these sedimentary sequences have been uplifted by up to 20 m with exposure of Miocene clays at the base of the cliffs, this uplift probably occurred between the deposition of the two loess units, and their associated *Helicella* gastropods, sometime between MIS 5e and MIS 3, and therefore prior to the Last Glacial Maximum.

Over long timescales D/L values in fossils are principally determined by the burial temperature regime, and by the extent to which diffusive leaching of amino acids has occurred over that period. There is no evidence in this case to suggest significant leaching of amino acids because the concentration of amino acids is consistent between modern and older samples. Therefore it is unlikely that there has been lowering of D/L values from the shells of BS-7-2 because of diffusive loss. Thus, the D/L values of the younger terrestrial gastropods from BS-7-2, near the base of a thick loess sequence suggests continuous cold conditions at this location since late MIS 3, with very cool burial conditions resulting in a very slow racemization rate and low D/L values.

7.8. Chapter summary

- Based on the results of this study, relative rates of racemization among the bivalve molluscs *Cardium edule*, *Chione gallina* and *Mytilus galloprovincialis* are; *Mytilus* > *Chione* > *Cardium*. This is not definitive, and requires further work.
- Results from the analysis of the extent of amino acid racemization on bivalve molluscs, foraminifera and whole-rock samples, supported by Uranium-series ages on bivalve molluscs indicate a last interglacial (MIS 5e) age, sensu lato, for the raised estuarine sequences at Eltigen, Kerch Peninsula and for correlative deposits on the Taman Peninsula at Maly Kut, Cape Krotkov and Cape Tuzla, Russia, northeastern Black Sea.
- These results are similar to Dodonov *et al.* (2000) who focused on the sedimentary sequences at Eltigen. However, there is no data in Dodonov *et al.* (2000) from for example Cape Krotkov with which to base a broader discussion.

Chapter Eight

Aminostratigraphy of the Gulf of Carpentaria: amino acid racemization in a tropical environment

8.1. Outline

Aminostratigraphic methods have been applied to samples from tropical environments in only a small number of cases. This study aims to determine the aminostratigraphic age of the marine and lacustrine strata from core MD32, central Gulf of Carpentaria. Results are presented from analyses undertaken on bivalve molluscs, a number of which were previously dated by gas chromatographic methods for the extent of amino acid racemization. Once the initial data (on bivalve molluscs) from this study were analysed, it was decided to focus on the most recent lacustrine phase of core MD32 using intracrystalline amino acids in bulk samples of the foraminifer *Ammonia beccarii* in an attempt to obtain better resolution, and thus better chronology, for the most recent phase of Lake Carpentaria.

8.2. Introduction

Extant semi-enclosed basins, influenced by the ingress of marine water above the level of their enclosing sill, commonly have preserved within them, sedimentary records that are readily associated with discrete environments and/or events. Examples include the clearly recognisable marine and lacustrine strata in the Black and Mediterranean Seas (Hsü, 1972; De Deckker *et al.*, 1988; Major *et al.*, 2006; Sliwinski-Strechie, 2007; Sorokin and Kuprin, 2007; Chapter 6), and the glacial and interglacial cycles evident in the Santa Barbara (Hendy *et al.*, 2002; Robert, 2004) and Cariaco basins (Heezen *et al.*, 1958; Peterson *et al.*, 2000; van Daele *et al.*, 2011). However there are also some epicontinental semi-enclosed basins where the sedimentary record is not so readily divisible into event- or environment-associated horizons. In these environments attempts to define a chronology of cyclic and acyclic processes may be problematic. This is because cyclic sedimentation within such basins is commonly the result of processes that largely operate outside of those locations, e.g. eustatic sea level change, and at regional to global scales (Peizhen *et al.*, 2001; Kershaw *et al.*, 2003). Additionally, processes that induce these allocyclic conditions in semi-enclosed environments more often than not result in autocyclic variations in sedimentation, i.e. the results of these external forcing mechanisms give rise to sedimentary deposits created only by processes within the sedimentary basin in question (Cecil, 2003). The lateral extent of autocyclic sedimentation is limited, because autocycles are restricted to the depositional basin, driven by local climatic

conditions. Thus, both allocyclic and autocyclic changes within semi-enclosed basins include variations in the supply and type of dissolved (i.e. chemical) and solid particulate matter. These processes affect the population, growth and longevity of benthic organisms including foraminifers and bivalve molluscs commonly sampled for chronological purposes. Minor changes in sea-level may produce significant effects on sedimentation because small rises or falls in water-level may result in floods or exposure of large portions of these basins (Cecil, 2003). These relationships in tropical epieric seas are comparatively less studied than those of temperate regions, and the interaction between the marine, and terrestrial environments, and the sediments and climate in these locations remains therefore less well understood.

This study focuses on the Gulf of Carpentaria, a monsoonally-influenced, shallow and tropical basin located on the southern margin of the Indo-Pacific Warm Pool between northern Australia and New Guinea. The deposition of late Pleistocene sediments recovered in cores from this basin are likely to have been heavily influenced by wet-dry seasonal to yearly climatic cycles, in addition to eustatic oscillations in sea-level. Marine water enters the Gulf once sea-level rises above – 53 m, the level of the Arafura Sill. However, the influence of the marine environment on the central gulf region during marine isotopic stages 2/3-5 is not clear, and the chronology is not resolved despite a number of recent attempts (Chivas *et al.*, 2001; Couapel *et al.*, 2007; Reeves, 2007; Reeves *et al.*, 2008).

Over the last full glacial cycle (from ~125 ka to the present interglacial), deposition in the Gulf has been driven by the interaction of climatic, terrestrial and oceanic processes. Two processes stand out as significant: these are processes associated with the monsoonal system including large fluvial discharge and cyclonic events, and eustatic changes in sea-level. During sea-level high stands, marine shells, microfossils and associated sediments are deposited while, in contrast, during periods of lowered sea-level, non-marine molluscs, foraminifers and ostracods may, or may not have been deposited. This, in turn, is particularly dependent on whether water was present in this shallow basin. Therefore this makes deriving an aminostratigraphy and/or aminochronology difficult because the species change as environments change and, the extent of racemization among taxa may be significantly different among environments, and among genera. While the general procedure for building an aminostratigraphy within a region is reliant on using a single genus (e.g. the foraminifer *Elphidium*, in Gulf St Vincent) common to all or at least most of the core or stratum being investigated (e.g. populations of shallow marine molluscs such as *Katelysia*, Kingscote, Kangaroo Island utilized in Chapter 5), this can be difficult to do in semi-enclosed basins because they commonly have strata that preserve different species in different sedimentary strata (e.g. the Black Sea, Chapter 6), and which may originate from vastly different habitats. The temporal extent of mixing of fauna of different ages, and from various environments in

these and similar regions is not well understood. The effects of the monsoonal system on the Gulf and its fauna during periods of low sea level, and the timing of monsoonal re-establishment after low stands of sea level are also poorly understood (Playà *et al.*, 2007).

A further question concerning core MD 32, is that the base of this core (Chivas *et al.*, 2001) recovered from the central basin (Fig. 8.1) and consisting of fluvially derived sediments has been dated to $\sim 123 \pm 16$ (TL), 124 ± 12 (OSL) ka (Chivas *et al.*, 2001; Couapel *et al.*, 2007). The location of MD 32 is in the central gulf, and over 100 km from land. For this location to have been fluvial, these sediments must have been deposited during a regressive phase of sea level, and at a time when the Arafura Sill was emergent. The extent of neotectonic influence is uncertain.

8.3. Study location

The Gulf of Carpentaria (Fig. 8.1) is a shallow epicontinental sea that has, over the Late Quaternary, experienced repeated oscillations in water-level associated with global eustatic fluctuations in ice-volume (Chivas *et al.*, 2001). These changes in water-level within this semi-enclosed basin are also directly and indirectly related to regional changes in climate, particularly that of the monsoonal system. The Gulf of Carpentaria is an important region for scientific exploration because the gulf is strongly influenced by the Australian monsoon and situated on the southern-most margin of the Indo-Pacific Warm Pool (Webster, 1994; Yan *et al.*, 1992; De Deckker *et al.*, 2002). It is a modern analogue for cratonic basins (Gluskoter *et al.*, 2001; Edgar *et al.*, 2003) because of the repeated oscillation between marginal marine sedimentary environments, from fully marine to saline lake conditions, and provides a record of climatically driven environmental change over the past ca. 125 ka or more (Chivas *et al.*, 2001; Reeves, 2007; Couapel *et al.*, 2007; Reeves *et al.*, 2007). An extensive lake, Lake Carpentaria, was formed when sea-level fell below -53 m, (the depth of the present Arafura Sill) during the Late Pleistocene (Torgersen, 1983; Chivas *et al.*, 2001; Reeves 2007; Couapel *et al.*, 2007; Reeves *et al.*, 2007). The discovery of submerged coral reefs in the southern gulf enhances the importance of this region because of issues related to anthropogenically driven increases in sea surface temperatures and coral survival in higher temperature environments (Harris *et al.*, 2004). The present gulf is the modern representation of several pre-existing stacked sedimentary basins. These are the Bamaga Basin (Palaeozoic age), Carpentaria Basin (Jurassic and Cretaceous age), and the Karumba Basin (Neogene and Quaternary) (Smart *et al.*, 1980; Passmore *et al.*, 1983; Playà *et al.*, 2007).

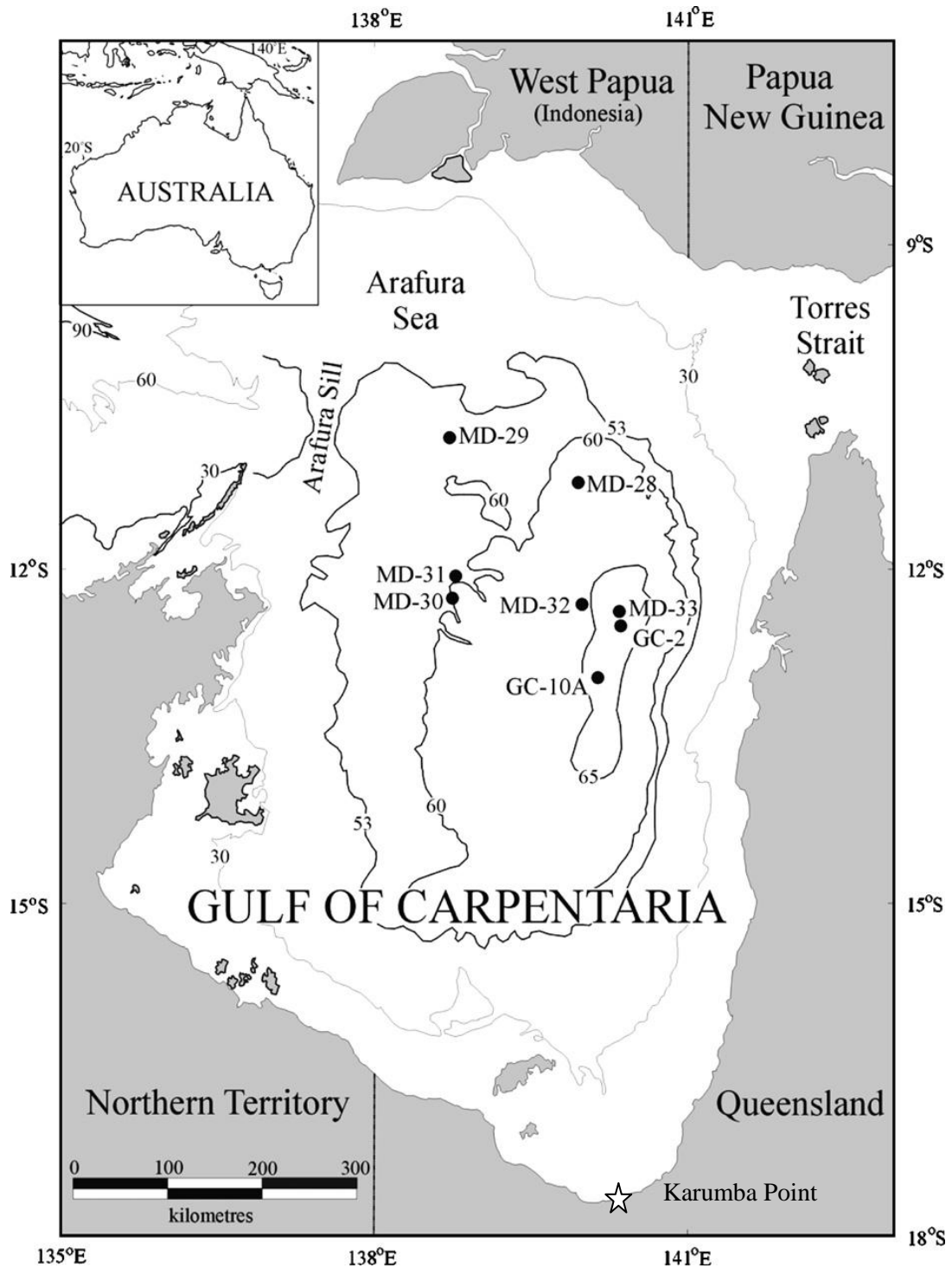


Figure 8.1. Map of the Gulf of Carpentaria and study site locations, modified from Chivas *et al.*, (2001). The principal core in this study, MD32 is located approximately in the centre of the northern portion of the basin. The locations of additional cores including MD31 from Chivas *et al.*, (2001) and previous studies (GC-10A and GC-2) are also illustrated as is the location of Karumba Point. The -53m contour represents the maximum possible extent of Lake Carpentaria, and is the current depth of the Arafura Sill, whereas Torres Strait is 12m deep.

Clastic sedimentation within the gulf is controlled in part by the fluvial water geochemistry (Playà *et al.*, 2007). More alkaline water enters the gulf west of Karumba, while more acidic

river water flows into the gulf from the quartzose sandstone river systems of Cape York. Surface water temperature in the estuary at Karumba was measured as 29.95 °C (2 Nov, 2007). The influence of the global ocean on the Gulf is determined to some extent by the presence of the shallow (12 m deep; Torgersen *et al.*, 1983; Hemer *et al.*, 2004) Torres Strait, and the broad shallow Arafura Sill at approximately 53 m depth. Small changes in sea level such as that of the Younger Dryas may have acted to further restrict the marine influence of the central basin, while large-scale eustatic regressions may have caused the Arafura Sill to become emergent during previous low stands. However, several channels cut the Arafura Sill (Edgar *et al.*, 2003), and the extent to which the Gulf was totally isolated from marine influence during low stands of the global ocean is uncertain. Seismic sections taken west of Weipa by the Canadian Superior Mining Company indicate a closed basin lake with a surface at 65 m below present sea level, and possible shoreline ridges at 63 m depth (Fig. 7 of Torgersen *et al.*, 1983). Sediment pinching out at 53 m below present sea level has been described by Torgersen *et al.* (1983) as corresponding to the maximum level of lake Carpentaria.

8.4. Previous amino acid racemization studies

Results from the analyses of *Tridacna* from the Great Barrier Reef and Huon Peninsula (PNG) (Hearty and Aharon, 1988) indicate that samples of *Tridacna* shell (giant clam) from the northern Great Barrier Reef (CMAT ~ 26-27 °C), and of Holocene age, have aiLe D/L values of up to 0.65 at 10 ka BP (Fig. 8.2). D/L values of 1.3 are reached in samples of 180 ka age. These studies, undertaken using older high pressure liquid chromatography methods (Miller and Mangerud, 1985; Hearty *et al.* 1986) to derive alloseleucine D/L values, were on large thick shells. By way of comparison, the results from the analysis on a single fragment of *Tridacna* from Huon by RP-HPLC (this study) are presented in Table 8.2.

An AAR study was undertaken on bivalve molluscs collected from core MD32 using gas chromatography (Chivas *et al.*, 2001; Table 8.1, Fig. 8.2). Two of these samples, UWGA 550 and 551, from near the bottom of core MD32 have glutamic D/L values close to racemic values but D/L values from the amino acids Asx, Leu and Val are lower. This variation in the apparent extent of racemization among the individual amino acids may be due to reversals in racemization rates over time for some of these amino acids. Sample UWGA 548, from 5.00 m depth in core MD32 has lower D/L values overall than the other samples from Chivas *et al.* (2001), yet some of these values are not significantly lower than the samples from near the base of this core.

In this earlier study a younger *Anadara granosa* sample recovered from core PCB#1 (4.61 m depth in core), Princess Charlotte Bay, Queensland, and dated to 7430 ± 130 a BP by radiocarbon methods, had significantly lower extents of racemization in the amino acids leucine and valine than those samples from core MD32. The data from this single sample were used to calibrate D/L values in the samples from MD32 to obtain numeric ages of 122 ± 18 (UWGA 550), 108 ± 16 (UWGA 551) and 72 ± 11 ka (UWGA 548) (Fig. 8.2). Glutamic acid D/L values for the samples UWGA 550 and 551 are high (0.977 and 0.925 respectively), yet aspartic acid D/L values (0.815 and 0.611) are lower, especially for sample UWGA 551 from 1318-1319 cm depth in MD 32. The valine D/L values are also lower, as would be expected, in these samples than the glutamic values. However, the leucine values are also comparatively low compared to glutamic. Some of these lowered D/L values may be due to reversals in the apparent racemization rate, but also perhaps due to diffusive loss of the more racemized free amino acid fraction.

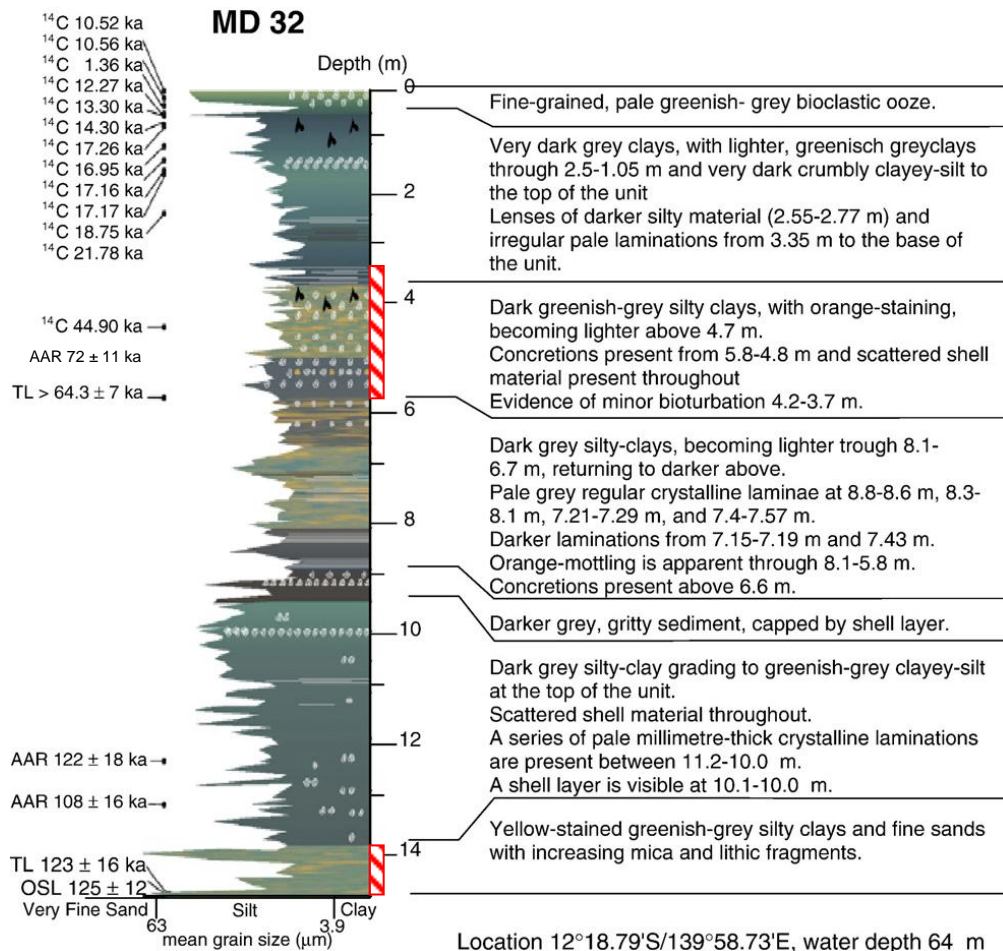


Figure 8.2. Log of core MD32 adapted from Couapel *et al.* (2007) with additional red striped rectangles indicating subaerial exposure.

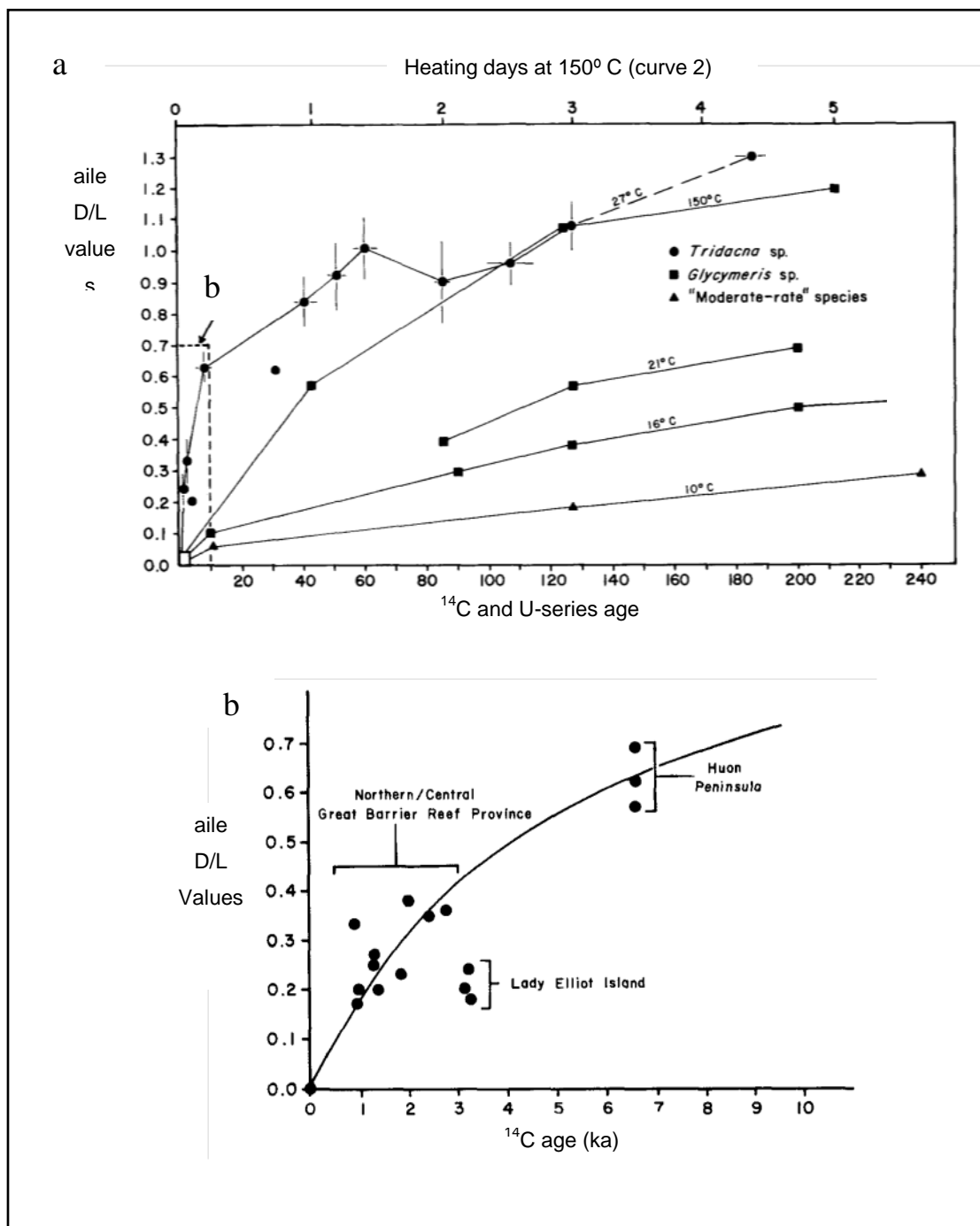


Figure 8.3, a and b. Adapted from Aharon and Hearty, 1988, indicating the extent of racemization in the bivalve mollusc *Tridacna* sp. from Huon Peninsula and the Great Barrier Reef, and other data derived from samples recovered from locations of lower mean annual temperature. Based upon these data, it would be expected that the possible maximum age of molluscs from the central Gulf of Carpentaria would be greater than last interglacial (MIS 5e) age (~ 125 ka) because there is an approximate 1-2° C difference in current mean annual temperature (CMAT) between these locations, with the gulf having the lower mean value. This is because lower rates of racemization occur due to lower temperatures. However, *Tridacna* is a large thick shell, while in contrast many shells from the Gulf of Carpentaria are small (< 1 cm length) and thinly constructed, and thus the extent of diffusive loss of indigenous amino acids may be comparatively greater in the smaller shells from the Gulf of Carpentaria than that of *Tridacna* sp.

The radiocarbon data from Chivas *et al.* (2001) and Reeves *et al.* (2007) indicate relative slow burial rates in the cores from the centre of the Gulf of Carpentaria compared with that of the sample from Princess Charlotte Bay. Comparatively longer periods of time at the surface, especially in locations of high to very high mean daily to annual temperatures, will give rise to higher extents of racemization prior to burial and thus the starting point from which measured D/L values are obtained may be significantly higher than for samples quickly buried and isolated from high temperatures such as sample UWGA 548. Attempts to calibrate with similar samples over long timescales, e.g. last interglacial (MIS 5e) or longer, will not significantly change the calibrated ages, but attempts to calibrate younger samples, including those of Holocene beach ridges and those from the recent lacustrine phase of the Gulf using these data are unlikely to be reliable because this procedure will result in differences in the slope of the curve (i.e. shallower against steeper) for lower values of D/L.

Table 8.1. D/L values for bivalve molluscs from Chivas *et al.* (2001).

Study site	Species	Lab (UWGA) code	Asx D/L	Glx D/L	Leu	Ala D/L	Val D/L
MD 32 5.00 m	<i>Bassina</i> sp. (disarticulated)	548	0.519 ± 0.014	0.614 ± 0.015	0.539 ± 0.002		0.531 ± 0.005
MD 32 12.38-12.40 m	<i>Bassina</i> sp. (articulated)	550	0.815 ± 0.002	0.977 ± 0.007	0.724 ± 0.015		0.688 ± 0.013
MD 32 13.18-13.19 m	<i>Anadara granosa</i> (articulated)	551	0.611 ± 0.088	0.925 ± 0.012	0.653 ± 0.001		0.649 ± 0.017
4.61 (PCB #1)	<i>Anadara granosa</i>	Murray-Wallace and Kimber (1988)			0.287 ± 0.005		0.171 ± 0.006

8.5. Methods

This study initially focused on larger shells, including examples of the bivalve mollusc *Anadara* present in cores (Chivas *et al.*, 2001). However, this focus shifted in an attempt to use fossil material (foraminifers) common to a large portion of the lacustrine section of core MD 32. In particular, this was an attempt to define an aminostratigraphy and chronology for the most recent lacustrine phase of Lake Carpentaria based on core MD 32.

Analyses were undertaken in two stages: the first stage involved AAR analyses of some shells previously dated by AAR (Chivas *et al.*, 2001) and of a number of small shells, foraminifers and ostracods to determine an appropriate approach to a detailed study of the lacustrine phase in the upper portion of core MD 32. Prior to analysis, shells and microfossils were subjected to a 1h soak in 12.5% NaOCl as part of preparatory procedures, with the aim

of removing any contamination. This method was adapted from Kaufman and Hearty (personal communication, 2005) who suggested the use of a 2h soak in H₂O₂ prior to digestion in 8M HCl, and subsequent hydrolysis for 22 hours at 110°C. The application of H₂O₂ was discontinued after the loss of microfossils due to the slightly acidic nature of this oxidizing agent and the thin walls of, for example, *Ammonia sp.* Bleach (12.5% NaOCl) was subsequently used (pH = 11.4) because it does not dissolve/destroy samples. Thereafter, only molluscs were analysed for the extent of racemization of the total hydrolysable amino acids.

The second stage involved dating by the intracrystalline amino acid method, bulk samples of the *Ammonia beccarii* and of ostracods, including *Cyprideis australiensis*. Samples consisting of multiples of individual microfossils were immersed in 12.5% NaOCl for 48 h to remove all organic components of the carbonate skeleton not enclosed within individual crystallites. 10-20 individual *Ammonia beccarii*, bleached for 48 h, were used as a single sample, and each sample was placed in 1ml reaction vial. 10µl of 8M HCl was used to digest each sample, and 5µl of rehydration solution was used upon post-hydrolysis drying to have sufficient sample for a single 4µl injection on the HPLC.

Calibration of amino acid D/L values was done using ¹⁴C ages on either the same material (this study), or on samples of bivalve molluscs, gastropods or ostracods from the same core horizon previously dated (Chivas *et al.*, 2001; Reeves *et al.*, 2008; Chivas, unpublished). Parabolic curve fitting was used to translate D/L values into numeric ages.

8.6. Results

8.6.1. Karumba beach ridges

Relative rates of racemization for *Tridacna* (Huon) and *Anadara* (Karumba Point) are consistent with expected relative racemization rates (Asx > Glu > Val) (Kvenvolden *et al.*, 1973; Lajoie *et al.*, 1980), suggesting that diffusive loss through leaching of amino acids from the carbonate matrix is minimal, and that significant reversals of racemization have not occurred. Similar aile D/L values to those of Hearty and Aharon (1988) were obtained from the analysis of a single sample of *Tridacna* (~ 125 ka) recovered from a last interglacial (MIS 5e) coral terrace on the Huon Peninsula (Table 8.2). The Aile D/L values from this sample, compared with the data from Hearty and Aharon (1988), suggest a latest last interglacial (MIS 5e) age (circled and arrowed, Fig. 8.4) of approximately 118 ka.

In comparison, *Anadara* shells from indurated beach ridges at Karumba, whose shore-parallel equivalents had previously been dated to between 630 ± 70 and 1320 ± 80 ¹⁴C a BP (Rhodes, 1982) had AiLe D/L values (0.390, 0.421, 0.390, 0.397 and 0.348) that indicate a substantially younger age than the sample from Huon. Comparison with Fig. 3 of Hearty and

Aharon (1988) suggests a Holocene age for the *Anadara* samples (Fig. 8.5). Valine D/L values for these *Anadara* samples are significantly higher (mean valine D/L = 0.363 ± 0.038) than that of the single sample of *Anadara granosa* from Princess Charlotte Bay, Queensland, dated to $7,430 \pm 130$ a BP (valine = 0.171 ± 0.006 ; Murray-Wallace and Kimber, 1988). Differences in the D/L values obtained between the *Anadara* from Karumba and that from Princess Charlotte Bay are likely to be the result of early and rapid burial of the sample at Princess Charlotte Bay soon after death, or death may have resulted from the rapid burial. In contrast, the higher extent of racemization in the samples from Karumba seems to imply shallow burial since original deposition in a beach ridge. In this case the shells were all disarticulated. The large numbers of relatively well preserved whole valves of *Anadara* in these strata suggest estuarine conditions were prevalent adjacent to where the beach ridges were deposited. Because of the strong likelihood that these shells, and the associated beach ridges have not been buried, the results from these shells were not used for age calibration elsewhere.

Table 8.2. AAR data obtained on the total hydrolysable amino acids (THAA) in a single sample of *Tridacna* from Huon Peninsula, Papua New Guinea, and samples of the bivalve mollusc *Anadara trapezia* from cemented beach ridges at Karumba Point. Also included are the results from two *Lentidium* shells from 500 cm depth in core MD32.

Study site	Species	Lab (UWGA) code	Asx D/L	Glx D/L	Ser D/L	Ala D/L	Val D/L	Aile D/L
Huon Peninsula last interglacial (MIS 5e) ~125 ka	<i>Tridacna</i>	8090	0.861 ± 0.005	0.959 ± 0.006	0 (no D-ser)	1.017 ± 0.050	0.771 ± 0.076	0.984 ± 0.057
Karumba Beach Ridge	<i>Anadara granosa</i>	6268	0.600 ± 0.001	0.442 ± 0.005	0.535 ± 0.045	0.759 ± 0.009	0.385 ± 0.023	0.390 ± 0.029
Karumba Beach Ridge	<i>Anadara granosa</i>	6269	0.616 ± 0.022	0.476 ± 0.013	0.470 ± 0.090	0.708 ± 0.023	0.395 ± 0.039	0.421 ± 0.100
Karumba Beach Ridge	<i>Anadara granosa</i>	6270	0.629 ± 0.006	0.455 ± 0.002	0.448 ± 0.163	0.777 ± 0.018	0.392 ± 0.0133	0.390 ± 0.043
Karumba Beach Ridge	<i>Anadara granosa</i>	6271	0.616 ± 0.000	0.484 ± 0.001	0.485 ± 0.000	0.781 ± 0.049	0.328 ± 0.030	0.397 ± 0.00
Karumba Beach Ridge	<i>Anadara granosa</i>	6272	0.611 ± 0.017	0.438 ± 0.042	0.463 ± 0.027	0.735 ± 0.007	0.316 ± 0.035	0.348 ± 0.061
	Mean		0.614	0.459	0.480	0.752	0.363	0.389
	Stdv		0.010	0.020	0.033	0.030	0.038	0.026
	CV (%)		1.7	4.4	6.9	4.1	10.6	6.7
MD32 500 cm	<i>Lentidium</i>	5476a	0.730	0.721	0.058	0.971	0.778	0.906
MD32 500 cm	<i>Lentidium</i>	5476b	0.786	0.718	0.068	0.982	0.796	0.951
	Mean		0.758	0.720	0.063	0.977	0.787	0.929
	Stdv		0.040	0.002	0.007	0.008	0.013	0.032
	CV (%)		5.2	0.3	11.2	0.8	1.6	3.4

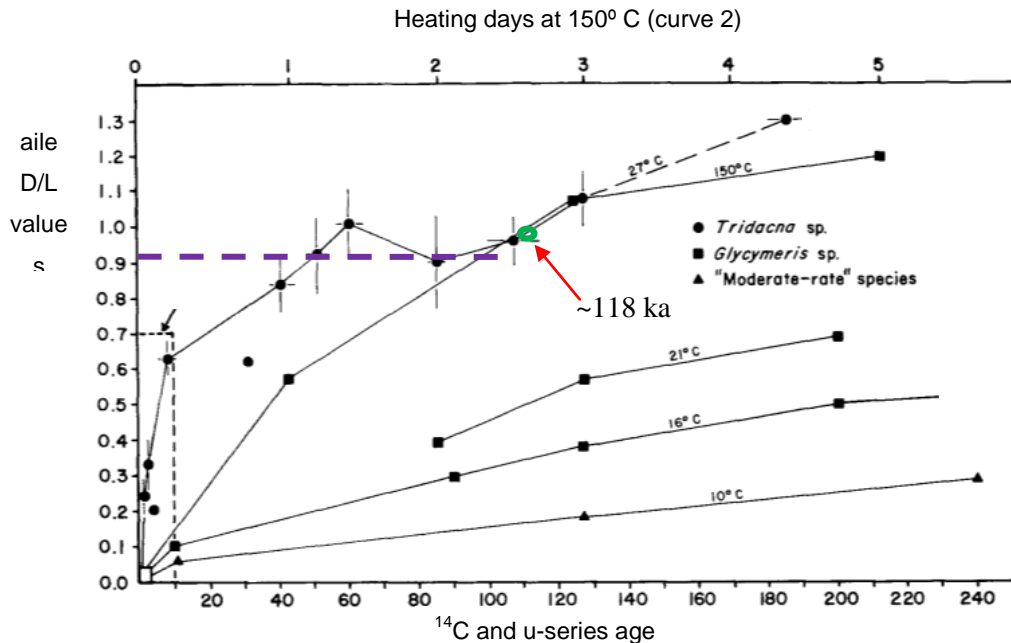


Figure 8.4. D/L value for alloisoleucine from a single sample of *Tridacna* of known last interglacial (MIS 5e) age (green circle) positioned on data for *Tridacna* from figure 2 of Hearty and Aharon (1988). This results in an approximate age of 140 ka for this sample, slightly higher than the previously determined last interglacial (MIS 5e) age. Also present above is a line (grey) indicating the mean D/L value obtained (mean aile D/L = 0.929 ± 0.032), and the possible range of ages from *Lentidium* at 500 cm depth in core MD32. A calibrated AAR age for *Lentidium* from 500 cm depth in core MD32, greater than 100 ka, would seem excessive in the light of the stratigraphy from this core (Chivas *et al.*, 2001; Reeves, 2007; Reeves *et al.*, 2008). In comparison, the arrowed box indicates previous results from Holocene samples (Hearty and Aharon, 1988).

8.6.2. Calibration and rates of racemization

Paired amino acid racemization and radiocarbon dating of 4 shells (Table 8.3) from the top of cores MD31 and MD32, suggest that racemization rates in these and similar shells in the Gulf of Carpentaria are high (CMAT = 25.4° C, Karumba Airport, for the years 1913-1951, Bureau of Meteorology; mean annual SST at the location of core MD 32 is ~ 26° C) compared to regions of lower temperature (e.g. the Black Sea, and Gulf St Vincent), and also compared to the *Anadara* sample from Princess Charlotte Bay (Murray-Wallace and Kimber, 1988). Mean annual Sea Surface Temperatures at Lady Elliot Island are at present approximately 24.5° C (based on fig 1 of Hearty and Aharon, 1988), and similar to that at Karumba. Though this conclusion is consistent with the data on *Anadara* sp from Karumba (Section 8.6.1), it is evident that this may not exactly be a fair comparison because the initial rates of racemization, commonly representing the period in a fossils existence of the highest rate of racemization, depend in part on the length of time the shells were located at the sediment-water interface,

and subsequent burial. The shells from beach ridges at Karumba Point are unlikely to have been buried, or at least only for a short period, while in contrast sedimentary particles in the cores will have been buried by subsequent deposition of sedimentary layers.

Table 8.3. Sample results and ages used for calibration of amino acid D/L values to obtain estimates of numerical ages on bivalve molluscs from MD 32.

Core and depth	Species	AAR and/or ANSTO code	Asx D/L	Glx D/L	Ser D/L	Ala D/L	Val D/L	¹⁴ C Age
Surface, (collected alive)	<i>Corbula</i>	7237c	0.1	0.04	0.181	0.152	0.018	5 est
Grab sample	<i>Lentidium</i>	5395	0.136	0.064	0.136	0.113	0.031	100 est
MD 28	<i>Bassina</i>	5354	0.543 ±	0.286 ±	0.463 ±	0.598 ±	0.266 ±	4,481
10 cm	(fragment)	(OZI756)	0.002	0.011	0.006	0.037	0.018	
MD 32	<i>Anadara</i>	5355	0.580 ±	0.326 ±	0.533 ±	0.605 ±	0.314 ±	11,112
05 cm	(fragment)	(OZI755)	0.001	0.001	0.057	0.004	0.022	
MD 31	<i>Tellenid</i>	5358	0.635 ±	0.384 ±	0.433 ±	0.695 ±	0.409 ±	10,603
02 cm		(OZI754)	0.001	0.006	0.081	0.009	0.027	
MD 32	<i>Lentidium</i>		0.565 ±	0.445 ±	0.337 ±	0.812 ±	0.450 ±	17170
145 cm			0.039	0.088	0.116	0.063	0.087	
MD 32	<i>Lentidium</i>		0.536 ±	0.406 ±	0.242 ±	0.709 ±	0.392 ±	18740
150 cm			0.051	0.031	0.037	0.133	0.063	

Because an exact comparison between the racemization rates of *Anadara* and *Tridacna* has not been conducted, it is therefore not possible to assign a definitive age to the *Anadara* based on these AAR data and therefore the precise rate of racemization for these samples at Karumba is unknown. The beach ridges at Karumba do not appear to have been buried to any depth. Indeed they may have not been ‘buried’ at all and may represent the position of the coast during the Holocene high stand, and it is therefore likely that higher extents of racemization will have occurred for bioclasts within the beach ridges, than for *Anadara* and other shells that were buried rapidly and/or to a significant depth, including those in the cores from the central gulf.

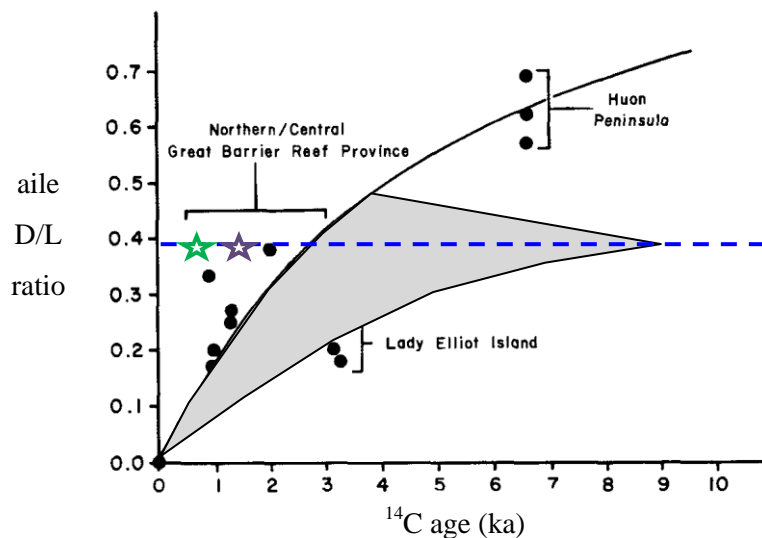


Figure 8.5. Holocene alloisoleucine D/L values. Dashed line drawn on Fig. 3 of Hearty and Aharon (1988) indicating an AiLe D/L value of approximately 0.389 (mean value from 5 *Anadara* shells from subaerially exposed beach ridges at Karumba, Queensland; Table 8.2). The curve for *Tridacna* from the Great Barrier Reef Province was used to estimate a similar trend of racemization, and one that passes through the samples from Lady Elliot Island. Based on the data from the Great Barrier Reef Province and from Lady Elliot Island, with lower mean annual temperatures than Huon, it is suggested that the data from *Anadara* indicate a minimum age of approximately 2.5 ka and a maximum age of 8.5 ka. However, the ages (indicated by stars above) obtained on adjacent beach ridges by radiocarbon methods is 630 ± 70 and $1,320 \pm 80$ a BP (Rhodes, 1980).

8.6.3 Age calibration using bivalve molluscs

Radiocarbon ages were obtained on three molluscs for the purpose of calibration of D/L values, one shell each was used from cores MD 28, MD 31 and MD 32, using accelerator mass spectrometry methods (Table 8.2). These data, combined with D/L values from modern samples, and AMS ages and D/L values from samples in core MD 32, were used to obtain numeric ages from either parabolic or power law equations (Figure 8.6). Of the now large dataset of radiocarbon ages for these cores (data from MD 32 presented in Tables 8.3, 8.4; Chivas *et al.*, 2001; Couapel *et al.*, 2007; Reeves *et al.*, 2007, 2008; Chivas unpublished), only samples where D/L values and radiocarbon ages exist on the same shell pieces, or from the same one centimetre horizon in core MD 32 were used for calibration.

The calibrated ages obtained in this study were first assessed against the stratigraphy and previously published chronology of core MD 32 (Chivas *et al.*, 2001; Couapel, 2005; Couapel *et al.*, 2007; Playá *et al.*, 2007; Reeves *et al.*, 2007, 2008). In particular, the basal sediments of core MD 32, indicative of fluvial conditions at 78-79 m below present sea level, can only have been deposited during a low stand of sea level, such as marine oxygen isotope (MIS) stage 2, 6, etc. When recovered the basal section of the core was mottled red in colour, indicating oxidising conditions, but the overlying sediments were not oxidised. Thus sea level

must have been sufficiently low for oxidation to take place. Luminescence dating (Chivas *et al.*, 2001; Couapel *et al.*, 2007; Reeves *et al.*, 2008) suggests a last interglacial (MIS 5e) age for the fluvial sediments, but when compared with the marine oxygen isotopic record, these ages are closest to, but younger than, the low stand of MIS 6 (Waelbroeck *et al.*, 2002). Additional age estimates by AMS ^{14}C and AAR dating suggest that the fluvial deposits are not MIS 2, in age, and also support an age of OIS 6 or older. However, there are no distinct unconformities in the core likely to suggest an age older than 140-150 ka for the basal sediments. A further consideration is the evaporitic gypsum from core MD 32 (Playa *et al.*, 2007). While the gypsum could be marine or non-marine in origin, an evaporative environment at this depth requires a sea level at least below the level of the Arafura Sill. The only possible time for this is during Marine Oxygen Isotope Stage 4 because it is only during this phase that sea levels would have been at the required height to allow evaporitic conditions to occur. Thus any calibration curve using amino acid racemization data must fit these constraints: oxygenating and fluvial conditions during MIS 6 or an older low stand of sea level, and an approximate age for the evaporitic gypsum horizons of MIS 4.

Calibrated ages obtained using parabolic equations were significantly lower than expected (Fig. 8.6). These ages were also low compared to previous dating of these cores (Chivas *et al.*, 2001; Couapel *et al.*, 2007; Reeves *et al.*, 2008), and low compared to the data from Huon Peninsula and Great Barrier Reef (Hearty and Aharon, 1988) and from Karumba beach ridges (Table 8.2). Using power law equations, possible calibrated ages for aspartic and valine were most similar. Calibrated ages using the power law equation for valine, $y = 0.0071x^{0.4164}$ provided the best fit to the previously obtained AAR ages on bivalve molluscs from core MD 32. Though specific techniques are different (Gas Chromatography and Reverse-Phase High Performance Liquid Chromatography), it would be expected that the end result (calibrated ages) would be the same. However, this does not give a good fit to an MIS 4 age for the gypsum layer in MD 32. Suitable ages were only obtained using the mean age obtained from individual power law equations for all of the amino acids aspartic, glutamic, alanine and valine together. While this approach to calibration is not common because most calibration attempts focus on a single amino acid (Wehmiller *et al.*, 2011), the method take here is similar to that of Penkman (2005) and Penkman *et al.* (2007, 2008), whereby several of the most reliable amino acids are used together for chronology. This latter approach assumes that the amino acids are isolated to a large extent from the external environment, and that the breakdown of peptide bonds are related among amino acids within a sample.

For both power law and parabolic models, the extent of racemization for glutamic acid was lower than valine (Fig. 8.5). This is similar to the actual D/L values obtained on samples from core MD 32 (Table 8.4), but does not fit with ‘expected’ rates of racemization as indicated by Lajoie *et al.* (1980). A racemic value using the power law equation $y = 0.0207x^{0.3049}$ for glutamic acid based on D/L values from calibration samples would give an approximate age of 335 ka, substantially higher than the 134 and 145 ka possible with the amino acids aspartic and valine respectively (Fig. 8.6). The possible 335 ka age for glutamic acid at first seems plausible because in contrast with Huon Peninsula (SST ~ CMAT = 27°C) the central Gulf has a lower mean annual temperature of approximately 26°C, and therefore an approximate doubling of the extent of racemization would theoretically be possible over that of Huon Peninsula. However, the application of this equation to glutamic values in MD 32 does not appear to fit the stratigraphy of MD 32, and results in ages for 5 m depth in core MD 32 of 100 ka. This seems excessive.

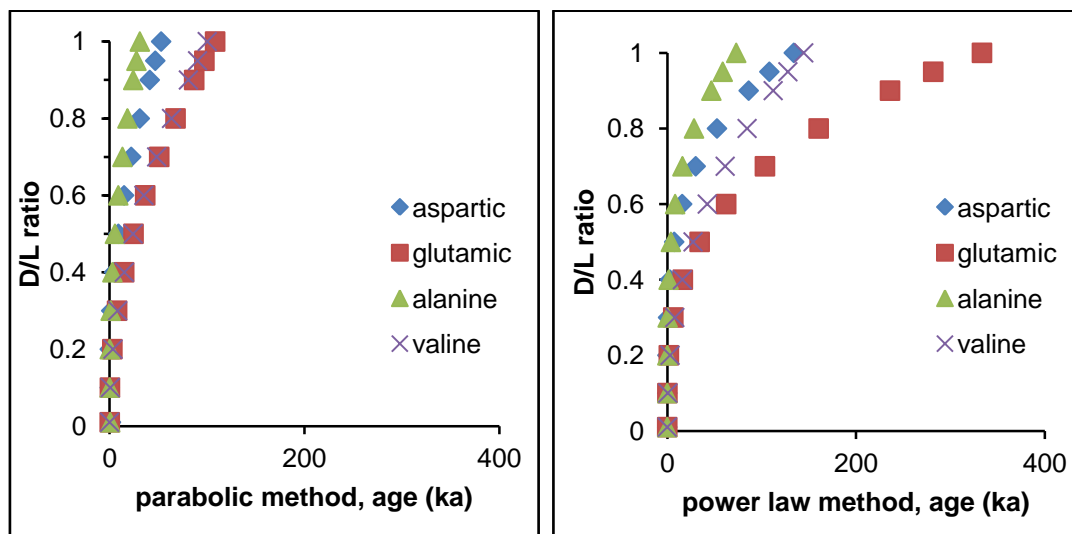


Fig. 8.6. Possible ages based on D/L values in calibration samples (Table 8.3) from parabolic (a) and power law (b) equations.

Table 8.4. Radiocarbon ages from core MD 32.

Depth (cm)	Sample type	ANSTO code	$\delta^{13}\text{C}_{\text{v-pdb}}$ ^{a, b} (‰)	^{14}C age (a BP)	1 σ	Cal age (mean, a BP)	1 σ	Reference
0-1	marine mollusc	OZF289	-1.3	9705	45	10520	50	Reeves et al., 2008
5-6	marine mollusc	OZI755		10150		11,112		This study
10-11	marine mollusc	OZG235	0.0	9700	80	10500	90	Reeves et al., 2008
20-21	marine mollusc	OZG384	0.0	1820	50	1320	60	Reeves et al., 2008
35-36	non-marine mollusc	OZF290	-0.3	10380	70	12260	130	Reeves et al., 2008
40-41	non-marine mollusc	OZF291	0.0	11440	80	13310	80	Reeves et al., 2008
70-71	non-marine mollusc	OZF292	7.3	12390	80	14390	260	Reeves et al., 2008
75-76	non-marine mollusc	OZG378	0.0	14390	80	17510	150	Reeves et al., 2008
100-101	non-marine mollusc	OZG385	0.0	14190	130	17270	210	Reeves et al., 2008
120-121	non-marine mollusc	OZG386	0.0	14330	90	17410	190	Reeves et al., 2008
145-146	non-marine mollusc	OZG388	0.0	14330	100	17410	200	Reeves et al., 2008
150-151	non-marine mollusc	OZF293	0.3	15390	110	18640	90	Reeves et al., 2008
158-159	ostracods	OZM159	-4.9	17950	100	21410	120	Chivas unpublished
161-162	non-marine mollusc	OZM160	1.1	15040	70	18190	130	Chivas unpublished
197-198	ostracods	OZM161	-5.0	18820	130	22400	170	Chivas unpublished
232-233	ostracods	OZM162	-5.1	18840	110	22410	150	Chivas unpublished
234-235	non-marine mollusc	OZI055	-4.4	18320	170	21840	250	Reeves et al., 2008
266-267	non-marine mollusc	OZM163	0	18490	200	22040	280	Chivas unpublished
273-274	ostracods	OZN456	-2.9	19130	100	22750	250	Chivas unpublished
371-372	non-marine gastropod	OZM164	-4.1	20210	130	24130	190	Chivas unpublished
371-372	ostracods	OZN457	0	20000	150	23920	240	Chivas unpublished
428-429	non-marine mollusc	OZI056	-2.3	23130	130	27970	190	Chivas unpublished
445-446	non-marine mollusc	OZM165	-1.3	44900	2400	48070	1630	Reeves et al., 2008
471-477	non-marine mollusc	OZM166	-1.9	41570	430	45070	350	Chivas unpublished
474-475	ostracods	OZN459	-7	49000	1200			Chivas unpublished
506-507	non-marine mollusc	OZM167	-4.0	31270	200	35520	190	Chivas unpublished

^a $\delta^{13}\text{C}_{\text{v-pdb}}$ values were obtained on the graphite derived from the original sample, and may not represent the actual value of the original bulk carbonate

^b actual values not available, values of 0.0 are estimated

8.6.4. Shell data and calibrated ages

The extent of racemization in relatively young samples from core MD 32 (Tables 8.3, 8.5) is high, but not as high as that of the *Anadara* samples from the indurated beach ridges at Karumba Point, Queensland (Table 8.2). The results from the majority of the shells examined do not follow the generally accepted relative rates of racemization for bivalve molluscs. This is because valine D/L values commonly exceed those of glutamic acid, whereas in a number of previous studies it was determined that the relative extents of racemization follow the general trend of Asx D/L > Glx D/L > Val D/L, and Val D/L > Aile (Lajoie *et al.*, 1980). Conforming to these relative rates of racemization has been determined to indicate reliable results (Penkman, 2005) because diffusive loss of indigenous amino acids from the fossil will result in one or more amino acids undergoing apparent reversals in racemization rate. Therefore the data produced here seem to require caution in their analysis and use. There is a greater amino acid concentration in the shells from Karumba compared with those *Lentidium* and other small samples including bulk foraminifers from MD 32. It is suggested that this concentration difference may be a source of different results, but this has not been investigated here due to time restrictions.

Two samples previously analysed for the extent of racemization by gas chromatography (Chivas *et al.*, 2001) were analysed here by RP-HPLC. The results differ significantly, with for example, comparatively low D/L values for valine by gas chromatography in *Bassina* (1238 cm depth; 0.688) and *Anadara* (1318 cm depth; 0.649) compared to 0.898 and 0.967 respectively by RP-HPLC. However, calibrated ages on these shells are similar (Table 8.5, Fig. 8.9).

Lentidium at 135 cm depth in MD32 have generally higher extents of racemization than those *Lentidium* from 145, 150 and 160 cm depth in the same core. Calibrated ages for these shells from 135 cm vary between 15 ± 1 and 37 ± 20 ka with a mean age of 23 ± 6 ka. In contrast, those from, for example, 150 cm have a mean age of 17 ± 5 ka, ranging from 13 ± 1 to 23 ± 4 ka. It is possible that the shells at 135 and 145 cm may have been close to the surface longer than those directly beneath, e.g. those at 150 cm. The length of time exposed at the surface will influence the initial extent of racemization, and extended time at the surface tends to result in higher extents of racemization over equivalent shells buried quickly. The case in point is the extent of racemization in the *Anadara* from Karumba beach ridges, with the extent of racemization in these shells being quite high compared to any others of comparable age, and this is likely due to a very high rate of racemization for these shells that remain relatively unburied.

The grouping of D/L values in bivalve molluscs from 500 and 910 cm in MD32 (Fig. 8.8a) suggests broadly similar ages (assuming the same thermal, i.e. burial, environment). The mean calibrated age for these shells from 500 cm was 67 ± 5 ka, while that from 910 cm depth was 72 ± 24 ka. This latter mean value was influenced by the oldest age of 101 ± 9 ka and the youngest of 34 ± 22 ka. Some data points do not fit well, with for example, D/L values in the two bivalve samples from 510 cm depth being significantly lower than those of 500 cm, and D/L values in shells from 1320 and 1340 cm are low when compared to adjacent horizons. These lower values are likely to reflect diffusive loss of amino acids from these shells, and/or contamination by younger amino acids.

To further test the above possibilities, the hydrolysable intracrystalline amino acids in bulk samples of *Ammonia beccarii* were used in an attempt to obtain a detailed chronology for the lacustrine phase in the upper sections of core MD32. These results are detailed in Section 8.6.2, the associated figures, and Table 8.8.

Table 8.5. Amino acid racemization data obtained from the analysis of the total hydrolysable amino acid pool in shells recovered from Gulf of Carpentaria cores (Chivas *et al.*, 2001). Calibrated ages are based on valine D/L values using a power law equation $y = 0.0071x^{0.4164}$. Single injections were used for each *Lentidium* or *Notocorbula*, and two injections used for other shells onto the reverse-phase column.

Core and depth (cm)	Species	Lab code	Asx D/L	Glx D/L	Ser D/L	Ala D/L	Val D/L	Calibrated age (ka)
MD32-135	<i>Lentidium</i>	5307-a	0.529	0.398	0.188	0.734	0.422	15.6
MD32-135	<i>Lentidium</i>	5307-b	0.550	0.388	0.269	0.765	0.379	15.6
MD32-135	<i>Lentidium</i>	5307-d	0.544	0.426	0.153	0.838	0.511	23.0
MD32-135	<i>Lentidium</i>	5307-e	0.572	0.479	0.205	0.894	0.637	33.3
MD32-135	<i>Lentidium</i>	5406h	0.535	0.393	0.295	0.765	0.437	16.8
MD32-135	<i>Lentidium</i>	5468	0.563	0.416	0.544	0.777	0.456	19.1
MD32-135	<i>Lentidium</i>	5469	0.593	0.436	0.433	0.818	0.498	23.3
MD32-135	<i>Lentidium</i>	5470	0.552	0.424	0.327	0.809	0.477	20.9
MD32-135	<i>Lentidium</i>	5471	0.545	0.419	0.272	0.794	0.462	19.6
MD32-135	<i>Lentidium</i>	5472	0.64	0.444	0.535	0.844	0.511	26.6
MD32-135	<i>Lentidium</i>	5473	0.533	0.434	0.277	0.801	0.483	20.8
MD32-135	<i>Lentidium</i>	5477	0.559	0.447	0.399	0.789	0.427	19.9
MD32-135	<i>Lentidium</i>	5479	0.563	0.386	0.218	0.751	0.443	16.9
MD32-135	<i>Lentidium</i>	5481	0.652	0.440	0.257	0.853	0.636	31.7
MD32-135	<i>Lentidium</i>	5483	0.552	0.357	0.330	0.724	0.409	14.2
	Mean		0.565	0.419	0.313	0.797	0.479	21.2
	Stdv		0.037	0.030	0.118	0.047	0.074	5.7
	CV (%)		6.5	7.3	37.7	5.9	15.5	26.9
MD32-145	<i>Lentidium</i>	5306a	0.562	0.410	0.561	0.803	0.357	17.5
MD32-145	<i>Lentidium</i>	5306c	0.611	0.607	0.258	0.793	0.409	31.3
MD32-145	<i>Lentidium</i>	5306d	0.613	0.478	0.344	0.914	0.604	34.2
MD32-145	<i>Lentidium</i>	5306e	0.539	0.418	0.251	0.841	0.489	22.1
MD32-145	<i>Lentidium</i>	5306f	0.515	0.400	0.277	0.798	0.430	17.7
MD32-145	<i>Lentidium</i>	5483	0.552	0.357	0.330	0.724	0.409	14.2
	Mean		0.565	0.445	0.337	0.812	0.450	22.8
	Stdv		0.039	0.088	0.116	0.063	0.087	8.1
	CV (%)		7.0	19.9	34.5	7.7	19.3	35.5
MD32-150	<i>Lentidium</i>	5309b	0.553	0.376	0.290	0.764	0.330	14.4
MD32-150	<i>Lentidium</i>	5309c	0.527	0.405	0.272	0.744	0.376	15.0
MD32-150	<i>Lentidium</i>	5309d	0.599	0.430	0.226	0.819	0.438	21.6
MD32-150	<i>Lentidium</i>	5309e	0.543	0.377	0.201	0.737	0.341	13.6
MD32-150	<i>Lentidium</i>	5562	0.540	0.444	0.403	0.823	0.477	22.0
	Mean		0.536	0.406	0.242	0.709	0.392	17.3
	Stdv		0.051	0.031	0.037	0.133	0.063	4.1
	CV (%)		9.5	7.5	15.4	18.7	16.1	23.9
32-160	<i>Lentidium</i>	5308 a	0.554	0.408	0.335	0.793	0.377	17.3
32-160	<i>Lentidium</i>	5308 b	0.539	0.432	0.125	0.811	0.413	19.4
32-160	<i>Lentidium</i>	5308 c	0.498	0.324	0.158	0.719	0.297	10.2
	Mean		0.530	0.388	0.206	0.774	0.362	15.6
	Stdv		0.029	0.057	0.113	0.049	0.059	4.8
	CV (%)		5	15	55	6	16	30.7
MD32-500	<i>Lentidium</i>	5393a	0.715	0.701	0.135	0.956	0.817	69.7
MD32-500	<i>Lentidium</i>	5393b	0.689	0.723	0 (no D-Ser)	0.905	0.772	65.6
MD32-500	<i>Lentidium</i>	5393c	0.629	0.626	0 (no D-Ser)	0.873	0.772	50.8
MD32-500	<i>Lentidium</i>	5393d	0.729	0.700	0 (no D-Ser)	0.959	0.807	69.9
	Mean		0.695	0.697	0.133	0.895	0.808	64.0
	Stdv		0.067	0.053	0.042	0.055	0.033	9.0
	CV (%)		9.6	7.6	31.5	6.1	4.1	14.1

MD32-510	<i>Lentidium</i>	5484	0.463	0.324	0.076	0.679	0.468	12.4
MD32-510	<i>Lentidium</i>	5485	0.534	0.4025	0.2325	0.706	0.4215	15.0
MD32-910	<i>Lentidium</i>	5559	0.615	0.760	0	0.933	0.818	72.3
MD32-910	<i>Lentidium</i>	5561	0.741	0.872	0	1.036	0.926	111.3
MD32-910	<i>Lentidium</i>	5563	0.379	0.429	0.028	0.764	0.643	23.1
MD32-910	<i>Lentidium</i>	5475	0.676	0.649	0.050	0.928	0.872	63.7
MD32-910	<i>Lentidium</i>	5476	0.708	0.723	0	0.958	0.864	75.1
	Mean		0.623	0.686	0.016	0.923	0.824	69.1
	Stdv		0.145	0.165	0.023	0.099	0.109	31.5
	CV (%)		23.2	24.0	146.2	10.7	13.2	45.6
MD32-1238	<i>Bassina</i> (articulated)	5169	0.794 ± 0.004	0.851 ± 0.021	0.299 ± 0.086	1.100 ± 0.013	0.898 ± 0.032	114.8
MD32-1290	301105-11	5406 d	0.855	0.781	0.098	1.027	0.953	104.3
MD32-1295	<i>Anadara</i> <i>granosa</i>	5169	0.930 ± 0.036	0.835 ± 0.035	0.325 ± 0.060	1.047 ± 0.004	0.967 ± 0.018	123.5
MD32-1318	<i>Anadara</i> <i>granosa</i> (articulated)	5169	0.928 ± 0.034	0.890 ± 0.032	0.453 ± 0.121	1.060± 0.019	0.967 ± 0.031	135.2
MD32-1320	<i>A.granosa</i> juv	5393	0.705	0.717	0.132	0.840	0.840	66.3
MD32-1340	<i>Notocorbula</i>	5289	0.673	0.645	0.118	0.868	0.751	52.9
MD32-1360	<i>Notocorbula</i>	5406 o	0.890	0.833	0.109	1.033	0.963	117.5
MD32-1360	<i>Notocorbula</i>	5443 a	0.884	0.825	0	1.026	0.967	115.2
MD32-1370	<i>Notocorbula</i>	5406a	0.854	0.851	noD-Ser	0.979	1.033	118.7
MD32-1380	<i>Notocorbula</i>	5406 e	0.880	0.889	0.113	1.023	0.985	128.2
MD31-1050	<i>Lentidium</i>	5565		0.847	0.214	1.043	0.890	95.2
MD31-1050	<i>Lentidium</i>	5567	0.801	0.826	0.142	1.044	0.934	107.7
MD31-1057	<i>articulated</i>	5570	0.776	0.791	0.131	1.002	0.897	94.1
MD31-1060	<i>Lentidium</i>	5568	0.551	0.376	0.026	0.850	0.687	28.8

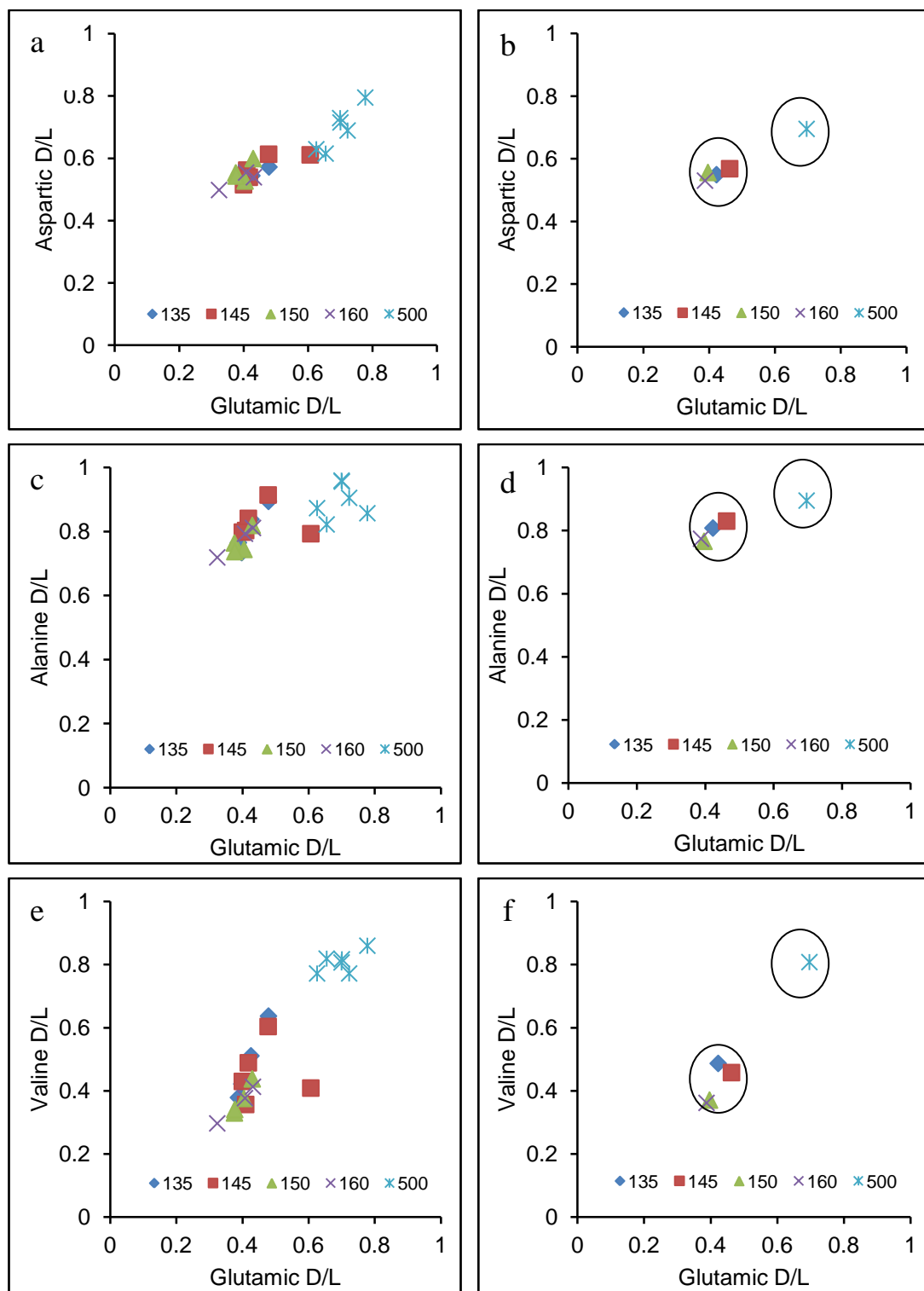


Figure 8.7. THAA D/L values in *Lentidium* sp. Figures on the left hand side (a, c, e) illustrate the covariance of amino acid pairs for individual shell samples, while the diagrams on the right (b, d, f) illustrate the covariance of mean D/L values for each horizon, located at 135, 145, 150, 160 and 500 cm depth in core MD32. Two aminozones are discernable, one consisting of samples from 135, 145, 150 and 160 cm and the second, consisting solely of samples from MD 32 500 cm depth.

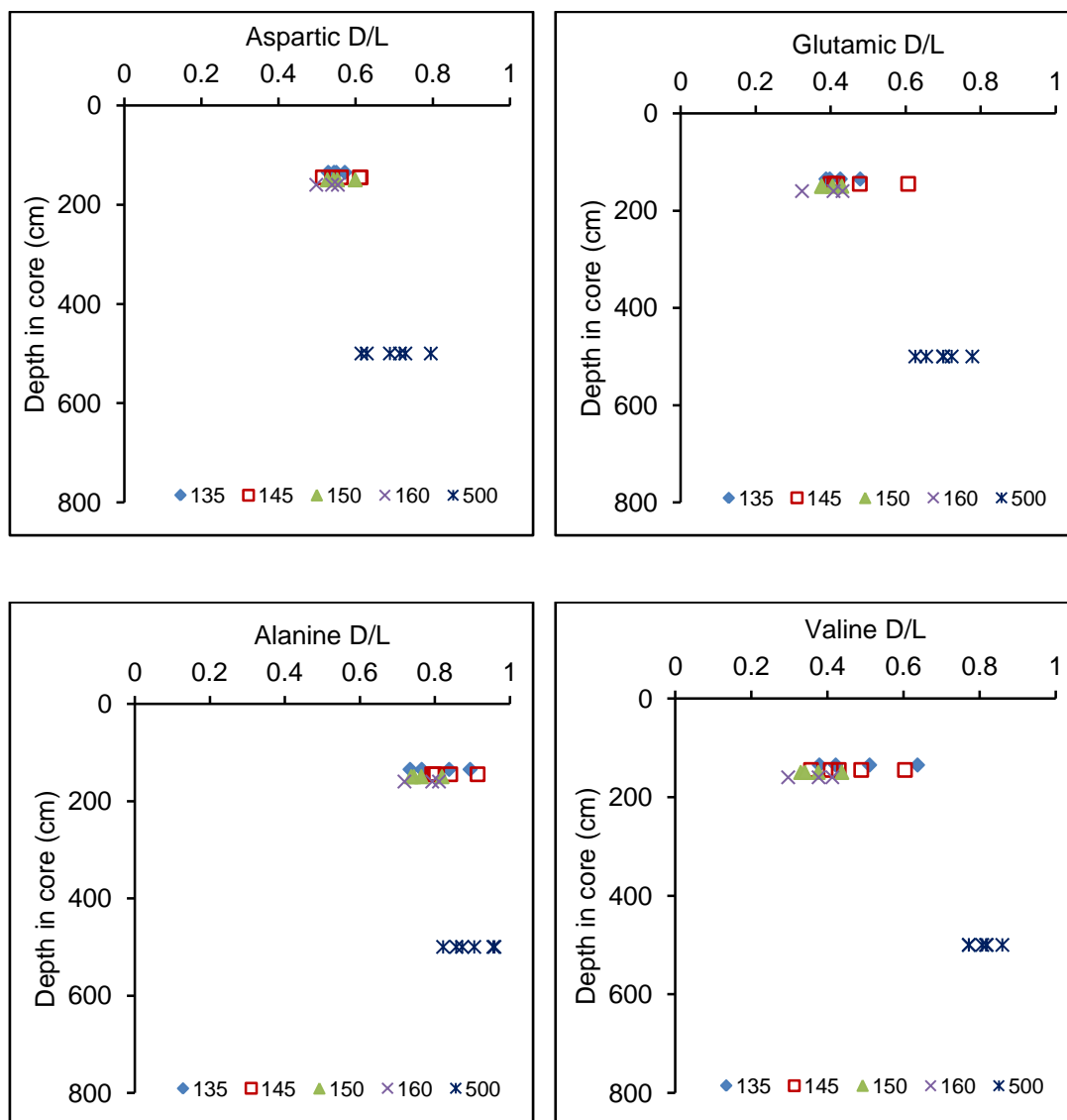


Figure 8.8. Distribution of amino acid D/L values from *Lentidium* in core MD32. The results for alanine change least from the horizons centred on 145 cm depth, to those of 500 cm depth. These high values for alanine, given the radiocarbon data previously published, probably indicate an environment of high burial temperatures because of the high alanine D/L values in the younger samples. The clustering of D/L values in these and the previous figures suggest two discrete ages for these strata.

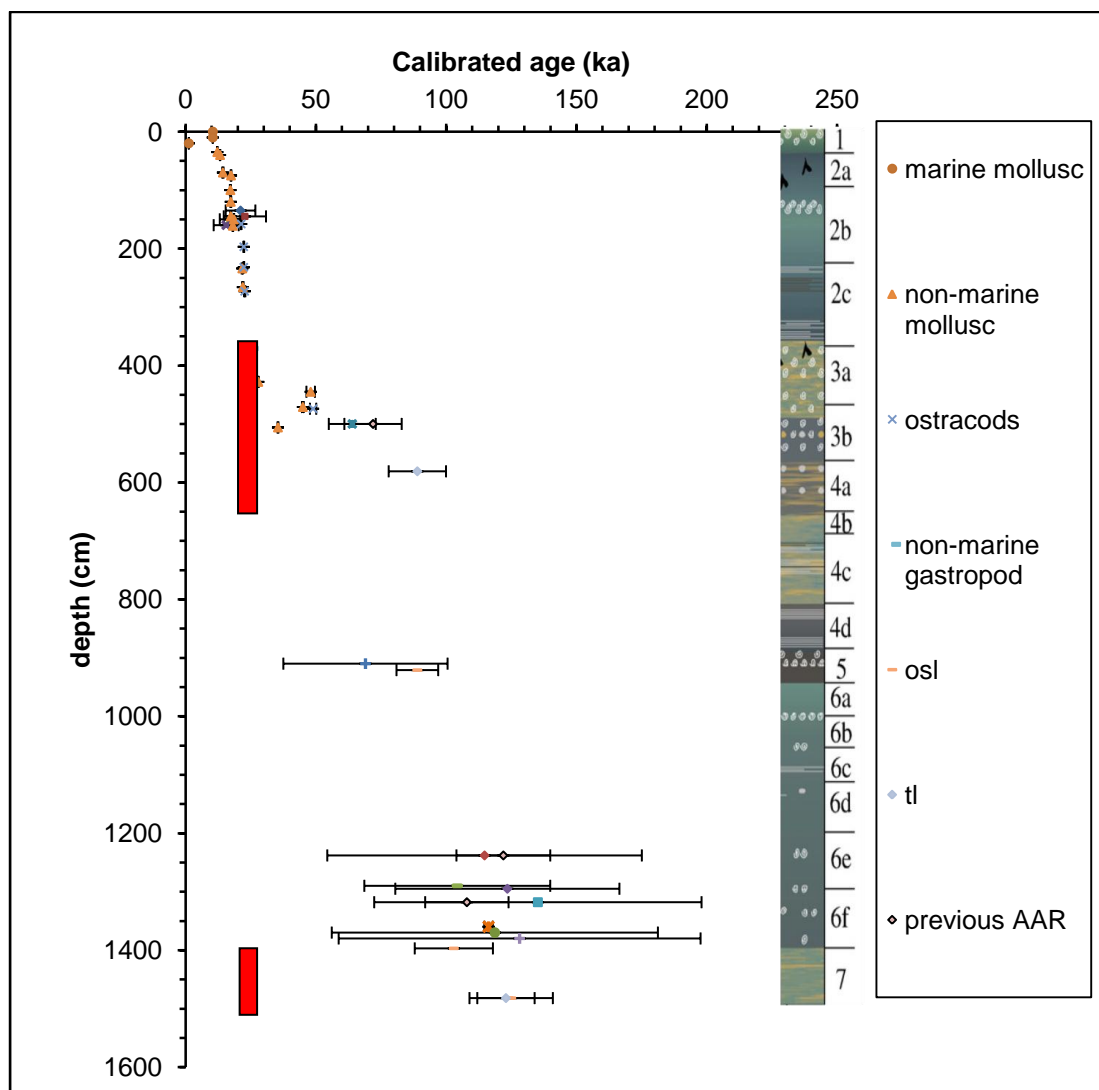


Figure 8.9. Distribution of mean calibrated ages on bivalve molluscs in core MD 32, and comparison with previous dating. Error bars are indicative of the 1σ uncertainty about the mean age obtained for the combined values of the amino acids aspartic, glutamic, alanine and valine. Uncertainty estimates are from individual mollusc samples from the section of core below 12 m, and on the mean value from multiple samples in the layers from 910 cm upwards. Vertical rectangles indicate subaerial exposure and oxidising conditions, the lowermost being fluvial. Uncertainties for radiocarbon ages are in many cases smaller than the associated symbols.

8.6.5. Hydrolysable amino acids in bulk samples of *Ammonia beccarii*

A limited study was undertaken on bulk samples of *Ammonia beccarii*, the results presented in Table 8.5 below. These results, obtained on samples picked from the same one-centimetre horizons were inconsistent, with for the samples obtained from 135 cm depth in core MD 32 having a coefficient of variation of 108 % for serine, and 22% for valine for example. However, the range of D/L values for these amino acids were similar to those from *Lentidium* from the same horizons, and suggested that an aminostratigraphy could be created using the results from samples of *Ammonia* and bivalve molluscs together. To this end, two studies

were undertaken (Section 8.7): one on a limited number of *Lentidium*, and the second on samples of *Ammonia beccarii*.

Table 8.6. D/L values from the hydrolysable amino acids within bulk samples of *Ammonia beccarii*. Each sample consisted of between 10 and 20 individual tests.

Core and depth	Species	Lab (UWGA) code	N = ?	Asx D/L	Glx D/L	Ser D/L	Ala D/L	Val D/L
MD32-135	<i>A. beccarii</i>	6256	2	0.638	0.398	0.456	0.749	0.495
MD32-135	<i>A. beccarii</i>	6251A	2	0.58	0.313	0.103	0.625	0.362
MD32-135	<i>A. beccarii</i>	6251B	2	0.594	0.291	0.076	0.619	0.369
MD32-135	<i>A. beccarii</i>	6251C	2	0.549	0.303	0.026	0.577	0.267
MD32-135	<i>A. beccarii</i>	6251D	2	0.608	0.353	0.129	0.661	0.403
		Mean		0.594	0.332	0.158	0.646	0.379
		Stdv		0.033	0.044	0.171	0.065	0.082
		CV (%)		5.6	13.2	108.2	10.0	21.7
MD32-145	<i>A. beccarii</i>	6265	3	0.599	0.318	0.221	0.708	0.480
MD32-150	<i>A. beccarii</i>	6267	2	0.482	0.241	0.507	0.366	0.187

8.7 Intracrystalline amino acids

8.7.1 Intracrystalline amino acids in *Lentidium* (bivalve molluscs)

To better understand why D/L values at 135 cm are generally higher than in those horizons immediately below, D/L values from intracrystalline amino acids in *Lentidium* were examined. A comparison of D/L values in individual shells from 135 cm compared to those from 150 cm depth in core MD32 are inconclusive. Both glutamic acid and valine D/L values in 135 cm are slightly higher than for 150 cm, similar to the previous results from *Lentidium* and *Ammonia* using the THAA pool. This may indicate that contamination is not a problem, but does not rule out significant reworking. However, *Lentidium* is only present in a limited number of horizons, and therefore this problem was investigated further using intracrystalline amino acids in *Ammonia*.

Table 8.7. Intracrystalline amino acid D/L values in *Lentidium* from core MD32.

Core and depth (cm)	UWGA code	Aspartic D/L	Glutamic D/L	Serine D/L	Alanine D/L	Valine D/L
MD32-135	8427 e	0.577	0.427	0.470	0.731	0.383
MD32-135	8427 d	0.582	0.433	0.474	0.649	0.364
MD32-135	8427 c	0.563	0.318	0.123	0.532	0.375
MD32-135	8427 b	0.562	0.413	0.529	0.699	0.335
MD32-135	8427 a	0.610	0.435	0.397	0.509	0.374
MD32-135	8427 f	0.577	0.419	0.319	0.754	0.402
MD32-135	8427 g	0.499	0.264	0.072	0.395	0.338
MD32-135	8427 h	0.586	0.385	0.201	0.524	0.394
	Mean	0.570	0.387	0.323	0.599	0.371
	Stdv	0.032	0.063	0.173	0.127	0.024
	CV (%)	5.7	16.2	53.6	21.3	6.5
MD32-150	8423 b	0.565	0.403	0.279	0.699	0.338
MD32-150	8423 a	0.590	0.415	0.213	0.743	0.403
MD32-150	8423 f	0.564	0.428	0.276	0.573	0.392
MD32-150	8423 d	0.558	0.416	0.31	0.644	0.343
MD32-150	8423 e	0.561	0.404	0.344	0.730	0.345
MD32-150	8423 c	0.348	0.154	0.04	0.320	0.170
MD32-150	8423 g	0.588	0.438	0.478	0.747	0.364
		0.539	0.380	0.277	0.637	0.336
		0.085	0.100	0.133	0.153	0.078
		15.8	26.4	48.0	24.0	23.1

8.7.2. Intracrystalline amino acids: *Ammonia beccarii*

The foraminifer *Ammonia beccarii* was chosen because it is present in a large proportion of the lacustrine section of core MD32. Overall, the data from the total hydrolysable amino acids are similar to those of the *Lentidium*. The data from *Ammonia* indicate a higher mean D/L value for glutamic acid from MD32 135 cm depth than for either 145 or 150 cm depths. However, valine results are higher for 145 cm than either for 135 or 150 cm depths. In most cases valine D/L values are higher than for glutamic acid, as is the case for most of the results from the bivalve mollusc samples listed above.

Fifty five samples were analysed from 14 one-centimetre horizons from core MD32 (Table 8.5, and Figures 8.7 and 8.8). Coefficients of variation among D/L values in samples from individual horizons, generally less than 0.2%, are very low, when compared with shell samples and single foraminifers (for any other investigation in this thesis) bleached with 12.5% NaOCl for one hour. The data can be divided into two subsets: those from 71 to 371 cm inclusive, and those data from 399 to 555 cm inclusive (Figures 8.7, 8.8). These subsets may be described as two individual aminozones. No data were obtained from below 555 cm

because the concentration of amino acids in these bulk samples below 555 cm was almost non-existent. This immediately is suggestive of diffusive loss of amino acids from the tests, but also may result from the breakdown of amino acids and perhaps production of secondary molecules. Of particular note are the results for the amino acid valine. In all samples, D/L values for valine are higher than for glutamic, and therefore not in accord with previously published relative racemization rates (Lajoie *et al.*, 1980). In two results from 444 cm, and one from 506 cm depth, valine D/L values exceed 1, theoretically not possible.

Coefficients of variation of D/L values for the sampled horizons at depths of 71, 98, 135, 150, 233, 256 and 371 cm are low compared to horizons lower down in core MD 32, particularly for 329 and 428 cm depth. These lower horizons have been suberially exposed (Fig. 8.8) with evidence for pedogenic alteration (strong oxidation) present in these basal fluvial sediments (Chivas *et al.*, 2001; Reeves *et al.*, 2008).

The closest correlation among amino acid D/L values was found to occur using aspartic and glutamic results (Fig. 8.11a). These data indicate a fast rate of racemization for aspartic acid, while glutamic D/L values increase much more gradually. A similar relationship exists between aspartic acid and valine D/L values (Fig. 8.11b). The relative rate of racemization in valine appears faster than for glutamic acid (Fig. 8.11c).

The distribution of D/L values in the slower racemising amino acids glutamic and valine, in addition to those results from aspartic acid (Fig. 8.12) indicates a significant change in conditions from that of the upper core between 71 and 371 cm, and that below the latter horizon. D/L values below 371 cm are erratic, but generally significantly higher than those above 371 cm. Notably, and similar to the results presented above, D/L values from 135 cm are higher than in those adjacent horizons, either above or below. In contrast, there is no pattern among results from the amino acid alanine.

Table 8.8. D/L values obtained on the hydrolysable intracrystalline amino acid (HIAA) fraction from samples consisting of multiple individual tests of the foraminifer *Ammonia beccarii*, core MD32. Each sample consisted of between 10 and 20 whole tests.

Core and depth (cm)	UWGA code	Aspartic D/L	Glutamic D/L	Serine D/L	Alanine D/L	Valine D/L
MD32-71	8434 d	0.592	0.330	0.264	0.782	0.473
MD32-71	8434 a	0.596	0.309	0.151	0.649	0.468
MD32-71	8434 b	0.611	0.343	0.259	0.646	0.496
	Mean	0.600	0.327	0.225	0.692	0.479
	Stdv	0.010	0.017	0.064	0.078	0.015
	CV	1.7	5.2	28.4	11.2	3.1
MD32-98	8436 c	0.617	0.373	0.305	0.744	0.475
MD32-98	8436 b	0.616	0.356	0.235	0.839	0.528
	Mean	0.617	0.365	0.270	0.792	0.502
	Stdv	0.001	0.012	0.049	0.067	0.037
	CV	0.1	3.3	18.3	8.5	7.5
MD32-135	8429 c	0.644	0.364	0.259	0.627	0.522
MD32-135	8429 b	0.650	0.378	0.242	0.582	0.511
MD32-135	8429 d	0.655	0.394	0.388	0.742	0.574
MD32-135	8429 a	0.654	0.399	0.371	0.662	0.546
	Mean	0.651	0.384	0.315	0.653	0.538
	Stdv	0.005	0.016	0.075	0.068	0.028
	CV	0.8	4.1	23.8	10.4	5.2
MD32-150	8425 a	0.632	0.354	0.235	0.787	0.508
MD32-150	8425 b	0.619	0.340	0.24	0.624	0.478
MD32-150	8425 c	0.622	0.343	0.273	0.587	0.664
MD32-150	8425 d	0.624	0.312	0.186	0.588	0.504
	Mean	0.624	0.337	0.234	0.647	0.539
	Stdv	0.006	0.018	0.036	0.095	0.085
	CV	0.9	5.3	15.4	14.7	15.7
MD32-233	8422 d	0.646	0.330	0.255	0.803	0.504
MD32-233	8422 b	0.641	0.343	0.171	0.628	0.517
MD32-233	8422 c	0.650	0.309	0.221	0.903	0.532
	Mean	0.646	0.327	0.216	0.778	0.518
	Stdv	0.005	0.017	0.042	0.139	0.014
	CV	0.7	5.2	19.6	17.9	2.7
MD32-256	8439 b	0.637	0.405	0.422	0.665	0.480
MD32-256	8439 c	0.656	0.402	0.387	0.618	0.471
MD32-256	8439 d	0.651	0.405	0.381	0.657	0.479
MD32-256	8439 e	0.653	0.400	0.421	0.618	0.430
MD32-256	8439 f	0.656	0.399	0.304	0.600	0.478
	Mean	0.651	0.402	0.383	0.632	0.468
	Stdv	0.008	0.003	0.048	0.028	0.021
	CV	1.2	0.7	12.5	4.4	4.6
MD32-371	8437 d	0.632	0.337	0.204	0.647	0.456
MD32-371	8437 c	0.601	0.321	0.120	0.753	0.494
MD32-371	8437 b	0.645	0.367	0.186	0.851	0.517
	Mean	0.626	0.342	0.170	0.750	0.489
	Stdv	0.023	0.023	0.044	0.102	0.031

	CV	3.6	6.8	26.0	13.6	6.3
MD32-399	8442 b	0.842	0.870	0.084	0.871	0.925
MD32-399	8442 c	0.599	0.835	0.044	0.885	0.802
MD32-399	8442 d	0.678	0.560	0.046	0.735	0.779
	Mean	0.706	0.755	0.058	0.830	0.835
	Stdv	0.124	0.170	0.023	0.083	0.079
	CV	17.5	22.5	38.9	10.0	9.4
MD32-428	8438 a	0.655	0.430	0.129	0.752	0.723
MD32-428	8438 b	0.553	0.327	0.087	0.563	0.637
MD32-428	8438 c	0.498	0.255	0.077	0.620	0.428
MD32-428	8438 d	0.723	0.540	0(no D-Ser)	0.862	0.687
MD32-428	8438 e	0.747	0.578	0(no D-Ser)	1.037	0.747
	Mean	0.635	0.426	0.098	0.767	0.644
	Stdv	0.107	0.137	0.028	0.191	0.128
	CV	16.9	32.2	28.3	24.9	19.8
MD32-444	8426 d	0.763	0.635	0.408	0.745	0.940
MD32-444	8426 c	0.786	0.697	0.207	0.832	1.086
MD32-444	8426 a	0.743	0.676	0.374	0.832	0.954
MD32-444	8426 b	0.793	0.648	0(no D-ser)	0.753	1.161
	Mean	0.771	0.664	0.330	0.791	1.035
	Stdv	0.023	0.028	0.108	0.048	0.107
	CV	3.0	4.2	32.6	6.1	10.3
MD32-506	8433 c	0.813	0.781	0(no D-Ser)	0.883	0.980
MD32-506	8433 d	0.880	0.742	0(no D-Ser)	0.761	1.156
MD32-506	8433 b	0.749	0.606	0(no D-Ser)	0.877	0.835
	Mean	0.814	0.710	0.000	0.840	0.990
	Stdv	0.066	0.092	0.000	0.069	0.161
	CV	8.0	12.9	0.0	8.2	16.2
MD32-515	8436 a	0.607	0.392	0.260	0.786	0.750
MD32-515	8436 b	0.594	0.356	0.388	0.770	0.718
MD32-515	8436 c	0.728	0.532	0(no D-Ser)	0.821	0.727
MD32-515	8436 d	0.660	0.457	0.328	0.850	0.800
	Mean	0.647	0.434	0.325	0.807	0.749
	Stdv	0.061	0.077	0.064	0.036	0.037
	CV	9.4	17.8	19.7	4.4	4.9
MD32-555	8437 a	0.696	0.516	0.204	0.892	0.788
MD32-555	8437 e	0.651	0.415	0.418	0.605	0.500
MD32-555	8437 b	0.767	0.623	0.371	0.883	0.650
MD32-555	8437 c	0.738	0.547	0.187	0.837	0.771
MD32-555	8437 f	0.737	0.553	0(no D-Ser)	0.853	0.758
MD32-555	8437 d	0.660	0.429	0.120	0.759	0.705
	Mean	0.708	0.514	0.260	0.805	0.695
	Stdv	0.047	0.079	0.128	0.109	0.108
	CV	6.6	15.5	49.2	13.5	15.6

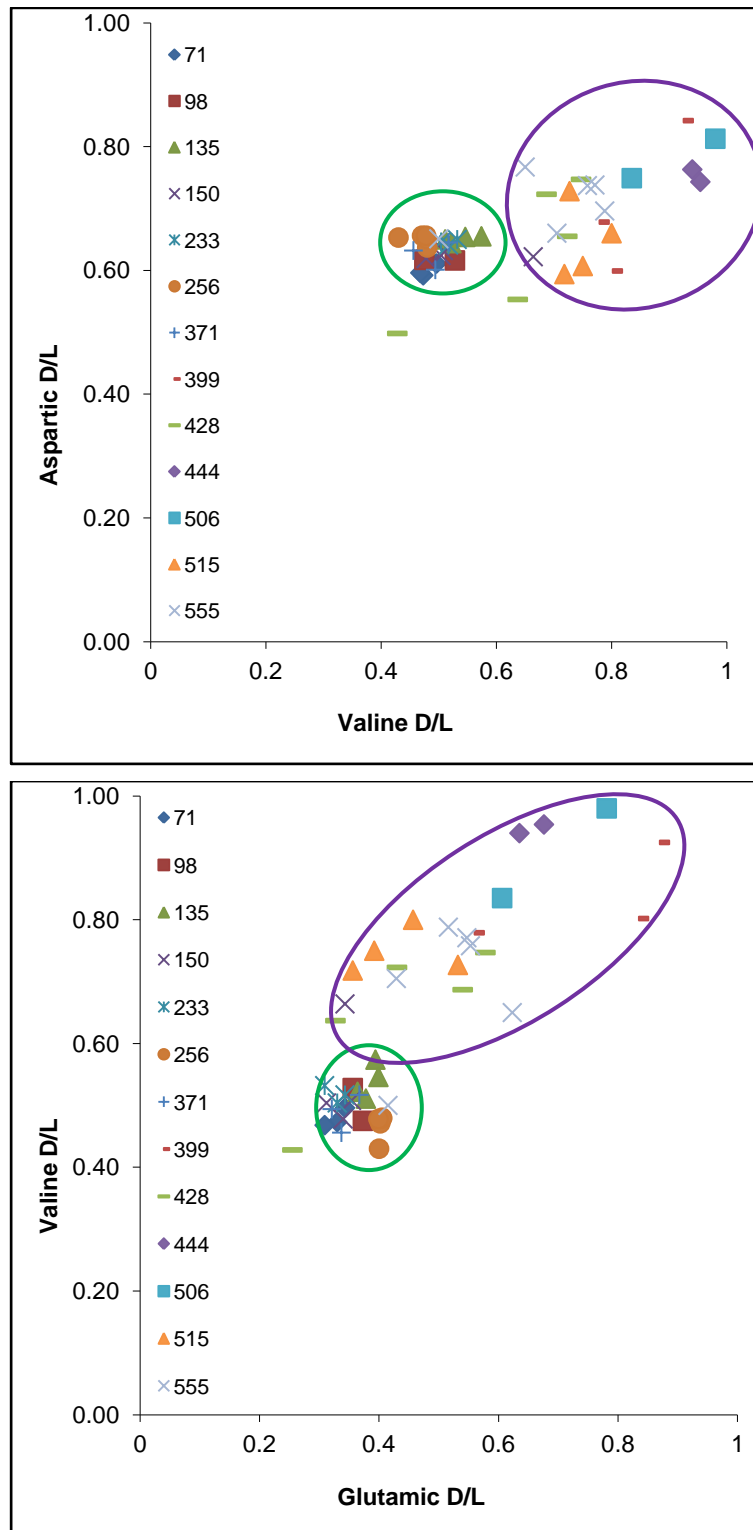


Figure 8.10. Amino acid D/L values in the foraminifer *Ammonia beccarii* from core MD32, Gulf of Carpentaria, indicating two associations of D/L values: those from 71 to 371 cm inclusive and those from 399 to 555 cm depth in core MD32. These two aminozones are partly the result of differing diagenetic histories between those in the upper sections of MD32 (approx 135 cm depth) and those from the subaerially exposed section of core.

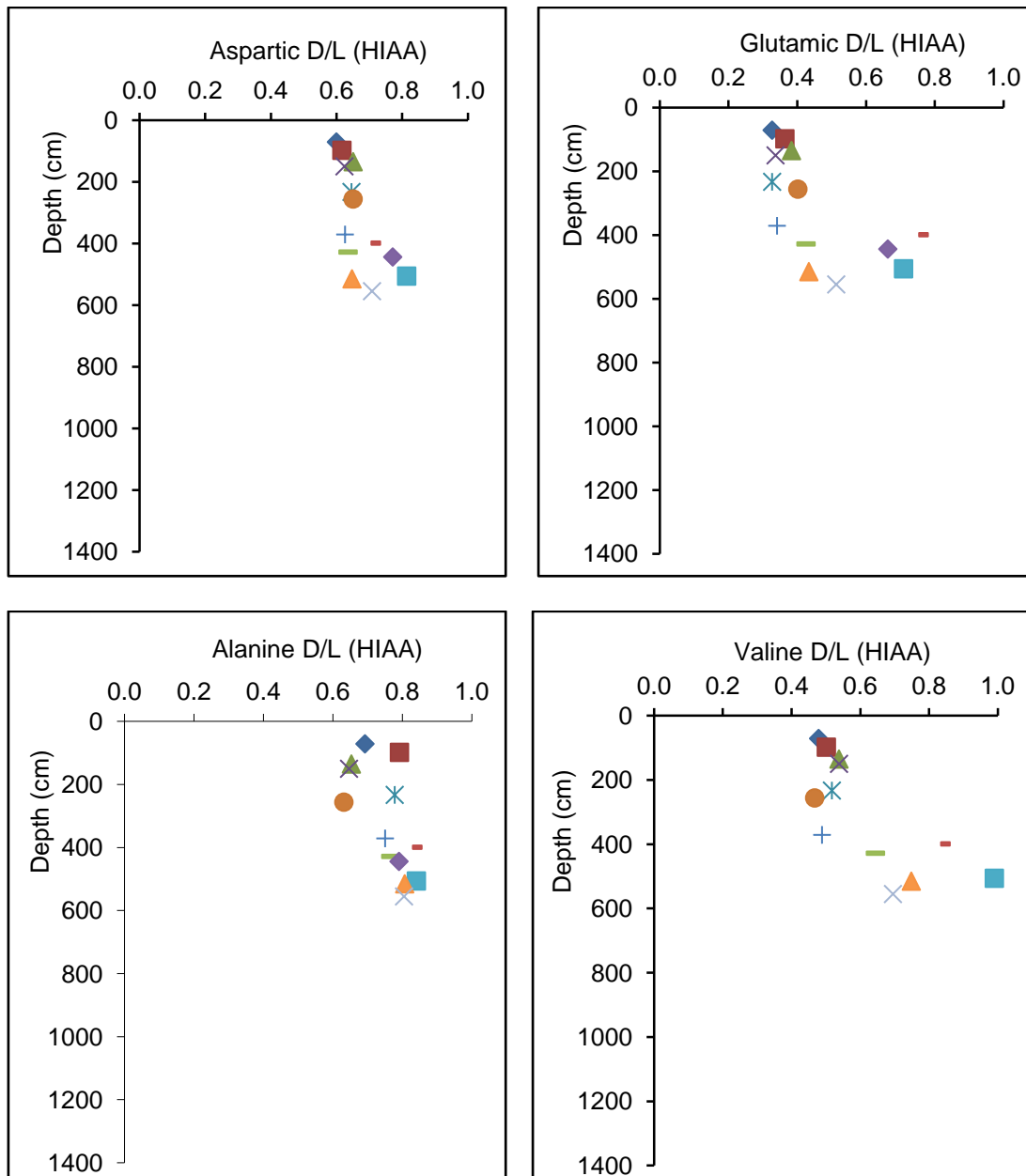


Figure 8.11. Mean amino acid D/L values for *Ammonia beccarii* plotted against depth in core MD32. Although there is some variance among results, there is a significant change in environment indicated between 371 and 399 cm depth. Below this depth the relatively close spacing of individual age-depth points increases, and D/L values increase significantly. This change approximately corresponds with the change from older horizons with pedogenic overprints, to younger and overlying lacustrine facies, without pedogenesis. It was not possible to obtain results from any deeper in this core using intracrystalline amino acids because concentrations were too low.

8.8 Discussion

Based on these AAR data, the sampled strata can be divided into four discrete groups. These are the samples from near the base of the core between 1238 and 1380 cm, samples at 910 cm, 555 to 399 cm, and 371 to 71 cm. It would seem unrealistic to subdivide these aminozones

further. Two recent models have been proposed for the evolution of the Gulf of Carpentaria from the last interglacial (MIS 5e) to the present (Couapel *et al.*, 2007; Reeves *et al.*, 2008) which describe the evidence for changes in sea level based on coccolith populations and luminescence dating (Couapel *et al.*, 2007) and from the evidence provided by ostracod and other fossil assemblages, and radiocarbon, luminescence and amino acid racemization dating methods (Reeves *et al.*, 2008), with both models focused on core MD 32. The results from this study, using samples from the same suite of core slices, are compared here with those two studies (Fig. 8.11).

Calibrated AAR ages based on power law equations using D/L values from two bivalve molluscs (Table 8.5; *Bassina* sp. 1238 cm, 115 ka, and *Anadara granosa*, 1318 cm, 135 ka), whether for the individual amino acid valine, or using the mean value from all four amino acids, aspartic, glutamic, alanine and valine together, are in broad agreement with ages previously published from the same shells (*Bassina* sp. 122 ± 18 ka, *Anadara granosa*, 108 ± 16 ka, Chivas *et al.*, 2001).

The samples from 1380 to 1238 cm were recovered from the marine section of the lower part of core MD 32. They are clearly separated from the younger units by an evaporitic gypsum-micrite unit, 873 to 853 cm depth, whose age has been interpolated as ‘approximately 70 ka’ (Playà *et al.*, 2007). The *Lentidium* (910 cm) are probably representative of a brackish lagoonal Gulf of Carpentaria, while *Anadara* (1295, 1318, and 1320 cm depth), an estuarine species, with the *Anadara* at 1318 cm depth being articulated, dated here to 124 ± 43 , 135 ± 63 , and 66 ± 40 ka, are representative of shallow marine/estuarine environments. Discounting the latter age, which is too low, and probably due to loss of indigenous highly racemized free amino acids with a resultant lowering of D/L values, these ages and environments fit the model described by Reeves *et al.* (2008; their Fig. 10) whereby the marine shells from the lower section of core MD 32 are dated to approximately OIS 5e, and the *Lentidium* at 910 cm depth dated here (69 ± 32 ka) to the transition from OIS 5a to 4 at a time when sea level was falling. The oxidized sediments at the base of the core, even though dated to 123 ± 16 and 124 ± 16 ka by thermoluminescence and optically stimulated luminescence methods respectively (Chivas *et al.*, 2001; Couapel *et al.*, 2007), must actually represent OIS 6 when the basin was without a marine signature. Unit 6f (Reeves *et al.*, 2008) is therefore probably representative of OIS 5e.

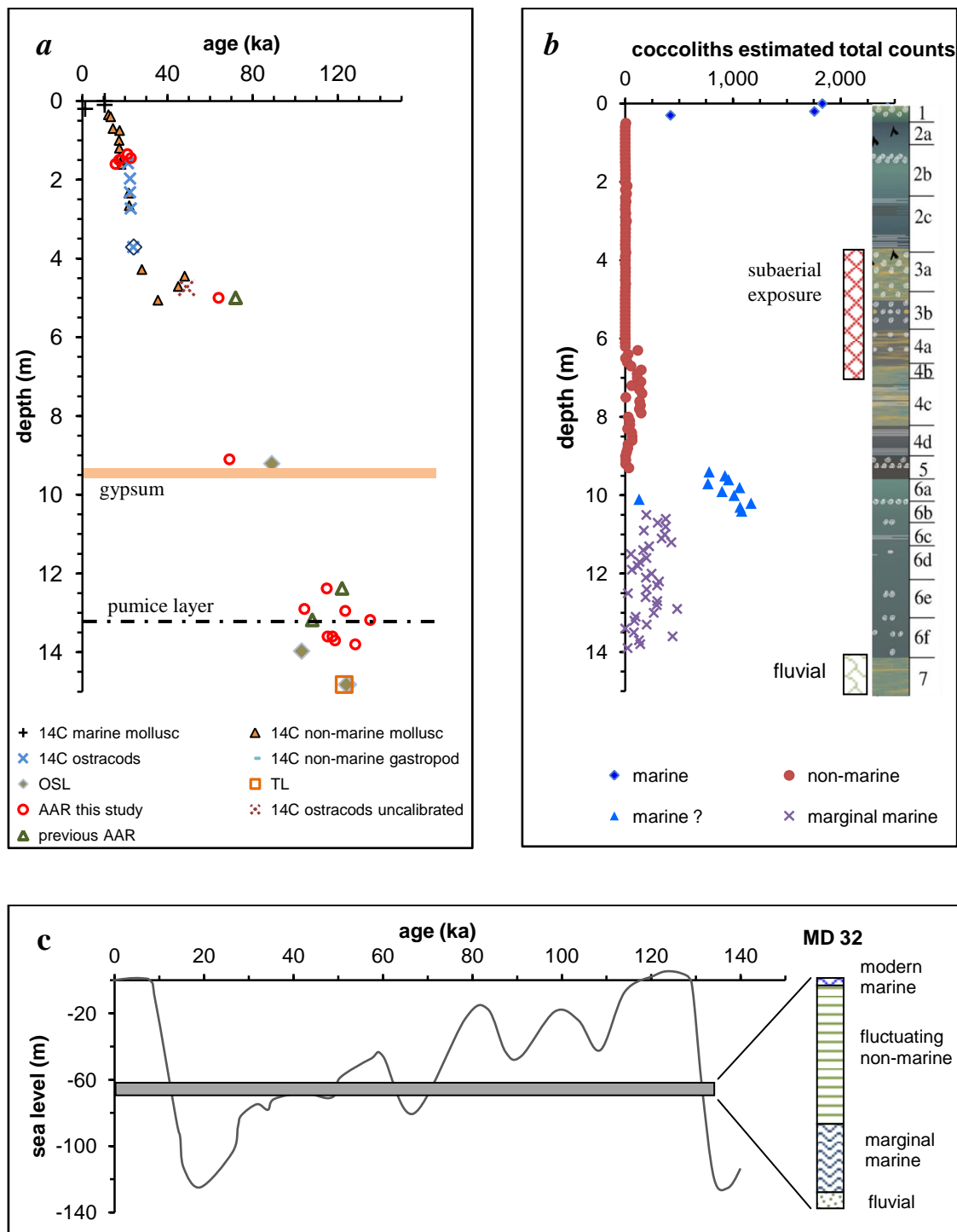


Figure 8.12. Summary diagram for core MD 32 (64 m water depth, 12° 18.79' S, 139° 58.73' E), Gulf of Carpentaria. 8.12a, chronology from multiple dating methods for MD 32. 8.12b, coccolith cumulative abundance as counts per gram of sediment from 1cm thick layers from MD 32 (Couapel, 2005, Couapel *et al.*, 2007). Sea level curve based on Waelbroeck *et al.*, 2002. 8.12c, principal depositional periods evident from core MD 32. Chronology from this study and Chivas *et al.*, 2001, Couapel, 2005, Reeves, 2005, Couapel *et al.*, 2007, Reeves *et al.*, 2007, 2008.

There is however, a problem with these interpretations because the bivalve molluscs dated here from the lower sections of MD 32 are marginal marine species. Their presence in the central gulf, suggests they were not deposited here during a high stand of sea level, but rather it is perhaps more likely they grew here during a period when sea level was lower than present, and thus during a time of rising or falling sea level. Furthermore, when coccolith abundances (Fig. 8.11c) are taken into account (based on Couapel, 2005) they do not indicate the same shallow marine conditions existed when sediments in core MD 32 were being deposited as at present. Indeed, the coccolith abundance for the lower marine section of MD 32 is particularly low compared to the modern environment (Fig. 8.11c; Couapel, 2005; Couapel *et al.*, 2007) and at 1340 cm in core MD 32 no coccoliths were recorded. This suggests that the deposition of these microfossils and therefore of the associated sediments is unlikely to be associated with a high stand of sea level and full marine conditions, but rather occurred when this part of the Gulf was more directly influenced by fluvial discharge (i.e. estuarine conditions) and thus lower sea level compared to present. This presence of a pumice layer (13.4-13.3 m; Reeves, 2005) is suggestive of an 'event', either from airfall, or from a cyclone. Pumice is common to northern Australia, but is not normally found in discrete layers, except in beach ridges. The concentration of pumice on modern coastlines of northern Australia is a process which may be attributed to cyclones impacting on the coastline, and formation of sedimentary units rich in pumice on the most landward extent of storm surge deposits. This suggests shallow inshore marine conditions, assuming the pumice is not from airfall. This may have occurred either during the transition between OIS 6 and 5.5, or between OIS 5.5 and 5.4. The ages on two *Notocorbula* from 1340 and 1360 cm depth are low, but are from shells recovered from the transition between unit 6f (open shallow marine) and 6e (restricted marine conditions). It seems likely that the bivalve molluscs, the enclosing sediment and the AAR ages do not represent OIS 5.5 *sensu stricto* but rather the transition from OIS 5.5 to 5.4 and a shallow nearshore environment.

This interpretation is tempered by the fact the amino acid racemization dating method does not provide sufficient resolution by itself to differentiate clearly, for example, between OIS 5.5 and 5.4. Secondly, there is little sedimentation occurring at present in the location where core MD 32 was recovered. The wind-driven circulation existing at present in the Gulf of Carpentaria results in a clockwise rotation of the Gulf waters (Burne and Graham, 1995). Most sedimentation occurs within the 0-20 m depth range (Jones and Torgersen, 1988), and tidal currents, sometimes disturbed by cyclones, bring sediment southwards along the eastern inner margin of the Gulf from Cape York to Karumba, and then west and northwestwards. The results from an examination of heavy mineral assemblages from the Gulf (Hareddy, 2007) are in agreement with this. It would seem unlikely then, that during the last interglacial (MIS

5e) (OIS 5e), with both Torres and Arafura Straits fully open, that significant sedimentation occurred within the central basin, in the location of core MD 32, if oceanographic conditions were similar to present (and 2-5 m deeper).

The presence of *Lentidium* and other mollusc species, dated here to ~ 69 ka, in core MD 32 from 910 cm depth (unit 5 of Reeves *et al.*, 2008), indicate together with the evidence provided by Reeves *et al.* (2008) that the Gulf was closed, and existing as an isolated basin. However, the presence of moderate concentrations of coccoliths (Fig. 8.11c) 1050-940 cm depth in MD 32 suggest a prior marine influence, while the *Lentidium* indicate fresh/fluviatile to brackish water environment (Hallan and Willan, 2010). Hallan and Willan noted that in some layers in the MD suite of cores from the Gulf of Carpentaria (Chivas *et al.*, 2001) that well preserved specimens of *Lentidium* have been found in fully marine sediments, although in only small numbers (Hallan and Willan, 2010). For the samples of *Lentidium* shells at 910 cm, the opposite is likely; the few coccoliths present are likely to have been reworked from underlying sediments in core MD 32 where coccoliths are ~ 2,000 % more abundant (Fig. 8.11). The recolonisation by coccoliths from 8.8 to 6.7 m depth, and described by Couapel *et al.*, (2007), of the area which MD 32 was recovered from, may instead also relate to reworking of coccolith-bearing sediments during a period of lowered sea level during a Lake Carpentaria phase. Based on the work of Waelbroeck *et al.* (2002) the existence of *Lentidium* in core MD 32 at 73 m depth (relative to modern sea level) would have to have occurred when the open marine water level was below this value, unless these brackish to freshwater bivalve molluscs were reworked over a large distance which seems unlikely, during OIS 4 or a similar low stand. It would seem more likely that, at this location, the conditions required for the proliferation of an abundance of *Lentidium* which require very low to nil salinity (Hallan and Willans, 2010) would only be achieved following a transgression, when sea level was falling or at a low stand. At a depth of 73 m, relative to present sea level, these *Lentidium* could only have existed sometime during OIS 4 at this location, because during earlier low stands the global sea level was above the level of the Arafura Sill, and the central Gulf must have had a significant marine influence.

Lentidium at 500 cm depth (69 m below present sea level), and dated here to ~ 64 ka, indicate much lower salinity conditions than that suggested by the presence of the estuarine-marine species, *Bassina*, and dated to 72 ka from 500 cm depth in MD 32 (Chivas *et al.*, 2001). Either the latter shell has been significantly reworked, because this species is not indicative of a brackish lake, nor of a fluvial environment (environments indicated by Reeves *et al.*, 2008) while *Lentidium* is (Hallan and Willans, 2010), or the identification may be incorrect. The calibrated AAR ages indicated here (this study; Chivas *et al.*, 2001) are not significantly

different, and radiocarbon dating of horizons just above these levels (Table 8.4) indicate ages of 49 ka (474 cm), thus the *Lentidium* were deposited during OIS 4.

Based on D/L values from bulk samples of *Ammonia* (Table 8.7) a significant change in the extent of racemization is indicated between 399 and 371 cm depth in core MD 32. This is consistent with the sedimentological data (Reeves, 2005; Reeves *et al.*, 2008) which indicate a transition at 3.73 m, between unit 3a and the overlying 2c. These results are suggestive of a different burial history for the lower sections of core MD 32 555-399 cm compared to those from 371 to 71 cm depth, and perhaps a comparatively long time gap. This is also consistent with evidence for subaerial exposure for the units from 6.3-3.73 m depth (Reeves, 2005; Reeves *et al.*, 2008).

The presence of coccoliths in unit ii of Couapel *et al.*, (2007), in sediments dated to the Last Glacial Maximum, during a period when the Gulf existed as a lake, must be relict fossils from the most immediate marine ingress prior to that time, especially given that the gulf in the central section is almost flat, and there is the likelihood that sediments have been reworked, especially if the core is in the transport route of a palaeo-channel/river. Couapel *et al.*, (2007) note in particular that a maximum of 20 individual coccoliths have been counted in samples analysed from 1 cm slices at 10 cm intervals. These include those from confined environments (cluster C1b; 3.9-2.0 m, 1.8-1.5 m, 1.3 m and 0.5 m depth in MD 32) or from non-marine conditions (cluster C1a; 1.9 m, 1.4 m and 1.2-0.4 m depth). Those samples from cluster C1b (confined environments) consisted of placolith-bearing opportunistic species more resistant to dissolution than other coccoliths because of their interlocking arrangement of plates. In a similar way to the shallow water sediments in the modern Gulf St Vincent, where MIS 3 age *Elphidium* (foraminifers) have been incorporated into Holocene sediments, it seems highly likely that the presence of coccoliths in the non-marine, Lake Carpentaria phase of the Last Glacial Maximum is because of reworking of sediments derived from shallow marine environments around the margins of the oscillating lake. Additionally, coccoliths may have lived in Lake Carpentaria in the brackish lake following a transgression. The brackish water of the lake would assist to preserve carbonate material, while the more recent oligohaline-fresh lake (Reeves *et al.*, 2008) would perhaps not be as suitable for the preservation of reworked coccoliths if freshwater flowing into the lake was in any way acidic.

The dating by AMS ^{14}C methods here of fossils in MD 32 suggests relative sea level heights for MIS 3 that are lower than those proposed for Gulf St Vincent (Chapter 5) at approximately the same time (48 ± 6 ka, 30-43 m). The minor marine incursion indicated by Reeves *et al.*, 2008, at this time is not reflected in significant coccolith populations in any part of this section of core. It seems likely that the subaerial exposure of this part of core MD 32 occurred after any MIS 3 highstand, and the evidence for this in the central basin may be largely missing.

8.9. Summary

- Amino acid racemization methods were utilised to determine the ages of marine and non-marine shells and non-marine foraminifers from the Gulf of Carpentaria, principally from core MD 32.
- Apart from the samples of the bivalve mollusc *Anadara* from Karumba beach ridges, and the single sample of *Tridacna* from Huon Peninsula, the D/L values obtained using the amino acid valine were generally higher than for glutamic acid. This conclusion is based on measurements made on the total hydrolysable amino acid *and* the hydrolysable intracrystalline amino acid populations within bivalve molluscs and foraminifers.
- The mean calibrated age obtained with power law equations and D/L values from the amino acids aspartic, glutamic, alanine and valine together was used for chronology.
- The base of core MD 32 is of MIS 6 age, and overlain by sediments including shells of MIS 5e to MIS 5d in age. If conditions in the Gulf were similar to present, the presence of estuarine species in the central Gulf are best explained by their proliferation when sea level was falling after the last interglacial (MIS 5e) (MIS 5e), and shallow marine/estuarine conditions existed in the central basin.
- *Lentidium* samples at 910 cm depth in core MD 32 (73 m total depth) are 69 ± 32 ka old. The *Lentidium* shells at 500 cm depth in this core, are dated by AAR methods to 64 ± 9 ka. This suggests that Lake Carpentaria existed throughout MIS 4. Coccoliths within Lake Carpentaria may have been reworked into this environment from older, and marine derived sediment, or may have lived within the brackish water body.
- A significant change in environment is indicated by amino acid D/L values obtained from intracrystalline amino acids in small samples of the foraminifer *Ammonia* sp, between 371 and 399 cm depth. This likely reflects the change indicated by sediments from the subaerially exposed section between 6.3 and 3.73 m (units 4a to 3a of Reeves *et al.*, 2008) to a permanent brackish lake above 3.73 m depth in core MD 32.
- The chronology of the sedimentary record within the central Gulf of Carpentaria seems to indicate sedimentation during falling or lowstand episodes of sea level rather than at periods of high sea levels, the exception being the present environment. These periods of sedimentation are likely related to the presence of more proximal shorelines, this combined with differences in fluvial discharge, into or via the central basin, and the absence and/or effects of monsoonal conditions.

Chapter 9

Summary, conclusions and suggestions for further research

9.1. Introduction

This chapter brings together the evidence from the previous chapters (4-8) on the extent of reworking in semi-enclosed basins. This evidence is presented by discussing aspects of problems in taphonomy and chronology, including time-averaging and analytical time-averaging, the recognition of reworked fossils, scales of age-mixing, the requirement for a source of material to be reworked, and particularly of relevance to chronology is the use of bulk samples, also discussed in chapter 6.

9.2. Thesis summary: reworked fossils in the Late Quaternary sedimentary record of semi-enclosed basins.

9.2.1. Time-averaging

Time-averaging (Walker and Bambach, 1971) is both a process and measure, whereby individual dead organisms, and taphonomic processes are assimilated into sedimentary strata over time-scales which are commonly not easily resolvable for a given study. Time-averaging is a function of the availability of old shells in the depositional system (Kowalewski *et al.*, 1998). The process of time-averaging and mixing of fossils both temporally and spatially, occurs through reworking, creating mixed-age assemblages that appear to be ubiquitous in most shallow marine regions (Henderson and Frey, 1986; Goodfriend, 1989). These processes blur the environmental signature within the sedimentary record (Goodwin *et al.*, 2004). Unrecognised time-averaged assemblages are problematic for obtaining estimates of age, and for quantifying rates of sedimentation based, for example, on radiocarbon ages of fossil molluscs. Therefore the palaeoenvironmental interpretation of time-averaged deposits and sedimentary sequences demands care. As indicated earlier (Chapter 2) neither a fossil's stratigraphic position, nor its taphonomic state, may be a reliable guide to its age and, as a result the presence of reworked fossils in time-averaged strata can be an underlying problem when attempting to construct relevant chronologies because they depend on the confident recognition of the stratigraphic disorder and physical mixing of fossils. The best example of

this problem is in the current debate on the post-glacial history of the Black Sea (chapter 6), where it has been common practice to describe sedimentary strata based on the dominant species or groups of species present. However, in this study such an approach has clearly been shown to be an incorrect method for attributing ages to the sedimentary units in question. The horizon of interest here for example, 342/3 in core 342, inshore Ukrainian shelf (chapter 6) was previously described as Bugazian (~7500 – 9000 a BP) based on the species present, dominantly *Dreissena*. However, radiocarbon dating of small *Mytilus* fragments indicates this deposit must be younger than 4365 ± 30 ^{14}C years, the youngest age of the *Mytilus* fragments. This is because these fragments can only have been broken after having lived, and therefore the depositional event post-dates (i.e. is younger than) the age of the shells. This stratum is time-averaged therefore, over 4,800 or more years. Furthermore, the *Mytilus* fragments point to ‘marine’ conditions, not fresh to very low salinity brackish conditions as implied by the dominant Dreissenids, and it appears logical to suggest this stratum was deposited in a marine environment. In particular, and common to a large proportion of the shelves in the Black Sea, the older Ponto-Caspian fauna exhibited medium to strong dissolution, abrasion, borings, and loss of colour. In contrast, though strongly fragmented the *Mytilus* in 342/3 retained original colour, were not dissolved and had no borings.

Accurate palaeoenvironmental interpretations based on fossil assemblages cannot exclude the subject of taphonomic alteration (cf. Schroeder-Adams, 2006) and attributing ages without in some way obtaining numerical ages is likely to lead to incorrect conclusions concerning the strata in question. Kowalewski and Bambach (2003) note that three aspects of temporal mixing need consideration when evaluating the temporal depositional resolution of a stratum: 1) the duration of temporal mixing, 2) the internal temporal structure, and 3) the completeness of the temporally mixed deposit. However, this study suggests one additional aspect requires consideration also – the correct identification of all of the individual elements of a deposit, because this will provide an immediate clue as to whether or not temporal mixing has occurred.

9.2.2. *Mass of samples*

Thus, determining the age of individual fossil elements within a sedimentary package is a fundamental issue where fine resolution is required. The phenomenon of reworked fossils and mixed-age assemblages has previously been investigated using paired AAR and ^{14}C dating (Goodfriend, 1989; Murray-Wallace and Belperio, 1994; Wehmiller *et al.*, 1995; Goodfriend and Stanley, 1996; Murray-Wallace *et al.*, 1996; Kowalewski *et al.*, 1998; Carroll, 2001; Barbour Wood *et al.*, 2003) but each of these studies has had to rely on, by comparison with RP-HPLC (Kaufman and Manley, 1998; Krause *et al.*, 2010; this study) large samples, either

of multiple foraminifer tests, large shells which can be uncommon in cores (e.g. the cores from central Gulf of Carpentaria, were dominated by microfossils and small to micro scale molluscs), or several shell pieces. This size (mass) restriction was determined principally by the technology available. By comparison, in this study single tests of the foraminifer, *Elphidium* were, where possible, utilized for chronology (with some individual *Elphidium* utilised as low as 50 µg in mass), to determine the extent of mixing of fossil material of varying ages. Effectively this means that each identifiable piece of suitable skeletal carbonate within a stratum, and of mass greater than only 50 µg may be used in similar, future studies, where necessary. This is significant because many temporal scales and processes may be recorded within individual sedimentary strata, and any attempt at understanding these records at fine scales of resolution requires an attention to the individual elements of such assemblages. This is especially so where relatively short-term changes in the depositional record exist. The use of known life habits, environmental tolerances, post-mortem shell alteration signatures (chapters 4, 5, 6, 7, 8), and amino acid racemization D/L values calibrated to sidereal years enable accurate determinations of the extent of mixing in time-averaged strata, and enable estimates of temporal scales over which changes in the depositional environment may have occurred to be produced (chapters 5, 6, 7).

9.2.3. Analytical time-averaging

A significant problem that amino acid racemization D/L values calibrated with radiometric dating to give an age in sidereal years can overcome is analytical time-averaging (Kowalewski *et al.*, 1998), whereby there may be insufficient age estimates to differentiate between reworked and *in-situ* material, an outcome commonly ensuing from pooling of samples (bulk sampling). In this study analytical time-averaging was readily overcome using single foraminifers for AAR dating and individual shells and shell pieces for AAR and ¹⁴C dating. This allowed for example the recognition of reworked tests in Gulf St Vincent, and in last interglacial (MIS 5e) sediments in Kerch Strait, where individual *Elphidium* were found to be significantly older than the strata in which they were deposited. The extent of time-averaging for single *Elphidium* and for *Katelsia* shell fragments in core SV5, Gulf St Vincent was found to be of the order of 45-50 ka.

9.2.4. Reworking in semi-enclosed basins

The extent of reworking of fossil material is dependent on a number of processes and pre-existing conditions. Of primary need for the reworking of older fossils and incorporation into younger strata to occur is the presence of a pre-existing sedimentary stratum which is not completely indurated or fossilized. In the MIS 3 sediments of Gulf St Vincent there was no evidence for a pre-existing semi-consolidated stratum in the samples examined. This was evident by the absence of last interglacial (MIS 5e) age foraminifera and molluscs present in the MIS 3 strata within the center of the gulf, and is consistent with the pervasive regional calcrite development on the last interglacial (MIS 5e) (MIS 5e) Glanville Formation which will reduce any possible erosion. This is in contrast to the Holocene sediments of central Gulf St Vincent, where large numbers of MIS 3 aged *Elphidium* were present, and whose presence is consistent with the semi-consolidated condition of these last interstadial skeletal carbonate-rich deposits.

Within last interglacial (MIS 5e) sediments of Kerch Strait there also is little or no evidence for reworking of pre-existing fossils, except for *Elphidium* tests recovered from lagoonal clays below the main marine sedimentary sequence. Throughout most of these sequences in Kerch Strait articulated bivalve molluscs were not present, except for where lagoonal or otherwise relatively quiet conditions were present, generally indicated by the presence of mud or silt-size sediment. The lack of *in-situ* molluscs has commonly been a problem in similar studies, and the case study used here is the post-glacial Black Sea. In this study few references to possible *in-situ* and articulated bivalve molluscs were noted (Giosan *et al.*, 2009; Ongan *et al.*, 2009). Here, using AAR D/L values calibrated with radiocarbon ages it was possible to estimate within each sedimentary unit investigated the extent of reworking, and based on the results in this study (Chapter 6) this appears to offer increased confidence in chronologies where *in-situ* articulated shells are not present.

Reworked bivalve molluscs, common in sediments within Holocene Black Sea shelf regions, are dominated either by Caspian-derived fresh to low salinity tolerant *Dreissena* and *Monodacna*, or by Mediterranean-sourced marine species including *Mytilus* and *Cardium*. The extent of time-averaging in both of these environments varied somewhat. The range of radiocarbon ages obtained on *Dreissena* from *Dreissena-coquina* on the outer Ukrainian shelf was 650 ¹⁴C a. In comparison, the extent of time-averaging in a single sedimentary stratum on the inner shelf (core 342/3) was 4,800 ¹⁴C a. It was not possible to determine with confidence the extent of time-averaging within the Gulf of Carpentaria. However, the evidence (preservational state, previous radiocarbon and AAR dating, combined with the sedimentology and stratigraphy) suggests that only during the Holocene, and following the most recent reconnection of this broad shallow basin with oceanic water has significant reworking

occurred, evidenced by the mixed assemblage of foraminifers, ostracods and molluscs within the uppermost and marine section of the cores (Chivas *et al.*, 2001).

9.2.5. *Scales of time-averaging*

Some workers have suggested that the scale of time-averaging may be up to ~125,000 years on high-energy shallow shelves (Martin *et al.*, 1996), and modern tidal-flat environments (Murray-Wallace, 1994), and that similar time-scales of time-averaging may be more common than previously thought. The evidence in this study, and from these previous studies make a serious point (cf. Flessa *et al.*, 1993), - a fossil's stratigraphic position, may be an unreliable guide to its age. However, it is argued here that the preservational state of the fossil may be used as a relatively reliable guide to relative ages in late Quaternary sedimentary environments, where two or more populations exist in the same or adjacent stratum, and are of substantially different age. The study at Kingscote (chapter 4) where the preservational state of bivalve molluscs and gastropods, taken as a population and not individually, and previously described as Holocene (Ludbruck, 1984) were found to be of last interglacial (MIS 5e) age by comparison of their D/L values with those previously published. These older shells were found to be less well preserved than Holocene aged shells of similar species, both populations dated in this study by AAR. Powell and Davies (1990) used a combined AAR and taphonomic method to answer the question "when is an old shell really old?", and asserted that shell discolouration was the only reasonable (but less than perfect) taphonomic age discriminant (see also Murray-Wallace *et al.*, 2005). In this present study shell discolouration, abrasion and dissolution and encrustation were all noted in the older, and last interglacial (MIS 5e) shells at Kingscote, previously described as Holocene (Ludbrook, 1984).

Numerical age and time-scale estimation from time-averaged shallow marine systems (deltas, aggrading clastic shelves, and carbonate platforms) are sparse and it has been suggested that time-averaging occurs over hundreds to thousands of years in these environments (Kidwell and Flessa, 1996; Kowalewski and Bambach, 2003). Estimates of remains which accumulated over only a few seasons or decades are quite rare. Using taphonomic grades and AAR analyses, Flessa *et al.*, (1993) note that surface shells may be up to 3,500 years old, and up to 10,000 years old in deeper shelf settings. Kidwell *et al.*, (2005) have found 5,000 year old shells in a modern tropical setting, and significantly note that time-averaging is greater in siliciclastic sediments than in carbonate sands. Yet the evidence presented here (chapter 5) indicates that the extent of time-averaging in the carbonate clastic setting of Gulf St Vincent is in the region of 30-40,000 years, but is in the range of 5-6,000 years in the Holocene Black Sea. Ultimately, the age and availability, in part determined by the susceptibility of older sedimentary successions to erosion, of the source material

determines the possible extent of time-averaging (Kowalewski *et al.*, 1998), while taphonomic processes determine the likelihood of the survival of those older shells and shell fragments while being reworked and incorporated into younger strata.

The susceptibility of sedimentary sequences to erosion and the subsequent incorporation of bioclasts into younger strata appears to be affected by regional-scale climatic and geochemical processes. These include for example the development of calcrete profiles (South Australia), the isolation of basins from the world ocean and the fauna inhabiting these semi-isolated seas (e.g. the *Ostrea*-rich bioherms in the Black Sea, and the Foraminifer-rich sediments within MIS3 and MIS1 sediments in Gulf St Vincent). Broadly speaking the three depositional basins investigated, Gulf St Vincent, the Black Sea and the Gulf of Carpentaria are distinctly different in their depositional styles. While Gulf St Vincent stands alone as a cool-temperate carbonate-dominated environment, the Black Sea and Gulf of Carpentaria differ because the sediments within the Gulf of Carpentaria are deposited in a very shallow environment, yet those fine sediments initially transported to the shelves of the Black Sea may ultimately be deposited in a basin 2 or more km deep. These results suggest that the plausibility of their being a taphonomic trade-off (Kidwell *et al.*, 2005) between relatively low temporal resolution and high compositional fidelity in tropical siliciclastic facies (Gulf of Carpentaria) may not apply to enclosed basins. These relationships appear more complex, and are driven by for example water chemistry, with poorer preservation associated in the Black Sea with shallow, lacustrine (fresh-water) conditions rather than marine. In contrast in the Gulf of Carpentaria poorer preserved bioclasts are common in present-day marine sediments, and within cores are associated with subaerial exposure. A separate model to that proposed for open coasts (Kidwell *et al.*, 2005) may be required to portray these relationships in semi-enclosed basins.

9.2.6. *Loss and contamination of amino acids and the utility of the intracrystalline approach*

The use of compromised fossil material compounds the problems alluded to above. For amino acid racemisation studies ‘compromised’ can mean contaminated with, or leached of amino acids, with the addition and loss of amino acids occurring in the taphonomic and diagenetic environment. Diffusive loss of amino acids, is commonly assumed to be the result of diagenetic and taphonomic processes, and results in lowered D/L values for the total hydrolysable amino acid pool because the more highly racemised free amino acids are lost from the skeletal carbonate, and this process therefore commonly produces significantly younger ages when calibrated than shells which have suffered no diffusive loss of indigenous amino acids, and with higher D/L values in the same stratum. While there has thus far been no significant work undertaken on marine bivalve molluscs using intracrystalline amino acids, nor on foraminifera using this method, this does offer a greater degree of confidence in results from

the analysis of amino acids for racemization-based chronological studies (chapter 4, 5, 7, 8), than the older (and perhaps standard) method of using the total hydrolysable amino acid content in a shell or foraminifer sample. Ultimately however, the purpose of the study must drive the method used, yet the failure of workers to differentiate between individual skeletal carbonate elements of varying age within a stratum is and will continue to be the biggest problem to overcome in attempts to determine accurate, reliable and useable chronologies. This is especially so where bulk samples are used for AAR radiocarbon and other dating purposes.

9.3. Suggestions for further research

The value of aminostratigraphy lies in the ability to differentiate between oxygen isotope stages of differing ages, but this method suffers from the inability to accurately portray chronologies to the detail that for example, radiocarbon routinely does. However, the sole use of intracrystalline amino acids may increase the level of detail possible with this method because of the use of these residues isolated from the diagenetic environment by the buffering affect of the skeletal carbonate and the associated intercrystalline proteins. This is where further research should perhaps focus. In particular, the use of amino acids whose stability is intertwined with that of the calcite or aragonite crystal lattice, may offer increased stability and repeatability in amino acid D/L values, and as a result improve the ability of this method to build reliable chronologies within individual marine isotope substages over 100 to 1,000's of years.

References

- Abelson, P. H., 1956. Paleobiochemistry. *Scientific American* 195, 83-92.
- Abrajno, T. A., Murphy, D. E., Fang, J., Comet, P., Brooks, J. M., 1994. C-13 C-12 values in individual fatty-acids of marine mytilids with and without bacterial symbionts. *Organic Geochemistry* 21, 611-617.
- Addadi, L., Joester, D., Nudelman, F., Weiner, S., 2006. Mollusc shell formation: A source of new concepts for understanding biomineralisation processes. *Chemistry, European Journal* 12, 980-987.
- Aguirre, M. L., Farinati, E. A., 1999. Taphonomic processes affecting late Quaternary molluscs along the coastal area of Buenos Aires Province (Argentina, Southwestern Atlantic). *Palaeogeography Palaeoclimatology Palaeoecology* 149, 283-304.
- Aharon, P., Schwarcz, H. P., Roberts, H. H., 1997. Radiometric dating of submarine hydrocarbon seeps in the Gulf of Mexico. *Geological Society of America Bulletin* 109, 568-579.
- Ainslie, R. C., Johnston, D. A., Offler, E. W., 1989. Intertidal communities of northern Spencer Gulf, South Australia. *Transactions of the Royal Society of South Australia* 113, 69-83.
- Aizenberg, J., 2000. Patterned crystallisation of calcite in vivo and in vitro. *Journal of Crystal Growth* 211, 143-148.
- Aizenberg, J., Hanson, J., Koetzle, T. F., Weiner, S., Addadi, L., 1997. Control of macromolecule distribution within synthetic and biogenic single calcite crystals. *Journal of the American Chemical Society* 119, 881-886.
- Akiyama, M., 1980. Diagenetic decomposition of peptide-linked serine residues in the fossil scallop shells. In: Hare, P. E., Hoering, T. C., & King, K. Jr., (Eds), *Biogeochemistry of Amino Acids*, pp. 115 – 120.
- Aksu, A. E., Hiscott, R. N., Yaşar, D., 1999. Oscillating Quaternary water levels of the Marmara Sea and vigorous outflow into the Aegean Sea from the Marmara Sea-Black Sea drainage corridor. *Marine Geology* 153, 275-302.
- Aksu, A. E., Hiscott, R. N., Yaşar, D., İşler, F. I., Marsh, S., 2002. Seismic stratigraphy of Late Quaternary deposits from the southwestern Black Sea shelf: evidence for non-catastrophic variations in sea-level during the last ~ 10000 yr. *Marine Geology* 190, 61-94.
- Albeck, S., Aizenberg, J., Addadi, L., Weiner, S., 1993. Interactions of various skeletal intracrystalline components with calcite crystals. *Journal of the American Chemical Society* 115, 11691-11697.
- Algan, O., Çağatay, N., Tchepalyga, A., Ongan, D., Eastoe, C., Gökaşan, E., 2001. Stratigraphy of the sediment infill in Bosphorus Strait: water exchange between the Black and Mediterranean Seas during the last glacial Holocene. *Geo-Marine Letters* 20, 209-218.
- Algan, O., Gökaşan, E., Gazioğlu, C., Yücel, Z., Alpar, B., Güneysu, C., Kırıcı, E., Demirel, S., Sarı, E., Ongan, D. 2002. A high-resolution seismic study in Sakarya Delta and Submarine Canyon, southern Black Sea shelf. *Continental Shelf Research* 22, 1511– 1527.
- Allen, J. R. L., 1990. The formation of coastal peat marshes under an upward tendency of relative sea-level. *Journal of the Geological Society, London* 147, 743-745.
- Allen, J. R. L., 1995. Salt-marsh growth and fluctuating sea level: implications of a simulation model for Flandrian coastal stratigraphy and peat-based sea-level curves. *Sedimentary Geology* 100, 21-45.
- Apakidze, A. M., Burchuladze, A. A., 1987. Radiouglerodnoe datirovanie arkeologicheskikh i paleobotanicheskikh abraztsov Gruzii (Radiocarbon dating of archaeological and paleobotanical samples in Georgia). *Metsniereba, Tbilisi*. (In Russian).
- Arslanov, Kh. A., 1993. Late Pleistocene geochronology of European Russia. *Radiocarbon* 35, 421-427.

- Arslanov, Kh. A., Tertychny, N. I., Kuznetsov, V. Yu., Chernov, S. B., Lokshin, N. V., Gerasimova, S. A., Maksimov, F. E., Dodonov, A. E., 2002. $^{230}\text{Th}/\text{U}$ and ^{14}C dating of mollusc shells from the coasts of the Caspian, Barents, White and Black Seas. *Geochronometria* 21, 49-56.
- Aswad, D., 1984. Determination of D- and L-aspartate in amino acid mixtures by high-performance liquid chromatography after derivatisation with a chiral adduct of o-phthalaldehyde. *Analytical Biochemistry* 137, 405-409.
- Atanassova, J., 2005. Palaeoecological setting of the western Black Sea area during the last 15000 years. *The Holocene* 15, 576-584.
- Bada, J. L., 1972. The dating of fossil bones using the racemization of isoleucine. *Earth and Planetary Science Letters* 15, 223-231.
- Bada, J. L., Shou, M-Y., Man, E. H., Schroeder, R. A., 1978. Decomposition of hydroxyl amino acids in foraminiferal tests: kinetics, mechanism and geochronological implications. *Earth and Planetary Science Letters* 41, 67-76.
- Bada, J. L., Wang, X. S., Hamilton, H., 1999. Preservation of key biomolecules in the fossil record: current knowledge and future challenges. *Philosophical Transactions of the Royal Society of London, B*, 354, 77-87.
- Badertscher, S., Fleitmann, D., Cheng, H., Edwards, R. L., Göktürk, O. M., Zumbühl, Leuenberger, M., Tüysüz, O., 2011. Pleistocene water intrusions from the Mediterranean and Caspian seas into the Black Sea. *Nature Geoscience* 4, 236-239.
- Badyukov, D. D., 1979. Sea level changes on the Soviet shores of the White, Baltic, and Black Seas during the past 15 thousand years. *Oceanology* 19, 177-181.
- Bahr, A., Arz, H. W., Lamy, F., Wefer, G., 2006. Late glacial to Holocene paleoenvironmental evolution of the Black Sea, reconstructed with stable oxygen isotope records obtained on ostracod shells. *Earth and Planetary Science Letters* 241, 863-875.
- Bahr, A., Lamy, F., Arz, H. W., Major, C., Kwiecien, O., Wefer, G., 2008. Abrupt changes of temperature and water chemistry in the late Pleistocene and early Holocene Black Sea. *Geochemistry Geophysics Geosystems* 9, 1-16.
- Bahr, A., Lamy, F., Arz, H., Kuhlmann, H., Wefer, G., 2005. Late Glacial to Holocene climate and sedimentation history in the NW Black Sea. *Marine Geology* 214, 309-322.
- Balabanov, I. P., 2007. Holocene sea-level changes of the Black Sea. In: Yanko-Hombach, V., Gilbert, A.S., Panin, N., Dolukhanov, P.M. (Eds.), *The Black Sea Flood Question: Changes in Coastline, Climate, and Human Settlement*. Springer, Dordrecht, pp. 711-730.
- Ballesteros, E., Gallego, M., Valcarcel, M., 1996. Sequential determination of D- and L-glutamic acid by continuous fractional crystallization. *Analytical Chemistry* 68, 322-326.
- Banerjee, D., Hildebrand, A. N., Murray-Wallace, C. V., Bourman, R. P., Brooke, B. P., Blair, M., 2003. New quartz SAR-OSL ages from the stranded beach dune sequence in south-east South Australia. *Quaternary Science Reviews* 22, 1019-1025.
- Barbieri, R., 2001. Taphonomic implications of foraminiferal composition and abundance in intertidal mud flats, Colorado River Delta (Mexico). *Micropaleontology* 47, 73-86.
- Barbieri, R., D'Onofrio, S., Melis, R., Westall, F., 1999. r-Selected benthic Foraminifera with associated bacterial colonies in Upper Pleistocene sediments of the Ross Sea (Antarctica): implications for calcium carbonate preservation. *Palaeogeography, Palaeoclimatology, Palaeoecology* 149, 41-57.
- Barbour Wood, S. L., Krause, R. A. Jr., Kowaleski, M., Wehmiller, J. F., Simoes, M. G., Goodfriend, G. A., 2003. A comparison of rates of time-averaging between the bivalve *Macoma cleryana* and brachiopod *Bouchardia rosea* on a shallow subtropical shelf. *Geological Society of America with Programs* 35, 273.
- Bedouet, L., Rusconi, F., Rousseau, M., Duplat, D., Marie, A., Dubost, L., Le Ny, K., Berland, S., Peduzzi, J., Lopez, E., 2006. Identification of low molecular weight molecules as new components of the nacre organic matrix. *Comparative Biochemistry and Physiology part B* 144, 532-543.

- Behrensmeyer, A. K., Kidwell, S. M., 1985. Taphonomy's contribution to paleobiology. *Paleobiology* 11, 105-119.
- Belperio, A. P., Cann, J. H., Murray-Wallace, C. V., 1996. Quaternary coastal evolution, sea level change and neotectonics: Coorong to Mount Gambier coastal plain, southeastern Australia. Excursion guide to 3rd annual meeting, Sydney, Australia, 4-14 November, 1996. IGCP Project 367 – Late Quaternary coastal records of rapid change: applications to present and future conditions.
- Belperio, A. P., Harvey, N., Bourman, R. P., 2002. Spatial and temporal variability in the Holocene sea-level record of the South Australian coastline. *Sedimentary Geology* 150, 153-169.
- Belperio, A. P., Murray-Wallace, C. V., Cann, J. H., 1995. The last interglacial shoreline in southern Australia: morphostratigraphic variations in a temperate carbonate setting. *Quaternary International* 26, 7-19.
- Berkeley, A., Perry, C. T., Smithers, S. G., Horton, B. P., Taylor, K. G., 2007. A review of the ecological and taphonomic controls on foraminiferal assemblage development in intertidal environments. *Earth Science Reviews* 83, 205-230.
- Blaine, C. C., 2003. The concept of autocyclic and allocyclic controls on sedimentation and stratigraphy, emphasizing the climatic variable. *Climate controls on stratigraphy*, SEPM Special Publication No. 77, 13-20.
- Boomer, I., Guichard, F., Lericolais, G., 2010. Late Pleistocene to recent ostracod assemblages from the western Black Sea. *Journal of Micropalaeontology* 29, 119-133.
- Borovskaya, R. V., Lomakin, P. D., 2008. Specific features of ice conditions in the Sea of Azov and the Kerch Strait in the winter season of 2005/06. *Russian Meteorology and Hydrology* 33, 453-457.
- Bourman, R. P., Belperio, A. P., Murray-Wallace, C. V., Cann, J. H., 1999. A last interglacial embayment fill at Normanville, South Australia, and its neotectonic implications. *Transactions of the Royal Society of South Australia* 123, 1-15.
- Bowen, C. E., Tang, H., 1996. Conchiolin-protein in aragonite shells of molluscs. *Comparative Biochemistry and Physiology, Part A: Physiology* 115, 269 – 275.
- Brandon, C., Tooze, J., 1999. *Introduction to Protein Structure*. 2nd edition. Garland Publishing Incorporated, New York. ISBN 0 8153 2305 0
- Brigham, J. K., 1983. Intrashell variations in amino acid concentrations and isoleucine epimerisation values in fossil *Hiatella arctica*. *Geology* 11, 509-513.
- Brückner, H., Kelterbaum, D., Marunchak, O., Porotov, A., Vött, A., 2010. The Holocene sea level story since 7500 BP – lessons from the Eastern Mediterranean, the Black Sea and the Azov Seas. *Quaternary International* 225, 160-179.
- Brückner, H., Wittner, R., Godel, H., 1991. Fully automated high-performance liquid chromatographic separation of DL-amino acids derivatised with o-Phthaldialdehyde together with N-isobutyryl-cysteine. Application to food samples. *Chromatographia* 32, 383-388.
- Bryant, E. A., Young, R. W., Price, D. M., Short, S. A., 1992: Evidence for Pleistocene and Holocene raised marine deposits, Sandon Point, New South Wales. *Australian Journal of Earth Sciences* 39, 481-493.
- Bryars, S., Neverauskas, V., Brown, P., Gilliland, J., Gray, L., Halliday, L., 2003. Degraded seagrass meadows and evidence of eutrophication in Western Cove, Kangaroo Island. Fish Habitat Program, Primary Industries and Resources South Australia, Adelaide.
- Buch, A., Glavin, D. P., Sternberg, R., Szopa, C., Rodier, C., Navarro-González, R., Raulin, F., Cabane, M., Mahaffy, P. R., 2006. A new extraction technique for in situ analyses of amino and carboxylic acids on Mars by gas chromatography mass spectrometry. *Planetary and Space Science* 54, 1592-1599.
- Burdige, D. J., Martens, C. S., 1988. Biogeochemical cycling in an organic-rich coastal marine basin: 10. The role of amino acids in sedimentary carbon cycling and nitrogen cycling. *Geochimica et Cosmochimica Acta* 52, 1571-1584.

- Burgess, S. N., McCulloch, M. T., Gagan, M. T., Ward, T., 2006. Long-term anthropogenic change in South Australian gulfs recorded by the faviid coral *Plesiastrea versipora*. *Geochimica et Cosmochimica Acta* 70, Supplement 1, August-September 2006, p A74.
- Burne, R. V., Graham, T. L., 1995. Coastal Environment Geoscience of Cape York Peninsula. Cape York Peninsula Land Use Strategy, Office of the Co-ordinator general of Queensland, Brisbane, Department of the Environment, Sport and Territories, Canberra, and Australian Geological Survey Organisation, Canberra. 71 pp.
- Burrows, K., 1979. Chapter 4, Climate. In: M. J. Tyler, C. R. Twidale, & J. K. Ling, (Eds), *Natural History of Kangaroo Island*, Royal Society of South Australia.
- Buynevich, I. V., Damušytė, A., Bitinas, A., Olenin, S., Mažeika, J., Petrošius, R., 2011. Pontic-Baltic pathways for invasive aquatic species: geoarchaeological implications. *The Geological Society of America, Special Paper* 473, 189-196.
- Bylinsky, E. N., Yanko, V. V., Motnenko, I. V., 1990. Sea-level changes at the Eltigen coastal exposure, East Crimea. *MBSS newsletter*, no 12.
- Cai, W.-J., Chen, F., Powell, E. N., Walker, S. E., Parsons-Hubbard, K. M., Staff, G. M., Wang, Y., Ashton-Alcox, K. A., Callender, W. R., Brett, C. E., 2006. Preferential dissolution of carbonate shells driven by petroleum seep activity in the Gulf of Mexico. *Earth and Planetary Science Letters* 248, 227-243.
- Cabioch, G., Ayliffe, L., 2001. 'Raised coral terraces at Malakula, Vanuatu, Southwest Pacific, indicate high sea level during marine isotope stage 3. *Quaternary Research* 56, 357-365.
- Cann, J. H., 1978. An exposed reference section for the Glanville Formation. *Quarterly Geological Notes, The Geological Survey of South Australia* 65, 2-4.
- Cann, J. H., Belperio, A. P., Gostin, V. A., Murray-Wallace, C. V., 1988. Sea-level history, 45,000 to 30,000 yrs B. P., inferred from benthic foraminifera, Gulf St. Vincent, South Australia, and a refined late Pleistocene sea level history. *Quaternary Research* 29, 153-175.
- Cann, J. H., Belperio, A. P., Gostin, V. A., Rice, R. L., 1993. Contemporary benthic foraminifera in Gulf St Vincent, South Australia, and a refined Late Pleistocene sea-level history. *Australian Journal of Earth Sciences* 40, 197-211.
- Cann, J. H., Belperio, A. P., Murray-Wallace, C. V., 2000. Late Quaternary paleosealevels and paleoenvironments inferred from foraminifera, northern Spencer Gulf, South Australia. *Journal of Foraminiferal Research* 30, 29-53.
- Cann, J. H., Clarke, J. D. A. 1993. The significance of *Marginopora vertebralis* (Foraminifera) in surficial sediments at Esperance, Western Australia, and in last interglacial sediments in northern Spencer Gulf, South Australia. *Marine Geology* 111, 171-187.
- Cann, J. H., Murray-Wallace, C. V., Riggs, N. J., Belperio, A. P., 2006. Successive foraminiferal faunas and inferred palaeoenvironments associated with the postglacial (Holocene) marine transgression, Gulf St. Vincent, South Australia. *The Holocene* 16, 1-11.
- Cann, J.H., Murray-Wallace, C.V., 1986. Holocene distribution and amino acid racemization of the benthic foraminifer *Massilina milletti*, northern Spencer Gulf, South Australia. *Alcheringa* 10, 45-54.
- Carrol, M., 2001. Quantitative estimates of time-averaging in brachiopod shell accumulations from a Holocene tropical shelf. MSc thesis, Virginia Polytechnic Institute and State University, Blacksburg, VA, USA.
- Casagrande, D. J., Given, P. H., 1980. Geochemistry of amino acids in some Florida peat accumulations – II. Amino acid distributions. *Geochimica et Cosmochimica Acta* 44, 1493-1507.
- Casford, J. S. L., Abu-Zied, R., Rohling, E. J., Cooke, S., Boessenkool, K. P., Brinkhuis, H., Castignetti, P., Manley, C. J., 1998. Benthic foraminiferal depth distribution within the sediment in a modern ria. *Terra Nova* 10, 37-41.
- Chappell, J., Omura, A., Esat, T., McCulloch, M., Pandolfi, J., Ota, Y., Pillans, B., 1996. Reconciliation of Late Quaternary sea levels derived from coral terraces at Huon Peninsula with deep sea oxygen isotope records. *Earth and Planetary Science Letters* 141, 227-236.

- Chateigner, D., Hedegaard, C., Wenk, H-R., 2000. Mollusc shell microstructures and crystallographic textures. *Journal of Structural Geology* 22, 1723-1735.
- Chave, K. E., Deffeyes, K. S., Garrels, R. M., Thompson, M. E., Weyl, P. K., 1962. Observations on the solubility of skeletal carbonates in aqueous solutions. *Science* 137, 33-34.
- Cheng, H., Edwards, R. L., Hoff, J., Gallup, C. D., Richards, D. A., Asmerom, Y., 2000. The half-lives of uranium-234 and thorium-230. *Chemical Geology* 169, 17-33.
- Chepalyga, A. L., 1984. Inland Sea Basins. In: Barnosky-Cathy, W. (Ed.), *Late Quaternary Environments of the Soviet Union*. University of Minnesota Press, Minneapolis, pp. 229-247.
- Chepalyga, A.L., 2007. Late Glacial great flood in the Ponto-Caspian basin. In: Yanko-Hombach, V., Gilbert, A.S., Panin, N., Dolukhanov, P.M. (Eds.), *The Black Sea Flood Question: Changes in Coastline, Climate, and Human Settlement*. Springer, Dordrecht, pp. 119-148.
- Chivas, A. R., Chappell, J., Polach, H., Pillans, B., Flood, P., 1986. Radiocarbon evidence for the timing and rate of island development, beach-rock formation and phosphatization at Lady Elliot Island, Queensland, Australia. *Marine Geology* 69, 273-287.
- Chivas, A. R., García, A., van der Kaars, S., Couapel, M. J. J., Holt, S., Reeves, J. M., Wheeler, D. M., Switzer, A. D., Murray-Wallace, C. V., Banerjee, D., Price, D. M., Wang, S. X., Pearson, G., Edgar, N. T., Beaufort, L., De Deckker, P., Lawson, E., Cecil, C. B., 2001. Sea-level and environmental changes since the last interglacial in the Gulf of Carpentaria, Australia: an overview. *Quaternary International* 83-85, 19-46.
- Clark, G. R. II., 2005. Daily growth lines in some living pectens (Mollusca: Bivalvia), and some applications in a fossil relative: Time and tide will tell. *Palaeogeography, Palaeoclimatology, Palaeoecology*, 228, 26-42.
- Clarke, G. R., II, 1999. Organic matrix taphonomy in some molluscan shell microstructures. *Palaeogeography, Palaeoclimatology, Palaeoecology* 149, 305-312.
- Clarke, S. J., Miller, G. H., Fogel, M. L., Chivas, A. R., Murray-Wallace, C. V., 2006. The amino acid and stable isotope biogeochemistry of elephant bird (*Aepyornis*) eggshells from southern Madagascar. *Quaternary Science Reviews* 25, 2343-2356.
- Clarke, S. J., Miller, G. H., Murray-Wallace, C. V., David, B., Pasveer, J. M., 2007. The geochronological potential of isoleucine epimerisation in cassowary and megapode eggshells from archaeological sites. *Journal of Archaeological Science* 34, 1051-1063.
- Clarke, S. J., Murray-Wallace, C. V., 2006. Mathematical expressions used in amino acid racemization geochronology – A review. *Quaternary Geochronology* 1, 261-278.
- Collins, M. J., Riley, M. S., 2000. Amino acid racemization in biominerals: the impact of protein degradation and loss. In: Goodfriend, G. A., Collins, M. J., Fogel, M. L., Macko, S. A., Wehmiller, J. F., (Eds), *Perspectives in Amino Acids and Protein Geochemistry*. Oxford University Press, pp. 108-119.
- Collins, M. J., Westbroek, P., Muyzer, G., De Leuw, J. W., 1992. Experimental evidence for condensation reactions between sugars and proteins in carbonate skeletons. *Geochimica et Cosmochimica Acta* 56, 1539-1544.
- Connor, S. E., 2006. A promethean legacy: Late Quaternary vegetation history of southern Georgia, Caucasus. PhD thesis, University of Melbourne, Australia.
- Connor, S. E., Kvavadze, E. V., 2008. Modelling late Quaternary changes in plant distribution, vegetation and climate using pollen data from Georgia, Caucasus. *Journal of Biogeography* 36, 529-545.
- Connor, S. E., Thomas, I., Kvavadze, E. V., 2007. A 5600-yr history of changing vegetation, sea-levels and human impacts from the Black Sea coast of Georgia. *The Holocene* 17, 25-36.
- Cooper, B. J., Lindsay, J. M., 1978. Marine entrance to the Cainozoic St Vincent Basin. *Quarterly Geological Notes of the Geological Survey of South Australia*, 67, 4-6.
- Couapel, M. J. J., Beaufort, L., Jones, B. G., Chivas, A. R., 2007. Late Quaternary marginal marine palaeoenvironments of northern Australia as inferred from cluster analysis of coccolith assemblages. *Marine Micropaleontology* 65, 213-231.

- Crenshaw, M. A., 1972. The soluble matrix from *Mercenaria mercenaria* shell. *Biom mineralization* 6, 6-11.
- Crusius, J., Bothner, M. H., Sommerfield, C. K., 2004. Bioturbation depths, rates and processes in Massachusettts Bay sediments inferred from modelling of ^{210}Pb and $^{239} + ^{240}\text{Pu}$ profiles. *Estuarine, Coastal and Shelf Science* 61, 643-655.
- Cutler, A. H., 1995. Taphonomic implications of shell surface textures in Bahia la Choya, northern Gulf of California. *Palaeogeography Palaeoclimatology Palaeoecology*, 114, 219-240.
- Cutler, A.H. and Flessa, K.W., 1990. Fossils out of sequence: Computer simulations and strategies for dealing with stratigraphic disorder. *Palaaios* 5, 227-235.
- Davies, D. J., Powell, E. N., Stanton, R. J. Jr., 1989. Taphonomic signatures as a function of environmental process: shells and shell beds in a hurricane-influenced inlet on the Texas coast. *Palaeogeography, Palaeoclimatology, Palaeoecology* 72, 317 – 356.
- De Deckker, P., Chivas, A. R., Shelley, J. M. G., 1988. Palaeoenvironment of the Messinian Mediterranean “Lago Mare” from strontium and magnesium in ostracode shells. *Palaaios* 3, 352-358.
- De Klerk, P., Haberl, A., Kaffke, A., Krebs, M., Matchutadze, I., Minke, M., Schulz, J., Joosten, H., 2009. Vegetation history and environmental development since ca 6000 cal yr BP in and around Ispani 2 (Kolkheti lowlands, Georgia). *Quaternary Science Reviews* 28, 890-910.
- De Silva Samarasinghe, J. R., 1998. Revisiting upper Gulf St. Vincent in South Australia: the salt balance and its implications. *Estuarine, Coastal and Shelf Science* 46, 51-63.
- De Silva Samarasinghe, J. R., Bode, L., Mason, L. B., 2003. Modelled response of Gulf St. Vincent (South Australia) to evaporation, heating and winds. *Continental Shelf Research* 23, 1285-1313.
- De Vries, C., Wefer, G., Geraga, M., Papatheodorou, G., Croudace, I., Thomson, J., Lykousis, V., 2001. Mediterranean climate variability during the Holocene. *Mediterranean Marine Science* 2, 45-55.
- Desrosiers, G., Savenkoff, C., Olivier, M., Stora, G., Juniper, K., Caron, A., Gagné, J.-P., Legendre, L., Mulsow, S., Grant, J., Roy, S., Grehan, A., Scaps, P., Silverberg, N., Klein, B., Tremblay, J.-É., Theriault, J.-C., 2000. Trophic structure of macrobenthos in the Gulf of St. Lawrence and on the Scotian Shelf. *Deep-Sea Research II* 47, 663-697.
- Devdariani, A. S., Novikova, Z. T., 1978. Tectonic movements on the northwestern shelf of the Black Sea during the Holocene, reconstructed from the mineralogic composition of the deposits. *Oceanology* 18, 453-457.
- Dickin, A. P., 2005. *Radiogenic Isotope Geology*. Cambridge University Press. 492 pp.
- Diefendorf, A. F., Patterson, W. P., Mullins, H. T., Tibert, N., Martini, A., 2006. Evidence for high-frequency late Glacial to mid-Holocene (16,800 to 5,500 cal yr B.P.) climate variability from oxygen isotope values of Lough Inchiquin, Ireland. *Quaternary Research* 65, 78-86.
- Dimitrov, L., 2002. Contribution to atmospheric methane by natural seepages on the Bulgarian continental shelf. *Continental Shelf Research* 22, 2429-2442.
- Dodonov, A. E., Tchepalyga, A. L., Mihailescu, C. D., Zhou, L. P., Markova, A. K., Trubidhin, V. M., Simakova, A. N., Konikov, E. G., 2000. Last-interglacial records from central Asia to the northern Black Sea shoreline: stratigraphy and correlation. *Geologie en Mijnbouw*, 79, 303-311.
- Dolukhanov, P. M., Kadurin, S. V., Larchenkov, E. P., 2009. Dynamics of the coastal North Black Sea area in Late Pleistocene and Holocene and early human dispersal. *Quaternary International* 197, 27-34.
- Dott, R. H. Jr., 1988. An episodic view of shallow marine clastic sedimentation. In: de Boer, P.L., van Gelder, A., Nio, S.D., (Eds), *Tide-influenced sedimentary environments and facies*. Reidel, Dordrecht, pp. 3-12.
- Dowling, L. A., Sejrup, H. P., Heijnis, H., & Coxon, P., 1998. Palynology, aminostratigraphy and U-series dating of marine Gortian interglacial sediments in Cork Harbour, southern Ireland. *Quaternary Science Reviews* 17, 945-962.
- Dungworth, G., 1976. Optical configuration and the racemization of amino acids in sediments and in fossils – a review. *Chemical Geology* 17, 135-153.

- Dzhanelidze, Z. Ch., Mikadze, I. P., 2007. Stratigraphy and water supply conditions of the Kobuleti peat bog. *Stratigraphy and Geological Correlation* 15, 437.
- Eastwood, W. J., Roberts, N., Lamb, H. F., Tibby, J. C., 1999. Holocene environmental change in southwest Turkey: a palaeoecological record of lake and catchment-related changes. *Quaternary Science Reviews* 18, 671-695.
- Edgar, N. T., Cecil, C. B., Mattick, R. E., Chivas, A. R., De Deckker, P., Djajadihardja, Y., 2003. A modern analogue for tectonic, eustatic, and climatic processes in cratonic basins: Gulf of Carpentaria, Northern Australia. In: Cecil, C. B., Edgar, N. T. (Eds.), *Climate Controls on Stratigraphy*, SEPM Special Publication No. 77, 193-205.
- Efremov, J. A., 1940. Taphonomy: New branch of palaeontology. *American Geologist* 74, 81-93.
- Eglinton, T. I., 1997. Variability in radiocarbon ages of individual organic compounds from marine sediments. *Science* 277, 796-799.
- Einsele, G., 1992. *Sedimentary Basins: Evolution, Facies, and Sediment Budget*. Springer-Verlag, Berlin. 628 pages
- Endo, K., Walton, D., Reymont, R. A., Curry, G. B., 1995. Fossil intra-crystalline biomolecules of brachiopod shells: diagenesis and preserved geo-biological information. *Organic Geochemistry* 23, 661-673.
- Estrela, C., Estrela, C. R. A., Barbin, E. L., Spanó, J. C. E., Marchesan, M. A., Pécora, J. D., 2002. Mechanism of action of sodium hypochlorite. *Brazilian Dentistry Journal* 13, 113-117.
- Falini, G., Albeck, S., Weiner, S., Addadi, L., 1996. Control of aragonite or calcite polymorphism by mollusc shell macromolecules. *Science* 271, 67 – 69.
- Feurdean, A., 2005. Holocene forest dynamics in northwestern Romania. *The Holocene* 15, 435-446.
- Feurdean, A., Mosbrugger, V., Onac, B. P., Polyak, V., Veres, D., 2007. Younger Dryas to mid-Holocene environmental history of the lowlands of NW Transylvania, Romania. *Quaternary Research* 68, 364-378.
- Feurdean, A., Mosbrugger, V., Onac, B. P., Polyak, V., Veres, D., 2007. Younger Dryas to mid-Holocene environmental history of the lowlands of NW Transylvania, Romania. *Quaternary Research* 68, 364-378.
- Filipova-Marinova, M., 2007. Archaeological and paleontological evidence of climate dynamics, sea-level change, and coastline migration in the Bulgarian sector of the circum-Pontic region. In: Yanko-Hombach, V., Gilbert, A.S., Panin, N., Dolukhanov, P.M. (Eds.), *The Black Sea Flood Question: Changes in Coastline, Climate, and Human Settlement*. Springer, Dordrecht, pp. 453-481.
- Firman, J. B., 1966. Stratigraphic units of Late Cainozoic age in the St Vincent Basin, South Australia. *Quarterly Geological Notes, Geological Survey, South Australia* 17, 6-9.
- Flessa, K. W., Brown, T. J., 1983. Selective solution of macroinvertebrate calcareous hard parts: a laboratory study. *Lethaia* 16, 193-205.
- Flessa, K. W., Cutler, A. H., and Meldahl, K. H., 1993. Time and taphonomy: quantitative estimates of time-averaging and stratigraphic disorder in a shallow marine habitat: *Paleobiology*, 19, 266-286.
- Fouache, E., Porotov, A., Müller, C., Gorlov, Y., 2004. The role of neo-tectonics in the variation of the relative mean sea level throughout the last 6000 years on the Taman Peninsula (Black Sea, Azov Sea, Russia). *IGCP 464, European Regional Conference, 2003: Rapid transgressions into semi-enclosed basins*, pp. 47-58.
- Fujiwara, O., Kamataki, T., Masuda, F., 2004. Sedimentological time-averaging and ¹⁴C dating of marine shells. *Nuclear Instruments and Methods in Physics Research B*, 223-224, 540-544.
- Gaffey, S. J., Bronnimann, C. E., 1993. Effects of Bleaching on organic and mineral phases in biogenic carbonates. *Journal of Sedimentary Research* 63, 752-754.
- Gerhardt, S., Henrich, R., 2001. Shell preservation of *Limacina inflata* (Pteropoda) in surface sediments from the Central and South Atlantic Ocean: a new proxy to determine the aragonite saturation state of water masses. *Deep-Sea Research* 1, 2051-2071.

- Gingele, F. X., De Deckker, P., Hillenbrand, C. D., 2004. Late Quaternary terrigenous sediments from the Murray Canyons area, offshore South Australia and their implications for sea level change, palaeoclimate and palaeodrainage of the Murray-Darling Basin. *Marine Geology* 212, 183-197.
- Giosan, L., Donnelly, J. P., Constantinescu, S., Filip, F., Ovejanu, I., Vespremeanu-Stroe, A., Vespremeanu, E., Duller, G. A. T., 2006. Young Danube delta documents stable Black Sea level since the middle Holocene: Morphodynamic, paleogeographic, and archaeological implications. *Geology* 34, 757-760.
- Giosan, L., Donnelly, J. P., Vespremeanu, E. I., Buonaiuto, F. S., 2005. River delta morphodynamics: examples from the Danube delta. In: Giosan, L., and Bhattacharya, J. P., (Eds). *River deltas – concepts, models, and examples*. SEPM Special Publication 83, 87-132.
- Giosan, L., Filip, F., Constantinescu, S., 2009. Was the Black Sea catastrophically flooded in the early Holocene? *Quaternary Science Reviews* 28, 1-6.
- Giunta, S., Morigi, C., Negri, A., Guichard, F., Lericolais, G., 2007. Holocene biostratigraphy and paleoenvironmental changes in the Black Sea based on calcareous nannoplankton. *Marine Micropaleontology* 63, 91-110.
- Gluskoter, H., Edgar, N. T., Cecil, C. B., Dulong, F. T., Damberger, H. H., 2001. The Gulf of Carpentaria as a modern tectonic and eustatic analogue for the Illinois Basin during the Pennsylvanian. Abstract, GSA Annual Meeting, November 5-8.
- Goldstein, S. T., Watkins, G. T., 1999. Taphonomy of salt marsh foraminifera: an example from coastal Georgia. *Palaeogeography, Palaeoclimatology, Palaeoecology* 149, 103-114.
- Goodfriend, G. A., 1989. Complementary use of amino acid epimerisation and radiocarbon analysis for dating of mixed-age assemblages. *Radiocarbon* 31, 1041-1047.
- Goodfriend, G. A., 1991. Patterns of racemization and epimerization of amino acids in land snails over the course of the Holocene. *Geochimica et Cosmochimica Acta* 55, 293-302.
- Goodfriend, G. A., Brigham-Grette, J., Miller, G. H., 1996. Enhanced age resolution of the marine quaternary record in the Arctic using aspartic acid racemization dating of bivalve shells. *Quaternary Research* 45, 176-187.
- Goodfriend, G. A., Flessa, K. W., Hare, P. E., 1997. Variation in amino acid epimerization rates and amino acid composition among shell layers in the bivalve *Chione* from the Gulf of California. *Geochimica et Cosmochimica Acta* 61, 1487-1493.
- Goodfriend, G. A., Meyer, V. A., 1991. A comparative study of the kinetics of amino acid racemization/epimerisation in fossil and modern mollusc shells. *Geochimica et Cosmochimica Acta* 55, 3355-3367.
- Goodfriend, G. A., Stanley, D. J., 1996. Reworking and discontinuities in Holocene sedimentation in the Nile Delta: documentation from amino acid racemization and stable isotopes in mollusc shells. *Marine Geology* 129, 271-283.
- Goodfriend, G. A., Weidman, C. R., 2001. Ontogenetic trends in aspartic acid racemization and amino acid composition within modern and fossil shells of the bivalve *Arctica*. *Geochimica et Cosmochimica Acta* 65, 1921-1932.
- Goodwin, D. H., Flessa, K. W., Téllez-Duarte, M. A., Dettman, D. L., Schöne, B. R., Avila-Serrano, G. A., 2004. Detecting time-averaging and spatial mixing using oxygen isotope variation: a case study. *Palaeogeography, Palaeoclimatology, Palaeoecology* 205, 1-21.
- Görür, N., Çağatay, M. M., Emre, Ö., Alpar, B., Sakinc, M., İslamoğlu, Y., Algan, O., Erkal, T., Kecer, M., Akkök, R., Karlik, G., 2001. Is the abrupt drowning of the Black Sea shelf at 7150 yr BP a myth? *Marine Geology* 176, 65-73.
- Grégoire, C., 1957. Topography of the organic components in mother of pearl. *Journal of Biophysical and Biochemical Cytology* 3, 797-821.
- Grégoire, C., 1972. Structure of the molluscan shell. In: Florkin, M., Scheer, B. T., (Eds), *Chemical Zoology*, (VII). Academic Press, New York, 45-102.
- Grégoire, C., Duchâteau, G., Florkin, M., 1955. La trame protidique des nacres et des perles. *Annals of the Institute of Oceanography, Monaco*, 31, 1-36.

- Gulin, S. B., Polikarpov, G. G., Egorov, V. N., 2003. The age of microbial carbonate structures grown at methane seeps in the Black Sea with an implication of dating of the seeping methane. *Marine Chemistry* 84, 67-72.
- Hails, J. R., Belperio, A. P., & Gostin, V. A., 1984. Quaternary sea levels, northern Spencer Gulf, Australia. *Marine Geology* 61, 373-389.
- Hallan, A., Willan, R. C., 2010. Two new species of *Lentidium* (Myida: Corbulidae) from tropical northern Australia: remarkable fresh/fluviatile to brackish-water bivalves. *Molluscan Research* 30, 143-153.
- Hare, P. E., 1963. Amino acids in proteins from aragonite and calcite in the shells of *Mytilus californianus*. *Science* 139, 216-217.
- Hare, P. E., 1988. Chiral mobile phases for the enantiomeric resolution of amino acids. In: Zef, M., Crane, L. J., (Eds), *Chromatographic chiral separations*. Marcel Dekker Inc, New York, pp. 165-177.
- Hare, P. E., Abelson, P. H., 1965. Amino acid composition of some calcified proteins. *Carnegie Institute of Washington Year Book* 64, 223.
- Hare, P. E., Abelson, P. H., 1967. Racemization of amino acids in fossil shells. *Carnegie Institution of Washington Year Book* 66, 526-528.
- Hareddy, R. A., 2008. Heavy minerals in marine and fluvial sediments: provenance indicators and distributions in the tropical southeastern shelf of the Gulf of Carpentaria and its hinterland, North Australia. PhD thesis, 298 pp.
- Harris, D. C., 2003. *Quantitative chemical analyses*. 6th edition. W. H. Freeman & company, New York. 903 pages.
- Harris, P. T., Heap, A. D., Wassenberg, T., Passlow, V., 2004. Submerged coral reefs in the Gulf of Carpentaria, Australia. *Marine Geology* 207, 185-191.
- Hart, H., 1991. *Organic Chemistry, a Short Course*. Eighth edition. Houghton Mifflin Company, Boston. 353 pages.
- Hasse, B., Ehrenberg, H., Marxen, J. C., Becker, W., Eppe, M., 2000. Calcium carbonate modifications in the mineralised shell of the freshwater snail *Biomphalaria glabrata*. *Chemistry - a European Journal* 6, 3679-3685.
- Head, M. J., 1999. Radiocarbon dating of arid zone deposits. In: Singhvi, A. K., Derbyshire, E., (Eds), *Paleoenvironmental reconstructions in arid lands*. Oxford & IBH Publishing Co. PVT. Ltd, New Delhi and Calcutta, pp. 293-396.
- Hearty, P. J., Kaufman, D. S., 2009. A Cerion-based chronostratigraphy and age model from the central Bahama Islands: amino acid racemization and ¹⁴C in land snails and sediments. *Quaternary Geochronology* 4, 148-159.
- Hearty, P. J., Miller, G. H., Stearns, C. E., Szabo, B. J., 1986. Aminostratigraphy of Quaternary shorelines around the Mediterranean basin. *Geological Society of America Bulletin* 97, 850-858.
- Hearty, P. J., O'Leary, M. J., Kaufman, D. S., Page, M., Bright, J., 2004. Amino acid geochronology of individual foraminifera (*Pulleniatina obliquiloculata*) tests, north Queensland margin, Australia: a new approach to correlating and dating Quaternary tropical marine sediment cores. *Paleoceanography* 19, PA4022, doi: 10.1029/2004PA001059.
- Hearty, P., O'Leary, M., Donald, A., Lachlan, T., 2006. The enigma of 3400 years BP coastal oolites in tropical northwest Western Australia...why then, why there? *Sedimentary Geology* 186, 171-185.
- Heezen, B. C., Menzies, R. J., Broecker, W. S., Ewing, M., 1958. Date of stagnation of the Cariaco Trench, southeast Caribbean. *Geological Society of America Bulletin* 69, 1579.
- Heinemann, F., Treccani, L., Fritz, M., 2006. Abalone nacre insoluble matrix induces growth of flat and oriented aragonite crystals. *Biochemical and Biophysical Research Communications* 344, 45-49.
- Heinrikson, R. L., Meredith, S. C., 1984. Amino acid analysis by reverse-phase high performance liquid chromatography: precolumn derivatisation with phenylisothiocyanate. *Analytical Biochemistry* 136, 65-74.

- Hemer, M. A., Harris, P. T., Coleman, R., Hunter, J., 2004. Sediment mobility due to currents and waves in the Torres Strait-Gulf of Papua region. *Continental Shelf Research* 24, 2297-2316.
- Hendy, I. L., Kennett, J. P., Roark, E. B., Ingram, B. L., 2002. Apparent synchronicity of submillennial scale climate events between Greenland and Santa Barbara Basin, California from 30-10 ka. *Quaternary Science Reviews* 21, 1167-1184.
- Hess, S., Gustafson, K. R., Milanowski, D. J., Alvira, E., Lipton, M. A., Pannell, L. K., 2004. Chirality determination of unusual amino acids using precolumn derivatization and HPLC-ESI-MS. *Journal of Chromatography* 1035, 211-219.
- Hill, P. J., De Deckker, P., von der Borch, C., Murray-Wallace, C. V., 2009. Ancestral Murray river on the Lacedpede Shelf, southern Australia: Late Quaternary migrations of a major river outlet and strandline development. *Australian Journal of Earth Sciences* 56, 135-157.
- Hill, R. L., 1965. Hydrolysis of proteins. *Advances in Protein Chemistry* 20, 30-107.
- Hiscott, R. N., Aksu, A. E., Mudie, P. J., Marrett, F., Abrajano, T., Kaminiski, M. A., Evans, J., Cakiroğlu, Yaşar, D., 2007. A gradual drowning of the southwestern Black Sea shelf: evidence for a progressive rather than abrupt Holocene reconnection with the eastern Mediterranean Sea through the Marmara Sea gateway. *Quaternary International* 167-168, 19-34.
- Hiscott, R. N., Aksu, A. E., Mudie, P. J., Marrett, F., Abrajano, T., Kaminiski, M. A., Evans, J., Cakiroğlu, Yaşar, D., 2010. Corrigendum to "A gradual drowning of the southwestern Black Sea shelf: Evidence for a progressive rather than abrupt Holocene reconnection with the eastern Mediterranean Sea through the Marmara Sea Gateway" [*Quaternary International*, 167-168 (2007) 19-34]. *Quaternary International* 226, 160.
- Holcová, K., 1997. Can detailed sampling and taphonomical analysis of foraminiferal assemblages offer new data for paleoecological interpretations? *Revue de Micropaléontologie* 40, 313-329.
- Hollin, J.T., Hearty, P.J., 1990. South Carolina interglacial sites and stage 5 sea levels. *Quaternary Research* 33, 1-17.
- Hovland, M., Risk, M., 2003. Do Norwegian deep-water coral reefs rely on seeping fluids? *Marine Geology* 198, 83-96.
- Howchin, W., 1909. Notes on the discovery of a large mass of living coral in Gulf St Vincent, with bibliographical references to the recent corals of South Australia. *Transactions and Proceedings and Report of the Royal Society of South Australia* 33, 242-252.
- Hsü, K. J., 1972. Origin of saline giants: a critical review after the discovery of the Mediterranean evaporite. *Earth Science Reviews* 8, 371-396.
- Hua, Q., Jacobsen, G. E., Zoppi, U., Lawson, E. M., Williams, A. A., Smith, A. M., McGann, M. J., 2001. Progress in radiocarbon target preparation at the ANTARES AMS centre. *Radiocarbon* 43, 275-282.
- Ingalls, A. E., Aller, R. C., Lee, C., Wakeham, S. G., 2004. Organic matter diagenesis in shallow water carbonate sediments. *Geochimica et Cosmochimica Acta* 68, 4363-4379.
- Ionin, A. S., Govberg, L. I., Novikova, Z. T., Yurkevich, M. G., P'P'rlchev, D., 1978. The result of morpholithodynamic studies in the northern part of the continental shelf of Bulgaria. *Oceanology* 18, 186-190.
- Ivanova, E. V., Murdmaa, I. O., Chepalyga, A. L., Cronin, T. M., Pasechnik, I. V., Levchenko, O. V., Howe, S. S., Manushkina, V., Platonova, E. A., 2007. Holocene sea-level oscillations and environmental changes on the Eastern Black Sea shelf. *Palaeogeography, Palaeoclimatology, Palaeoecology* 246, 228-259.
- Ivy-Ochs S., Kerschner, H., Maisch, M., Christi, M., Kubik, P. W., Schlüchter, C., 2009. Latest Pleistocene and Holocene glacier variations in the European Alps. *Quaternary Science Reviews* 28, 2137-2149.
- Jakubke, H. D., Jeschkeit, H., 1977. *Amino Acids, Peptides and Proteins – an Introduction*. Macmillan Press Ltd, London. 336 pages.
- James, M. L., Schrek, J. O., 1982. *General, Organic, and Biological Chemistry: a brief Introduction*. D. C. Heath & Company. 480 pages.

- James, P. R., Clark, I. F., 2002. Geology. In: Davies, M., Twidale, C. R., Tyler, M. J., (Eds), Natural History of Kangaroo Island, 2nd edition. Royal Society of South Australia Inc, pp. 1-22.
- Jensen, J. B., Bennike, O., Witkowski, A., Lemke, W., Kuijpers, A., 1999. Early Holocene history of the southwestern Baltic Sea: The Ancylus Lake stage. *Boreas* 28, 437-453.
- Jian, S., Wenyi, T., Wuyong, C., 2008. Ultrasound-accelerated enzymatic hydrolysis of solid leather waste. *Journal of Cleaner Production*, 16, 591-597.
- Johnson, B. J., Miller, G. H., 1997. Archaeological applications of amino acid racemization. *Archaeometry* 39, 265-287.
- Jones, D. S., 1980. Annual cycle of shell growth increment formation in two continental shelf bivalves and its paleoecologic significance. *Paleobiology* 6, 331-340.
- Jones, G. A., Gagnon, A. R., 1994. Radiocarbon chronology of Black Sea Sediments. *Deep-Sea Research I* 41, 531-557.
- Jordan, J. W., Mason, O. K., 1999. A 5000 year record of intertidal peat stratigraphy and sea level change from northwest Alaska. *Quaternary International* 60, 37-47.
- Karrow, P. F., Bada, J. L., 1980. Amino acid racemization dating of Quaternary raised marine terraces in San Diego County, California. *Geology* 8, 200-204.
- Katz, B. J., Man, E.H., 1980. The effects and implications of ultrasonic cleaning on the amino acid geochemistry of Foraminifera. In: Hare, P. E., Hoering, T. C., King, K. Jr., (Eds), *Biogeochemistry of amino acids*. John Wiley & Sons, pp. 215-222.
- Kaufman, D. S. & Manley, W. F. 1998. A new procedure for determining DL amino acid values in fossils using reverse phase liquid chromatography. *Quaternary Science Reviews* 17, 987-1000.
- Kaufman, D. S., 2000. Amino acid racemization in ostracodes. In: Goodfriend, G. A., Fogel, M. L., Macko, S. A., Wehmiller, J. F., (Eds.), *Perspectives in Amino Acid and Protein Geochemistry*. Oxford University Press, New York, pp. 145-160.
- Kaufman, D. S., 2003. Dating deep-lake sediments by using amino acid racemization in fossil ostracodes. *Geology* 31, 1049-1052.
- Kaufman, D. S., 2005. Amino acid racemization in ostracodes from Bear Lake cores BL96-1 and BL96-2, Utah and Idaho. U.S. Geological Survey Open-File Report 2005-1129, 8 pages.
- Kaufman, D. S., 2006. Temperature sensitivity of aspartic and glutamic acid racemization in the foraminifera *Pulleniatina*. *Quaternary Geochronology* 1, 188-207.
- Kaufman, D. S., Forman, S. L., Bright, J., 2001. Age of the Cutler Dam alloformation (Late Pleistocene), Bonneville Basin, Utah. *Quaternary Research* 56, 322 – 334.
- Kaufman, D. S., Manley, W. F., 1998. A new procedure for determining enantiomeric (D/L) amino acid values in fossils using reverse phase liquid chromatography. *Quaternary Science Reviews* 17, 987-1000.
- Kaufman, D. S., Miller, G. H., 1995. Isoleucine epimerisation and amino acid composition in molecular-weight separations of Pleistocene *Genyornis* eggshell. *Geochimica et Cosmochimica Acta* 59, 2757-2765.
- Kaufman, D. S., Sejrup, H-P., 1995. Isoleucine epimerisation in the high-molecular-weight fraction of Pleistocene *Arctica*. *Geochimica et Cosmochimica Acta* 14, 337-350.
- Kaufman, D.S. 2003. Amino acid paleothermometry of Quaternary ostracodes from the Bonneville Basin, Utah: *Quaternary Science Reviews* 22, 899-914.
- Keenan, E. M., Ortlieb, L., Wehmiller, J. F., 1987. Amino acid dating of Quaternary marine terraces, Bahia Asunción, Baja California Sur, Mexico. *Journal of Coastal Research* 3, 297-305.
- Keigwin, L. D., 2002. Late Pleistocene-Holocene palaeoceanography and ventilation of the Gulf of California. *Journal of Oceanography* 58, 421-432.
- Keil, R. G., Tsamakis, E., Giddings, J. C., Hedges, J. I., 1998. Biochemical distributions (amino acids, neutral sugars, and lignin phenols) among size-classes of modern marine sediments from the Washington coast. *Geochimica et Cosmochimica Acta* 62, 1347-1364.

- Keil, R. G., Tsamakis, E., Hedges, J. I., 2000. Early diagenesis of particulate amino acids in marine systems. In: Goodfriend, G. A., Collins, M. J., Fogel, M. L., Macko, S. A., & Wehmiller, J. F., (Eds), *Perspectives in Amino Acid and Protein Geochemistry*. Oxford University Press, pp. 69-82.
- Keith, M. L., Anderson, G. M., 1963. Radiocarbon dating: fictitious results with mollusc shells. *Science* 141, 634-637.
- Kendrick, G. W., Wyrwoll, K-H. Szabo, B. J. 1991. Pliocene-Pleistocene coastal events and history along the western margin of Australia. *Quaternary Science Reviews* 10, 419-439.
- Kershaw, A. P., van der Kaars, S., Moss, P. T., 2003. Late Quaternary Milankovitch-scale climatic change and variability and its impact on monsoonal Australasia. *Marine Geology*, 201, 81-95.
- Kessler, J. D., Reeburgh, W. S., Southon, J., Seifert, R., Michaelis, W., Tyler, S. C., 2006. Basin-wide estimates of the input of methane from seeps and clathrates to the Black Sea. *Earth and Planetary Science Letters* 243, 366-375.
- Kidwell, S. M., 2001. Preservation of species abundance in marine death assemblages. *Science* 294, 1091-1094.
- Kidwell, S. M., 2002. Mesh-size effects on the ecological fidelity of death assemblages: a meta analysis of molluscan live-dead studies. *Geobios, Mémoire spécial* 24, 107-119.
- Kimber, R. W. L. & Milnes, A. R. 1984. The extent of racemization of amino acids in Holocene and Pleistocene marine molluscs in southern South Australia: preliminary data on a time-framework for calcrete formation. *Australian Journal of Earth Sciences* 31, 279-286.
- Kimber, R. W. L., Griffin, C. V., 1987. Further evidence of the complexity of the racemization process in fossil shells with implications for amino acid racemization dating. *Geochimica et Cosmochimica Acta*, 51, 839-846.
- Kimber, R. W. L., Griffin, C. V., Milnes, A. R., 1986. Amino acid racemization dating: evidence of apparent reversal in aspartic acid racemization with time in shells of *Ostrea*. *Geochimica et Cosmochimica Acta* 50, 1159-1161.
- Kimber, R. W. L., Milnes, A. R., 1984. The extent of racemization of amino acids in Holocene and Pleistocene marine molluscs in southern South Australia: preliminary data on a time-framework for calcrete formation. *Australian Journal of Earth Sciences* 31, 279-286.
- Köhler-Rink, S., Köhl, M., 2000. Microsensor studies of photosynthesis and respiration in larger symbiotic foraminifera. 1. The physico-chemical microenvironment of *Marginopora vertebralis*, *Amphistegina lobifera* and *Amphisorus hemprichii*. *Marine Biology* 137, 473-486.
- Konikov, E., G., 2007. Sea-level fluctuations and coastline migration in the northwestern Black Sea area over the last 18 ky based on high-resolution lithological-genetic analysis of sediment architecture. In: Yanko-Hombach, V., Gilbert, A. S., Panin, N., Dolukhanov, P. M. (Eds.), *The Black Sea Flood Question: Changes in Coastline, Climate and Human settlement*. Springer, Dordrecht, pp. 405-435.
- Konikov, E., Likhodedova, O., Pedan, G., 2007. Paleogeographic reconstructions of sea-level change and coastline migration on the northwestern Black Sea shelf over the past 18 kyr. *Quaternary International* 167-168, 49-60.
- Koral, H., 2007. Modes, rates and geomorphological consequences of active tectonics in the Marmara region, NW Turkey – a critical overview based on seismotectonic field observations. *Quaternary International* 167-168, 149-161.
- Kowaleski, M., Goodfriend, G. A., Flessa, K. W., 1998. High-resolution estimates of temporal mixing within shell beds: the evils and virtues of time-averaging. *Paleobiology* 24, 287-304.
- Kowalewski, M., Bambach, R. K., 2003. The limits of paleontological resolution. In: Harries, P. J., (Ed), *Approaches in High-Resolution Stratigraphic Palaeontology*. Kluwer academic/Plenum Publishers, New York, pp 1-48.
- Krause, R. A., Barbour, S. L., Kowalewski, M., Kaufman, D. S., Romanek, C. S., Simões, M. G., Wehmiller, J. F., 2010. Quantitative comparisons and models of time-averaging in bivalve and brachiopod shell accumulations. *Paleobiology* 36, 428-452.

- Kriausakul, N., Mitterer, R. M., 1980. Comparison of isoleucine epimerisation in a model dipeptide and fossil protein. *Geochimica et Cosmochimica Acta* 44, 753-758.
- Kroepelin, H., 1968. Racemization of amino acids on silicates. In: Schenk, P. A., Havenaar, J., (Eds), *Advances in Organic Geochemistry*. Pergamon Press, Oxford, pp. 535-541.
- Kvavadze, E. V., Connor, S. E., 2005. *Zelkova carpinifolia* (Pallas) K. Koch in Holocene sediments of Georgia – an indicator of climatic optima. *Review of Palaeobotany and Palynology* 133, 69-89.
- Kvenvolden, K. A., 1975. Advances in the geochemistry of amino acids. *Annual Reviews of Earth and Planetary Science* 3, 183-212.
- Kvenvolden, K. A., Blunt, D. J., 1980. Amino acid dating of *Saxidomus giganteus* at Willapa Bay, Washington, by racemization of glutamic acid. In: Hare, P. E., Hoering, T. C., King, K. Jr., (Eds), *Biogeochemistry of Amino Acids*. John Wiley & Sons, pp. 393-399.
- Kvenvolden, K. A., Peterson, E., Wehmiller, J., Hare, P. E., 1973. Racemization of amino acids in marine sediments determined by gas chromatography. *Geochimica et Cosmochimica Acta* 37, 2215-2225.
- Kwiecien, O., Arz, H. W., Lamy, F., Wulf, S., Bahr, A., Röhl, U., Haug, G. H., 2008. Estimated reservoir ages of the Black Sea since the Last Glacial. *Radiocarbon* 50, 99-118.
- Lajoie, K. R., Wehmiller, J. F., Kennedy, G. L., 1980. Inter- and intra-generic trends in apparent racemization kinetics of amino acids in Quaternary mollusks. In: Hare, P. E., Hoering, T. C., King, K. Jr., (Eds), *Biogeochemistry of Amino Acids*. John Wiley & Sons, pp. 393-399.
- Lambeck, K., Smither, C., Johnston, P., 1998. Sea-level change, glacial rebound and mantle viscosity for northern Europe. *Geophysical Journal International* 134, 102-144.
- Laprida, C., Bertels-Psotka, A., 2003. Benthic foraminifers and paleoecology of a Holocene shelly concentration, Salado Basin, Argentina. *Geobios* 36, 559-572.
- Larchenkov, E., Kadurin, S., 2011. Palaeogeography of the Pontic Lowland and northwestern Black Sea shelf for the past 25 k.y. In: Buynevich, I. V., Yanko-Hombach, V., Gilbert, A. S., Martin, R. E., (Eds.), *Geology and Geoarchaeology of the Black Sea Region: Beyond the Flood Hypothesis*. Geological Society of America, Special Paper 473, 71-87.
- Lawrence, D. R., 1968. Taphonomy and information loss in fossil communities. *Geological Society of America Bulletin* 79, 1315-1330.
- Lee, S. W., Choi, C. S., 2007. The correlation between organic matrices and biominerals (myostracal prism and folia) of the adult oyster shell, *Crassostrea gigas*. *Micron* 38, 58-64.
- Lemke, G. and Sturm, M., 1997. $\delta^{18}\text{O}$ and trace element measurements as proxy for the reconstruction of climate changes at Lake Van (Turkey): Preliminary results. In: Dalfes, N.D., Kukla, G., Weiss, H., (Eds.) *Third Millennium BC Climate Change and Old World Collapse*, NATO ASI Series, Vol 149. Springer, Berlin, 654-678.
- Lericolais, G., Bulois, C., Gillet, H., Guichard, F., 2009. High frequency sea level fluctuations recorded in the Black Sea since the LGM. *Global and Planetary Change* 66, 65-75.
- Lericolais, G., Guichard, F., Morigi, C., Minereau, A., Popescu, I., Radan, S., 2010. A post Younger Dryas Black Sea regression identified from sequence stratigraphy correlated to core analysis and dating. *Quaternary International* 225, 199-209.
- Lericolais, G., Guichard, F., Morigi, C., Popescu, I., Bulois, C., Gillet, H., and Ryan, W. B. F., 2011. Assessment of Black Sea water-level fluctuations since the Last Glacial Maximum. In: Buynevich, I., Yanko-Hombach, V., Gilbert, A. S., and Martin, R. E., *Geology and Geoarchaeology of the Black Sea Region: Beyond the Flood Hypothesis*. The Geological Society of America, Boulder, Colorado, 33-50.
- Li, Q., James, N. P., Bone, Y., Cann, J., 1998. Synergetic influence of water masses and Kangaroo Island barrier on foraminiferal distribution, Lincoln and Lacepede Shelves, South Australia: a synthesis. *Alcheringa* 22, 153-176.
- Lindroth, P., Mopper, K., 1979. High performance liquid chromatographic determination of sub-picomole amounts of amino acids by precolumn fluorescence derivatisation with o-phthalaldehyde. *Analytical Chemistry* 51, 1667-1674.

- Linsley, B. K., 1996. Oxygen isotope evidence of sea level and climatic variations in the Sulu Sea over the past 150,000 years. *Nature* 380, 234-237.
- Lowenstam, H. A., 1980. Bioinorganic constituents of hard parts. In: Hare, P. E., Hoering, T. C., King, K. Jr., (Eds), *Biogeochemistry of Amino Acids*. John Wiley & Sons, pp. 3-16.
- Ludbrook, N. H. 1976. The Glanville Formation at Port Adelaide. South Australia. Geological Survey. Quarterly Geological Notes 57, 4-7.
- Ludbrook, N. H. 1984. Quaternary molluscs of South Australia. Department of Mines and Energy, South Australia, Handbook, 9.
- Ludwig, K. R., Simmons, K. R., Szabo, B. J., Winograd, I. J., Landwehr, I. J., Landwehr, J. M., Riggs, A. C., Hoffman, R. J., 1992. Mass-spectrometric Th^{230} - U^{234} - U^{238} dating of the Devils-Hole calcite vein. *Science* 258, 284-287.
- Magny, M., Bégeot, C., 2004. Hydrological changes in the European midlatitudes associated with freshwater outbursts from Lake Agassiz during the Younger Dryas event and the early Holocene. *Quaternary Research* 61, 181-192.
- Magny, M., Guiot, J., Schoellammer, P., 2001. Quantitative reconstruction of Younger Dryas to mid-Holocene paleoclimates at Le Locle, Swiss Jura, using pollen and lake-level data. *Quaternary Research* 56, 170-180.
- Major, C. O., 2002. Non-eustatic controls on sea-level change in semi-enclosed basins. PhD thesis, Columbia University.
- Major, C. O., Goldstein, S. L., Ryan, W. B. F., Lericolais, G., Piotrowski, A. M., Hajdas, I., 2006. The co-evolution of Black Sea level and composition through the last deglaciation and its paleoclimatic significance. *Quaternary Science Reviews* 25, 2031-2047.
- Major, C., Ryan, W., Lericolais, G., Hajdas, I., 2002. Constraints on Black Sea outflow to the Sea of Marmara during the last glacial-interglacial transition. *Marine Geology* 190, 19-34.
- Manley, W. F., Miller, G. H., Czywczynski, J., 2000. Kinetics of aspartic acid racemization in *Mya* and *Hiatella*: modelling age and paleotemperature of high-latitude quaternary molluscs. In: Goodfriend, G. A., Collins, M. J., Fogel, M. L., Macko, S. A., Wehmiller, J. F., (Eds), *Perspectives in Amino Acids and Protein Geochemistry*. Oxford University Press, pp. 108-119.
- Marin, F., Luquet, G., 2004. Molluscan shell proteins. *Comptus Rendus Palevol*, 3, 469-492.
- Marin, F., Pokroy, B., Luquet, G., Layrolle, P., De Groot, K., 2007. Protein mapping of calcium carbonate biominerals by immunogold. *Biomaterials* 28, 2368-2377.
- Marret, F., Mudie, P., Aksu, A., Hiscott, R. N., 2009. A Holocene dinocyst record of a two-step transformation of the Neoeuxinian brackish water lake into the Black Sea. *Quaternary International* 197, 72-86.
- Marret, F., Mudie, P., Aksu, A., Hiscott, R. N., 2010. Corrigendum to "A Holocene dinocyst record of a two-step transformation of the Neoeuxinian brackish water lake into the Black Sea"[*Quaternary International*, 197 (2009) 72-86]. *Quaternary International* 226, 161.
- Martin, R. E., 1999. *Taphonomy: a Process Approach*. Cambridge University Press. 484 pages.
- Martin, R. E., Goldstein, S. T., Patterson, R. T., 1999. Taphonomy as an environmental science. *Palaeogeography, Palaeoclimatology, Palaeoecology*, 149, vii-viii.
- Martin, R. E., Harris, M. S., Liddell, W. D., 1995. Taphonomy and time-averaging of foraminiferal assemblages in Holocene tidal flat sediments, Bahia la Choya, Sonora, Mexico (northern Gulf of California). *Marine Micropaleontology* 26, 187-206.
- Martin, R. E., Wehmiller, J. F., Harris, M. S., Liddell, W. D., 1996. Comparative taphonomy of bivalves and foraminifera from Holocene tidal flat sediments, Bahia la Choya, Sonora, Mexico, (Northern Gulf of California): taphonomic grades and temporal resolution. *Paleobiology* 22, 80-90.
- McCulloch, M. T., Esat, T., 2000. The coral record of last interglacial sea levels and sea surface temperatures. *Chemical Geology* 169, 107-129.

- McNichol, A. P., Aluwihare, L. I., 2007. The power of radiocarbon in biogeochemical studies of the marine carbon cycle: insights from studies of dissolved and particulate organic carbon (DOC and POC). *Chemical Reviews*, 107, 443-466.
- Meldahl, K. H., Flessa, K. W., 1990. Taphonomic pathways and comparative biofacies and taphofacies in a recent intertidal/shallow shelf environment. *Lethaia* 23, 43-60.
- Mendes, I., Gonzalez, R., Dias, J. M. A., Lobo, F., Martins, V., 2004. Factors influencing recent benthic foraminifera distribution on the Guadiana shelf (Southwestern Iberia). *Marine micropaleontology* 51, 171-192.
- Michenfelder, M., Fu, G., Lawrence, C., Weaver, J. C., Wustman, B. A., Taranto, L., Evans, J. S., Morse, D. E., 2003. Characterization of two molluscan crystal-modulating biomineralization proteins and identification of putative mineral binding domains. *Biopolymers* 70, 522-533.
- Middleburg, J. J., Calvert, S. E., Karlin, R., 1991. Organic-rich transitional facies in silled basins: Response to sea-level change. *Geology* 19, 679-682.
- Miller, G. H., Clarke, S. J., 2007. Amino acid dating. In: Elias, S.A., (Ed), *Encyclopaedia of Quaternary Sciences*. Elsevier, 41-52.
- Miller, G. H., Hare, P. E., 1980. Amino acid geochronology: integrity of the carbonate matrix and potential of molluscan fossils. In: Hare, P.E., Hoering, T. C., King, K. Jr., (Eds), *Biogeochemistry of Amino Acids*. John Wiley & Sons, pp. 415-444.
- Miller, G. H., Hart, C. P., Roark, E. B., Johnson, B. J., 2000. Isoleucine epimerisation in eggshells of the flightless Australian birds *Genyornis* and *Dromaius*. In: Goodfriend, G. A., Collins, M. J., Fogel, M. L., Macko, S. A., Wehmler, J. F., (Eds), *Perspectives in Amino Acid and Protein Geochemistry*. Oxford University Press, pp. 161-181.
- Miller, G. H., Hopkins, D. M., 1980. Degradation of molluscan shell protein by lava-induced transient heat flow, Pribilof Islands, Alaska: Implications for amino acid geochronology and radiocarbon dating. In: Hare, P.E., Hoering, T. C., King, K. Jr., (Eds), *Biogeochemistry of Amino Acids*. John Wiley & Sons, pp. 445-451.
- Miller, G. H., Mangerud, J., 1986. Aminostratigraphy of European marine interglacial deposits. *Quaternary Science Reviews* 4, 215-278.
- Milnes, A. R., Ludbrook, N. H., Lindsay, J. M., Cooper, B. J., 1983. The succession of Cainozoic marine sediments on Kangaroo Island, South Australia. *Transactions of the Royal Society of South Australia* 107, 1-35.
- Mitterer, R. M., Kriausakul, N., 1989. Calculation of amino acid racemization ages based on apparent parabolic kinetics. *Quaternary Science Reviews* 8, 353-357.
- Miura, O., Nishi, S., Chiba, S., 2007. Temperature-related diversity of shell colour in the intertidal gastropod *Batillaria*. *Journal of Molluscan Studies* 73, 235-240.
- Molodkov, A. N., Bolikhovskaya, N. S., 2002. Eustatic sea-level and climate changes over the last 600 ka as derived from mollusc-based ESR-chronostratigraphy and pollen evidence in Northern Eurasia. *Sedimentary Geology* 150, 185-201.
- Mudie, P. J., Rochon, A., Aksu, A. E., 2002. Pollen stratigraphy of Late Quaternary cores from Marmara Sea: land-sea correlation and paleoclimatic history. *Marine Geology* 190, 233-260.
- Muratov, V. M., Ostrovsky, A. B., Fridenberg, E. O., 1974. Quaternary stratigraphy and palaeogeography on the Black Sea coast of Western Caucasus. *Boreas* 3, 49-60.
- Murray, J.W., Stewart, K., Kassakian, S., Krynytzky, M., Di Julio, D. 2007. Oxic, suboxic, and anoxic conditions in the Black Sea. In: Yanko-Hombach V., Gilbert, A.S., Panin, N., Dolukhanov, P.M., (Eds.), *The Black Sea Flood Question: Changes in Coastline, Climate and Human Settlement*. Springer, pp. 1-22.
- Murray-Wallace, C. V., 1993. A review of the application of the amino acid racemization reaction to archaeological dating. *The Artifact* 16, 19-26.
- Murray-Wallace, C. V., 1995. Aminostratigraphy of Quaternary coastal sequences in southern Australia – an overview. *Quaternary International* 26, 69-86.

- Murray-Wallace, C. V., 2000. Quaternary coastal aminostratigraphy: Australian data in a global context. In: Goodfriend, G. A., Collins, M. J., Fogel, M. L., Macko, S. A., Wehmiller, J. F., (Eds). Perspectives in amino acid and protein geochemistry. Oxford university press, pp. 279-300.
- Murray-Wallace, C. V., 2002. Pleistocene coastal stratigraphy, sea-level highstands and neotectonism of the southern Australian passive continental margin – a review. *Journal of Quaternary Science* 17, 469-489.
- Murray-Wallace, C. V., Belperio, A. P., 1991. The Last interglacial shoreline in Australia – a review. *Quaternary Science Reviews* 10, 441-461.
- Murray-Wallace, C. V., Belperio, A. P., 1994. Identification of remanié fossils using amino acid racemization. *Alcheringa* 18, 219-227.
- Murray-Wallace, C. V., Kimber, R. W. L., 1987. Evaluation of the amino acid racemization reaction in studies of Quaternary marine sediments in South Australia. *Australian Journal of Earth Sciences* 34, 279-292.
- Murray-Wallace, C. V., Kimber, R. W. L., 1989. Quaternary marine aminostratigraphy: Perth Basin, Western Australia. *Australian Journal of Earth Sciences* 36, 553-568.
- Murray-Wallace, C. V., Kimber, R. W. L., 1993. Further evidence for apparent parabolic racemization kinetics in Quaternary molluscs. *Australian Journal of Earth Sciences* 40, 313-317.
- Murray-Wallace, C. V., Belperio, A. P., Picker, K., Kimber, R. W. L., 1991. Coastal aminostratigraphy of the last interglaciation in Southern Australia. *Quaternary Research* 35, 63-71.
- Murray-Wallace, C. V., Belperio, A., Gostin, V. A., Cann, J. H., 1993: Amino acid racemization and radiocarbon dating of interstadial marine strata (oxygen isotope stage 3), Gulf St. Vincent, South Australia. *Marine Geology* 110, 83 – 92.
- Murray-Wallace, C. V., Beu, A. G., Kendrick, G. W., Brown, L. J., Belperio, A. P., Sherwood, J. E., 2000. Palaeoclimatic implications of the occurrence of the arcoid bivalve *Anadara trapezia* (Deshayes) in the Quaternary of Australasia. *Quaternary Science Reviews* 19, 559-590.
- Murray-Wallace, C. V., Bourman, R. P. 2002. Amino acid racemization dating of a raised gravel beach deposit, Sellicks Beach, South Australia. *Transactions of the Royal Society of South Australia* 126, 21-28.
- Murray-Wallace, C. V., Ferland, M. A., Roy, P. S., 2005. Further amino acid racemization evidence for glacial age, multiple lowstand deposition on the New South Wales outer continental shelf, southeastern Australia. *Marine Geology* 214, 235-250.
- Murray-Wallace, C. V., Ferland, M. A., Roy, P. S., Sollar, A., 1996. Unravelling patterns of reworking in lowstand shelf deposits using amino acid racemization and radiocarbon dating. *Quaternary Science Reviews (Quaternary Geochronology)* 15, 685-697.
- Murray-Wallace, C. V., Ferland, M. A., Roy, P. S., Sollar, A., 1996. Unravelling patterns of reworking in lowstand shelf deposits using amino acid racemization and radiocarbon dating. *Quaternary Science Reviews* 15, 685-697.
- Murray-Wallace, C. V., Bourman, R. P., Prescott, J. R., Williams, F., Price, D. M., Belperio, A. P., 2010. Aminostratigraphy and thermoluminescence dating of coastal aeolianites and the later Quaternary history of a failed delta: The River Murray mouth region, South Australia. *Quaternary Geochronology* 5, 28-49.
- Naddeo, V., Belgiorno, V., Napoli, R. M. A., 2007. Behaviour of natural organic matter during ultrasonic irradiation. *Desalination* 210, 175-182.
- Nanson, G. C., Price, D.M., Short, S. A., Young, R. W., Jones, B. G., 1991. Comparative uranium-thorium and thermoluminescence dating of weathered Quaternary alluvium in the tropics of northern Australia. *Quaternary Research* 35, 347-366.
- Naudts, L., Greinert, J., Artemov, Y., Beaubien, S. E., Borowski, C., De Batist, M., 2008. Anomalous sea-floor backscatter patterns in methane venting areas, Dnepr paleo-delta, NW Black Sea. *Marine Geology* 251, 253-267.
- Neuberger, A., 1948. Stereochemistry of amino acids. *Advances in Protein Chemistry* 4, 297-383.

- Neveeskaya, L. A., 1965. Posdnechetvertichnye dvustvorchatye mollyuski Chernogo moray, ich sistemata, ecologia. Moskva, isdatelstvo nauka. 391 pages.
- Neveeskaya, L. A., 1974. Molluscan Shells in Deep-Water Sediments of Black Sea. In: Degens, E. T., Ross, D. A., (Eds.), The Black Sea - Geology, Chemistry and Biology. The American Association of Petroleum Geologists, Memoir 20, Tulsa, Oklahoma, pp. 349-352.
- Nicholas, W. A., Chivas, A. R., Murray-Wallace, C. V., Fink, D., 2011. Prompt transgression and gradual salinisation of the Black Sea during the early Holocene constrained by amino acid racemization and radiocarbon dating. Quaternary Science Reviews 30, 3769-3790.
- Noakes, J. E., Herz, N., 1983. University of Georgia Radiocarbon Dates VII. Radiocarbon 25, 919-929.
- Norman, M. F., 1936. The oxidation of amino-acids by hypochlorite: 1. Glycine. The Biochemical Journal 30, 484-96.
- Nunes, R. A., Lennon, G. W., 1986. Physical property distributions and seasonal trends in Spencer Gulf, South Australia: an inverse estuary. Australian Journal of Marine and Freshwater Research 37, 39-53.
- Nyman, J. A., Walters, R. J., Delaune, R. D., Patrick, W. H. Jr., 2006. Marsh vertical accretion via vegetative growth. Estuarine, Coastal and Shelf Science 69, 370-380.
- O'Donnell, T. 2003. $\delta^{13}\text{C}$ composition of amino acids from the Shells of modern and fossil *Mercenaria*. Geological Society of America Abstracts with Programs 35, No. 6, September 2003, p. 274.
- O'Leary, M., Hearty, P. J. & McCulloch, M. T. 2008. U-series evidence for widespread reef development in Shark Bay during the Last interglacial. Palaeogeography, Palaeoclimatology, Palaeoecology 259, 424-435.
- O'Neal, M. L., Wehmiller, J. F., Newell, W. L., 2000. Amino acid geochronology of Quaternary coastal terraces on the northern margin of Delaware Bay, southern New Jersey, U.S.A. In: Goodfriend, G. A., Collins, M. J., Fogel, M. L., Macko, S. A., Wehmiller, J. F., (Eds), Perspectives in Amino Acid and Protein Geochemistry. Oxford University Press, pp. 301-319.
- Ogawa, Y., Takahashi, K., Yamanaka, T., Onodera, J., 2009. Significance of euxinic condition in the middle Eocene paleo-Arctic basin: a geochemical study on the IODP Arctic Coring Expedition 302 sediments. Earth and Planetary Science Letters 285, 190-197.
- Oguz, T., Su, J., 2004. Semi-enclosed seas, islands and Australia pan-regional overview. In, Robinson, Allan R., and Brink, Kenneth, H., (Eds.) The Sea, Volume 14, 83-116.
- Oguz, T., Tugrul, S., Kideys, A. E., Ediger, V., Kubilay, N., 2004. Physical and biochemical characteristics of the Black Sea. In, Robinson, A. R., Brink, K. H., (Eds), The Sea: The global coastal ocean. Harvard University Press, pp.1331-1369.
- Ojala, A. E. K., Heinsalu, A., Saarnisto, M., Tiljander, M., 2005. Annually laminated sediments date the drainage of the Ancylus Lake and early Holocene shoreline displacement in central Finland. Quaternary International 130, 63-73.
- Ongan, D., Algan, O., Kapan-Yeşilyurt, S., Nazik, A., Ergin, M., Eastoe, C., 2009. Benthic faunal assemblages of the Holocene sediments from the southwest Black Sea shelf. Turkish Journal of Earth Sciences 18, 1-59.
- Orlova, M. I., Therriault, T. W., Antonov, P. I., Shcherbina, G. Kh., 2005. Invasion ecology of quagga mussels (*Dreissena rostriformis bugensis*): a review of evolutionary and phylogenetic impacts. Aquatic Ecology 39, 401-418.
- Orme, C.A., Noy, A., Wierzbicki, A., McBride, M. T., Grantham, M., Teng, H. H., Dove, P. M., DeYoreo, J. J., 2001. Formation of chiral morphologies through selective binding of amino acids to calcite surface steps. Nature 411, 775-779.
- Otsmann, M., Suursaar, Ü., Kullas, T., 2001. The oscillatory nature of the flows in the system of straits and small semienclosed basins of the Baltic Sea. Continental Shelf Research 21, 1577-1603.
- Owen, L. A., Bright, J., Finkel, R. C., Jaiswal, M. K., Kaufman, D. S., Mahan, S. Radtke, U., Schneider, J. S., Sharp, W., Singhvi, A. K. W., Claude N., 2007. Numerical dating of a Late Quaternary spit-shoreline complex at the northern end of Silver Lake playa, Mojave Desert,

- California: A comparison of the applicability of radiocarbon, luminescence, terrestrial cosmogenic nuclide, electron spin resonance, U-series and amino acid racemization methods. *Quaternary International* 166, 87-110.
- Oxburgh, R., Pierson-Wickmann, A.-C., Reisberg, L., Hemming, S., 2007. Climate-correlated variations in seawater $^{187}\text{Os}/^{188}\text{Os}$ over the past 200,000 yr: evidence from the Cariaco Basin, Venezuela. *Earth and Planetary Science Letters* 263, 246-258.
- Panin, N., Panin, S., Herz, N., Noakes, J. E., 1983. Radiocarbon dating of the Danube Delta deposits. *Quaternary Research* 19, 245-255.
- Parfitt, S. A., Barendregt, R. W., Breda, M., Candy, I., Collins, M. J., Coope, G. R., Durbridge, P., Field, M. H., Lee, J. R., Lister, A. M., Mutch, R., Penkman, K. E. H., Preece, R. C., Rose, J., Stringer, C. B., Symmons, R., Whittaker, J. E., Wymer, J. J., Stuart, A. J., 2005. The earliest record of human activity in northern Europe. *Nature*, 438, 1008-1012.
- Passmore, V. L., Williamson, P. E., Maung, T. U., Gray, A. R. G., 1993. The Gulf of Carpentaria – a new basin and new exploration targets. *Australian Petroleum Exploration Association Journal*, 33, 297-314.
- Patterson, R. T., Guilbault, J.-P., Clague, J. J., 1999. Taphonomy of tidal marsh foraminifera: implications of surface sample thickness for high-resolution sea-level studies. *Palaeogeography, Palaeoclimatology, Palaeoecology*, 149, 199-211.
- Peizhen, Z., Molnar, P., Downs, W. R., 2001. Increased sedimentation rates and grain sizes 2 ± 4 Myr ago due to the influence of climate change on erosion rates. *Nature* 410, 891-897.
- Penkman, K. E. H., 2005. Amino Acid Geochronology: a closed system approach to test and refine the UK model. Unpublished PhD thesis, University of Newcastle.
- Penkman, K. E. H., Kaufman, D. S., Maddy, D., Collins, M. J., 2008. Closed-system behavior of the intra-crystalline fraction of amino acids in mollusk shells. *Quaternary Geochronology* 3, 2-25.
- Penkman, K. E. H., Preece, R. C., Keen, D. H., Maddy, D., Schreve, D. C., Collins, M. J., 2007. Testing the aminostratigraphy of fluvial archives: the evidence from intra-crystalline proteins within freshwater shells. *Quaternary Science Reviews* 26, 2958-2969.
- Pereira-Mouries, L., Almeida, M. J., Ribeiro, C., Peduzzi, J., Barthelemy, M., Milet, C., Lopez, E., 2002. Soluble silk-like organic matrix in the nacreous layer of the bivalve *Pinctada maxima*: a new insight in the biomineralization field. *European Journal of Biochemistry* 269, 4994-5003.
- Peterson, L. C., Haug, G. H., Murray, R. W., Yarincik, K. M., King, J. W., Bralower, T. J., Kameo, K., Rutherford, S. D., Pearce, R. B., 2000. Late Quaternary stratigraphy and sedimentation at site 1002, Cariaco Basin (Venezuela). In: R. M. Leckie, H. Sigurdsson, G. D. Acton, G. Draper (Eds.) *Proceedings of the Ocean Drilling Program Scientific Results Volume* 165.
- Pietrzak, J. E., Bates, J. M., Scott, R. M., 1973. Constituents of unionid extrapallial fluid. I. Electrophoretic and immunological studies of protein components. *Biology Bulletin* 144, 391-399.
- Pingitore, N. E. Jr., Fretzdorff, S. B., Seitz, B. P., Estrada, L. Y., Borrego, P. M., Crawford, G. M., Love, K. M., 1993. Dissolution kinetics of CaCO_3 in common laboratory solvents. *Journal of Sedimentary Petrology* 63, 641-645.
- Playá, E., Cendón, D. I., Travé, A., Chivas, A. R., García, A., 2007. Non-marine evaporites with both inherited marine and continental signatures: The Gulf of Carpentaria, Australia, at ~ 70 ka. *Sedimentary Geology* 201, 276-285.
- Pokroy, B., Fitch, A. N., Lee, P. L., Quintana, J. P., Caspi, E. N., Zolotoyabko, E., 2006. Anisotropic lattice distortions in the mollusc-made aragonite: A widespread phenomenon. *Journal of Structural Biology* 153, 145-150.
- Popescu, I., 2008. Processus sédimentaires récents dans l'éventail profond du Danube (Mer Noire). *GeoEcoMarina*, 14, special publication 2, 201 pages.
- Popescu, I., De Batist, M., Lericolais, G., Nouzé, H., Poort, J., Panin, N., Versteeg, W., Gillet, H., 2006. Multiple bottom-simulating reflections in the Black Sea: potential proxies of past climate conditions. *Marine Geology* 227, 163-176.

- Popescu, I., De Batist, M., Lericolais, G., Nouzé, H., Poort, J., Panin, N., Versteeg, W., Gillet, H., 2006. Multiple bottom-simulating reflections in the Black Sea: potential proxies of past climate conditions. *Marine Geology* 227, 163-176.
- Popescu, I., Lericolais, G., Panin, N., De Batist, M., Gillet, H., 2007. Seismic expression of gas and gas hydrates across the western Black Sea. *Geo-Marine Letters* 27, 173-183.
- Popescu, I., Lericolais, G., Panin, N., Normand, A., Dinu, C., LeDrezen, E., 2004. The Danube submarine canyon (Black Sea): morphology and sedimentary processes. *Marine Geology* 206, 249-265.
- Popescu, I., Lericolais, G., Panin, N., Wong, H. K., Droz, L., 2001. Late Quaternary channel avulsions on the Danube deep-sea fan, Black Sea. *Marine Geology* 179, 25-37.
- Powell, E. N., Parsons-Hubbard, K. M., Callender, W. R., Staff, G. M., Rowe, G. T., Brett, C. E., Walker, S. E., Raymond, E., Carlson, D. D., White, S., Heise, E. A., 2002. Taphonomy on the continental shelf and slope: two-year trends – Gulf of Mexico and Bahamas. *Palaeogeography, Palaeoclimatology, Palaeoecology* 184, 1-35.
- Prebble, M., Sim, R., Finn, J., Fink, D., 2005. A Holocene pollen and diatom record from Vanderlin Island, Gulf of Carpentaria, lowland tropical Australia. *Quaternary Research* 64, 357-371.
- Preiss, W. V., 2000. The Adelaide Geosyncline of South Australia and its significance in Neoproterozoic continental reconstruction. *Precambrian Research* 100, 21-63.
- Puverel, S., Houlbrèque, F., Tambutté, E., Zoccola, D., Payan, P., Caminiti, N., Tambutté, S., Allemand, D., 2007. Evidence of low molecular weight components in the organic matrix of the reef building coral, *Stylophora pistillata*. *Comparative Biochemistry and Physiology A* 147, 850-856.
- Reading, H. G., 1996. *Sedimentary Environments: Processes, Facies and Stratigraphy*. Blackwell Science Ltd, Oxford. 688 pages
- Reeburgh, W. S., 2007. Oceanic methane biogeochemistry. *Chemical Reviews* 107, 486-513.
- Reeburgh, W. S., Tyler, S. C., Carrol, J.-L., 2006. Stable carbon and hydrogen isotope measurements on Black Sea water-column methane. *Deep-Sea Research II* 53, 1893-1900.
- Reimer, P. J., Baillie, M. G. L., Bard, E., Bayliss, A., Beck, J. W., Blackwell, P. G., Ramsey, C. B., Buck, C. E., Burr, G. S., Edwards, R. L., Friedrich, M., Grootes, P. M., Guilderson, T. P., Hajdas, I., Heaton, T. J., Hogg, A. G., Hughen, K. A., Kaiser, K. F., Kromer, B., McCormac, F. G., Manning, S. W., Reimer, R. W., Richards, D. A., Southon, J. R., Talamo, S., Turney, C. S. M., van der Plicht, J., Weyhenmeyer, C. E., 2009. Intcal09 and Marine09 Radiocarbon Age Calibration Curves, 0-50,000 Years Cal BP. *Radiocarbon* 51, 1111-1150.
- Renaud, P. E., Riggs, S. R., Ambrose, W. G. Jr., Schmid, K., Snyder, S. W., 1997. Biological-geological interactions: storm effects on macroalgal communities mediated by sediment characteristics and distribution. *Continental Shelf Research* 17, 37-56.
- Reubsæet, J. L. E., Beijnen, J. H., Bult, A., van Maanen, R. J., Marchal, J. A. D., Underberg, W. J. M., 1998. Analytical techniques used to study the degradation of proteins and peptides: chemical instability. *Journal of Pharmaceutical and Biomedical Analysis* 17, 955-978.
- Rhodes, E. G., 1982. Depositional model for a chenier plain, Gulf of Carpentaria, Australia. *Sedimentology* 29, 201-221.
- Riggs, N., 2002. Post-glacial palaeosealevels, inferred from foraminifers in Gulf St Vincent, South Australia. Unpublished thesis, B. Sc. Honours, University of Wollongong.
- Rivas-Martinez, S., 1996-2005. Phytosociological Research Center, Spain. <http://www.globalbioclimatics.org/station/ru-kerch.htm>
- Robbins, L. L., Andrews, S., Ostrom, P. H., 2000. Characterisation of ultrastructural and biochemical characteristics of modern and fossil shells. In: Goodfriend, G. A., Collins, M. J., Fogel, M. L., Macko, S. A., Wehmiller, J. F., (Eds), *Perspectives in Amino Acids and Protein Geochemistry*. Oxford University Press, pp. 108-119.
- Robbins, L. L., Brew, K., 1990. Proteins from the organic matrix of core-top and fossil planktonic foraminifera. *Geochim Cosmochim Acta* 54, 2285-2292.

- Robert, C., 2004. Late Quaternary variability of precipitation in southern California and climatic implications: clay mineral evidence from the Santa Barbara Basin, ODP Site 893. *Quaternary Science Reviews* 23, 1029-1040.
- Robinson, A. B., Rudd, C. J., 1974. Deamidation of glutaminy and asparaginy residues in peptides and proteins. *Current topics in Cellular Regulation* 8, 247-295.
- Rossignol-Strick, M., 1995. Sea-land correlation of pollen records in the eastern Mediterranean for the glacial-interglacial transition: biostratigraphy versus radiometric timescale. *Quaternary Science Reviews* 14, 893-915.
- Rousseau, M., Pereira-Mouriès, Almeida, M.-J., Milet, C., Lopez, E., 2003. The water-soluble matrix fraction from the nacre of *Pinctada maxima* produces earlier mineralisation of MC3T3-E1 mouse pre-osteoblasts. *Comparative Biochemistry and Physiology*, B 135, 1-7.
- Ryan, W. B. F., Major, C. O., Lericolais, G., Goldstein, S. L., 2003. Catastrophic flooding of the Black Sea. *Annual Reviews of Earth and Planetary Science* 31, 525-524.
- Ryan, W. B. F., Pitman, W. C. III, Major, C. O., Shimkus, K., Moskalenko, V., Jones, G. A., Diminitrov, P., Görür, N., Sakiç, M., Yüce, H., 1997. An abrupt drowning of the Black Sea shelf. *Marine Geology* 138, 119-126.
- Ryan, W.B.F., 2007. Status of the Black sea flood hypothesis. In: Yanko- Hombach, V., Gilbert, A.S., Panin, N., Dolukhanov, P.M. (Eds.), *The Black Sea Flood Question: Changes in Coastline, Climate and Human Settlement*, Springer, pp. 63-88.
- Salvador, A., 1994. *International Stratigraphic Guide: a guide to stratigraphic classification, terminology and procedure*. International Subcommission on Stratigraphic Classification of IUGS International Commission on Stratigraphy. 2nd edition, Geological Society of America, 214 pp.
- Sandiford, M., 2002. Neotectonics of southeastern Australia: linking the Quaternary faulting record with seismicity and in situ stress. *Geological Society of Australia Special Publication* 22, 101-113.
- Sarashina, I., Endo, K., 1998. Primary structure of a soluble matrix of scallop shell: implications for calcium carbonate biomineralisation. *American Mineralogist* 83, 1510-1515.
- Schroeder, R. A., Bada, J. L., 1973. Glacial-Postglacial temperature difference deduced from aspartic acid racemization in fossil bones. *Science*, 182, 479-481.
- Schroeder, R. A., Bada, J. L., 1976. A review of the geochemical applications of the amino acid racemization reaction. *Earth-Science Reviews* 12, 347-391.
- Schröder-Adams, C., 2006. Estuaries of the past and present: a biofacies perspective. *Sedimentary Geology* 190, 289-298.
- Seed, R., 1980. Shell growth and form in the bivalvia. In: Rhoads, D. C., Lutz, R. A., (Eds), *Skeletal Growth of Aquatic Organisms*. Plenum Press, pp. 23-67.
- Sejrup, H. P., Iversen, M., Larsen, E., Landvik, J. Y., Janocko, J., 1999. A stage 7 marine interglacial record (the Grødeland Interglacial) on Jæren, southwestern Norway; foraminiferal, stable isotopes and amino acid evidence. *Boreas* 28, 326-346.
- Sejrup, H. P., Nagy, J., Brigham-Grette, J., 1989. Foraminiferal stratigraphy and amino acid geochronology of interglacial and glacial sediments in the Norwegian Channel, northern North Sea. *Norsk Geologisk Tidsskrift* 69, 111-124.
- Seto, J., Zhang, Y., Hamilton, P., Wilt, F., 2004. The localisation of occluded matrix proteins in calcareous spicules of sea urchin larvae. *Journal of Structural Biology* 134, 56-66.
- Shcherbakov, F. A. and Babak, Ye. V., 1979. Stratigraphic subdivision of the Neoeuxinian deposits in the Black Sea. *Oceanology* 19, 298.
- Shcherbakov, F. A., 1991. Lithodynamic conditions of sedimentation on the Black Sea shelf of Crimea. *Oceanology* 31, 353-355.
- Shcherbakov, F. A., Babak, Ye. V., 1979. Stratigraphic subdivision of the Neoeuxinian deposits in the Black Sea. *Oceanology* 19, 298-300.
- Shlyukov, A. I., Tsyryapkin, V. A., Nedospasova, L. V., Parunin, O. B., 1989. Amino-acid composition and geochronometry based on fossil mollusks of the Caspian. 107-110. Translated from:

- Aminokislrotnyy sostav I geokhronometriya po iskopayemym mollyuskam Kaspiya. Doklady Akademii Nauk SSSR, 1989, vol 309, 681-685.
- Short, A. D., Fotheringham, D. G., 1986. Coastal morphodynamics and Holocene evolution of the Kangaroo Island coast, South Australia. Coastal Studies Unit Technical Report No. 86/1. Coastal Studies Unit, Department of Geography, The University of Sydney, Sydney, NSW, 2006, Australia, 112 pages.
- Siani, G., Paterne, M., Arnold, M., Bard, E., Métiévier, B., Tisnerat, N., Bassinot, F., 2000. Radiocarbon reservoir ages in the Mediterranean Sea and Black Sea. Radiocarbon 42, 271-280.
- Siddall, M., Pratt, L. J., Helfrich, K. R., Giosan, L., 2004. Testing the physical oceanographic implications of the suggested sudden Black Sea infill 8400 years ago. Paleoclimatology 19, PA 1024, doi:10.1029/2003PA000903.
- Slack, J. F., Turner, R. J. W., Ware, P. L. G., 1998. Boron-rich mud volcanoes of the Black Sea region: Modern analogues to ancient sea-floor tourmalinites associated with Sullivan-type Pb-Zn deposits? Geology 26, 439-442.
- Sloss, C. R., Jones, B. G., McClennen, C. E., de Carli, J., Price, D. M., 2006. The geomorphological evolution of a wave-dominated barrier estuary: Burrill Lake, New South Wales, Australia. Sedimentary Geology 187, 229-249.
- Sloss, C. R., Murray-Wallace, C. V., Jones, B. G., 2006. Aminostratigraphy of two Holocene wave-dominated barrier estuaries in southeastern Australia. Journal of Coastal Research 22, 113-136.
- Sloss, C. R., Murray-Wallace, C. V., Jones, B. G., Wallin, T., 2004. Aspartic acid racemization dating of mid-Holocene to recent estuarine sedimentation in New South Wales, Australia: a pilot study. Marine Geology 212, 45-59.
- Smart, T., Grimes, K. G., Douth, H. F., Pinchin, J., 1980. The Carpentaria and Karumba Basins, North Queensland, Australia. Bureau of Mineral Resources, Geology and Geophysics, Bulletin 202, 73 pp.
- Smith, G. G., Evans, R. C., 1980. The effect of structure and conditions on the rate of racemization of free and bound amino acids. In: Hare, P. E., Hoering, T. C., King, K. Jr., (Eds), The Biogeochemistry of Amino Acids. John Wiley and Sons, pp. 257-282.
- Smith, G. G., Williams, K. M., Wonnacott, D. M., 1978. Factors affecting the rate of racemization of amino acids and their significance to geochronology. The Journal of Organic Chemistry 43, 1-5.
- Sone, E. D., Weiner, S., Addadi, L., 2007. Biomineralisation of limpet teeth: a cryo-TEM study of the organic matrix and the onset of mineral deposition. Journal of Structural Biology 158, 428-444.
- Sorokin, V. M., Kuprin, P. N., 2007. On the character of Black Sea level rise during the Holocene. Moscow University Geology Bulletin 62, 334-341. Original Russian text: 2007, Vestnik Moskovskogo Universiteta Geologiya 5, 40-46.
- Soulet, G., Ménot, G., Garreta, V., Rostek, F., Zaragosi, S., Lericolais, G., Bard, E., 2011b. Black Sea "Lake" reservoir age evolution since the Last Glacial – Hydrologic and climatic implications. Earth and Planetary Science Letters 308, 245-258.
- Soulet, G., Ménot, G., Lericolais, G., Bard, E., 2011a. A revised calendar age for the last reconnection of the Black Sea to the global ocean. Quaternary Science Reviews 30, 1019-1026.
- Staas, W. H., Spurlock, L. A., 1975. Chemistry of ultrasound. Part IV. Effects of ultrasound on some amino acids. JCS Perkin 1, 1675-1679.
- Stadnitskaia, A., Ivanov, M. K., Poludetkina, E. N., Kreulen, R., van Weering, T. C. E., 2008. Sources of hydrocarbon gases in mud volcanoes from the Sorokin Trough, NE Black Sea, based on molecular and carbon isotopic compositions. Marine and Petroleum Geology 25, 309-322.
- Stadnitskaia, A., Ivanov, M. K., Poludetkina, E. N., Kreulen, R., van Weering, T. C. E., 2008. Sources of hydrocarbon gases in mud volcanoes from the Sorokin Trough, NE Black Sea, based on molecular and carbon isotopic compositions. Marine and Petroleum Geology 25, 309-322.
- Stanev, E. V., Beckers, J. M., Lancelot, C., Staneva, J. V., LeTraon, P. Y., Peneva, E. L., Gregoire, M., 2002. Coastal-open sea exchange in the Black Sea: Observations and modelling. Estuarine Coastal Shelf Science 54, 601– 620.

- Stanley, D. J., Hait, A. K., 2000. Deltas, radiocarbon dating, and measurements of sediment storage and subsidence. *Geology* 28, 295-298.
- Stathoplos, L., Hare, P. E. 1993. Bleach removes labile amino acids from deep sea planktonic foraminiferal shells. *Journal of Foraminiferal Research* 23, 102-107.
- Stirling, C. H., Esat, T. M., Lambeck, K., McCulloch, M. T., 1998. Timing and duration of the Last Interglacial: evidence for a restricted interval of widespread coral reef growth. *Earth and Planetary Science Letters* 160, 745-762.
- Stirling, C. H., Esat, T. M., McCulloch, M. T., Lambeck, K., 1995. High-precision U-series dating of corals from Western Australia and implications for the timing and duration of the Last Interglacial. *Earth and Planetary Science Letters* 135, 115-130.
- Strechie-Sliwinski, C., 2007. Changements environnementaux récents dans la zone de Nord-Ouest de la Mer Noire. *GeoEcoMarina* 13, special publication 1, 270 p.
- Stuart, W. J. Jnr., von Sanden, A. T., 1972. Palaeozoic history of the St. Vincent Gulf region, South Australia. *The APEA Journal*, 9-16.
- Su, X., Belcher, A. M., Zaremba, C. M., Morse, D. E., Stucky, G. D., Heuer, A. H., 2002. Structural and microstructural characterization of the growth lines and prismatic microarchitecture in red abalone shell and the microstructures of abalone "flat pearls". *Chemistry of Materials* 14, 3106-3117.
- Sur, H. İ, Özsoy, E., Ilyin, Y. P., Ünlüata, Ü., 1996. Coastal/deep ocean interactions in the Black Sea and their ecological/environmental impacts. *Journal of Marine Systems* 7, 293-320.
- Surge, D. M., Lohmann, K. C., Goodfriend, G. A., 2003. Reconstructing estuarine conditions: oyster shells as recorders of environmental change, Southwest Florida. *Estuarine, Coastal and Shelf Science* 57, 737-756.
- Svitoch, A. A., 2009. Karangatian stratotypes in the Taman and Kerch Peninsulas (Comparative Analysis). *Doklady Earth Sciences* 425, 210-212.
- Svitoch, A. A., 2009. Khvalynian transgression of the Caspian Sea was not a result of water overflow from the Siberian proglacial lakes, nor a prototype of the Noachian flood. *Quaternary International* 197, 115-125.
- Swain, G., Woodhouse, A., Hand, M., Barovich, K., Schwarz, M., Fanning, C. M., 2005. Provenance and tectonic development of the late Archaean Gawler Craton, Australia; U-Pb zircon, geochemical and Sm-Nd isotopic implications. *Precambrian Research* 141, 106 – 136.
- Swanson, K., van der Lingen, G., 1997. Late Quaternary ostracod and planktonic foraminiferal dissolution signals from the eastern Tasman Sea – palaeoenvironmental implications. *Palaeogeography, Palaeoclimatology, Palaeoecology* 131, 303-314.
- Sykes, G. A., Collins, M. J., Walton, D. I., 1995. The significance of a geochemically isolated intracrystalline organic fraction within biominerals. *Organic Geochemistry* 23, 1059-1065.
- Szabo, B. J. 1979. Uranium-series age of coral reef growth on Rottneest Island, Western Australia. *Marine Geology*, 29, M11 – M15.
- Terashima, M., 1991. Abundances of acidic amino acids and non-protein amino acids in carbonates and muddy sediments, and their relationship to diagenetic decomposition. *Chemical Geology* 90, 123-131.
- Therriault, T. W., Docker, M. F., Orlova, M. I., Heath, D. D., MacIsaac, H. J., 2004. Molecular resolution of the family Dreissenidae (Mollusca: Bivalvia) with emphasis on Ponto-Caspian species, including first report of *Mytilopsis leucophaea* in the Black Sea basin. *Molecular Phylogenetics and Evolution* 30, 479-489.
- Thom, N., 2010. A hydrological model of the Black and Caspian Seas in the late Pleistocene and early-middle Holocene. *Quaternary Science Reviews* 29, 2989-2995.
- Thompson, W. G., Spiegelman, M. W., Goldstein, S. L., Speed, R. C., 2003. An open-system for U-series age determinations of fossil corals. *Earth and Planetary Science Letters* 210, 365-381.
- Toler, S. K., Hallock, P., 1998. Shell malformation in stressed *Amphistegina* populations: relation to biomineralisation and paleoenvironmental potential. *Marine Micropaleontology* 34, 107-115.

- Tonkov, S., 2003. Holocene palaeovegetation of the northwestern Pirin Mountains (Bulgaria) as reconstructed from pollen analysis. *Review of Palaeobotany and Palynology* 124, 51-61.
- Tonkov, S., Bozilova, E., Possnert, G., Velčev, A., 2008. A contribution to the postglacial vegetation history of the Rila Mountains, Bulgaria: the pollen record of Lake Trilistnika. *Quaternary International* 190, 58-70.
- Torgersen, T., Hutchinson, M. F., Searle, D. E., Nix, H. A., 1983. General bathymetry of the Gulf of Carpentaria and the Quaternary physiography of Lake Carpentaria. *Palaeogeography, Palaeoclimatology, Palaeoecology* 41, 207-225.
- Twidale, C. R., Bourne, J. A., 2002. The land surface. In: Davies, M., Twidale, C. R., Tyler, M. J., (Eds), *Natural History of Kangaroo Island*, 2nd edition. Royal Society of South Australia Inc, 159-168.
- Uchupi, E., Ross, D. A., 2000. Early Holocene marine flooding of the Black Sea. *Quaternary Research* 54, 68-71.
- Urban, E. R., Sundby, B., Malanotte-Rizzoli, P., Melillo, J. M., (Eds) 2009. *Watersheds, Bays, and Bounded Seas: the science and management of semi-enclosed marine systems*. Island Press, 269 pp.
- Vallentyne, J. R., 1964. Biogeochemistry of organic matter – II Thermal reaction kinetics and transformation products of amino compounds. *Geochimica et Cosmochimica Acta* 28, 157-188.
- Van Daele, M., van Welden, A., Moernaut, J., Beck, C., Audemard, F., Sanchez, J., Jouanne, F., Carrillo, E., Malave, G., Lemus, A., De Batist, M., 2011. Reconstruction of Late-Quaternary sea- and lake-level changes in a tectonically active marginal basin using seismic stratigraphy: the Gulf of Cariaco, NE Venezuela. *Marine Geology* 279, 37-51.
- Van der Zwaan, G. J., Duijnste, I. A. P., den Dulk, M., Ernst, S. R., Jannink, N. T., Kouwenhoven, T. J., 1999. Benthic foraminifers: proxies or problems? A review of paleocological concepts. *Earth-Science Reviews* 46, 213-236.
- Van Duin, A. C. T., Collins, M. J., 1998. The effects of conformational constraints on aspartic acid racemization. *Organic Geochemistry* 29, 1227-1232.
- Van Duin, A., Collins, M., 2000. Investigation into amino acid racemization pathways using computational chemical methods. *Goldschmidt 2000, Journal of conference abstracts*, 5, 1036.
- Veevers, J. J., 2006. Updated Gondwana (Permian – Cretaceous) earth history of Australia. *Gondwana Research* 9, 231-260.
- Vermoere, M., Degryse, P., Vanhecke, L., Muchez, Ph., Paulissen, E., Smets, E., Waelkens, M., 1999. Pollen analysis of two travertine sections in Basköy (southwestern Turkey): implications for environmental conditions during the early Holocene. *Review of Palaeobotany and Palynology* 105, 93-110.
- Veron, J. E. N., 1986. *Corals of Australia and the Indo-Pacific*. Angus and Robertson, Australia. 644 pages.
- Veron, J. E. N., Marsh, L. M., 1988. *Hermatypic corals of Western Australia. Records and annotated species list. Records of the Western Australian Museum. Supplement no. 29*, 1-136.
- von Der Borch, C. C., Bada, J. L., Schwebel, D.L., 1980. Amino acid racemization dating of Late Quaternary strandline events of the coastal plain sequence near Robe, southeastern South Australia. *Transactions of the Royal Society of South Australia* 104, 167-170.
- Waelbroeck, C., Labeyrie, L., Michel, E., Duplessy, J. C., McManus, J. F., Lambeck, K., Balbon, E., Labracherie, M., 2002. Sea-level and deep water temperature changes derived from benthic foraminifera isotopic records. *Quaternary Science Reviews* 21, 295-305.
- Wakeham, S.F., Beier, J.A., Clifford, C.H., 1991. Organic matter sources in the Black Sea as inferred from hydrocarbon distributions. In: Murray, J. W., Izdar, E., (Eds), *Black Sea Oceanography*. NATO Advance Studies Institute, Kluwer, Dordrecht, pp. 319-341.
- Walker, K. R., Bambach, R. K., 1971. The significance of fossil assemblages from fine-grained sediments: time-averaged communities. *Geological Society of America Abstracts with Program* 3, 783-784.

- Walker, M. J. C., 2005. Quaternary Dating Methods. John Wiley & Sons Ltd. 286 pages.
- Walton, D., 1998. Degradation of intracrystalline proteins and amino acids in fossil brachiopods. *Organic Geochemistry* 28, 389-410.
- Walton, D., Curry, G. B., 1994. Extraction, analysis and interpretation of intracrystalline amino acids in fossils. *Lethaia* 27, 179-184.
- Webster, P. J., 1994. The role of hydrological processes in ocean-atmosphere interactions. *Review of Geophysics* 32, 427-476.
- Wehmiller, J. F., 1980. Intergeneric differences in apparent racemization kinetics in molluscs and foraminifera: implications for models of diagenetic racemization. In: Hare, P. E., Hoering, T. C., King, K. Jr., (Eds), *Biogeochemistry of amino acids*. John Wiley and Sons, pp. 342-355.
- Wehmiller, J. F., 1984. Interlaboratory comparison of amino acid enantiomeric values in fossil Pleistocene mollusks. *Quaternary Research* 22, 109-120.
- Wehmiller, J. F., 1984. Relative and absolute dating of Quaternary molluscs with amino acid racemization: evaluation, applications and questions. In: Mahaney, W. C., (Eds), *Quaternary Dating Methods*. Developments in Palaeontology and Stratigraphy 7, 171-193.
- Wehmiller, J. F., Miller, G. H., 2000. Aminostratigraphic dating methods in Quaternary geology. In: Noller, J. S., Sowers, J. M., Letts, W. R., (Eds), *Quaternary Geochronology: methods and applications*. American Geophysical Union, pp. 187 - 220.
- Wehmiller, J. F., Stecher, H. A., York, L. L., Friedman, I., 2000. The thermal environment of fossils: effective ground temperatures at aminostratigraphic sites on the U. S. Atlantic Coastal Plain. In: G.A. Goodfriend, M. J. Collins, M. L. Fogel, S. A. Macko, J. F. Wehmiller, (Eds), *Perspectives in amino acids and protein geochemistry*. Oxford University Press, pp. 219 – 250.
- Wehmiller, J. F., York, L. L., Bart, M. L., 1995. Amino acid racemization geochronology of reworked Quaternary molluscs on U.S. Atlantic coast beaches: implications for chronostratigraphy, taphonomy, and coastal sediment transport. *Marine Geology* 124, 303-337.
- Weiner, S., Erez, J., 1984. Organic matrix of the shell of the foraminifer, *Heterostegina depressa*. *Journal of Foraminiferal Research* 14, 206-212.
- Weiss, I. M., Tuross, N., Addadi, L., Weiner, S., 2002. Mollusc larval shell formation: amorphous calcium carbonate is a precursor phase for aragonite. *Journal of Experimental Zoology* 293, 478-491.
- Whitelaw, M. J., Batts, B. D., Murray-Wallace, C. V., McRae, C. R., 2001. Diagenesis of the organic matrix in *Anadara trapezia* during the late Quaternary: preliminary findings. *Proceedings of the Linnean Society of New South Wales* 123, 225-234.
- Wick, L., Lemcke, G., Sturm, M., 2003. Evidence of Lateglacial and Holocene climatic change and human impact in eastern Anatolia: high-resolution pollen, charcoal, isotopic and geochemical records from the laminated sediments of Lake Van, Turkey. *The Holocene* 13, 665-675.
- Wilbur, K. M., 1964. Shell formation and regeneration. In: Wilbur, K. M., Yonge, C. M., (Eds), *Physiology of Mollusca*, 1. New York, Academic Press, pp. 243-277.
- Williams, K. M., Smith, G. G., 1977. A critical evaluation of the application of amino acid racemization to geochronology and geothermometry. *Origins of Life* 8, 91-144.
- Wilt, F. H., 2005. Developmental biology meets materials science: morphogenesis of biomineralised structures. *Developmental Biology* 280, 15-25.
- Woodroffe, C. D., Brooke, B. P., Linklater, M., Kennedy, D. M., Jones, B. G., Buchanan, C., Mleczko, R., Hua, Q., Zhao, J-x., 2010. Response of coral reefs to climate change: expansion and demise of the southernmost Pacific coral reef. *Geophysical Research Letters*, 37, doi: 10.1029/2010GL044067.
- Yamashita, Y., Tanoue, E., 2004. Chemical characteristics of amino acid-containing dissolved organic matter in seawater. *Organic Geochemistry* 35, 679-692.
- Yan, X. -H., HO, C. -R., Zheng, Q., Klemas, V., 1992. Temperature and size variabilities of the Western Pacific Warm Pool. *Science* 258, 1643-1645.

- Yanko, V. V., Troitskaya, T. S., 1987. Pozdnechetvertichnye foraminifery Chernogo Moria (Late Quaternary Foraminifera of the Black Sea). Nauka, Moscow. In Russian.
- Yanko-Hombach, V. V., 2007. Controversy over Noah's Flood in the Black Sea: Geological and foraminiferal evidence from the shelf. In: Yanko-Hombach, V., Gilbert, A. S., Panin, N., Dolukhanov, P. M. (Eds.), The Black Sea Flood Question: Changes in Coastline, Climate, and Human Settlement. Springer, New York, pp. 149-203.
- Yanko-Hombach, V., Gilbert, A. S., Dolukhanov, P., 2007. Controversy over the great flood hypotheses in the Black Sea in light of geological, paleontological, and archaeological evidence. Quaternary International 167-168, 91-113.
- Yu K.-F., Zhao J.-X., Shi Q., Chen T.-G., Wang P.-X., Collerson K. D., Liu T.-S., 2006. U-series dating of dead Porites corals in the South China Sea: evidence for episodic coral mortality over the past two centuries. Quaternary Geochronology 1, 129-141.
- Zhang, C., Xie, L., Huang, J., Liu, X., Zhang, R., 2006. A novel matrix protein family participating in the prismatic layer framework formation of pearl oyster, *Pinctada fucata*. Biochemical and Biophysical Research Communications 344, 735-740.
- Zhao J. X., Hu K., Collerson K. D., Xu H. K., 2001. Thermal ionization mass spectrometry U-series dating of a hominid site near Nanjing, China. Geology 29, 27-30.
- Zhao, J.-X., Xia, Q. & Collerson, D. 2001. Timing and duration of the Last Interglacial inferred from high resolution U-series chronology of stalagmite growth in Southern Hemisphere. Earth and Planetary Science Letters 184, 635-644.
- Zhou, W. J., Chen, M. B., Liu, Y. H., Dohanue, D., Head, J., Lu, X. F., Jull, A. J. T., Deng, L., 2000. Radiocarbon determinations using a minicyclotron: applications in archaeology. Nuclear Instruments and Methods in Physics Research B 173, 201-205.
- Zhu, Z. R., Wyrwoll, K.-H., Collins, L. B., Chen, J. H., Wasserburg, G. J., Eisenhauer, A. 1993. High-precision U-series dating of Last Interglacial events by mass spectrometry: Houtman Abrolhos Islands, Western Australia. Earth and Planetary Science Letters 118, 281-293.
- Zubakov, V. A., 1988. Climatostratigraphic scheme of the Black Sea Pleistocene and its correlation with the oxygen-isotope scale and glacial events. Quaternary Research 29, 1-24.
- Zuschin, M., Stachowitsch, M., Stanton, R. J., Jr. 2003. Patterns and processes of shell fragmentation in modern and ancient marine environments. Earth-Science Reviews 63, 33-82.

Appendices

Abstract A

INQUA 501- IGCP 521 Sixth Plenary Meeting and Field Trip, Rhodes, Greece, 27 September – 5 October 2010

Oral presentation

Nicholas, W. A., Chivas, A. R., Murray-Wallace, C. V., Fink, D.,

Radiocarbon and amino acid racemization dating of the post-glacial Black Sea: rapid transgression and gradual salinisation of the palaeo-lake by Mediterranean-sourced water

Keywords: age-mixing, molluscs, continental shelf, *Cardium*, *Mytilus*

Introduction

Amino acid racemization (AAR) dating is reliant on the preservation of amino acids in the carbonate skeletons of molluscs, foraminifers and ostracods for relative dating. It is reliant on additional chronological methods, particularly ^{14}C , uranium-series, and luminescence dating to calibrate D/L values to obtain numeric ages. The aminostratigraphic chronometer has been used with success in a range of environments from glacial to tropical, and from deep marine to fluvial. Paired AAR and accelerator mass spectrometer (AMS) ^{14}C dating methods have been used to determine the extent of reworking in several continental shelf localities. These include studies on individual molluscs (Murray-Wallace *et al.*, 1995), and single foraminifers (Nicholas *et al.*, 2010).

This study determined the extent of reworking of shells on the continental shelf of the Black Sea using paired AAR and AMS ^{14}C radiocarbon dating methods. Because we have focused on the extent of mixing of shells with different ages the results of this study have allowed us a fresh perspective into the post-glacial history of the Black Sea. Here we present new radiocarbon data, summarise the results of this study, and draw conclusions on the utility of the AAR method to future studies in the Black Sea and similar basins. Furthermore, we evaluate the use of radiocarbon dating methods in the Black Sea in light of our new and previous ^{14}C ages.

Results

Three *Cardium edule* shells from core BS37A-82, previously dated by AAR methods (Nicholas *et al.*, 2009) were determined to be $5,005 \pm 45$ ^{14}C a (UWGA 7221, 1.68 m in core), $5,255 \pm 50$ ^{14}C a (UWGA 7220, 1.85 m in core) and $5,500 \pm 50$ ^{14}C a (UWGA 7224, 1.95 m in core) – ages uncalibrated and uncorrected for reservoir effect. Two *Mytilus* fragments, from 0.85 m depth in core 342, were determined to be $4,365 \pm 30$ and $5,765 \pm 35$ ^{14}C a.

Discussion

These new radiocarbon ages, each on an individual bivalve mollusc shell or shell fragment, illustrate some of the complexities in attempts to use paired AAR-AMS dating methods at fine scales of resolution. Previously, the range of amino acid racemization ages, calibrated using AMS data was estimated to be of the order of 3,600 a in adjacent horizons in core BS37A-82 (Nicholas *et al.*, 2009), and based on the previous data a significant amount of vertical mixing was evident in the core section 1.49-1.95 m. However, the radiocarbon ages from this section of core increase downcore, indicating

stratigraphic order. Using these additional ^{14}C ages in calibrating AAR D/L values increases the estimated extent of time averaging (now 4,200) between shells in adjacent horizons (1.93 and 1.95 m depth) in core BS37A-82.

In contrast, based on the ^{14}C age of *Mytilus* from core 45B, outer Ukrainian shelf, an AMS calibrated AAR age of 6,200 a was indicated for the age of *Mytilus* fragments from core sample 342/3, 0.85 m depth in core (Nicholas *et al.*, 2009). The new AMS determinations, each on a single *Mytilus* fragment from 342/3 indicates ^{14}C ages of $4,365 \pm 30$ and $5,765 \pm 35$ a for these fragments recovered from sediment dominated by *Dreissena*, but which also includes *Cardium* dated to $9,140 \pm 60$ ^{14}C a. These ages are younger than the previous calibrated AAR age (6,200 a) for this horizon using a single ^{14}C age determination on *Mytilus*. Recalibration of D/L values using these new ^{14}C ages in addition to the first ^{14}C determination on *Mytilus* results in a mean calibrated age of $5,099 \pm 1,435$ a for the horizon 342/3 ($n = 5$; 0.85 m in core 342), and a mean calibrated age of $7,377 \pm 621$ a for the horizon 342/2 ($n = 2$; 0.55 m in core 342). These new ^{14}C ages indicate the minimum depositional age for sediments in core 342/3 are $4,365 \pm 30$ ^{14}C a, underneath which are fluvial and lacustrine sediments of $8,920 \pm 60$ to $9,620 \pm 60$ ^{14}C a (Nicholas *et al.*, 2009). Both marine and non-marine shells and sediments in the samples from this core are reworked.

Conclusion

The value of AAR studies in the Black Sea and similar semi-enclosed basins lies in the use of this method as a preliminary and exploratory stratigraphic tool. Where burial histories for the strata of interest are similar, this allows the separation of strata into time-equivalent aminostratigraphic units prior to applying appropriate isotopic or exposure dating methods to refine stratigraphies and calibrate D/L values.

We conclude that sedimentary strata on the shelves of the Black Sea are the result of a prompt transgression of the pre-existing restricted lake by marine water through the Bosphorus Strait, giving rise to a basic three-layer stratigraphy that varies among locations. The basal lacustrine unit on the outer Ukrainian and Romanian shelf, consisting of *Dreissena* shells, commonly partially to completely bleached and strongly dissolved, formed in response to the prompt ingress of warmer water derived from the Marmara Sea. The overlying units, in core 342 for example, indicate a stabilizing water column, with significant mixing on the inner shelf of older and younger shells. This transgression raised the water level from approximately -100 m (-107 m, core 45B) to the level of the Bosphorus Sill (-35 m) in 300 a, yet salinity took significantly longer to change. This gradual transition from lacustrine to marine conditions is indicated by the progression from Caspian-type *Dreissena*-dominated shells (salinity range < 3-12 psu) to a brackish water fauna that includes *Monodacna caspia*, to marine species dominated by Mytilids. This model indicates that proponents of the ‘flood’ hypothesis and those proposing a gradual salinisation are both correct, with simple calculations indicating it would be impossible to suddenly salinise a pre-existing very low salinity lake.

The onset of significant salinisation is indicated by the earliest sapropel at 7,500 a BP, and by the significant presence of *Mytilus* and *Cardium* in cores at several depths on the continental shelf from the same time period.

Radiocarbon ages on bulk samples consisting of multiple individual shells dated by scintillation-counting, and commonly of mixed species, point to high water-levels existing on the shelves of the Black Sea prior to the marine ingress. There are however, no AMS ages older than approximately 12 ka BP on molluscs from the shelves of the Black Sea – and this suggests that the shelves may have been subaerially exposed at some point in time since the LGM lowstand. We suggest that the use of AMS ^{14}C ages on single shells not be utilized alongside radiocarbon ages on samples consisting of multiple individual shells. While the environmental data from individual shell samples may be readily utilized,

determining the relevance of data obtained from shells commonly mixed from a variety of environments and of differing ages is problematic.

Acknowledgements

We gratefully acknowledge the assistance of Prof. V. Yanko-Hombach and Sergei Kadurin for providing us with samples from cores 721, 342 and 45B. Prof. E. Konikov provided samples from cores BS37-82 and BS37A-82.

References

- Hua, Q., Jacobsen, G. E., Zoppi, U., Lawson, E. M., Williams, A. A., Smith, A. M., and McGann, M. J., 2001. Progress in radiocarbon target preparation at the Antares AMS centre. *Radiocarbon* 43, 275-285.
- Kaufman, D. S., Manley, W. F., 1998. A new procedure for determining DL amino acid values in fossils using reverse phase liquid chromatography. *Quaternary Science Reviews* 17, 987-1000.
- Konikov, E., Likhodedova, O., and Pedan, G., 2007. Paleogeographic reconstructions of sea-level change and coastline migration on the northwestern Black Sea shelf over the past 18 kyr. *Quaternary International* 167-168, 49-60.
- Murray-Wallace, C. V., 1995. Aminostratigraphy of Quaternary coastal sequences in southern Australia – an overview. *Quaternary International* 26, 69-86.
- Nicholas, W. A., Chivas, A. R., Kadurin, S., Murray-Wallace, C. V., Fink, D., 2009. Chronology of an early Holocene transgressive Black Sea. In, Gilbert, A., and Yanko-Hombach, V., eds., *Extended Abstracts of the Fifth Plenary Meeting and Field Trip of IGCP-521 "Black Sea – Mediterranean corridor during the last 30 ky: Sea level change and human adaptation" (2008-2010) – INQUA 0501 "Caspian-Black Sea-Mediterranean Corridor during last 30 ky: Sea level change and human adaptive strategies" (2008-2010)*. Izmir-Çanakkale (Turkey), August 22-31, 2009, pp. 129-131.
- Nicholas, W. A., Murray-Wallace, C. V., Kaufman, D., Chivas, A. R., 2010. Aminostratigraphy of Late Quaternary Gulf St Vincent, South Australia: amino acid racemization dating of single foraminifera, *Elphidium*. Australian Earth Sciences Convention, Canberra, 4-8 July, 2010.
- Yanko-Hombach, V., Gilbert, A. S., Dolukhanov, P., 2007. Controversy over the Great Flood Hypotheses in the Black Sea in light of geological, paleontological, and archaeological evidence. *Quaternary International* 167-168, 91-113.

Abstract B

Australian Earth Science Convention, 4-8 July, 2010

Oral Presentation

Nicholas, W. A., Murray-Wallace, C. V., Kaufman, D., Chivas, A. R.

Aminostratigraphy of Late Quaternary Gulf St Vincent, South Australia: amino acid racemization dating of single foraminifera, *Elphidium*

Gulf St Vincent is a semi-enclosed basin within the southern Australian margin. It is isolated from the Southern Ocean by the presence of Kangaroo Island, whose northern coast provides the southernmost margin to this basin. The Late Quaternary sediments from Gulf St Vincent have been the subject of several studies investigating changes in sea level primarily attributed to eustatic oscillations over Last interglacial (MIS 5e, 125 ka) to Holocene time-scales (Cann *et al.*, 1988; Murray-Wallace *et al.*, 1993). A significant discrepancy exists between estimated palaeo-water depths for the Gulf during MIS 3 (-22 to -30 m; Cann *et al.*, 1988; Murray-Wallace *et al.*, 1993) and that of the coral record at Huon Peninsula (-37 to -53 m; Chappell *et al.*, 1996; Murray-Wallace, 2002; Waelbroek *et al.*, 2002). The aims of this study were to derive an amino acid racemization based chronology for Gulf St Vincent using single *Elphidium* tests (foraminifers), and to estimate sea-level within the Gulf during MIS3. Reverse-Phase High Performance Liquid Chromatography (RP-HPLC; Kaufman and Manley, 1998) was undertaken on samples consisting of single *Elphidium* and *Marginopora* (foraminifers) and multiple *Elphidium* tests, on single bivalve shells and on whole-rock samples. Accelerator Mass Spectrometric ^{14}C dating at ANSTO was undertaken on four bulk samples consisting of multiple *Elphidium* tests, the results of which were used for calibration of amino acid D/L values to obtain numeric ages. Uranium-series dating was undertaken at the University of Queensland on a single coral specimen, *Goniopora lobata*, recovered during this work from coastal outcrop at Kingscote, Kangaroo Island.

The utility of single *Elphidium* tests as subject material for AAR studies was examined using a visual preservation index and D/L values. After screening AAR results for covariance of racemization among amino acids in each test, and for contamination, the results from 492 individual foraminifer tests were utilised (63 rejected) from core SV#5, (394 of which were from the core section 0.53-3.85 m).

Core SV#5 was differentiated into two units, Holocene and Marine Isotopic Stage 3, based on D/L values in single *Elphidium* tests, with the boundary at 52-53 cm. The mean calibrated age using all tests (mean glutamic acid D/L = 0.256 ± 0.022 , $n = 394$ *Elphidium* tests) for the pre-Holocene section of SV#5 was $47,800 \pm 8,100$ a. Using only the best preserved tests (mean glutamic acid D/L = 0.260 ± 0.024 , $n = 256$ *Elphidium* tests) this age was $49,300 \pm 9,000$ a. These AAR data demonstrate the stability of amino acids in calcite tests of foraminifera. In contrast with bivalve molluscs, leaching of amino acids may occur in less-well preserved shells, indicated by lowered D/L values. This was not observed in these results. Our data indicate the foraminifer *Elphidium* can be considered robust for this type of study. Therefore an additional 177 individual *Elphidium* were analysed from 22 further sediment samples from core ($n = 16$) and outcrops ($n = 6$) in Gulf St Vincent. Despite the differences in AAR methods between RP-HPLC (this study) and gas chromatography (e.g. Murray-Wallace *et al.* 1993), and the different sample types (principally foraminifer tests here, molluscs in previous studies) the conclusions are similar.

Single foraminifer tests of Last Interstadial age are present in sediments in water depths of > 30 m, and suggest a palaeo-sealevel for Gulf St Vincent during MIS 3 of -20 to -30 m. This is higher than global estimates for this isotopic stage, yet consistent with previous estimates for this location. The presence of last interglacial (MIS 5e) age coral, *Goniopora lobata* at Kingscote, whose southern-most habitat at present is in Shark Bay, W. Australia, and Elizabeth Reef, eastern Australia, indicates a strengthened Leeuwin Current in Southern Australian waters during the last interglacial (MIS 5e), and sea-surface temperatures 2-3° higher than at present.

Abstract C

Australian Earth Science Convention, 4-8 July, 2010

Poster Abstract

Nicholas, W. A., Chivas, A. R., Murray-Wallace, C. V., Fink, D.,

Post-glacial development of the Black Sea: a problem of two radiocarbon-based chronologies

The Black Sea Flood hypothesis (Ryan and Pitman, 1997) proposed a catastrophic early Holocene transgression of the Black Sea region by Mediterranean sourced water through the Bosphorus Strait, while outflow hypotheses argue the converse. This debate has been dependent on radiocarbon methods for numeric ages. Here we present a new radiocarbon-based chronology based upon new accelerator mass spectrometry (AMS) ^{14}C ages on individual molluscs and peat samples, and a reassessment of previous AMS ^{14}C and conventional radiocarbon ages on peat and shells. These data, supported by the first amino acid racemization dating of bivalve molluscs in the Black Sea, indicates prompt infilling of the Black Sea from an initial depth (~100m) below that of the Bosphorus Sill (-35 m).

Amino acid racemization (AAR) and AMS ^{14}C methods were used for chronology on shells, and AMS ^{14}C was used on peat samples. Four peat and 56 shell samples were analysed from five cores, BS37-82, BS37A-82 (Odessa Bay, Ukrainian shelf, water depth 18 m), core 721 (Sukhumi Bay, Georgia, 14.9 m water depth) core 342 (western Ukrainian shelf, 30 m water depth) and core 45 (outer Ukrainian shelf, water depth 107 m). Four shell samples consisted of bulk samples of juvenile *Cardium*, and 52 were of individual valves. Samples of core material were selected at Odessa National University and analysed at the School of Earth and Environmental Sciences, University of Wollongong, for the extent of amino acid racemization in molluscs. AMS was undertaken at the laboratories of the Australian Nuclear Science and Technology Organisation using methods detailed in Hua *et al.*, (2001). Reverse-Phase High Performance Liquid Chromatography was used to examine the extent of AAR in the bivalve molluscs *Dreissena*, *Cardium edule*, *Chione gallina* and *Mytilus*. The AAR method used (Kaufman and Manley, 1998) was modified by strong bleaching (12.5% NaOCl) for one hour.

We have found that our AMS ^{14}C ages on peat in core 721, Sukhumi Bay, Georgia, are broadly comparable with earlier data (Apakidze, 1987; Yanko and Troitskaya, 1987) from the same core using β -counting radiocarbon methods. Thus, our results suggest that earlier ^{14}C data using β -counting (mostly from eastern European laboratories) are as valid as those from western laboratories. In light of these results we have integrated previously published ^{14}C ages on peat and bivalve molluscs to model the development of the early Holocene Black Sea.

A basinwide transgressive event is recorded in the sedimentary record on the shelves of the Black Sea. This signature is visible in each of the examined cores. In core 721 this transgressive event is dated to just after 8530 ^{14}C yr BP on peat but prior to 8210 ± 120 ^{14}C yr BP on marine molluscs. This is also recorded in core 45 (107 m depth, outer Ukrainian shelf) after 8695 ± 50 ^{14}C a BP (lacustrine phase) but prior to 6530 ± 45 ^{14}C a BP (marine). Reworked shells in core 342 (30 m water depth, inner Ukrainian shelf) testify to the change from alluvial and lagoonal (peat, and *Dreissena* and *Monodacna* bivalves) to marine conditions (indicated by the presence of the Mediterranean bivalve mollusc, *Mytilus*) after 9020 ^{14}C a BP but prior to 6200 a BP (AAR).

Integrating the data presented here with those of previously published ages on peat (Balabanov, 2007; Gorur *et al.*, 2001; Filipova-Marinova, 2007) and molluscs (Lericolais *et al.*, 2009) indicate a

transgression into the Black Sea from 8760 ^{14}C yr BP, and a near-zero radiocarbon reservoir age in *Dreissena* shells (indicative of low to near-zero salinity) marking a rapidly transgressing coastline. This transgression took c. 300 yr to reach the level of the Bosphorus sill from an initial water depth of c. 100 m, occurring after drawdown of the pre-existing lake initiated at the beginning of the Younger Dryas.

We conclude that two radiocarbon chronologies on shells have been used to debate the history of the Black Sea: AMS ^{14}C ages on single valves, and conventional ^{14}C ages on bulk shell samples. These do not appear equivalent because the AMS ^{14}C ages on single valves appear to give younger ages than the bulk samples, and many of the bulk shell samples dated by conventional ^{14}C methods consist of marine and non-marine shells which, based on stratigraphic relationships in cores, inhabited the Black Sea at different times. Thus the use of ^{14}C ages on bulk shell samples from the Black Sea has muddled the scientific waters in these investigations.

Abstract D

IGCP 521 Fifth Plenary Meeting and Field Trip, Izmir-Çanakkale (Turkey), August 22-31, 2009

Oral presentation

Nicholas W. A., Chivas A. R., Kadurin, S., Murray-Wallace C.V., Fink, D.

Chronology of an Early Holocene transgressive Black Sea

Keywords: Radiocarbon, Amino Acid Racemization, Peat, *Dreissena*, *Mytilus*, *Cardium*

Introduction

Debate on the post-glacial connection of the Black Sea with the Mediterranean through the narrow Bosphorus Strait and Marmara Sea has been dependent on radiocarbon methods for numeric ages (e.g. Uchupi and Ross, 2000; Görür *et al.*, 2001; Aksu *et al.*, 2002; Ryan *et al.*, 2003; Bahr *et al.*, 2006; Major *et al.*, 2006; Ivanova *et al.*, 2007; Yanko-Hombach *et al.*, 2007; Bahr *et al.*, 2008; Giosan *et al.*, 2009; Lericolais *et al.*, 2009). Here, we present a chronology for the Holocene Black Sea based upon accelerator mass spectrometry (AMS) ages on individual molluscs, and both AMS and conventional radiocarbon ages on peat deposits.

Methods

Amino acid racemization (AAR) and AMS methods were used for chronology on shells, and AMS was used on peat samples. Four peat and 56 shell samples were analysed from five cores, BS37-82, BS37A-82 (Konikov *et al.*, 2007), core 721 (Yanko-Hombach *et al.*, 2007) core 342, (Ukrainian shelf, 45°43'09" N, 30°34'28" E, water depth 30 m) and core 45, (Ukrainian shelf, 44°40'16" N 31°17'30" E, water depth 107 m). Four shell samples consisted of bulk samples of juvenile *Cardium*, and 52 were of individual valves. Samples of core material were selected at Odessa National University and analysed at the School of Earth & Environmental Sciences, University of Wollongong, Australia for the extent of amino acid racemization in molluscs. AMS was undertaken at the laboratories of the Australian Nuclear Science and Technology Organisation using methods detailed in Hua *et al.*, (2001). Reverse-Phase High Performance Liquid Chromatography was used to examine the extent of AAR in the bivalve molluscs *Dreissena*, *Cardium edule*, *Chione gallina* and *Mytilus*. The AAR method used (Kaufman and Manley, 1998) was modified by strong bleaching (12.5% NaOCl) for one hour. Amino acid racemization D/L values from molluscs were calibrated with AMS ^{14}C ages, uncorrected for reservoir effect, obtained from the same shell samples.

Results

Reworked valves of *Cardium edule* from core BS 37A, inner Ukrainian shelf (water depth 19.6 m), have ^{14}C -calibrated AAR ages of between 2445 (1.93 m) and 6045 yr (1.95 m) in adjacent horizons. These indicate the extent of age-mixing in closely spaced horizons is up to 3,600 a in BS 37A.

Peat in core 721, Sukhumi Bay, Georgia, recovered from 14.9 m water depth, was dated to 9370 ± 70 ^{14}C a BP (26.5 m depth) and 8530 ± 110 ^{14}C a BP (26.2 m) (Nicholas *et al.*, 2008). These are overlain by marine molluscs (*Cardium*) dated to 8210 ± 120 ^{14}C a BP (22.0 m depth in core). Ages on *Cardium* above this are 3495 ± 50 (17.25 m), 3190 ± 90 (15.0 m), 2530 ± 80 (8.0 m), and 1790 ± 90 ^{14}C a BP (2.0 m). These data indicate a high sedimentation rate (0.9 cm a^{-1}) between 1790 and 3495 ^{14}C a BP, and a comparatively low rate at this location in the early to mid Holocene (0.1 cm a^{-1}).

Peat in core 342, Ukrainian Shelf (1.15 m in core, 30 m water depth) was dated to 9020 ± 70 ^{14}C a BP, while peat from 1.65 m depth in the same core was dated to 8920 ± 60 ^{14}C a BP. A single *Dreissena polymorpha* valve recovered from the peat at 1.15 m was dated to 9600 ± 60 ^{14}C a BP, while a single *Cardiid* (0.85 m depth, core 342) was dated to 9140 ± 60 ^{14}C a BP.

Two *Dreissena rostriformis* valves sampled from a bleached shell hash layer, (0.44 m depth, core 45), recovered from 107 m water depth on the outer Ukrainian shelf were dated to 8695 ± 50 and 8820 ± 70 ^{14}C a BP. These were overlain by a *Mytilus* layer composed of broken but unbleached *Mytilus* fragments, and dated to 6530 ± 45 ^{14}C a BP on a single valve. The top 15 cm of core 45 consists of mud with the bivalve *Modiolus*.

Discussion

Our results suggest that earlier ^{14}C data using beta-counting (mostly from former eastern European laboratories) are as valid as those from western laboratories. We have found that our AMS ages on peat in core 721, Sukhumi Bay, Georgia, are broadly comparable with those of Yanko and Troit-skaya, (1987) using conventional radiocarbon methods. Our reassessment of previously published ages on peat and molluscs (Appendix 1, 2 of Yanko-Hombach *et al* 2007) supports this conclusion. The youngest age on peat granules (8530 ± 110 ^{14}C a BP) in core 721, recovered from below the level of the Bosphorus sill (-35 m), is similar to recent estimates (Lericolais *et al.*, 2009) for the onset of the most recent transgression of the Black Sea. The low sedimentation rate in Sukhumi Bay between 8210 and 3495 ^{14}C a BP is similar to that found by Connor (2004) with reduced sedimentation in the Georgian Mountains Between 4450 and 9540 ^{14}C a BP.

Conclusion

A transgressive event is recorded in core 721, dated to just after 8530 ^{14}C a BP on peat but prior to 8210 ± 120 ^{14}C yr BP on marine molluscs. A transgression is also recorded in core 45 at -107 m depth occurring after 8695 ± 50 ^{14}C a BP but prior to 6530 ± 45 ^{14}C a BP. A change in conditions in core 342 from alluvial and lagoonal to marine (indicated by the presence of the Mediterranean taxa, *Cardium*) after 9020 ^{14}C a BP at -30 m on the Ukrainian shelf also points to a transgression. We conclude that these three local events are evidence for a transgression of the Black Sea in the Early Holocene, whose signature is recorded basin-wide. Comparison of the data presented here with those of previously published ages on peat (Balabanov, 2007; Gorur *et al.*, 2001; Filipova-Marinova, 2007) and molluscs (Lericolais *et al.*, 2009) suggest a transgression into the Black Sea from 8760 ^{14}C a BP, and a near-zero radiocarbon reservoir age in the pre-existing lacustrine phase.

References

- Aksu, A. E., Hiscott, R. N., Yaşar, D., İşler, F. I., Marsh, S., 2002. Seismic stratigraphy of Late Quaternary deposits from the southwestern Black Sea shelf: evidence for non-catastrophic variations in sea-level during the last ~ 10000 yr. *Marine Geology* 190, 61-94.
- Bahr, A., Arz, H. W., Lamy, F., Wefer, G., 2006. Late glacial to Holocene paleoenvironmental evolution of the Black Sea, reconstructed with stable oxygen isotope records obtained on ostra-cod shells. *Earth and Planetary Science Letters* 241, 863-875.
- Bahr, A., Lamy, F., Arz, H., Major, C., Kwiecien, O., Wefer, G., 2008. Abrupt changes of temperature and water chemistry in the late Pleistocene and early Holocene Black Sea. *Geochemistry, Geophysics, Geosystems* (G-cubed) 9(1). DOI:10.1029/2007GC001683.
- Balabanov, I. P., 2007. Holocene sea-level changes of the Black Sea. In, V. Yanko-Hombach et al eds, *The Black Sea Flood Question*, Ch 30, 711-730.
- Filipova-Marinova, M., 2007. Archaeological and paleontological evidence of climate dynamics, sea-level change, and coastline migration in the Bulgarian sector of the circum-Pontic region. In, V. Yanko-Hombach et al., (eds), *The Black Sea Flood Question*, 453-481.

- Giosan, L., Filip, F., Constatinescu, S., 2009. Was the Black Sea catastrophically flooded in the early Holocene? *Quaternary Science Reviews*, 28, 1-6.
- Görür, N., Çağatay, M. M., Emre, Ö., Alpar, B., Sakıncı, M., İslamoğlu, Y., Algan, O., Erkal, T., Kecer, M., Akkök, R., Karlık, G., 2001. Is the abrupt drowning of the Black Sea shelf at 7150 yr BP a myth? *Marine Geology* 176, 65-73.
- Hua, Q., Jacobsen, G. E., Zoppi, U., Lawson, E. M., Williams, A. A., Smith, A. M., McGann, M. J., 2001. Progress in radiocarbon target preparation at the Antares AMS centre. *Radiocarbon* 43, 275-282.
- Ivanova, E. V., Murdmaa, I. O., Chepalyga, A. L., Cronin, T. M., Pasechnik, I. V., Levchenko, O. V., Howe, S. S., Manushkina, V., Platonova, E. A., 2007. Holocene sea-level oscillations and environmental changes on the Eastern Black Sea shelf. *Palaeogeography, Palaeoclimatology, Palaeoecology*, 246, 228-259.
- Kaufman, D. S., Manley, W. F., 1998. A new procedure for determining DL amino acid values in fossils using reverse phase liquid chromatography. *Quaternary Science Reviews* 17, 987-1000.
- Konikov, E., Likhodedova, O., Pedan, G., 2007. Paleogeographic reconstructions of sea-level change and coastline migration on the northwestern Black Sea shelf over the past 18 kyr. *Quaternary International* 167-168, 49-60.
- Lericolais, G., Bulois, C., Gillet, H., and Guichard, F., (2009). High frequency sea level fluctuations recorded in the Black Sea since the LGM. *Global and Planetary Change* 66, 65-75.
- Major, C. O., Goldstein, S. L., Ryan, W. B. F., Lericolais, G., Piotrowski, A. M., Hajdas, I., 2006. The co-evolution of Black Sea level and composition through the last deglaciation and its paleoclimatic significance. *Quaternary Science Reviews* 25, 2031-2047.
- Nicholas, W. A., Chivas, A. R., Murray-Wallace, C. V., Yanko-Hombach, V., 2008. Amino acid racemisation and AMS radiocarbon dating of Holocene Black Sea core sediments. In, extended abstracts, IGCP 521-INQUA 0501 Fourth Plenary Meeting and Field Trip, Bucharest (Romania)-Varna (Bulgaria), 4-16 October. p. 125-126.
- Ryan, W. B. F., Pitman, W. C. III, Major, C. O., Shimkus, K., Moskalenko, V., Jones, G. A., Diminitrov, P., Görür, N., Sakıncı, M., Yüce, H., 1997. An abrupt drowning of the Black Sea shelf. *Marine Geology* 138, 119-126.
- Ryan, W. B. F., Major, C. O., Lericolais, G., Goldstein, S. L., 2003. Catastrophic flooding of the Black Sea. *Annual Reviews of Earth and Planetary Science* 31, 525-524.
- Uchupi, E., Ross, D. A., 2000. Early Holocene marine flooding of the Black Sea. *Quaternary Research* 54, 68-71.
- Yanko, V. V., Troitskaya, T. S., 1987. Pozdnechetvertichnye foraminifery Chernogo Moria (Late Quaternary Foraminifera of the Black Sea). Nauka, Moscow. In Russian
- Yanko-Hombach, V., Gilbert, A. S., Dolukhanov, P., 2007. Controversy over the great flood hypotheses in the Black Sea in light of geological, paleontological, and archaeological evidence. *Quaternary International* 167-168, 91-113.
- Yanko-Hombach, V., Gilbert, A. S., Panin, N., Dolukhanov, P. M. (Eds) 2007 *The Black Sea Flood Question: Changes in Coastline, Climate and Human settlement*. Springer, Dordrecht

Abstract E

IGCP 521 Fifth Plenary Meeting and Field Trip, Izmir-Çanakkale (Turkey), August 22-31, 2009

Oral presentation

Nicholas, W. A., Chivas, A. R., Murray-Wallace, C. V., Fink, D., Yanko-Hombach, V., Chepalyga, A., Kadurin, S.

Last Interglacial Kerch Strait: an aminostratigraphic perspective

Keywords: Amino Acid Racemization, *Cardium edule*, *Chione gallina*, *Helicella*,

Introduction

Shallow marine fauna of last interglacial (MIS 5e) age exist at a number of locations within the Black Sea region, distal from their source – the Mediterranean Sea. These taxa, having been transported during the Karangatian transgression (~125 ka), indicate a time period in which salinity rose to approximately 30‰ in this restricted sea (Muratov *et al.*, 1974; Dodonov *et al.*, 2000). In the northern Black Sea region, sedimentary units of Karangatian age exist on the Caucasus coast, inner Ukrainian shelf, and Kerch Strait. This latter location is the site of Karangatian stratotypes at Eltigen, Kerch Peninsula, Ukraine and at Cape Tuzla, Taman Peninsula, Krasnodor Territory, Russia (Dodonov *et al.*, 2003; Svitoch, 2009).

Marine coastal sedimentary sequences at Eltigen in Kerch Strait have been ascribed a last interglacial age (MIS 5e, Eemian, Mikulino) based on U/Th dating techniques (Zubakov, 1988; Arslanov, 1993; Dodonov *et al.*, 2000; Arslanov *et al.*, 2002). However, the range of ages obtained using U/Th methods on molluscs from Kerch Strait, spans up to 75 ka (Arslanov *et al.*, 2002), though the most recent analyses suggest ages between approximately 90 and 130 ka for the sedimentary sequence at Eltigen (Arslanov *et al.*, 2002). The southernmost section at Eltigen has also been dated to MIS 7a and 7c (Bylinsky *et al.*, 1990).

Earlier data from the coastal deposits at Eltigen, Maly Kut, Cape Tuzla and Cape Krotkov obtained using luminescence and radiocarbon dating methods are inconsistent in many instances with the most recent uranium-thorium ages (Zubakov, 1988). The principal chronological methods used to ascertain the timing of sea-level and environmental change for last interglacial (MIS 5e) sedimentary sequences from coastal successions have been uranium-series and luminescence dating. An alternative to these, and used with success in a number of studies on Australian, North American and European sedimentary sequences, is the amino acid racemization geochronological technique. Therefore the focus of this study was to date these coastal sedimentary sequences in Kerch Strait, using aminostratigraphic methods, and where possible to correlate among these deposits located on the eastern and western coasts of Kerch Strait.

Methods

Fieldwork was undertaken in May 2007. Amino acid racemization (AAR, Kaufman and Manley, 1998), ¹⁴C accelerator mass spectrometry (AMS, Hua *et al.*, 2001), and uranium-series (Zhao *et al.*, 2001) dating were undertaken on shells recovered from Eltigen, Cape Tuzla, Maly Kut, Cape Krotkov and Feodosia. Reverse-Phase High Performance Liquid Chromatography (Kaufman and Manley, 1998) was used to examine the extent of AAR in the bivalve molluscs *Cardium edule*, *Chione gallina* and *Mytilus*, and in the gastropod *Helicella*. A limited number of additional AAR analyses were performed on whole-rock and single foraminifera (*Elphidium*) samples. ¹⁴C AMS ages were obtained on two *Helicella*

recovered from loess-like sediments, Eltigen. Six uranium-series analyses were undertaken on single valves from articulated *Cardium edule* and *Chione gallina*.

Results

These results indicate that the bivalve molluscs from the study sites in Kerch Strait are broadly speaking of the same aminostratigraphic age, and suggest an early MIS 5 age based on comparison with the results from previous AAR studies. In general, *Mytilus* had the highest D/L values and higher concentration of amino acids. *Cardium edule* had the lowest amino acid concentrations, but similar D/L values to that of *Chione gallina*. Articulated *Cardium edule* from Cape Krotkov had lower D/L values to the same species from Eltigen, and had a mean calibrated age of 108 ka. *Helicella* of last interglacial (MIS 5e) and MIS 3 age were recovered from Eltigen. The mean uranium-series ages, each from two valves, were 85.1 ± 0.65 ka (*Cardium edule*, Eltigen), 80.4 ± 0.8 ka (*Chione gallina*, Eltigen), and 147.4 ± 1.5 ka (*Cardium edule*, Maly Kut). In contrast with these results, the lowest D/L values for articulated *Chione gallina* (Glutamic acid D/L = 0.195) were obtained on samples from Maly Kut. Lower D/L values were obtained on *Chione gallina* valves from stratigraphically lower horizons at Eltigen (Glutamic D/L = 0.254) than from those highest in the sequence (Glutamic D/L = 0.283).

Discussion

The global record of last interglacial (MIS 5e) sedimentary sequences indicates a significant lowering of sea-level between MIS 5e and MIS 5c. It is difficult to discern how marine sedimentary sequences may be preserved in Kerch Strait, and attributed ages (here) of MIS 5e and 5c, without connection to the Mediterranean unless Kerch Strait and the Sea of Azov existed as an enclosed saline lake once the Mediterranean influence receded from the Black Sea following the regression during MIS 5d. In this regard this study is inconclusive, though given the broadly similar D/L values at each of these study sites in Kerch Strait it is suggested that these sedimentary sequences are all of MIS 5e age.

References

- Arslanov, Kh. A., 1993: Late Pleistocene geochronology of European Russia. *Radiocarbon* 35, 421 – 427.
- Arslanov, Kh. A., Tertychny, N. I., Kuznetsov, V. Yu., Chernov, S. B., Lokshin, N. V., Gerasimova, S. A., Maksimov, F. E., Dodonov, A. E., 2002: $^{230}\text{Th}/\text{U}$ and ^{14}C dating of mollusc shells from the coasts of the Caspian, Barents, White and Black seas. *Geochronometria* 21, 49-56.
- Bylinsky, E. N., Yanko, V. V., Motnenko, I. V., 1990: Sea-level changes at the Eltigen coastal exposure, East Crimea. MBSS newsletter, no 12.
- Dodonov, A. E., Tchepalyga, A. L., Mihailescu, C. D., Zhou, L. P., Markova, A. K., Trubikhin, V. M., Simakova, A. N., Konikov, E. G., 2000: Last interglacial records from central Asia to the northern Black Sea shoreline: stratigraphy and correlation. *Geologie en Mijnbouw* 79, 303 – 311.
- Hua, Q., Jacobsen, G. E., Zoppi, U., Lawson, E. M., Williams, A. A., Smith, A. M., McGann, M. J., 2001. Progress in radiocarbon target preparation at the Antares AMS centre. *Radiocarbon* 43, 275-282.
- Kaufman, D. S., Manley, W. F., 1998: A new procedure for determining DL amino acid values in fossils using reverse phase liquid chromatography. *Quaternary Science Reviews* 17, 987-1000.
- Muratov, V. M., Ostrovsky, A. B., Fridenberg, E. O., 1974. Quaternary stratigraphy and palaeogeography on the Black Sea coast of Western Caucasus. *Boreas* 3, 49-60.
- Svitoch, A. A., 2009. Karangatian stratotypes in the Taman and Kerch Peninsulas (Comparative Analysis). *Doklady Earth Sciences* 425, 210-212.
- Zhao J. X., Hu K., Collerson K. D., Xu H. K., 2001: Thermal ionization mass spectrometry U-series dating of a hominid site near Nanjing, China. *Geology* 29, 27-30.
- Zubakov, V. A., 1988: Climatostratigraphic scheme of the Black Sea Pleistocene and its correlation with the oxygen-isotope scale and glacial events. *Quaternary Research* 29, 1 -24.

Abstract F

IGCP 521 Fourth Plenary Meeting and Field Trip, Bucharest (Romania) - Varna (Bulgaria), October 4-16, 2008

Oral presentation.

Nicholas, W. A., Chivas, A. R., Murray-Wallace, C. V., Yanko-Hombach, V.

Amino acid racemization and AMS radiocarbon dating of Holocene Black Sea core sediments

Keywords: Aminostratigraphy, *Cardium edule*, micro-molluscs, reworking, Black Sea Flood

Introduction The timing, extent and direction of sea-level change within the Black Sea Basin, has become a topic of some discussion since Ryan *et al.*'s (1997) proposition for a Black Sea Flood from the Mediterranean during the early Holocene. One particular debate concerns the scientific merit of using fossil material for dating and/or palaeoenvironmental reconstruction (e.g. Yanko-Hombach *et al.*, 2007) because of the possibility of misassociation of specific habitats and environments. Such diagnosis is, in part, contingent on the absence and/or recognition of reworked material. The predominant method used to chronologically investigate the reworking phenomena in fossils has been the use of paired AAR and ^{14}C dating (e.g. Goodfriend, 1989; Murray-Wallace & Belperio, 1994). The aim of this pilot study is to utilise the amino acid racemization (AAR) geo-chronological technique to date a number of shells in Holocene cores from the Black Sea, and investigate the possible extent of time-averaging in Black Sea sediments.

Methods Reverse-Phase High Performance Liquid Chromatography was used to examine the extent of amino acid racemisation in 10 *Cardium edule* molluscs from core BS 37A, and 1 *Cardium edule* from core BS 37, Ukrainian shelf (see Konikov *et al.*, 2007). The amino acid racemisation analytical method used here is based on Kaufman and Manley (1998) with modification by the addition of strong bleaching (12.5% NaOCl) for one hour. Four mollusc samples were subjected to AMS radiocarbon dating at the ANSTO facility, Lucas Heights, Sydney, with the results from two being used to obtain radiocarbon-calibrated amino acid ages on these molluscs analysed for AAR. Initial AMS radiocarbon results were reported in Konikov *et al.*, (2007). Seven AMS radiocarbon ages were also obtained on selected samples – two from peat and five from micromolluscs, from core 721, recovered from 14.9 m water depth, Sukhumi Bay, Georgian Shelf, eastern Black Sea (Kvavadze and Connor, 2005; Yanko-Hombach, 2007; Yanko-Hombach *et al.*, 2007). All ^{14}C dates presented here are uncalibrated and uncorrected radiocarbon ages. These micromollusc ages represent the only ^{14}C dates from the marine section of core 721 (0 – 26.1 m).

Results Nine amino acid racemization ages were obtained for core BS 37A using glutamic acid. These D/L values were calibrated with 2 AMS dated shells (uncalibrated and uncorrected ^{14}C AMS years) to give a parabolic equation ($y = 0.001362x + 0.011216$). Shell ages range between 2000 and 4250 yrs. Two shells, from 1.83 – 1.86 m and 1.92 – 1.94 m depth, had the same glutamic acid D/L values and thus the same AMS-AAR ages (1992 years BP). Coefficients of variation (CV %) for shells in BS 37A ranged between 0 and 13%, with a mean CV of 5.6%. In general, these variations in results are slightly higher than for similarly analysed *Cardium edule* from Eltigen, Kerch Strait.

Seven ages were obtained on material from core 721, Sukhumi Bay, Georgian shelf, Black Sea. These include five ages on micro-molluscs, and two on peat. Peat recovered from 26.2 m depth was dated to 8530 ± 110 yr BP, and the peat sample from 26.5 m depth was dated to 9370 ± 70 a BP. Using these data, an age of 8250 a BP is obtained for the top of the peat at 26.1 m. The silt unit immediately above

the peat between approximately 19.2 and 26.1 m contains mollusc remains including those of *Dreissena polymorpha* and *Cardium edule* (Fig. 9, Yanko-Hombach *et al.*, 2007). An age of 8210 ± 120 ^{14}C a BP was obtained on micromolluscs from 22.0 m depth. Ages above this are 3495 ± 50 (17.25 m), 3190 ± 90 (15.0 m), 2530 ± 80 (8.0 m), and 1790 ± 90 ^{14}C a BP (2.0 m).

Discussion These results indicate that *Cardium edule* valves in core BS 37A between approximately 1.5 and 2.0 m depth are reworked with, for example, shells at 1.49 m depth being older than those at 1.85 and 1.93 m depth. The maximum extent of time-averaging between shells is up to 2,300 yrs in equivalent horizons (1.93 and 1.95 m depth) of the sampled section. There are no preservational differences between samples that would suggest a significant diagenetic influence on results. Based on the extent of racemization in the mollusc samples from BS 37A these AAR results indicate that the use of individual or bulk shell samples for ^{14}C dating requires caution in dating Black Sea sedimentary events because of the likelihood of overestimating the age of the event under scrutiny.

Peat ages reported here from core 721 are similar to those previously measured (26.7 m depth, 9580 ± 80 yr B.P., Yanko and Troitskaya, 1987; Yanko-Hombach, 2007). It is not possible to directly compare radiocarbon ages on peat with those of micromolluscs because there is no accepted reservoir correction for molluscs from the Black Sea. Radiocarbon ages obtained here indicate a linear sedimentation rate of 0.9 cm a^{-1} for the strata between 2.0 m (1790 ± 90 ^{14}C a BP) and 17.25 m depth (3495 ± 50 ^{14}C a BP) in core 721. Comparison of the sedimentation rate and ages with the older age of 8210 ± 120 ^{14}C a BP on micromolluscs at 22.0 m depth point to a change in deposition rates at a depth of approximately 18.2–19.2 m. This corresponds with the transition from sand to silt lithologies (Fig. 9, Yanko-Hombach *et al.*, 2007) and may represent a period of significantly reduced sedimentation.

References

- Goodfriend, G. A. 1989. Complementary use of amino acid epimerization and radiocarbon analysis for dating mixed-age fossil assemblages. *Radiocarbon* 31, 1041–1047.
- Konikov, E., Likhodedova, O., Pedan, G., 2007. Paleogeographic reconstructions of sea-level change and coastline migration on the northwestern Black Sea shelf over the past 18 kyr. *Quaternary International* 167–168, 49–60.
- Kaufman, D. S., Manley, W. F., 1998. A new procedure for determining DL amino acid values in fossils using reverse phase liquid chromatography. *Quaternary Science Reviews* 17, 987–1000.
- Murray-Wallace, C.V., Belperio, A.P., 1994. Identification of remanié fossils using amino acid racemisation. *Alcheringa* 18, 219–227.
- Ryan, W. B. F., Pitman III, W. C., Major, C. O., Shimkus, K., Moskalenko, V., Jones, G. A., Dimitrov, P., Görür, N., Sakinc, M., Yüce, H., 1997. An abrupt drowning of the Black Sea Shelf. *Marine Geology* 138, 119–126.
- Yanko, V.V., T.S. Troitskaya, T. S., 1987. Pozdnechetvertichnye foraminifery Chernogo moria [Late Quaternary Foraminifera of the Black Sea]. Nauka, Moscow. (In Russian)
- Yanko-Hombach, V. V., 2007. Controversy over Noah's Flood in the Black Sea: geological and foraminiferal evidence from the shelf. In Yanko-Hombach V., Gilbert A.S., Panin N., and Dolukhanov P., eds, *The Black Sea Flood Question: Changes in Coastline, Climate and Human Settlement*, Springer, Dordrecht, The Netherlands, pp. 149–203.
- Yanko-Hombach, V., Gilbert, A. S., Dolukhanov, P., 2007. Controversy over the great flood hypotheses in the Black Sea in light of geological, paleontological, and archaeological evidence. *Quaternary International* 167–168, 91–113.

Abstract G

IGCP 521 Fourth Plenary Meeting and Field Trip, Bucharest (Romania) - Varna (Bulgaria), October 4-16, 2008

Keynote

Nicholas, W. A., Chivas, A. R., Murray-Wallace, C. V., Yanko-Hombach, V., Chepalyga, A., Kadurin, S.

Aminostratigraphy of coastal sedimentary sequences, Kerch Strait, northeastern Black Sea

Keywords: Amino Acid Racemization, *Cardium edule*, *Chione gallina*, last interglacial (MIS 5e), whole-rock, reworking

Introduction

The principal methods used to constrain the timing of sea-level and environmental change for last interglacial (MIS 5e) sedimentary sequences have been Uranium-series and luminescence dating. An alternative to these, and used with success in studies on Australian coastal sedimentary sequences, is the amino acid racemization geochronological technique. Recent technological (Bruckner *et al.*, 1991) and methodological developments (Kaufman and Manley, 1998; Hearty *et al.*, 2004) now allow for calibrated age determinations on suitable skeletal carbonate including individual foraminifers and ostracods.

Marine coastal sedimentary sequences at Eltigen in Kerch Strait have been ascribed a last interglacial age (MIS 5e, 125 ka) based on U/Th dating techniques (Zubakov, 1988; Arslanov, 1993; Dodonov *et al.*, 2000; Arslanov *et al.*, 2002). However, the southernmost section at Eltigen (our BS-4, Fig. 1) has also been dated to MIS 7a and 7c (Bylinsky *et al.*, 1990). The focus of this study is to date the coastal sedimentary sequences at Eltigen, Kerch Strait, Ukraine, using aminostratigraphy, and where possible to correlate these deposits with similar sediments from the Taman Peninsula, Krasnodar Territory, Russia.

Methods

Reverse-Phase High Performance Liquid Chromatography was used to examine the extent of amino acid racemization (AAR) in the bivalve molluscs *Cardium edule*, *Chione gallina* and *Mytilus*. The extent of AAR was additionally analysed in whole-rock samples, - a term referring to the total content of skeletal carbonate material within a sediment sample. The AAR method used is based on Kaufman and Manley (1998) for shells and Hearty *et al.* (2006) for whole-rock samples, with modification of both by strong bleaching (12.5% NaOCl) for one hour. This method uses pre-column derivatisation with o-phthalaldehyde (OPA) and N-isobutyryl-L-cysteine (IBLC) to produce fluorescent chiral primary amino acids as diastereomeric derivatives, separable with a reverse-phase column.

Results

D/L values from whole-rock samples indicate that the sediments from BS-4 (Fig. 1) are older than those recovered from BS-5, 6 and 8 (Fig. 1), and the sediments of those latter study sites are of an equivalent aminostratigraphic age. D/L values from articulated and disarticulated single mollusc shells, principally *Chione gallina*, suggest that the age of the fossils at these locations (BS-4 and BS-6) are the same. Results from a limited number of articulated *Chione gallina* from Maly Kut (BS-11) indicate the shells from this study site are younger than those of Eltigen. Results from *Chione gallina* from Cape Tuzla are inconclusive (only two samples to date), but also suggest that these sediments are younger than those of Eltigen. D/L values from disarticulated valves (Eltigen) are not different to D/L values on articulated samples, suggesting that reworking of shell material for most of the sedimentary sequence at Eltigen is

intraformational. However, the older whole-rock samples from the southern study site at Eltigen indicate that at the initial time of sedimentation, reworking of pre-existing bioclastic sediments may have occurred.

Discussion

Based on the extent of racemization in the amino acids glutamic, valine and alioi-soleucine, a MIS 5e age seems appropriate for the raised sedimentary sequence at Eltigen. However, D/L values in articulated *Chione* are generally lower for study site BS-4 than for BS-6 (Fig. 1) – the opposite of the apparent stratigraphic sequence. Accepting a MIS 5e age for Eltigen and using a parabolic method for age estimation, the articulated *Chione gallina* from Cape Tuzla are of MIS 5e (using valine) or 5c age (using glutamic acid), while those from Maly Kut are early MIS 3 (valine or glutamic acid).

The AAR age of the sedimentary sequence at Maly Kut, previously correlated with Eltigen on the presence of *Chione gallina* and similar marine molluscs, appears erroneously young. The distribution of D/L ratio based ages correlates with preservational differences in these shells. The best preserved shells (BS-6) have the higher D/L values, those more poorly preserved (BS – 9, 11) have lower D/L values. AAR age differences between these molluscs are therefore likely to be related to differences in physical and diagenetic environments between the individual study sites rather than large chronological variations.

References

- Arslanov, Kh. A., 1993: Late Pleistocene geochronology of European Russia. *Radiocarbon* 35, 421 – 427.
- Arslanov, Kh. A., Tertychny, N. I., Kuznetsov, V. Yu., Chernov, S. B., Lokshin, N. V., Gerasimova, S. A., Maksimov, F. E., Dodonov, A. E., 2002: $^{230}\text{Th}/\text{U}$ and ^{14}C dating of mollusc shells from the coasts of the Caspian, Barents, White and Black seas. *Geochronometria* 21, 49-56.
- Brückner, H., Wittner, R., Godel, H., 1991: Fully automated high-performance liquid chromatographic separation of DL-amino acids derivatised with o-Phthaldialdehyde together with N-isobutyryl-cysteine. Application to food samples. *Chromatographia* 32, 383-388.
- Bylinsky, E. N., Yanko, V. V., Motnenko, I. V., 1990: Sea-level changes at the Eltigen coastal exposure, East Crimea. *MBSS newsletter*, no 12.
- Dodonov, A. E., Tchepalyga, A. L., Mihailescu, C. D., Zhou, L. P., Markova, A. K., Trubikhin, V. M., Simakova, A. N., Konikov, E. G., 2000: Last Interglacial records from central Asia to the northern Black Sea shoreline: stratigraphy and correlation. *Geologie en Mijnbouw* 79, 303 – 311.
- Hearty, P., O'Leary, M., Donald, A., Lachlan, T., 2006: The enigma of 3400 years BP coastal oolites in tropical northwest Western Australia...why then, why there? *Sedimentary Geology* 186, 171-185.
- Kaufman, D. S., Manley, W. F., 1998: A new procedure for determining DL amino acid values in fossils using reverse phase liquid chromatography. *Quaternary Science Reviews* 17, 987-1000.
- Zubakov, V. A., 1988: Climatostratigraphic scheme of the Black Sea Pleistocene and its correlation with the Oxygen-isotope scale and glacial events. *Quaternary Research* 29, 1 -24.